

Dissertation zur Erlangung des Doktorgrades
der Fakultät für Chemie und Pharmazie
der Ludwig-Maximilians-Universität München

**Quantification of Electrophilic Reactivities of Ketones and
Heteroallenes**

Zhen Li

aus

Baotou, Nei Mongol, China

2018

Erklärung

Diese Dissertation wurde im Sinne von § 7 der Promotionsordnung vom 28. November 2011 von Herrn Prof. Dr. Herbert Mayr betreut.

Eidesstattliche Versicherung

Diese Dissertation wurde eigenständig und ohne unerlaubte Hilfe erarbeitet.

München, 14.06.2018

Zhen Li

Dissertation eingereicht am 14.06.2018

1. Gutachter: Prof. Dr. Herbert Mayr
2. Gutachter: Prof. Dr. Hendrik Zipse

Mündliche Prüfung am 10.07.2018

...dedicated to my family

Acknowledgements

First and foremost, I would like to express my sincere gratitude to my supervisor Prof. Dr. Herbert Mayr for giving me the opportunity to work in his lab. I really appreciate all his help during my PhD period. His broad knowledge of science and rigorous working attitude have impacted on me very much. Numerous open discussions with him always gave me some new ideas and encouraged me to work well in the next period. I cannot overemphasize my gratitude for all the things I learned from him.

Furthermore, I would like to thank Prof. Dr. Hendrik Zipse for contribution to our joint project, reviewing my thesis, and also the board of examiners for their participation in my defense examination.

The financial support by the China Scholarship Council is gratefully acknowledged and I also thank the Consulate General of China in München for their kind help.

I must thank Dr. Armin R. Ofial for all his contributions on my PhD projects. His excellent suggestions and critical comments help me a lot. Owing to his routine management of our labs, we have such a good research environment.

I am also thankful to my past and present group members, Hildegard Lipfert, Brigitte Janker, Nathalie Hampel, Dr. Peter A. Byrne, Dr. Quan Chen, Dr. Guillaume Berionni, Dr. Xingwei Guo, Follet Elsa, Elija Wiedemann, Dr. Ángel Puente, Feng An, Artem Leonov, Daria Timofeeva, Patrick Jüstel, Robert Mayer, Le Li. I also thank Harish Jangra, Yihung Chen, Zhiliang Shen, Hongdong Hao, Bichu Cheng. Thank you for all kinds of help to me during my PhD period.

I would like to thank Frau Claudia Dubler and Dr. David Stephenson for the measurement of NMR spectra and Dr. Peter Mayer for solving crystal structures.

The last but not least, I really appreciate my whole family, especially my parents, for their unconditional support over the years.

Parts of this Ph.D. thesis have been published

“Nucleophilicity parameters of arylsulfonyl-substituted halomethyl anions”

Li, Z.; Chen, Q.; Mayer, P.; Mayr, H. *J. Org. Chem.* **2017**, 82, 2011–2017.

“Quantification and theoretical analysis of the electrophilicities of Michael acceptors”

Allgäuer, D. S.; Jangra, H.; Asahara, H.; Li, Z.; Chen, Q.; Zipse, H.; Ofial, A. R.; Mayr, H. *J. Am. Chem. Soc.* **2017**, 139, 13318–13329.

“Kinetics and mechanism of oxirane-formation by Darzens condensation of ketones: quantification of the electrophilicities of ketones”

Li, Z.; Jangra, H.; Chen, Q.; Mayer, P.; Ofial, A. R.; Zipse, H.; Mayr, H. *J. Am. Chem. Soc.* **2018**, 140, 5500–5515. (Selected in Spotlights on Recent JACS Publications “Ketone Electrophilicity Quantified” *J. Am. Chem. Soc.* **2018**, 140, 5659–5660.)

Conference Attended:

Kinetics and mechanism of oxirane-formation by Darzens Condensation of ketones

26th ISHC congress Sep 3-8, 2017 in Regensburg, Germany

(Poster Presentation)

Table of Contents

Chapter 0 Summary	1
Chapter 1 Introduction	11
Chapter 2 Nucleophilicity Parameters of Arylsulfonyl-Substituted Halomethyl Anions	23
Chapter 3 Kinetics and Mechanism of Oxirane-Formation by Darzens Condensation of Ketones:	
Quantification of the Electrophilicities of Ketones	53
Chapter 4 Quantification of Electrophilicities of Carbon Dioxide and Other Heteroallenes	211
Chapter 5 Kinetics and Mechanism of Corey-Chaykovsky Reactions of Acceptor-Substituted	
Ketones	251

Chapter 0: Summary

0.1 General

In previous work, the Mayr group has developed scales of nucleophilicities and electrophilicities based on linear free-energy relationship (1) which covers a reactivity range of 40 orders of magnitude.

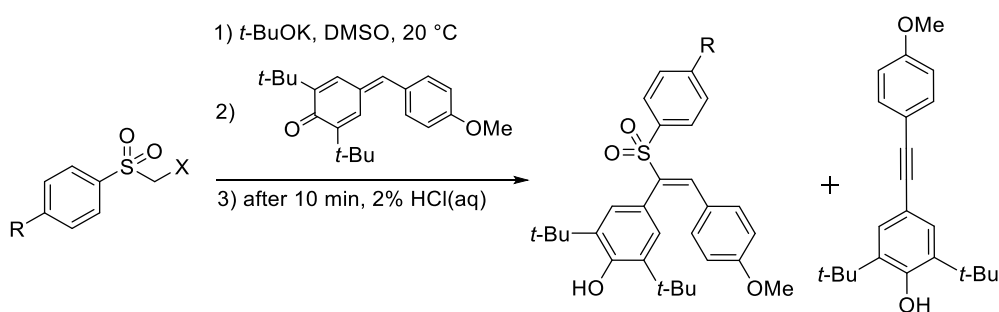
$$\log k_2(20\text{ }^{\circ}\text{C}) = s_N(N + E) \quad (1)$$

The purpose of this thesis is to examine the applicability of eq (1) for quantifying the electrophilic reactivities of ketones and heteroallenes.

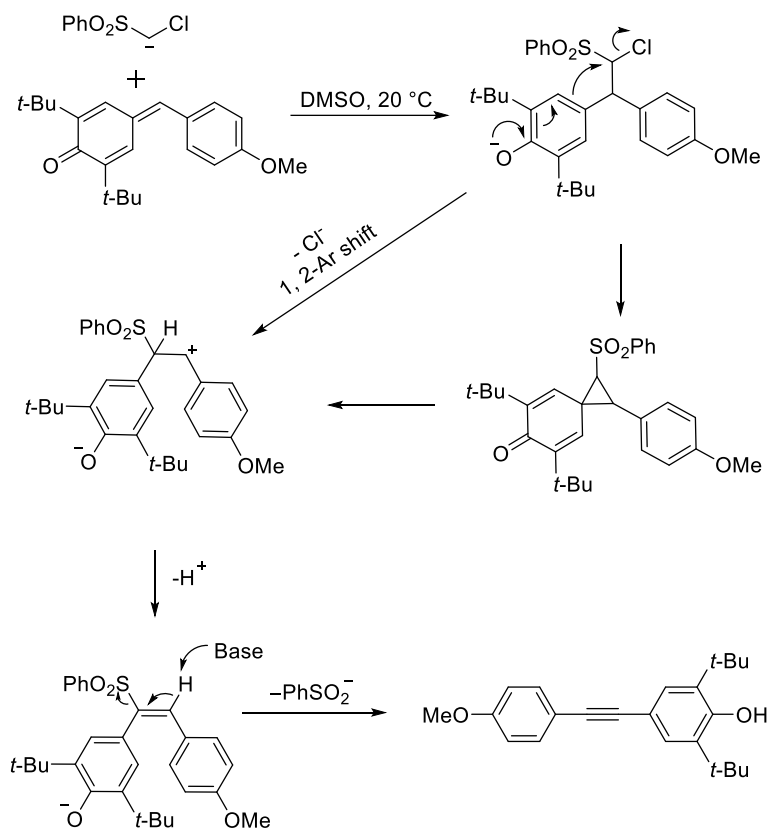
0.2 Nucleophilicity parameters of arylsulfonyl-substituted halomethyl anions

The rates of the reactions of the arylsulfonyl substituted carbanions carrying α -chloro and α -bromo substituents with quinone methides and benzyldenemalonates in DMSO were determined by UV-Vis spectroscopy at 20 $^{\circ}\text{C}$. When the reactions of halomethyl anions with quinone methides were carried out in DMSO at 20 $^{\circ}\text{C}$ and quenched with 2% aqueous HCl after 10 min, mixtures of products were obtained (Scheme 1). Scheme 2 suggests a plausible reaction mechanism.

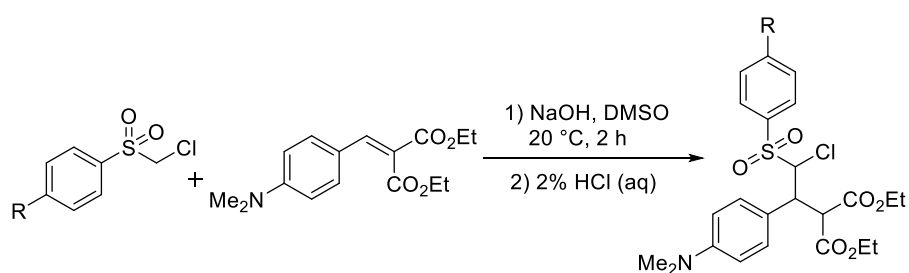
Scheme 1. Reaction of Arylsulfonyl-Substituted Halomethyl Anions with a Quinone Methide at 20 $^{\circ}\text{C}$



Scheme 2. Plausible Mechanism for the Reaction of Phenylsulfonyl-Substituted Chloromethyl Anion with a Quinone Methide



Scheme 3. Reaction of a Benzylidenemalonate with Arylsulfonyl-Substituted Chloromethyl Anions



The NaOH induced reaction of arylsulfonyl-substituted chloromethane with a benzylidenemalonate in DMSO gave a Michael adduct (Scheme 3).

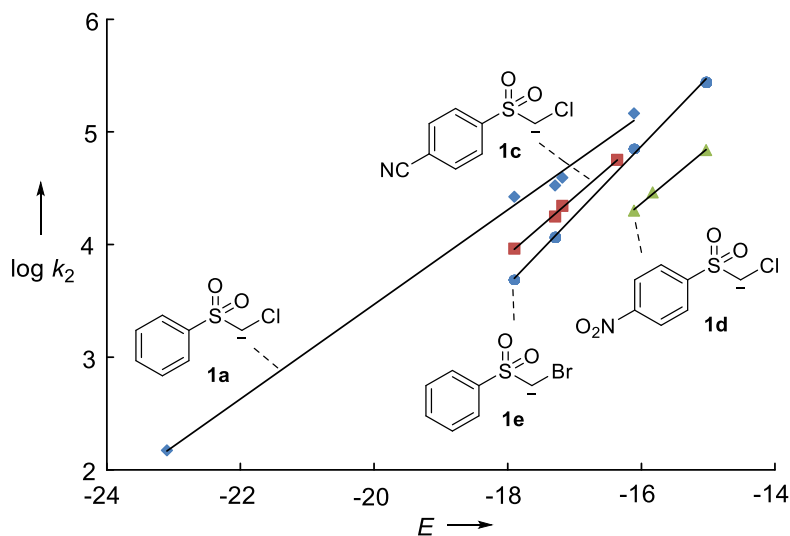


Figure 1. Correlation of $\log k_2$ for the reactions of the carbanions **1a** and **1c–e** with the quinone methides **2a–g** and benzylidenemalonates **2h–i** versus the electrophilicity parameters E of the corresponding electrophiles.

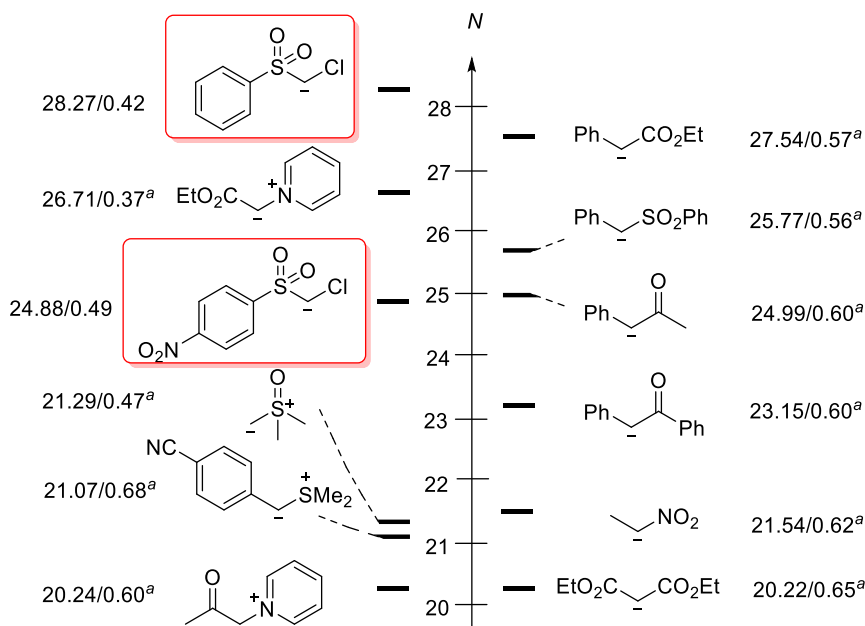


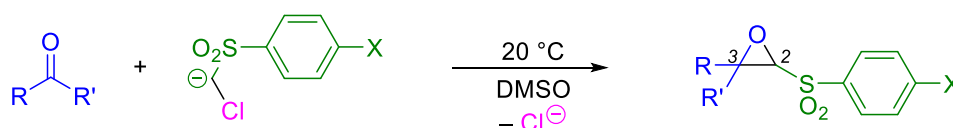
Figure 2. Comparison of the nucleophilicity parameters N (in DMSO at 20 °C) of arylsulfonyl-substituted chloromethyl anions with other classes of nucleophiles

Figure 1 shows that $\log k_2$ for these reactions correlate linearly with E as required by eq 1 and thus allow the calculation of the nucleophile-specific parameters N and s_N . The comparison of nucleophilicity parameters N of carbanions in this work with other classes of nucleophiles is shown in Figure 2.

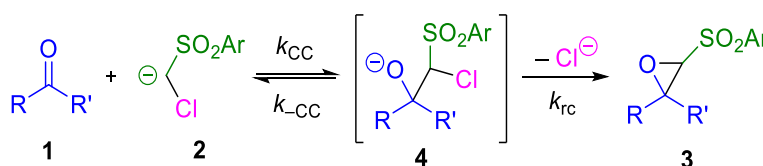
0.3 Kinetics and mechanism of oxirane-formation by Darzens condensation of ketones: quantification of the electrophilicities of ketones

The kinetics of epoxide formation by Darzens condensations of aliphatic ketones with arylsulfonyl-substituted chloromethyl anions ($\text{ArSO}_2\text{CH}^-\text{Cl}$) have been determined photometrically in DMSO solution at 20 °C. The corresponding reactions in DMSO proceeded smoothly at room temperature (Scheme 4) and gave the epoxides in good yields.

Scheme 4. Reactions of Arylsulfonyl-Substituted Chloromethyl Anions with Ketones



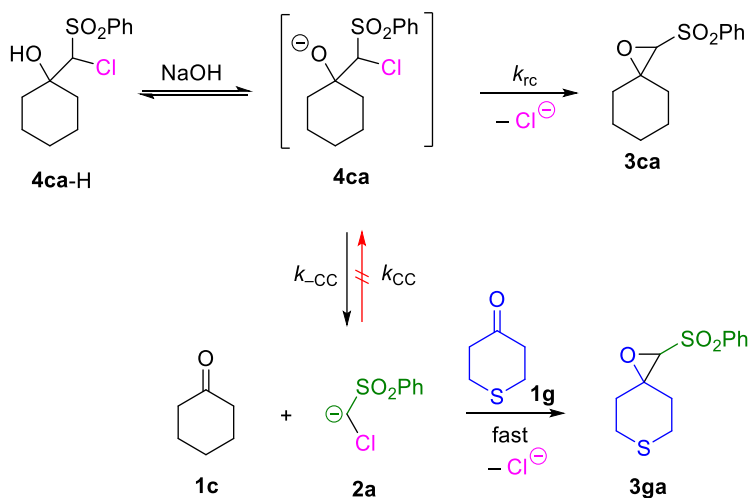
Scheme 5. Mechanism of the Reactions of Arylsulfonyl-Substituted Chloromethyl Anions with Ketones



As shown in Scheme 5, nucleophilic attack of **2** at the ketone **1** yields the intermediate alkoxide anion **4**, which either cyclizes with formation of the epoxide **3** or undergoes retroaddition with regeneration of ketone **1** and carbanion **2**. According to equation (2), the rate of the attack of **2** at the carbonyl group (k_{CC}) can be derived from the measured rate constant k_2^{exp} if the ratio $k_{-\text{CC}}/k_{\text{rc}}$ is known. The ratio $k_{-\text{CC}}/k_{\text{rc}}$ was derived from a crossover experiment with independently synthesized **4-H** as starting material (Scheme 6).

$$k_2^{\text{exp}} = k_{\text{CC}} / (k_{-\text{CC}}/k_{\text{rc}} + 1) \quad (2)$$

The principle of the crossover experiments is illustrated in Scheme 6. When the independently synthesized halohydrin **4ca-H** was treated with NaOH in the presence of the highly reactive ketone **1g**, the generated intermediate **4ca** has the choice of either undergoing ring closure with formation of the epoxide **3ca** or retroaddition with regeneration of **1c** and **2a**. As **1g** is considerably more reactive and present in higher concentration than **1c**, any regenerated carbanion **2a** will exclusively be converted into the crossover product **3ga**, and the ratio $[\mathbf{3ga}]/[\mathbf{3ca}]$ equals the ratio $k_{-\text{CC}}/k_{\text{rc}}$.

Scheme 6. Crossover Experiment with the Cyclohexanone Adduct **4ca-H**

Substitution of k_{CC} (derived from k_{-CC}/k_{rc} and k_2^{exp} based on equation 2) and the published parameters N and s_N for **2** into equation 1 yielded the electrophilicity parameters E of the ketones **1**. As illustrated in Figure 3, the electrophilicities of saturated aliphatic ketones are comparable to the C=C bond reactivities of β -phenyl substituted α,β -unsaturated ketones, much lower than the C=C bond reactivities of terminally unsaturated vinyl ketones. As for the electrophilic reactivities

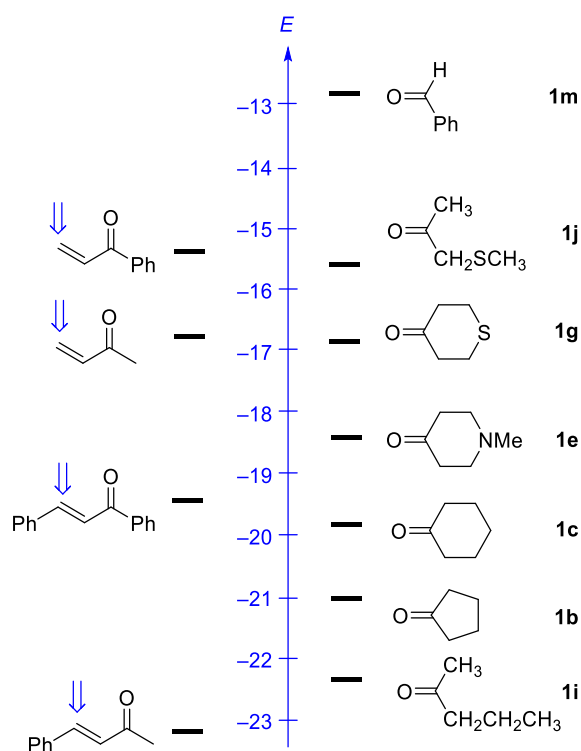


Figure 3. Comparison of the empirical electrophilicities E of carbonyl groups and Michael acceptors in DMSO.

of Michael acceptors, the electrophilicities E of the ketones **1a–1j** correlate well with the calculated methyl anion affinities in DMSO. (Figure 4).

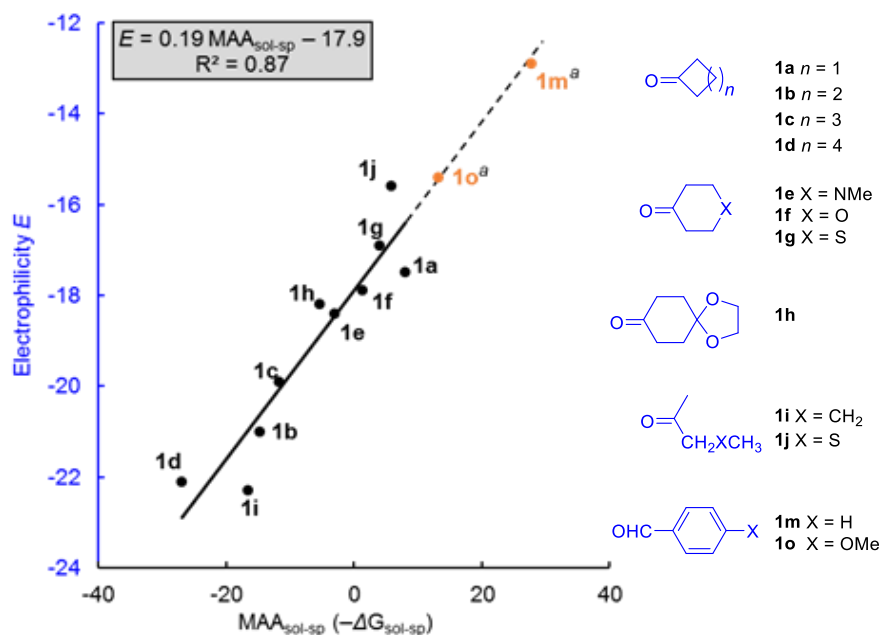


Figure 4. Correlation between electrophilicities (E) of ketones with their MAA_{sol-sp} values ($-\Delta G_{sol-sp}$, kJ mol^{-1}) calculated at SMD(DMSO)/B3LYP/6-311++G(3df,2pd) //B3LYP/6-31G(d,p) level of theory. ^a Aldehydes **1m** and **1n** were not used for the construction of the correlation line.

0.4 Quantification of electrophilic reactivities of carbon dioxide and other heteroallenes

The kinetics of the reactions of heteroallenes **1** with reference nucleophiles (carbanions **2** and enamines **3**) have been investigated in DMSO or CH_3CN solution at 20°C and their second order rate constants k_2 were obtained. The corresponding reactions in DMSO or CH_3CN proceeded smoothly at room temperature (Scheme 7).

Scheme 7. Reactions of Heteroallenes **1** with Carbanions **2**.

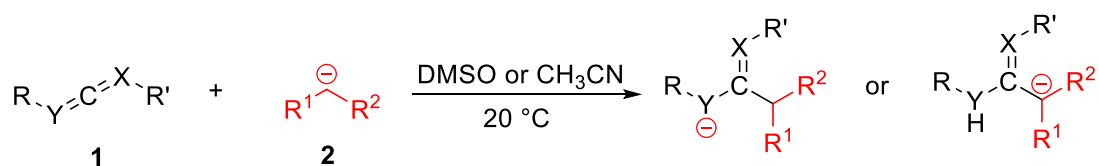


Figure 5 shows that the correlations of $(\log k_2)/s_N$ for the reactions of heteroallenes **1** with carbanions **2** and enamines **3** versus the corresponding nucleophilicity parameters N are linear

with a slope of roughly 1.0 as required by eq 1. It indicates that the reactions of cumulative π system with enamines and carbanions follow the linear free-energy relationship (1) as the corresponding reactions of benzhydrylium ions and other π electrophiles. A comparison of the electrophilicities E of heteroallenes is shown in Figure 6.

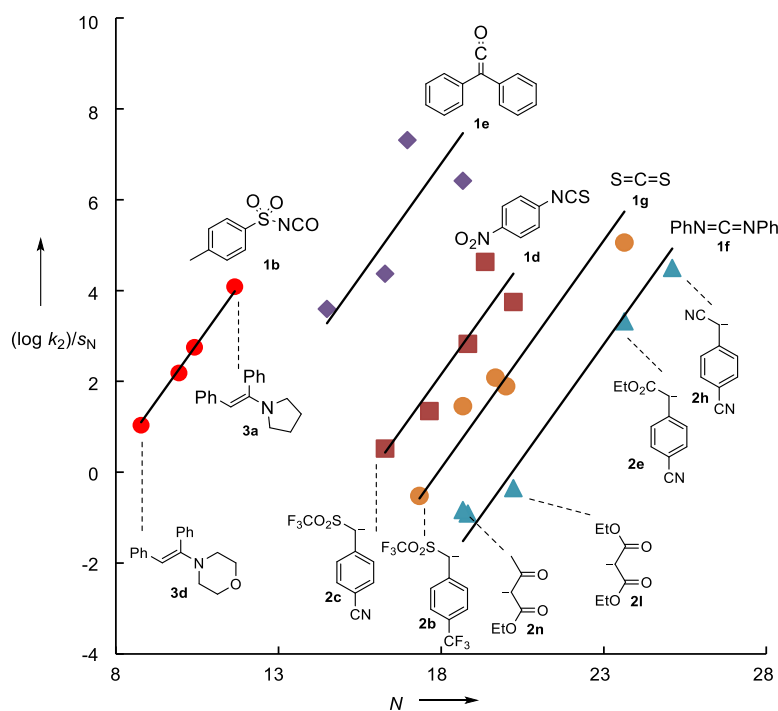


Figure 5. Plot of $(\log k_2)/S_N$ vs N for the reactions of heteroallenes **1** with carbanions **2** and enamines **3** in DMSO or CH_3CN at 20 °C (the slope is enforced to 1). For the sake of clarity, the correlation lines for PhNCO (**1a**) and PhNCS (**1c**) are shown only in the experimental section of Chapter 4.

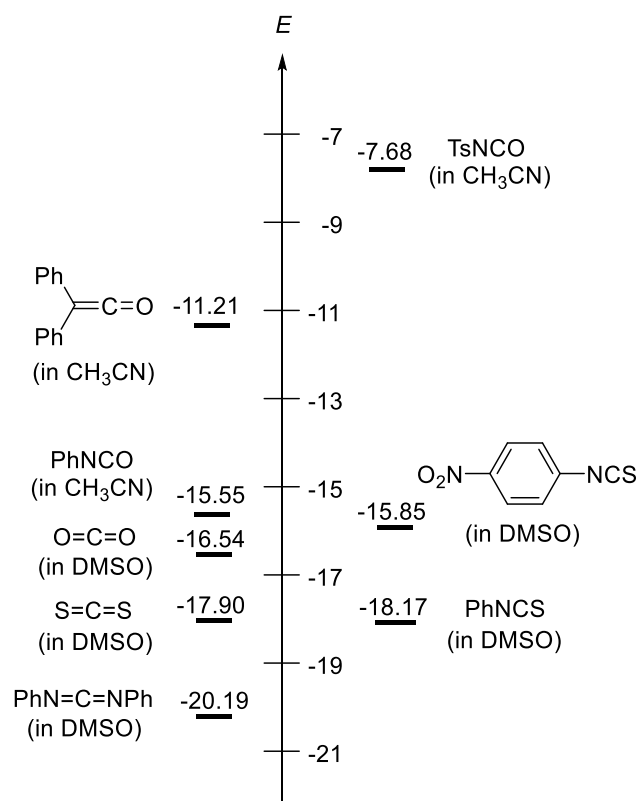
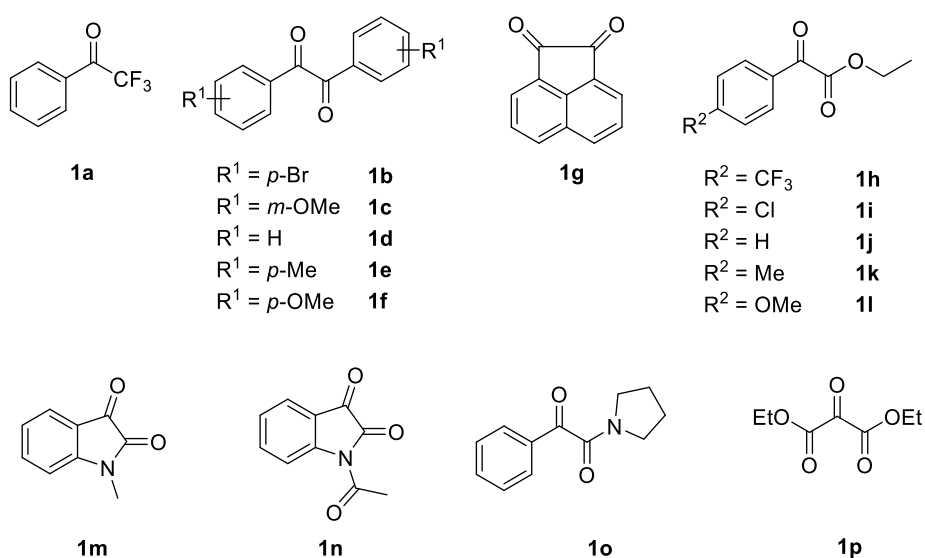


Figure 6. Comparison of the electrophilicities of heteroallenes

0.5 Kinetics and mechanism of Corey-Chaykovsky reactions of acceptor-substituted ketones

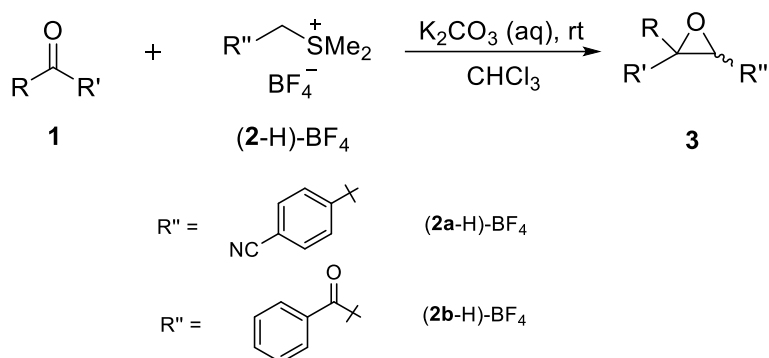
Scheme 8. Activated Ketones Studied in This Work



The kinetics of epoxide formation by Corey-Chaykovsky reaction of activated ketones **1** (Scheme 8) with sulfonium ylides **2** (Scheme 9) have been determined photometrically in DMSO solution

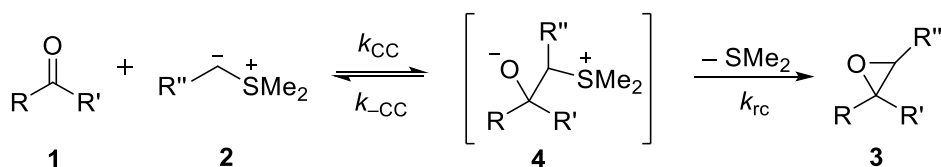
at 20 °C. The corresponding reactions proceeded smoothly at room temperature under phase transfer conditions (CHCl_3 /aqueous solution of K_2CO_3) to give the epoxides **3** in good yields (Scheme 9).

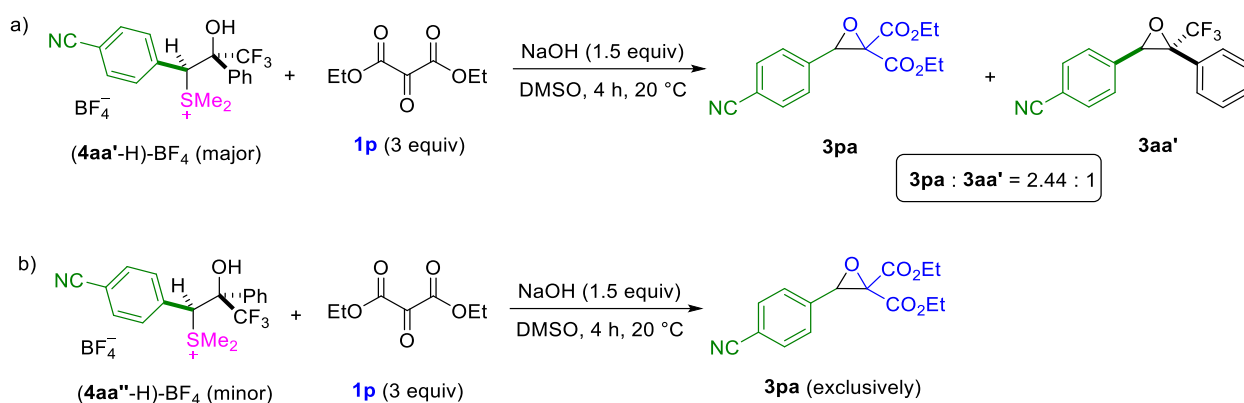
Scheme 9. Reactions of Sulfonium Ylides **2** with Activated Ketones **1**.



As shown in Scheme 10, the sulfur ylide mediated epoxidations (Corey-Chaykovsky reaction) proceed via initial nucleophilic attack of sulfonium ylide **2** at ketone **1** to give the zwitterion **4** which either undergoes retroaddition (k_{CC}) or intramolecular substitution with elimination of dimethyl sulfide and formation of epoxide **3**. In order to determine the degree of reversibility, we synthesized and separated the diastereomeric intermediates **4aa'**-H and **4aa''**-H and subjected them to the crossover experiments shown in Scheme 11. The intermediate **4aa'** undergoes ring closure with formation of epoxide **3aa'** as well as retroaddition with generation of ketone **1a** and carbanion **2a** which is quantitatively intercepted by ketonmalonate **1p** to form epoxide **3pa**, while the other intermediate **4aa''** exclusively undergoes retroaddition to form the crossover product **3pa** under the same reaction condition (Scheme 11). The results of the crossover experiments suggest the preferred formation of product **3aa'** with Ar and CF₃ trans to each other, since the rate of cyclization of **4aa''** is much slower than the rate of retroaddition with regeneration of **1a** and **2a**.

Scheme 10. Mechanism of the Reactions of Sulfonium Ylides **2** with Ketones **1**



Scheme 11. Crossover Experiments of **4aa'**-H and **4aa''**-H

Whereas the diastereoselectivity of initial attack of sulfonium ylide **2a** at the ketone **1a** is unknown in DMSO solution at 20 °C under the conditions of the kinetic experiments, we cannot derive k_{CC} and subsequently derive the E parameter.

Chapter 1: Introduction

1.1 General

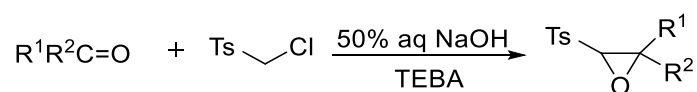
Ketones and heteroallenes are common electrophiles which are widely used in organic synthesis. It was the goal of my work to quantify their electrophilic reactivities, to include them in the comprehensive electrophilicity scale of the Mayr group, and thus compare their reactivities with those of other electrophiles. The obtained electrophilicity parameters could be employed by organic chemists to predict scope and selectivities of the reactions of these electrophiles with nucleophiles.

Ordinary acceptor-stabilized carbanions are not suitable as reference nucleophiles for the determination of the *E* parameters of ketones in aprotic solvents as the nucleophilic attack of such carbanions at the carbonyl group is usually endergonic in aprotic solvents and these reactions only proceed in the presence of a suitable proton source. For that reason, carbanions carrying a leaving group in α -position are used as reference nucleophiles since the initially formed intermediates may undergo cyclization with formation of epoxides. Whereas acceptor-substituted sulfonium ylides are not sufficiently nucleophilic to react with typical ketones, arylsulfonyl-substituted halomethyl anions were known to react with typical ketones to form epoxides. As their nucleophilicity parameters have not yet been reported, my first task was the determination of *N* and *s_N* of arylsulfonyl-substituted halomethyl anions.

1.2 Arylsulfonyl-substituted halomethyl anions

Carbanions bearing leaving groups at position α are useful reagents in organic synthesis. They are widely used in Darzens condensations, cyclopropanations, aziridinations, and vicarious nucleophilic substitutions.

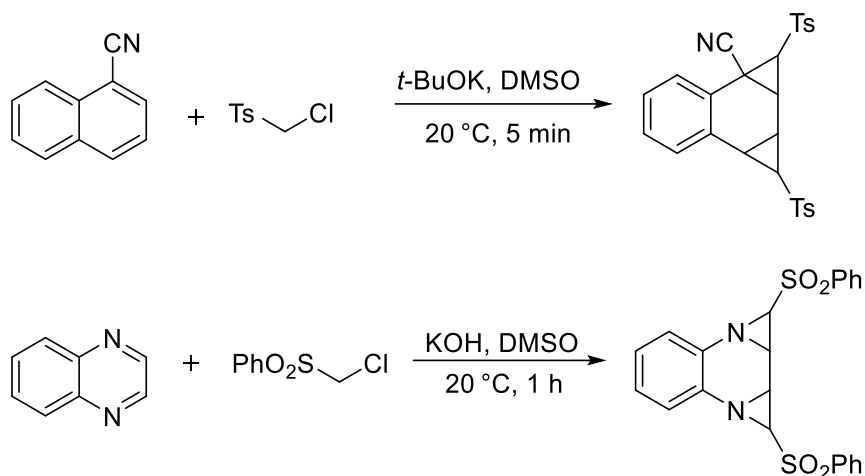
Scheme 1. Darzens Condensation of Carbonyl Compounds with Tosyl-Substituted Chloromethyl Anion



Makosza group developed a method to synthesize epoxy sulfones by the reaction of the arylsulfonyl-stabilized chloromethyl anion with carbonyl compounds. A one-pot Darzens

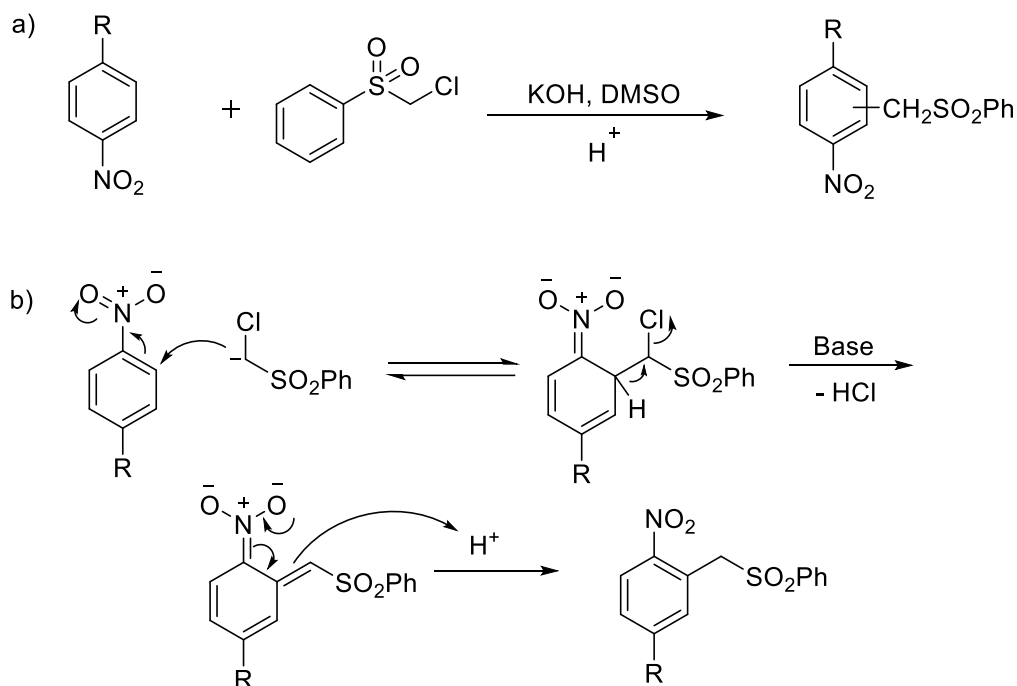
condensation was achieved by using a phase transfer catalyst, benzyltriethylammonium chloride, in 50% sodium hydroxide solution.¹

Scheme 2. Cyclopropanation and Aziridination Reactions of Arylsulfonyl-Substituted Chloromethyl Anions



Makosza group also employed this type of anions to perform cyclopropanation and aziridination reactions with different electrophilic arenes.²

Scheme 3. Vicarious Nucleophilic Substitution of Nitroarenes with Phenylsulfonyl Chloromethyl Anion and Corresponding Reaction Mechanism.



The vicarious nucleophilic substitution (VNS) is a special type of nucleophilic aromatic substitution. A nucleophile replaces a hydrogen atom on the aromatic ring rather than leaving groups such as halogen substituents which are commonly used in S_NAr. Numerous studies have

been performed by Professor Makosza and his coworkers.³ The VNS is a two-step reaction which proceeds via initial formation of the σ -adducts, followed by a base-induced β -elimination (Scheme 3).^{3a} Apart from nitroarenes, heteroarenes such as nitropyrroles,^{3b} nitrothiophenes,^{3b} nitrofuranes,^{3b} etc. also react efficiently with arylsulfonyl chloromethyl anions.

1.3 Reactivities of aliphatic ketones

Ketones belong to the most frequently employed electrophiles in organic synthesis. Several reports on their electrophilic reactivities have previously been studied. Herbert C. Brown and coworkers have studied the kinetics of reactions of carbonyl compounds with sodium borohydride in *isopropyl* alcohol.⁴ The rates of reaction of sodium borohydride with a number of cyclanones were determined at various temperature and shown in Table 1.^{4c} From Table 1, one can see that cyclobutanone and cyclohexanone are the most reactive compounds among the examined ketones, and cyclohexanone is more reactive than cyclopentanone. There is a drop in reactivity from 7- to 10-ring derivatives and the 10-ring cyclanone is the least reactive ketone in this table. From 10-ring to open chain derivative, di-*n*-hexylketone, the reactivity increases slightly. The results were explained by changes in internal strain.

Geneste and associates have also performed numerous investigations of the reactivities of ketones. They studied the kinetics of the reactions of 26 ketones with BH_4^- ,^{5a} CN^- ,^{5b} SO_3^{2-} ,^{5b,5c} NH_2OH ,^{5b,5d} and RS^- ^{5e} in water and reported linear correlations^{5f} between the different sets of data. A linear relationship $\log k = A \log k_0 + B$, where k is the rate constant for the reaction of the ketone under consideration with a given nucleophile and k_0 is the corresponding rate constant for cyclohexanone, was reported by Geneste. Because cyclohexanone is a strain-free molecule it was selected as reference. Values of A and B for several ketones are recorded in Table 2.^{5f} One can see in most cases, the susceptibilities A are close to 1, and Geneste's equation can, therefore, be simplified to $\log k/k_0 = B$. Positive values of B indicate that the test ketone is more reactive than cyclohexanone. A values close to 1 indicate that the relative reactivities of ketones are independent of the nature of the nucleophiles. Geneste furthermore reported that the ketone reactivities B did not give a good correlation with the strain energy f (ketone strain energy – cyclohexanone strain energy) developed by Allinger.⁶

Table 1. Rate Constants and Derived Data for the Reaction of the Cyclanones with Sodium Borohydride in *Isopropyl Alcohol* Solution.

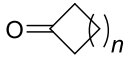
	Temp. (°C)	Rate constant $k_2 \times 10^4$	$E_{\text{act.}}$ (kcal mol ⁻¹)	log <i>A</i>	ΔH^\ddagger (kcal mol ⁻¹)	ΔS^\ddagger (e.u.)
1	-24.1 -14.5 0.1	56.9 115 266	8.6	5.4	8.1	-36.4
2	0.0 25.0 35.1	7.01 31.8 54.1	9.8	4.7	9.3	-38.8
3	-23.7 -9.2 0.0	61.7 115 161	5.8	2.9	5.1	-48.1
4	0.0 25.0 35.1	1.02 4.90 8.54	10.2	4.1	9.6	-41.6
5	0.0 25.0 35.1	0.0781 0.411 0.963	11.9	4.4	11.3	-41.2
6	25.0 35.1 45.0	0.203 0.381 0.732	12.2	4.3	11.6	-41.4
7	25.0 35.1 45.0	0.103 0.218 0.416	13.1	4.6	12.6	-43.5
8	25.0 35.1 45.1	0.152 0.290 0.537	12.0	4.0	11.4	-42.4
9	25.0 35.1 45.1	1.05 1.98 3.42	11.3	4.3	10.7	-41.0
10	0.0 25.0 35.0	0.194 1.22 2.22	11.8	4.7	11.1	-39.2
12	0.0 25.0 35.1	0.420 2.41 4.61	11.5	4.9	10.8	-38.9
14	0.0 25.0 35.0	0.583 3.07 5.56	10.7	4.4	10.2	-40.5
di-n-hexyl ketone	25.0 35.1 45.0	2.67 5.05 9.00	11.5	4.9	10.8	-38.8

Table 2. Ketones and Corresponding Values of *A* and *B*

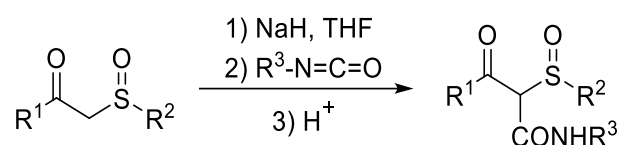
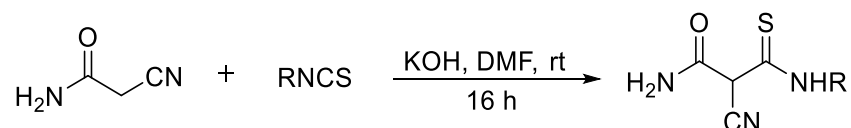
ketones	slope <i>A</i>	intercept <i>B</i>	corr coeff
cyclohexanone	1.00	0.00	Reference
cyclobutanone	1.02	0.09	0.999
4-tert-butylcyclohexanone	1.01	-0.008	
3-methylcyclohexanone	0.99	-0.05	0.999
4-methylcyclohexanone	1.01	-0.08	0.999
2-methylcyclohexanone	1.06	-0.48	0.999
cycloheptanone	0.95	-0.95	0.991
cyclopentanone	0.97	-1.18	0.981
acetone	1.10	-1.19	0.991
2-butanone	1.14	-1.45	

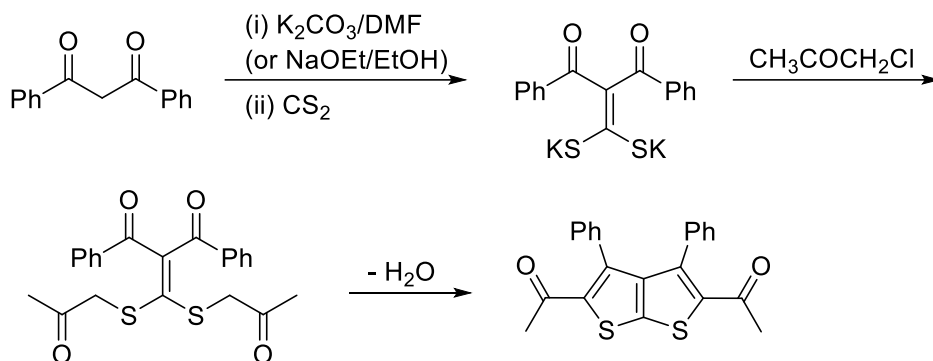
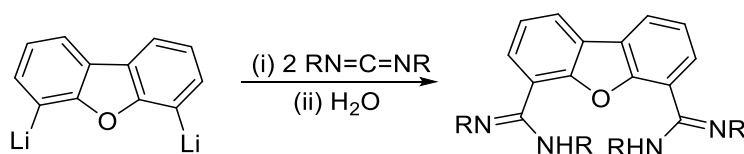
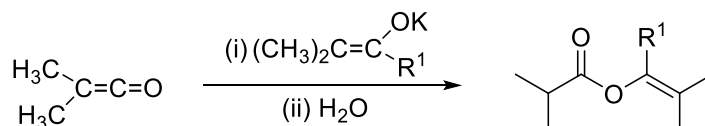
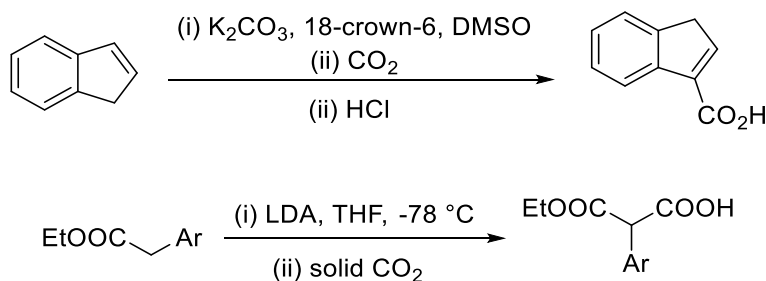
1.4 Heteroallenes

Heteroallenes, organic compounds derived from allene by replacing one or more CH₂ groups by heteroatom, are important reagents and intermediates in organic chemistry. They include isocyanates, isothiocyanates, carbodiimides, carbon disulfides, ketenes, carbon dioxide, etc.⁷ Nucleophilic addition and cycloaddition are two main reaction modes for heteroallenes.

1.3.1 Nucleophilic additions to heteroallenes

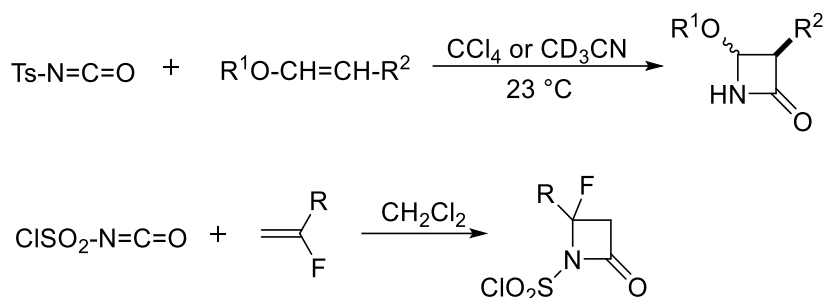
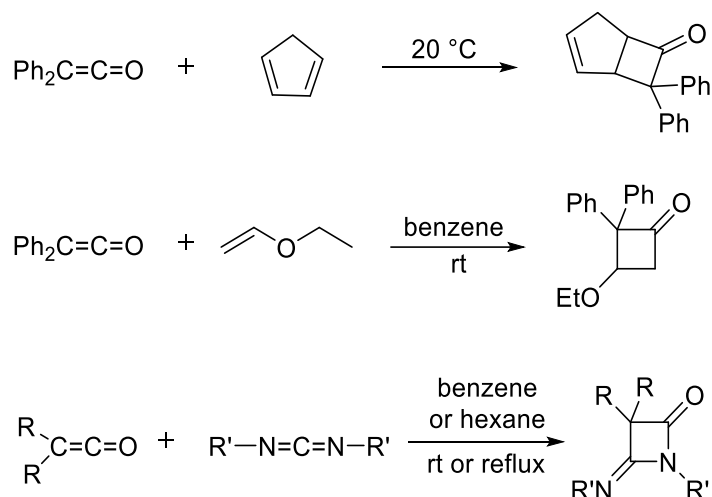
As shown in Schemes 4–9, all kinds of heteroallenes undergo nucleophilic additions with different nucleophiles (carbanions and enolates).^{8–13}

Scheme 4. Nucleophilic Additions of Stabilized Carbanions to Isocyanates^{8a}**Scheme 5.** Nucleophilic Additions of a Stabilized Carbanion to Isothiocyanates^{9a}

Scheme 6. Nucleophilic Addition of a Dibenzoyl-Stabilized Carbanion to Carbon Disulfide and Subsequent Reactions^{10a}**Scheme 7.** Nucleophilic Additions of an Aryllithium Reagent to Carbodiimides^{11a}**Scheme 8.** Nucleophilic Additions of Enolates to Ketene^{12a}**Scheme 9.** Nucleophilic Additions of Carbanions to Carbon Dioxide^{13a,b}

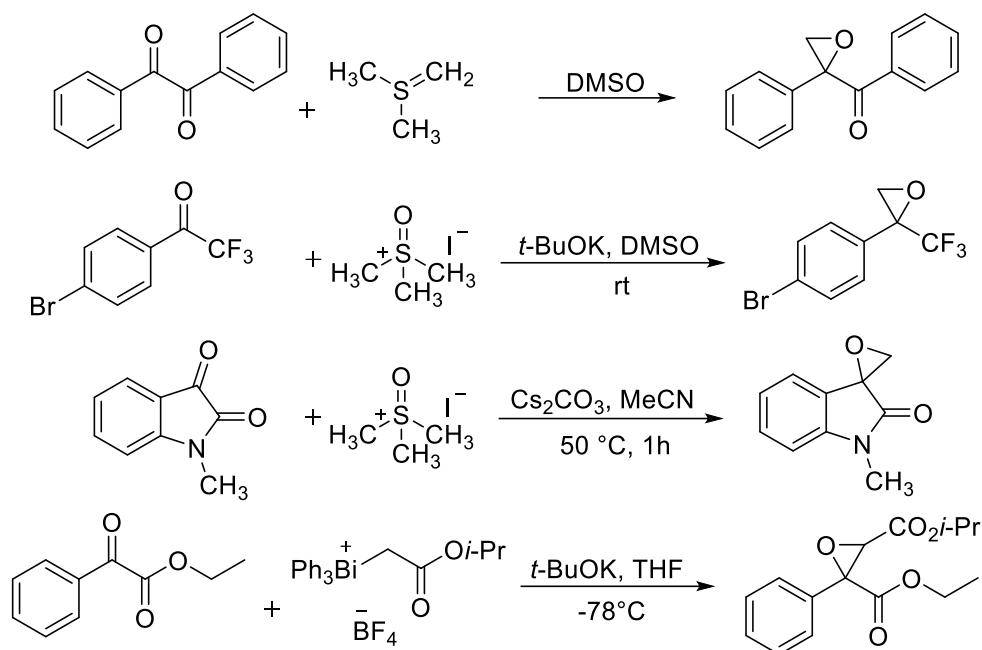
1.3.2 Cycloaddition reactions of heteroallenes

Selected examples of cycloaddition reactions of isocyanates and ketenes with various nucleophiles, such as enol ethers, alkenes, and carbodiimides are shown in Schemes 10 and 11.^{14,15,16} Numerous articles have reported that [2+2] cycloadditions may proceed by concerted or stepwise mechanisms.¹⁶

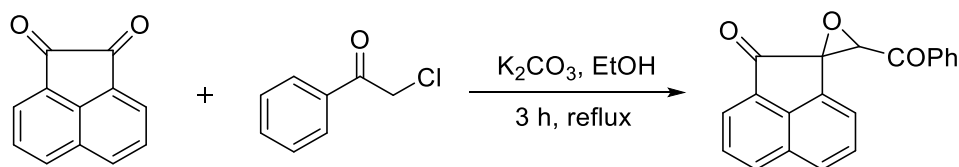
Scheme 10. Cycloadditions of Isocyanates with Enol Ethers and Vinyl Fluorides^{16a,c}**Scheme 11.** Cycloadditions of Ketenes with Cyclopentadiene, Ethyl Vinyl Ether, and Carbodiimides^{15b,c, 16d}**1.5 Acceptor-substituted ketones**

Ketones with acceptor substituted groups in α -position, such as trifluoromethyl, carbonyl, ester, amide, have high electrophilic reactivities. Due to their high reactivities, they undergo a variety of reactions under milder conditions than ordinary ketones. Several reactions of common activated ketones with nucleophiles are shown below.

Scheme 12. Previously Reported Reactions of Activated Ketones with Sulfur Ylides^{17a,b,c} and Bismuthonium Ylide^{17d}



Scheme 13. Previously Reported Reaction of Activated Ketone with Phenacyl Chloride anion^{17e}



From Scheme 12 and 13, one can see a number of reactions of activated ketones with sulfur ylides, bismuthonium ylide and analog phenacyl chloride have been studied previously.¹⁷ All reactions proceed with initial nucleophilic addition to the carbonyl group followed by intramolecular cyclization to form epoxides.

1.6 References

- (1) Jonczyk, A.; Banko, K.; Makosza, M. *J. Org. Chem.* **1975**, *40*, 266–267.
- (2) Makosza, M.; Glinka, T.; Ostrowski, S.; Rykowski, A. *Chem. Lett.* **1987**, *16*, 61–64.
- (3) (a) Makosza, M.; Winiarski, J. *Acc. Chem. Res.* **1987**, *20*, 282–289. (b) Makosza, M. *Synthesis* **1991**, 103–111. (c) Makosza, M.; Kwast, A. *J. Phys. Org. Chem.* **1998**, *11*, 341–349. (d) Makosza, M.; Wojciechowski, K. *Chem. Rev.* **2004**, *104*, 2631–2666. (e) Makosza, M. *Chem. Soc. Rev.* **2010**, *39*, 2855–2868. (f) Makosza, M. *Synthesis* **2011**, 2341–2356. (g) Błaziak, K.; Danikiewicz, W.; Makosza, M. *J. Am. Chem. Soc.* **2016**, *138*, 7276–7281.
- (4) (a) Brown, H. C.; Mead, E. J.; Rao, B. C. S. *J. Am. Chem. Soc.* **1955**, *77*, 6209–6213. (b)

- Brown, H. C.; Wheeler, O. H.; Ichikawa, K. *Tetrahedron* **1957**, *1*, 214–220. (c) Brown, H. C.; Ichikawa, K. *Tetrahedron* **1957**, *1*, 221–230. (d) Brown, H. C.; Ichikawa, K. *J. Am. Chem. Soc.* **1962**, *84*, 373–376. (e) Brown, H. C.; Muzzio, J. *J. Am. Chem. Soc.* **1966**, *88*, 2811–2822. (f) Brown, H. C.; Wang, K. K.; Chandrasekharan, J. *J. Am. Chem. Soc.* **1983**, *105*, 2340–2343.
- (5) (a) Geneste, P.; Durand, R.; Hugon, I.; Reminiac, C. *J. Org. Chem.* **1979**, *44*, 1971–1973. (b) Geneste, P.; Lamaty, G.; Moreau, C.; Roque, J. P. *Tetrahedron Lett.* **1970**, *11*, 5011–5014. (c) Geneste, P.; Lamaty, G.; Roque, J. P. *Tetrahedron* **1971**, *27*, 5539–5559. (d) Geneste, P.; Lamaty, G.; Roque, J. P. *Tetrahedron* **1971**, *27*, 5561–5578. (e) Fournier, L.; Lamaty, G.; Natat, A.; Roque, J. P. *Tetrahedron* **1975**, *31*, 1031–1034. (f) Finiels, A.; Geneste, P. *J. Org. Chem.* **1979**, *44*, 1577–1578.
- (6) Allinger, N. L.; Tribble, M. T.; Miller, M. A. *Tetrahedron*, **1972**, *28*, 1173–1190.
- (7) (a) Brandsma, L. *Eur. J. Org. Chem.* **2001**, 4569–4581. (b) Louie, J. *Curr. Org. Chem.* **2005**, *9*, 605–623. (c) Schenk, S.; Notni, J.; Köhn, U.; Wermann, K.; Anders, E. *Dalton Trans.* **2006**, 4191–4206.
- (8) Nucleophilic additions to isocyanates: (a) Messinger, P.; Kunick, C. *Arch. Pharm.* **1985**, *318*, 1086–1090. (b) Basheer, A.; Mishima, M.; Rappoport, Z. *Arkivoc*, **2015**, (iii) 18–37. (c) Leslie-Smith, M. G.; Paton, R. M.; Webb, N. *Tetrahedron Lett.* **1994**, *35*, 9251–9254. (d) Boiteau, L.; Boivin, J.; Liard, A.; Quiclet-Sire, B.; Zard, S. Z. *Angew. Chem. Int. Ed.* **1998**, *37*, 1128–1131. (e) Malamidou-Xenikaki, E.; Vlachou, C.; Stampelos, X. N. *Tetrahedron* **2006**, *62*, 9931–9941.
- (9) Nucleophilic additions to isothiocyanates: (a) Varaprasad, C. V. N. S.; Barawakar, D.; Abdellaoui, H. E.; Chakravarty, S.; Allan, M.; Chen, H.; Zhang, W.; Wu, J. Z.; Tam, R.; Hamatake, R.; Lang, S.; Hong, Z. *Bioorg. Med. Chem. Lett.* **2006**, *16*, 3975–3980. (b) Assy, M. G.; Moustafa, H. Y. *Phosphorus, Sulfur Silicon Relat. Elem.* **1995**, *105*, 213–216. (c) Mohareb, R. M.; Wardakhan, W. W. *Med. Chem. Res.* **2015**, *24*, 2043–2054. (d) Fishwick, B. R.; Rowles, D. K.; Stirling, J. M. *J. Chem. Soc. Perkin Trans. I* **1986**, 1171–1179.
- (10) Nucleophilic additions to carbon disulfide: (a) Mabkhot, Y. N.; Aldawsari, F. D.; Al-Shoiman, S. S.; Barakat, A.; Soliman, S. M.; Choudhary, M. I.; Yousuf, S.; Mubarak, M. S.; Hadda, T. B. *Chem. Cent. J.* **2015**, *9*:24. (b) El-Shafei, A. K.; El-Sayed, A. M.; El-Saghier, A. M. M. *Phosphorus, Sulfur Silicon Relat. Elem.* **1994**, *90*, 213–218. (c) Elgemeie, G. H.; Elsayed, S. H.; Hassan, A. S. *Synth. Commun.* **2009**, *39*, 1781–1792. (d) Liu, X. R.; Wu, H.; He, Z. Y.; Ma, Z. Q.; Feng, J. T.; Zhang, X. *Molecules* **2014**, *19*, 14036–14051. (e) De Jong, R. L. P.; Brandsma, L. *J. Organomet. Chem.* **1986**, *312*, 277–282.

- (11) Nucleophilic additions to carbodiimides: (a) Kazeminejad, N.; Munzel, D.; Gamer, M. T.; Roesky, P. W. *Chem. Commun.* **2017**, 53, 1060–1063. (b) Chlupaty, T.; Padelkova, Z.; Lycka, A.; Ruzicka, A. *J. Organomet. Chem.* **2011**, 696, 2346–2354. (c) Skötsch, C.; Breitmaier, E. *Chem. Ber.* **1978**, 111, 2003–2009.
- (12) Nucleophilic additions to ketenes: (a) Gong, L.; Leung-Toung, R.; Tidwell, T. T. *J. Org. Chem.* **1990**, 55, 3634–3639. (b) Eventova, I.; Nadler, E. B.; Rochlin, E.; Frey, J.; Rappoport, Z. *J. Am. Chem. Soc.* **1993**, 115, 1290–1302. (c) Bairgrie, L. M.; Leung-Toung, R.; Tidwell, T. T. *Tetrahedron Lett.* **1988**, 29, 1673–1676. (d) Fehr, C.; Galindo, J. *Angew. Chem.* **1994**, 106, 1967–1969.
- (13) Nucleophilic additions to carbon dioxide: (a) Chiba, K.; Tagaya, H.; Miura, S.; Karasu, M. *Chem. Lett.* **1992**, 21, 923–926. (b) Volonterio, A.; Zanda, M. *J. Org. Chem.* **2008**, 73, 7486–7497. (c) Recio, A.; Heinzman, J. D.; Tunge, J. A. *Chem. Commun.* **2012**, 48, 142–144.
- (14) Cycloadditions of isocyanates: (a) Effenberger, F.; Gleiter, R. *Angew. Chem.* **1963**, 75, 450–451. (b) Effenberger, F.; Gleiter, R. *Chem. Ber.* **1964**, 97, 1576–1583. (c) Inaba, S.; Ojima, I.; Yoshida, K.; Nagai, M. *J. Organomet. Chem.* **1979**, 164, 123–134. (d) Moriconi, E. J.; Hummel, C. F. *J. Org. Chem.* **1976**, 41, 3583–3586. (e) Moriconi, E. J.; Kelly, J. F. *J. Org. Chem.* **1968**, 33, 3036–3046.
- (15) Cycloadditions of ketenes: (a) Staudinger, H. *Liebigs Ann. Chem.* **1907**, 356, 51–94. (b) Huisgen, R.; Otto, P. *Chem. Ber.* **1969**, 102, 3475–3485. (c) Huisgen, R.; Feiler, L. A.; Otto, P. *Chem. Ber.* **1969**, 102, 3405–3427. (d) Brady, W. T.; R. R. J. *J. Am. Chem. Soc.* **1971**, 93, 1662–1664. (e) Rulliere, P.; Carret, S.; Milet, A.; Poisson, J. F. *Chem. - Eur. J.* **2015**, 21, 3876–3881. (f) Rasik, C. M.; Brown, M. K. *J. Am. Chem. Soc.* **2013**, 135, 1673–1676. (g) Hasek, R. H.; Martin, J. C. *J. Org. Chem.* **1961**, 26, 4775–4776.
- (16) (a) Effenberger, F.; Prossel, G.; Fischer, P. *Chem. Ber.* **1971**, 104, 2002–2012. (b) Effenberger, F.; Fischer, P.; Prossel, G.; Kiefer, G. *Chem. Ber.* **1971**, 104, 1987–2001. (c) Schellhamer, D. F.; Bunting, S. A.; Hickie, K. R.; Horn, P. C.; Milligan, J. C.; Shipowick, D. E.; Smith, L. B.; Vandenbroek, D. J.; Perry, M. C.; Boatz, J. A. *J. Org. Chem.* **2013**, 78, 246–252. (d) Brady, W. T.; Dorsey, E. D.; Parry, F. H. *J. Org. Chem.* **1969**, 34, 2846–2848. (e) Huisgen, R.; Mayr, H. *Tetrahedron Lett.* **1975**, 34, 2965–2968. (f) Huisgen, R.; Mayr, H. *Tetrahedron Lett.* **1975**, 34, 2969–2972. (g) Schellhamer, D. F.; Alexander, K. L.; Bunting, S. A.; Elwin, S. L.; Licata, C. J.; Milligan, J. C.; Robinson, R. D.; Shipowick, D. E.; Smith, L. B.; Perry, M. C. *Synthesis* **2015**, 47, 1944–1950. (h) Burke, L. A. *J. Org. Chem.* **1985**, 50,

- 3149–3155. (i) Bernardi, F.; Bottoni, A.; Robb, M. A.; Venturini, A. *J. Am. Chem. Soc.* **1990**, *112*, 2106–2114.
- (17) (a) Pierre, J. L. et al *Bulletin de la Societe Chimique de France*, **1967**, *4*, 1439. (b) Molinaro, C.; Guilbault, A. A.; Kosjek, B. *Org. Lett.* **2010**, *12*, 3772–3775. (c) Chouhan, M.; Senwar, K. R.; Sharma, R.; Grover, V.; Nair, V. A. *Green Chem.* **2011**, *13*, 2553–2560. (d) Matano, Y.; Rahman, M. M.; Yoshimune, M.; Suzuki, H. *J. Org. Chem.* **1999**, *64*, 6924–6927. (e) El-Sawi, E. A.; Mostafa, T. B.; Radwan, H. A. *Chem. Heterocycl. Compd.* **2009**, *45*, 981–989.

Chapter 2. Nucleophilicity parameters of arylsulfonyl-substituted halomethyl anions

Zhen Li, Quan Chen, Peter Mayer, and Herbert Mayr*

J. Org. Chem. **2017**, 82, 2011–2017

2.1 Introduction

Carbanions bearing leaving groups at the α -position are useful reagents in organic synthesis. They are widely used in Darzens condensations,¹ cyclopropanations,² and vicarious nucleophilic substitutions.³ Knowledge of the nucleophilic reactivities of these carbanions would be a valuable tool for designing their use in synthesis. In previous work, we had demonstrated that the rates of the reactions of nucleophiles with carbocations and Michael acceptors can be predicted by eq 1, where nucleophiles are characterized by two solvent-dependent parameters, the nucleophilicity parameter N and the susceptibility parameter s_N , whereas electrophiles are characterized by one parameter, the electrophilicity E .⁴

$$\log k_2(20\text{ }^\circ\text{C}) = s_N(N + E) \quad (1)$$

On the basis of this linear free-energy relationship, we have developed the most comprehensive nucleophilicity and electrophilicity scale presently available.⁵ We have now employed this method for characterizing the nucleophilicities of arylsulfonyl substituted carbanions carrying α -chloro and α -bromo substituents **1a–e** (Scheme 1). Quinone methides **2a–g** and benzylidenemalonates **2h–i** (Table 1) were used as reference electrophiles for these investigations.

Scheme 1. Cl-Stabilized Carbanions **1a–d**, and Br-Stabilized Carbanion **1e**

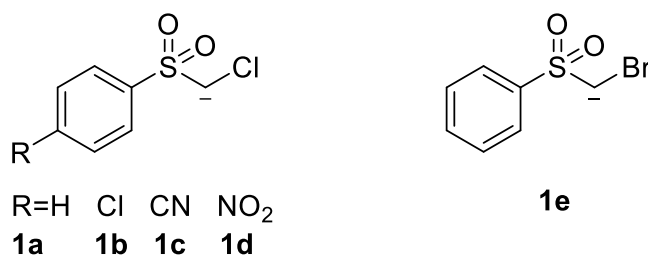
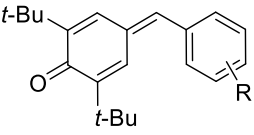
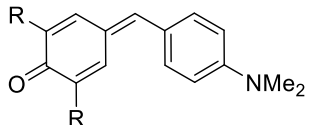
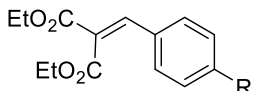
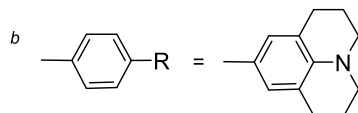


Table 1. Quinone Methides **2a–g** and Diethyl Benzylidenemalonates **2h–i**.

Electrophile		R	E^a
	2a	3-F	-15.03
	2b	4-Me	-15.83
	2c	4-OMe	-16.11
	2d	4-NMe ₂	-17.29
	2e	jul ^b	-17.90
	2f	Me	-16.36
	2g	OMe	-17.18
	2h	NMe ₂	-23.10
	2i	jul ^b	-23.80

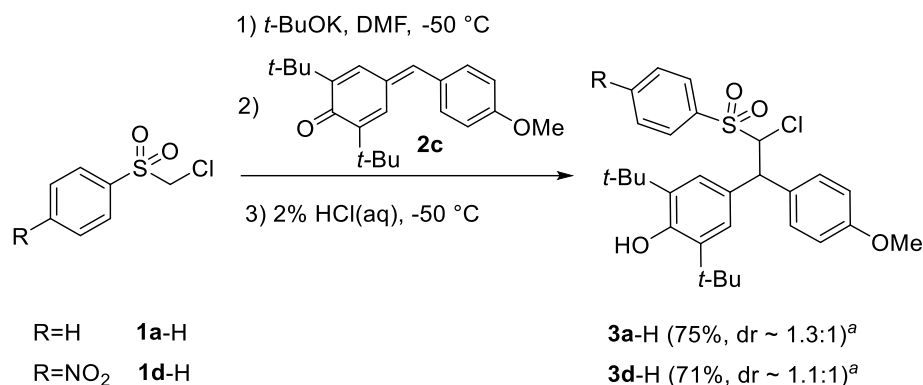
^a Electrophilicity parameters E of **2a**, **2f** and **2g** were taken from ref 6a, of **2b–e** from ref 6b, of **2h–i** from ref 6c.



2.2 Results and Discussion

Product studies. As representative examples for the reactions of carbanions **1** with quinone methides **2a–g**, we have investigated the corresponding reactions with **2c**. Treatment of **1a–H** with 1 equivalent of *t*-BuOK in DMF at -50 °C and subsequent addition of 0.5 equivalent of **2c** gave a phenolate which was treated with 2% aqueous HCl after 5 min at -50 °C to yield 75% of **3a–H** as a mixture of two diastereomers. The reaction of **1d** with **2c** proceeded analogously (Scheme 2).

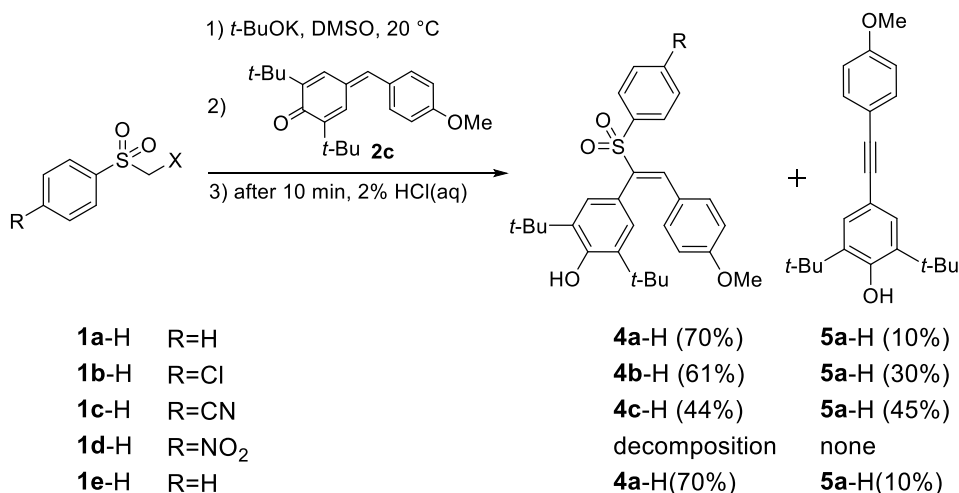
Scheme 2. Synthesis of Michael Adducts **3-H** by the Reactions of Carbanions **1** with Quinone Methide **2c**



^a Diastereomeric ratios dr correspond to isolated products.

When the reactions of **1a–c** and of **1e** with **2c** were carried out in DMSO at 20 °C and quenched with 2% aqueous HCl after 10 min, mixtures of **4-H** and **5a-H** were obtained, while **1d** gave a complex mixture of products (Scheme 3). Because of the high melting point of DMSO, low temperature studies were not possible as in DMF (see above).

Scheme 3. Reaction of Carbanions **1** with Quinone Methide **2c** at 20 °C



The structure of **4a-H** was confirmed by single crystal X-ray crystallography (Figure 1). Treatment of isolated **4a-H** with *t*-BuOK led to formation of **5a-H** (Scheme 4). In order to investigate whether the weaker Brønsted base **1a-K** which may be the effective base under the conditions of Scheme 3 can also affect this elimination, **4a-H** was also treated with **1a-K**. As shown in Scheme 4, this reaction proceeded slowly, and after 10 min a similar amount of **5a-H** was obtained as in the reaction of **1a** with **2c** described in Scheme 3.

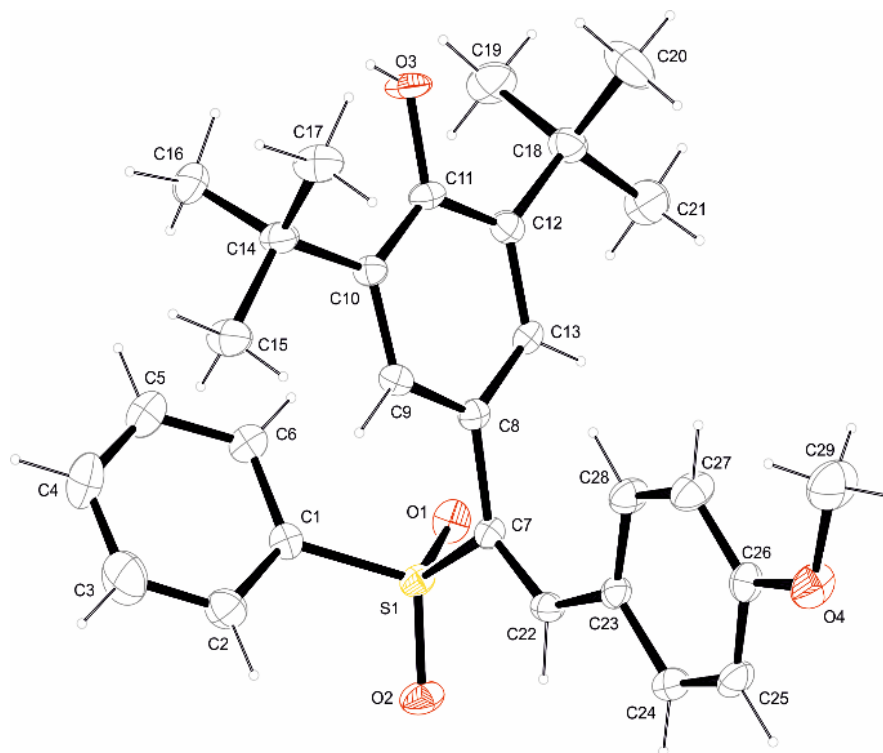
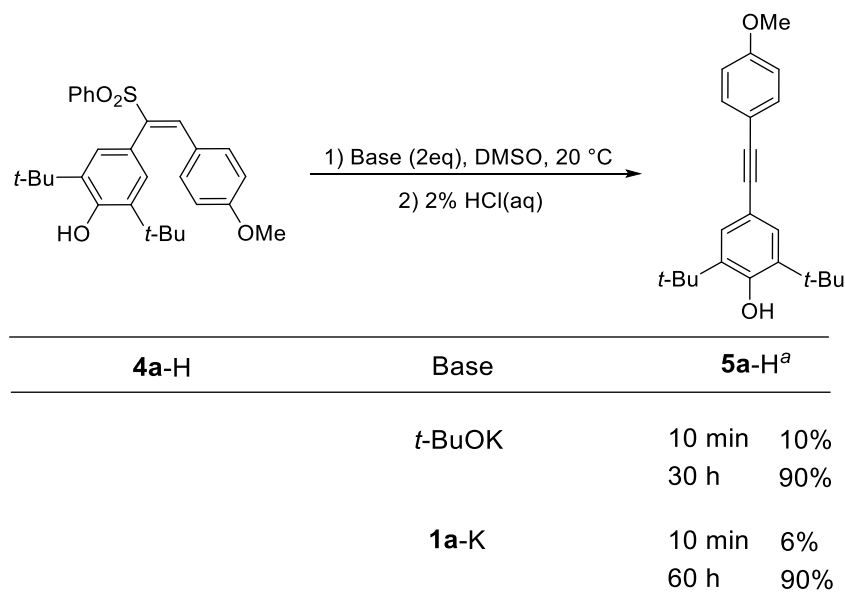


Figure 1. ORTEP-drawing of the crystal structure of **4a-H**. (The ellipsoid probability level is 50%)

Scheme 4. Transformation of **4a-H** into **5a-H**.

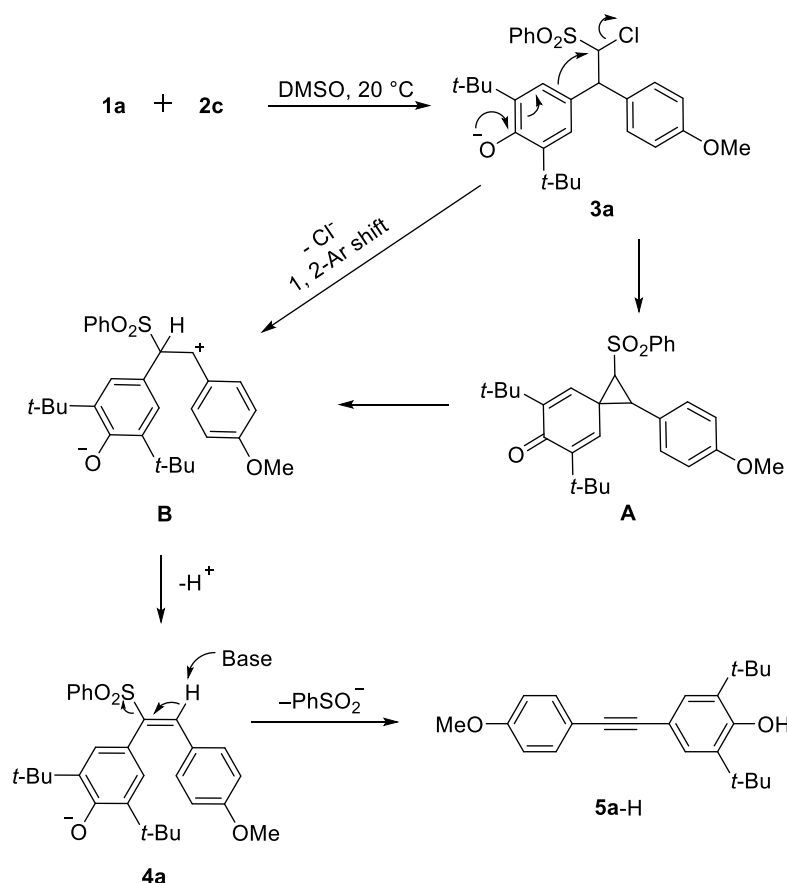


^a Yield of isolated product.

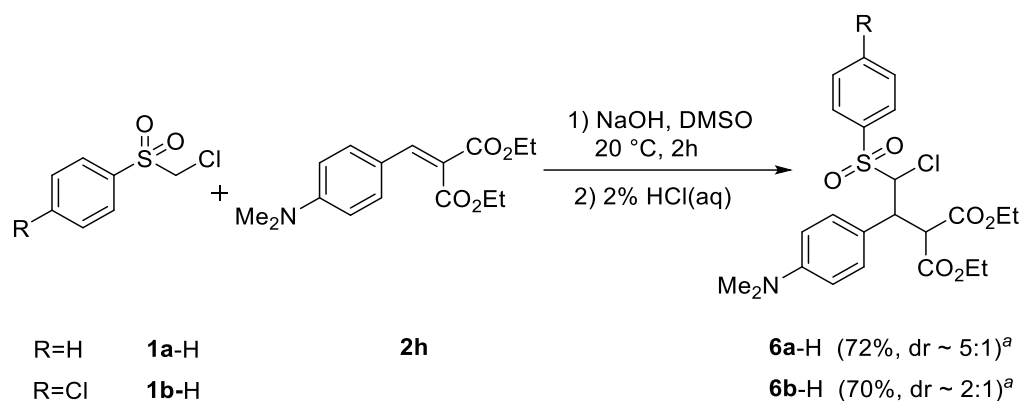
These observations suggest the reaction mechanism described in Scheme 5. Michael addition of the carbanion **1a** to the electrophilic double bond of the quinone methide **2c** yields the phenolate anion **3a**. This intermediate was trapped by protonation with 2% aqueous HCl, when the reaction was carried out in DMF at -50 °C (Scheme 2). At 20 °C, intramolecular

cyclization may lead to the formation of spirodienone **A**, which undergoes spontaneous ring opening with formation of the mesomerically stabilized zwitterion **B**. As an alternative to this mechanism suggested by Groszek,⁷ phenoxide-migration with substitution of Cl^- gives **B** directly through a transition state resembling **A**. Deprotonation yields the phenolate **4a** (**4a-H** was isolated, Scheme 3 and Figure 1), which is selectively formed as the (*E*)-diastereomer, probably because of attractive intramolecular π - π interaction of the two aryl rings in the intermediate zwitterion **B**, as previously suggested by Groszek. Slow elimination of PhSO_2^- from **4a** yields the alkynyl substituted phenol **5a-H**. The formation of Michael adducts of type **3-H** and of the rearranged elimination products **4-H** from the reaction of tolylsulfonyl chloromethyl anion **1** ($\text{R} = \text{Me}$) with quinone methides has previously been reported by Groszek and coworkers.⁷

Scheme 5. Plausible Mechanism for the Reaction of **1a** with **2c**



The NaOH induced reaction of **1a-H** with benzylidenemalonate **2h** in DMSO gave the Michael adduct **6a-H**, as previously reported for the corresponding reaction in DMF.⁸ The reaction of **1b-H** with **2h** proceeded analogously (Scheme 6).

Scheme 6. Reaction of Benzyldenemalonate **2h** with Carbanions **1**

^a Diastereomeric ratios dr correspond to crude products.

Kinetic investigations. All kinetic investigations were performed in DMSO solution at 20 °C and monitored photometrically by following the disappearance of the colored quinone methides or benzyldenemalonates. Generally a high excess of the carbanions over the electrophiles was used to achieve first-order kinetics. As reported earlier,⁹ the carbanions **1a–e** disproportionate slowly at room temperature. For that reason, the double-mixing mode of stopped flow UV-Vis spectrometers was used to generate solutions of the carbanions **1a–e** by mixing the CH acids (**1a–e**)-H with *t*BuOK. After a user-defined delay period (1 – 30s), the solutions of carbanions were combined with the electrophiles **2a–i**.

Figure 2 illustrates the decay of the absorption of **2c** ($\lambda_{\text{max}} = 393 \text{ nm}$) in DMSO at 20 °C after addition of 20 equivalents of **1a** (pseudo-first-order conditions). The absorbance decreases to about 15% of its initial value within 50 ms and then shows a very slow increase. Separate UV-Vis measurements showed that the residual absorbance after 50 ms is due to the generation of **4a**, which has an absorption maximum at 504 nm. The subsequent slow increase (insert of Figure 2) is due to the formation of **5a** by elimination of PhSO₂H from **4a**. (Depending on the excess of base used for these experiments, the alkyne is either formed as the anion **5a** or its conjugate acid **5a-H**.) While an analogous behavior was observed for all other reactions of **1** with the quinone methides **2a–g**, the corresponding reactions with the benzyldenemalonates **2h,i** showed only the fast decay of the absorption band of **2h,i**.

The first-order rate constants k_{obs} were obtained by least-squares fitting of the exponential function $A = A_0 \exp(-k_{\text{obs}}t) + C$ to the observed time-dependent absorbances A of the quinone methides **2a–g** (in the initial period) and of the benzyldenemalonates **2h,i**. According to eq 2 and eq 3, the pseudo-first-order rate constant k_{obs} should be proportional to

the concentration of the carbanions **1**. As shown for the reaction of **1a** with **2c** in Figure 3, k_{obs} correlates linearly with the concentrations of the carbanions **1**, and the negative intercept may be due to partial decomposition of the carbanions **1**. Though the intercept is small and negligible in most of these correlations (SI), in few cases even small positive intercepts were observed. The second-order rate constants k_2 listed in Table 2 correspond to the slopes of the k_{obs} versus $[\mathbf{1}]$ correlations. The experimental second-order rate constant k_2 for the reaction of **1a** with **2h** ($149 \text{ M}^{-1} \text{ s}^{-1}$) is close to that ($200 \text{ M}^{-1} \text{ s}^{-1}$) extrapolated for this reaction in DMF at 20°C from the measured rate constant at -40°C .⁸

$$-\text{d}[\mathbf{2}]/\text{dt} = k_2[\mathbf{1}][\mathbf{2}] \quad (2)$$

$$\text{for } [\mathbf{1}]_0 \gg [\mathbf{2}]_0 \Rightarrow k_{\text{obs}} = k_2[\mathbf{1}]_0$$

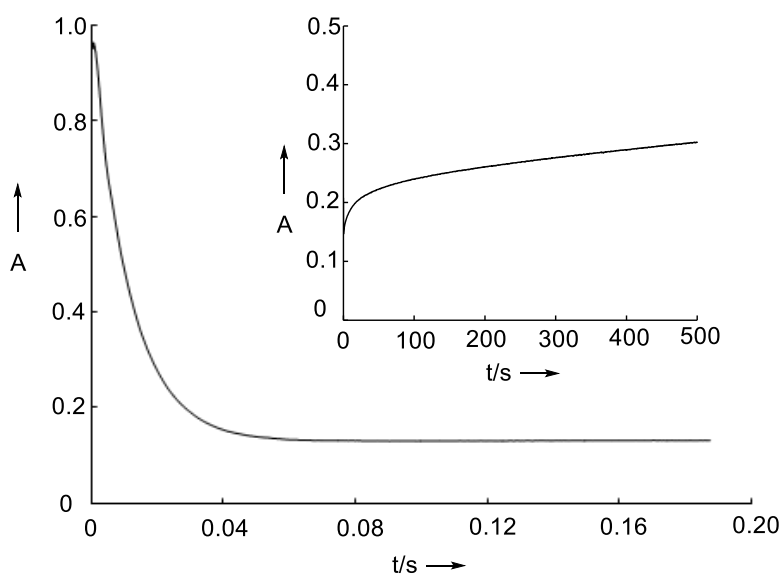


Figure 2. Monoexponential decay of the absorbance A (at 393 nm) during the first 200 ms of the reaction of **1a** ($1.00 \times 10^{-3} \text{ mol L}^{-1}$) with **2c** ($5.00 \times 10^{-5} \text{ mol L}^{-1}$) in DMSO at 20°C . Inset: slow increase of the absorbance at 393 nm at 20°C between 0.05 and 500 s.

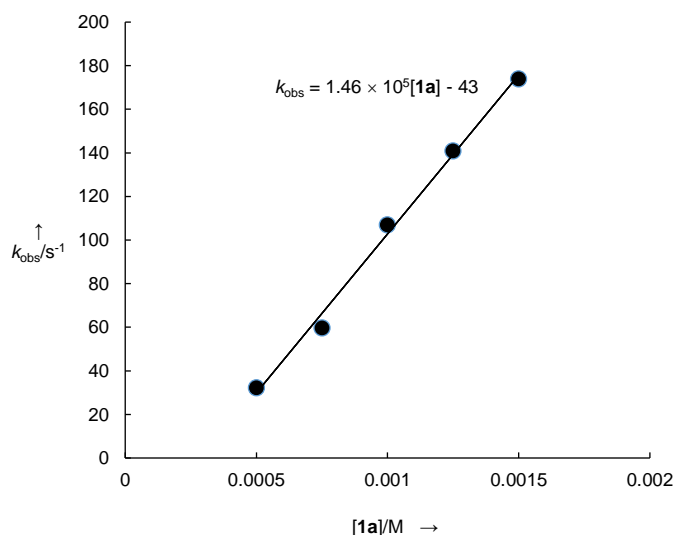


Figure 3. Correlation of k_{obs} for reaction of **1a** with **2c** versus the concentration of **1a**.

In order to determine the nucleophile-specific parameters N and s_N of the carbanions **1a–e** according to eq 1, the second-order rate constants ($\log k_2$) of their reactions with electrophiles **2** (see Table 2) were plotted against the previously reported electrophilicity parameters E of **2a–i** (Table 1). Figure 4 and Figure S1 (SI) show that $\log k_2$ for these reactions correlate linearly with E as required by eq 1 and thus allow the calculation of the nucleophile-specific parameters N and s_N listed in Table 2. The similarities of the slopes of the correlations for the carbanions **1b–d** (Figure 4 and Figure S1), which are numerically expressed by the s_N parameters in Table 2, imply that the relative nucleophilicities of the carbanions **1b–d** depend only slightly on the electrophilicities of the reaction partners. The Hammett correlation for the reactions of carbanions **1a–d** with benzylidenemalonate **2h** is of moderate quality and gives rise to the Hammett reaction constant $\rho = -1.50$ (Figure 5). Since the substituted aryl ring is separated from the nucleophilic reaction center by the sulfonyl group, the Hammett reaction constant ρ has a small negative value.

Table 2. Second-Order Rate Constants (k_2) for the Reactions of Carbanions **1a–e** with Quinone Methides **2a–g** and Benzyldenemalonates **2h–i** in DMSO at 20°C

Carbanion	Electrophile	k_2 (M ⁻¹ S ⁻¹)	N , s_N^a
1a	2c	1.46×10^5	28.27, 0.42
	2d	3.35×10^4	
	2e	2.65×10^4	
	2g	3.92×10^4	
	2h	1.49×10^2	
1b	2b	1.08×10^5	26.90, 0.45
	2c	8.87×10^4	
	2d	2.01×10^4	
	2h	4.90×10^1	
	2i	2.85×10^1	
1c	2d	1.77×10^4	25.59, 0.51
	2e	9.19×10^3	
	2f	5.65×10^4	
	2g	2.21×10^4	
1d	2a	6.89×10^4	24.88, 0.49
	2b	2.90×10^4	
	2c	2.00×10^4	
1e	2a	2.78×10^5	23.90, 0.62
	2c	7.11×10^4	
	2d	1.17×10^4	
	2e	4.90×10^3	

^a The nucleophile-specific parameters s_N and N were derived from the slopes and the intercepts on the abscissa of the correlations between $\log k_2$ (this table) and the electrophilicity parameters E from Table 1. For details see text.

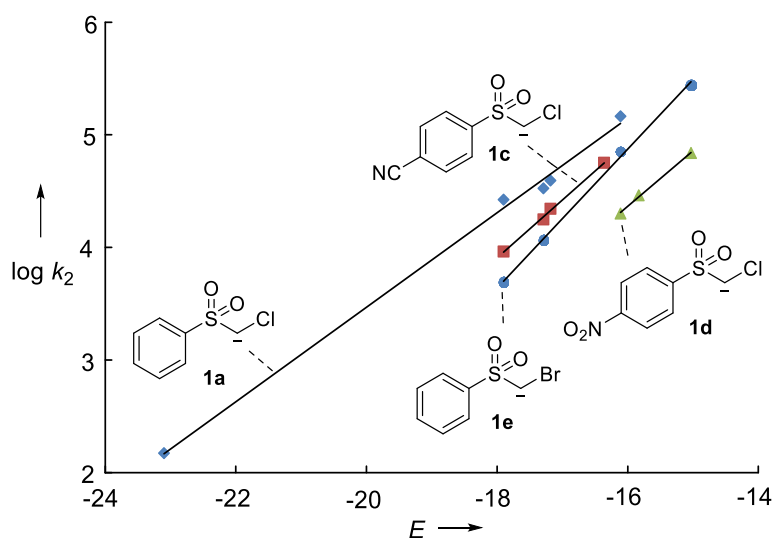


Figure 4. Correlation of $\log k_2$ for the reactions of the carbanions **1a** and **1c–e** with the quinone methides **2a–g** and benzylidenemalonates **2h–i** versus the electrophilicity parameters E of the corresponding electrophiles. For the sake of clarity, the correlation line for **1b** is only shown in the SI.

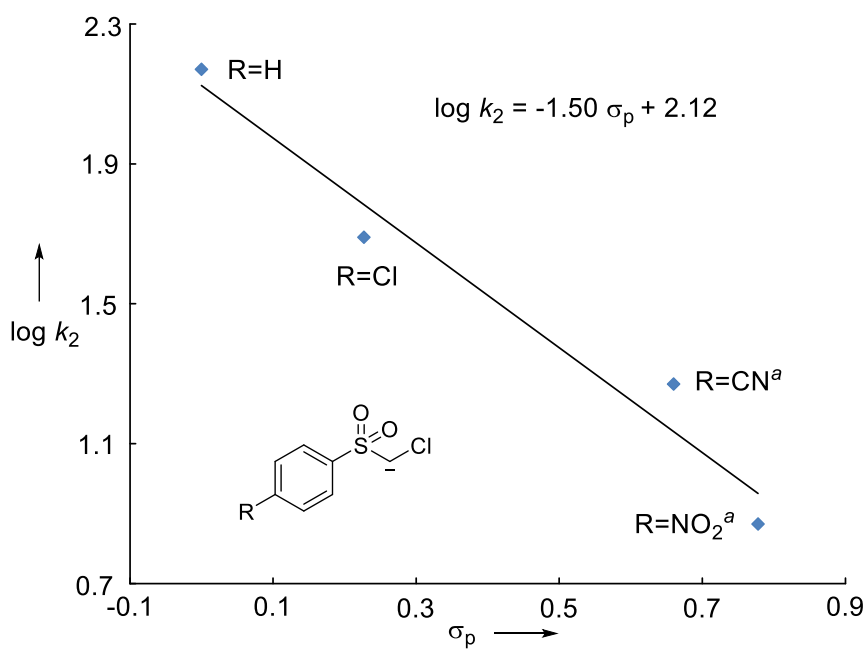


Figure 5. Correlation of $\log k_2$ of the reactions of carbanions **1a–d** with benzylidenemalonate **2h** versus the Hammett σ_p values for R. ^a $\log k_2$ calculated by eq 1 with E from Table 1.

Figure 6 compares the reactivities of **1a–e** with that of the previously characterized phenylsulfonyl substituted benzyl anion **1f**. As the s_N values for these carbanions differ slightly, their relative nucleophilic reactivities depend somewhat on the electrophilicity of the

reaction partner. The reactivities of the arylsulfonyl substituted halomethyl anions **1a–e** towards **2c** differ by less than a factor of 7. The chloro-substituted carbanion **1a** is two times more reactive than the corresponding bromo-derivative **1e**. The similar nucleophilic reactivities of the phenylsulfonyl substituted carbanions **1a** and **1f** show that α -chloro and α -phenyl substitution has a similar effect on nucleophilic reactivities as on the corresponding basicities in DMSO (**1a-H** : $pK_a = 23.8$,¹⁰ **1f-H**: $pK_a = 23.43$ ¹¹).

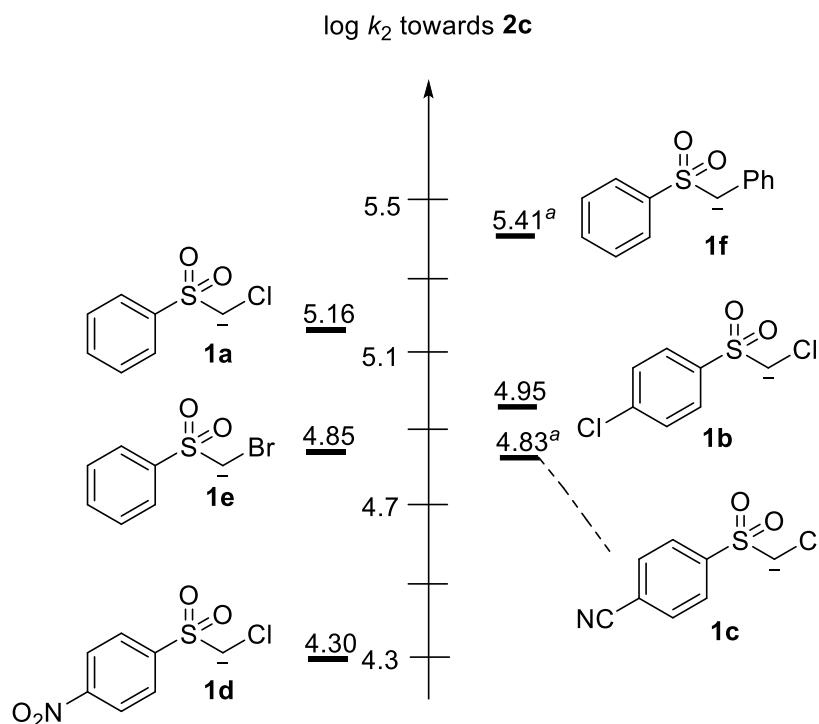


Figure 6. Comparison of log k_2 for the reactions of carbanions **1a–f** with electrophile **2c** in DMSO at 20 °C. ^a log k_2 (**2c**) calculated by eq 1 with E from Table 1. N and s_N values of **1f** from ref 12d.

2.3 Conclusion

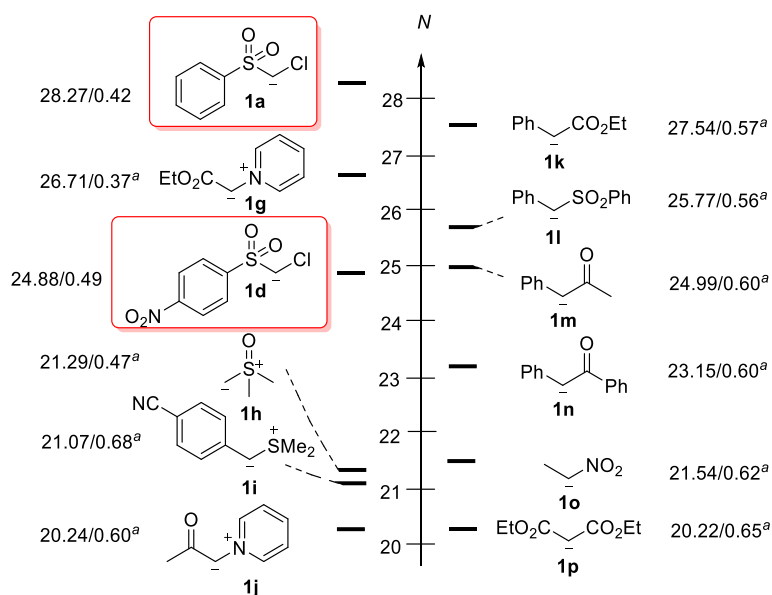


Figure 7. Comparison of nucleophilicity parameters N (in DMSO at 20 °C) of **1a** and **1d** with other classes of nucleophiles. ^a N and s_N values of **1g** and **1j** were taken from ref 12a, of **1h** and **1i** from ref 12b, of **1k** from ref 12c, of **1l**, **1m** and **1n** from ref 12d, of **1o** from ref 12e, of **1p** from ref 4b.

The rate constants for the reaction of the Cl-, Br-substituted carbanions **1a–e** with quinone methides and diethyl benzylidenemalonates in DMSO follow the linear free-energy relationship eq 1, allowing us to include these compounds in our comprehensive nucleophilicity scale and to compare their reactivities with those of other nucleophiles (Figure 7). As they contain halogens in α -position, which can be nucleophilically substituted, carbanions **1** show carbenoid character and yield epoxides¹, aziridines^{1c,13} and cyclopropanes² by reaction with carbonyl compounds, imines, and Michael acceptors, respectively. In this aspect they resemble the behavior of sulfur and nitrogen ylides, some representatives of which are also shown on the left side of Figure 7. Though the relative reactivities of these nucleophiles depend somewhat on the electrophilicity of the reaction partner due to the different values of s_N , the ranking based on N in Figure 7 gives a rough orientation. Thus, one can see that the arylsulfonyl substituted chloromethyl anions are stronger nucleophiles than semistabilized sulfur ylides, and therefore, can be used for the synthesis of epoxides from non-activated ketones. The high nucleophilic reactivities of **1a–e** combined with the high nucleofugality of chloride and bromide, also explains their versatile applications in vicarious nucleophilic substitutions.³

2.4 Experimental Section

(1) Product study

Chloromethyl aryl sulfones (1a–d)-H and bromomethyl phenyl sulfone 1e-H. Chloromethyl phenyl sulfone **1a-H** (>97%) and bromomethyl phenyl sulfone **1e-H** (98%) are commercially available compounds. Compounds (**1b–d**)-H were prepared by chlorination of the corresponding 4-substituted thioanisoles¹⁴, and subsequent *m*-CPBA oxidation¹⁵ following literature procedures.^{14,15} **1b-H** is a known compound fully characterized already.¹⁶ For the reason of simplicity, the ¹H NMR signals of AA'BB'-spin systems of *p*-disubstituted aromatic rings of all compounds described below were treated as doublets. NMR signal assignments were based on additional 2D-NMR experiments (COSY, HSQC, HMBC).

Chloromethyl 4-nitrophenyl sulfone (1d-H) (General procedure 1). 4-Nitrothioanisole (3.50 g, 20.7 mmol) was treated with *N*-chlorosuccinimide (3.18 g, 23.8 mmol) in dry carbon tetrachloride (21 mL) at 35 °C for 24 h. Succinimide precipitated and was removed by filtration. After evaporation of the solvent the residue was dissolved in 65 mL of DCM, cooled in an ice-water bath with stirring, and 77% *m*-chloroperoxybenzoic acid (11.0 g, 49.1 mmol) was added in portions within 5 min. The mixture was stirred at 0 °C for 40 min and 5 h at room temperature. After addition of ether, the solution was washed with water, 10% aqueous NaOH, an aqueous solution of Na₂S₂O₃-NaI-NaOH, and a saturated aqueous solution of NaCl. The organic extract was dried over MgSO₄, and the solvent was removed using a rotary evaporator. The residue was recrystallized from EtOAc and pentane to give a yellow solid **1d-H** (3.42 g, 14.5 mmol, 70%), mp 138–143 °C. ¹H NMR (400 MHz, DMSO-*d*₆) δ 8.50 (d, *J* = 8.8 Hz, 2 H, H-3 and H-5), 8.23 (d, *J* = 8.9 Hz, 2 H, H-2 and H-6), 5.50 (s, 2 H, H-1). ¹³C NMR (101 MHz, DMSO-*d*₆) δ 151.1 (C-4), 141.2 (C-7), 130.6 (C-2 and C-6), 124.6 (C-3 and C-5), 57.1 (C-1). HRMS (EI) *m/z*: [M⁺] calcd for C₇H₆ClNO₄S 234.9701, found 234.9702. IR (ATR) ν (cm⁻¹) = 2942, 1607, 1531, 1475, 1401, 1334, 1236, 1209, 1155, 1131, 1083, 1011, 873, 854, 796, 755, 723, 679.

Chloromethyl 4-cyanophenyl sulfone (1c-H). General procedure 1 was applied to 4-cyanothioanisole (1.49 g, 10.0 mmol), *N*-chlorosuccinimide (1.40 g, 10.5 mmol) and 77% *m*-chloroperoxybenzoic acid (5.31 g, 23.7 mmol). **1c-H** was obtained as a white solid (1.62 g, 7.53 mmol, 75%) mp 133–138 °C. ¹H NMR (400 MHz, DMSO-*d*₆) δ 8.21 (d, *J* = 8.7 Hz, 2 H, H-2 and H-7), 8.13 (d, *J* = 8.7 Hz, 2 H, H-3 and H-6), 5.46 (s, 2 H, H-1). ¹³C NMR (101 MHz, DMSO-*d*₆) δ 139.9 (C-8), 133.5 (C-2 and C-7), 129.6 (C-3 and C-6), 117.4 (C-5), 117.1 (C-4), 57.0 (C-1). HRMS (EI) *m/z*: [M⁺] calcd for C₈H₆ClNO₂S 214.9802, found 214.9796. IR

(ATR) ν (cm^{-1}) = 3019, 2240, 1387, 1327, 1293, 1146, 1081, 1015, 850, 841, 794, 778, 732, 693.

Reaction of carbanion 1a with quinone methide 2c in DMF at -50 °C (General procedure 2). To a solution of *t*-BuOK (112 mg, 1.00 mmol) in anhydrous DMF (5 mL) at -50 °C was added a solution of **1a-H** (190 mg, 1.00 mmol) in anhydrous DMF (5 mL) and successively a solution of **2c** (162 mg, 0.500 mmol) in anhydrous DMF (5 mL). After 5 min, 100 mL of 2% aqueous HCl was added and the mixture was extracted with CHCl_3 . The organic phase was washed by water three times to remove remaining DMF, dried with anhydrous MgSO_4 and filtered. The solvent was evaporated under reduced pressure and the residue was purified by column chromatography to give a pale yellow liquid: 2,6-Di-*tert*-butyl-4-(2-chloro-1-(4-methoxyphenyl)-2-(phenylsulfonyl)ethyl)phenol (**3a-H**), ~ 1.3:1 mixture of diastereomers. (193 mg, 0.375 mmol, 75%). Diastereomer A: ^1H NMR (599 MHz, CDCl_3) δ 7.73 (d, J = 7.6 Hz, 2 H, H-15 x 2), 7.57 (t, J = 7.3 Hz, 1 H, H-17), 7.43 (dd, J = 7.2, 7.2 Hz, 2 H, H-16 x 2), 7.33 (d, J = 8.2 Hz, 2 H, H-4 x 2), 7.12 (s, 2 H, H-8 x 2), 6.81 (d, J = 8.0 Hz, 2 H, H-5 x 2), 5.41 – 5.38 (m, 1 H, H-1, overlap with B), 5.14 (s, 1 H, OH), 5.06 (d, J = 4.7 Hz, 1 H, H-2), 3.78 (s, 3 H, H-7 x 3), 1.39 (s, 18 H, H-11 x 18). ^{13}C NMR (151 MHz, CDCl_3) δ 158.79 (C-6), 153.03 (C-12), 137.05 (C-14), 136.02 (C-9 x 2), 134.04 (C-17), 131.04 (C-3), 130.90 (C-13), 130.82 (C-4 x 2), 129.66 (C-15 x 2), 128.79 (C-16 x 2), 124.98 (C-8 x 2), 113.63 (C-5 x 2), 79.36 (C-1), 55.26 (C-7), 50.55 (C-2), 34.44 (C-10 x 2), 30.33 (C-11 x 6). Diastereomer B: ^1H NMR (599 MHz, CDCl_3) δ 7.67 (d, J = 7.5 Hz, 2 H, H-15 x 2), 7.54 (t, J = 7.1 Hz, 1 H, H-17), 7.38 (dd, J = 7.4, 7.4 Hz, 2 H, H-16 x 2), 7.25 (d, J = 9.3 Hz, 2 H, H-4 x 2), 7.15 (s, 2 H, H-8 x 2), 6.81 (d, J = 8.0 Hz, 2 H, H-5 x 2), 5.41 – 5.38 (m, 1 H, H-1, overlap with A), 5.12 (s, 1 H, OH), 4.97 (d, J = 5.3 Hz, 1 H, H-2), 3.77 (s, 3 H, H-7 x 3), 1.38 (s, 18 H, H-11 x 18). ^{13}C NMR (151 MHz, CDCl_3) δ 158.72 (C-6), 153.15 (C-12), 136.57 (C-14), 135.52 (C-9 x 2), 133.91 (C-17), 132.44 (C-3), 130.01 (C-15 x 2), 129.41 (C-4 x 2), 128.79 (C-13), 128.54 (C-16 x 2), 126.36 (C-8 x 2), 114.11 (C-5 x 2), 79.76 (C-1), 55.32 (C-7), 51.20 (C-2), 34.36 (C-10 x 2), 30.41 (C-11 x 6). HRMS (EI) m/z : $[\text{M}^+]$ calcd for $\text{C}_{29}\text{H}_{35}\text{ClO}_4\text{S}$ 514.1939, found 514.1948. IR (ATR) ν (cm^{-1}) = 3634, 2956, 1610, 1511, 1435, 1361, 1322, 1309, 1250, 1212, 1179, 1150, 1135, 1081, 1032, 887, 836, 810, 685, 667.

(*E*)-2,6-Di-*tert*-butyl-4-(2-(4-methoxyphenyl)-1-((4-nitrophenyl)sulfonyl)vinyl)phenol (3d-H): General procedure 2 was applied to **1d-H** (235 mg, 1.00 mmol), **2c** (162 mg, 0.500 mmol) and *t*-BuOK (112 mg, 1.00 mmol). **3d-H** was obtained as a pale yellow liquid and a mixture of diastereomers. (199 mg, 0.355 mmol, 71%, dr ~ 1.1:1). Diastereomer A: ^1H NMR (599 MHz, CDCl_3) δ 8.20 (d, J = 9.0 Hz, 2 H, H-16 x

2), 7.84 (d, $J = 9.0$ Hz, 2 H, H-15 x 2), 7.29 (d, $J = 8.8$ Hz, 2 H, H-4 x 2), 7.08 (s, 2 H, H-8 x 2), 6.78 (d, $J = 8.9$ Hz, 2 H, H-5 x 2), 5.42 (d, $J = 5.5$ Hz, 1 H, H-1), 5.16 (s, 1 H, OH), 5.01 (d, $J = 5.5$ Hz, 1 H, H-2), 3.77 (s, 3 H, H-7 x 3), 1.37 (s, 18 H, H-11 x 18). ^{13}C NMR (151 MHz, CDCl_3) δ 159.19 (C-6), 153.35 (C-12), 150.77 (C-17), 142.55 (C-14), 136.28 (C-9 x 2), 131.16 (C-15 x 2), 130.80 (C-4 x 2), 130.42 (C-3), 130.07 (C-13), 125.06 (C-8 x 2), 123.67 (C-16 x 2), 113.83 (C-5 x 2), 79.77 (C-1), 55.38 (C-7), 50.92 (C-2), 34.51 (C-10 x 2), 30.39 (C-11 x 6). Diastereomer B: ^1H NMR (599 MHz, CDCl_3) δ 8.14 (d, $J = 9.1$ Hz, 2 H, H-16 x 2), 7.75 (d, $J = 9.0$ Hz, 2 H, H-15 x 2), 7.20 (d, $J = 8.9$, 2 H, H-4 x 2), 7.12 (s, 2 H, H-8 x 2), 6.79 (d, $J = 8.8$ Hz, 2 H, H-5 x 2), 5.45 (d, $J = 6.0$ Hz, 1 H, H-1), 5.15 (s, 1 H, OH), 4.93 (d, $J = 5.9$ Hz, 1 H, H-2), 3.75 (s, 3 H, H-7 x 3), 1.34 (s, 18 H, H-11 x 18). ^{13}C NMR (151 MHz, CDCl_3) δ 159.06 (C-6), 153.55 (C-12), 150.67 (C-17), 142.15 (C-14), 135.88 (C-9 x 2), 131.53 (C-15 x 2), 131.48 (C-3), 129.45 (C-4 x 2), 128.19 (C-13), 126.45 (C-8 x 2), 123.39 (C-16 x 2), 114.28 (C-5 x 2), 80.29 (C-1), 55.34 (C-7), 51.38 (C-2), 34.41 (C-10 x 2), 30.32 (C-11 x 6). HRMS (EI) m/z : $[\text{M}^+]$ calcd for $\text{C}_{29}\text{H}_{34}\text{ClNO}_6\text{S}$ 559.1790, found 559.1795. IR (ATR) ν (cm^{-1}) = 3631, 2956, 1608, 1531, 1511, 1434, 1346, 1309, 1251, 1179, 1150, 1080, 1032, 908, 853, 752, 681.

Reaction of carbanion 1a with quinone methide 2c in DMSO at 20 °C (General procedure 3). To a solution of **1a** (190 mg, 1.00 mmol) in anhydrous DMSO (5 mL) was added a solution of *t*-BuOK (112 mg, 1.00 mmol) in anhydrous DMSO (5 mL) at room temperature. After 2 min, a solution of **2c** (162 mg, 0.500 mmol) in anhydrous DMSO (10 mL) was added to the resulting solution. The completion of the reaction was checked by TLC and quenched by 100 mL 2% aqueous HCl followed with CHCl_3 extraction. The organic extract was washed by water three times to remove remaining DMSO, dried with anhydrous MgSO_4 and filtered. The solvent was evaporated under reduced pressure and the crude product was purified by column chromatography to obtain white solid **4a-H** (167 mg, 0.351 mmol, 70%) and byproduct colorless liquid **5a-H** (16.8 mg, 0.0499 mmol, 10%).

(E)-2,6-Di-tert-butyl-4-(2-(4-methoxyphenyl)-1-(phenylsulfonyl)vinyl)phenol (4a-H): white solid, mp 147–152 °C. ^1H NMR (599 MHz, CDCl_3) δ 7.84 (s, 1 H, H-1), 7.66 – 7.57 (m, 2 H, H-15 x 2), 7.50 (t, $J = 7.4$ Hz, 1 H, H-17), 7.37 (dd, $J = 8.5$, 7.1 Hz, 2 H, H-16 x 2), 7.05 (d, $J = 8.9$ Hz, 2 H, H-3 x 2), 6.71 (s, 2 H, H-9 x 2), 6.69 (d, $J = 9.0$ Hz, 2 H, H-4 x 2), 5.31 (s, 1 H, OH), 3.75 (s, 3 H, H-6 x 3), 1.28 (s, 18 H, H-13 x 18). ^{13}C NMR (151 MHz, CDCl_3) δ 161.03 (C-5), 154.60 (C-11), 139.54 (C-14), 139.47 (C-7), 136.62 (C-1), 136.55 (C-10 x 2), 132.83 (C-17), 132.35 (C-3 X 2), 128.83 (C-15 x 2), 128.58 (C-16 x 2), 127.71 (C-9 x 2), 125.96 (C-2), 122.10 (C-8), 113.96 (C-4 x 2), 55.41 (C-6), 34.39 (C-12 x 2), 30.33 (C-13 x 6).

HRMS (EI) m/z : $[M^+]$ calcd for $C_{29}H_{34}O_4S$ 478.2172, found 478.2172. IR (ATR) ν (cm^{-1}) = 3552, 2949, 1606, 1513, 1444, 1419, 1376, 1305, 1282, 1256, 1236, 1177, 1147, 1110, 1036, 1023, 981, 895, 840, 804, 765, 751, 714, 689, 666.

2,6-Di-tert-butyl-4-((4-methoxyphenyl)ethynyl)phenol (5a-H): colorless liquid. 1H NMR (599 MHz, $CDCl_3$) δ 7.46 (d, J = 8.7 Hz, 2 H, H-4 x 2), 7.34 (s, 2 H, H-9 x 2), 6.86 (d, J = 8.7 Hz, 2 H, H-3 x 2), 5.35 (s, 1 H, OH), 3.82 (s, 3 H, H-1 x 3), 1.45 (s, 18 H, H-12 x 18). ^{13}C NMR (151 MHz, $CDCl_3$) δ 159.4 (C-2), 154.3 (C-13), 136.2 (C-10 x 2), 133.0 (C-4 x 2), 128.6 (C-9 x 2), 116.1 (C-5), 114.5 (C-8), 114.1 (C-3 x 2), 89.3 (C-7), 87.0 (C-6), 55.4 (C-1), 34.5 (C-11 x 2), 30.4 (C-12 x 6). HRMS (EI) m/z : $[M^+]$ calcd for $C_{23}H_{28}O_2$ 336.2084, found 336.2081. IR (ATR) ν (cm^{-1}) = 3625, 2956, 1606, 1509, 1433, 1287, 1174, 1152, 1119, 1105, 1031, 885, 830, 806, 774, 757.

(E)-2,6-Di-tert-butyl-4-(1-((4-chlorophenyl)sulfonyl)-2-(4-methoxyphenyl)vinyl)phenol (4b-H). General procedure 3 was applied to **1b-H** (225 mg, 1.00 mmol), **2c** (162 mg, 0.500 mmol) and *t*-BuOK (112 mg, 1.00 mmol). **4b-H** was obtained as a pale yellow liquid (156 mg, 0.305 mmol, 61%) 1H NMR (400 MHz, $CDCl_3$) δ 7.82 (s, 1 H, H-1), 7.52 (d, J = 8.6 Hz, 2 H, H-15 x 2), 7.34 (d, J = 8.5 Hz, 2 H, H-16 x 2), 7.06 (d, J = 8.8 Hz, 2 H, H-3 x 2), 6.72 (s, 2 H, H-9 x 2), 6.70 (d, J = 8.8 Hz, 2 H, H-4 x 2), 5.34 (s, 1 H, OH), 3.76 (s, 3 H, H-6 x 3), 1.30 (s, 18 H, H-13 x 18). ^{13}C NMR (101 MHz, $CDCl_3$) δ 161.19 (C-5), 154.72 (C-11), 139.52 (C-17), 139.21 (C-7), 138.03 (C-14), 136.82 (C-1), 136.76 (C-10 x 2), 132.42 (C-3 x 2), 130.29 (C-15 x 2), 128.80 (C-16 x 2), 127.76 (C-9 x 2), 125.78 (C-2), 121.88 (C-8), 114.02 (C-4 x 2), 55.43 (C-6), 34.42 (C-12 x 2), 30.33 (C-13 x 6). HRMS (EI) m/z : $[M^+]$ calcd for $C_{29}H_{33}ClO_4S$ 512.1783, found 512.1792. IR (ATR) ν (cm^{-1}) = 3628, 2955, 1601, 1510, 1474, 1436, 1375, 1303, 1253, 1176, 1145, 1029, 982, 828, 765, 706, 669.

(E)-2,6-Di-tert-butyl-4-(1-((4-cyanophenyl)sulfonyl)-2-(4-methoxyphenyl)vinyl)phenol (4c-H): General procedure 3 was applied to **1c-H** (215 mg, 1.00 mmol), **2c** (162 mg, 0.500 mmol) and *t*-BuOK (112 mg, 1.00 mmol). **4c-H** was obtained as a yellow solid (111 mg, 0.220 mmol, 44%) mp 135–140 °C. 1H NMR (400 MHz, $CDCl_3$) δ 7.85 (s, 1 H, H-1), 7.71 (d, J = 8.1 Hz, 2 H, H-15 x 2), 7.66 (d, J = 8.2 Hz, 2 H, H-16 x 2), 7.06 (d, J = 8.4 Hz, 2 H, H-3 x 2), 6.74 (s, 2 H, H-9 x 2), 6.71 (d, J = 8.4 Hz, 2 H, H-4 x 2), 5.38 (s, 1 H, OH), 3.77 (s, 3 H, H-6 x 3), 1.30 (s, 18 H, H-13 x 18). ^{13}C NMR (101 MHz, $CDCl_3$) δ 161.5 (C-5), 154.9 (C-11), 144.1 (C-14), 138.2 (C-1 and C-7), 137.0 (C-10 x 2), 132.6 (C-3 x 2), 132.2 (C-16 x 2), 129.4 (C-15 x 2), 127.8 (C-9 x 2), 125.5 (C-2), 121.4 (C-8), 117.4 (C-18), 116.4 (C-17), 114.1 (C-4 x 2), 55.5 (C-6), 34.4 (C-12 x 2), 30.4 (C-13 x 6).

HRMS (EI) m/z : $[M^+]$ calcd for $C_{30}H_{33}NO_4S$ 503.2125, found 503.2124. IR (ATR) ν (cm^{-1}) = 3598, 2956, 2232, 1664, 1603, 1511, 1436, 1422, 1358, 1310, 1174, 1120, 1081, 1033, 978, 892, 826, 755, 670.

Reaction of carbanion 1 with benzylidenemalonate 2h (General procedure 4). To a solution of **1a** (98.0 mg, 0.516 mmol) and **2h** (100 mg, 0.344 mmol) in anhydrous DMSO (5 mL) was added anhydrous NaOH (20.6 mg, 0.515 mmol). The resulting solution was stirred for 2h at room temperature and then quenched by saturated NH_4Cl solution followed with $CHCl_3$ extraction. The organic extract was washed by water three times to remove remaining DMSO, dried with anhydrous $MgSO_4$ and filtered. The solvent was evaporated under reduced pressure and the residue was purified by column chromatography to obtain yellow liquid diethyl 2-(2-chloro-1-(4-(dimethylamino)phenyl)-2-(phenylsulfonyl)ethyl)malonate (**6a-H**) (119 mg, 0.248 mmol, 72%, dr ~ 5:1). The major diastereomer could be isolated in pure form and its full characterization is as same as literature reported.⁷

Diethyl 2-(2-chloro-2-((4-chlorophenyl)sulfonyl)-1-(4-(dimethylamino)phenyl)ethyl)malonate (6b-H). General procedure 4 was applied to **1b-H** (117 mg, 0.520 mmol), **2h** (100 mg, 0.344 mmol) and NaOH (20.6 mg, 0.515 mmol). **6b-H** was obtained as a pale yellow liquid (123 mg, 0.238 mmol, 70%, dr ~ 2:1), minor diastereomer decomposed during purification. Major diastereomer: 1H NMR (599 MHz, $CDCl_3$) δ 7.60 (d, J = 8.7 Hz, 2 H, H-16 x 2), 7.36 (d, J = 8.6 Hz, 2 H, H-17 x 2), 7.16 (d, J = 8.8 Hz, 2 H, H-11 x 2), 6.49 (d, J = 8.3 Hz, 2 H, H-12 x 2), 5.66 (d, J = 7.3 Hz, 1 H, H-1), 4.44 (d, J = 8.6 Hz, 1 H, H-3), 4.18 – 4.09 (m, 3 H, H-2 and H-8 x 2), 4.01 (q, J = 7.1 Hz, 2 H, H-5 x 2), 2.91 (s, 6 H, H-14 x 6), 1.21 (t, J = 7.2 Hz, 3 H, H-9 x 3), 1.08 (t, J = 7.1 Hz, 3 H, H-6 x 3). ^{13}C NMR (151 MHz, $CDCl_3$) δ 168.0 (C-7), 167.6 (C-4), 150.4 (C-13), 140.5 (C-18), 136.4 (C-15), 131.1 (C-11 x 2), 130.6 (C-16 x 2), 129.3 (C-17 x 2), 121.5 (C-10), 112.0 (C-12 x 2), 76.5 (C-1), 62.0 (C-8), 61.7 (C-5), 55.4 (C-3), 47.4 (C-2), 40.5 (C-14 x 2), 14.1 (C-9), 13.9 (C-6). HRMS (EI) m/z : $[M^+]$ calcd for $C_{23}H_{27}Cl_2NO_6S$ 515.0931, found 515.0925. IR (ATR) ν (cm^{-1}) = 2981, 2929, 1728, 1613, 1523, 1475, 1445, 1394, 1332, 1279, 1256, 1089, 1012, 947, 819, 751, 666.

(2) Kinetics of the reactions of carbanions 1a–e with electrophiles 2a–i

The rates of all investigated reactions were determined spectrophotometrically (UV-Vis) either by following the disappearance of the colored quinone methides or benzylidenemalonates. The temperature of the solutions during all kinetics studies was kept constant (20.0 ± 0.1 °C) by using a circulating bath thermostat. The kinetics investigations

were performed with a high excess of the carbanions over the electrophiles to achieve first-order kinetics. As the carbanions **1a–e** decompose slowly at room temperature. Thus we employed double-mixing mode of stopped flow UV-vis spectrometers to generate the carbanions by mixing of two reagents (**1a–e-H** + *t*-BuOK) with a first mixing drive and after a user defined delay period, mixed the aged solution with a third reagent (electrophiles) to achieve kinetics curve of the reaction. All the kinetics measurements were measured by a commercial stopped-flow spectrophotometer system. Rate constants k_{obs} (s^{-1}) were obtained by fitting the single exponential decay $A_t = A_0 \exp(-k_{\text{obs}}t) + C$ (exponential decrease) to the observed time-dependent absorbance (in the case of the stopped-flow spectrophotometer, an average from at least 5 kinetics runs for each nucleophile concentration was done). Second-order rate constants k_2 ($\text{M}^{-1} \text{s}^{-1}$) were derived from the slopes of the linear correlations of k_{obs} with nucleophile concentrations.

Chapter 2: Nucleophilicity parameters of arylsulfonyl-substituted halomethyl anions

Table S1. Kinetics of the reactions of **1a** with **2c** in DMSO at 20 °C (deprotonated with 1.00–1.05 equiv. *t*-BuOK, stopped-flow UV-Vis spectrometer, $\lambda = 393$ nm).

[2c]/mol L ⁻¹	[1a]/mol L ⁻¹	$k_{\text{obs}}/\text{s}^{-1}$
2.50E-05	5.00E-04	3.23E+01
2.50E-05	7.50E-04	5.98E+01
2.50E-05	1.00E-03	1.07E+02
2.50E-05	1.25E-03	1.41E+02
2.50E-05	1.50E-03	1.74E+02

$k_2 = 1.46 \times 10^5 \text{ L mol}^{-1} \text{ s}^{-1}$

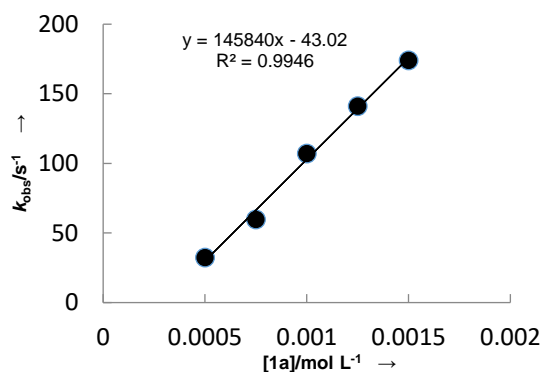


Table S2. Kinetics of the reactions of **1a** with **2d** in DMSO at 20 °C (deprotonated with 1.00–1.05 equiv. *t*-BuOK, stopped-flow UV-Vis spectrometer, $\lambda = 486$ nm).

[2d]/mol L ⁻¹	[1a]/mol L ⁻¹	$k_{\text{obs}}/\text{s}^{-1}$
4.93E-05	9.98E-04	5.85E+01
4.93E-05	1.50E-03	8.15E+01
4.93E-05	2.49E-03	1.11E+02
4.93E-05	2.99E-03	1.27E+02

$k_2 = 3.35 \times 10^4 \text{ L mol}^{-1} \text{ s}^{-1}$

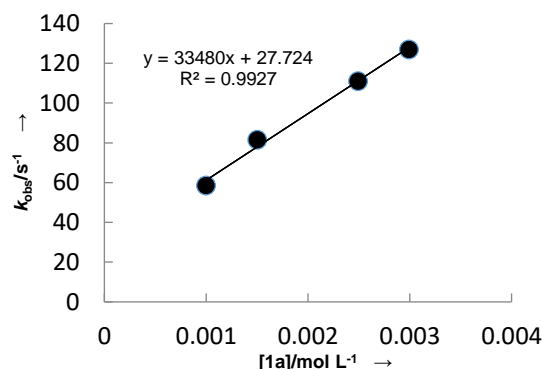


Table S3. Kinetics of the reactions of **1a** with **2e** in DMSO at 20 °C (deprotonated with 1.00–1.05 equiv. *t*-BuOK, stopped-flow UV-Vis spectrometer, $\lambda = 521$ nm).

[2e]/mol L ⁻¹	[1a]/mol L ⁻¹	$k_{\text{obs}}/\text{s}^{-1}$
9.75E-05	9.95E-04	2.89E+01
9.75E-05	1.49E-03	3.46E+01
9.75E-05	1.99E-03	4.83E+01
9.75E-05	2.49E-03	6.06E+01
9.75E-05	2.98E-03	8.17E+01

$k_2 = 2.65 \times 10^4 \text{ L mol}^{-1} \text{ s}^{-1}$

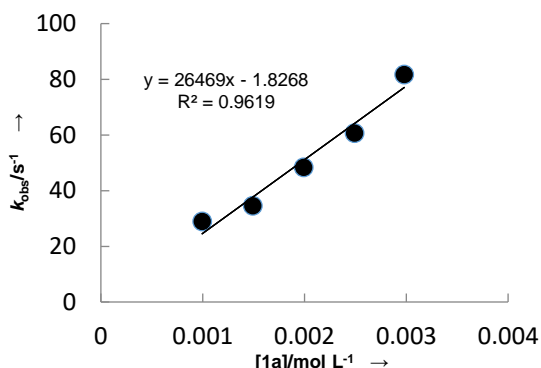
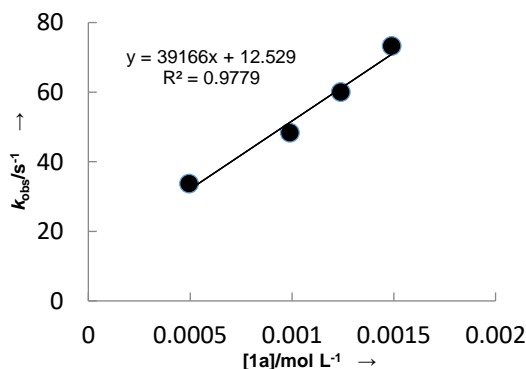


Table S4. Kinetics of the reactions of **1a** with **2g** in DMSO at 20 °C (deprotonated with 1.00–1.05 equiv. *t*-BuOK, stopped-flow UV-Vis spectrometer, $\lambda = 490$ nm).

[2g]/mol L ⁻¹	[1a]/mol L ⁻¹	$k_{\text{obs}}/\text{s}^{-1}$
3.78E-05	4.95E-04	3.37E+01
3.78E-05	9.90E-04	4.83E+01
3.78E-05	1.24E-03	6.00E+01
3.78E-05	1.49E-03	7.32E+01

$k_2 = 3.92 \times 10^4 \text{ L mol}^{-1} \text{ s}^{-1}$



Chapter 2: Nucleophilicity parameters of arylsulfonyl-substituted halomethyl anions

Table S5. Kinetics of the reactions of **1a** with **2h** in DMSO at 20 °C (deprotonated with 1.00–1.05 equiv. *t*-BuOK, stopped-flow UV-Vis spectrometer, $\lambda = 383$ nm).

[2h]/mol L ⁻¹	[1a]/mol L ⁻¹	$k_{\text{obs}}/\text{s}^{-1}$
2.50E-05	7.58E-04	6.70E-02
2.50E-05	1.01E-03	1.05E-01
2.50E-05	1.26E-03	1.43E-01
2.50E-05	1.52E-03	1.78E-01
2.50E-05	1.77E-03	2.19E-01

$k_2 = 1.49 \times 10^2 \text{ L mol}^{-1} \text{ s}^{-1}$

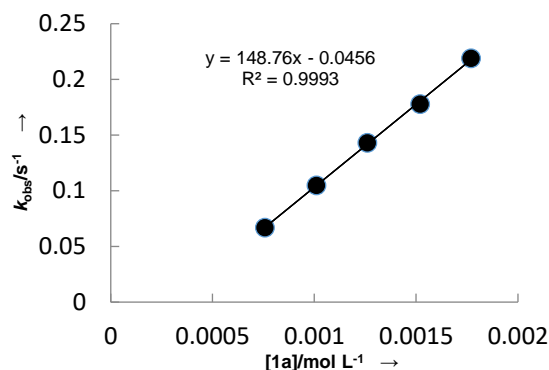


Table S6. Kinetics of the reactions of **1b** with **2b** in DMSO at 20 °C (deprotonated with 1.00–1.05 equiv. *t*-BuOK, stopped-flow UV-Vis spectrometer, $\lambda = 371$ nm).

[2b]/mol L ⁻¹	[1b]/mol L ⁻¹	$k_{\text{obs}}/\text{s}^{-1}$
2.50E-05	2.56E-04	1.76E+01
2.50E-05	3.83E-04	3.14E+01
2.50E-05	5.11E-04	4.12E+01
2.50E-05	6.39E-04	6.02E+01

$k_2 = 1.08 \times 10^5 \text{ L mol}^{-1} \text{ s}^{-1}$

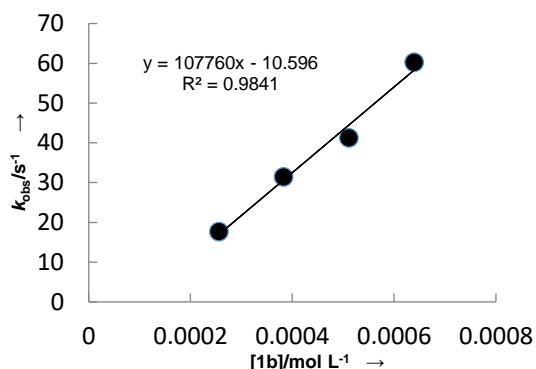


Table S7. Kinetics of the reactions of **1b** with **2c** in DMSO at 20 °C (deprotonated with 1.00–1.05 equiv. *t*-BuOK, stopped-flow UV-Vis spectrometer, $\lambda = 393$ nm).

[2c]/mol L ⁻¹	[1b]/mol L ⁻¹	$k_{\text{obs}}/\text{s}^{-1}$
2.50E-05	2.56E-04	1.69E+01
2.50E-05	3.83E-04	3.18E+01
2.50E-05	5.11E-04	4.35E+01
2.50E-05	6.39E-04	5.16E+01
2.50E-05	7.67E-04	6.37E+01

$k_2 = 8.87 \times 10^4 \text{ L mol}^{-1} \text{ s}^{-1}$

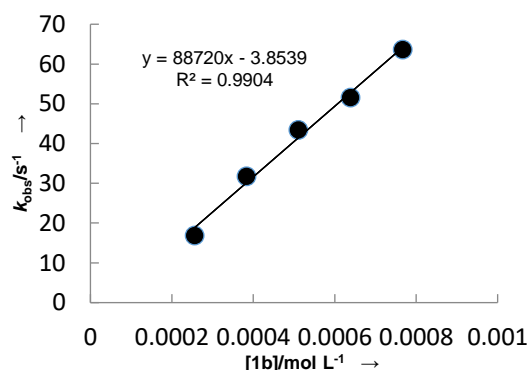
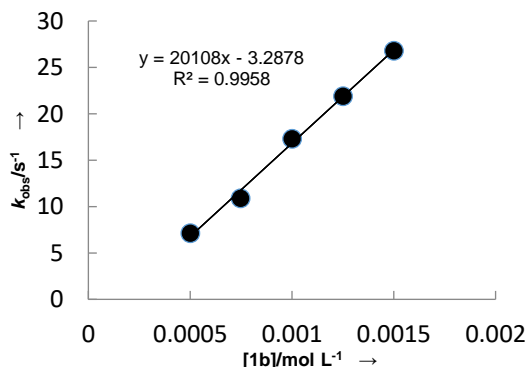


Table S8. Kinetics of the reactions of **1b** with **2d** in DMSO at 20 °C (deprotonated with 1.00–1.05 equiv. *t*-BuOK, stopped-flow UV-Vis spectrometer, $\lambda = 486$ nm).

[2d]/mol L ⁻¹	[1b]/mol L ⁻¹	$k_{\text{obs}}/\text{s}^{-1}$
2.50E-05	5.00E-04	7.14E+00
2.50E-05	7.47E-04	1.09E+01
2.50E-05	1.00E-03	1.73E+01
2.50E-05	1.25E-03	2.19E+01
2.50E-05	1.50E-03	2.68E+01

$k_2 = 2.01 \times 10^4 \text{ L mol}^{-1} \text{ s}^{-1}$



Chapter 2: Nucleophilicity parameters of arylsulfonyl-substituted halomethyl anions

Table S9. Kinetics of the reactions of **1b** with **2h** in DMSO at 20 °C (deprotonated with 1.00–1.05 equiv. *t*-BuOK, stopped-flow UV-Vis spectrometer, $\lambda = 390$ nm).

[2h]/mol L ⁻¹	[1b]/mol L ⁻¹	$k_{\text{obs}}/\text{s}^{-1}$
4.12E-05	6.05E-04	1.57E-02
4.12E-05	8.07E-04	2.35E-02
4.12E-05	1.01E-03	3.25E-02
4.12E-05	1.21E-03	4.57E-02

$k_2 = 4.90 \times 10^1 \text{ L mol}^{-1} \text{ s}^{-1}$

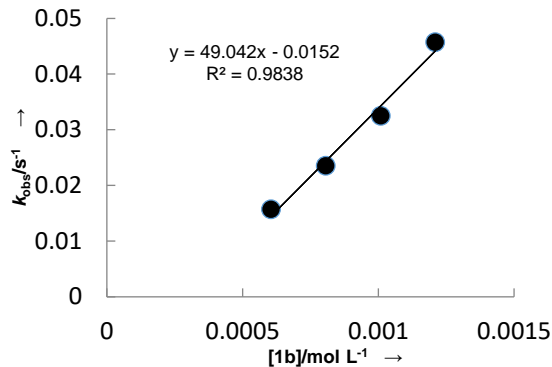


Table S10. Kinetics of the reactions of **1b** with **2i** in DMSO at 20 °C (deprotonated with 1.00–1.05 equiv. *t*-BuOK, stopped-flow UV-Vis spectrometer, $\lambda = 409$ nm).

[2i]/mol L ⁻¹	[1b]/mol L ⁻¹	$k_{\text{obs}}/\text{s}^{-1}$
2.50E-05	1.26E-03	2.96E-02
2.50E-05	1.51E-03	3.63E-02
2.50E-05	1.76E-03	4.34E-02
2.50E-05	2.02E-03	5.17E-02
2.50E-05	2.27E-03	5.79E-02

$k_2 = 2.85 \times 10^1 \text{ L mol}^{-1} \text{ s}^{-1}$

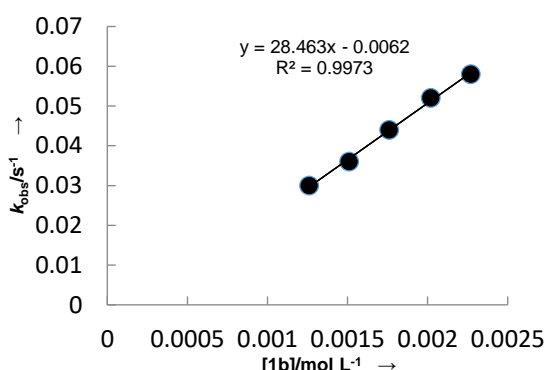


Table S11. Kinetics of the reactions of **1c** with **2d** in DMSO at 20 °C (deprotonated with 1.00–1.05 equiv. *t*-BuOK, stopped-flow UV-Vis spectrometer, $\lambda = 486$ nm).

[2d]/mol L ⁻¹	[1c]/mol L ⁻¹	$k_{\text{obs}}/\text{s}^{-1}$
5.00E-05	1.04E-03	2.74E+01
5.00E-05	1.55E-03	3.63E+01
5.00E-05	2.59E-03	5.11E+01
5.00E-05	3.11E-03	6.59E+01

$k_2 = 1.77 \times 10^4 \text{ L mol}^{-1} \text{ s}^{-1}$

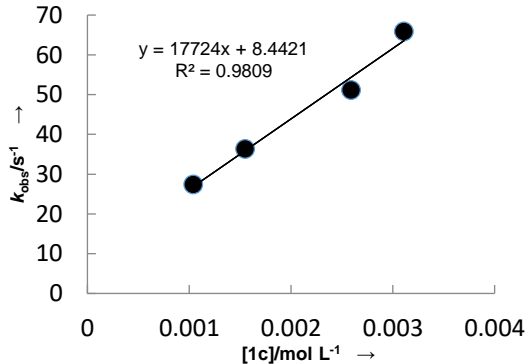
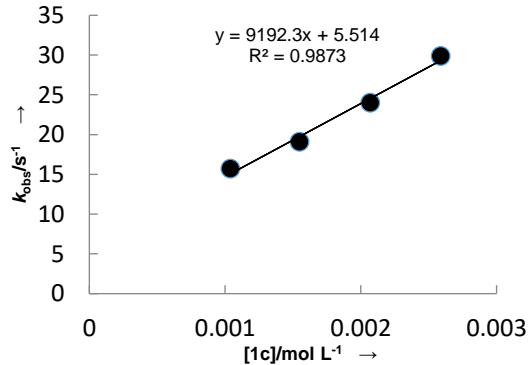


Table S12. Kinetics of the reactions of **1c** with **2e** in DMSO at 20 °C (deprotonated with 1.00–1.05 equiv. *t*-BuOK, stopped-flow UV-Vis spectrometer, $\lambda = 521$ nm).

[2e]/mol L ⁻¹	[1c]/mol L ⁻¹	$k_{\text{obs}}/\text{s}^{-1}$
5.00E-05	1.04E-03	1.57E+01
5.00E-05	1.55E-03	1.91E+01
5.00E-05	2.07E-03	2.40E+01
5.00E-05	2.59E-03	2.99E+01

$k_2 = 9.19 \times 10^3 \text{ L mol}^{-1} \text{ s}^{-1}$



Chapter 2: Nucleophilicity parameters of arylsulfonyl-substituted halomethyl anions

Table S13. Kinetics of the reactions of **1c** with **2f** in DMSO at 20 °C (deprotonated with 1.00–1.05 equiv. *t*-BuOK, stopped-flow UV-Vis spectrometer, $\lambda = 490$ nm).

[2f]/mol L ⁻¹	[1c]/mol L ⁻¹	$k_{\text{obs}}/\text{s}^{-1}$
5.00E-05	1.55E-03	7.08E+01
5.00E-05	2.07E-03	1.10E+02
5.00E-05	2.59E-03	1.33E+02
5.00E-05	3.11E-03	1.61E+02

$k_2 = 5.65 \times 10^4 \text{ L mol}^{-1} \text{ s}^{-1}$

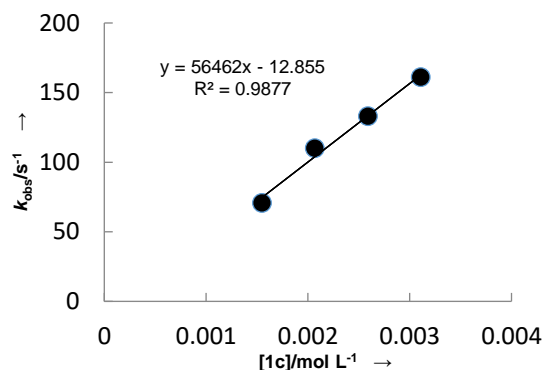


Table S14. Kinetics of the reactions of **1c** with **2g** in DMSO at 20 °C (deprotonated with 1.00–1.05 equiv. *t*-BuOK, stopped-flow UV-Vis spectrometer, $\lambda = 490$ nm).

[2g]/mol L ⁻¹	[1c]/mol L ⁻¹	$k_{\text{obs}}/\text{s}^{-1}$
5.00E-05	1.55E-03	2.59E+01
5.00E-05	2.07E-03	3.66E+01
5.00E-05	2.59E-03	5.02E+01
5.00E-05	3.11E-03	5.96E+01

$k_2 = 2.21 \times 10^4 \text{ L mol}^{-1} \text{ s}^{-1}$

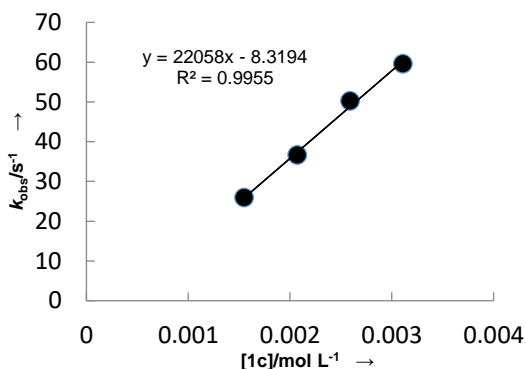


Table S15. Kinetics of the reactions of **1d** with **2a** in DMSO at 20 °C (deprotonated with 1.00–1.05 equiv. *t*-BuOK, stopped-flow UV-Vis spectrometer, $\lambda = 370$ nm).

[2a]/mol L ⁻¹	[1d]/mol L ⁻¹	$k_{\text{obs}}/\text{s}^{-1}$
5.00E-05	4.98E-04	2.42E+01
5.00E-05	9.96E-04	4.98E+01
5.00E-05	1.24E-03	7.76E+01

$k_2 = 6.89 \times 10^4 \text{ L mol}^{-1} \text{ s}^{-1}$

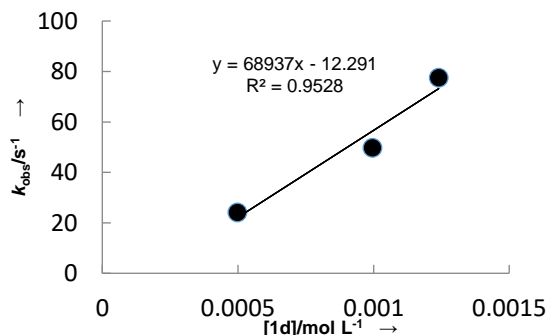
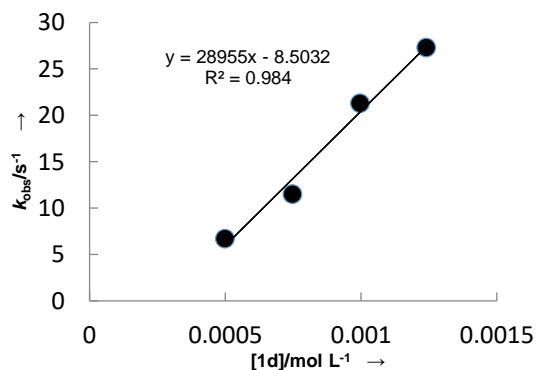


Table S16. Kinetics of the reactions of **1d** with **2b** in DMSO at 20 °C (deprotonated with 1.00–1.05 equiv. *t*-BuOK, stopped-flow UV-Vis spectrometer, $\lambda = 380$ nm).

[2b]/mol L ⁻¹	[1d]/mol L ⁻¹	$k_{\text{obs}}/\text{s}^{-1}$
5.00E-05	4.98E-04	6.68E+00
5.00E-05	7.47E-04	1.15E+01
5.00E-05	9.96E-04	2.13E+01
5.00E-05	1.24E-03	2.73E+01

$k_2 = 2.90 \times 10^4 \text{ L mol}^{-1} \text{ s}^{-1}$



Chapter 2: Nucleophilicity parameters of arylsulfonyl-substituted halomethyl anions

Table S17. Kinetics of the reactions of **1d** with **2c** in DMSO at 20 °C (deprotonated with 1.00–1.05 equiv. *t*-BuOK, stopped-flow UV-Vis spectrometer, $\lambda = 393$ nm).

[2c]/mol L ⁻¹	[1d]/mol L ⁻¹	$k_{\text{obs}}/\text{s}^{-1}$
5.00E-05	4.98E-04	5.24E+00
5.00E-05	7.47E-04	9.93E+00
5.00E-05	9.96E-04	1.52E+01

$k_2 = 2.00 \times 10^4 \text{ L mol}^{-1} \text{ s}^{-1}$

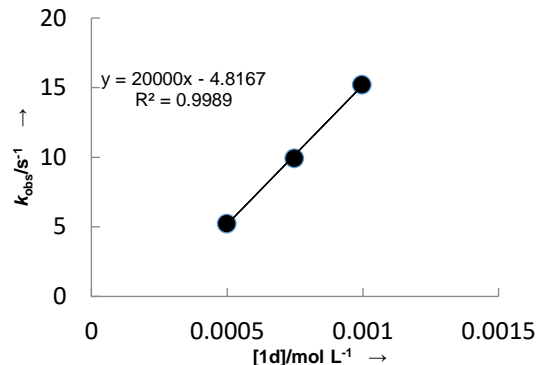


Table S18. Kinetics of the reactions of **1e** with **2a** in DMSO at 20 °C (deprotonated with 1.00–1.05 equiv. *t*-BuOK, stopped-flow UV-Vis spectrometer, $\lambda = 354$ nm).

[2a]/mol L ⁻¹	[1e]/mol L ⁻¹	$k_{\text{obs}}/\text{s}^{-1}$
2.50E-05	2.50E-04	6.40E+01
2.50E-05	5.00E-04	1.50E+02
2.50E-05	7.50E-04	2.03E+02

$k_2 = 2.78 \times 10^5 \text{ L mol}^{-1} \text{ s}^{-1}$

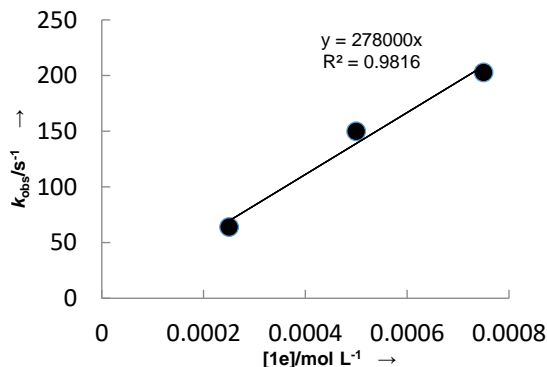


Table S19. Kinetics of the reactions of **1e** with **2c** in DMSO at 20 °C (deprotonated with 1.00–1.05 equiv. *t*-BuOK, stopped-flow UV-Vis spectrometer, $\lambda = 393$ nm).

[2c]/mol L ⁻¹	[1e]/mol L ⁻¹	$k_{\text{obs}}/\text{s}^{-1}$
4.00E-05	1.01E-03	2.78E+01
4.00E-05	1.51E-03	6.63E+01
4.00E-05	2.01E-03	9.23E+01
4.00E-05	2.51E-03	1.41E+02
4.00E-05	3.02E-03	1.69E+02

$k_2 = 7.11 \times 10^4 \text{ L mol}^{-1} \text{ s}^{-1}$

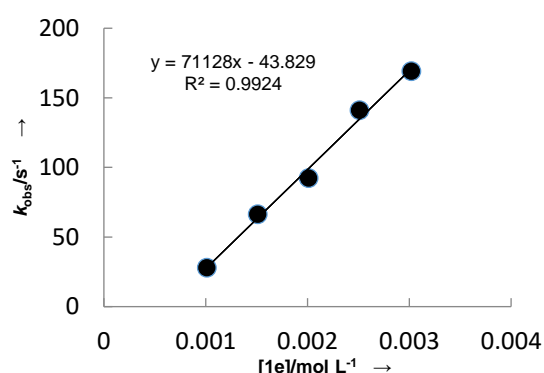


Table S20. Kinetics of the reactions of **1e** with **2d** in DMSO at 20 °C (deprotonated with 1.00–1.05 equiv. *t*-BuOK, stopped-flow UV-Vis spectrometer, $\lambda = 486$ nm).

[2d]/mol L ⁻¹	[1e]/mol L ⁻¹	$k_{\text{obs}}/\text{s}^{-1}$
5.00E-05	1.01E-03	7.84E+00
5.00E-05	1.51E-03	1.18E+01
5.00E-05	2.01E-03	1.88E+01
5.00E-05	2.51E-03	2.50E+01

$k_2 = 1.17 \times 10^4 \text{ L mol}^{-1} \text{ s}^{-1}$

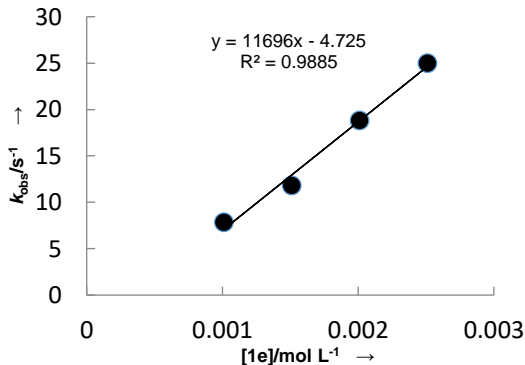
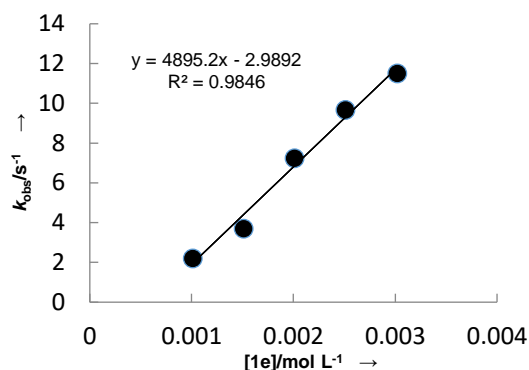


Table S21. Kinetics of the reactions of **1e** with **2e** in DMSO at 20 °C (deprotonated with 1.00–1.05 equiv. *t*-BuOK, stopped-flow UV-Vis spectrometer, $\lambda = 521$ nm).

[2e]/mol L ⁻¹	[1e]/mol L ⁻¹	$k_{\text{obs}}/\text{s}^{-1}$
4.00E-05	1.01E-03	2.20E+00
4.00E-05	1.51E-03	3.69E+00
4.00E-05	2.01E-03	7.24E+00
4.00E-05	2.51E-03	9.67E+00
4.00E-05	3.02E-03	1.15E+01

$k_2 = 4.90 \times 10^3 \text{ L mol}^{-1} \text{ s}^{-1}$



(3) Correlation of the $\log k_2$ for the reaction of carbanion **1b with electrophiles versus the corresponding electrophilicity parameters E**

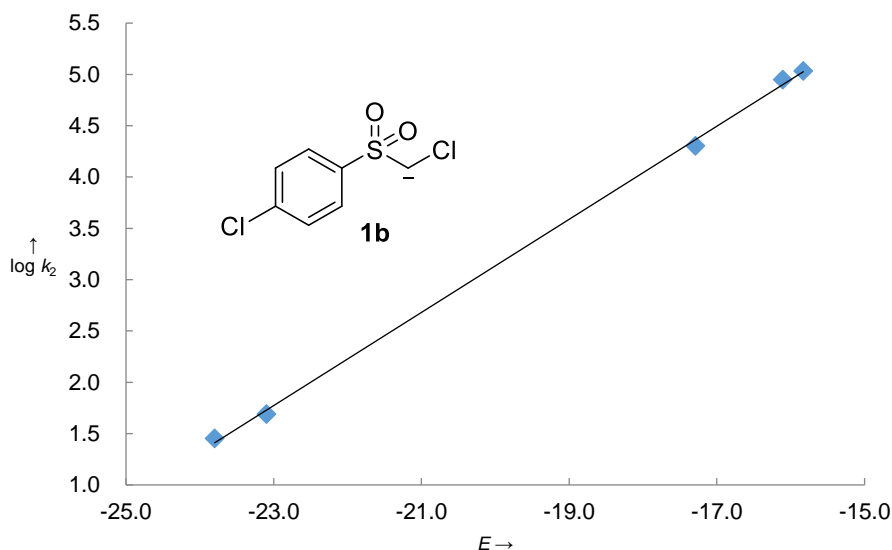


Figure S1. Correlation of $\log k_2$ for the reactions of the carbanion **1b** with the quinone methides **2b–d** and benzylidenemalonates **2h–i** versus the electrophilicity parameters E of the corresponding electrophiles.

(4) Crystallographic data

Single crystal of **4a**-H of suitable quality for X-ray analysis was obtained by dissolving about 50 mg of the solid in 2 mL of CH₂Cl₂ and allowing the solvents to evaporate slowly (two days). Crystallographic data have been deposited with the Cambridge Crystallographic Data Centre (CCDC number: 1512461). These supplementary crystallographic data can be obtained free of charge from The Cambridge Crystallographic Data Centre via www.ccdc.cam.ac.uk/data_request/cif

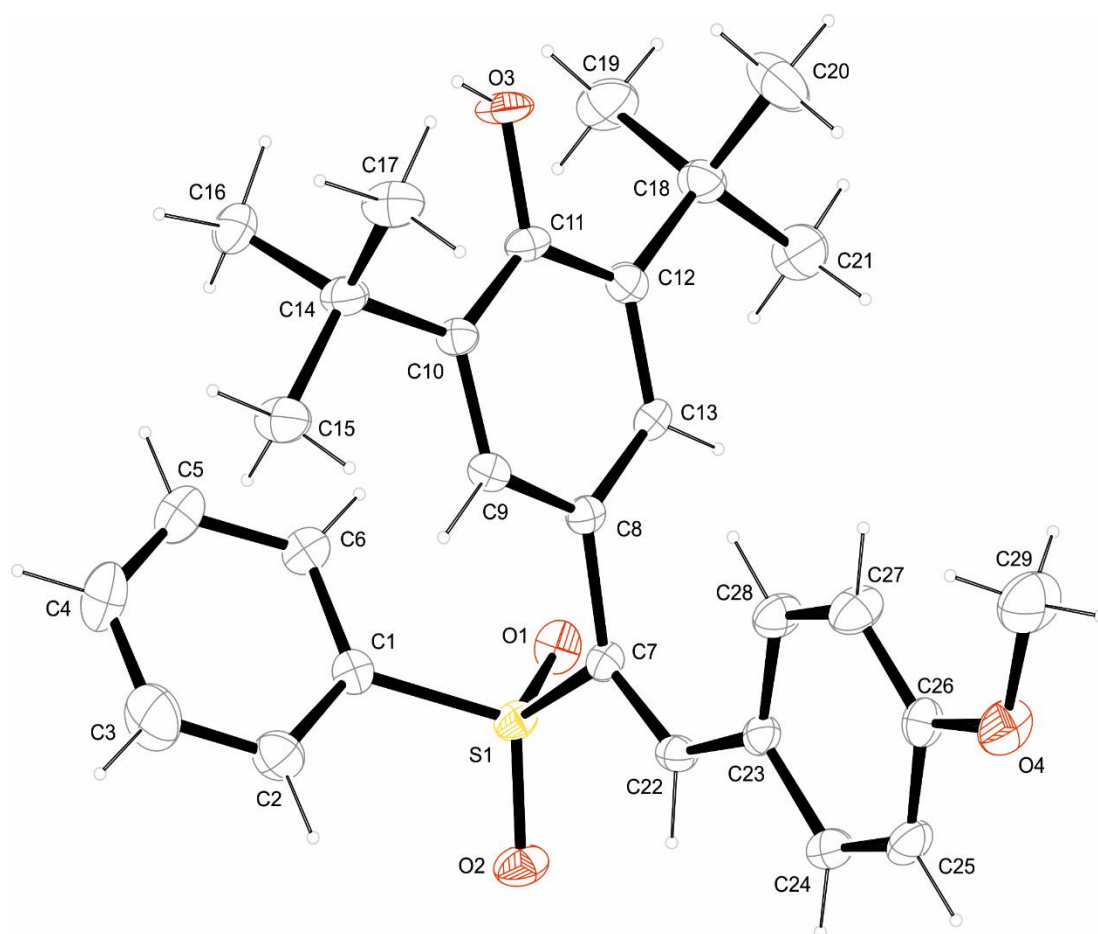


Figure S2. ORTEP-drawing of the crystal structure of **4a**-H. (The ellipsoid probability level is 50%)

Table S22. Crystallographic data for **4a-H**.

	4a-H
net formula	C ₂₉ H ₃₄ O ₄ S
$M_r/\text{g mol}^{-1}$	478.62
crystal size/mm	0.100 × 0.070 × 0.030
T/K	153.(2)
radiation	MoK α
diffractometer	'Bruker D8 Venture TXS'
crystal system	monoclinic
space group	'P 1 21 1'
$a/\text{\AA}$	9.3489(5)
$b/\text{\AA}$	15.6494(9)
$c/\text{\AA}$	18.4534(10)
$\alpha/^\circ$	90
$\beta/^\circ$	102.884(2)
$\gamma/^\circ$	90
$V/\text{\AA}^3$	2631.8(3)
Z	4
calc. density/ g cm^{-3}	1.208
μ/mm^{-1}	0.155
absorption correction	Multi-Scan
transmission factor range	0.9176–0.9705
refls. measured	24982
R_{int}	0.0350
mean $\sigma(I)/I$	0.0433
θ range	3.398–25.024
observed refls.	8656
x, y (weighting scheme)	0.0476, 1.2603
hydrogen refinement	C-H: constr, O-H: refxyz
Flack parameter	0.04(2)
refls in refinement	9268

parameters	633
restraints	10
$R(F_{\text{obs}})$	0.0419
$R_w(F^2)$	0.1050
S	1.083
shift/error _{max}	0.001
max electron density/e Å ⁻³	0.746
min electron density/e Å ⁻³	-0.274

2.5 References

- (1) (a) Rosen, T. Darzens Glycidic Ester Condensation. In *Comprehensive Organic Synthesis*, 1st ed.; Trost, B. M., Fleming, I., Eds.; Pergamon Press: Oxford, **1991**; Vol. 2, pp 409–439. (b) Aggarwal, V. K.; Crimmin, M.; Riches, S. Synthesis of Epoxide by Carbonyl Epoxidation. In *Science of Synthesis*, 2008.; Forysth, C. J., Jacobsen, E. N., Eds.; Thieme: Stuttgart, **2008**; Vol. 37, pp 321–406. (c) Reutrakul, V.; Pohmakotr, M. Chloromethyl Phenyl Sulfone. In *Encyclopedia of Reagents for Organic Synthesis*, 2nd ed.; Paquette, L. A., Crich, D., Fuchs, P. L., Molander, G. A., Eds.; Wiley: Chichester, **2009**; Vol. 4, pp 2375–2378. (d) Bako, P.; Rapi, Z.; Keglevich, G. *Curr. Org. Synth.* **2014**, 11, 361–376.
- (2) (a) Verhe, R.; Kimpe, N. D. Synthesis and reactivity of electrophilic cyclopropanes. In *The Chemistry of the Cyclopropyl Group*, 1st ed.; Rappoport, Z., Ed.; Wiley & Sons: New York, **1987**; Part 1, pp 445–564. (b) Lebel, H.; Marcoux, J-F.; Molinaro, C.; Charette, A. *Chem. Rev.* **2003**, 103, 977–1050.
- (3) (a) Makosza, M.; Winiarski, J. *Acc. Chem. Res.* **1987**, 20, 282–289. (b) Makosza, M. *Synthesis* **1991**, 103–111. (c) Makosza, M.; Kwast, A. *J. Phys. Org. Chem.* **1998**, 11, 341–349. (d) Makosza, M.; Wojciechowski, K. *Chem. Rev.* **2004**, 104, 2631–2666. (e) Makosza, M. *Chem. Soc. Rev.* **2010**, 39, 2855–2868. (f) Makosza, M. *Synthesis* **2011**, 2341–2356. (g) Blaziak, K.; Danikiewicz, W.; Makosza, M. *J. Am. Chem. Soc.* **2016**, 138, 7276–7281.
- (4) (a) Mayr, H.; Bug, T.; Gotta, M. F.; Hering, N.; Irrgang, B.; Janker, B.; Kempf, B.; Loos, R.; Ofial, A. R.; Remennikov, G.; Schimmel, H. *J. Am. Chem. Soc.* **2001**, 123, 9500–9512. (b) Lucius, R.; Loos, R.; Mayr, H. *Angew. Chem., Int. Ed.* **2002**, 41, 91–95; *Angew. Chem.* **2002**, 114, 97–102; (c) Mayr, H.; Kempf, B.; Ofial, A. R. *Acc. Chem. Res.* **2003**, 36, 66–77.
- (5) For a list of nucleophilicity parameters N and s_N and electrophilicity parameters E , see: <http://www.cup.lmu.de/oc/mayr/DBintro.html>.
- (6) (a) Richter, D.; Hampel, N.; Singer, T.; Ofial, A. R.; Mayr, H. *Eur. J. Org. Chem.* **2009**, 3203–3211. (b) Lucius, R.; Loos, R.; Mayr, H. *Angew. Chem., Int. Ed.* **2002**, 41, 91–95. (c) Kaumanns, O.; Lucius, R.; Mayr, H. *Chem.–Eur. J.* **2008**, 14, 9675–9682.
- (7) Groszek, G.; Blazej, S.; Brud, A.; Swierczynski, D.; Lemek, T. *Tetrahedron* **2006**, 62, 2622–2630.
- (8) Seeliger, F.; Blazej, S.; Bernhardt, S.; Makosza, M.; Mayr, H. *Chem.–Eur. J.* **2008**, 14, 6108–6118.

- (9) Galvagni, M.; Kelleher, F.; Paradisi, C.; Scorrano, G. *J. Org. Chem.* **1990**, 55, 4454–4456.
- (10) (a) Bordwell, F. G. *Acc. Chem. Res.* **1988**, 21, 456–463. (b) For a comprehensive list of pK_a values, see: <http://ibond.nankai.edu.cn/>.
- (11) Bordwell, F. G.; Drucker, G. E.; McCollum, G. J. *J. Org. Chem.* **1982**, 47, 2504–2510.
- (12) (a) Allgäuer, D. S.; Mayer, P.; Mayr, H. *J. Am. Chem. Soc.* **2013**, 135, 15216–15224. (b) Appel, R.; Hartmann, N.; Mayr, H. *J. Am. Chem. Soc.* **2010**, 132, 17894–17900. (c) Corral-Bautista, F.; Mayr, H. *Eur. J. Org. Chem.* **2013**, 4255–4261. (d) Corral-Bautista, F.; Appel, R.; Frickel, J. S.; Mayr, H. *Chem.–Eur. J.* **2015**, 21, 875–884. (e) Lemek, T.; Mayr, H. *J. Org. Chem.* **2003**, 68, 6880–6886.
- (13) (a) Golinski, J.; Makosza, M.; Rykowski, A. *Tetrahedron Lett.* **1983**, 24, 3279–3280. (b) Reutrakul, V.; Prapansiri, V.; Panyachotipun, C. *Tetrahedron Lett.* **1984**, 25, 1949–1952. (c) Calet, S.; Alper, H. *Tetrahedron Lett.* **1986**, 27, 2739–2742. (d) Makosza, M.; Glinka, T.; Ostrowski, S.; Rykowski, A. *Chem. Lett.* **1987**, 61–64.
- (14) Beckwith, A. L. J.; Pigou, P. E. *Aust. J. Chem.* **1986**, 39, 77–87.
- (15) Creary, X.; Sky, A. F.; Phillips, G.; Alonso, D. E. *J. Am. Chem. Soc.* **1993**, 115, 7584–7592.
- (16) Staniszewska, M.; Bondaryk, M.; Ochal, Z. *Bioorg. Med. Chem.* **2015**, 23, 314–321.

Chapter 3. Kinetics and Mechanism of Oxirane-Formation by Darzens Condensation of Ketones: Quantification of the Electrophilicities of Ketones

Zhen Li, Harish Jangra, Quan Chen, Peter Mayer,
Armin R. Ofial*, Hendrik Zipse*, and Herbert Mayr*

J. Am. Chem. Soc. **2018**, *140*, 5500–5515.

3.1 Introduction

Combinations of electrophiles with nucleophiles are the most important reactions in organic synthesis. In order to predict scope and selectivities of such reactions we have developed scales of nucleophilicity and electrophilicity on the basis of equation 1, which characterizes electrophiles by one parameter, E (electrophilicity), and nucleophiles by two solvent-dependent parameters, N (nucleophilicity) and s_N (susceptibility).¹

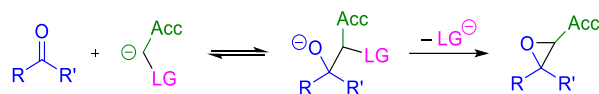
$$\log k_2(20\text{ }^\circ\text{C}) = s_N(N + E) \quad (1)$$

Though carbonyl compounds belong to the most frequently employed electrophiles in organic synthesis, there was only one previous attempt to integrate aldehydes in these scales.² The major problem for the quantitative determination of the electrophilic reactivities of carbonyl compounds is the fact that the nucleophilic attack at the carbonyl group is often a reversible process, which is followed by an irreversible rate-determining step.³

In the late 1950s kinetic investigations of the reactions of ketones and aldehydes with sodium borohydride in protic solvents have been reported by H. C. Brown.⁴ Geneste and associates studied the kinetics of the reactions of ketones with BH_4^- ,^{5a} CN^- ,^{5b} SO_3^{2-} ,^{5b,5c} NH_2OH ,^{5b,5d} and RS^- ^{5e} in water and reported linear correlations^{5f} between the different sets of data. Thermodynamics accounts for the fact that ordinary acceptor-stabilized carbanions (e. g. malonate anions), which have previously been used as reference nucleophiles for the quantification of electrophilic reactivities,^{1b,6} are not suitable for the determination of the E parameters of carbonyl compounds in aprotic solvents: Due to the high basicity of the initially formed alkoxide anions ($\text{p}K_{\text{aH}} = 29.0$ for MeO^- in DMSO),⁷ additions of weakly basic carbanions ($\text{p}K_{\text{aH}} \approx 16$ for dimethyl malonate in DMSO)⁸ to ordinary ketones and aldehydes are highly endergonic in aprotic solvents and only proceed in the presence of a suitable proton source. For that reason, reference nucleophiles are needed, which yield intermediates that undergo fast subsequent irreversible reactions to form stable products. One possibility is to

use carbanions carrying a leaving group LG in α -position, since the resulting intermediates may undergo cyclization with formation of epoxides (Scheme 1).

Scheme 1. Epoxides from Carbonyl Compounds



For LG = Hal, the reaction depicted in Scheme 1 corresponds to the Darzens condensation,^{9,10} which has mechanistically been investigated by Ballester¹¹ and others.^{3a,12} Whereas early work has preferentially been performed with α -halogen-substituted esters, ketones, and aldehydes (Acc = CO₂R or COR), Vogt and Tavares reported that α -halo-substituted sulfones (Acc = ArSO₂) also undergo the reaction sequence shown in Scheme 1 to give sulfonyl-substituted epoxides.^{3b} For LG = R₂S⁺, the nucleophile in Scheme 1 is a sulfonium ylide, and the sequence depicted in Scheme 1 then corresponds to the Corey-Chaykovsky epoxidation.^{13,14}

In previous work, we have determined the nucleophile-specific reactivity parameters for acceptor-substituted sulfonium ylides¹⁵ and for arylsulfonyl-substituted chloromethyl anions.¹⁶ Since acceptor-substituted sulfonium ylides are not sufficiently nucleophilic to react with typical ketones, we have employed anions **2** (Scheme 2) as reference nucleophiles to quantify the electrophilicities of ketones.

3.2 Results

Product study. The reactions of the ketones **1a–l** with the carbanions **2a,b** in anhydrous DMSO proceeded smoothly at room temperature (Scheme 2) and gave the epoxides **3** in good yields. The asymmetric ketones **1i–l** generally reacted with low diastereoselectivity. Only in the reaction of **1l** with **2b**, the formation of the diastereomer with ArSO₂ and CF₃ trans to each other is highly preferred (d.e. 88%) (Scheme 2). The different stereoselectivity of **2a** and **2b** in reactions with **1l** has been observed in numerous experiments where **1l** was used as trapping reagent in crossover experiments (see below). As shown in the Experimental Section of this chapter, **2a** always gave 2/1 mixtures of two diastereomers, while **2b** gave one diastereomer almost exclusively, possibly because **1l** reacts with **2a**, but not with **2b**, under diffusion control.¹⁷

Scheme 2. Reactions of Carbanions **2** with Ketones **1** and Corresponding Gross Second-Order Rate Constants k_2^{exp}

Ketones 1		X	k_2^{exp} ($\text{M}^{-1} \text{s}^{-1}$) ^b	Oxiranes 3 (yield)
	1a $n = 1$	2b CN	7.05×10^3	3ab (80%) ^c
	1b $n = 2$	2a H		3ba (87%) ^d
		2b CN	1.31×10^2	3bb (73%) ^d
	1c $n = 3$	2a H	2.98×10^3	3ca (95%) ^c
		2b CN	2.61×10^2	3cb (75%) ^c
	1d $n = 4$	2a H	8.49×10^1	3da (90%) ^c
	1e X = NMe	2a H	1.77×10^4	3ea (90%) ^c
	1f X = O	2b CN	1.82×10^3	3eb (90%) ^c
		2b CN	7.62×10^3	3fb (70%) ^c
	1g X = S	2a H	very fast ^e	3ga (95%) ^c
		2b CN	1.81×10^4	3gb (85%) ^c
		2a H	2.12×10^4	3ha (80%) ^c
2b CN		3.00×10^3	3hb (75%) ^c	
	1i X = CH ₂	2a H	7.42×10^1	3ia (90%, rel-2S,3S/rel-2R,3S = 2.6) ^c
	1j X = S	2b CN	3.21×10^4	3jb (80%, rel-2S,3S/rel-2R,3S = 2.2) ^d
	1k X = O	2b CN	very fast ^e	3kb (89%, rel-2R,3R/rel-2R,3S = 2.3) ^c
	2a H	very fast ^e	3la (90%, rel-2R,3R/rel-2R,3S = 2.0) ^c	
	2b CN	very fast ^e	3lb (80%, rel-2S,3S/rel-2R,3S > 15) ^c	

^a Counterion: K⁺ for kinetics, Na⁺ for product studies. ^b Carbanions **2a,b** generated by treatment of (**2a,b**)-H with *t*-BuOK, as described in the section Kinetic Investigations. ^c Isolated yield obtained after chromatographic purification. ^d Yield determined by ¹H NMR spectroscopy using *m*-xylene as internal standard. ^e Too fast to be measured by the stopped-flow technique.

Kinetic investigations. All kinetic investigations were performed in anhydrous DMSO solution at 20 °C by following the disappearance of the UV/Vis absorptions of the carbanions **2a** (320 nm) or **2b** (405 nm) under pseudo-first-order conditions ($[\mathbf{1}]_0/[\mathbf{2}]_0 > 10$). As the carbanions **2a,b** decompose on the minute time-scale at 20 °C (depending on the way of preparation), they were generated by treatment of their conjugate CH acids with 1.00–1.05 equiv of *t*-BuOK in dry THF at –78 °C. Small amounts of these solutions were dissolved in DMSO at 20 °C immediately before the ketones **1** were added. The first-order rate constants k_{obs} were obtained by least-squares fitting of the exponential function $A = A_0 \exp(-k_{\text{obs}}t) + C$ to the observed time-dependent absorbances A of **2** (Figure 1a). The slopes of the linear correlations between k_{obs} and the different concentrations of **1a–j** (Figure 1b) correspond to the second-order rate constants k_2^{exp} listed in Scheme 2.

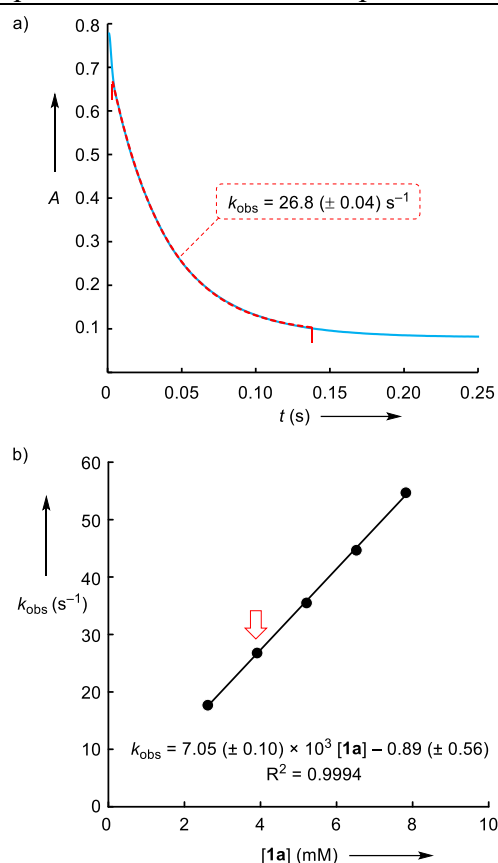


Figure 1. a) Monoexponential decay of the absorbance A of **2b** (at 405 nm) during the reaction of **1a** ($3.91 \times 10^{-3} \text{ mol L}^{-1}$) with **2b** ($2.50 \times 10^{-4} \text{ mol L}^{-1}$) in DMSO at 20 °C (the remaining absorbance is due to products generated by degradation of carbanion **2b**). b) Plot of k_{obs} for the reaction of **1a** with **2b** versus the concentration of **1a**.

Table 1 shows the role of counterions on the reaction kinetics. Neither addition of 18-crown-6 ether to the potassium salts of **2a** or **2b**, nor exchange of t -BuOK by Schwesinger's base P₄- t Bu¹⁸ for the generation of **2b** from its conjugate acid had a significant effect on the second-order rate constants k_2^{exp} .

Table 1. Second-Order Rate Constants k_2^{exp} (in $\text{M}^{-1} \text{ s}^{-1}$)^a for the Reactions of the Ketones **1** with Carbanions **2** under Various Conditions

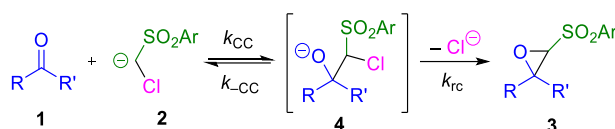
Ketone	Nucleophile	$k_2^{\text{exp } a}$	$k_2^{\text{exp}}(18\text{-crown-6})^b$	$k_2^{\text{exp}}(\text{P}_4\text{-}t\text{Bu})$
1e	2a	$1.77 (\pm 0.13) \times 10^4$	$1.79 (\pm 0.11) \times 10^4$	-
1f	2b	$7.62 (\pm 0.35) \times 10^3$	$7.65 (\pm 0.47) \times 10^3$	-
1g	2b	$1.81 (\pm 0.07) \times 10^4$	$1.71 (\pm 0.04) \times 10^4$	$1.66 (\pm 0.05) \times 10^4$
1j	2b	$3.21 (\pm 0.55) \times 10^4$	$3.59 (\pm 0.33) \times 10^4$	-

^a Data from Scheme 2. ^b 18-Crown-6 (2.0 to 2.5 equiv) was added to the potassium salts of **2a,b**.

Determination of the rate-limiting step

As shown in Scheme 3, nucleophilic attack of **2** at the ketone **1** yields the intermediate alkoxide anion **4**, which either cyclizes with formation of the epoxide **3** or undergoes retroaddition with regeneration of ketone **1** and carbanion **2**.

Scheme 3. Mechanism of the Reactions of Arylsulfonyl-Substituted Chloromethyl Anions with Ketones



The time-dependent concentrations of **2**, **4**, and **3** can be expressed by equations 2–4.

$$d[\mathbf{2}]/dt = -k_{CC}[\mathbf{1}][\mathbf{2}] + k_{-CC}[\mathbf{4}] \quad (2)$$

$$d[\mathbf{4}]/dt = k_{CC}[\mathbf{1}][\mathbf{2}] - k_{-CC}[\mathbf{4}] - k_{rc}[\mathbf{4}] \quad (3)$$

$$d[\mathbf{3}]/dt = k_{rc}[\mathbf{4}] \quad (4)$$

As the intermediate β -chloro-alkoxide anion **4** is formed as a short-lived species, the Bodenstein approximation holds ($d[\mathbf{4}]/dt = 0$), and the concentration of **4** is given by equation 5. Substitution into equation 4 yields equation 6, and k_2^{exp} is a function of k_{CC} , k_{-CC} , and k_{rc} as shown by equation 7.

$$[\mathbf{4}] = k_{CC}[\mathbf{1}][\mathbf{2}]/(k_{-CC} + k_{rc}) \quad (5)$$

$$\Rightarrow d[\mathbf{3}]/dt = -d[\mathbf{2}]/dt = k_{CC}k_{rc}[\mathbf{1}][\mathbf{2}]/(k_{-CC} + k_{rc}) \quad (6)$$

$$\Rightarrow k_2^{\text{exp}} = k_{CC}/(k_{-CC}/k_{rc} + 1) \quad (7)$$

According to equation 7, the rate of the attack of **2** at the carbonyl group (k_{CC}) can be derived from the measured rate constant k_2^{exp} (Scheme 2) if the ratio k_{-CC}/k_{rc} is known. In order to determine k_{-CC}/k_{rc} , we have developed an independent access to the intermediate **4**.

Synthesis of the halohydrins 4-H. Whereas treatment of **2-H** with base in the presence of ketones **1** at ambient temperature led to the formation of the epoxides **3** (Scheme 2), the reactions of **2a-H** with BuLi or of **2b-H** with lithium diisopropylamide (LDA) in THF at -78°C , followed by addition of the ketones **1a-j**, and subsequent acidification at low temperature yielded the halohydrins **4-H** in good yields (Scheme 4).¹⁹ In the case of the acyclic ketones **1i** and **1j**, two diastereomeric compounds were formed, which were separated by column chromatography on silica gel and fully characterized. The structure of **4ca-H** was confirmed

Chapter 3: Kinetics and mechanism of oxirane-formation by Darzens condensation of ketones: quantification of the electrophilicities of ketones
by single-crystal X-ray crystallography and showed a conformer with chlorine *gauche* to the hydroxyl group (Figure 2).

Scheme 4. Synthesis of the Halohydrins **4-H**

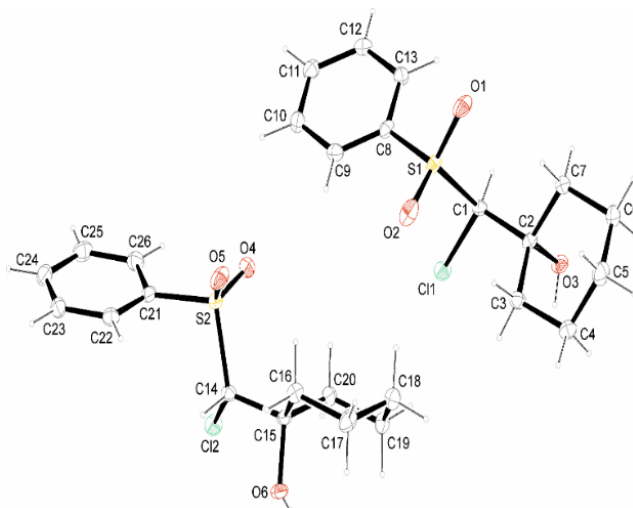
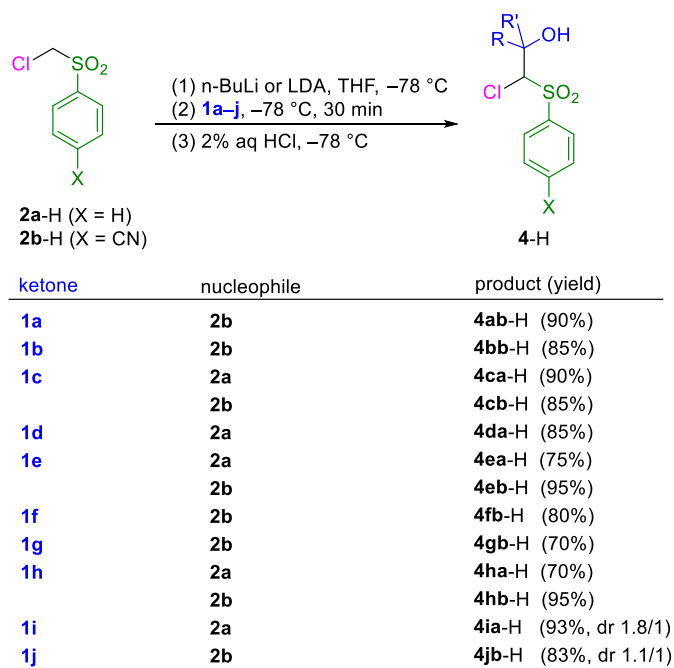


Figure 2. ORTEP drawing of the crystal structure of **4ca-H** (the ellipsoid probability level is 50%)

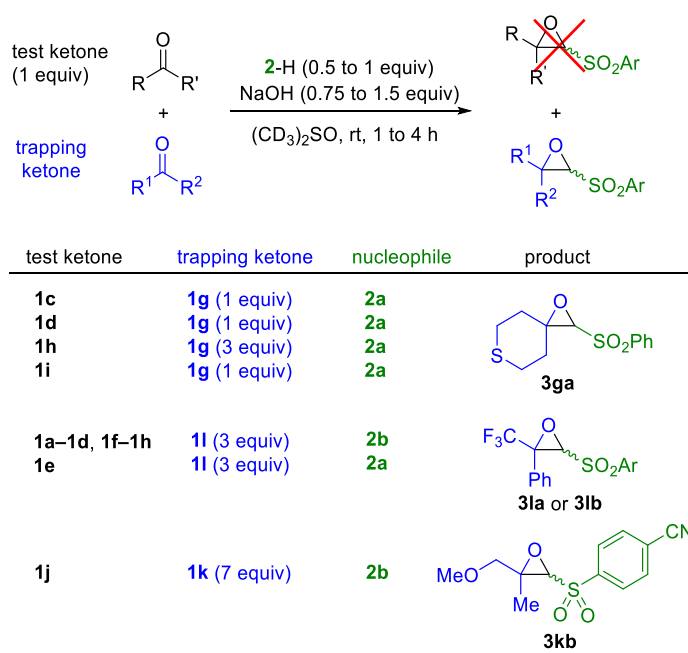
Examination of the reversibility of the attack of **2 at the ketones **1**.** In order to examine whether the intermediates **4**, generated by treatment of the halohydrins **4-H** with base, undergo ring closure with formation of **3** (k_{rc} , Scheme 3) or retroaddition with regeneration of **1** and **2** (k_{cc} , Scheme 3), it was necessary to find a trapping reagent, which rapidly intercepts

2 after its generation from **4**. In view of their high reaction rates (Scheme 2), ketones **1g**, **1j**, **1k**, and **1l** were considered to be suitable trapping agents. Ketone **1j** was then eliminated from this series because the resulting oxirane **3jb** turned out not to be stable at 20 °C.

When 1/1 mixtures of **1g** on one side, and of **1c**, **1d**, or **1i** on the other, were combined with 0.5 equiv of the carbanion **2a**, the oxiranes derived from **1g** (i.e. **3ga**) were formed exclusively (Scheme 5). Since **1g** is only 6-times more reactive than **1h**, 3 equiv of **1g** were employed to obtain **3ga** exclusively from a mixture of **1h** and **1g**.

The oxiranes **3la** and **3lb** were the only products obtained from the reactions of 3/1 mixtures of **1l** and **1a–h** with **2** (1 equiv with respect to **1a–h**). Since the product obtained by treatment of a mixture of **1j** and **1l** with **2b** was difficult to analyze, **1k** was used as a trapping agent, and treatment of a 7/1 mixture of **1k** and **1j** with 1 equiv of **2b** gave the oxirane **3kb** exclusively.

Scheme 5. Competition Reactions to Examine the Suitability of Ketones **1g,k,l** as Trapping Agents

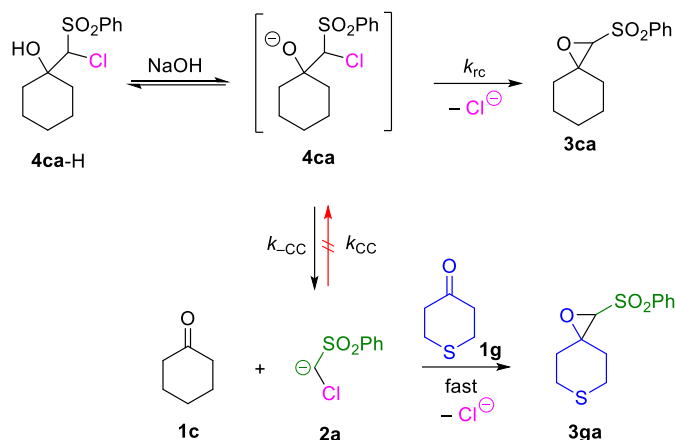


The principle of the crossover experiments is illustrated in Scheme 6. When the independently synthesized halohydrin **4ca-H** was treated with NaOH in the presence of the highly reactive ketone **1g**, the generated intermediate **4ca** has the choice of either undergoing ring closure with formation of the epoxide **3ca** or retroaddition with regeneration of **1c** and **2a**. As **1g** is considerably more reactive and present in higher concentration than **1c**, any regenerated

Chapter 3: Kinetics and mechanism of oxirane-formation by Darzens condensation of ketones: quantification of the electrophilicities of ketones

carbanion **2a** will exclusively be converted into the crossover product **3ga**, and the ratio $[3ga]/[3ca]$ equals the ratio k_{cc}/k_{rc} .

Scheme 6. Crossover Reaction of the Cyclohexanone Adduct **4ca-H**



Scheme 7. Crossover Reactions of **4-H**

entry	halohydrin	trapping ketone	$P_{cc}/P_{rc} = k_{cc}/k_{rc}$ ^a
1	4ab-H	1l (4 equiv)	0.89
2	4bb-H	1l (4 equiv)	0.63
3	4ca-H	1g (3 equiv) ^b	0.60
4	4cb-H	1l (4 equiv) ^b	0.86
5	4da-H	1g (3 equiv) ^b	3.5
6		1g (3 equiv) ^c	3.3
7		1l (3 equiv)	4.1
8	4ea-H	1l (4 equiv)	0.37
9		1l (4 equiv) ^c	0.29
10	4eb-H	1l (4 equiv)	0.33
11	4fb-H	1l (4 equiv)	0.13
12	4gb-H	1l (4 equiv)	0.57
13	4ha-H	1g (4 equiv)	0.19
14		1l (4 equiv)	0.24
15	4hb-H	1l (4 equiv)	0.21
16	4ia'-H	1g (3 equiv) ^b	2.2
17	4ia''-H	1g (3 equiv)	6.9
18	4jb'-H	1k (8 equiv)	2.2
19	4jb''-H	1k (8 equiv)	5.1

^a Determined by ¹H NMR spectroscopic analysis of the crude product. ^b Product yields determined by using 1,3,5-trimethoxybenzene as internal standard (Supporting Information). ^c KOH was used as base instead of NaOH.

Scheme 7 shows that in all crossover experiments at least 3 equiv of trapping agents were employed to ensure that they will quantitatively intercept the regenerated carbanions **2**. In Scheme 7 one can furthermore see that in most cases investigated, ring closure (k_{rc}) is up to 6 times faster than retroaddition. Entries 5–7 show, however, that the intermediates generated

from cycloheptanone (**1d**) undergo retroaddition 3–4 times faster than ring closure. Comparison of entry 5 with 7 and of entry 13 with 14 indicates that almost the same $k_{\text{CC}}/k_{\text{rc}}$ ratio is obtained with different trapping agents and entries 5/6 and 8/9 show that the nature of the counterion (K^+ vs Na^+) has only a small influence on this ratio. The similarity of $k_{\text{CC}}/k_{\text{rc}}$ in entries 3/4, 8/10, and 13/15 implies that the ratio retroaddition vs ring closure is almost independent of the substituents at the arylsulfonyl groups. Entries 16/17 as well as 18/19 show that the two diastereomeric halohydrins obtained from the asymmetric ketones **1i** and **1j** react with significantly different $k_{\text{CC}}/k_{\text{rc}}$ ratios.

Table 2. Determination of Second-Order Rate Constants k_{CC} from Measured Rate Constants k_2^{exp} and Ratios $k_{\text{CC}}/k_{\text{rc}}$

Ketone	Nucleophile	$k_2^{\text{exp}} (\text{M}^{-1} \text{s}^{-1})^a$	$(k_{\text{CC}}/k_{\text{rc}} + 1)^b$	$k_{\text{CC}} (\text{M}^{-1} \text{s}^{-1})$	E	$k^{\text{calc}}/k_{\text{CC}}$
1a	2b	7.05×10^3	1.89	1.33×10^4	−17.5	identical
1b	2b	1.31×10^2	1.63	2.14×10^2	−21.0	identical
1c	2a	2.98×10^3	1.60	4.77×10^3	−19.9 ^c	0.69
	2b	2.61×10^2	1.86	4.85×10^2		1.6
1d	2a	8.49×10^1	4.5	3.8×10^2	−22.1	identical
1e	2a	1.77×10^4	1.37	2.42×10^4	−18.4 ^c	0.58
	2b	1.82×10^3	1.33	2.42×10^3		1.9
1f	2b	7.62×10^3	1.13	8.61×10^3	−17.9	identical
1g	2b	1.81×10^4	1.57	2.84×10^4	−16.9	identical
1h	2a	2.12×10^4	1.19	2.52×10^4	−18.2 ^c	0.67
	2b	3.00×10^3	1.21	3.63×10^3		1.6
1i	2a	7.42×10^1	3.2 ^d	3.3×10^2 ^e	−22.3	identical
			7.9 ^d			
1j	2b	3.21×10^4	3.2 ^d	1.3×10^5 ^e	−15.6	identical
			6.1 ^d			identical

^a From Scheme 2. ^b From Scheme 7. ^c Calculated by averaging the individual E parameters. ^d Ratios ($k_{\text{CC}}/k_{\text{rc}}$) for the individual halohydrin diastereoisomers. ^e $k_{\text{CC}} = k'_{\text{CC}} + k''_{\text{CC}}$ (see text for calculation).

Combination of the $k_{\text{CC}}/k_{\text{rc}}$ ratios from Scheme 7 with k_2^{exp} from Scheme 2 according to equation 7 yields the rate constants for nucleophilic attack of **2** at the ketones **1** (k_{CC}), which are listed in Table 2. While this procedure is straightforward for the reactions with symmetrical ketones, the situation is more complex for unsymmetrical ketones because their

Chapter 3: Kinetics and mechanism of oxirane-formation by Darzens condensation of ketones: quantification of the electrophilicities of ketones

reactions with the carbanions **2** yield mixtures of diastereomeric halohydrins **4**-H, as specified for **1i** and **1j** in the last two entries of Table 2.

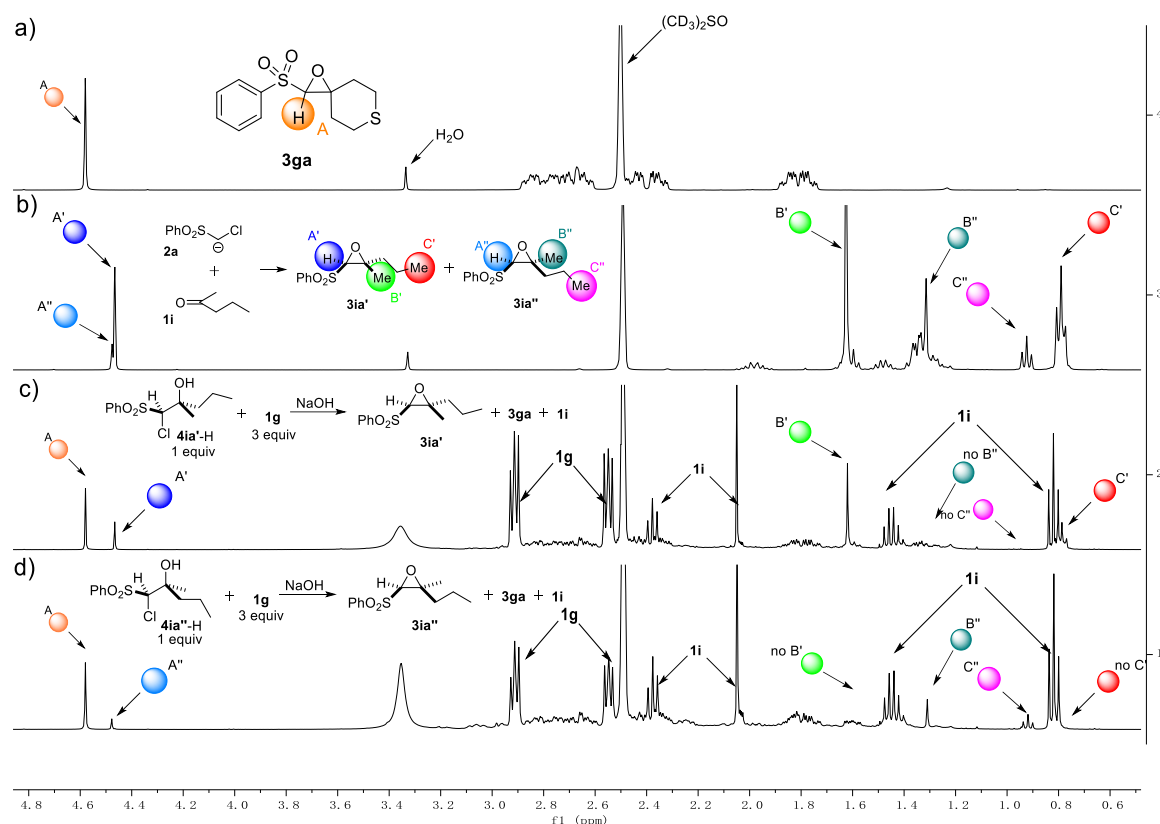


Figure 3. Examination of the stereospecificity of ring closure of the diastereomeric halohydrins **4ia'**-H and **4ia''**-H by ^1H NMR spectroscopy: a) Independently synthesized trapping product of regenerated **2a**. b) Mixture of **3ia'** and **3ia''** obtained from the reaction of **2a** with **1i**. c) Exclusive formation of **3ia'** and **3ga** ($1/2.2 = k'_{\text{rc}}/k'_{\text{-CC}}$) by treatment of **4ia'**-H with NaOH in the presence of **1g**. d) Exclusive formation of **3ia''** and **3ga** ($1/6.9 = k''_{\text{rc}}/k''_{\text{-CC}}$) by treatment of **4ia''**-H with NaOH in the presence of **1g**.

The stereospecificity of ring closure has exemplarily been studied for the reaction of **2a** with pentan-2-one (**1i**). The diastereomeric halohydrins **4ia'**-H and **4ia''**-H either undergo stereospecific ring closure with formation of epoxides or retroaddition with regeneration of **1i** and **2a**. Figure 3a shows the ^1H NMR spectrum of **3ga**, the product formed by trapping the regenerated carbanion **2a** with the ketone **1g**. Treatment of ketone **1i** with anion **2a** yielded a mixture of the diastereomeric epoxides **3ia'** and **3ia''** (Figure 3b). Since the ring protons A' and A'' of the epoxides **3ia'** and **3ia''** have similar chemical shifts, their ratio was derived from the ^1H NMR signals of the methyl groups B'/B'' and C'/C''. NOE experiments show that the methyl resonances at lower field (B' and C'') arise from the groups *cis* to the phenylsulfonyl substituent.²⁰ Figures 3c and 3d reveal that the epoxides **3ia'** and **3ia''** are

formed stereospecifically from the diastereomeric halohydrins **4ia'**-H and **4ia''**-H, respectively. When **4ia'**-H is treated with NaOH in the presence of **1g**, epoxides **3ia'** and **3ga** are formed in the ratio 1/2.2, as derived from the integrals of protons A' and A in Figure 3c. Since there are no peaks at δ 1.32 and 0.93, the chemical shifts of the methyl protons (B'' and C'') of the diastereomer **3ia''**, we can conclude that **4ia'** either cyclizes with formation of **3ia'** or fragments with formation of **1i** and **2a**, the latter of which is subsequently trapped by **1g** to give **3ga**.

Analogously, treatment of the other diastereomer (**4ia''**-H) with NaOH in the presence of **1g** yields the epoxides **3ia''** and **3ga** in a ratio of 1/6.9 (from integrals A'' and A, Figure 3d). The stereospecificity of this cyclization, i.e., the exclusive formation of **3ia''** from **4ia''**-H can be derived from the absence of **3ia'** in the product mixture, which would be detectable by a ^1H NMR signal for the methyl group B' at δ 1.63 and less clearly by the methyl triplet at δ 0.80 for C'.

With the product ratio **3ia'**/**3ia''** = 2.6 given in Scheme 2 we can split the measured gross second-order rate constant $k_2^{\text{exp}} = 74.2 \text{ M}^{-1} \text{ s}^{-1}$ for the reaction of **1i** with **2a** (Scheme 2) into the partial rate constants $k_2'^{(\text{exp})} = 53.6 \text{ M}^{-1} \text{ s}^{-1}$ and $k_2''^{(\text{exp})} = 20.6 \text{ M}^{-1} \text{ s}^{-1}$ for the formation of **3ia'** and **3ia''**, respectively. The ratio of these partial rate constants corresponds to the observed product ratio (equation 8) given in Scheme 2, and their sum corresponds to the measured rate constants (k_2^{exp} in Scheme 2, equation 9).

$$k_2'^{(\text{exp})}/k_2''^{(\text{exp})} = 2.6 \quad (8)$$

$$k_2'^{(\text{exp})} + k_2''^{(\text{exp})} = k_2^{\text{exp}} = 74.2 \text{ M}^{-1} \text{ s}^{-1} \quad (9)$$

Application of equation 7 to the two parallel reactions with $k'_{\text{-CC}}/k'_{\text{rc}} = 2.2$ (Figure 3c and Scheme 7, entry 16) and $k''_{\text{-CC}}/k''_{\text{rc}} = 6.9$ (Figure 3d and Scheme 7, entry 17) we obtain $k'_{\text{CC}} = (2.2 + 1) \times 53.6 \text{ M}^{-1} \text{ s}^{-1} = 1.7 \times 10^2 \text{ M}^{-1} \text{ s}^{-1}$ and $k''_{\text{CC}} = (6.9 + 1) \times 20.6 \text{ M}^{-1} \text{ s}^{-1} = 1.6 \times 10^2 \text{ M}^{-1} \text{ s}^{-1}$, i.e., both halohydrins are formed with similar rates, and the stereoselectivity originates from the different rates of cyclization as illustrated in Figure 4. In contrast, in THF at -78°C **4ia'**-Li is formed 1.8 times faster than **4ia''**-Li (Scheme 4).

An analogous calculation gave $k'_{\text{CC}} = 7.1 \times 10^4 \text{ M}^{-1} \text{ s}^{-1}$ and $k''_{\text{CC}} = 6.1 \times 10^4 \text{ M}^{-1} \text{ s}^{-1}$ for the reaction of **2b** with the unsymmetrical ketone **1j**.

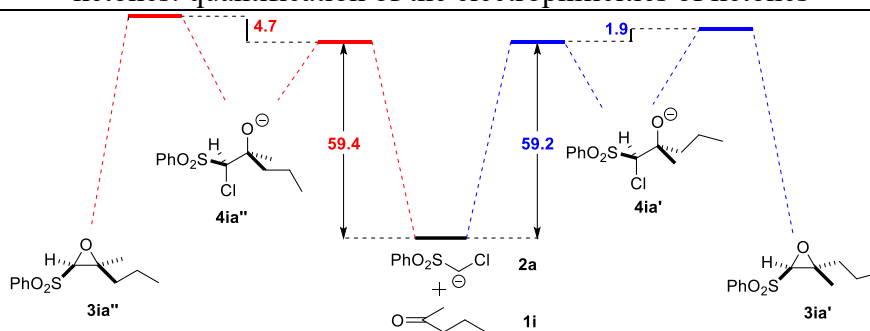
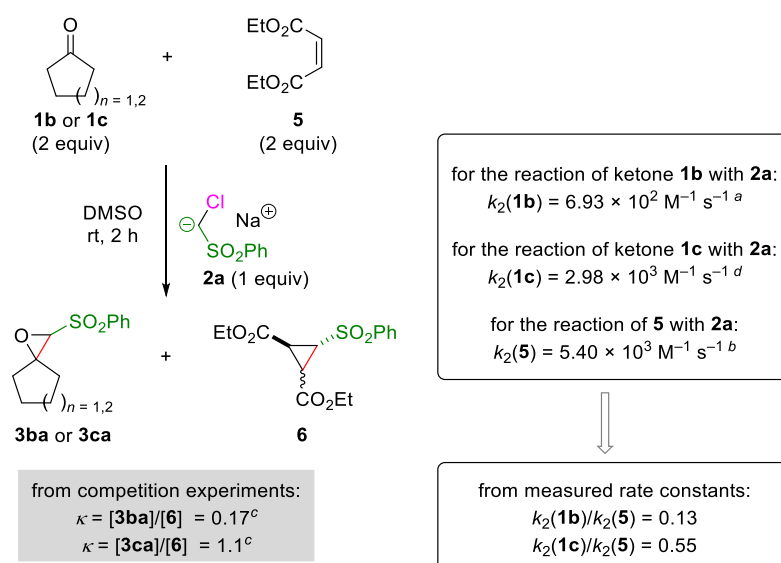


Figure 4. Gibbs energy profile (kJ mol^{-1}) for the reaction of carbanion **2a** with pentan-2-one **1i** at 20 °C in DMSO derived from rate measurements (Scheme 2) and crossover experiments (Figure 3, Table 2)

Substitution of k_{CC} and the published parameters N and s_N for **2a,b** into equation 1 yielded the electrophilicity parameters E of the ketones **1**. In cases where the electrophilicity parameters E were derived from reactions with **2a** and **2b**, both rate constants should ideally give the same value of E . As this is not the case, the E values derived from different reactions were averaged and listed in Table 2. The last column of Table 2, which compares the rate constants calculated by equation 1 with the directly determined rate constants, shows that in this series, equation 1 reproduces the rate constants k_{CC} within a factor of two.

A confirmation for the ketone reactivities derived in this way was obtained by competition experiments. When a mixture of diethyl maleate (**5**) ($E = -19.49$) and cycloalkanone **1b** or **1c** was treated with **2a** (in situ generated from **2a-H** and NaOH), mixtures of the epoxides **3** and the cyclopropane **6** were obtained. Their ratio was determined by ^1H NMR spectroscopy and used to calculate the ratio $k_2^{\text{exp}}(\mathbf{1})/k_2^{\text{exp}}(\mathbf{5})$ given in Scheme 8. The ratios of direct rate measurements, $k_2(\mathbf{1})/k_2(\mathbf{5})$, agree with product ratios from competition experiments, $\kappa = [\mathbf{3}]/[\mathbf{6}]$, within a factor of two. This suggests that diethyl maleate (**5**) and cyclohexanone (**1c**) have similar electrophilicities E , one order of magnitude greater than the electrophilic reactivity of cyclopentanone (**1b**).

Scheme 8. Examination of the *E* Parameters of Ketones **1**



^a Equation 1 gives $k_{CC} = 1.13 \times 10^3 \text{ M}^{-1} \text{ s}^{-1}$, which was corrected for reversibility by applying equation 7 with $k_{-CC}/k_{rc} = 0.63$. ^b This work (Table S20, Supporting Information). ^c Calculation see Supporting Information. ^d From Scheme 2.

Intrinsic reaction pathway calculations. The mechanistic picture derived from the kinetic studies was subsequently complemented by reaction path calculations. Geometry optimizations and calculations of intrinsic reaction pathways (IRC) have been performed at the B3LYP²¹-D3²²/6-31+G(d,p)²³ level of theory in combination with the PCM²⁴ model for DMSO as the solvent and UA0 radii. Improved energies for ground and transition states have been calculated at the PCM(DMSO,UA0)/B2PLYP²⁵-D3/def2TZVPP²⁶ level. Combination of energies with thermochemical corrections obtained at a lower level then yields the reaction Gibbs energies reported in the Experimental Section of this chapter and summarized in Figures 5–7.

For the reaction of carbanion **2a** with cyclohexanone (**1c**) (a ketone of intermediate electrophilicity, $E = -19.9$) the Gibbs energy surface is shown in Figure 5. Two distinct pathways have been identified for the addition of anion **2a** to the C=O double bond in ketone **1c**, which differ by the relative orientation of the two reactants. The enlisted energies are those of the energetically best conformers for each pathway (for full details see Experimental Section of this chapter). The blue, energetically less favorable reaction pathway ($\Delta G^\ddagger = +61.5 \text{ kJ mol}^{-1}$) directly yields an adduct with the C-Cl bond *anti* to the C-O bond. Chloride expulsion through epoxide ring closure is possible from this adduct with a barrier of $+44.8 \text{ kJ mol}^{-1}$ (relative to separate reactants). A second, red reaction pathway ($\Delta G^\ddagger = +47.4 \text{ kJ mol}^{-1}$) leads to a primary adduct where the C-Cl bond assumes a *gauche* orientation relative to the C-

O bond. Epoxide ring closure from this adduct is not immediately possible, but requires rotation around the newly formed C-C bond such that the C-Cl and C-O bonds attain the *anti* orientation required for cyclization. The barrier for this rotation is higher ($\Delta G^\ddagger = +58.5$ kJ mol⁻¹ relative to separate reactants) than the barrier for the reversal to the separate reactants **2a** and **1c**. The comparable heights of the barriers for initial nucleophilic addition and conformational reorientation are in line with the results derived from the cross-over experiments with halohydrin **4ca-H** described in Scheme 7. Guided by the conformational analysis of halohydrin **4ca-H** and its deprotonated form **4ca**, we assume that **4ca-H** exists as a mixture of conformers in solution, from which only that with the C-Cl and C-O bonds in *gauche* conformation had crystallized (see Figure 2 and Figure S15). Deprotonation of **4ca-H** will give both adduct conformers shown in Figure 5. While the adduct **4ca** with *gauche* C-Cl and C-O bonds will revert back to reactants, the conformer with *anti* C-Cl/C-O orientation will cyclize to epoxide **3ca**.

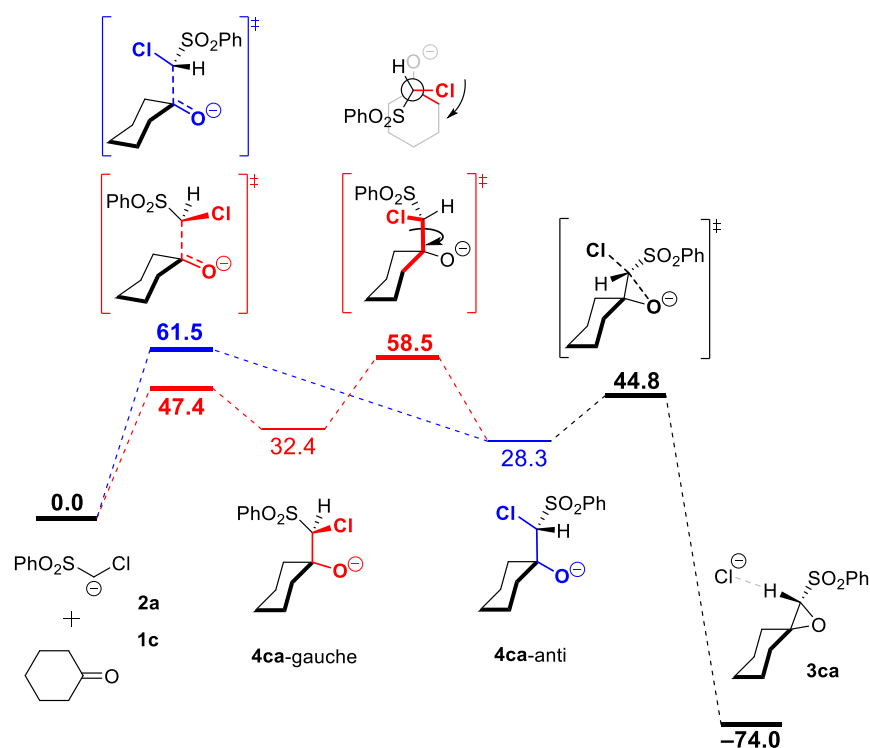


Figure 5. Gibbs energy surface (25 °C) for the reaction of **1c** with **2a** [at PCM(DMSO,UA0)/B2PLYP-D3/def2TZVPP//PCM(DMSO,UA0)/B3LYP-D3/6-31+G(d,p) level, in kJ mol⁻¹].

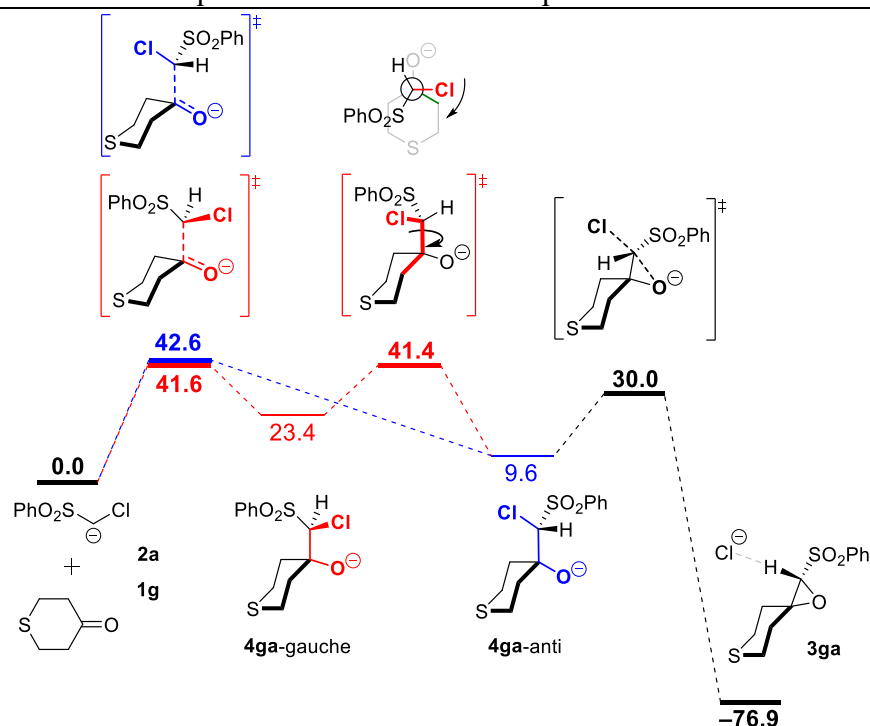


Figure 6. Gibbs energy surface (25 °C) for the reaction of **1g** with **2a** [at PCM(DMSO,UA0)/B2PLYP-D3/def2TZVPP//PCM(DMSO,UA0)/B3LYP-D3/6-31+G(d,p) level, in kJ mol⁻¹].

The reaction of anion **2a** with the more reactive ketone **1g** ($E = -16.9$) has been studied analogously. The resulting Gibbs energy surface in Figure 6 shows that the nucleophilic addition can also lead to intermediates **4ga** with C-Cl/C-O *gauche* or *anti* orientation, and the rotational barrier for their interconversion ($\Delta G^\ddagger = +41.4$ kJ mol⁻¹ relative to separate reactants) is again comparable to the barriers of the reverse reaction. The barrier for epoxide ring closure is, in comparison, lower at $\Delta G^\ddagger = +30.0$ kJ mol⁻¹, which again implies that adducts with C-Cl/C-O *anti* orientation will move forward to epoxide product rather than revert to separate reactants. In agreement with the larger E value of ketone **1g** as compared to **1c** (-16.9 vs. -19.9) the calculated overall Gibbs energy barrier for reaction with anion **2a** is much lower for **1g** than for **1c** ($+41.6$ vs. $+58.5$ kJ mol⁻¹).

In order to test whether the mechanistic picture obtained for the ketone addition reaction is comparable to that for addition to electron-poor alkenes (Michael acceptors), the reaction of anion **2a** with dimethyl maleate (**5***), as a model for the experimentally studied diethyl maleate (**5**), was also treated computationally (Figure 7). While the same sequence of initial nucleophilic addition, *gauche/anti* reorientation, and ring closure was also found for this system, the relative barriers for the individual steps differ significantly from those found for

the ketones: While the barrier for the initial addition step ($\Delta G^\ddagger = +46.2 \text{ kJ mol}^{-1}$) is similar to that for ketone **1c** (in line with the kinetic measurements described above), the barriers for rotation and cyclopropane ring closure are much lower than the barrier for the reverse reaction. This implies that the initial addition step of anion **2a** to alkene **5*** is practically irreversible, irrespective of the *gauche*/*anti* orientation in the initial addition step.

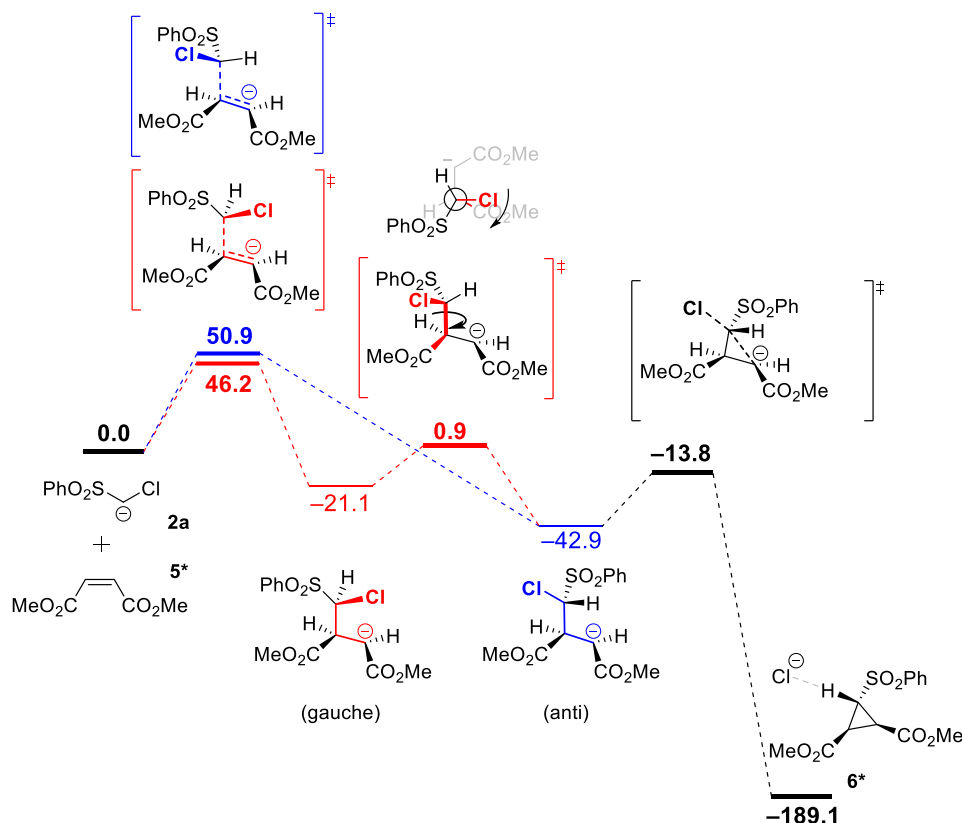
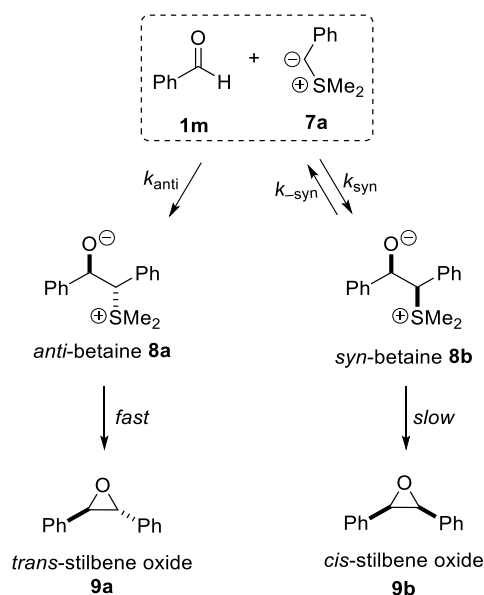


Figure 7. Gibbs energy surface (25 °C) for the reaction of **5*** with **2a** [PCM(DMSO,UA0)/B2PLYP-D3/def2TZVPP//PCM(DMSO,UA0)/B3LYP-D3/6-31+G(d,p) level, in kJ mol^{-1}]. Dimethyl maleate **5*** is used as model substrate for diethyl maleate **5**.

Electrophilicities of benzaldehydes

According to Table 2, most of the ketones characterized in this work have *E* parameters similar to that previously reported for benzaldehyde (**1m**, $E = -19.5$),² in contrast to common experience that aldehydes are generally more electrophilic than ordinary ketones. How can this discrepancy be explained?

Scheme 9. Aggarwal's Mechanism Accounting for the High *Trans* Selectivity in the Epoxidation Reaction of Benzaldehyde with Semistabilized Sulfur Ylide **7a**



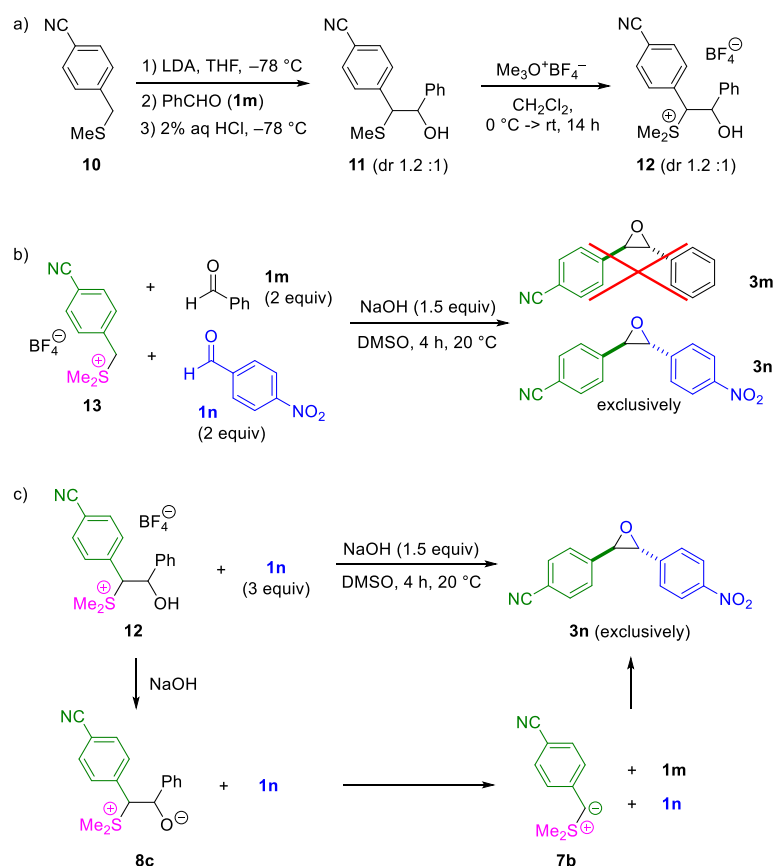
Based on Aggarwal's report that the independently synthesized *anti*-betaine **8a**, formed from sulfonium ylide **7a** and benzaldehyde (**1m**), does not undergo retroaddition but rapidly cyclizes with formation of *trans*-stilbene oxide **9a** (Scheme 9),^{3c} we had extrapolated that the same was true for the betaine generated from benzaldehyde **1m** and *p*-cyano-substituted sulfonium ylide **7b**.²

This conclusion was obviously incorrect as shown by the following experiments. Treatment of the benzylthioether **10** with LDA and benzaldehyde (**1m**) yielded the β -thio substituted alcohol **11**, which was converted into the sulfonium tetrafluoroborate **12** by treatment with trimethyloxonium tetrafluoroborate (Scheme 10a). As shown in Scheme 10b, the sulfonium ylide generated by treatment of the sulfonium ion **13** with NaOH in the presence of *p*-nitrobenzaldehyde (**1n**) and benzaldehyde (**1m**) reacts exclusively with the former to yield the epoxide **3n**. As expected, *p*-nitrobenzaldehyde (**1n**) is much more reactive than the parent benzaldehyde (**1m**).

The crossover experiment in Scheme 10c shows the exclusive formation of the epoxide **3n** when **12** was treated with base in the presence of *p*-nitrobenzaldehyde (**1n**). This observation implies that the betaine **8c**, which is formed by deprotonation of **12**, does not cyclize, but rather undergoes retroaddition with regeneration of benzaldehyde (**1m**) and the sulfonium ylide **7b**, which is quantitatively intercepted by *p*-nitrobenzaldehyde **1n**. The rate-determining step for the reaction of the sulfonium ylide **7b** with benzaldehyde (**1m**) thus is the cyclization and not the nucleophilic attack of the ylide at the carbonyl group, as assumed for the

derivation of the electrophilic reactivity of benzaldehyde (**1m**) in ref 2. The electrophilicity parameters of aldehydes reported in ref 2 thus do not refer to the initial attack of nucleophiles at the carbonyl group but describe the gross rate constants for the reactions of carbonyl groups with the sulfonium ylide **7b**.

Scheme 10. Synthesis of Sulfonium Tetrafluoroborate **12** and Crossover Experiment to Elucidate the Rate-Determining Step in the Epoxidation of Benzaldehyde with the Sulfonium Ylide **7b**

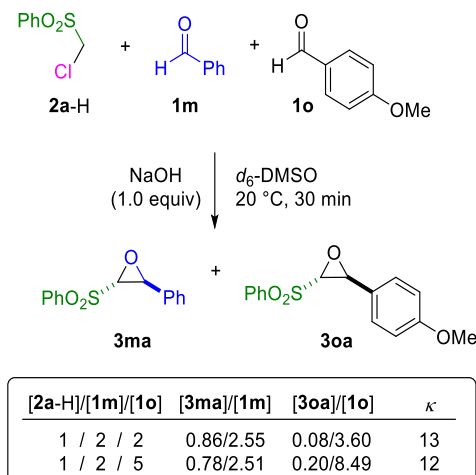


How can the rate of the initial nucleophilic attack at aldehydes be determined? Are the chloro-substituted carbanions **2a,b** suitable reference nucleophiles, because the corresponding intermediates cyclize with lower barriers than the intermediates formed from sulfur ylides? In line with the expected higher electrophilic reactivity of benzaldehyde **1m**, its reactions with the carbanions **2a,b** were found to be too fast for direct measurements with our stopped-flow techniques. We succeeded, however, to measure the rate of the reaction of **2b** with the less electrophilic *p*-methoxybenzaldehyde (**1o**) in the same way as described above for the corresponding reactions with ketones and obtained the second-order rate constant $k_2^{\text{exp}} = 2.69 \times 10^4\text{ M}^{-1}\text{ s}^{-1}$ which will be used in Table 3. Subsequently, the relative reactivities of

Chapter 3: Kinetics and mechanism of oxirane-formation by Darzens condensation of ketones: quantification of the electrophilicities of ketones

benzaldehyde (**1m**) and *p*-methoxybenzaldehyde (**1o**) towards **2a** were determined by the competition experiment illustrated in Scheme 11.²⁷

Scheme 11. Competition Experiments for Determining the Relative Reactivities of Benzaldehyde (**1m**) and *p*-Methoxybenzaldehyde (**1o**) toward **2a**



From the composition of the reaction mixtures given in Scheme 11, we derived the competition constant κ using equation 10,²⁸ which is applicable when the competing reagents are not used in high excess and the ratio of their concentrations changes during the reaction.

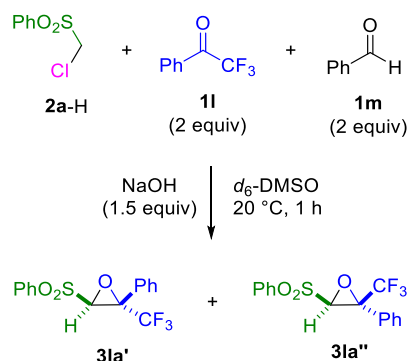
$$\kappa = \frac{k_2^{\text{exp}}(\mathbf{1m})}{k_2^{\text{exp}}(\mathbf{1o})} = \frac{\log\left(\frac{[\mathbf{1m}]_0}{[\mathbf{1m}]_t}\right)}{\log\left(\frac{[\mathbf{1o}]_0}{[\mathbf{1o}]_t}\right)} = \frac{\log\left(1 + \frac{[\mathbf{3ma}]_t}{[\mathbf{1m}]_t}\right)}{\log\left(1 + \frac{[\mathbf{3oa}]_t}{[\mathbf{1o}]_t}\right)} \quad (10)$$

From the directly measured rate constant for the reaction of **2b** with **1o** and the competition constant κ (Scheme 11) one can calculate the rate constant k_2^{exp} for the reaction of **2b** with benzaldehyde (**1m**) according to equation 11.

$$k_2^{\text{exp}}(\mathbf{1m}) = \kappa k_2^{\text{exp}}(\mathbf{1o}) \quad (11)$$

As described in Scheme 3 and equations 2–7 the rate constants k_2^{exp} thus obtained refer to the rates of the overall reactions. In order to derive the rate of attack of the anions **2** at the carbonyl groups of the aldehydes **1m** and **1o** (k_{CC}), we must know the degree of reversibility of the initial addition step, which again was determined by crossover experiments. For their design, it was necessary to identify trapping agents which can quantitatively intercept the carbanions **2** generated by reverse addition of the halohydrin anions. As shown in Scheme 12, the epoxides **3la'** and **3la''** are formed exclusively when a 1/1 mixture of benzaldehyde (**1m**) and trifluoroacetophenone (**1l**) is treated with 0.5 equiv of **2a**, indicating that the fluorinated ketone **1l** is much more electrophilic than benzaldehyde (**1m**).

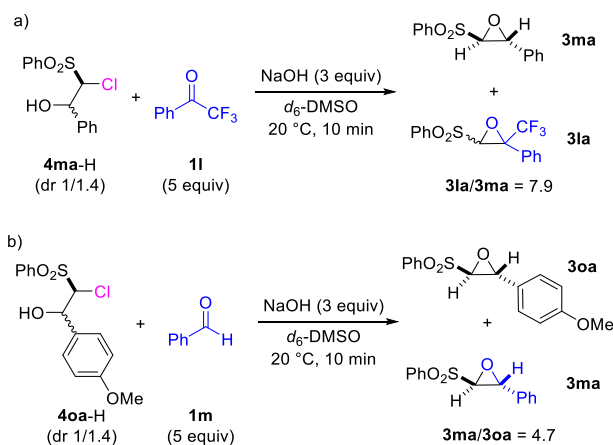
Scheme 12. Competition Experiment to Demonstrate the Much Higher Reactivity of Ketone **1l** Compared to Benzaldehyde (**1m**)



In analogy to the procedure described in Scheme 4, the chlorohydrins **4ma-H** and **4oa-H** (Scheme 13) were synthesized in THF at $-78\text{ }^{\circ}\text{C}$ by the reaction of **2a-Li** with the aldehydes **1m** and **1o**, respectively, and subsequent acidification. As illustrated in Scheme 13, treatment of a 1/5 mixture of **4ma-H** and **1l** gave the crossover product **3la** in addition to **3ma**, the cyclization product of **4ma**, in a ratio of 7.9/1. Since **1l** is much more electrophilic than **1m** (Scheme 12), we can conclude that **3ma** is exclusively formed by direct cyclization of the deprotonated chlorohydrin **4ma**, whereas the carbanion **2a**, which is formed by reversal of **4ma**, is quantitatively converted into **3la**. The ratio $[\mathbf{3la}]/[\mathbf{3ma}] = 7.9$ (Scheme 13a) thus reflects the ratio $k_{\text{CC}}/k_{\text{rc}}$ given in Table 3.

Since the competition experiment in Scheme 11 showed **1m** to be 12 times more reactive than **1o**, benzaldehyde **1m** could be used as a trapping reagent for the crossover experiment in Scheme 13b, and the ratio $[\mathbf{3ma}]/[\mathbf{3oa}] = 4.7$ (Scheme 13b) again reflects the ratio $k_{\text{CC}}/k_{\text{rc}}$ given in Table 3.

Scheme 13. Crossover Reactions of aldehydes **1m**, **1o**



Equation 7 was then used to calculate the rate constants k_{CC} for the nucleophilic attack of **2b** at the aldehydes **1o,m** from the gross rate constants k_2^{exp} listed in Table 3 and the k_{-CC}/k_{rc} ratios from Scheme 13. Substitution into equation 1 with the N and s_N parameters of **2b** eventually yielded the electrophilicity parameters E of the aldehydes **1m** and **1o** in the last column of Table 3. It should be admitted, however, that there are two uncertainties in this derivation. First, the mixtures of diastereomers of the chlorohydrins **4ma-H** and **4oa-H**, which are used for the crossover experiments in Scheme 13, are formed by the reactions with the lithiated nucleophiles **2a-Li** in THF at -78°C and may differ somewhat from the diastereomeric ratios of the halohydrins generated under the conditions of the kinetic experiments. Secondly, we had to use the k_{-CC}/k_{rc} ratios for the adducts of **2a** for the calculation of k_{CC} in Table 3 because the epoxides obtained from **2b** were not stable. The plausibility of this assumption is based on the comparison of entries 3/4, 8/10, and 13/15 in Scheme 7, which indicated that the ratio retroaddition vs ring closure (k_{-CC}/k_{rc}) is almost independent of the substituents at the arylsulfonyl groups.

Table 3. Derivation of the Rate Constants k_{CC} for Nucleophilic Attack of **2b** at the Aldehydes **1o** and **1m** and the Resulting E Parameters

Aldehyde	Nucleophile	k_2^{exp} ($\text{M}^{-1} \text{s}^{-1}$)	k_{-CC}/k_{rc}^a	k_{CC}^b ($\text{M}^{-1} \text{s}^{-1}$)	approx. E
1m	2b	3.36×10^5 ^c	7.9	3.0×10^6	-12.9
1o	2b	2.69×10^4 ^d	4.7	1.5×10^5	-15.4

^a From Scheme 13. ^b From equation 7. ^c From equation 11 using the averaged κ from Scheme 11, $k_2^{\text{exp}} = 12.5 \cdot (2.69 \times 10^4 \text{ M}^{-1} \text{s}^{-1})$. ^d Direct rate measurement.

These uncertainties prompted us to examine the E value for benzaldehyde thus derived by an independent experiment. Substitution of the E values for **1m** and **14** and of the N and s_N parameters for **2a** into equation 1 gives k_{CC} , the rate constant for the initial nucleophilic attack of **2a** at these electrophiles. Since the attack of **2a** at **1m** (in contrast to the attack at **14**) is reversible, k_{CC} was corrected by the splitting ratio k_{-CC}/k_{rc} according to equation 7 to obtain the overall rate constant k_2^{exp} for the formation of the epoxide **3ma**.

In the competition experiment described in Scheme 14, which compares the electrophilic reactivity of benzaldehyde (**1m**) with that of the N-tosyl-imine **14**, we observed the ratios $[\mathbf{3ma}]/[\mathbf{1m}] = 0.22/3.31$ and $[\mathbf{15}]/[\mathbf{14}] = 1.08/2.04$ from which the reactivity ratio $\kappa = k(\mathbf{14})/k(\mathbf{1m}) = 6.6$ was derived by equation 10 as summarized in Table 4. The fair agreement between the relative reactivities of **1m** and **14** and the rate constants calculated by equation 1 confirms the electrophilicity parameter of benzaldehyde (**1m**) derived above.

Scheme 14. Competition Experiment to Determine the Relative Reactivities of Benzaldehyde (**1m**) and Imine **14**

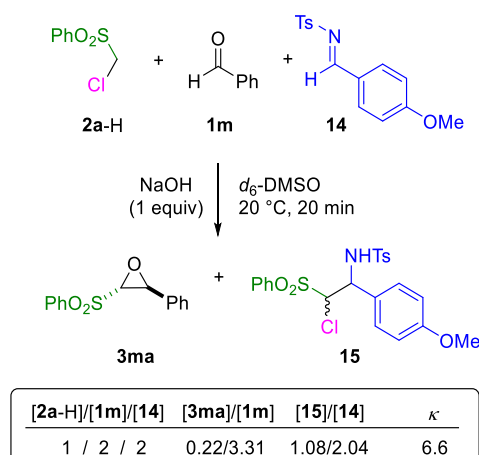


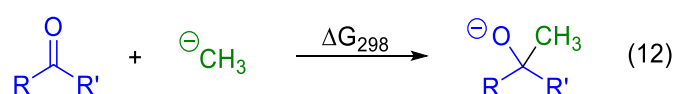
Table 4. Comparison of the Relative Reactivities of Benzaldehyde (**1m**) and Imine **14** Towards **2a** Derived from Rate Measurements and Competition Studies

electrophile	E	$k_{CC} (M^{-1} s^{-1})^a$	$k_2^{exp} (M^{-1} s^{-1})$	$k_{rel} (rates)$	$k_{rel} (competition)$
1m	-12.9	2.85×10^6	3.20×10^5 ^b	1	1
14	-13.05 ^c	2.47×10^6	2.47×10^6	7.7	6.6 ^d

^a From equation 1 with E from this table and $N = 28.27$ and $s_N = 0.42$ for **2a**. ^b Calculated with equation 7 using $k_{CC}/k_{rc} = 7.9$ from Table 3. ^c Ref 2. ^d From Scheme 14; for a competition experiment with $[2a-H]/[1m]/[14] = 1/5/2$ a $\kappa = 6.65$ was obtained (see Experimental Section of this chapter).

Correlation Analysis

In order to elucidate the origin of the corresponding electrophilic reactivities, we have determined various properties of the investigated carbonyl compounds by quantum chemical calculations (Table 5). As specified in Tables 5 and S25, the computational methods used in these calculations differ from those employed in the reaction path calculations (see above) in order to make them strictly comparable to our earlier work on nucleophilic additions to Michael acceptors and carbenium ions.²⁹



Methyl anion affinities (MAAs) have been calculated as the negative of the reaction Gibbs energies for the addition of methyl anion to ketones and aldehydes (equation 12). In addition, we calculated Parr electrophilicity indices ω (equation 13) for 12 carbonyl compounds,³⁰ from the chemical hardness η (equation 14) and the electronic chemical potential μ (equation 15). The values of η and μ have been calculated from the energies of the lowest unoccupied molecular orbital ($\varepsilon_{\text{LUMO}}$) and the highest occupied molecular orbital ($\varepsilon_{\text{HOMO}}$), which were derived at gas phase B3LYP/6-31G(d,p) level. As in previous studies, the Parr electrophilicity indices are expressed in eV.

$$\omega = \mu^2/2\eta \quad (13)$$

$$\eta = (\varepsilon_{\text{LUMO}} - \varepsilon_{\text{HOMO}}) \quad (14)$$

$$\mu = \frac{1}{2}(\varepsilon_{\text{LUMO}} + \varepsilon_{\text{HOMO}}) \quad (15)$$

$$\omega_c = \omega f_c^+ \quad (16)$$

The local electrophilicity indices ω_c at the carbonyl carbon were calculated as the product of Parr's electrophilicity index ω with the nucleophilic Fukui function (f_k^+) according to equation 16. The Fukui function for nucleophilic attack is defined as the change of partial charge q at a certain atom k by adding an electron to the corresponding compound, that is $f_k^+ = q(k, N+1) - q(k, N)$ with N = total number of electrons.³¹

Table 5. Quantum Chemically Calculated Frontier Orbital Energies (Hartree), Global (ω) and Local (ω_C) Parr Electrophilicity Indices (in eV) as well as Methyl Anion Affinities (MAAs, in kJ mol⁻¹) of Ketones and Aldehydes

Electrophile	E^a	$\varepsilon_{\text{HOMO}}^b$	$\varepsilon_{\text{LUMO}}^b$	Global ω^b	Local ω_C^b	$\Delta G_{\text{gas}}(-\text{MAA})^c$	$\Delta G_{\text{sol-sp}}(-\text{MAA})^d$
1a	-17.5	-0.24245	-0.02117	1.07	0.16	-131.6	-8.0
1b	-21.0	-0.23597	-0.01449	0.96	0.15	-114.2	14.6
1c	-19.9	-0.23443	-0.01201	0.93	0.15	-126.7	11.7
1d	-22.1	-0.23483	-0.01104	0.92	0.14	-116.3	26.8
1e	-18.4	-0.22444	-0.01456	0.93	0.15	-136.2	2.9
1f	-17.9	-0.24378	-0.02071	1.07	0.18	-147.3	-1.4
1g	-16.9	-0.23250	-0.02310	1.06	0.19	-158.3	-4.1
1h	-18.2	-0.23481	-0.01233	0.93	0.15	-138.5	5.3
1i	-22.3	-0.24272	-0.00948	0.93	0.15	-114.3	16.4
1j	-15.6	-0.22563	-0.02762	1.10	0.14	-144.4	-5.9
1m	\approx -12.9	-0.25521	-0.06342	1.80	0.22	-155.2	-27.8
1o	\approx -15.4	-0.23442	-0.05149	1.52	0.18	-143.7	-13.2

^a Empirical electrophilicity parameters from Tables 2 and 3, as defined in equation 1. ^b Calculated at B3LYP/6-31G(d,p) level in the gas phase. ^c Calculated at B3LYP/6-311+G(3df,2pd)³²//B3LYP/6-31G(d,p) level in the gas phase. ^d Based on methyl anion affinities (ΔG_{gas}), which were corrected for solvent effects by adding single point solvation energies calculated at B3LYP/6-31G(d,p) using the SMD³³ (solvent = DMSO) solvation model on gas phase optimized geometries at the same level.

Previously, good correlations between electrophilicities of benzhydrylium ions and their LUMO energies were reported by Liu^{34a} and Yu.^{34b} Figure 8 shows a moderate correlation between the electrophilicity parameters E of ketones and their LUMO energies in the gas phase. This correlation improves slightly when the correlation with LUMO energies in DMSO solution is considered (as depicted in Figure S29(B), Experimental Section of this chapter). Though the correlation between the electrophilicity parameters E and LUMO energies of Michael acceptors has been reported to be very poor,^{29a} Figure 8 shows that ketones are generally more electrophilic than Michael acceptors of equal LUMO energies.

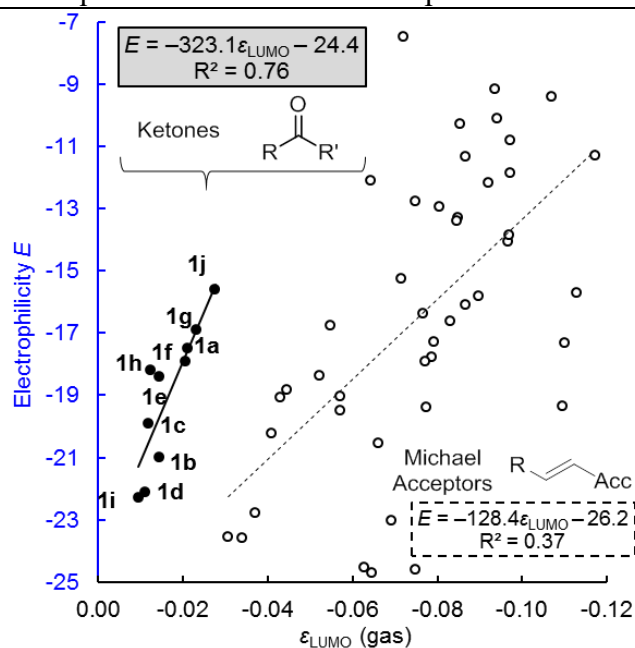


Figure 8. Correlation of the electrophilicities (E) of ketones with their gas phase lowest unoccupied molecular orbital energies (ϵ_{LUMO}) calculated at B3LYP/6-31G(d,p) level of theory compared with the corresponding correlation for Michael acceptors.

Whereas Figure 9 shows a moderate correlation between electrophilicities E and Parr's global electrophilicity index ω , a plot of E vs the local electrophilicity index ω_{β} (Figure S33A, Experimental Section of this chapter) has a correlation coefficient of $R^2 = 0.30$ (!), i.e., ω_{β} is inadequate to predict electrophilic reactivities of ketones.³⁵

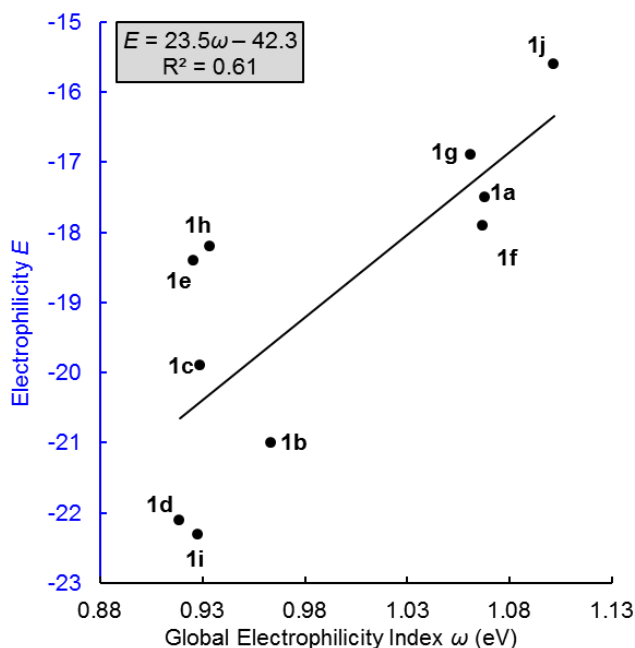


Figure 9. Correlation between electrophilicities (E) of ketones **1a–1j** and Parr's global electrophilicity index (ω) calculated at B3LYP/6-31G(d,p) level of theory.

As in our previous investigation of the electrophilic reactivities of Michael acceptors,^{29a} the electrophilicities E of the ketones **1a–1j** correlate fairly with the calculated gas phase methyl anion affinities ($R^2 = 0.77$, Figure S17B, Experimental Section of this chapter),^{21,23,32,36} and this correlation improves further, when solvation is included in the calculated methyl anion affinities (Figure 10). Obviously, the solvation energy of the methyl anion is overestimated by this model, since negative MAAs were calculated for several additions. Though the data for the benzaldehydes **1m** and **1o** were not used for the correlation because of the uncertainty of the experimental E parameters, they also are on this best-fit line, thus justifying the approximations made for the derivation of their E parameters.

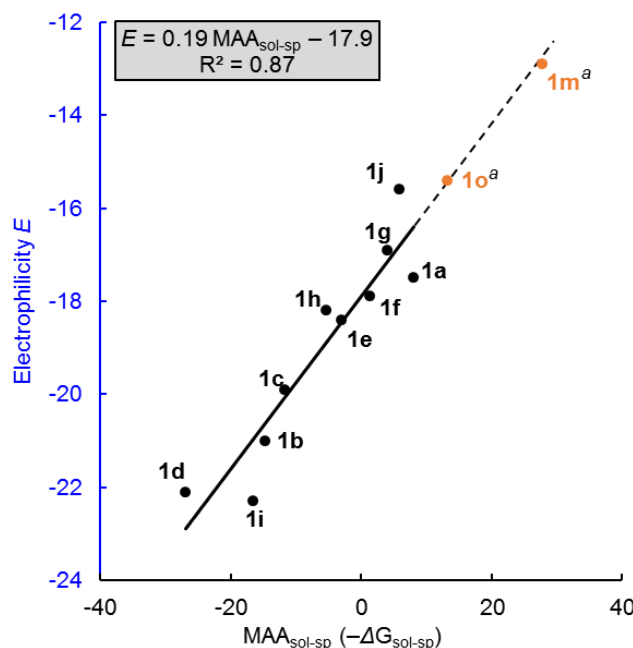


Figure 10. Correlation between electrophilicities (E) of ketones with their MAA_{sol-sp} values ($-\Delta G_{sol-sp}$, kJ mol^{-1}) calculated at SMD(DMSO)/B3LYP/6-311++G(3df,2pd)//B3LYP/6-31G(d,p) level of theory. ^a Not used for the construction of the correlation line.

When the plots of E vs MAA for carbonyl compounds and Michael acceptors are drawn in the same graph (Figure 11), one can clearly see two correlation lines, which differ in two aspects. First, the slope for the ketones is significantly larger than that for Michael acceptors. As pointed out previously, the slope of the Michael acceptor correlation implies that in reactions with a nucleophile of $s_N = 0.7$ (see equation 1) about 43 % of the differences of the Gibbs reaction energies are reflected in the Gibbs activation energies.^{29a} A significantly higher percentage (75 %) of the Gibbs reaction energies is mirrored by the activation energies of the additions of nucleophiles with the typical value $s_N = 0.7$ to carbonyl compounds.³⁷ Secondly, the different positions of the two correlation lines imply that carbonyl compounds are

significantly more electrophilic than Michael acceptors of equal thermodynamic driving force ($\Delta_r G^0$). In Marcus terminology^{38a-e} this means that Michael additions proceed with significantly higher reorganization energies than nucleophilic additions to carbonyl groups, which can be explained by the much greater movements of electrons and structural changes occurring in Michael additions (Scheme 15).^{38f}

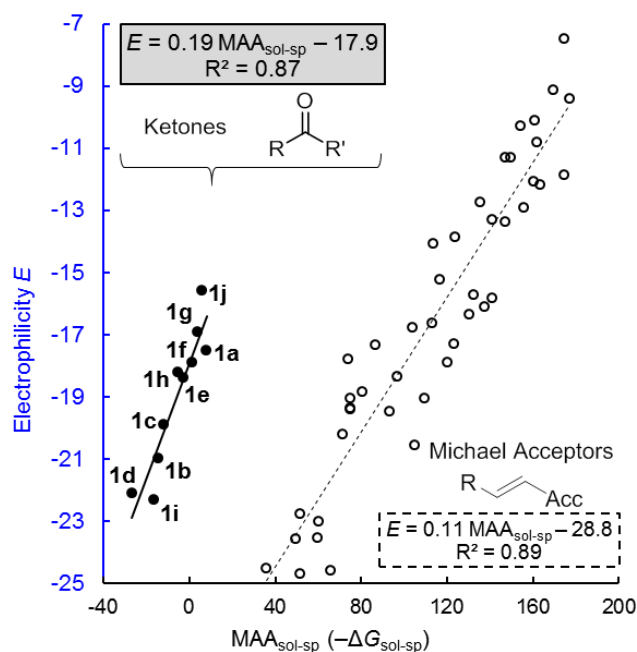
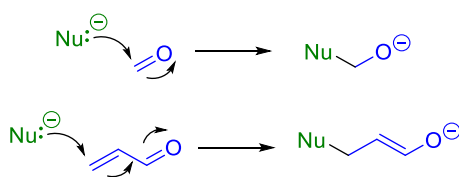


Figure 11. Correlation between the empirical electrophilicities (E , equation 1) and MAAs ($-\Delta G_{\text{sol-sp}}$, kJ mol^{-1}) values calculated at SMD(DMSO)/B3LYP/6-311++G(3df,2pd)//B3LYP/6-31G(d,p) level of theory for ketones and Michael acceptors.

Scheme 15. Less Movement of Electrons and Nuclei Required in Nucleophilic Additions to Carbonyl Groups than to Michael Acceptors



Structure Reactivity Relationships

As shown in Table 6, the reactivity order cyclobutanone (**1a**) > cyclohexanone (**1c**) > cyclopentanone (**1b**) > cycloheptanone (**1d**), which we found for reactions with carbanions **2a,b**, had previously been observed in reactions with other nucleophiles, though the relative reactivities of the different cycloalkanones depend on the reaction partner and conditions.³⁹ The uniformly higher electrophilic reactivity of cyclobutanone (**1a**) can partially be explained by the higher release of ring strain during conversion of the sp^2 carbon in the four-membered

ring into an sp^3 carbon. Table 5 shows, however, that the gas phase methyl anion affinity of **1a** is only 5 kJ mol⁻¹ higher than that of cyclohexanone (**1c**) indicating that release of strain can only account for part of the reactivity difference of **1a** and **1c**. Since the MAA of **1a** is almost 20 kJ mol⁻¹ higher than that of **1c** in DMSO solution, we must conclude that differences of solvation are the major reason for the higher reactivity of cyclobutanone (**1a**) toward **2b** in solution. Let us analyze the origin of the solvation effect in the following comparison of cyclohexanone with cyclopentanone.

H. C. Brown rationalized the 23 times faster reaction of NaBH₄ with cyclohexanone compared to cyclopentanone by a change of torsional strain: As the hybridization of the carbonyl carbon changes from sp^2 to sp^3 , the torsional strain increases in the 5-membered ring (eclipsed bonds), but decreases in the 6-membered ring because the equatorial hydrogens are nearly eclipsed with carbonyl oxygen in cyclohexanone and attain staggered arrangements in the chair conformation of cyclohexanol.⁴⁰ Since the opposite rehybridization takes place in the rate-determining step of S_N1 reactions of cycloalkyl halides, differences in torsional strain were analogously used to explain the much larger solvolysis rates of cyclopentyl halides compared to cyclohexyl halides.⁴⁰ We had already doubted that the change from C_{sp3} to C_{sp2} is the major contribution to this difference of the S_N1 reactivities because methylenecyclopentane was found to react 50 times faster with benzhydrylium ions than methylenecyclohexane though the rate-determining step does not involve rehybridization of a ring carbon.⁴¹

The 12.5 kJ mol⁻¹ higher gas phase methyl anion affinity of cyclohexanone (**1c**) compared to cyclopentanone (**1b**) in Table 5 supports the torsional strain argument. However, the difference between the MAAs of **1c** and **1b** shrinks to 2.9 kJ mol⁻¹ in DMSO solution. As discussed in detail in Figures S24 and S25, this change is due to the fact that the cyclohexanolate conformer with oxygen in axial position, which is most stable in the gas phase, is less efficiently solvated and becomes even less stable in DMSO solution than the conformer with equatorial oxygen. Thus, the overall poorer solvation of the cyclohexanolate ion accounts for the fact that the MAA of cyclohexanone, which is much higher than that of cyclopentanone in the gas phase, is only slightly higher in solution. The poor solvation of the cyclohexanolate anion with oxygen in axial position analogously accounts for the finding (Table 5) that the MAAs of cyclobutanone and cyclohexanone differ only slightly in the gas phase (5 kJ mol⁻¹) but strongly in solution (20 kJ mol⁻¹).

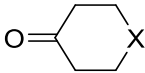
Table 6. Comparison of the Reactivities of the Cycloalkanones **1a–d** towards Different Nucleophiles.

	$k_{CC}(\mathbf{2b})^a$ ($M^{-1} s^{-1}$)	$k_2(NaBH_4)^b$ ($M^{-1} s^{-1}$)	$k_{rel}(\mathbf{2b})^a$	$k_{rel}(NaBH_4)^b$	$k_{rel}(Nu)^c$
1a	1.33×10^4	2.66×10^{-2}	27	1.6	1.2
1b	2.14×10^2	7.01×10^{-4}	0.44	0.044	0.066
1c	4.85×10^2	1.61×10^{-2}	1	1	1
1d	3.88×10^1 ^d	1.02×10^{-4}	0.080	0.0063	0.11

^a In DMSO, 20 °C, from Table 2. ^b In *i*PrOH, 0 °C, from ref 4c. ^c Averaged value derived from reactions with NH_2OH , SO_3^{2-} , CN^- , BH_4^- , $HOC_2H_4S^-$ in aqueous solution; $k_{rel}(Nu) = 10^B$ calculated from Geneste's *B* values defined by the relation $\log k = A \log k_0 + B$ in ref. 5f. ^d From rate constant with **2a** (Table 2) divided by 9.8 the reactivity ratio **2a/2b** toward cyclohexanone (**1c**).

As shown in Table 7, the introduction of electronegative elements in 4-position of cyclohexanone leads to an increase of the electrophilic reactivity toward carbanion **2b** as well as toward BH_4^- . Possibly different solvation accounts for the fact that the relative reactivities in the two reaction series correlate only moderately. From the fact that the data for the four six-membered ring ketones **1c**, **1e**, **1f**, and **1g** are perfectly on the correlation line of Figure 10, one can conclude that the relative reactivities of these ketones are predominantly controlled by the thermodynamics of the CC-bond forming step. Though oxygen is more electronegative than sulfur, tetrahydrothiopyranone (**1g**) is more electrophilic than tetrahydropyranone (**1f**), which may be due to through bond interaction.⁴²

Table 7. Influence of Heteroatoms in γ -Position on the Reactivities of Cyclic Ketones



Ketones 1	$k_{rel}(\mathbf{2b})^a$	$k_{rel}(BH_4^-)^b$
1c (X = CH ₂)	1.0	1.0
1e (X = NMe)	5.0	9.9
1f (X = O)	18	
1g (X = S)	59	11.2

^a k_{CC} in DMSO from Table 2. ^b In water/dioxane (1/1) at 25 °C (from ref 5a)

When the β -carbon of ketones is replaced by sulfur (**1i** \rightarrow **1j**) or oxygen (**1i** \rightarrow **1k**), the heteroatom effect is larger (by a factor of 400 for S and not measurable for O) than the γ -heteroatom effect shown in Table 7 and follows the electronegativity order O \gg S.

3.3 Conclusions

The arylsulfonyl substituted chloromethyl anions **2a,b** are suitable reference nucleophiles for the determination of the electrophilic reactivities of ordinary aliphatic ketones. The rate constants k_{CC} for the initial nucleophilic attack are accessible by combination of the directly measured gross rate constants (k_2^{exp}) for the formation of the epoxides **3** from the reactants **1** and **2** with the degree of reversibility of the initial step (k_{-CC}/k_{rc}). This ratio was derived from crossover experiments with the independently synthesized intermediates **4**. Two reaction pathways have been identified for the reactions of the carbanions **2** with the ketones **1**: One, which yields the intermediate halohydrin anions **4** with the C-Cl and C-O⁻ bonds in *anti*-arrangements that can undergo direct cyclization to the epoxides **3**, and a second one which gives the halohydrin anions **4-gauche** with C-Cl and C-O⁻ in gauche orientation. The latter undergo retroaddition with regeneration of the reactants **1** and **2**, because the barrier for reversal is lower than the barrier for rotation to give the *anti*-conformer suitable for cyclization. The cyclopropanation of diethyl maleate with **2a** proceeds via an analogous mechanism, with the difference that the initial CC-bond forming step, which also gives different conformers, is irreversible.

The electrophilicity parameters E of the ketones **1** were calculated by equation 1 from the rate constants k_{CC} and the previously reported reactivity parameters N and s_N for the carbanions **2**. The E parameters, which refer to the nucleophilic attack of **2** at the carbonyl groups, correlate moderately with the gas phase LUMO energies of the ketones ($R^2 = 0.76$, Figure 8), poorly with Parr's global electrophilicity index ω ($R^2 = 0.61$, Figure 9), very poorly with Parr's local electrophilicity index ω_C ($R^2 = 0.30$, Figure S33A in Experimental Section of this chapter), and best with the methyl anion affinities calculated for DMSO solution ($R^2 = 0.88$, Figure 10). We thus do not consider Parr's electrophilicity indices suitable measures for electrophilic reactivities, though electrophilic reactivities within series of structurally closely related Michael acceptors correlate well with Parr's indices.³⁰

Comparison of the electrophilicities E of ketones with those of Michael acceptors show that ketones are significantly more electrophilic than Michael acceptors of equal methyl anion

affinity (\triangleq Lewis acidity), indicating that nucleophilic additions to ketones proceed over much lower Marcus intrinsic barriers due to less electronic and geometrical reorganization than in Michael additions.

Crossover experiments showed that the initial attack of the *p*-cyanophenyl sulfonium ylide at aldehydes is reversible (in contrast to previous extrapolations), with the consequence that the previously reported *E* parameters for aldehydes correspond to the gross rate constants for these epoxidations and do not reflect the rates of initial attack of nucleophiles at the carbonyl group. By using the carbanions **2** as reference nucleophiles, estimates for the rate of nucleophilic attack at aldehydes have been obtained, showing that the electrophilicity parameter *E* of benzaldehyde (**1m**) is approximately 7 units greater than that of cyclohexanone (**1c**).

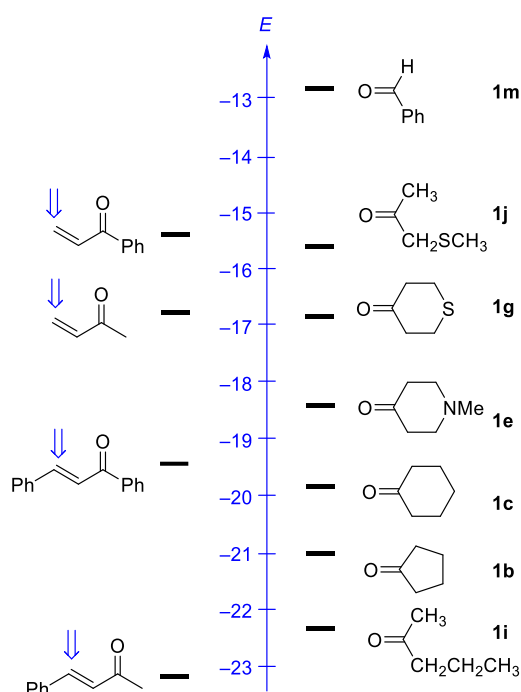


Figure 12. Comparison of the empirical electrophilicities *E* of carbonyl groups and Michael acceptors in DMSO.

As illustrated in Figure 12, the electrophilicities of saturated aliphatic ketones are comparable to the C=C bond reactivities of β -phenyl substituted α,β -unsaturated ketones, much lower than the C=C bond reactivities of terminally unsaturated vinyl ketones. Benzaldehyde, on the other hand, is more electrophilic than the α,β -unsaturated carbonyl compounds depicted in Figure 12, in line with the observation that α,β -unsaturated aldehydes usually undergo 1,2-additions under kinetically controlled conditions. In earlier applications of equation 1, we have shown that in reactions of nucleophiles with carbenium ions and a variety of Michael

acceptors the electrophilicity parameters E can be treated as solvent-independent quantities, with the consequence that all solvent effects were shifted into the nucleophile-specific parameters N and s_N . Because of the high basicity of alkoxide ions in aprotic media, this approximation does probably not hold for the electrophilicities of carbonyl compounds, and systematic investigations of solvent effects are now needed to arrive at reliable predictions of carbonyl reactivities in different solvents.

3.4 References

- (1) (a) Mayr, H.; Bug, T.; Gotta, M. F.; Hering, N.; Irrgang, B.; Janker, B.; Kempf, B.; Loos, R.; Ofial, A. R.; Remennikov, G.; Schimmel, H. *J. Am. Chem. Soc.* **2001**, *123*, 9500–9512. (b) Lucius, R.; Loos, R.; Mayr, H. *Angew. Chem., Int. Ed.* **2002**, *41*, 91–95. (c) Mayr, H.; Kempf, B.; Ofial, A. R. *Acc. Chem. Res.* **2003**, *36*, 66–77.
- (2) Appel, R.; Mayr, H. *J. Am. Chem. Soc.* **2011**, *133*, 8240–8251.
- (3) (a) Zimmerman, H. E.; Ahramjian, L. *J. Am. Chem. Soc.* **1960**, *82*, 5459–5466. (b) Vogt, P. F.; Tavares, D. F. *Can. J. Chem.* **1969**, *47*, 2875–2881. (c) Aggarwal, V. K.; Calamai, S.; Ford, J. G. *J. Chem. Soc., Perkin Trans. I* **1997**, 593–599.
- (4) (a) Brown, H. C.; Mead, E. J.; Rao, B. C. S. *J. Am. Chem. Soc.* **1955**, *77*, 6209–6213. (b) Brown, H. C.; Wheeler, O. H.; Ichikawa, K. *Tetrahedron* **1957**, *1*, 214–220. (c) Brown, H. C.; Ichikawa, K. *Tetrahedron* **1957**, *1*, 221–230. (d) Brown, H. C.; Ichikawa, K. *J. Am. Chem. Soc.* **1962**, *84*, 373–376. (e) Brown, H. C.; Muzzio, J. *J. Am. Chem. Soc.* **1966**, *88*, 2811–2822. (f) Brown, H. C.; Wang, K. K.; Chandrasekharan, J. *J. Am. Chem. Soc.* **1983**, *105*, 2340–2343.
- (5) (a) Geneste, P.; Durand, R.; Hugon, I.; Reminiac, C. *J. Org. Chem.* **1979**, *44*, 1971–1973. (b) Geneste, P.; Lamaty, G.; Moreau, C.; Roque, J. P. *Tetrahedron Lett.* **1970**, *11*, 5011–5014. (c) Geneste, P.; Lamaty, G.; Roque, J. P. *Tetrahedron* **1971**, *27*, 5539–5559. (d) Geneste, P.; Lamaty, G.; Roque, J. P. *Tetrahedron* **1971**, *27*, 5561–5578. (e) Fournier, L.; Lamaty, G.; Natat, A.; Roque, J. P. *Tetrahedron* **1975**, *31*, 1031–1034. (f) Finiels, A.; Geneste, P. *J. Org. Chem.* **1979**, *44*, 1577–1578.
- (6) (a) Zenz, I.; Mayr, H. *J. Org. Chem.* **2011**, *76*, 9370–9378. (b) Kaumanns, O.; Lucius, R.; Mayr, H. *Chem. - Eur. J.* **2008**, *14*, 9675–9682. (c) Lemek, T.; Mayr, H. *J. Org. Chem.* **2003**, *68*, 6880–6886. (d) For a comprehensive database of nucleophilicity parameters N and s_N as well as electrophilicity parameters E , see

- (7) (a) Olmstead, W. N.; Margolin, Z.; Bordwell, F. G. *J. Org. Chem.* **1980**, *45*, 3295–3299. (b) Bordwell, F. G. *Acc. Chem. Res.* **1988**, *21*, 456–463.
- (8) (a) Arnett, E. M.; Maroldo, S. G.; Schilling, S. L.; Harrelson, J. A. *J. Am. Chem. Soc.* **1984**, *106*, 6859–6767. (b) For a comprehensive list of pK_a values, see <http://ibond.nankai.edu.cn/>.
- (9) (a) Darzens, G. *Comp. Rend.* **1904**, *139*, 1214–1217. (b) Darzens, G. *Comp. Rend.* **1905**, *141*, 766–768. (c) Darzens, G. *Comp. Rend.* **1906**, *142*, 214–215. (d) Darzens, G.; Lefébure, P. *Comp. Rend.* **1906**, *142*, 714–715.
- (10) (a) Newman, M. S.; Magerlein, B. J. *Org. React.* **1949**, *5*, 413–440. (b) Rosen, T. In *Comprehensive Organic Synthesis*, 1st ed.; Trost, B. M., Fleming, I., Eds.; Pergamon Press: Oxford, **1991**; Vol. 2, pp 409–439. (c) Aggarwal, V. K.; Crimmin, M.; Riches, S. In *Science of Synthesis*, 2008.; Forysth, C. J., Jacobsen, E. N., Eds.; Thieme: Stuttgart, **2008**; Vol. 37, pp 321–406. (d) Reutrakul, V.; Pohmakotr, M. In *Encyclopedia of Reagents for Organic Synthesis*, 2nd ed.; Paquette, L. A., Crich, D., Fuchs, P. L., Molander, G. A., Eds.; Wiley: Chichester, **2009**; Vol. 4, pp 2375–2378. (e) Bako, P.; Rapi, Z.; Keglevich, G. *Curr. Org. Synth.* **2014**, *11*, 361–376. For diastereoselective or asymmetric Darzens reactions, see: (f) Liu, Y.; Provencher, B. A.; Bartelson, K. J.; Deng, L. *Chem. Sci.* **2011**, *2*, 1301–1304. (g) Kuang, Y.; Lu, Y.; Tang, Y.; Liu, X.; Lin, L., Feng, X. *Org. Lett.* **2014**, *16*, 4244–4247. (h) Li, B.; Li, C. *J. Org. Chem.* **2014**, *79*, 8271–8277. (i) Sakowicz, A.; Loska, R.; Małosza, M. *Synlett* **2016**, *27*, 2443–2446. (j) Chai, G.-L.; Han, J.-W.; Wong, H. N. C. *Synthesis* **2017**, *49*, 181–187. (k) Chai, G.-L.; Han, J.-W.; Wong, H. N. C. *J. Org. Chem.* **2017**, *82*, 12647–12654.
- (11) Ballester, M. *Chem. Rev.* **1955**, *55*, 283–300.
- (12) (a) Bachelor, F. W.; Bansal, R. K. *J. Org. Chem.* **1969**, *34*, 3600–3604. (b) Sipos, G.; Schöbel, G.; Sirokmán, F. *J. Chem. Soc., Perkin Trans. 2* **1975**, 805–808.
- (13) (a) Corey, E. J.; Chaykovsky, M. *J. Am. Chem. Soc.* **1965**, *87*, 1353–1363. (b) Johnson, A. W.; LaCount, R. B. *J. Am. Chem. Soc.* **1961**, *83*, 417–423.
- (14) (a) Aggarwal, V. K.; Winn, C. L. *Acc. Chem. Res.* **2004**, *37*, 611–620. (b) McGarrigle, E. M.; Myers, E. L.; Illa, O.; Shaw, M. A.; Riches, S. L.; Aggarwal, V. K. *Chem. Rev.* **2007**, *107*, 5841–5883.

- (15) (a) Appel, R.; Mayr, H. *Chem. - Eur. J.* **2010**, *16*, 8610–8614. (b) Appel, R.; Hartmann, N.; Mayr, H. *J. Am. Chem. Soc.* **2010**, *132*, 17894–17900.
- (16) Li, Z.; Chen, Q.; Mayer, P.; Mayr, H. *J. Org. Chem.* **2017**, *82*, 2011–2017.
- (17) Mayr, H.; Ofial, A. R. *Angew. Chem., Int. Ed.* **2006**, *45*, 1844–1854.
- (18) Schwesinger, R.; Schlemper, H.; Hasenfratz, C.; Willaredt, J.; Dambacher, T.; Breuer, T.; Ottaway, C.; Fletschinger, M.; Boele, J.; Fritz, H.; Putzas, D.; Rotter, H. W.; Bordwell, F. G.; Satish, A. V.; Ji, G. Z.; Peters, E. M.; Peters, K.; v. Schnering, H. G.; Walz, L. *Liebigs Ann.* **1996**, 1055–1081.
- (19) (a) Durst, T., Tin, K.-C.; De Reinach-Hirtzbach, F.; Decesare, J. M., Ryan, M. D. *Can. J. Chem.* **1979**, *57*, 258–266. (b) Reutrakul, V.; Jarussophon, S.; Pohmakotr, M.; Chaiyasut, Y.; U-Thet, S.; Tuchinda, P. *Tetrahedron Lett.* **2002**, *43*, 2285–2288.
- (20) Arai, S.; Shioiri, T. *Tetrahedron* **2002**, *58*, 1407–1413.
- (21) Becke, A. D. *J. Chem. Phys.* **1993**, *98*, 5648–5652.
- (22) (a) Grimme, S. *J. Comput. Chem.* **2006**, *27*, 1787–1799. (b) Grimme, S.; Antony, J.; Ehrlich, S.; Krieg, H. *J. Chem. Phys.* **2010**, *132*, 154104. (c) Wagner, J. P.; Schreiner, P. R. *Angew. Chem., Int. Ed.* **2015**, *54*, 12274–12296.
- (23) (a) Ditchfield, R.; Hehre, W. J.; Pople, J. A. *J. Chem. Phys.* **1971**, *54*, 724–728. (b) Krishnan, R.; Binkley, J. S.; Seeger, R.; Pople, J. A. *J. Chem. Phys.* **1980**, *72*, 650–654.
- (24) (a) Cancès, E.; Mennucci, B.; Tomasi, J. *J. Chem. Phys.* **1997**, *107*, 3032–3041. (b) Tomasi, J.; Mennucci, B.; Cammi, R. *Chem. Rev.* **2005**, *105*, 2999–3094. (c) Mayer, R. J.; Tokuyasu, T.; Mayer, P.; Gomar, J.; Sabelle, S.; Mennucci, B.; Mayr, H.; Ofial, A. R. *Angew. Chem. Int. Ed.* **2017**, *56*, 13279–13282.
- (25) Grimme, S. *J. Chem. Phys.* **2006**, *124*, 034108.
- (26) (a) Weigend, F.; Ahlrichs, R. *Phys. Chem. Chem. Phys.* **2005**, *7*, 3297–3305. (b) Weigend, F. *Phys. Chem. Chem. Phys.* **2006**, *8*, 1057–1065.
- (27) The corresponding competition experiment with **2b** could not be performed because of the low stability of the resulting oxiranes.
- (28) Huisgen, R. *Angew. Chem., Int. Ed. Engl.* **1970**, *9*, 751–762.
- (29) Allgäuer, D. S.; Jangra, H.; Asahara, H.; Li, Z.; Chen, Q.; Zipse, H.; Ofial, A. R.; Mayr, H. *J. Am. Chem. Soc.* **2017**, *139*, 13318–13329. (b) Mayr, H.; Ammer, J.; Baidya, M.;

Maji, B.; Nigst, T. A.; Ofial, A. R.; Singer, T. *J. Am. Chem. Soc.* **2015**, *137*, 2580–2599.

- (30) Domingo, L. R.; Pérez, P.; Contreras, R. *Tetrahedron* **2004**, *60*, 6585–6591.
- (31) Contreras, R. R.; Fuentealba, P.; Galván, M.; Pérez, P. *Chem. Phys. Lett.* **1999**, *304*, 405–413. (b) Yang, W.; Mortier, W. J. *J. Am. Chem. Soc.* **1986**, *108*, 5708–5711.
- (32) Li-F, Clark, T.; Chandrasekhar, J.; Spitznagel, G. W.; Schleyer, P. v. R. *J. Comput. Chem.* **1983**, *4*, 294–301.
- (33) Marenich, A. V.; Cramer, C. J.; Truhlar, D. G. *J. Phys. Chem. B.* **2009**, *113*, 6378–6396.
- (34) (a) Wang, C.; Fu, Y.; Guo, Q.-X.; Liu, L. *Chem. - Eur. J.* **2010**, *16*, 2586–2598. (b) Zhuo, L.-G.; Liao, W.; Yu, Z.-X. *Asian J. Org. Chem.* **2012**, *1*, 336–345.
- (35) (a) Aizman, A.; Contreras, R.; Pérez, P. *Tetrahedron* **2005**, *61*, 889–895. (b) Pérez, P.; Domingo, L. R.; Aizman, A.; Contreras, R. In *Theoretical Aspects of Chemical Reactivity* (Theoretical and Computational Chemistry Vol. 19); Toro-Labbé, A., Ed.; Elsevier, Amsterdam: 2007; Chapt. 9, pp 139–201. (c) Chamorro, E.; Duque-Noreña, M.; Pérez, P. *J. Mol. Struct. THEOCHEM* **2009**, *896*, 73–79. (d) Chamorro, E.; Duque-Noreña, M.; Pérez, P. *J. Mol. Struct. THEOCHEM* **2009**, *901*, 145–152.
- (36) Byrne, P. A.; Kobayashi, S.; Würthwein, E.-U.; Ammer, J.; Mayr, H. *J. Am. Chem. Soc.* **2017**, *139*, 1499–1511.
- (37) $\Delta\Delta G^\ddagger = 2.303RT\Delta\log k = 2.303RT_{\text{SN}}\Delta E$
- (38) (a) I, Marcus, R. A. *J. Chem. Phys.* **1956**, *24*, 966–978; (b) Marcus, R. A. *J. Phys. Chem.* **1968**, *72*, 891–899; (c) Albery, W. J. *Annu. Rev. Phys. Chem.* **1980**, *31*, 227–263; (d) Murdoch, J. R.; Magnoli, D. E. *J. Am. Chem. Soc.* **1982**, *104*, 3792–3800; (e) Chen, M. Y.; Murdoch, J. R. *J. Am. Chem. Soc.* **1984**, *106*, 4735–4743. (f) The ‘Principle of Least Nuclear Motion’ provides a qualitative rationalization for this phenomenon: Hine, J. *Adv. Phys. Org. Chem.* **1977**, *15*, 1–61.
- (39) Carey, F. A., Sundberg, R. J. *Advanced Organic Chemistry Part A: Structure and Mechanisms*, 5th ed; Springer: New York: 2007; pp 632–637.
- (40) Brown, H. C.; Borkowski, M. *J. Am. Chem. Soc.* **1962**, *74*, 1894–1902.
- (41) Roth, M.; Schade, C.; Mayr, H. *J. Org. Chem.* **1994**, *59*, 169–172.
- (42) Hoffmann, R. *Acc. Chem. Res.* **1971**, *4*, 1–9.

3.5 Experimental Section

(1) Chemical

DMSO (99.7%, extra dry, over molecular sieves, AcroSeal) was purchased and used without further purification. Compound **2b**-H was prepared according to ref [S1](#). The sulfonium tetrafluoroborate **9** and imine **5b** were prepared according to ref [S2](#). The sulfide **6** was prepared according to ref [S3](#). Diethyl maleate **5a** and benzaldehyde **5m** were purchased and then purified by vacuum distillation prior to use. NaOH pellet and KOH pellet were ground into powder by mortar and then stored in glovebox. All other chemicals were purchased from commercial sources and used without purification.

(2) Analytics

^1H and ^{13}C NMR spectra were recorded in CDCl_3 (δ_{H} 7.26, δ_{C} 77.16) on 300, 400 or 600 MHz NMR spectrometers and are given in ppm. The following abbreviations were used to designate chemical shift multiplicities: s = singlet, d = doublet, t = triplet, q = quartet, m = multiplet, br = broad, app = apparent. The assignments of individual NMR signals were based on additional 2D-NMR experiments (COSY, NOESY, HSQC, HMBC). Diastereomeric ratios (dr) were determined by ^1H NMR of the crude reaction products if not stated otherwise. HRMS and MS were recorded on a Finnigan MAT 95Q (EI) mass spectrometer or Thermo Finnigan LTQ FT Ultra (ESI). The melting points were recorded on a Büchi Melting Point B-540 device and are not corrected.

(3) Product studies

Oxiranes **3**

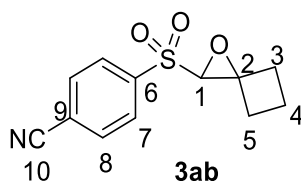
Procedure A for the synthesis of epoxides **3.** To a solution of **1** (0.30 mmol) and **2**-H (0.20 mmol) in anhydrous DMSO (2 mL) at room temperature was added NaOH (12 mg, 0.30 mmol). After 2 h, 2% aq HCl (10 mL) was added and the mixture was extracted with CHCl_3 (3×15 mL). The organic phase was washed with water (2×30 mL) and brine (1×30 mL) to remove remaining DMSO, dried with anhydrous MgSO_4 , and filtered. The solvent was

Chapter 3: Kinetics and mechanism of oxirane-formation by Darzens condensation of ketones: quantification of the electrophilicities of ketones

evaporated under reduced pressure, and the residue was purified by column chromatography to give epoxides.

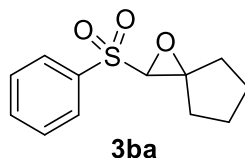
Procedure B for the synthesis of epoxides 3. To a solution of **1** (0.20 mmol) and **2-H** (0.30 mmol) in anhydrous DMSO (2 mL) at room temperature was added NaOH (12 mg, 0.30 mmol). After 2 h, 2% aq HCl (10 mL) was added and the mixture was washed with CHCl₃ (2 × 15 mL). Then the aqueous phase was neutralized by adding NaHCO₃. Afterwards, the water phase was extracted by CHCl₃ (3 × 15 mL). The combined organic phase was washed with water (2 × 30 mL) and brine (1 × 30 mL) to remove remaining DMSO, dried with anhydrous MgSO₄, and filtered. The solvent was evaporated under reduced pressure, and the residue was product **3** without further purification.

4-((1-Oxaspiro[2.3]hexan-2-yl)sulfonyl)benzonitrile (3ab) was obtained according to Procedure A from **1a** (21 mg, 0.30 mmol) and **2b-H** (43 mg, 0.20 mmol): white solid (40 mg, 80%); mp 124–129 °C.

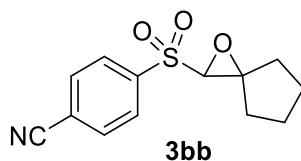


¹H NMR (400 MHz, CDCl₃) δ 8.05 (d, *J* = 8.0 Hz, 2 H, H-7), 7.88 (d, *J* = 8.1 Hz, 2 H, H-8), 3.87 (s, 1 H, H-1), 3.10–2.94 (m, 1 H, H-3), 2.82–2.74 (m, 1 H, H-3), 2.60–2.42 (m, 2 H, H-5), 2.10–2.01 (m, 2 H, H-4). **¹³C NMR** (101 MHz, CDCl₃) δ 142.3 (C-6), 133.2 (C-8), 129.3 (C-7), 118.2 (C-9), 117.2 (C-10), 70.2 (C-1), 68.6 (C-2), 31.6 (C-5), 29.9 (C-3), 14.1 (C-4). **HRMS** (EI) *m/z*: [*M*⁺] calcd for [C₁₂H₁₁NO₃S]⁺ 249.0454, found 249.0465. **IR** (ATR) *ν* (cm⁻¹) = 3063, 3105, 3091, 3043, 3005, 2955, 2231, 1420, 1396, 1324, 1150, 1084, 833.

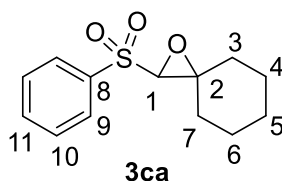
2-(Phenylsulfonyl)-1-oxaspiro[2.4]heptane (3ba) was not isolated as it decomposed during the attempted purification. Formation of the oxirane **3ba** was studied directly by NMR spectroscopy after mixing from **1b** (8.4 mg, 0.10 mmol), **2a-H** (19 mg, 0.10 mmol), and NaOH (6.0 mg, 0.15 mmol) in 0.6 mL *d*₆-DMSO. The yield was 87% which was determined by using *m*-xylene as internal standard compound.



4-((1-Oxaspiro[2.4]heptan-2-yl)sulfonyl)benzonitrile (3bb) was not isolated as it decomposed during the attempted purification. The formation of the oxirane **3bb** was studied by NMR spectroscopy after mixing **1b** (8.4 mg, 0.10 mmol), **2b-H** (22 mg, 0.10 mmol), and NaOH (6.0 mg, 0.15 mmol) in 0.6 mL *d*₆-DMSO. After 1h, 2% aq HCl (10 mL) was added and the mixture was extracted with CHCl₃ (3 × 15 mL). The organic phase was washed with water (2 × 30 mL) and brine (1 × 30 mL) to remove remaining DMSO, dried with anhydrous MgSO₄, and filtered. The solvent was evaporated under reduced pressure, and the residue was analyzed by ¹H NMR spectroscopy (in CDCl₃). The yield was 73% which was determined by using m-xylene as internal standard compound.



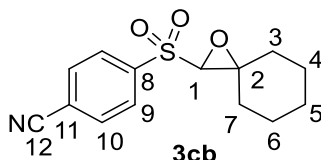
2-(Phenylsulfonyl)-1-oxaspiro[2.5]octane (3ca)^{S4} was obtained according to Procedure A from **1c** (29 mg, 0.30 mmol) and **2a-H** (38 mg, 0.20 mmol): colorless liquid (48 mg, 95%).



¹H NMR (400 MHz, CDCl₃) δ 7.95 (d, *J* = 7.2 Hz, 2 H, H-9), 7.68 (t, *J* = 7.4 Hz, 1 H, H-11), 7.59 (t, *J* = 7.6 Hz, 2 H, H-10), 3.76 (s, 1 H, H-1), 2.32–2.12 (m, 2 H, H-7), 1.91–1.69 (m, 3 H, H-4 × 2, H-6), 1.66–1.42 (m, 5 H, H-3 × 2, H-5 × 2, H-6). **¹H NMR** (400 MHz, (CD₃)₂SO) δ 7.92 (d, *J* = 7.4 Hz, 2 H), 7.82 (t, *J* = 7.4 Hz, 1 H), 7.72 (t, *J* = 7.6 Hz, 2 H), 4.50 (s, 1 H), 2.17–2.11 (m, 1 H), 2.05–1.98 (m, 1 H), 1.74–1.58 (m, 2 H), 1.57–1.43 (m, 6 H). **¹³C NMR** (101 MHz, CDCl₃) δ 139.2 (C-8), 134.2 (C-11), 129.5 (C-10), 128.3 (C-9), 74.9 (C-1), 69.5 (C-2), 35.4 (C-3), 28.4 (C-7), 25.2/25.1/25.0 (C-4, C-5 and C-6). **HRMS** (ESI⁺) *m/z*:

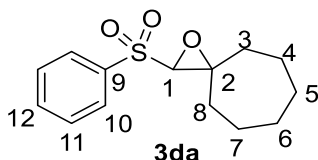
$[M+NH_4]^+$ calcd for $[C_{13}H_{20}NO_3S]^+$ 270.1158, found 270.1159. **IR** (ATR) ν (cm^{-1}) = 2935, 2859, 1447, 1421, 1321, 1310, 1269, 1152, 1086, 935, 747, 719, 686.

4-((1-Oxaspiro[2.5]octan-2-yl)sulfonyl)benzonitrile (3cb) was obtained according to Procedure A from **1c** (29 mg, 0.30 mmol) and **2b-H** (43 mg, 0.20 mmol): white solid (42 mg, 75%).



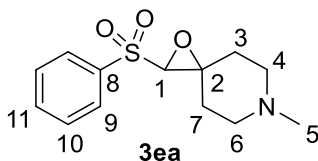
1H NMR (400 MHz, $CDCl_3$) δ 8.08 (d, J = 8.0 Hz, 2 H), 7.89 (d, J = 8.0 Hz, 2 H), 3.75 (s, 1 H), 2.27–2.18 (m, 2 H), 1.91–1.69 (m, 3 H), 1.66–1.46 (m, 5 H). **1H NMR** (200 MHz, $(CD_3)_2SO$) δ 8.22 (d, J = 8.3 Hz, 2H), 8.09 (d, J = 8.3 Hz, 2H), 4.65 (s, 1H), 2.23–1.93 (m, 2H), 1.65–1.45 (m, 8H). **^{13}C NMR** (101 MHz, $CDCl_3$) δ 143.0, 133.3, 129.1, 118.1, 117.2, 74.5, 70.4, 35.5, 28.6, 25.14, 25.07. **HRMS** (EI) m/z : $[M^+]$ calcd for $[C_{14}H_{15}NO_3S]^+$ 277.0767, found 277.0749. **IR** (ATR) ν (cm^{-1}) = 2961, 2951, 2934, 2859, 2232, 1421, 1332, 1322, 1124, 1085, 934, 843, 769, 703.

2-(Phenylsulfonyl)-1-oxaspiro[2.6]nonane (3da) was obtained according to Procedure A: from **1d** (34 mg, 0.30 mmol) and **2a-H** (38 mg, 0.20 mmol): colorless liquid (49 mg, 90%).



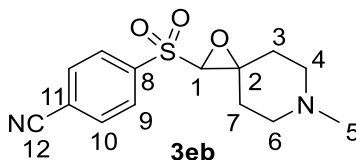
1H NMR (400 MHz, $CDCl_3$) δ 7.96 (d, J = 7.3 Hz, 2 H, H-10), 7.68 (t, J = 7.4 Hz, 1 H, H-12), 7.59 (t, J = 7.7 Hz, 2 H, H-11), 3.77 (s, 1 H, H-1), 2.46–2.39 (m, 1 H, H-3), 2.33–2.26 (m, 1 H, H-3), 1.83–1.52 (m, 10 H). **1H NMR** (400 MHz, $(CD_3)_2SO$) δ 7.92 (d, J = 7.6 Hz, 2 H), 7.82 (t, J = 7.4 Hz, 1 H), 7.72 (t, J = 7.6 Hz, 2 H), 4.50 (s, 1 H), 2.29–2.22 (m, 1 H), 2.20–2.11 (m, 1 H), 1.76–1.42 (m, 10 H). **^{13}C NMR** (101 MHz, $CDCl_3$) δ 139.2 (C-9), 134.3 (C-12), 129.5 (C-11), 128.4 (C-10), 75.6 (C-1), 71.1 (C-2), 37.6/30.7/28.8/28.7/24.6/24.5 (C-8, C-3, C-4, C-7, C-5, C-6). **HRMS** (ESI $^+$) m/z : $[M+NH_4]^+$ calcd for $[C_{14}H_{22}NO_3S]^+$ 284.1315, found 284.1315. **IR** (ATR) ν (cm^{-1}) = 2927, 2857, 1447, 1321, 1309, 1149, 1087, 716, 687.

6-Methyl-2-(phenylsulfonyl)-1-oxa-6-azaspiro[2.5]octane (3ea) was obtained according to Procedure B from **1e** (23 mg, 0.20 mmol) and **2a-H** (57 mg, 0.30 mmol): colorless liquid (47 mg, 90%).



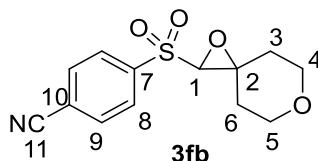
¹H NMR (599 MHz, CDCl₃) δ 7.96 (d, J = 8.5, 2 H, H-9), 7.70 (t, J = 7.4 Hz, 1 H, H-11), 7.63–7.56 (t, J = 8.4 Hz, 2 H, H-10), 3.81 (s, 1 H, H-1), 2.76–2.70 (m, 1 H, H-4), 2.65–2.59 (m, 1 H, H-6), 2.58–2.52 (m, 1 H, H-4), 2.50–2.45 (m, 1 H, H-6), 2.43–2.38 (m, 2 H, H-3), 2.33 (s, 3 H, H-5), 1.98–1.87 (m, 1 H, H-7), 1.55–1.45 (m, 1 H, H-7). **¹³C NMR** (151 MHz, CDCl₃) δ 138.9 (C-8), 134.5 (C-11), 129.6 (C-10), 128.4 (C-9), 74.1 (C-1), 67.2 (C-2), 54.1 (C-4), 53.9 (C-6), 46.1 (C-5), 34.6 (C-7), 28.2 (C-3). **HRMS** (EI) m/z : [M⁺] calcd for [C₁₃H₁₇NO₃S]⁺ 267.0924, found 267.0923. **IR** (ATR) ν (cm⁻¹) = 2925, 2788, 1446, 1322, 1284, 1152, 1082, 1069, 789, 748, 719, 686.

4-((6-Methyl-1-oxa-6-azaspiro[2.5]octan-2-yl)sulfonyl)benzonitrile (3eb) was obtained according to Procedure B from **1e** (23 mg, 0.20 mmol) and **2b-H** (65 mg, 0.30 mmol): yellow solid (53 mg, 90%), mp 140–145 °C.



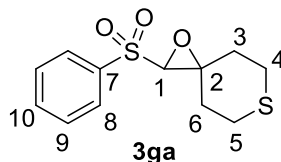
¹H NMR (400 MHz, CDCl₃) δ 8.07 (d, J = 8.5 Hz, 2 H, H-9), 7.90 (d, J = 8.7 Hz, 2 H, H-10), 3.79 (s, 1 H, H-1), 2.76–2.68 (m, 1 H, H-4), 2.66–2.60 (m, 1 H, H-6), 2.58–2.36 (m, 4 H, H-3 \times 2, H-4, H-6), 2.33 (s, 3 H, H-5), 1.99–1.89 (m, 1 H, H-7), 1.48–1.51 (m, 1 H, H-7). **¹³C NMR** (101 MHz, CDCl₃) δ 142.8 (C-8), 133.3 (C-10), 129.1 (C-9), 118.2 (C-11), 117.1 (C-12), 73.8 (C-1), 68.1 (C-2), 54.0 (C-4), 53.9 (C-6), 46.0 (C-5), 34.6 (C-7), 28.3 (C-3). **HRMS** (ESI⁺) m/z : [M+H]⁺ calcd for [C₁₄H₁₇N₂O₃S]⁺ 293.0954 found 293.0953. **IR** (ATR) ν (cm⁻¹) = 2968, 2918, 2798, 2233, 1446, 1375, 1332, 1286, 1152, 1136, 1083, 1016, 953, 839, 763.

4-((1,6-Dioxaspiro[2.5]octan-2-yl)sulfonyl)benzonitrile (3fb) was obtained according to Procedure A from **1f** (20 mg, 0.20 mmol) and **2b**-H (65 mg, 0.30 mmol): white solid (39 mg, 70%), mp 165–170 °C.



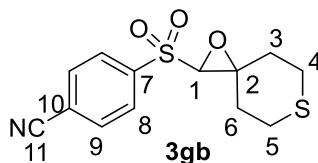
¹H NMR (400 MHz, CDCl₃) δ 8.09 (d, *J* = 7.9 Hz, 2 H, H-8), 7.91 (d, *J* = 7.9 Hz, 2 H, H-9), 4.05–3.70 (m, 5 H, H-1, H-4, H-5), 2.58–2.40 (m, 1 H, H-3), 2.42–2.23 (m, 1 H, H-3), 2.05–1.85 (m, 1 H, H-6), 1.57–1.39 (m, 1 H, H-6). **¹³C NMR** (101 MHz, CDCl₃) δ 142.6 (C-7), 133.4 (C-9), 129.2 (C-8), 118.4 (C-10), 117.1 (C-11), 73.7 (C-1), 67.4 (C-2), 66.5 (C-4), 66.3 (C-5), 35.2 (C-6), 29.5 (C-3). **HRMS** (ESI[−]) *m/z*: [M+HCOO][−] calcd for [C₁₄H₁₄NO₆S][−] 324.0547 found 324.0551. **IR** (ATR) *ν* (cm^{−1}) = 3093, 3039, 2974, 2863, 2233, 1380, 1324, 1228, 1152, 1100, 1085, 1018, 952, 841, 767, 654.

2-(Phenylsulfonyl)-1-oxa-6-thiaspiro[2.5]octane (3ga) was obtained according to Procedure A from **1g** (35 mg, 0.30 mmol) and **2a**-H (38 mg, 0.20 mmol): colorless liquid (51 mg, 95%).



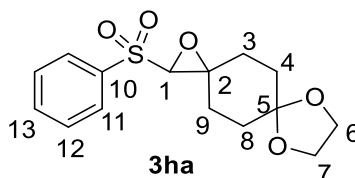
¹H NMR (400 MHz, CDCl₃) δ 7.94 (d, *J* = 7.0 Hz, 2 H, H-8), 7.70 (t, *J* = 7.5 Hz, 1 H, H-10), 7.60 (t, *J* = 7.5 Hz, 2 H, H-9), 3.74 (s, 1 H, H-1), 2.98–2.89 (m, 1 H, H-4), 2.90–2.79 (m, 2 H, H-4, H-5), 2.73–2.66 (m, 1 H, H-5), 2.63–2.52 (m, 2 H, H-3), 1.99–1.90 (m, 1 H, H-6), 1.84–1.73 (m, 1 H, H-6). **¹H NMR** (400 MHz, (CD₃)₂SO) δ 7.93 (d, *J* = 7.3 Hz, 2 H), 7.84 (t, *J* = 7.4 Hz, 1 H), 7.73 (t, *J* = 7.6 Hz, 2 H), 4.58 (s, 1 H), 2.88–2.82 (m, 1 H), 2.81–2.59 (m, 3 H), 2.48–2.41 (m, 1 H), 2.38–2.32 (m, 1 H), 1.88–1.82 (m, 1 H), 1.81–1.73 (m, 1 H). **¹³C NMR** (101 MHz, CDCl₃) δ 138.8 (C-7), 134.5 (C-10), 129.6 (C-9), 128.3 (C-8), 74.6 (C-1), 67.8 (C-2), 37.1 (C-6), 30.6 (C-3), 27.8 (C-5), 27.6 (C-4). **HRMS** (ESI⁺) *m/z*: [M+NH₄]⁺ calcd for [C₁₂H₁₈NO₃S₂]⁺ 288.0723, found 288.0724. **IR** (ATR) *ν* (cm^{−1}) = 3064, 2920, 2830, 1584, 1447, 1430, 1322, 1271, 1150, 1086, 900, 748, 720, 686.

4-((1-Oxa-6-thiaspiro[2.5]octan-2-yl)sulfonyl)benzonitrile (3gb) was obtained according to Procedure A from **1g** (35 mg, 0.30 mmol) and **2b-H** (43 mg, 0.20 mmol): white solid (50 mg, 85%), mp 160–165 °C.



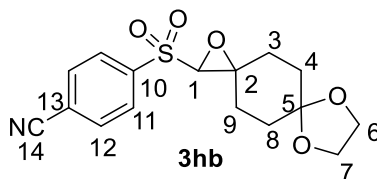
¹H NMR (400 MHz, CDCl₃) δ 8.08 (d, *J* = 8.1 Hz, 2 H, H-8), 7.91 (d, *J* = 8.1 Hz, 2 H, H-9), 3.72 (s, 1 H, H-1), 3.00–2.91 (m, 1 H, H-4), 2.91–2.81 (m, 2 H, H-4, H-5), 2.78–2.67 (m, 1 H, H-5), 2.66–2.52 (m, 2 H, H-3), 2.03–1.93 (m, 1 H, H-6), 1.84–1.76 (m, 1 H, H-6). **¹³C NMR** (101 MHz, CDCl₃) δ 142.7 (C-7), 133.4 (C-9), 129.1 (C-8), 118.4 (C-10), 117.1 (C-11), 74.3 (C-1), 68.8 (C-2), 37.1 (C-6), 30.8 (C-3), 27.9 (C-5), 27.6 (C-4). **HRMS** (EI) *m/z*: [*M*⁺] calcd for [C₁₃H₁₃NO₃S₂]⁺ 295.0331, found 295.0331. **IR** (ATR) *ν* (cm⁻¹) = 3090, 3039, 2920, 2234, 1396, 1325, 1305, 1150, 1085, 951, 904, 844, 827, 771, 707.

2-(Phenylsulfonyl)-1,7,10-trioxadispiro[2.2.4⁶.2³]dodecane (3ha) was obtained according to Procedure A from **1h** (31 mg, 0.20 mmol) and **2a-H** (57 mg, 0.30 mmol): colorless liquid (50 mg, 80%).



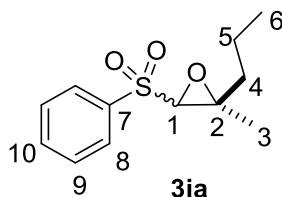
¹H NMR (599 MHz, CDCl₃) δ 7.96 (d, *J* = 7.2 Hz, 2 H, H-11), 7.72–7.66 (t, *J* = 7.8 Hz, 1 H, H-13), 7.62–7.58 (t, *J* = 8.4 Hz, 2 H, H-12), 4.00–3.95 (m, 4 H, H-6, H-7), 3.85 (s, 1 H, H-1), 2.50–2.43 (m, 1 H, H-3), 2.40–2.33 (m, 1 H, H-3), 1.98–1.83 (m, 4 H), 1.80–1.76 (m, 1 H), 1.56–1.51 (m, 1 H). **¹H NMR** (400 MHz, (CD₃)₂SO) δ 7.92 (d, *J* = 7.7 Hz, 2 H), 7.83 (t, *J* = 7.4 Hz, 1 H), 7.73 (t, *J* = 7.6 Hz, 2 H), 4.64 (s, 1 H), 3.89 (s, 4 H), 2.24–2.12 (m, 2 H), 1.79–1.53 (m, 6 H). **¹³C NMR** (101 MHz, CDCl₃) δ 138.94 (C-10), 134.43 (C-13), 129.61 (C-12), 128.36 (C-11), 107.52 (C-5), 74.50 (C-1), 67.95 (C-2), 64.63 (C-6 and C-7), 33.02/32.96/32.40/25.15 (C-3, C-4, C-8, C-9). **HRMS** (ESI⁺) *m/z*: [*M*+H]⁺ calcd for [C₁₅H₁₉O₅S]⁺ 311.0948, found 311.0955. **IR** (ATR) *ν* (cm⁻¹) = 2957, 2887, 1447, 1323, 1293, 1152, 1084, 1033, 936, 910, 748, 720, 687.

4-((1,7,10-Trioxadispiro[2.2.4⁶.2³]dodecan-2-yl)sulfonyl)benzonitrile (3hb) was obtained according to Procedure A from **1h** (31 mg, 0.20 mmol) and **2b-H** (65 mg, 0.30 mmol): white solid (50 mg, 75%), mp 164–168 °C.



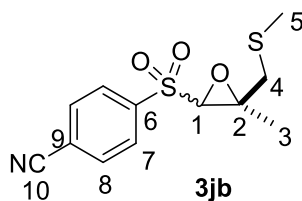
¹H NMR (400 MHz, CDCl₃) δ 8.08 (d, *J* = 8.7 Hz, 2 H, H-11), 7.90 (d, *J* = 8.7 Hz, 2 H, H-12), 4.01–3.95 (m, 4 H, H-6, H-7), 3.83 (s, 1 H, H-1), 2.49–2.34 (m, 2 H, H-3), 1.99–1.75 (m, 5 H), 1.60–1.49 (m, 1 H). **¹H NMR** (400 MHz, (CD₃)₂SO) δ 8.22 (d, *J* = 8.0 Hz, 2 H), 8.10 (d, *J* = 8.0 Hz, 2 H), 4.78 (s, 1 H), 3.90 (s, 4 H), 2.32–2.13 (m, 2 H), 1.77–1.67 (m, 5 H), 1.63–1.52 (m, 1 H). **¹³C NMR** (101 MHz, CDCl₃) δ 142.9 (C-10), 133.3 (C-12), 129.1 (C-11), 118.2 (C-13), 117.1 (C-14), 107.3 (C-5), 74.2 (C-1), 68.8 (C-2), 64.69/64.66 (C-6, C-7), 33.1/33.0/32.5/25.3 (C-3, C-4, C-8, C-9). **HRMS** (ESI[−]) *m/z*: [M+HCOO][−] calcd for [C₁₇H₁₈NO₇S][−] 380.0810, found 380.0808. **IR** (ATR) *ν* (cm^{−1}) = 3100, 2958, 2883, 2232, 1445, 1331, 1267, 1151, 1083, 1032, 910, 840, 767, 677.

2-Methyl-3-(phenylsulfonyl)-2-propyloxirane (3ia) was obtained according to Procedure A from **1i** (26 mg, 0.30 mmol) and **2a-H** (38 mg, 0.20 mmol): pale yellow liquid (43 mg, 90%), dr 2.6 : 1. Only the resonances of the major diastereomer are listed below.



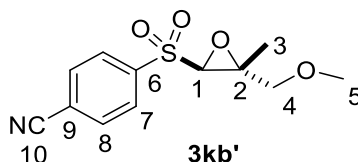
¹H NMR (400MHz, CDCl₃) major diastereomer **3ia**⁺: δ 7.96 (d, *J* = 7.0 Hz, 2 H, H-8), 7.71–7.67 (t, *J* = 7.2 Hz, 1 H, H-10), 7.60 (t, *J* = 7.6 Hz, 2 H, H-9), 3.78 (s, 1 H, H-1), 1.77 (s, 3 H, H-3), 1.69–1.59 (m, 2 H, H-4), 1.47–1.40 (m, 2 H, H-5), 0.89 (t, *J* = 7.2 Hz, 3 H, H-6). **¹³C NMR** (101 MHz, CDCl₃) major diastereomer **3ia**⁺: δ 139.1 (C-7), 134.3 (C-10), 129.5 (C-9), 128.3 (C-8), 74.0 (C-1), 66.9 (C-2), 40.5 (C-4), 18.2 (C-5), 16.2 (C-3), 13.8 (C-6). **HRMS** (EI) *m/z*: [M⁺] calcd for [C₁₂H₁₆O₃S]⁺ 240.0815, found 240.0818.

4-((3-Methyl-3-((methylthio)methyl)oxiran-2-yl)sulfonyl)benzonitrile (3jb) was studied directly by NMR spectroscopy according to Procedure A by mixing **1j** (10.4 mg, 0.10 mmol) and **2b-H** (21.6 mg, 0.10 mmol), and NaOH (6.0 mg, 0.15 mmol) in 0.6 mL *d*₆-DMSO: the yield was 80% determined by using m-xylene as internal standard compound, dr 2.2 : 1. Only the resonances of the major diastereomer are listed below.



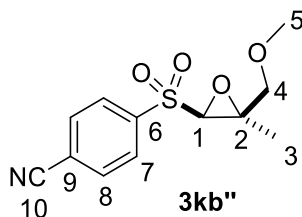
¹H NMR (400MHz, (CD₃)₂SO) major diastereomer **3jb'**: δ 8.22 (d, *J* = 8.1 Hz, 2 H, H-7), 8.10 (d, *J* = 8.1 Hz, 2 H, H-8), 4.76 (s, 1 H, H-1), 2.77–2.64 (m, 2 H, H-4), 2.02 (s, 3 H, H-5), 1.77 (s, 3 H, H-3). **¹³C NMR** (101 MHz, (CD₃)₂SO) major diastereomer **3jb'**: δ 142.1 (C-6), 133.9 (C-8), 128.8 (C-7), 117.4 (C-9), 117.0 (C-10), 71.8 (C-1), 65.6 (C-2), 39.9 (C-4), 15.1 (C-5), 14.8 (C-3). **HRMS** (EI) *m/z*: [*M*⁺] calcd for [C₁₂H₁₃NO₃S₂]⁺ 283.0331, found 283.0333.

4-((3-(Methoxymethyl)-3-methyloxiran-2-yl)sulfonyl)benzonitrile (3kb) was obtained according to Procedure A from **1k** (40 mg, 0.45 mmol), **2b-H** (65 mg, 0.30 mmol), and NaOH (18 mg, 0.45 mmol): **3kb'** (rel-2R,3R, 50.0 mg, 62%), **3kb''** (rel-2R,3S, 22.0 mg, 27%).



pale yellow liquid

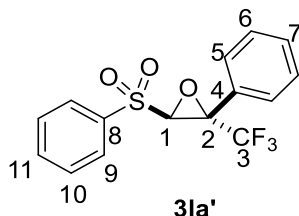
¹H NMR (400 MHz, CDCl₃) δ 8.08 (d, *J* = 7.2 Hz, 2 H, H-7), 7.89 (d, *J* = 7.6 Hz, 2 H, H-8), 4.11 (s, 1 H, H-1), 3.57–3.44 (m, 2 H, H-4), 3.30 (s, 3 H, H-5), 1.78 (s, 3 H, H-3). **¹H NMR** (400 MHz, (CD₃)₂SO) δ 8.22 (d, *J* = 8.4 Hz, 2 H), 8.11 (d, *J* = 8.4 Hz, 2 H), 4.66 (s, 1 H), 3.46 (d, *J* = 11.7 Hz, 1 H), 3.35 (d, *J* = 11.7 Hz, 1 H), 3.22 (s, 3 H), 1.67 (s, 3 H). **¹³C NMR** (101 MHz, CDCl₃) δ 142.9 (C-6), 133.3 (C-8), 129.1 (C-7), 118.2 (C-9), 117.1 (C-10), 73.1 (C-4), 70.2 (C-1), 65.9 (C-2), 59.5 (C-5), 14.2 (C-3). **HRMS** (ESI⁺) *m/z*: [*M*+H]⁺ calcd for [C₁₂H₁₄NO₄S]⁺ 268.0638, found 286.0638. **IR** (ATR) *ν* (cm⁻¹) = 2936, 2235, 1397, 1331, 1196, 1153, 1117, 1085, 968, 835, 753, 732.



pale yellow liquid

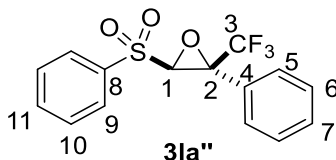
¹H NMR (599 MHz, CDCl₃) δ 8.09 (br s, 2 H, H-7), 7.91 (br s, 2 H, H-8), 4.02 (m, 2 H, H-4), 3.84 (s, 1 H, H-1), 3.46 (s, 3 H, H-5), 1.49 (s, 3 H, H-3). **¹H NMR** (599 MHz, (CD₃)₂SO) δ 8.22 (d, *J* = 8.4 Hz, 2 H), 8.10 (d, *J* = 8.3 Hz, 2 H), 4.80 (s, 1 H), 3.92 (d, *J* = 11.1 Hz, 1 H), 3.85 (d, *J* = 11.1 Hz, 1 H), 3.33 (s, 3 H), 1.38 (s, 3 H). **¹³C NMR** (151 MHz, CDCl₃) δ 142.5 (C-6), 133.3 (C-8), 129.3 (C-7), 118.3 (C-9), 117.1 (C-10), 73.5 (C-4), 71.6 (C-1), 67.1 (C-2), 59.4 (C-5), 20.1 (C-3). **HRMS** (ESI⁺) *m/z*: [M+H]⁺ calcd for [C₁₂H₁₄NO₄S]⁺ 268.0638, found 268.0648. **IR** (ATR) *ν* (cm⁻¹) = 2934, 2235, 1397, 1331, 1288, 1195, 1153, 1110, 1080, 931, 838, 754.

2-Phenyl-3-(phenylsulfonyl)-2-(trifluoromethyl)oxirane (3la) was obtained according to Procedure A from **1l** (78 mg, 0.45 mmol), **2a-H** (57 mg, 0.30 mmol), and NaOH (18 mg, 0.45 mmol): **3la'** (rel-2R,3R, 59 mg, 60%), **3la''** (rel-2R,3S, 30 mg, 30%).



white solid, mp 75–80 °C

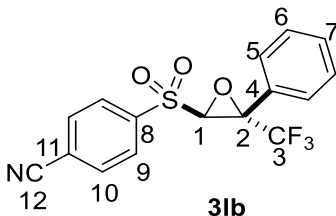
¹H NMR (400 MHz, CDCl₃) δ 7.68 (d, *J* = 7.0 Hz, 2 H, H-9), 7.63 (d, *J* = 7.6 Hz, 1 H, H-11), 7.50–7.42 (m, 5 H, H-5, H-7, H-10), 7.40–7.34 (m, 2 H, H-6), 4.61 (s, 1 H, H-1). **¹H NMR** (400 MHz, (CD₃)₂SO) δ 7.82 (t, *J* = 7.4 Hz, 1 H), 7.76 (d, *J* = 7.8 Hz, 2 H), 7.65 (t, *J* = 7.7 Hz, 2 H), 7.54–7.40 (m, 5 H), 5.79 (s, 1 H). **¹³C NMR** (101 MHz, CDCl₃) δ 136.8 (C-8), 134.7 (C-5), 130.5 (C-11), 129.4 (C-10), 129.0 (C-9), 128.7 (C-7), 128.5 (C-6), 125.3 (C-4), 121.7 (q, *J* = 280.5 Hz, C-3), 69.9 (q, *J* = 2.0 Hz, C-1), 63.8 (q, *J* = 37.3 Hz, C-2). **HRMS** (ESI⁺) *m/z*: [M+NH₄]⁺ calcd for [C₁₅H₁₅F₃NO₃S]⁺ 346.0719, found 346.0719. **IR** (ATR) *ν* (cm⁻¹) = 3007, 1448, 1337, 1280, 1156, 1085, 960, 801, 751, 683, 593, 576.



white solid, mp 73–78 °C

¹H NMR (599 MHz, CDCl₃) δ 8.02 (d, *J* = 7.7 Hz, 2 H, H-9), 7.74 (t, *J* = 7.5 Hz, 1 H, H-11), 7.64 (t, *J* = 7.7 Hz, 2 H, H-10), 7.51–7.33 (m, 5 H, H-5, H-6, H-7), 4.14 (s, 1H, H-1). **¹H NMR** (599 MHz, (CD₃)₂SO) δ 8.01 (d, *J* = 7.1 Hz, 2 H), 7.86 (t, *J* = 7.5 Hz, 1 H), 7.74 (t, *J* = 7.9 Hz, 2 H), 7.49 (d, *J* = 7.9 Hz, 3 H), 7.45 (d, *J* = 6.1 Hz, 2 H), 5.26 (s, 1 H). **¹³C NMR** (151 MHz, CDCl₃) δ 138.2 (C-8), 135.0 (C-11), 130.4 (C-7), 130.3 (C-4), 129.7 (C-10), 129.0 (C-6), 128.8 (C-9), 126.6 (C-5), 121.9 (q, *J* = 279.6 Hz, C-3), 75.6 (C-1), 66.0 (q, *J* = 40.1 Hz, C-2). **HRMS** (EI) *m/z*: [M⁺] calcd for [C₁₅H₁₁F₃O₃S]⁺ 328.0376, found 328.0369. **IR** (ATR) *ν* (cm⁻¹) = 3066, 1693, 1449, 1350, 1152, 1084, 967, 915, 794, 737, 720, 685.

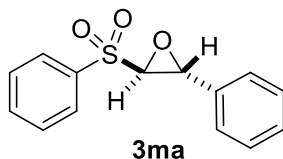
rel-2S,3S-4-((3-Phenyl-3-(trifluoromethyl)oxiran-2-yl)sulfonyl)benzonitrile (3lb) was obtained according to Procedure A from **11** (52 mg, 0.30 mmol) and **2b-H** (43 mg, 0.20 mmol): white solid (56 mg, 80%), mp 143–148 °C.



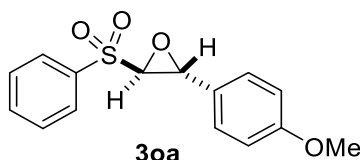
¹H NMR (599 MHz, CDCl₃) δ 7.70 (s, 4 H, H-9, H-10), 7.46 (t, *J* = 7.0 Hz, 1 H, H-7), 7.40–7.32 (m, 4 H, H-5, H-6), 4.67 (s, 1 H, H-1). **¹H NMR** (400 MHz, (CD₃)₂SO) δ 8.12 (d, *J* = 7.8 Hz, 2 H), 7.89 (d, *J* = 7.9 Hz, 2 H), 7.52 (d, *J* = 5.7 Hz, 1 H), 7.47–7.41 (m, 4 H), 5.96 (s, 1 H). **¹⁹F NMR** (377 MHz, CDCl₃) δ -75.55. **¹³C NMR** (151 MHz, CDCl₃) δ 140.1 (C-8), 132.8 (C-10), 130.8 (C-7), 129.8 (C-9), 128.6 (C-5, C-6), 124.8 (C-4), 121.4 (q, *J* = 280.5 Hz, C-3), 118.3 (C-11), 116.9 (C-12), 70.2 (C-1), 63.9 (q, *J* = 37.5 Hz, C-2). **HRMS** (EI) *m/z*: [M⁺] calcd for [C₁₆H₁₀F₃NO₃S]⁺ 353.0328, found 353.0325. **IR** (ATR) *ν* (cm⁻¹) = 3051, 3003, 2239, 1450, 1401, 1350, 1271, 1179, 1153, 1084, 1018, 914, 845, 794, 763, 697, 672.

rel-2R,3R-2-Phenyl-3-(phenylsulfonyl)oxirane (3ma) was not isolated as it decomposed during the attempted purification. The formation of the oxirane **3ma** was studied directly by

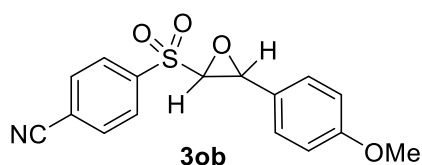
NMR spectroscopy after mixing **1m** (17 mg, 0.16 mmol), **2a-H** (30 mg, 0.16 mmol), and NaOH (19 mg, 0.48 mmol) in 0.6 mL *d*₆-DMSO.



rel-2R,3R-2-(4-Methoxyphenyl)-3-(phenylsulfonyl)oxirane (3oa) was not isolated as it decomposed during the attempted purification. The formation of the oxirane **3oa** was studied directly by NMR spectroscopy after mixing **1o** (22 mg, 0.16 mmol), **2a-H** (30 mg, 0.16 mmol), and NaOH (19 mg, 0.48 mmol) in 0.6 mL *d*₆-DMSO.



4-((3-(4-Methoxyphenyl)oxiran-2-yl)sulfonyl)benzonitrile (3ob) was not isolated as it decomposed during the attempted purification. The formation of **3ob** was studied directly by NMR spectroscopic analysis of a mixture of **1o** (7.6 mg, 0.056 mmol), **2b-H** (8.0 mg, 0.037 mmol), and NaOH (4.4 mg, 0.11 mmol) in 0.6 mL *d*₆-DMSO.



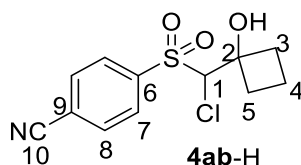
Halohydrins 4-H.

Procedure C for the synthesis of halohydrin 4-H: To a solution of **2-H** (0.2 mmol) in anhydrous THF (1 mL) at $-78\text{ }^{\circ}\text{C}$ was added dropwise a freshly prepared solution of LDA (0.24 mmol) or *n*-BuLi (0.24 mmol) in 1 mL anhydrous THF. After 10 min, a solution of **1** (0.30 mmol) in 0.5 mL anhydrous THF was added dropwise at $-78\text{ }^{\circ}\text{C}$. After another 30 min, 2% aq HCl (10 mL) was added at $-78\text{ }^{\circ}\text{C}$ and the mixture was extracted with CHCl_3 (3×15

mL). The combined organic phase was washed with brine, dried with anhydrous MgSO_4 , and filtered. The solvent was evaporated under reduced pressure, and the residue was purified by column chromatography to give halohydrin **4-H**.

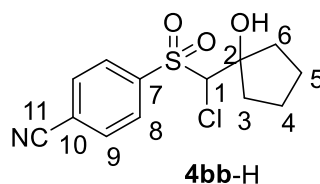
Procedure D for the synthesis of halohydrin 4-H: To a solution of **2-H** (0.2 mmol) in anhydrous THF (1 mL) at -78°C was added dropwise a freshly prepared solution of LDA (0.24 mmol) or $n\text{-BuLi}$ (0.24 mmol) in 1 mL anhydrous THF. After 10 min, a solution of **1** (0.30 mmol) in 0.5 mL anhydrous THF was added dropwise at -78°C . After another 30 min, 2% aq HCl (10 mL) was added at -78°C and the mixture was washed with CHCl_3 (2×15 mL). Then the aqueous phase was neutralized by adding NaHCO_3 . Afterwards, the aqueous phase was extracted with CHCl_3 (3×15 mL). The combined organic phases were washed with brine (1×30 mL), dried with anhydrous MgSO_4 , and filtered. The solvent was evaporated under reduced pressure, and the residue was product **4-H** and analyzed without further purification.

4-((Chloro(1-hydroxycyclobutyl)methyl)sulfonyl)benzonitrile (4ab-H) was obtained according to Procedure C from **1a** (21 mg, 0.30 mmol), **2b-H** (43 mg, 0.20 mmol), and LDA (0.24 mmol): white solid (50 mg, 90%), mp $120\text{--}124^\circ\text{C}$.



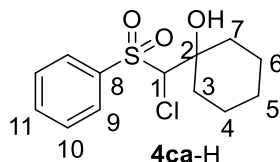
^1H NMR (400 MHz, CDCl_3) δ 8.11 (d, $J = 8.4$ Hz, 2 H, H-7), 7.87 (d, $J = 8.4$ Hz, 2 H, H-8), 4.88 (s, 1H, H-1), 2.92 (s, 1 H, OH), 2.85–2.76 (m, 1 H, H-3), 2.41–2.30 (m, 2 H, H-3 and H-5), 2.17–2.03 (m, 2 H, H-4 and H-5), 1.87–1.74 (m, 1 H, H-4). **^{13}C NMR** (101 MHz, CDCl_3) δ 141.0 (C-6), 132.7 (C-8), 131.0 (C-7), 118.4 (C-9), 117.1 (C-10), 78.9 (C-1), 77.0 (C-2), 35.2 (C-5), 33.9 (C-3), 13.7 (C-4). **HRMS** (EI) m/z : $[\text{M}^+]$ calcd for $[\text{C}_{12}\text{H}_{12}\text{ClNO}_3\text{S}]^+$ 285.0221, found 285.0221. **IR** (ATR) ν (cm^{-1}) = 3496, 2948, 2240, 1332, 1267, 1168, 1147, 1080, 1014, 865, 841, 788, 739, 662.

4-((Chloro(1-hydroxycyclopentyl)methyl)sulfonyl)benzonitrile (4bb-H) was obtained according to Procedure C from **1b** (25 mg, 0.30 mmol), **2b-H** (43 mg, 0.20 mmol), and LDA (0.24 mmol): white solid (51 mg, 85%), mp 116–121 °C.



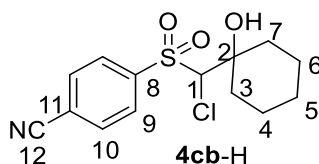
¹H NMR (599 MHz, CDCl₃) δ 8.11 (d, *J* = 8.4 Hz, 2 H, H-8), 7.88 (d, *J* = 8.4 Hz, 2 H, H-9), 4.82 (s, 1 H, H-1), 2.94 (s, 1 H, OH), 2.15–2.01 (m, 2 H, H-3), 1.99–1.90 (m, 3 H, H-4, H-6), 1.89–1.82 (m, 1 H, H-5), 1.81–1.68 (m, 2 H, H-4 and H-5). **¹³C NMR** (151 MHz, CDCl₃) δ 141.3 (C-7), 132.8 (C-9), 130.6 (C-8), 118.4 (C-10), 117.1 (C-11), 83.9 (C-2), 79.5 (C-1), 39.1 (C-3), 38.9 (C-6), 24.5 (C-4), 23.3 (C-5). **HRMS** (EI) *m/z*: [*M*⁺] calcd for [C₁₃H₁₄ClNO₃S]⁺ 299.0377, found 299.0395. **IR** (ATR) *ν* (cm⁻¹) = 3535, 3096, 2962, 2232, 1392, 1321, 1285, 1204, 1142, 1080, 1022, 838, 810, 745.

1-(Chloro(phenylsulfonyl)methyl)cyclohexan-1-ol (4ca-H) was obtained according to Procedure C from **1c** (29 mg, 0.30 mmol), **2a-H** (38 mg, 0.20 mmol), and *n*-BuLi (0.24 mmol): white solid (52 mg, 90%), mp 150–154 °C. (mp 150–151 °C in ref [S5](#))



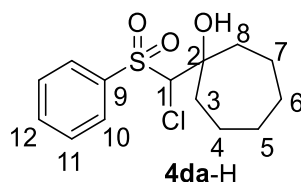
¹H NMR (400MHz, CDCl₃) δ 7.97 (d, *J* = 7.1 Hz, 2 H, H-9), 7.70 (t, *J* = 7.4 Hz, 1 H, H-11), 7.63–7.51 (t, *J* = 8.0 Hz, 2 H, H-10), 4.61 (s, 1 H, H-1), 3.15 (s, 1 H, OH), 2.13 (m, 1 H, H-7), 1.97–1.60 (m, 8 H, H-3, H-4, H5, H-6, H-7), 1.26–1.19 (m, 1 H, H-5). **¹³C NMR** (101 MHz, CDCl₃) δ 137.9 (C-8), 134.7 (C-11), 129.5 (C-10), 129.3 (C-9), 80.3 (C-1), 76.2 (C-2), 35.6 (C-3), 32.9 (C-7), 25.3 (C-5), 21.4/21.3 (C-4, C-6). **HRMS** (EI) *m/z*: [*M*⁺] calcd for [C₁₃H₁₇ClO₃S]⁺ 288.0581, found 288.0579. **IR** (ATR) *ν* (cm⁻¹) = 3470, 2936, 2863, 1584, 1446, 1380, 1307, 1291, 1145, 1081, 978, 944, 811, 772, 751, 720, 699, 684.

4-((Chloro(1-hydroxycyclohexyl)methyl)sulfonyl)benzonitrile (4cb-H) was obtained according to Procedure C from **1c** (29 mg, 0.30 mmol), **2b-H** (43 mg, 0.20 mmol), and LDA (0.24 mmol): white solid (53 mg, 85%), mp 120–124 °C.



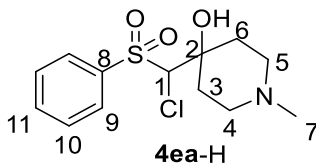
¹H NMR (400 MHz, CDCl₃) δ 8.09 (d, *J* = 8.5 Hz, 2 H, H-9), 7.88 (d, *J* = 8.4 Hz, 2 H, H-10), 4.63 (s, 1 H, H-1), 3.17 (d, *J* = 1.6 Hz, 1 H, OH), 2.13–2.02 (m, 1 H, H-7), 1.97–1.77 (m, 3 H, H-3 × 2, H-7), 1.76–1.56 (m, 5 H, H-4 × 2, H-5, H-6 × 2), 1.30–1.16 (m, 1 H, H-5). **¹³C NMR** (101 MHz, CDCl₃) δ 141.8 (C-8), 132.9 (C-10), 130.2 (C-9), 118.4 (C-11), 117.1 (C-12), 80.4 (C-1), 76.2 (C-2), 35.5/33.5 (C-3, C-7), 25.2 (C-5), 21.4/21.3 (C-4, C-6). **HRMS** (ESI[−]) *m/z*: [M-H][−] calcd for [C₁₄H₁₅ClNO₃S][−] 312.0467, found 312.0468. **IR** (ATR) ν (cm^{−1}) = 3522, 2935, 2860, 2235, 1448, 1394, 1327, 1287, 1146, 1079, 982, 912, 841, 804, 752, 661.

1-(Chloro(phenylsulfonyl)methyl)cycloheptan-1-ol (4da-H) was obtained according to Procedure C from **1d** (34 mg, 0.30 mmol), **2a-H** (38 mg, 0.20 mmol), and n-BuLi (0.24 mmol): white solid (52 mg, 85%), mp 135–140 °C.



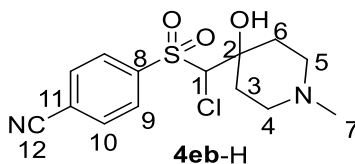
¹H NMR (400 MHz, CDCl₃) δ 7.97 (d, *J* = 7.1 Hz, 2 H, H-10), 7.70 (t, *J* = 7.5 Hz, 1 H, H-12), 7.59 (t, *J* = 7.7 Hz, 2 H, H-11), 4.63 (s, 1 H, H-1), 3.70 (s, 1 H, OH), 2.21 (m, 2 H, H-8), 2.11 (dd, *J* = 15.3, 9.9 Hz, 1 H, H-3), 1.85–1.68 (m, 4 H, H-3, H-6 × 2, H-7), 1.68–1.52 (m, 4 H, H-4 × 2, H-5, H-7), 1.50–1.40 (m, 1 H, H-5). **¹³C NMR** (101 MHz, CDCl₃) δ 137.9 (C-9), 134.7 (C-12), 129.5 (C-11), 129.3 (C-10), 81.4 (C-1), 79.7 (C-2), 40.4 (C-3), 36.7 (C-8), 29.5 (C-5), 29.1 (C-6), 22.5 (C-7), 22.3 (C-4). **HRMS** (EI) *m/z*: [M⁺] calcd for [C₁₄H₁₉ClO₃S]⁺ 302.0738, found 302.0736. **IR** (ATR) ν (cm^{−1}) = 3473, 2945, 2860, 1584, 1446, 1309, 1290, 1148, 1084, 998, 811, 749, 717, 686.

4-(Chloro(phenylsulfonyl)methyl)-1-methylpiperidin-4-ol (4ea-H) was obtained according to Procedure D from **1e** (23 mg, 0.20 mmol), **2a-H** (57 mg, 0.30 mmol), and n-BuLi (0.30 mmol): white solid (47 mg, 75%), mp 160–164 °C.



¹H NMR (400 MHz, CDCl₃) δ 7.97 (d, *J* = 7.2 Hz, 2 H, H-9), 7.71 (t, *J* = 7.4 Hz, 1 H, H-11), 7.60 (t, *J* = 7.7 Hz, 2 H, H-10), 4.60 (s, 1 H, H-1), 3.62 (s, 1 H, OH), 2.80–2.61 (m, 2 H, H-5), 2.44–2.35 (m, 2 H, H-4), 2.31 (s, 3 H, H-7), 2.24 (td, *J* = 12.9, 4.5 Hz, 1 H, H-3), 2.15–2.07 (m, 2 H, H-6), 1.86–1.79 (m, 1 H, H-3). **¹³C NMR** (101 MHz, CDCl₃) δ 137.6 (C-8), 134.8 (C-11), 129.6 (C-10), 129.3 (C-9), 79.5 (C-1), 73.8 (C-2), 50.64 (C-4), 50.62 (C-5), 46.2 (C-7), 35.5 (C-3), 33.1 (C-6). **HRMS** (EI) *m/z*: [M⁺] calcd for [C₁₃H₁₈ClNO₃S]⁺ 303.0690, found 303.0695. **IR** (ATR) *ν* (cm⁻¹) = 2953, 2804, 1467, 1450, 1383, 1311, 1173, 1151, 1083, 1060, 1009, 948, 795, 778, 735, 712, 687.

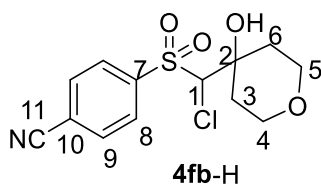
4-((Chloro(4-hydroxy-1-methylpiperidin-4-yl)methyl)sulfonyl)benzonitrile (4eb-H) was obtained according to Procedure D from **1e** (23 mg, 0.20 mmol), **2b-H** (65 mg, 0.30 mmol), and LDA (0.30 mmol): white solid (62 mg, 95%), mp 140–145 °C.



¹H NMR (400 MHz, CDCl₃) δ 8.10 (d, *J* = 6.7 Hz, 2 H, H-9), 7.89 (d, *J* = 6.8 Hz, 2 H, H-10), 4.62 (s, 1 H, H-1), 3.26 (s, 1 H, OH), 2.76–2.66 (m, 2 H, H-4 and H-5), 2.37 (t, *J* = 11.9 Hz, 2 H, H-4 and H-5), 2.31 (s, 3 H, H-7), 2.22 (td, *J* = 12.7, 4.2 Hz, 1 H, H-3), 2.09–2.03 (m, 2 H, H-6), 1.90 (d, *J* = 12.8 Hz, 1 H, H-3). **¹³C NMR** (101 MHz, CDCl₃) δ 141.5 (C-8), 132.9 (C-10), 130.3 (C-9), 118.4 (C-11), 117.0 (C-12), 79.9 (C-1), 73.6 (C-2), 50.6/50.5 (C-4, C-5), 46.0 (C-7), 35.3 (C-3), 33.8 (C-6). **HRMS** (EI) *m/z*: [M⁺] calcd for [C₁₄H₁₇ClN₂O₃S]⁺ 328.0643, found 328.0647. **IR** (ATR) *ν* (cm⁻¹) = 3090, 2981, 2806, 2236, 1465, 1386, 1328, 1310, 1173, 1152, 1061, 1010, 950, 847, 788, 744.

4-((Chloro(4-hydroxytetrahydro-2H-pyran-4-yl)methyl)sulfonyl)benzonitrile (4fb-H)

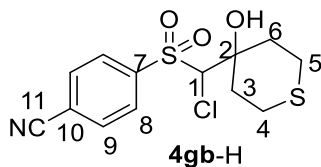
was obtained according to Procedure C from **1f** (30 mg, 0.30 mmol), **2b-H** (43 mg, 0.20 mmol), and LDA (0.24 mmol): colorless liquid (51 mg, 80%).



¹H NMR (400 MHz, CDCl₃) δ 8.10 (d, *J* = 8.4 Hz, 2 H, H-8), 7.90 (d, *J* = 8.3 Hz, 2 H, H-9), 4.62 (s, 1 H, H-1), 3.91–3.74 (m, 4 H, H-4, H-5), 3.39 (s, 1 H, OH), 2.34–2.18 (m, 1 H, H-3), 2.17–2.00 (m, 1 H, H-6), 1.93 (dd, *J* = 13.9, 2.6 Hz, 1 H, H-6), 1.86–1.76 (m, 1 H, H-3). **¹³C NMR** (101 MHz, CDCl₃) δ 141.3 (C-7), 133.0 (C-9), 130.3 (C-8), 118.7 (C-10), 117.0 (C-11), 79.5 (C-1), 73.7 (C-2), 62.95/62.92 (C4, C-5), 35.8 (C-3), 34.1 (C-6). **HRMS** (EI) *m/z*: [M⁺] calcd for [C₁₃H₁₄ClNO₄S]⁺ 315.0327, found 315.0327. **IR** (ATR) *ν* (cm⁻¹) = 3509, 2962, 2872, 2236, 1394, 1330, 1158, 1141, 1020, 911, 844, 749, 676.

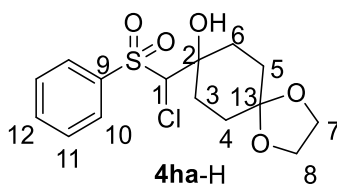
4-((Chloro(4-hydroxytetrahydro-2H-thiopyran-4-yl)methyl)sulfonyl)benzonitrile (4gb-H)

was obtained according to Procedure C from **1g** (35 mg, 0.30 mmol), **2b-H** (43 mg, 0.20 mmol), and LDA (0.24 mmol): white solid (46 mg, 70%), mp 120–124 °C.



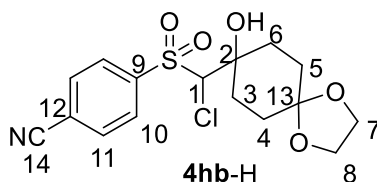
¹H NMR (599 MHz, CDCl₃) δ 8.10 (d, *J* = 7.9 Hz, 2 H, H-8), 7.91 (d, *J* = 8.0 Hz, 2 H, H-9), 4.53 (s, 1 H, H-1), 3.51 (s, 1 H, OH), 3.15–3.11 (m, 2 H, H-5), 2.52–2.40 (m, 3 H, H-4 × 2, H-6), 2.32–2.20 (m, 2 H, H-3 and H-6), 2.03 (m, 1 H, H-3). **¹³C NMR** (151 MHz, CDCl₃) δ 141.4 (C-7), 133.1 (C-9), 130.2 (C-8), 118.7 (C-10), 116.9 (C-11), 79.9 (C-1), 75.5 (C-2), 36.7 (C-3), 33.9 (C-6), 23.4 (C-4 and C-5). **HRMS** (EI) *m/z*: [M⁺] calcd for [C₁₃H₁₄ClNO₃S₂]⁺ 331.0098, found 331.0097. **IR** (ATR) *ν* (cm⁻¹) = 3506, 2924, 2235, 1427, 1394, 1320, 1284, 1214, 1147, 1077, 934, 911, 841, 753, 656.

8-(Chloro(phenylsulfonyl)methyl)-1,4-dioxaspiro[4.5]decan-8-ol (4ha-H) was obtained according to Procedure C from **1h** (31 mg, 0.20 mmol), **2a-H** (57 mg, 0.30 mmol), and *n*-BuLi (0.30 mmol): white solid (49 mg, 70%), 122–126 °C.



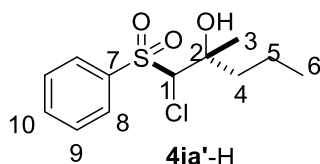
¹H NMR (400 MHz, CDCl₃) δ 7.97 (d, *J* = 7.0 Hz, 2 H, H-10), 7.71 (t, *J* = 7.5 Hz, 1 H, H-12), 7.60 (t, *J* = 7.8 Hz, 2 H, H-11), 4.63 (s, 1 H, H-1), 4.04–3.84 (m, 4 H, H-7, H-8), 3.67 (d, *J* = 2.0 Hz, 1 H, OH), 2.28–1.96 (m, 5 H, H-3, H-4, H-6), 1.88–1.80 (m, 1 H, H-3), 1.73–1.54 (m, 2 H, H-5). **¹³C NMR** (101 MHz, CDCl₃) δ 137.7 (C-9), 134.8 (C-12), 129.5 (C-11), 129.3 (C-10), 107.9 (C-13), 79.6 (C-1), 75.3 (C-2), 64.6 (C-8), 64.4 (C-7), 33.6 (C-3), 30.6/30.0 (C-4, C-6), 29.9 (C-5). **HRMS** (EI) *m/z*: [*M*⁺] calcd for [C₁₅H₁₉ClO₅S]⁺ 346.0636, found 346.0648. **IR** (ATR) *ν* (cm⁻¹) = 3447, 2945, 2889, 1583, 1446, 1310, 1279, 1167, 1112, 1080, 1005, 972, 951, 799, 738, 688.

4-((Chloro(8-hydroxy-1,4-dioxaspiro[4.5]decan-8-yl)methyl)sulfonyl)benzonitrile (4hb-H) was obtained according to Procedure C from **1h** (31 mg, 0.20 mmol), **2b-H** (43 mg, 0.20 mmol), and LDA (0.24 mmol): colorless liquid (69 mg, 95%).



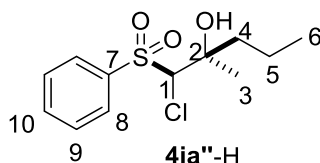
¹H NMR (599 MHz, CDCl₃) δ 8.10 (d, *J* = 8.6 Hz, 2 H, H-10), 7.90 (d, *J* = 8.4 Hz, 2 H, H-11), 4.65 (s, 1 H, H-1), 4.05–3.87 (m, 4 H, H-7 and H-8), 3.31 (d, *J* = 1.8 Hz, 1 H, OH), 2.26–2.15 (m, 2 H, H-3 and H-6), 2.14–2.07 (m, 1 H, H-6), 2.06–1.97 (m, 2 H, H-5), 1.95–1.90 (m, 1 H, H-3), 1.71–1.64 (m, 2 H, H-4). **¹³C NMR** (151 MHz, CDCl₃) δ 141.6 (C-9), 133.0 (C-11), 130.3 (C-10), 118.5 (C-12), 117.0 (C-14), 107.7 (C-13), 79.7 (C-1), 75.3 (C-2), 64.6 (C-8), 64.4 (C-7), 33.5 (C-3), 31.2 (C-6), 30.0 (C-4), 29.9 (C-5). **HRMS** (ESI⁻) *m/z*: [*M*+HCOO]⁻ calcd for [C₁₇H₁₉ClNO₇S]⁻ 416.0576 found 416.0583. **IR** (ATR) *ν* (cm⁻¹) = 3510, 2933, 2235, 1395, 1326, 1146, 1098, 1035, 993, 842, 804, 750, 682.

1-Chloro-2-methyl-1-(phenylsulfonyl)pentan-2-ol (4ia-H) was obtained according to Procedure C from **1i** (26 mg, 0.30 mmol), **2a-H** (38 mg, 0.20 mmol), and n-BuLi (0.24 mmol): **4ia'**-H (34 mg, 60%) and **4ia''**-H (18 mg, 33%).



white solid, mp 69–73 °C

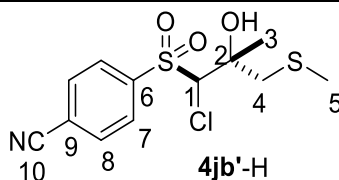
¹H NMR (400 MHz, CDCl₃) δ 7.97 (d, *J* = 7.2 Hz, 2 H, H-8), 7.71 (t, *J* = 7.5 Hz, 1 H, H-10), 7.67–7.51 (t, *J* = 8.0 Hz, 2 H, H-9), 4.66 (s, 1 H, H-1), 3.51 (br s, 1 H, OH), 2.06–1.91 (m, 2 H, H-4), 1.64–1.53 (m, 1 H, H-5), 1.49–1.38 (m, 4 H, H-3, H-5), 0.99 (t, *J* = 7.3 Hz, 3 H, H-6). **¹³C NMR** (101 MHz, CDCl₃) δ 137.8 (C-7), 134.7 (C-10), 129.5 (C-9), 129.3 (C-8), 80.2 (C-1), 77.1 (C-2), 40.1 (C-4), 25.3 (C-3), 16.9 (C-5), 14.6 (C-6). **HRMS** (EI) *m/z*: [M⁺] calcd for [C₁₂H₁₇ClO₃S]⁺ 276.0581, found 276.0580. **IR** (ATR) *ν* (cm⁻¹) = 3519, 2937, 2874, 1582, 1447, 1395, 1302, 1250, 1159, 1139, 1076, 1022, 966, 914, 825, 790, 759, 716, 683, 618, 562.



white solid, mp 68–72 °C

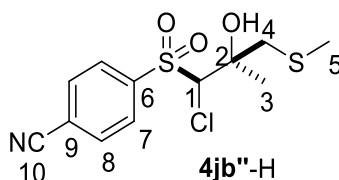
¹H NMR (400 MHz, CDCl₃) δ 7.98 (d, *J* = 7.3 Hz, 2 H, H-8), 7.72 (t, *J* = 7.5 Hz, 1 H, H-10), 7.64–7.51 (t, *J* = 8.0 Hz, 2 H, H-9), 4.62 (s, 1 H, H-1), 3.91 (s, 1 H, OH), 1.77–1.68 (m, 1 H, H-4), 1.66–1.59 (m, 4 H, H-3, H-4), 1.57–1.46 (m, 1 H, H-5), 1.40–1.23 (m, 1 H, H-5), 0.91 (t, *J* = 7.3 Hz, 3 H, H-6). **¹³C NMR** (101 MHz, CDCl₃) δ 137.8 (C-7), 134.8 (C-10), 129.5 (C-9), 129.4 (C-8), 78.5 (C-1), 76.8 (C-2), 43.4 (C-4), 23.6 (C-3), 16.0 (C-5), 14.3 (C-6). **HRMS** (EI) *m/z*: [M⁺] calcd for [C₁₂H₁₇ClO₃S]⁺ 276.0581, found 276.0597. **IR** (ATR) *ν* (cm⁻¹) = 3473, 2944, 2873, 1583, 1447, 1307, 1140, 1081, 1023, 902, 863, 815, 751, 714, 685, 611, 566.

4-((1-Chloro-2-hydroxy-2-methyl-3-(methylthio)propyl)sulfonyl)benzonitrile (4jb-H) was obtained according to Procedure C from **1j** (47 mg, 0.45 mmol), **2b-H** (65 mg, 0.30 mmol), and LDA (0.36 mmol): **4jb'**-H (41 mg, 43%) and **4jb''**-H (37 mg, 40%).



pale yellow liquid

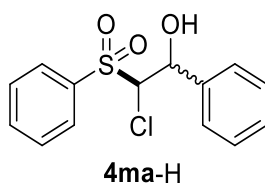
¹H NMR (400 MHz, CDCl₃) δ 8.10 (d, *J* = 7.6 Hz, 2 H, H-7), 7.89 (d, *J* = 7.7 Hz, 2 H, H-8), 5.17 (s, 1 H, H-1), 3.27 (d, *J* = 13.9 Hz, 1 H, H-4), 3.05 (s, 1 H, OH), 2.99 (d, *J* = 13.5 Hz, 1 H, H-4), 2.25 (s, 3 H, H-5), 1.68 (s, 3 H, H-3). **¹³C NMR** (101 MHz, CDCl₃) δ 141.7 (C-6), 133.0 (C-8), 130.3 (C-7), 118.4 (C-9), 117.0 (C-10), 78.9 (C-1), 77.4 (C-2), 44.6 (C-4), 25.2 (C-3), 18.1 (C-5). **HRMS** (EI) *m/z*: [*M*⁺] calcd for [C₁₂H₁₄ClNO₃S₂]⁺ 319.0098, found 319.0100. **IR** (ATR) *ν* (cm⁻¹) = 3496, 2923, 2235, 1395, 1329, 1288, 1151, 1079, 913, 841, 808, 753, 731.



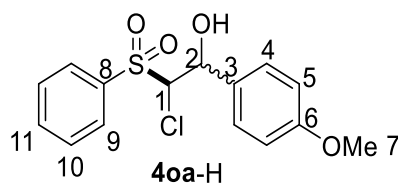
pale yellow liquid

¹H NMR (400 MHz, CDCl₃) δ 8.13 (d, *J* = 7.8 Hz, 2 H, H-7), 7.91 (d, *J* = 7.7 Hz, 2 H, H-8), 5.14 (s, 1 H, H-1), 3.80 (s, 1 H, OH), 2.93–2.79 (m, 2 H, H-4), 2.24 (s, 3 H, H-5), 1.70 (s, 3 H, H-3). **¹³C NMR** (101 MHz, CDCl₃) δ 141.5 (C-6), 133.1 (C-8), 130.3 (C-7), 118.6 (C-9), 117.0 (C-10), 78.5 (C-1), 77.4 (C-2), 45.6 (C-4), 23.7 (C-3), 18.1 (C-5). **HRMS** (EI) *m/z*: [*M*⁺] calcd for [C₁₂H₁₄ClNO₃S₂]⁺ 319.0098, found 319.0095. **IR** (ATR) *ν* (cm⁻¹) = 3516, 2924, 2236, 1396, 1324, 1287, 1148, 1081, 1017, 913, 842, 808, 753, 732.

2-Chloro-1-phenyl-2-(phenylsulfonyl)ethan-1-ol (4ma-H) was obtained according to Procedure C from **1m** (48 mg, 0.45 mmol), **2a-H** (57 mg, 0.30 mmol), and *n*-BuLi (0.36 mmol): colorless liquid (80 mg, 0.27 mmol, 90%, dr = 1/1.4). NMR characterizations are as reported in ref. [S6](#).



2-Chloro-1-(4-methoxyphenyl)-2-(phenylsulfonyl)ethan-1-ol (4oa-H) was obtained according to Procedure C from **1o** (61 mg, 0.45 mmol), **2a-H** (57 mg, 0.30 mmol), and n-BuLi (0.36 mmol): colorless liquid (83 mg, 83%, dr = 1/1.4).

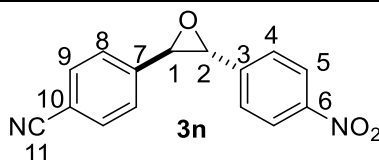


¹H NMR (400 MHz, CDCl₃) major diastereomer: δ 8.03–7.98 (m, 2H, H-9), 7.77–7.70 (m, 1 H, H-11), 7.65–7.56 (m, 2 H, H-10), 7.36–7.27 (m, 2 H, H-4), 6.88 (m, 2 H, H-5), 5.14 (dd, *J* = 8.9, 2.2 Hz, 1 H, H-2), 4.80 (d, *J* = 8.9 Hz, 1 H, H-1), 4.17 (d, *J* = 2.2 Hz, 1 H, OH), 3.79 (s, 3 H, H-7). minor diastereomer: δ 8.03–7.98 (m, 2 H, H-9), 7.77–7.70 (m, 1 H, H-11), 7.65–7.56 (m, 2 H, H-10), 7.36–7.27 (m, 2 H, H-4), 6.88 (m, 2 H, H-5), 5.85 (d, *J* = 3.5 Hz, 1 H, H-2), 4.73 (d, *J* = 1.4 Hz, 1 H, H-1), 3.79 (s, 3 H, H-7), 3.18 (d, *J* = 3.6 Hz, 1 H, OH). **¹³C NMR** (101 MHz, CDCl₃) major diastereomer: δ 160.21 (C-6), 135.55 (C-11), 135.07 (C-8), 130.35 (C-3), 130.08 (C-9), 129.38 (C-10), 128.93 (C-4), 113.97 (C-5), 76.09 (C-1), 73.76 (C-2), 55.39 (C-7). minor diastereomer: δ 159.91 (C-6), 135.65 (C-11), 134.98 (C-8), 130.32 (C-3), 130.01 (C-9), 129.33 (C-10), 130.01 (C-4), 114.07 (C-5), 78.84 (C-1), 69.45 (C-2), 55.43 (C-7). **HRMS** (EI) *m/z*: [*M*⁺] calcd for [C₁₅H₁₅ClO₄S]⁺ 326.0374, found 326.0369.

Other products

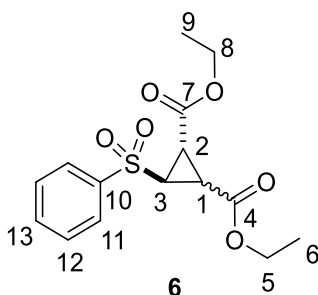
4-((rel-2R,3R)-3-(4-Nitrophenyl)oxiran-2-yl)benzonitrile (**3n**)

To a solution of **1n** (30 mg, 0.20 mmol) and **13** (80 mg, 0.30 mmol) in anhydrous DMSO (2 mL) at room temperature was added NaOH (12 mg, 0.30 mmol). After 4 h, 2% aq HCl (10 mL) was added and the mixture was extracted with CHCl₃ (3 × 15 mL). The organic phase was washed with water (2 × 30 mL) and brine (1 × 30 mL) to remove remaining DMSO, dried over anhydrous MgSO₄, and filtered. The solvent was evaporated under reduced pressure, and the residue was purified by column chromatography to give epoxide **3n**: yellow solid (44.2 mg, 83%), mp 190–195 °C.



¹H NMR (400 MHz, CDCl₃) δ 8.26 (d, *J* = 8.7 Hz, 2 H, H-5), 7.70 (d, *J* = 8.2 Hz, 2 H, H-9), 7.52 (d, *J* = 8.7 Hz, 2 H, H-4), 7.47 (d, *J* = 8.2 Hz, 2 H, H-8), 3.95 (d, *J* = 1.7 Hz, 1 H, H-2), 3.92 (d, *J* = 1.8 Hz, 1 H, H-1). **¹³C NMR** (101 MHz, CDCl₃) δ 148.2 (C-6), 143.5 (C-3), 141.5 (C-7), 132.7 (C-9), 126.5 (C-4), 126.4 (C-8), 124.1 (C-5), 118.5 (C-11), 112.7 (C-10), 62.4 (C-1), 62.1 (C-2). **HRMS** (EI) *m/z*: [*M*⁺] calcd for [C₁₅H₁₀N₂O₃]⁺ 266.0686, found 266.0687. **IR** (ATR) *ν* (cm⁻¹) = 2923, 2228, 1601, 1516, 1344, 1094, 1016, 855, 821, 752, 719, 688.

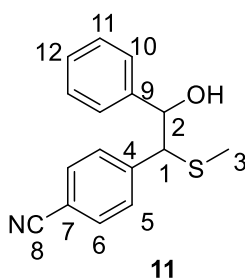
Diethyl 3-(phenylsulfonyl)cyclopropane-1,2-dicarboxylate (6)^{S7} was obtained according to Procedure A from **5** (52 mg, 0.30 mmol), **2a-H** (57 mg, 0.30 mmol), and NaOH (14 mg, 0.35 mmol): colorless liquid (78 mg, 80%, rel-1*R*,2*S*,3*s*/rel-1*S*,2*S* = 1/0.45)



¹H NMR (599 MHz, CDCl₃) rel-1*R*,2*S*,3*s*: δ 7.92 (t, *J* = 8.6 Hz, 2 H, H-11), 7.70–7.64 (m, 1 H, H-13), 7.58 (t, *J* = 7.7 Hz, 2 H, H-12), 4.16–4.07 (m, 4 H, H-5, H-8), 3.54 (t, *J* = 5.7 Hz, 1 H, H-3), 2.82 (d, *J* = 5.8 Hz, 2 H, H-1 and H-2), 1.21 (t, *J* = 7.2 Hz, 6 H, H-6 and H-9). rel-1*S*,2*S*: δ 7.92 (t, *J* = 8.6 Hz, 2 H, H-11), 7.70–7.64 (m, 1 H, H-13), 7.58 (t, *J* = 7.7 Hz, 2 H, H-12), 4.28–4.18 (m, 2 H, H-8), 4.17–4.14 (m, 2 H, H-5), 3.20 (dd, *J* = 9.6, 5.6 Hz, 1 H, H-3), 3.15 (t, *J* = 6.0 Hz, 1 H, H-2), 2.67 (dd, *J* = 9.3, 6.8 Hz, 1 H, H-1), 1.29 (t, *J* = 7.1 Hz, 3 H, H-9), 1.26 (t, *J* = 7.2 Hz, 3 H, H-6). **¹³C NMR** (151 MHz, CDCl₃) rel-1*R*,2*S*,3*s*: δ 166.1 (C-4 and C-7), 139.1 (C-10), 134.3 (C-13), 129.6 (C-12), 127.8 (C-11), 62.1 (C-5 and C-8), 43.0 (C-3), 26.8 (C-1 and C-2), 14.1 (C-6 and C-9). rel-1*S*,2*S*: δ 169.0 (C-4), 165.0 (C-7), 139.8 (C-10), 134.2 (C-13), 129.4 (C-12), 128.0 (C-11), 62.3 (C-5), 62.2 (C-8), 45.4 (C-3), 29.9 (C-1), 24.2 (C-2), 14.0 (C-6 and C-9). **HRMS** (EI) *m/z*: [*M*⁺] calcd for [C₁₅H₁₈O₆S]⁺ 326.0819, found 326.0818.

4-(2-Hydroxy-1-(methylthio)-2-phenylethyl)benzonitrile (11)

To a solution of **10** (82 mg, 0.50 mmol) in anhydrous THF (3 mL) at -78 °C was dropwise added a freshly prepared solution of LDA (0.60 mmol) in anhydrous THF (1 mL). After 10 min, a solution of **1m** (80 mg, 0.75 mmol) in anhydrous THF (1mL) was added at -78 °C dropwise. Then the cooling bath was removed and the reaction was stirred for 30 min at room temperature. Afterwards, 2% aq HCl (10 mL) was added, and the mixture was extracted with CHCl₃. The organic phase was washed with brine, dried over anhydrous MgSO₄, and filtered. The solvent was evaporated under reduced pressure, and the residue was purified by column chromatography to give **11**: yellow liquid (129 mg, 96%, dr = 1.2 : 1).

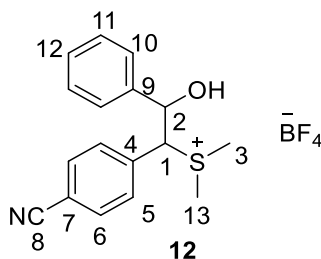


¹H NMR (400 MHz, CDCl₃) Diastereomer A: δ 7.53 (d, J = 7.9 Hz, 2 H, H-6), 7.36 (d, J = 7.9 Hz, 2 H, H-5), 7.31–7.25 (m, 2 H, H-11), 7.21–7.16 (m, 3 H, H-10, H-12), 5.03 (d, J = 6.0 Hz, 1 H, H-2), 3.98 (d, J = 5.9 Hz, 1 H, H-1), 3.21 (br s, 1 H, OH), 1.86 (s, 3 H, H-3). Diastereomer B: δ 7.46 (d, J = 7.8 Hz, 2 H, H-6), 7.31–7.25 (m, 2 H, H-11), 7.23 (d, J = 8.1 Hz, 2 H, H-5), 7.21–7.16 (m, 1 H, H-12), 7.12–7.07 (m, 2 H, H-10), 4.84 (d, J = 7.9 Hz, 1 H, H-2), 3.98 (d, J = 5.9 Hz, 1 H, H-1), 2.69 (br s, 1 H, OH), 1.97 (s, 3 H, H-3). **¹³C NMR** (101 MHz, CDCl₃) Diastereomer A : δ 144.27 (C-4), 140.73 (C-9), 131.91 (C-6), 129.97 (C-5), 128.31 (C-11), 128.25 (C-12), 126.46 (C-10), 118.80 (C-8), 111.15 (C-7), 76.04 (C-2), 59.16 (C-1), 15.16 (C-3). Diastereomer B : δ 144.91 (C-4), 140.31 (C-9), 132.00 (C-6), 129.49 (C-5), 128.26 (C-11), 128.19 (C-12), 126.66 (C-10), 118.66 (C-8), 111.02 (C-7), 76.75 (C-2), 61.00 (C-1), 15.00 (C-3). **HRMS** (ESI⁻) m/z : [M+HCOO]⁻ calcd for [C₁₇H₁₆NO₃S]⁻ 314.0856 found 314.0858.

(1-(4-Cyanophenyl)-2-hydroxy-2-phenylethyl)dimethylsulfonium tetrafluoroborate (12)

To a suspension of trimethyloxonium tetrafluoroborate (29.6 mg, 0.200 mmol) in CH₂Cl₂ (1 mL) was added a solution of sulfide **11** (53.9 mg, 0.200 mmol) in CH₂Cl₂ (1 mL) at 0 °C. The reaction mixture was stirred for 1 h at 0 °C and then for 14 h at room temperature. After

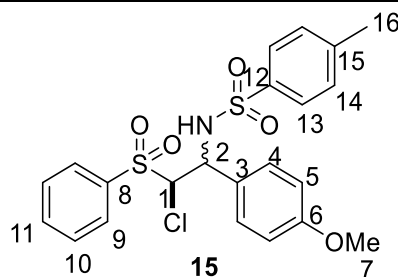
removal of the solvent, the solid residue was washed with CH₂Cl₂ to give the sulfonium tetrafluoroborate **12** as a mixture of diastereomers (68 mg, 90%, dr = 1.2/1)



¹H NMR (400 MHz, CD₃CN) Diastereomer A: δ 7.75 (d, J = 8.5 Hz, 2 H, H-6), 7.52 (d, J = 6.5 Hz, 2 H, H-5), 7.26 (s, 5 H, H-10, H-11, H-12), 5.45 (d, J = 9.8 Hz, 1 H, H-2), 5.01 (d, J = 9.8 Hz, 1 H, H-1), 4.81 (brs, 1 H, OH), 2.97 (s, 3 H, H-3), 2.45 (s, 3 H, H-13). Diastereomer B: δ 7.66 (d, J = 8.6 Hz, 2 H, H-6), 7.50 (d, J = 6.6 Hz, 2 H, H-5), 7.22–7.15 (m, 5 H, H-10, H-11, H-12), 5.61 (d, J = 4.0 Hz, 1 H, H-2), 4.93 (d, J = 4.1 Hz, 1 H, H-1), 4.69 (brs, 1 H, OH), 3.05 (s, 3 H, H-3), 2.58 (s, 3 H, H-13). **¹³C NMR** (101 MHz, CD₃CN) Diastereomer A: δ 140.3 (C-9), 135.3 (C-4), 134.3 (C-6), 132.0 (C-5), 129.9 (C-12), 129.7 (C-11), 128.0 (C-10), 118.7 (C-8), 114.9 (C-7), 75.6 (C-2), 67.4 (C-1), 28.2 (C-3), 24.1 (C-13). Diastereomer B: δ 139.4 (C-9), 134.8 (C-4), 133.6 (C-6), 132.6 (C-5), 129.3 (C-11), 129.2 (C-12), 126.9 (C-10), 118.9 (C-8), 114.5 (C-7), 71.6 (C-2), 66.2 (C-1), 24.8 (C-3), 24.6 (C-13). **HRMS** (ESI⁺) m/z : [M–BF₄]⁺ calcd for [C₁₇H₁₈NOS]⁺ 284.1104 found 284.1104.

N-(2-Chloro-1-(4-methoxyphenyl)-2-(phenylsulfonyl)ethyl)-4-methylbenzenesulfonamide (**15**)

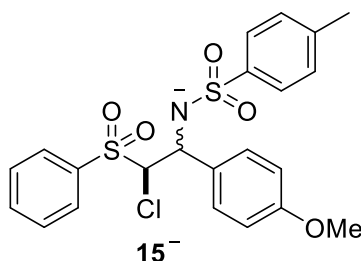
To a solution of **14** (58 mg 0.20 mmol) and **2a**-H (38 mg, 0.20 mmol) in anhydrous DMSO (2 mL) at room temperature was added NaOH (8 mg, 0.2 mmol). After 2 h, saturated NH₄Cl solution (10 mL) was added, and the mixture was extracted with CHCl₃. The organic phase was washed with water (2 × 30 mL) and brine (1 × 30 mL) to remove remaining DMSO, dried over anhydrous MgSO₄, and filtered. The solvent was evaporated under reduced pressure, and the residue was purified by column chromatography to give **15**: colorless liquid (77 mg, dr = 5.7 : 1). NMR chemical shifts for the major diastereomer are listed below.



¹H NMR (599 MHz, CDCl₃) δ 7.82 (d, *J* = 7.3 Hz, 2 H, H-9), 7.66 (t, *J* = 7.5 Hz, 1 H, H-11), 7.57 (d, *J* = 8.3 Hz, 2 H H-13), 7.51 (t, *J* = 7.8 Hz, 2 H, H-10), 7.15 (d, *J* = 7.6 Hz, 2 H, H-14), 7.11 (d, *J* = 8.7 Hz, 2 H, H-4), 6.67 (d, *J* = 8.8 Hz, 2 H, H-5), 5.90 (d, *J* = 6.7 Hz, 1 H, NH), 5.18 (dd, *J* = 6.9, 4.7 Hz, 1 H, H-2), 5.15 (d, *J* = 4.7 Hz, 1 H, H-1), 3.73 (s, 3 H, H-7), 2.36 (s, 3 H, H-16). **¹H NMR** (400 MHz, (CD₃)₂SO) δ 8.62 (d, *J* = 9.2 Hz, 1 H), 7.87–7.77 (m, 3 H), 7.65 (t, *J* = 7.7 Hz, 2 H), 7.41 (d, *J* = 8.0 Hz, 2 H), 7.14 (d, *J* = 8.0 Hz, 2 H), 7.08 (d, *J* = 8.5 Hz, 2 H), 6.64 (d, *J* = 8.4 Hz, 2 H), 5.46 (d, *J* = 4.9 Hz, 1 H), 5.11 (dd, *J* = 9.2, 5.0 Hz, 1 H), 3.68 (s, 3 H), 2.28 (s, 3 H). **¹³C NMR** (151 MHz, CDCl₃) δ 160.01 (C-6), 143.75 (C-15), 136.64 (C-12), 135.93 (C-8), 134.75 (C-11), 129.83 (C-4), 129.78 (C-9), 129.64 (C-14), 129.20 (C-10), 127.29 (C-13), 126.13 (C-3), 113.73 (C-5), 77.00 (C-1), 56.73 (C-2), 55.29 (C-7), 21.61 (C-16). **HRMS** (EI) *m/z*: [M⁺] calcd for [C₂₂H₂₂ClNO₅S₂]⁺ 479.0622, found 479.0624.

N-(-2-Chloro-1-(4-methoxyphenyl)-2-(phenylsulfonyl)ethyl)-4-methylbenzenesulfonamide anion (**15⁻**)

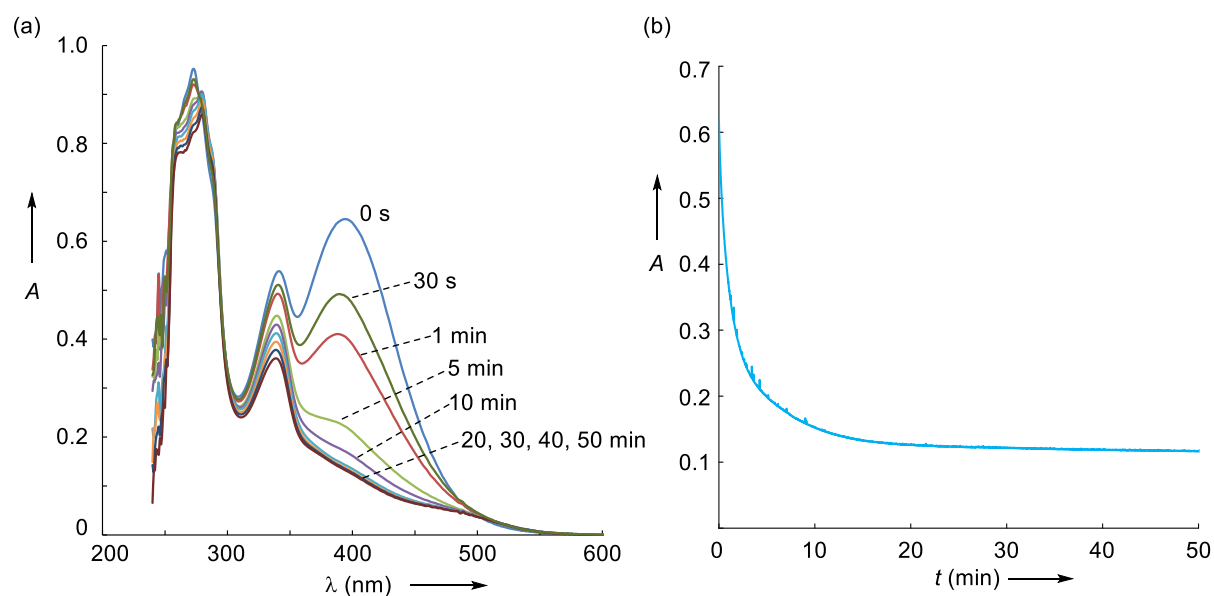
To a solution of **14** (46 mg 0.16 mmol) and **2a-H** (30 mg, 0.16 mmol) in *d*₆-DMSO (0.6 mL) at 20 °C was added NaOH (6.4 mg, 0.16 mmol). After 2 h, the reaction mixture was analyzed by ¹H NMR spectroscopy without workup.



¹H NMR (400 MHz, (CD₃)₂SO) major diastereomer **15'⁻**: δ 7.72 (m, 3 H), 7.65–7.57 (m, 2 H), 7.41 (d, *J* = 8.1 Hz, 2 H), 7.22 (d, *J* = 8.7 Hz, 2 H), 7.06 (d, *J* = 7.6 Hz, 2 H), 6.68 (d, *J* = 8.7 Hz, 2 H), 5.27 (d, *J* = 3.6 Hz, 1 H), 5.00 (d, *J* = 3.6 Hz, 1 H), 3.69 (s, 3 H), 2.26 (s, 3 H).

(4) Kinetics of the reactions of the ketones 1a–j, aldehyde 1o, and Michael acceptor 5 with the reference nucleophiles 2

The rates of all investigated reactions were determined spectrophotometrically (UV-Vis) by following the disappearance of the colored carbanions **2a,b**. The temperature of the solutions during all kinetics studies was kept constant (20.0 ± 0.1 °C) by using a circulating bath thermostat. The kinetic investigations were performed with a high excess of the electrophiles over the carbanions to achieve first-order kinetics. The carbanions **2a,b** decompose on the minute time-scale at room temperature (see graphs below). Thus we prepared stock solutions of the carbanions **2a,b** by deprotonation of the corresponding CH acids **2a,b-H** in dry THF at -78 °C with 1.00–1.05 equiv *t*-BuOK. Small amounts of these stock solutions were dissolved in DMSO (99.7%, extra dry, over molecular sieves, AcroSeal) at room temperature directly before each kinetic experiment. The kinetics were followed by a commercial stopped-flow spectrophotometer system. Rate constants k_{obs} (s^{-1}) were obtained by fitting the single exponential decay $A_t = A_0 \exp(-k_{\text{obs}}t) + C$ (exponential decrease) to the observed time-dependent absorbance (in the case of the stopped-flow spectrophotometer, at least 5 kinetic runs for each nucleophile concentration were averaged). Second-order rate constants k_2 ($\text{M}^{-1} \text{s}^{-1}$) were derived from the slopes of the linear correlations of k_{obs} with electrophile concentrations.



(a) Time-dependent UV-vis absorbance of **2b** ($2.50 \times 10^{-4} \text{ mol L}^{-1}$) in DMSO at 20 °C (decomposition in the absence of electrophile). (b) Decay of the absorbance A of **2b** ($2.50 \times 10^{-4} \text{ mol L}^{-1}$) at 405 nm in DMSO at 20 °C.

Chapter 3: Kinetics and mechanism of oxirane-formation by Darzens condensation of ketones: quantification of the electrophilicities of ketones

Table S1. Kinetics of the reactions of **1a** with **2b** in DMSO at 20 °C (deprotonated with 1.00–1.05 equiv. *t*-BuOK, stopped-flow UV-Vis spectrometer, $\lambda = 405$ nm).

[2b]/mol L ⁻¹	[1a]/mol L ⁻¹	$k_{\text{obs}}/\text{s}^{-1}$
2.50×10^{-4}	2.61×10^{-3}	1.77×10^1
2.50×10^{-4}	3.91×10^{-3}	2.68×10^1
2.50×10^{-4}	5.21×10^{-3}	3.55×10^1
2.50×10^{-4}	6.52×10^{-3}	4.47×10^1
2.50×10^{-4}	7.82×10^{-3}	5.47×10^1

$$k_2 = 7.05 (\pm 0.10) \times 10^3 \text{ L mol}^{-1} \text{ s}^{-1}$$

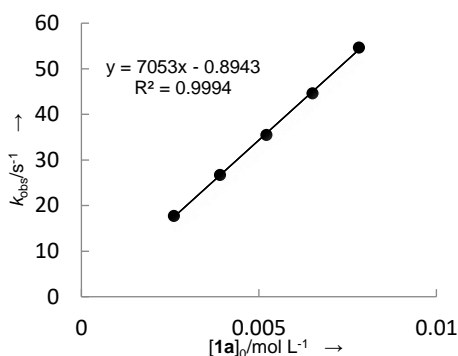


Table S2. Kinetics of the reactions of **1b** with **2b** in DMSO at 20 °C (deprotonated with 1.00–1.05 equiv. *t*-BuOK, stopped-flow UV-Vis spectrometer, $\lambda = 405$ nm).

[2b]/mol L ⁻¹	[1b]/mol L ⁻¹	$k_{\text{obs}}/\text{s}^{-1}$
2.50×10^{-4}	3.01×10^{-3}	4.21×10^{-1}
2.50×10^{-4}	4.51×10^{-3}	6.09×10^{-1}
2.50×10^{-4}	6.01×10^{-3}	7.51×10^{-1}
2.50×10^{-4}	7.51×10^{-3}	9.43×10^{-1}
2.50×10^{-4}	9.02×10^{-3}	1.24×10^0

$$k_2 = 1.31 (\pm 0.10) \times 10^2 \text{ L mol}^{-1} \text{ s}^{-1}$$

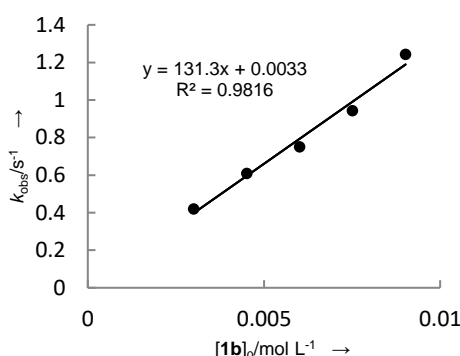


Table S3. Kinetics of the reactions of **1c** with **2a** in DMSO at 20 °C (deprotonated with 1.00–1.05 equiv. *t*-BuOK, stopped-flow UV-Vis spectrometer, $\lambda = 320$ nm).

[2a]/mol L ⁻¹	[1c]/mol L ⁻¹	$k_{\text{obs}}/\text{s}^{-1}$
2.50×10^{-4}	8.78×10^{-3}	2.66×10^1
2.50×10^{-4}	1.32×10^{-2}	4.15×10^1
2.50×10^{-4}	1.76×10^{-2}	5.04×10^1
2.50×10^{-4}	2.20×10^{-2}	6.50×10^1
2.50×10^{-4}	2.64×10^{-2}	8.04×10^1

$$k_2 = 2.98 (\pm 0.14) \times 10^3 \text{ L mol}^{-1} \text{ s}^{-1}$$

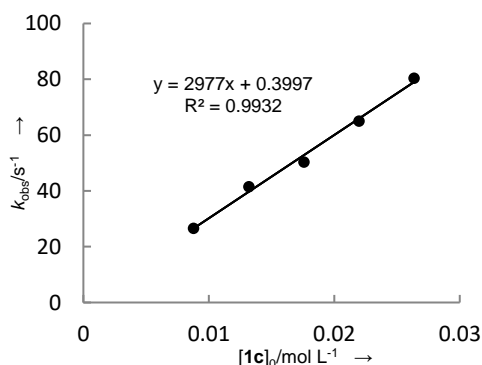
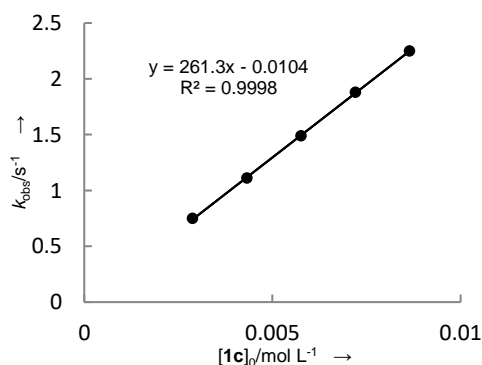


Table S4. Kinetics of the reactions of **1c** with **2b** in DMSO at 20 °C (deprotonated with 1.00–1.05 equiv. *t*-BuOK, stopped-flow UV-Vis spectrometer, $\lambda = 405$ nm).

[2b]/mol L ⁻¹	[1c]/mol L ⁻¹	$k_{\text{obs}}/\text{s}^{-1}$
2.50×10^{-4}	2.88×10^{-3}	7.50×10^{-1}
2.50×10^{-4}	4.32×10^{-3}	1.11×10^0
2.50×10^{-4}	5.77×10^{-3}	1.49×10^0
2.50×10^{-4}	7.21×10^{-3}	1.88×10^0
2.50×10^{-4}	8.65×10^{-3}	2.25×10^0

$$k_2 = 2.61 (\pm 0.02) \times 10^2 \text{ L mol}^{-1} \text{ s}^{-1}$$



Chapter 3: Kinetics and mechanism of oxirane-formation by Darzens condensation of ketones: quantification of the electrophilicities of ketones

Table S5. Kinetics of the reactions of **1d** with **2a** in DMSO at 20 °C (deprotonated with 1.00–1.05 equiv. *t*-BuOK, stopped-flow UV-Vis spectrometer, $\lambda = 320$ nm).

[2a]/mol L ⁻¹	[1d]/mol L ⁻¹	$k_{\text{obs}}/\text{s}^{-1}$
2.50×10^{-4}	5.54×10^{-3}	4.36×10^{-1}
2.50×10^{-4}	8.31×10^{-3}	6.70×10^{-1}
2.50×10^{-4}	1.11×10^{-2}	1.04×10^0
2.50×10^{-4}	1.66×10^{-2}	1.36×10^0

$k_2 = 8.49 (\pm 0.10) \times 10^1 \text{ L mol}^{-1} \text{ s}^{-1}$

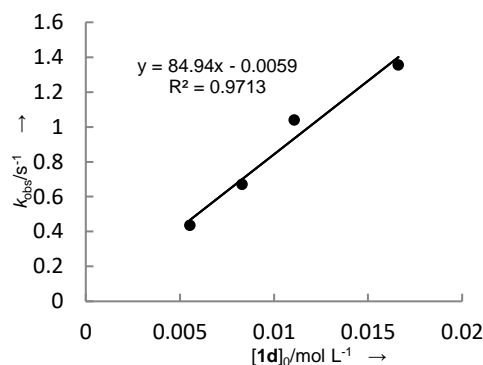


Table S6. Kinetics of the reactions of **1e** with **2a** in DMSO at 20 °C (deprotonated with 1.00–1.05 equiv. *t*-BuOK, stopped-flow UV-Vis spectrometer, $\lambda = 320$ nm).

[2a]/mol L ⁻¹	[1e]/mol L ⁻¹	$k_{\text{obs}}/\text{s}^{-1}$
2.50×10^{-4}	2.62×10^{-3}	4.42×10^1
2.50×10^{-4}	3.92×10^{-3}	6.20×10^1
2.50×10^{-4}	5.23×10^{-3}	8.60×10^1
2.50×10^{-4}	6.54×10^{-3}	1.04×10^2
2.50×10^{-4}	7.85×10^{-3}	1.39×10^2

$k_2 = 1.77 (\pm 0.13) \times 10^4 \text{ L mol}^{-1} \text{ s}^{-1}$

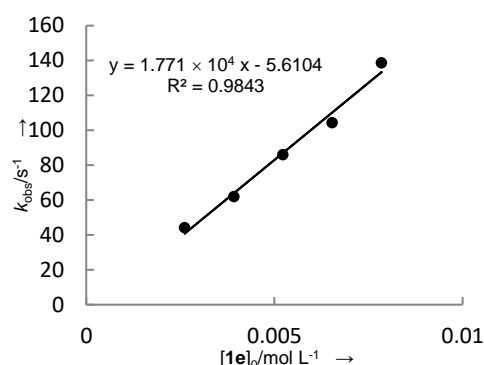


Table S7. Kinetics of the reactions of **1e** with **2a** in DMSO at 20 °C (deprotonated with 1.00–1.05 equiv. *t*-BuOK, stopped-flow UV-Vis spectrometer, $\lambda = 320$ nm).

[2a]/mol L ⁻¹	[18-crown-6]	[1e]/mol L ⁻¹	$k_{\text{obs}}/\text{s}^{-1}$
2.50×10^{-4}	6.10×10^{-4}	2.62×10^{-3}	4.03×10^1
2.50×10^{-4}	6.10×10^{-4}	3.92×10^{-3}	6.63×10^1
2.50×10^{-4}	6.10×10^{-4}	5.23×10^{-3}	7.97×10^1
2.50×10^{-4}	6.10×10^{-4}	6.54×10^{-3}	1.09×10^2
2.50×10^{-4}	6.10×10^{-4}	7.85×10^{-3}	1.36×10^2

$k_2 = 1.79 (\pm 0.11) \times 10^4 \text{ L mol}^{-1} \text{ s}^{-1}$

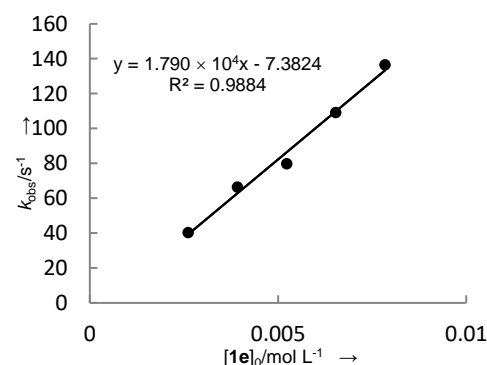
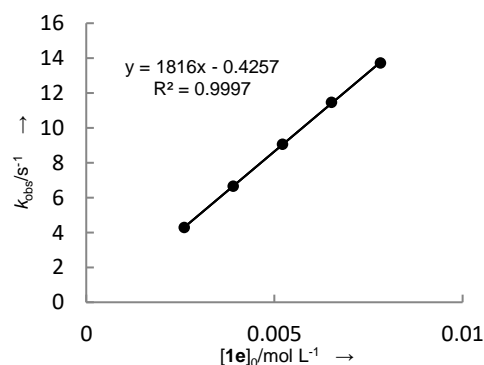


Table S8. Kinetics of the reactions of **1e** with **2b** in DMSO at 20 °C (deprotonated with 1.00–1.05 equiv. *t*-BuOK, stopped-flow UV-Vis spectrometer, $\lambda = 405$ nm).

[2b]/mol L ⁻¹	[1e]/mol L ⁻¹	$k_{\text{obs}}/\text{s}^{-1}$
2.50×10^{-4}	2.61×10^{-3}	4.29×10^0
2.50×10^{-4}	3.91×10^{-3}	6.66×10^0
2.50×10^{-4}	5.21×10^{-3}	9.06×10^0
2.50×10^{-4}	6.52×10^{-3}	1.15×10^1
2.50×10^{-4}	7.82×10^{-3}	1.37×10^1

$k_2 = 1.82 (\pm 0.02) \times 10^3 \text{ L mol}^{-1} \text{ s}^{-1}$



Chapter 3: Kinetics and mechanism of oxirane-formation by Darzens condensation of ketones: quantification of the electrophilicities of ketones

Table S9. Kinetics of the reactions of **1f** with **2b** in DMSO at 20 °C (deprotonated with 1.00–1.05 equiv. *t*-BuOK, stopped-flow UV-Vis spectrometer, $\lambda = 405$ nm).

[2b]/mol L ⁻¹	[1f]/mol L ⁻¹	$k_{\text{obs}}/\text{s}^{-1}$
2.50×10^{-4}	2.55×10^{-3}	1.81×10^1
2.50×10^{-4}	3.83×10^{-3}	3.01×10^1
2.50×10^{-4}	5.10×10^{-3}	3.73×10^1
2.50×10^{-4}	6.38×10^{-3}	4.67×10^1
2.50×10^{-4}	7.65×10^{-3}	5.84×10^1

$k_2 = 7.62 (\pm 0.35) \times 10^3 \text{ L mol}^{-1} \text{ s}^{-1}$

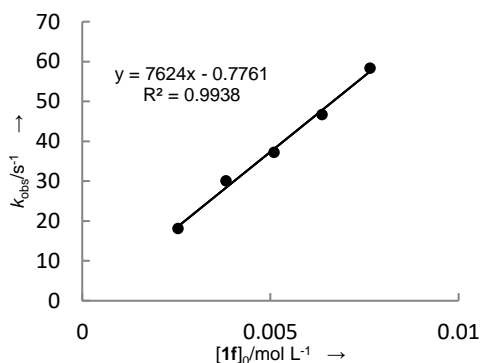


Table S10. Kinetics of the reactions of **1f** with **2b** in DMSO at 20 °C (deprotonated with 1.00–1.05 equiv. *t*-BuOK, stopped-flow UV-Vis spectrometer, $\lambda = 405$ nm).

[2b]/mol L ⁻¹	[18-crown-6]	[1f]/mol L ⁻¹	$k_{\text{obs}}/\text{s}^{-1}$
2.50×10^{-4}	5.68×10^{-4}	2.38×10^{-3}	1.84×10^1
2.50×10^{-4}	5.68×10^{-4}	3.57×10^{-3}	2.79×10^1
2.50×10^{-4}	5.68×10^{-4}	4.76×10^{-3}	3.81×10^1
2.50×10^{-4}	5.68×10^{-4}	5.95×10^{-3}	4.85×10^1
2.50×10^{-4}	5.68×10^{-4}	7.14×10^{-3}	5.36×10^1

$k_2 = 7.65 (\pm 0.47) \times 10^3 \text{ L mol}^{-1} \text{ s}^{-1}$

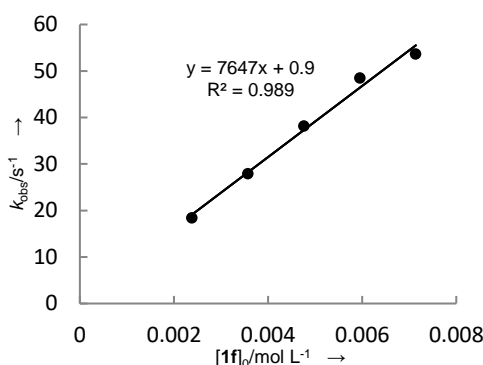


Table S11. Kinetics of the reactions of **1g** with **2b** in DMSO at 20 °C (deprotonated with 1.00–1.05 equiv. *t*-BuOK, stopped-flow UV-Vis spectrometer, $\lambda = 405$ nm).

[2b]/mol L ⁻¹	[1g]/mol L ⁻¹	$k_{\text{obs}}/\text{s}^{-1}$
2.50×10^{-4}	2.48×10^{-3}	3.99×10^1
2.50×10^{-4}	3.72×10^{-3}	6.83×10^1
2.50×10^{-4}	4.96×10^{-3}	8.93×10^1
2.50×10^{-4}	6.20×10^{-3}	1.09×10^2
2.50×10^{-4}	7.44×10^{-3}	1.32×10^2

$k_2 = 1.81 (\pm 0.07) \times 10^4 \text{ L mol}^{-1} \text{ s}^{-1}$

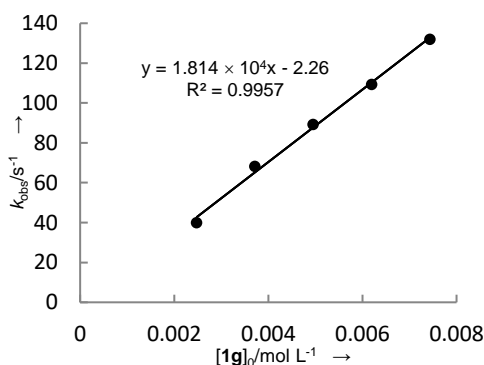
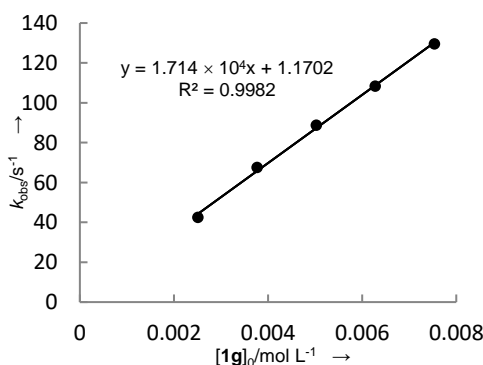


Table S12. Kinetics of the reactions of **1g** with **2b** in DMSO at 20 °C (deprotonated with 1.00–1.05 equiv. *t*-BuOK, stopped-flow UV-Vis spectrometer, $\lambda = 405$ nm).

[2b]/mol L ⁻¹	[18-crown-6]	[1g]/mol L ⁻¹	$k_{\text{obs}}/\text{s}^{-1}$
2.50×10^{-4}	5.68×10^{-4}	2.51×10^{-3}	4.25×10^1
2.50×10^{-4}	5.68×10^{-4}	3.77×10^{-3}	6.75×10^1
2.50×10^{-4}	5.68×10^{-4}	5.03×10^{-3}	8.87×10^1
2.50×10^{-4}	5.68×10^{-4}	6.28×10^{-3}	1.08×10^2
2.50×10^{-4}	5.68×10^{-4}	7.54×10^{-3}	1.30×10^2

$k_2 = 1.71 (\pm 0.04) \times 10^4 \text{ L mol}^{-1} \text{ s}^{-1}$



Chapter 3: Kinetics and mechanism of oxirane-formation by Darzens condensation of ketones: quantification of the electrophilicities of ketones

Table S13. Kinetics of the reactions of **1g** with **2b** in DMSO at 20 °C (deprotonated with 1.00–1.05 equiv. $P_4^{-1}Bu$, stopped-flow UV-Vis spectrometer, $\lambda = 405$ nm).

[2b]/mol L ⁻¹	[1g]/mol L ⁻¹	k_{obs}/s^{-1}
2.50×10^{-4}	2.49×10^{-3}	4.47×10^1
2.50×10^{-4}	3.74×10^{-3}	6.75×10^1
2.50×10^{-4}	4.98×10^{-3}	8.82×10^1
2.50×10^{-4}	6.23×10^{-3}	1.05×10^2
2.50×10^{-4}	7.47×10^{-3}	1.29×10^2

$k_2 = 1.66 (\pm 0.05) \times 10^4 \text{ L mol}^{-1} \text{ s}^{-1}$

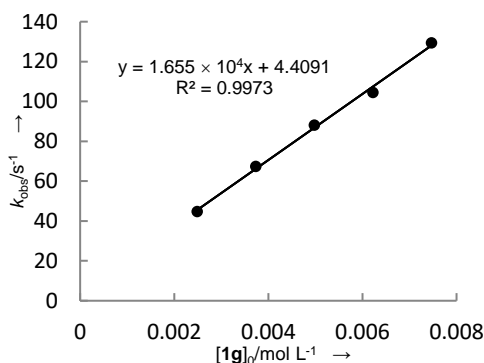


Table S14. Kinetics of the reactions of **1h** with **2a** in DMSO at 20 °C (deprotonated with 1.00–1.05 equiv. $t\text{-BuOK}$, stopped-flow UV-Vis spectrometer, $\lambda = 320$ nm).

[2a]/mol L ⁻¹	[1h]/mol L ⁻¹	k_{obs}/s^{-1}
2.50×10^{-4}	2.56×10^{-3}	4.51×10^1
2.50×10^{-4}	3.84×10^{-3}	6.51×10^1
2.50×10^{-4}	5.12×10^{-3}	9.65×10^1
2.50×10^{-4}	6.39×10^{-3}	1.26×10^2
2.50×10^{-4}	7.67×10^{-3}	1.50×10^2

$k_2 = 2.12 (\pm 0.08) \times 10^4 \text{ L mol}^{-1} \text{ s}^{-1}$

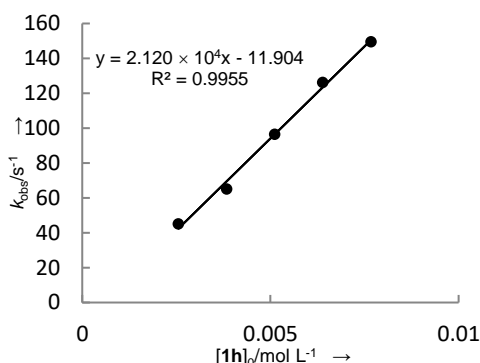


Table S15. Kinetics of the reactions of **1h** with **2b** in DMSO at 20 °C (deprotonated with 1.00–1.05 equiv. $t\text{-BuOK}$, stopped-flow UV-Vis spectrometer, $\lambda = 405$ nm).

[2b]/mol L ⁻¹	[1h]/mol L ⁻¹	k_{obs}/s^{-1}
2.50×10^{-4}	2.52×10^{-3}	6.73×10^0
2.50×10^{-4}	3.78×10^{-3}	1.04×10^1
2.50×10^{-4}	5.05×10^{-3}	1.39×10^1
2.50×10^{-4}	6.31×10^{-3}	1.80×10^1
2.50×10^{-4}	7.57×10^{-3}	2.19×10^1

$k_2 = 3.00 (\pm 0.05) \times 10^3 \text{ L mol}^{-1} \text{ s}^{-1}$

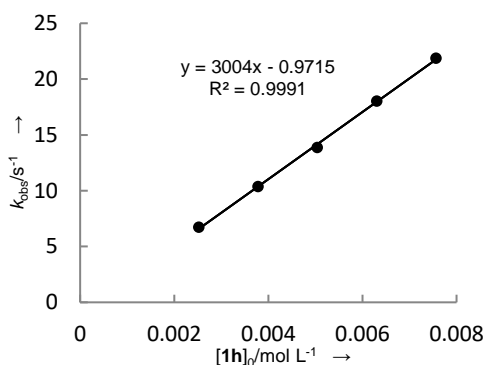
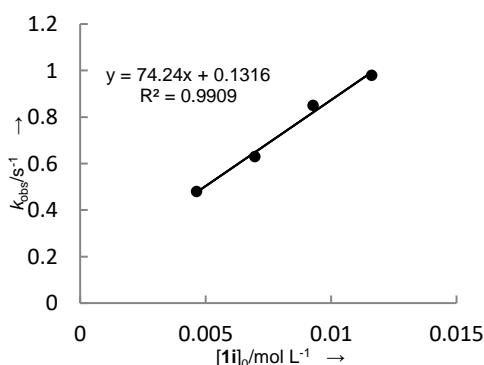


Table S16. Kinetics of the reactions of **1i** with **2a** in DMSO at 20 °C (deprotonated with 1.00–1.05 equiv. $t\text{-BuOK}$, stopped-flow UV-Vis spectrometer, $\lambda = 320$ nm).

[2a]/mol L ⁻¹	[1i]/mol L ⁻¹	k_{obs}/s^{-1}
2.50×10^{-4}	4.65×10^{-3}	4.80×10^{-1}
2.50×10^{-4}	6.97×10^{-3}	6.30×10^{-1}
2.50×10^{-4}	9.29×10^{-3}	8.50×10^{-1}
2.50×10^{-4}	1.16×10^{-2}	9.80×10^{-1}

$k_2 = 7.42 (\pm 0.50) \times 10^1 \text{ L mol}^{-1} \text{ s}^{-1}$



Chapter 3: Kinetics and mechanism of oxirane-formation by Darzens condensation of ketones: quantification of the electrophilicities of ketones

Table S17. Kinetics of the reactions of **1j** with **2b** in DMSO at 20 °C (deprotonated with 1.00–1.05 equiv. *t*-BuOK, stopped-flow UV-Vis spectrometer, $\lambda = 405$ nm).

[2b]/mol L ⁻¹	[1j]/mol L ⁻¹	$k_{\text{obs}}/\text{s}^{-1}$
2.50×10^{-4}	5.23×10^{-3}	2.32×10^2
2.50×10^{-4}	6.54×10^{-3}	2.80×10^2
2.50×10^{-4}	7.85×10^{-3}	3.52×10^2
2.50×10^{-4}	1.05×10^{-2}	3.99×10^2

$k_2 = 3.21 (\pm 0.55) \times 10^4 \text{ L mol}^{-1} \text{ s}^{-1}$

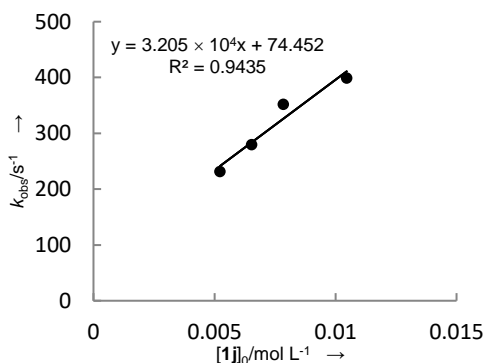


Table S18. Kinetics of the reactions of **1j** with **2b** in DMSO at 20 °C (deprotonated with 1.00–1.05 equiv. *t*-BuOK, stopped-flow UV-Vis spectrometer, $\lambda = 405$ nm).

[2b]/mol L ⁻¹	[18-crown-6]	[1j]/mol L ⁻¹	$k_{\text{obs}}/\text{s}^{-1}$
2.50×10^{-4}	5.00×10^{-4}	4.05×10^{-3}	1.82×10^2
2.50×10^{-4}	5.00×10^{-4}	5.40×10^{-3}	2.26×10^2
2.50×10^{-4}	5.00×10^{-4}	6.75×10^{-3}	3.10×10^2
2.50×10^{-4}	5.00×10^{-4}	8.11×10^{-3}	3.56×10^2
2.50×10^{-4}	5.00×10^{-4}	9.46×10^{-3}	3.70×10^2
2.50×10^{-4}	5.00×10^{-4}	1.08×10^{-2}	4.26×10^2

$k_2 = 3.59 (\pm 0.33) \times 10^4 \text{ L mol}^{-1} \text{ s}^{-1}$

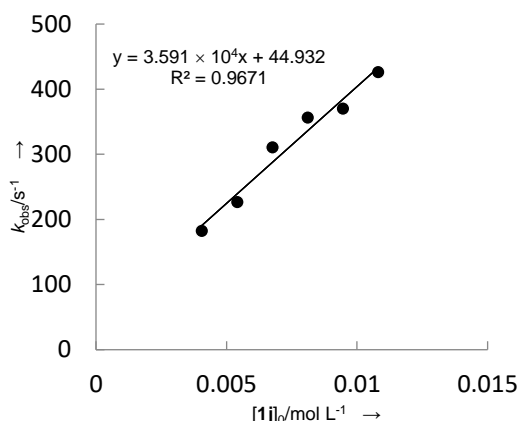


Table S19. Kinetics of the reactions of **1o** with **2b** in DMSO at 20 °C (deprotonated with 1.00–1.05 equiv. *t*-BuOK, stopped-flow UV-Vis spectrometer, $\lambda = 405$ nm).

[2b]/mol L ⁻¹	[1o]/mol L ⁻¹	$k_{\text{obs}}/\text{s}^{-1}$
2.50×10^{-4}	2.68×10^{-3}	6.78×10^1
2.50×10^{-4}	4.02×10^{-3}	1.06×10^2
2.50×10^{-4}	5.36×10^{-3}	1.41×10^2
2.50×10^{-4}	6.70×10^{-3}	1.76×10^2
2.50×10^{-4}	8.04×10^{-3}	2.13×10^2

$k_2 = 2.69 (\pm 0.02) \times 10^4 \text{ L mol}^{-1} \text{ s}^{-1}$

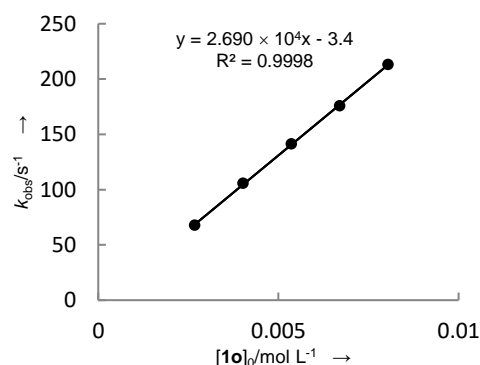
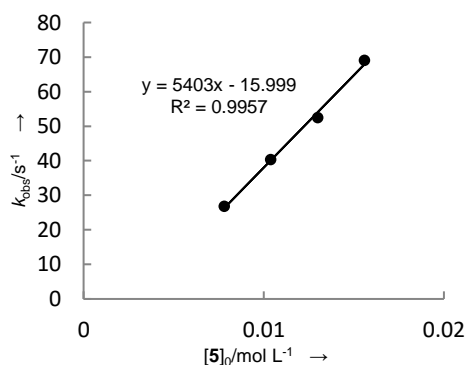


Table S20. Kinetics of the reactions of **5** with **2a** in DMSO at 20 °C (deprotonated with 1.00–1.05 equiv. *t*-BuOK, stopped-flow UV-Vis spectrometer, $\lambda = 320$ nm).

[2a]/mol L ⁻¹	[5]/mol L ⁻¹	$k_{\text{obs}}/\text{s}^{-1}$
2.50×10^{-4}	7.81×10^{-3}	2.68×10^1
2.50×10^{-4}	1.04×10^{-2}	4.01×10^1
2.50×10^{-4}	1.30×10^{-2}	5.26×10^1
2.50×10^{-4}	1.56×10^{-2}	6.94×10^1

$k_2 = 5.40 (\pm 0.25) \times 10^3 \text{ L mol}^{-1} \text{ s}^{-1}$



(5) Competition experiments

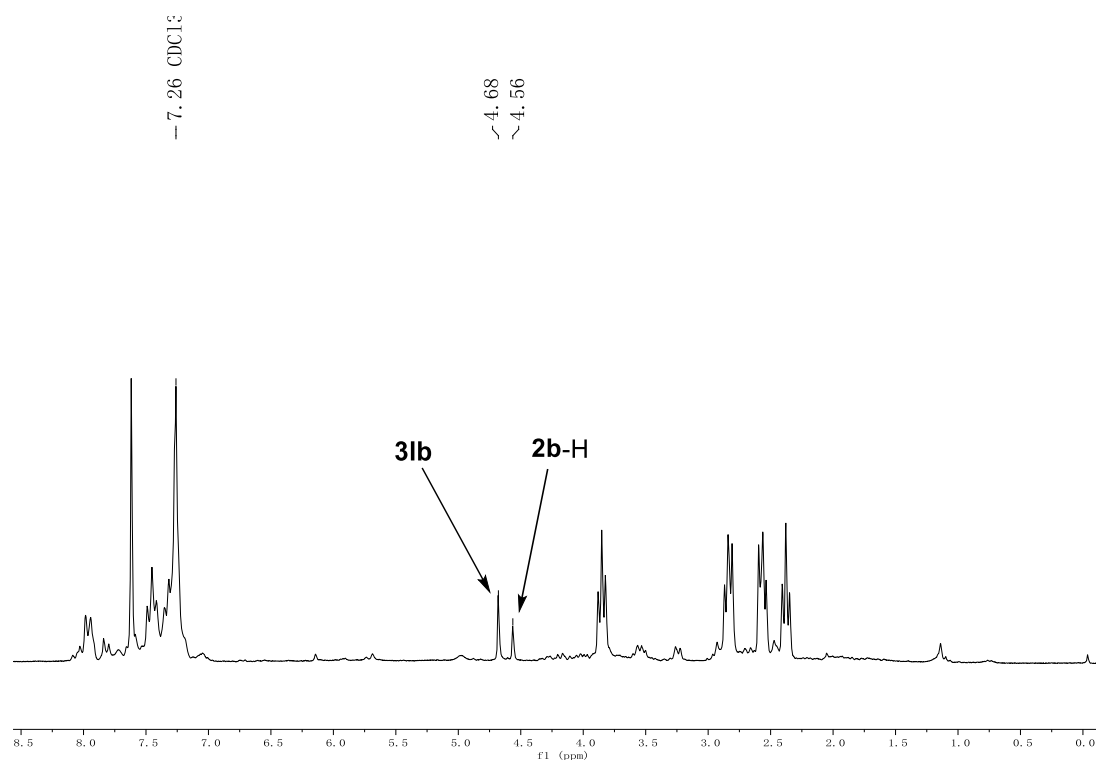
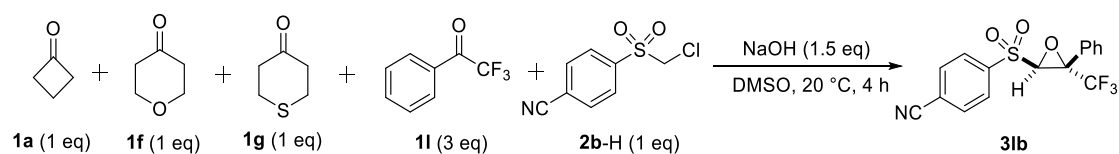
Procedure E for competition experiments: One (0.10 mmol) or several (0.10 mmol each) of the ketones **1**, a carbanion precursor (**2-H** or **13**; 0.10 mmol), and a reactive trapping electrophile (**1l**, **1n**, or **5**; 0.30 mmol) were dissolved in DMSO (1.0 mL). Then NaOH (0.15 mmol) was added. After 4 h at 20 °C, 2% aq HCl (10 mL) was added, and the mixture was extracted with CHCl₃ (3 × 15 mL). The organic phases were combined and subsequently washed with water (2 × 30 mL) and brine (1 × 30 mL) to remove remaining DMSO. After drying with anhydrous MgSO₄ and filtration, the solvent was evaporated under reduced pressure. The residue was dissolved in CDCl₃ and analyzed by ¹H NMR spectroscopy.

Procedure F for competition experiments: One (0.20 mmol) or several (0.20 mmol each) of the ketones **1**, a carbanion precursor (**2-H**; 0.10 mmol), and a reactive trapping electrophile (**1g**, **1k**, **1l**, or **5**; 0.20 mmol) were dissolved in *d*₆-DMSO (1.0 mL). Then NaOH (0.15 mmol) was added. After 4 h at 20 °C, the reaction mixture was analyzed by ¹H NMR spectroscopy without further workup.

Procedure G for competition experiments: Two different electrophiles, the carbanion precursor **2a-H** (0.10 mmol), and Me₂SO₂ (4.7 mg, 50 μmol, as integration standard, δ_H = 3.02 ppm) were dissolved in *d*₆-DMSO (0.7 mL). A ¹H NMR spectrum of the solution was recorded. Then NaOH (0.10 mmol) was added. After 30 min at 20 °C, the reaction mixture was analyzed by ¹H NMR spectroscopy without further workup.

Competition between **1a**, **1f**, **1g**, and **1l** (trapping agent) for carbanion **2b** (this chapter, Scheme 5)

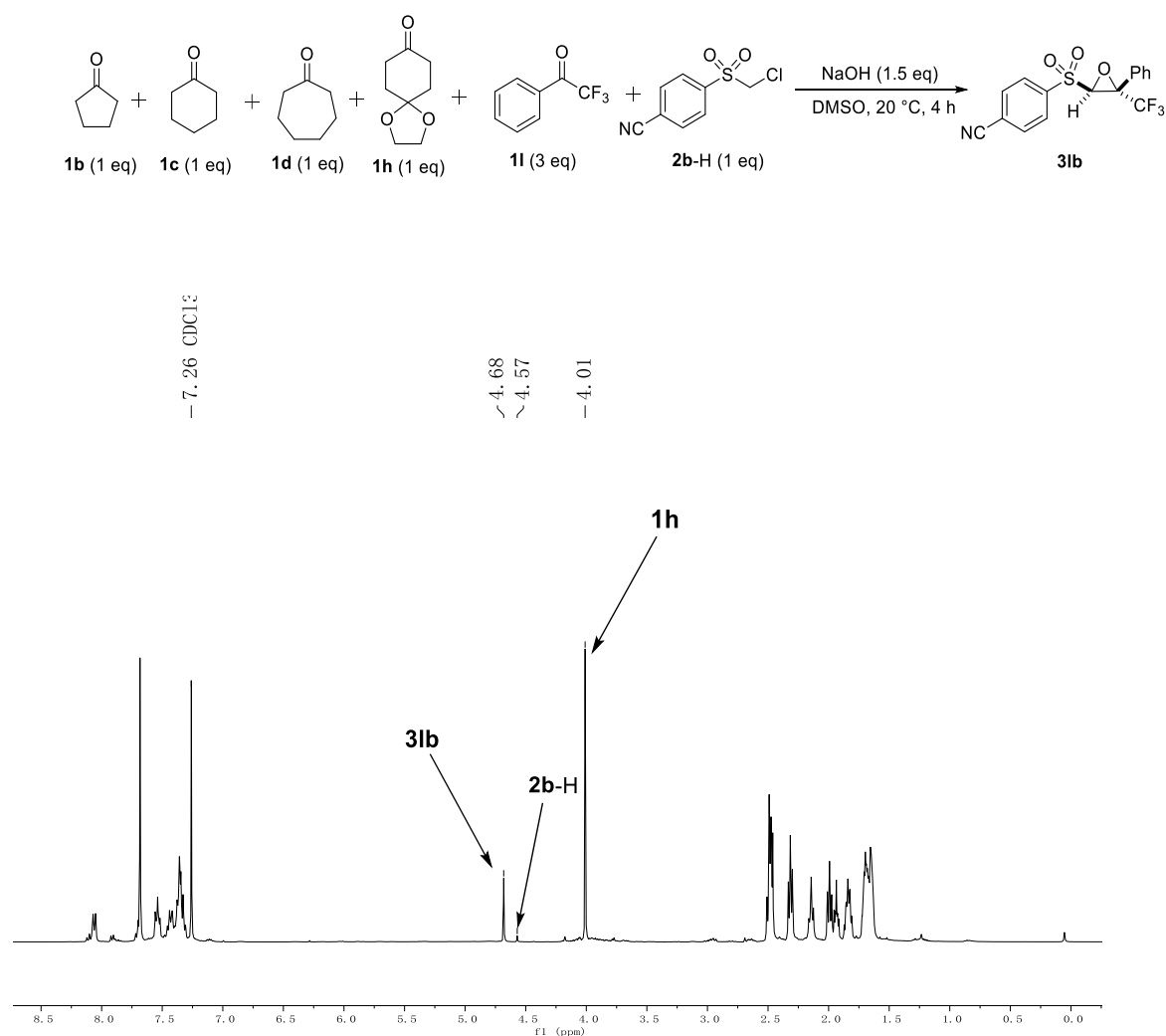
According to Procedure E, **1a** (7.0 mg, 0.10 mmol), **1f** (10 mg, 0.10 mmol), **1g** (12 mg, 0.10 mmol), **1l** (52 mg, 0.30 mmol), and **2b-H** (22 mg, 0.10 mmol), and NaOH (6.0 mg, 0.15 mmol) were combined.



¹H NMR spectroscopy shows selective formation of **3b** (from **1l**) under the above mentioned experimental conditions ($[\mathbf{1l}]_0/[\mathbf{1a,f,g}]_0 \geq 3$).

Competition between **1b**, **1c**, **1d**, **1h** and **1l** (trapping agent) for carbanion **2b** (this chapter, Scheme 5)

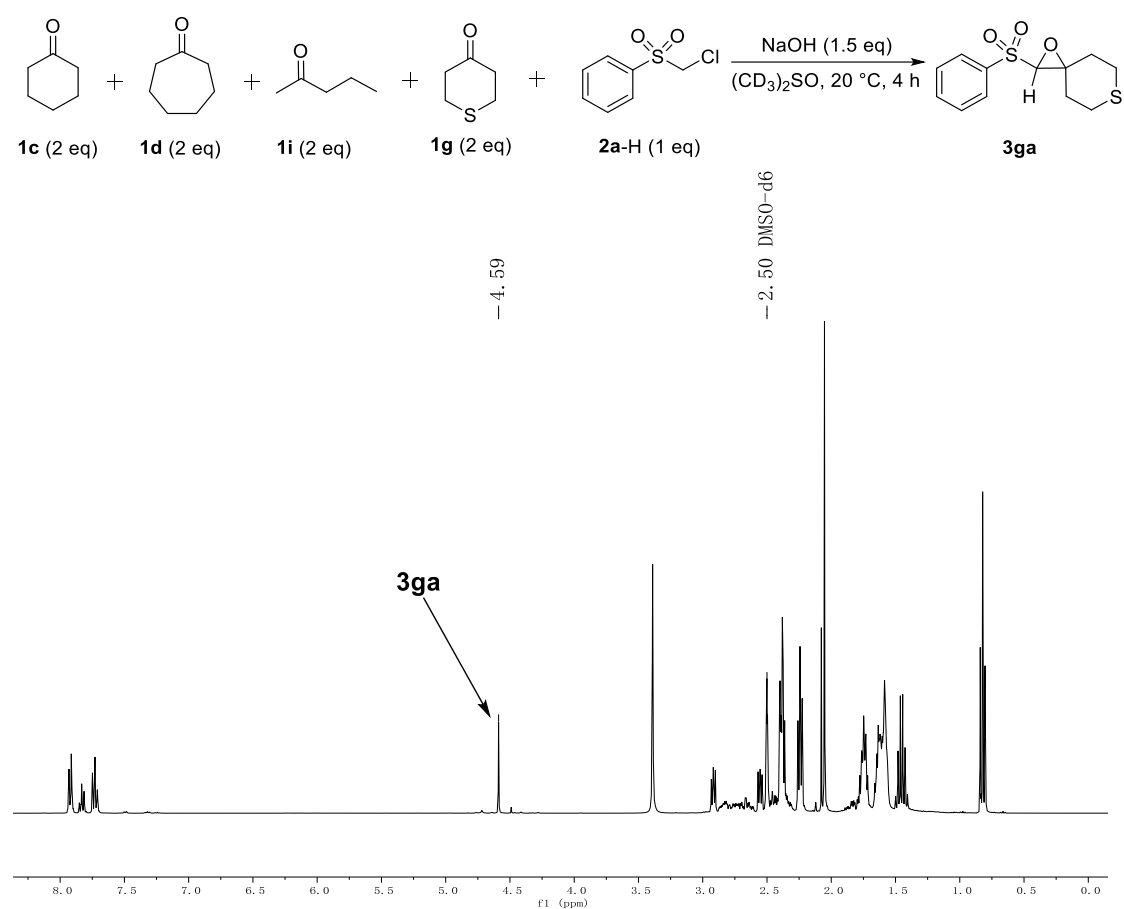
In analogy to Procedure E, **1b** (5.8 mg, 0.069 mmol), **1c** (6.8 mg, 0.069 mmol), **1d** (7.7 mg, 0.069 mmol), **1h** (11 mg, 0.069 mmol), **1l** (37 mg, 0.21 mmol), and **2b-H** (15 mg, 0.069 mmol), and NaOH (4.0 mg, 0.10 mmol) were combined.



¹H NMR spectroscopy shows selective formation of **3b** (from **1l**) under the above mentioned experimental conditions ($[\mathbf{1l}]_0/[\mathbf{1b,c,d,h}]_0 \geq 3$).

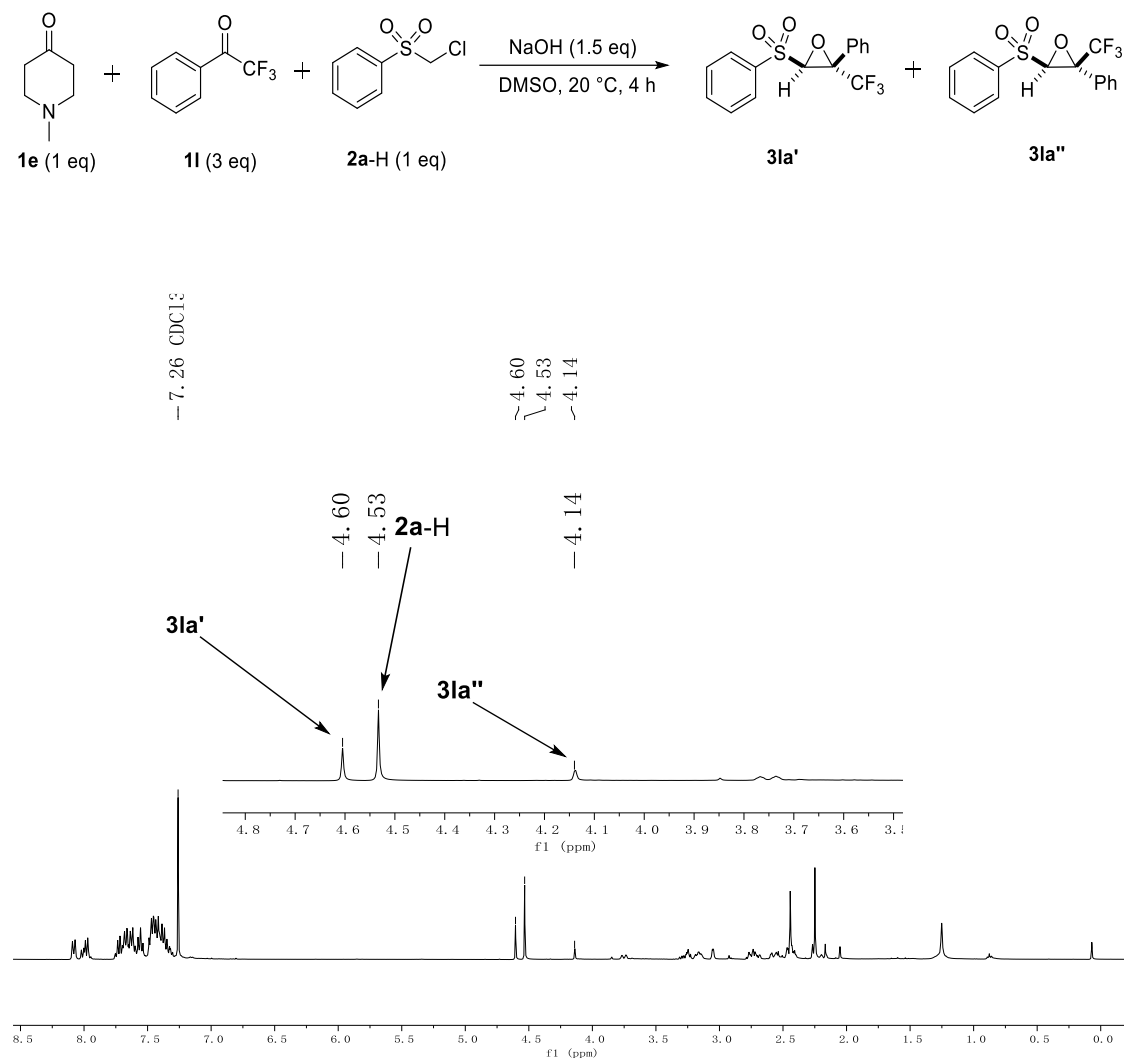
Competition between **1c**, **1d**, **1i**, and **1g** (trapping agent) for carbanion **2a** (this chapter, Scheme 5)

According to Procedure F, **1c** (20 mg, 0.20 mmol), **1d** (22 mg, 0.20 mmol), **1i** (17 mg, 0.20 mmol), **1g** (23 mg, 0.20 mmol), and **2a**-H (19 mg, 0.10 mmol), and NaOH (6.0 mg, 0.15 mmol) were combined.



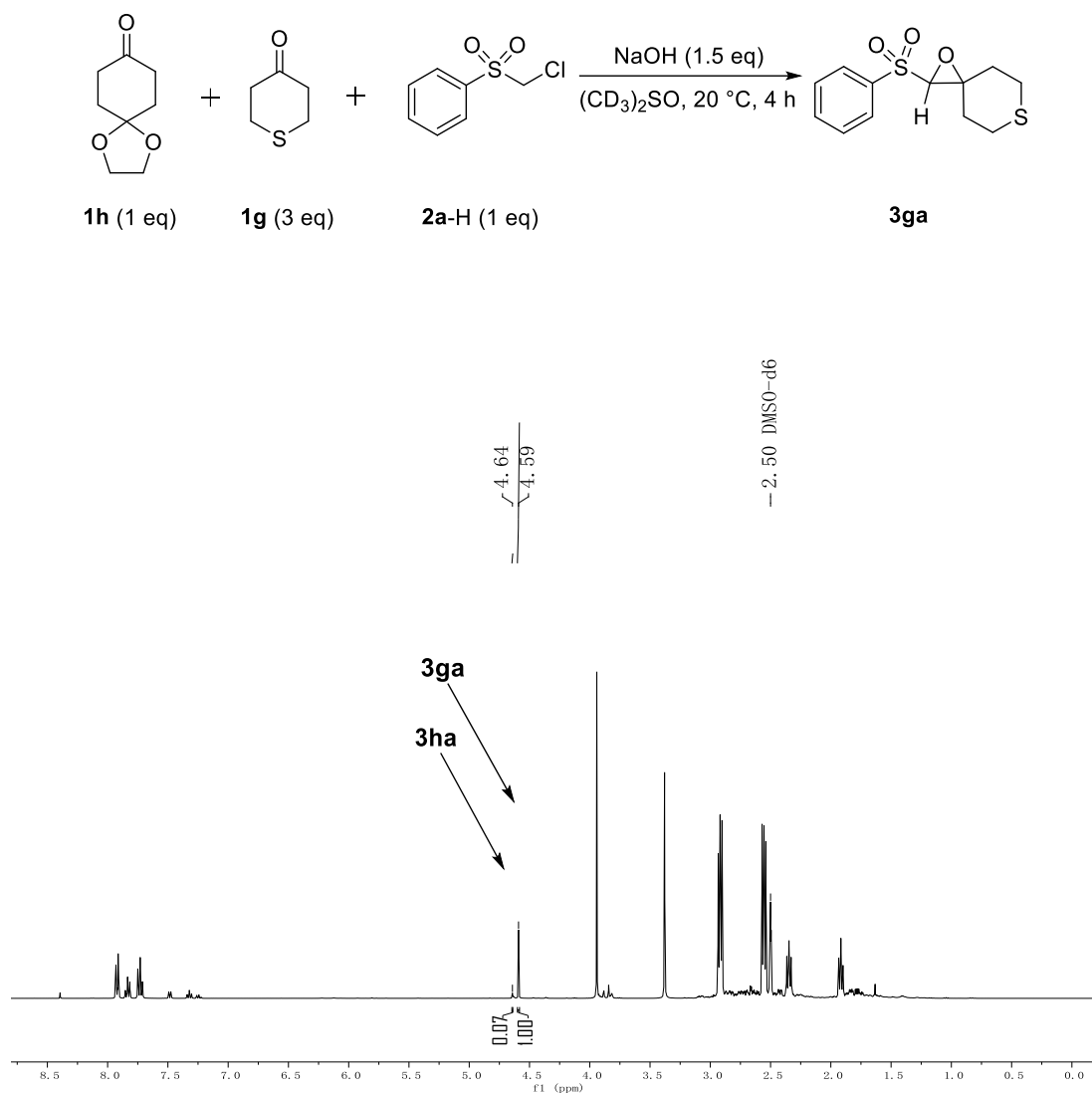
^1H NMR spectroscopy shows selective formation of **3ga** (from **1g**) under the above mentioned experimental conditions ($[\mathbf{1g}]_0/[\mathbf{1c,d,i}]_0 = 1$).

In analogy to Procedure E but workup by saturated NH_4Cl solution instead of 2% aq HCl , **1e** (5.7 mg, 0.050 mmol), **1l** (26 mg, 0.15 mmol), and **2a-H** (9.5 mg, 0.050 mmol), and NaOH (3.0 mg, 0.075 mmol) were combined.



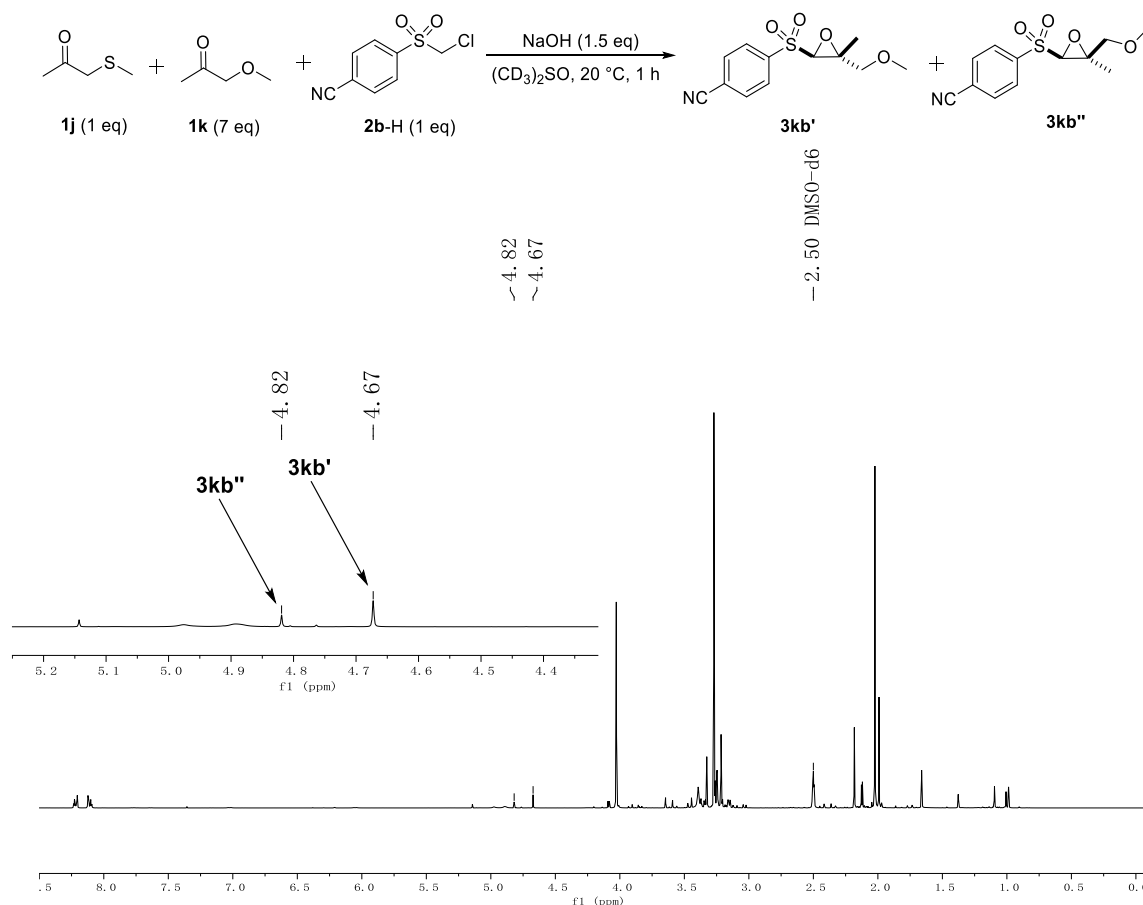
^1H NMR spectroscopy shows selective formation of **3la** (from **1l**) under the above mentioned experimental conditions ($[\mathbf{1l}]_0/[\mathbf{1e}]_0 \geq 3$).

In analogy to Procedure F, **1h** (7.8 mg, 0.050 mmol), **1g** (17 mg, 0.15 mmol), and **2a**-H (9.5 mg, 0.050 mmol), and NaOH (3.0 mg, 0.075 mmol) were combined.



¹H NMR spectroscopy shows almost selective formation of **3ga** (from **1g**) under the above mentioned experimental conditions ($[\mathbf{1g}]_0/[\mathbf{1h}]_0 \geq 3$).

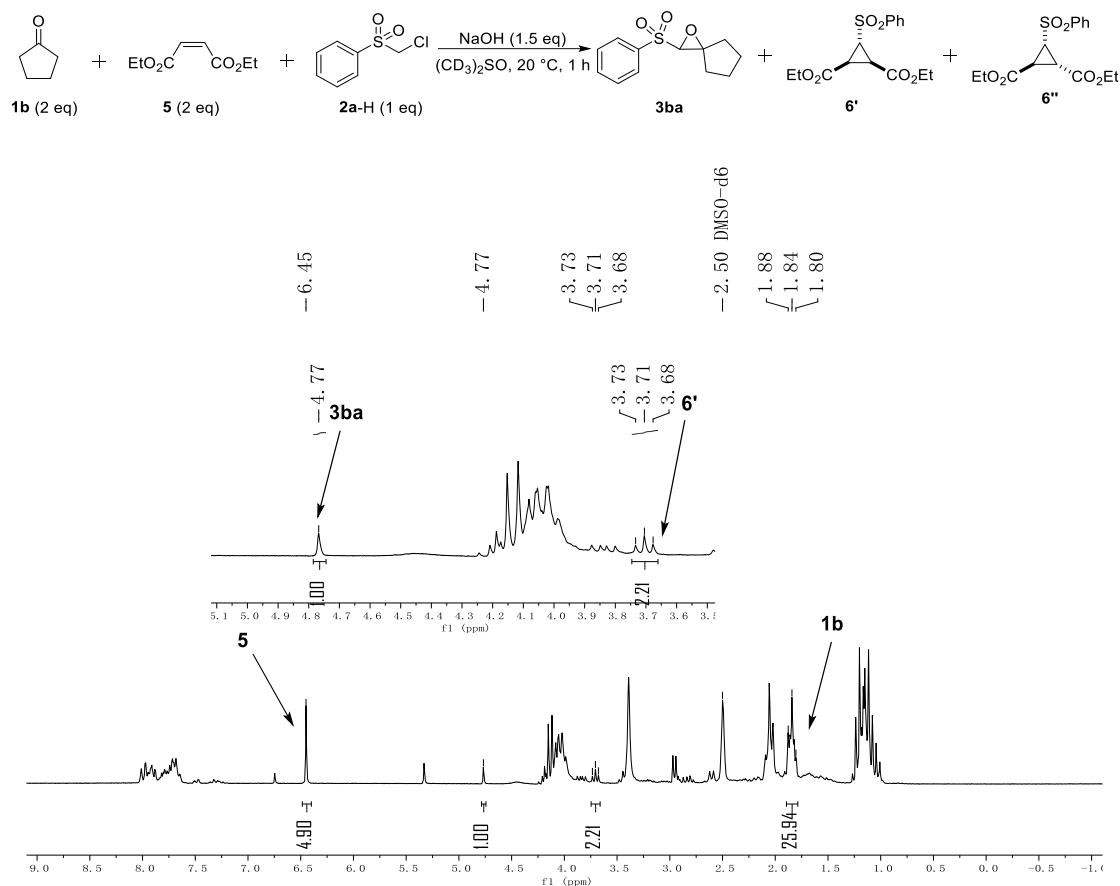
In analogy to Procedure F, **1j** (5.2 mg, 0.050 mmol), **1k** (31 mg, 0.35 mmol), **2b**-H (11 mg, 0.050 mmol) and NaOH (3.0 mg, 0.075 mmol) were combined.



¹H NMR spectroscopy shows selective formation of **3kb** (from **1k**) under the above mentioned experimental conditions ([**1k**]₀/[**1j**]₀ ≥ 7).

Competition of **1b** and **5** for carbanion **2a** (this chapter, Scheme 8)

In analogy to Procedure F, **1b** (17 mg, 0.20 mmol), **5** (34 mg, 0.20 mmol), **2a**-H (19 mg, 0.10 mmol) and NaOH (6.0 mg, 0.15 mmol) were combined in *d*₆-DMSO. After 1h, the reaction mixture was analyzed by ¹H NMR spectroscopy without further workup.



Based on the relative concentrations of remaining starting materials and formed products, the competition constant κ was determined:

The characteristic resonance of **6''** superimposed with resonances of other compounds.

Therefore, **6''** was derived as 0.99 based on dr (**6'**/**6''** = 1/0.45) from the product study of **5** with **2a**.

$$\mathbf{6} : \mathbf{5} = (\mathbf{6}' + \mathbf{6}'') : \mathbf{5} = (2.21 + 0.99) : (4.90/2) = 1.30$$

$$\mathbf{3ba} : \mathbf{1b} = 1 : (25.94/4) = 0.15$$

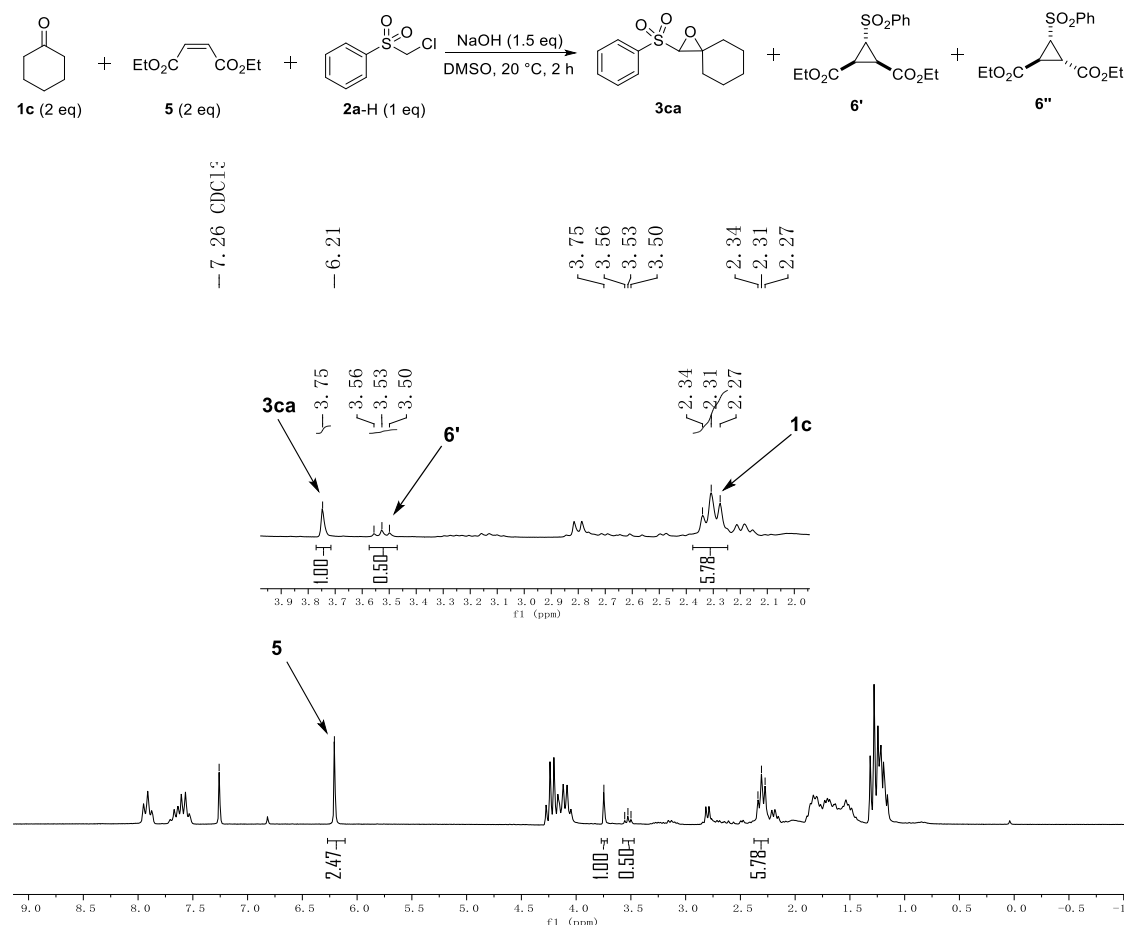
The relative reactivity of **1b** and **5** can be expressed by the competition constant κ .

$$\kappa = \frac{k_2^{\text{exp}(\mathbf{1b})}}{k_2^{\text{exp}(\mathbf{5})}} = \frac{\log\left(\frac{[\mathbf{1b}]_0}{[\mathbf{1b}]_t}\right)}{\log\left(\frac{[\mathbf{5}]_0}{[\mathbf{5}]_t}\right)} = \frac{\log\left(1 + \frac{[\mathbf{3ba}]_t}{[\mathbf{1b}]_t}\right)}{\log\left(1 + \frac{[\mathbf{6}]_t}{[\mathbf{5}]_t}\right)} = \frac{\log(1 + 0.15)}{\log(1 + 1.30)} = 0.17$$

Chapter 3: Kinetics and mechanism of oxirane-formation by Darzens condensation of ketones: quantification of the electrophilicities of ketones

Competition of **1c** and **5** for carbanion **2a** (this chapter, Scheme 8)

In analogy to Procedure E, **1c** (20 mg, 0.20 mmol), **5** (34 mg, 0.20 mmol), **2a**-H (19 mg, 0.10 mmol), and NaOH (6.0 mg, 0.15 mmol) were combined.



Based on the relative concentrations of remaining starting materials and formed products, the competition constant κ was determined:

The characteristic resonance of **6''** superimposed with resonances of other compounds.

Therefore, **6''** was derived as 0.23 based on dr (**6'**/**6''** = 1/0.45) from the product study of **5** with **2a**.

$$\mathbf{6} : \mathbf{5} = (\mathbf{6}' + \mathbf{6}'') : \mathbf{5} = (0.50 + 0.23) : (2.47/2) = 0.59$$

$$\mathbf{3ca} : \mathbf{1c} = 1 : (5.78/4) = 0.69$$

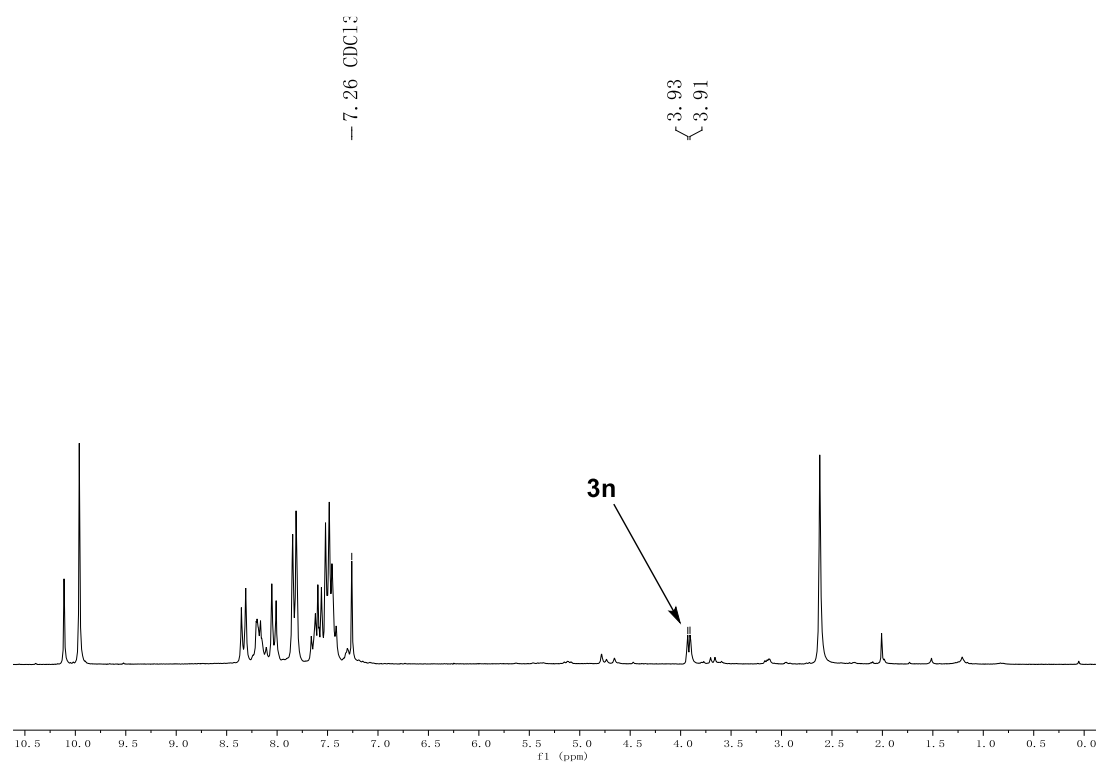
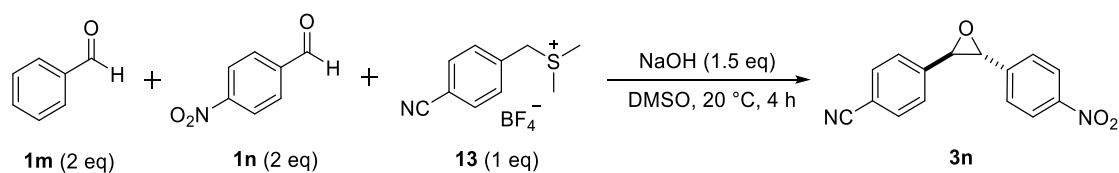
The relative reactivity of **1c** and **5** can be expressed by the competition constant κ .

$$\kappa = \frac{k_2^{\text{exp}}(\mathbf{1c})}{k_2^{\text{exp}}(\mathbf{5})} = \frac{\log\left(\frac{[\mathbf{1c}]_0}{[\mathbf{1c}]_t}\right)}{\log\left(\frac{[\mathbf{5}]_0}{[\mathbf{5}]_t}\right)} = \frac{\log\left(1 + \frac{[\mathbf{3ca}]_t}{[\mathbf{1c}]_t}\right)}{\log\left(1 + \frac{[\mathbf{6}]_t}{[\mathbf{5}]_t}\right)} = \frac{\log(1 + 0.69)}{\log(1 + 0.59)} = 1.13$$

Chapter 3: Kinetics and mechanism of oxirane-formation by Darzens condensation of ketones: quantification of the electrophilicities of ketones

Competition between **1m** and **1n** (trapping agent) for sulfur ylide **13** (this chapter, Scheme 10)

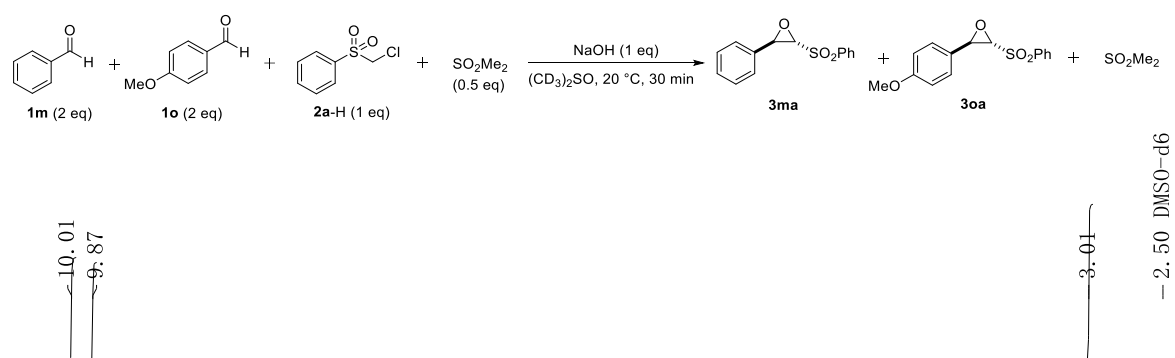
In analogy to Procedure E, **1m** (106 mg, 1.00 mmol), **1n** (151 mg, 1.00 mmol), **13** (132 mg, 0.500 mmol) and NaOH (30 mg, 0.75 mmol) were combined.



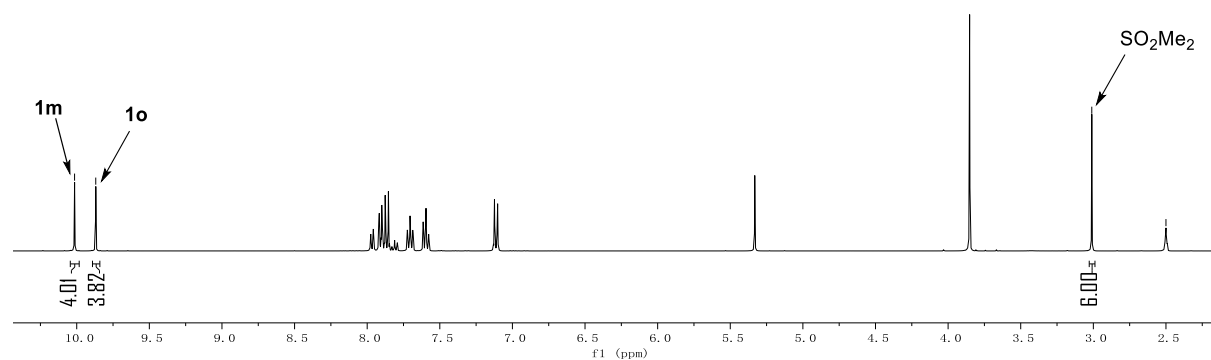
^1H NMR spectroscopy shows selective formation of **3n** (from **1n**) under the above mentioned experimental conditions ($[\mathbf{1n}]_0/[\mathbf{1m}]_0 = 1$).

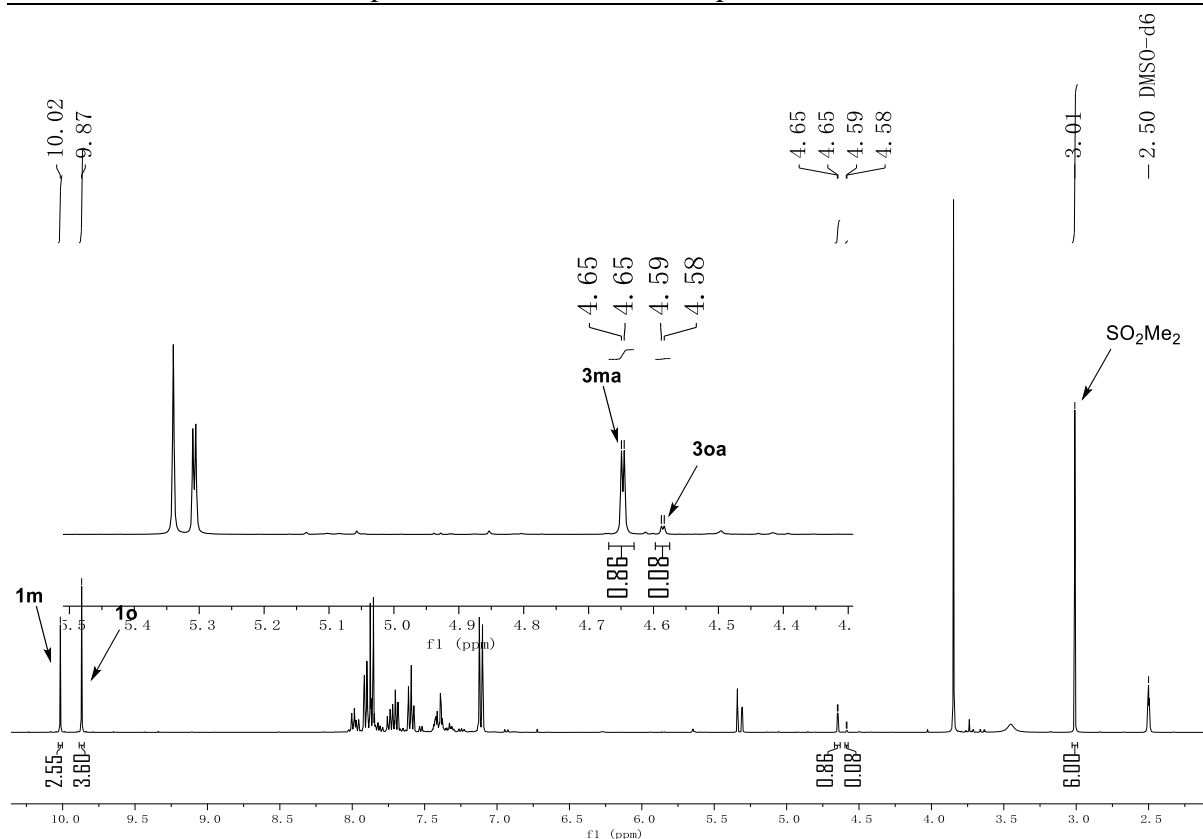
Competition of **1m** and **1o** for carbanion **2a** (this chapter, Scheme 11)

According to Procedure G, **1m** (21 mg, 0.20 mmol), **1o** (27 mg, 0.20 mmol), Me₂SO₂ (4.7 mg, 0.050 mmol), **2a**-H (19 mg, 0.10 mmol) and NaOH (4.0 mg, 0.10 mmol) were combined. After 30 min, the reaction mixture was analyzed by ¹H NMR spectroscopy without further workup.



before reaction
(NaOH was not added)





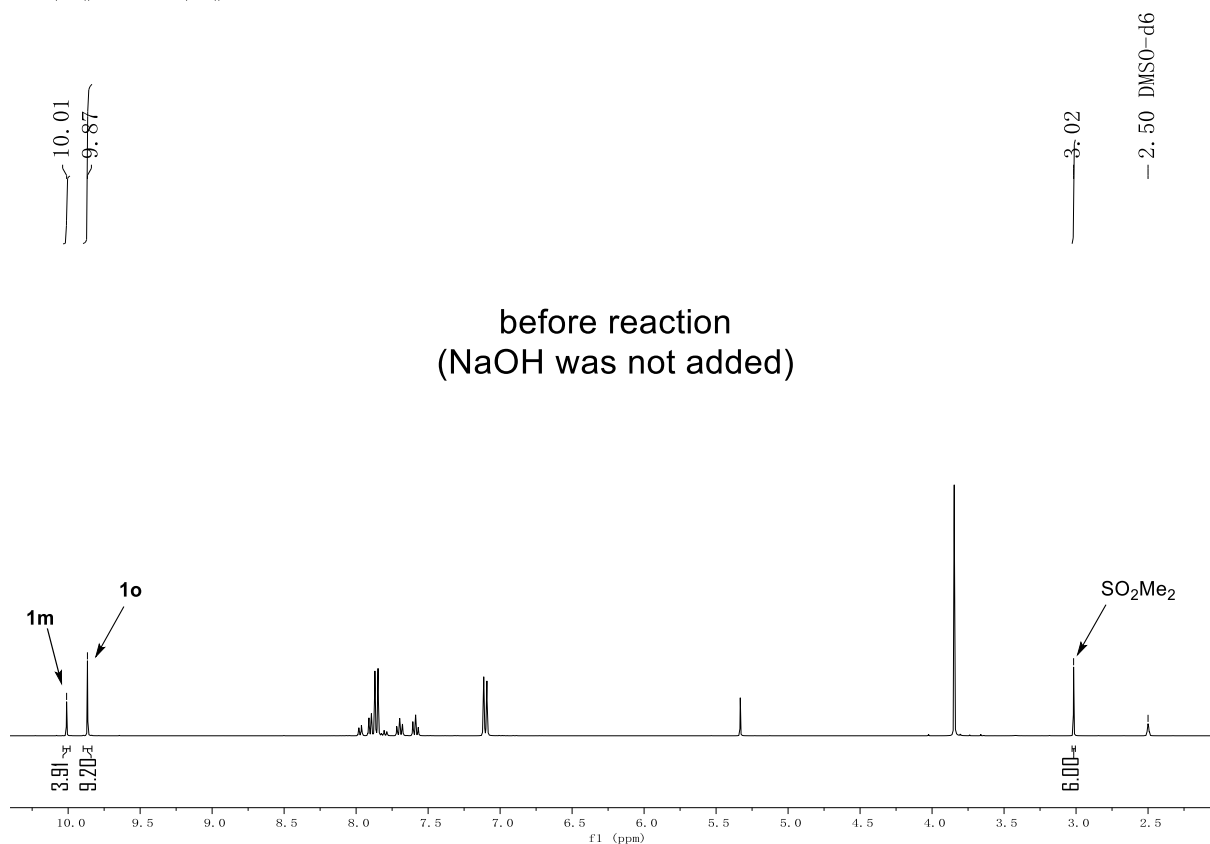
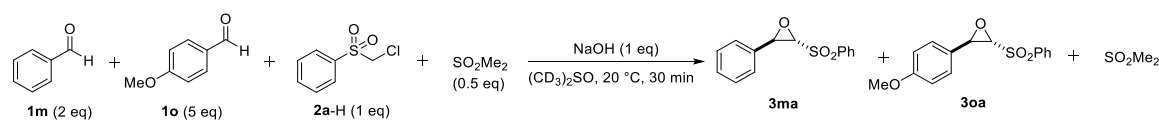
Based on the relative concentrations of remaining starting materials and formed products, the competition constant κ was determined:

$$\kappa = \frac{k_2^{\text{exp}}(\mathbf{1m})}{k_2^{\text{exp}}(\mathbf{1o})} = \frac{\log\left(\frac{[\mathbf{1m}]_o}{[\mathbf{1m}]_t}\right)}{\log\left(\frac{[\mathbf{1o}]_o}{[\mathbf{1o}]_t}\right)} = \frac{\log\left(1 + \frac{[\mathbf{3ma}]_t}{[\mathbf{1m}]_t}\right)}{\log\left(1 + \frac{[\mathbf{3oa}]_t}{[\mathbf{1o}]_t}\right)} = \frac{\log\left(1 + \frac{0.86}{2.55}\right)}{\log\left(1 + \frac{0.08}{3.60}\right)} = 13.22$$

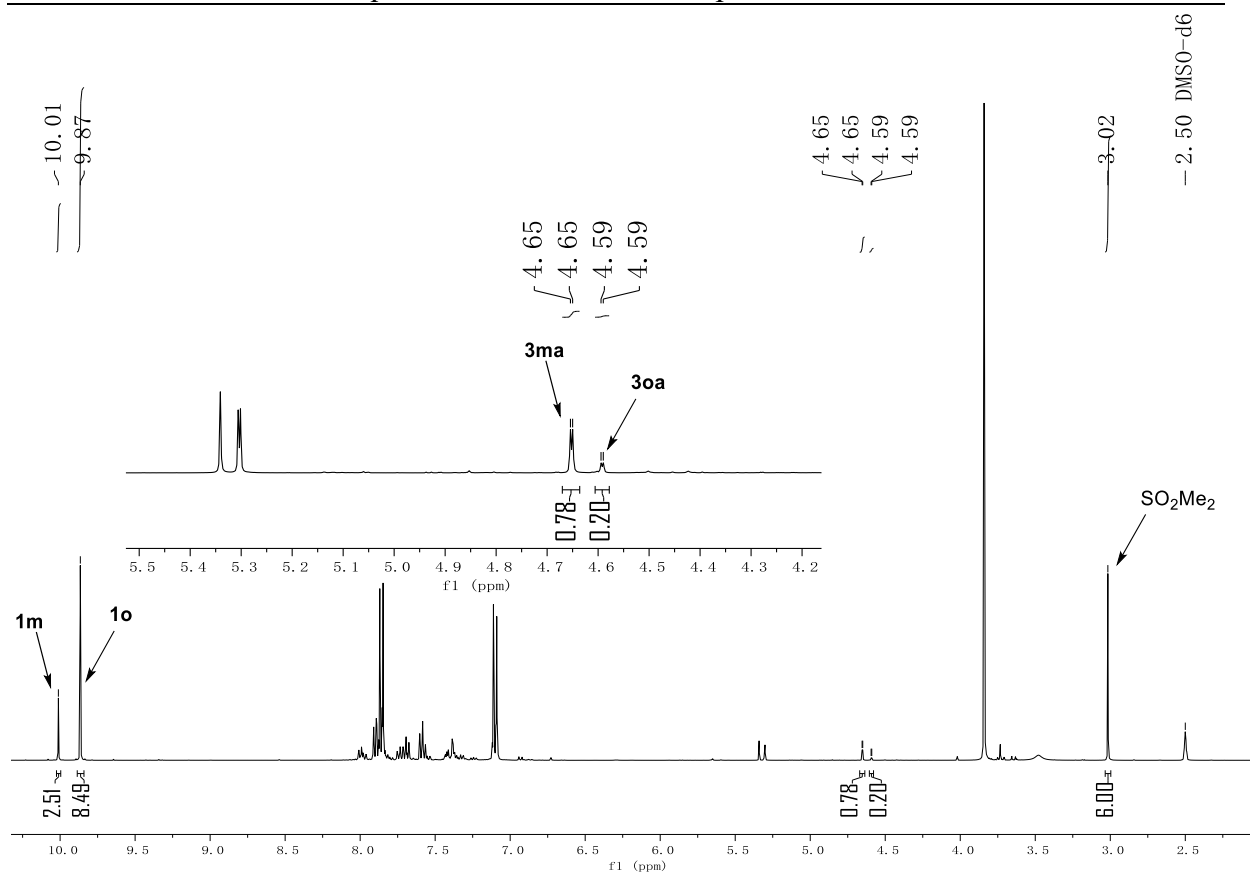
Chapter 3: Kinetics and mechanism of oxirane-formation by Darzens condensation of ketones: quantification of the electrophilicities of ketones

Competition of **1m** and **1o** for carbanion **2a** (this chapter, Scheme 11)

According to Procedure G, **1m** (21 mg, 0.20 mmol), **1o** (68 mg, 0.50 mmol), Me₂SO₂ (4.7 mg, 0.05 mmol), **2a**-H (19 mg, 0.10 mmol) and NaOH (4.0 mg, 0.10 mmol) were combined. After 30 min, the reaction mixture was analyzed by ¹H NMR spectroscopy without further workup.



before reaction
(NaOH was not added)

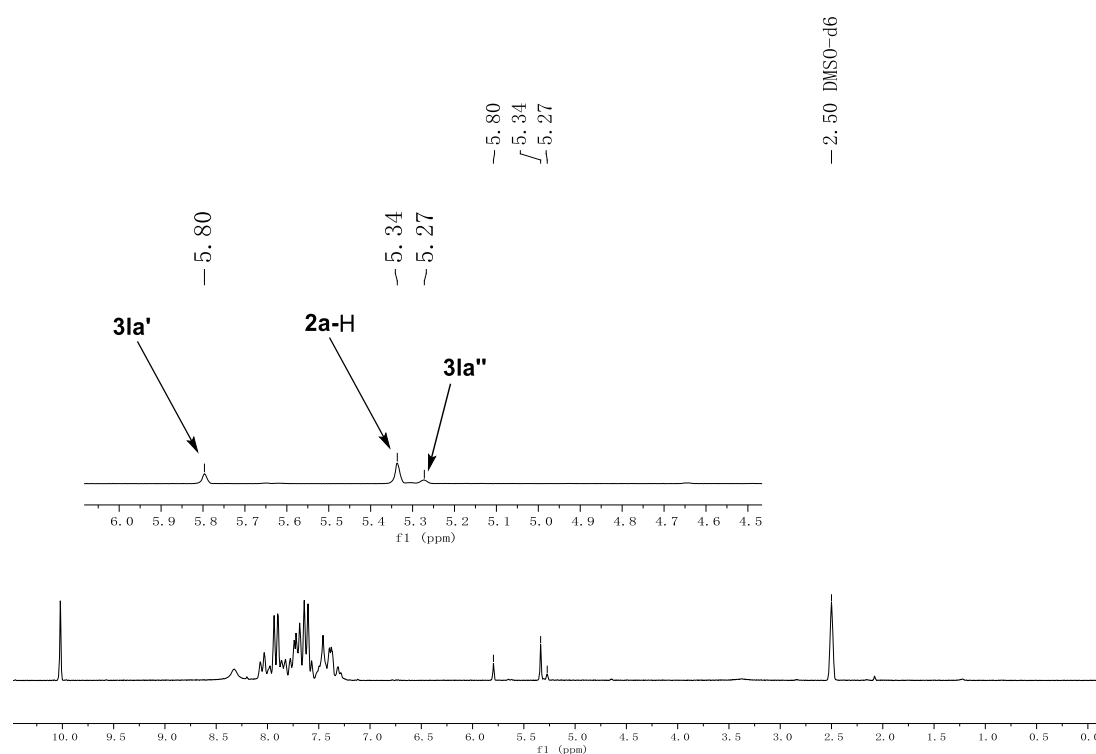
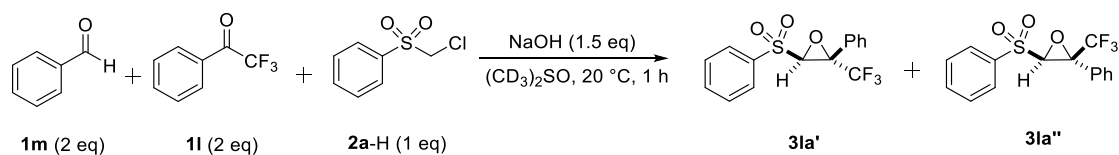


Based on the relative concentrations of remaining starting materials and formed products, the competition constant κ was determined:

$$\kappa = \frac{k_2^{\text{exp}}(\mathbf{1m})}{k_2^{\text{exp}}(\mathbf{1o})} = \frac{\log\left(\frac{[\mathbf{1m}]_o}{[\mathbf{1m}]_t}\right)}{\log\left(\frac{[\mathbf{1o}]_o}{[\mathbf{1o}]_t}\right)} = \frac{\log\left(1 + \frac{[\mathbf{3ma}]_t}{[\mathbf{1m}]_t}\right)}{\log\left(1 + \frac{[\mathbf{3oa}]_t}{[\mathbf{1o}]_t}\right)} = \frac{\log\left(1 + \frac{0.78}{2.51}\right)}{\log\left(1 + \frac{0.20}{8.49}\right)} = 11.62$$

Final κ is averaged from the individual κ of both control experiments, namely $\kappa = (13 + 12)/2 = 12.5$

Analogy to Procedure F, **1m** (21 mg, 0.20 mmol), **1l** (35 mg, 0.20 mmol), **2a**-H (19 mg, 0.10 mmol) and NaOH (6.0 mg, 0.15 mmol) were combined.

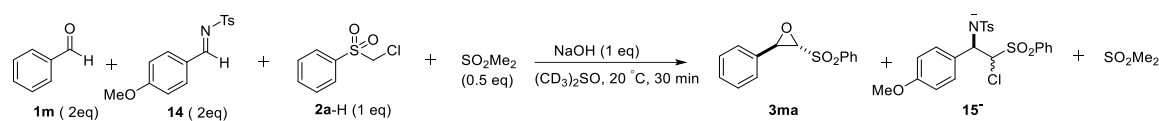


^1H NMR spectroscopy shows selective formation of **3la** (from **1l**) under the above mentioned experimental conditions ($[\text{1l}]_0/[\text{1m}]_0 = 1$).

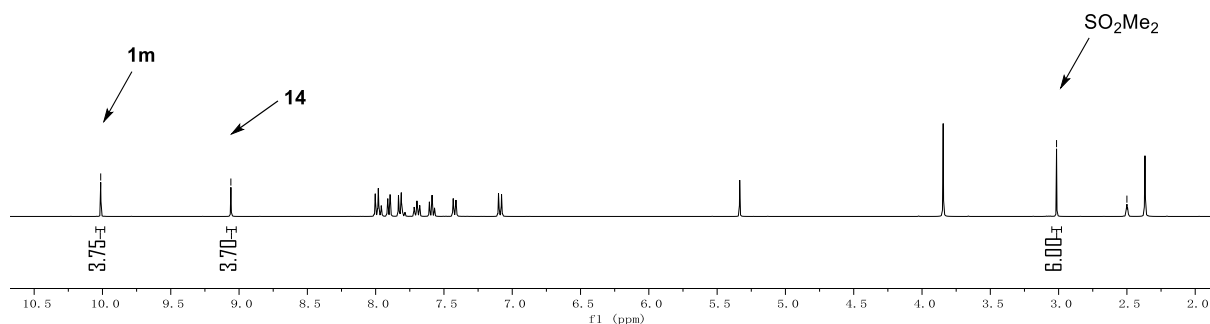
Chapter 3: Kinetics and mechanism of oxirane-formation by Darzens condensation of ketones: quantification of the electrophilicities of ketones

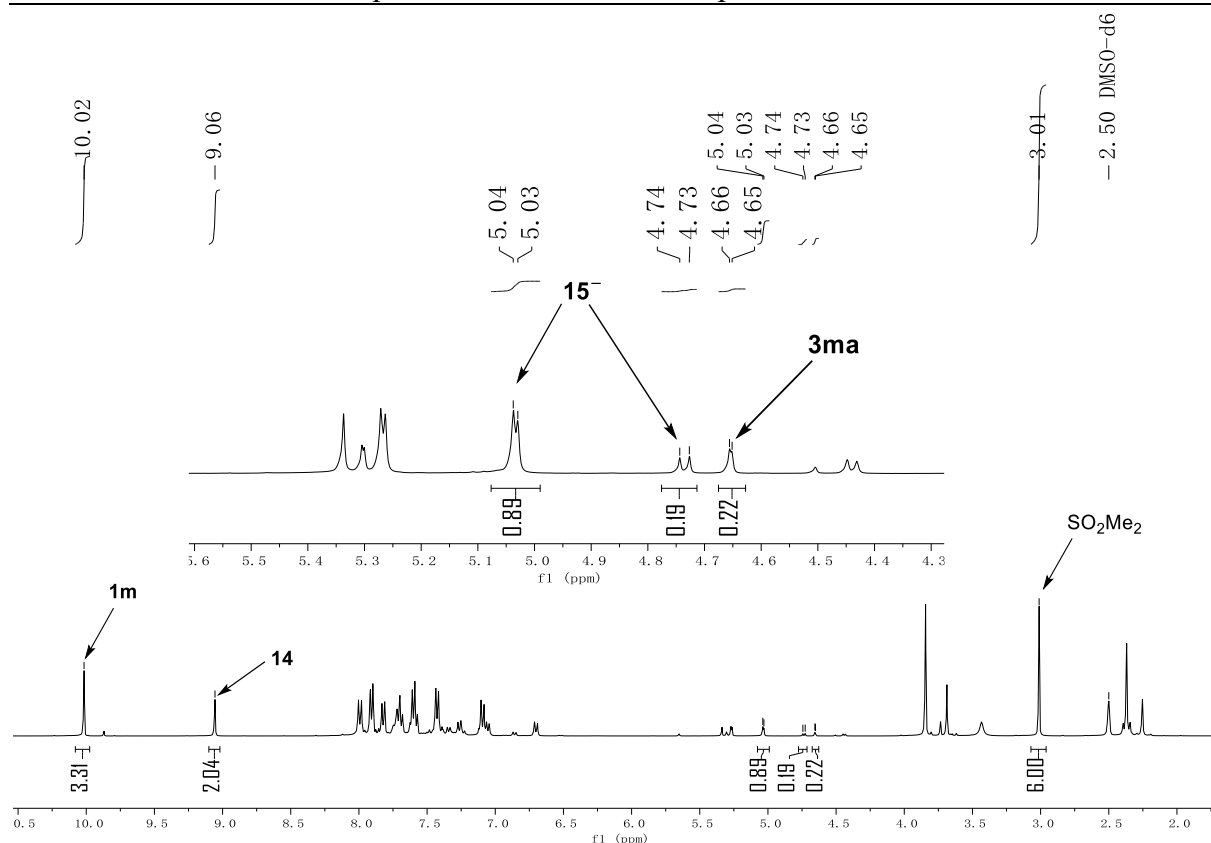
Competition of **14** and **1m** for carbanion **2a** (this chapter, Scheme 14)

According to Procedure G, **1m** (21 mg, 0.20 mmol), **14** (34 mg, 0.20 mmol), Me₂SO₂ (4.7 mg, 0.050 mmol), **2a**-H (19 mg, 0.10 mmol), and NaOH (4.0 mg, 0.10 mmol) were combined. After 30 min, the reaction mixture was analyzed by ¹H NMR spectroscopy without further workup.



before reaction
(NaOH was not added)





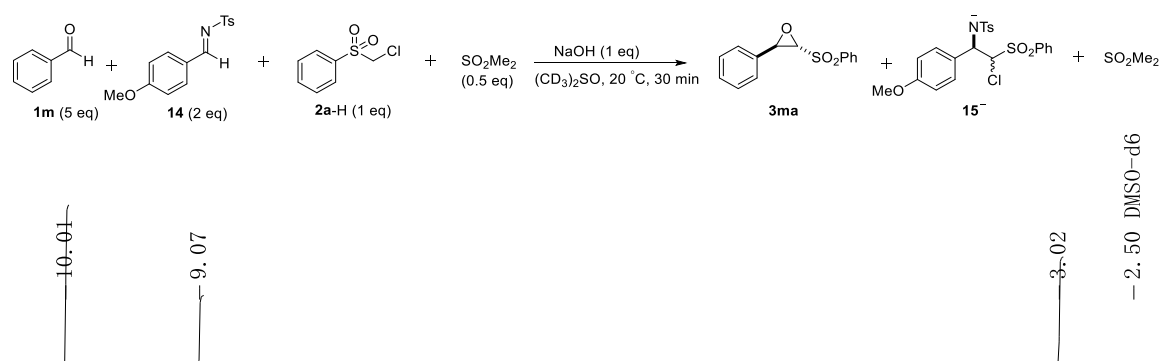
Based on the relative concentrations of remaining starting materials and formed products, the competition constant κ was determined:

$$\kappa = \frac{k_2^{\text{exp}}(\mathbf{14})}{k_2^{\text{exp}}(\mathbf{1m})} = \frac{\log\left(\frac{[\mathbf{14}]_o}{[\mathbf{14}]_t}\right)}{\log\left(\frac{[\mathbf{1m}]_o}{[\mathbf{1m}]_t}\right)} = \frac{\log\left(1 + \frac{[\mathbf{15}^-]_t}{[\mathbf{14}]_t}\right)}{\log\left(1 + \frac{[\mathbf{3ma}]_t}{[\mathbf{1m}]_t}\right)} = \frac{\log\left(1 + \frac{0.89 + 0.19}{2.04}\right)}{\log\left(1 + \frac{0.22}{3.31}\right)} = 6.61$$

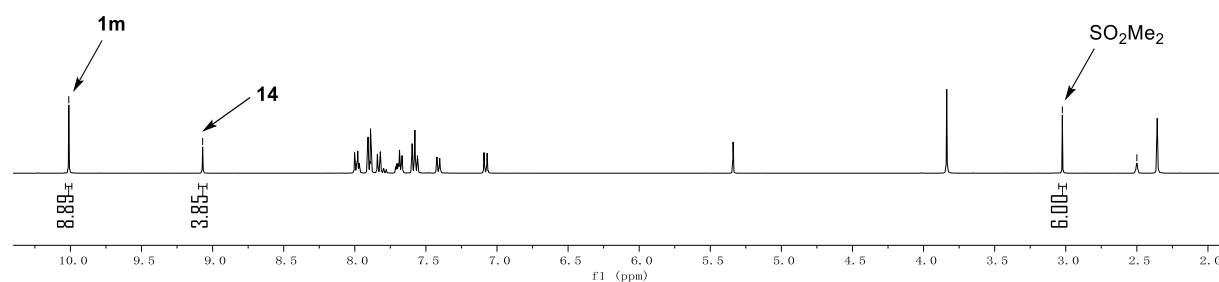
Chapter 3: Kinetics and mechanism of oxirane-formation by Darzens condensation of ketones: quantification of the electrophilicities of ketones

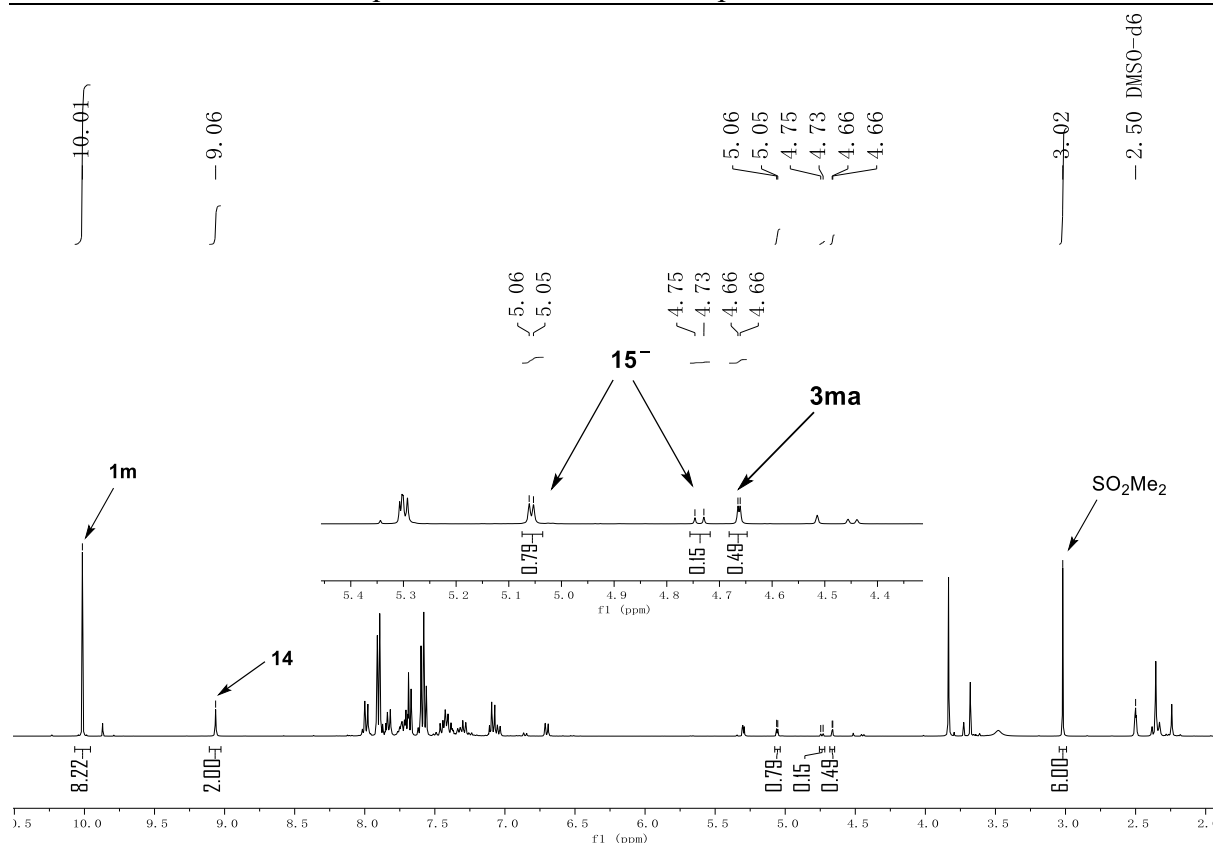
Competition of **14** and **1m** for carbanion **2a** (this chapter, Scheme 14)

According to Procedure G, **1m** (53 mg, 0.50 mmol), **14** (34 mg, 0.20 mmol), Me₂SO₂ (4.7 mg, 0.050 mmol), **2a**-H (19 mg, 0.10 mmol) and NaOH (4.0 mg, 0.10 mmol) were combined. After 30 min, the reaction mixture was analyzed by ¹H NMR spectroscopy without further workup.



before reaction
(NaOH was not added)





Based on the relative concentrations of remaining starting materials and formed products, the competition constant κ was determined:

$$\kappa = \frac{k_2^{\text{exp}(\mathbf{14})}}{k_2^{\text{exp}(\mathbf{1m})}} = \frac{\log\left(\frac{[\mathbf{14}]_o}{[\mathbf{14}]_t}\right)}{\log\left(\frac{[\mathbf{1m}]_o}{[\mathbf{1m}]_t}\right)} = \frac{\log\left(1 + \frac{[\mathbf{15}^-]_t}{[\mathbf{14}]_t}\right)}{\log\left(1 + \frac{[\mathbf{3ma}]_t}{[\mathbf{1m}]_t}\right)} = \frac{\log\left(1 + \frac{0.79 + 0.15}{2.00}\right)}{\log\left(1 + \frac{0.49}{8.22}\right)} = 6.65$$

Final κ is averaged from the individual κ of both control experiments, namely $\kappa = (6.61 + 6.65)/2 = 6.63$

(6) Crossover experiments

Procedure H for crossover experiments

A solution of **4-H** (0.050 mmol) and trapping reagent **1** (0.20 mmol) in DMSO (1.0 mL) was prepared. Then NaOH (0.075 mmol) was added at 20 °C. After the given time at 20 °C, 2% aq HCl (10 mL) was added, and the mixture was extracted with CHCl₃ (3 × 15 mL). The organic phases were combined, subsequently washed with water (2 × 30 mL) and brine (1 × 30 mL) to remove remaining DMSO, and then dried over anhydrous MgSO₄, and filtered. The solvent was evaporated under reduced pressure and the residue (in CDCl₃) was analyzed by ¹H NMR spectroscopy.

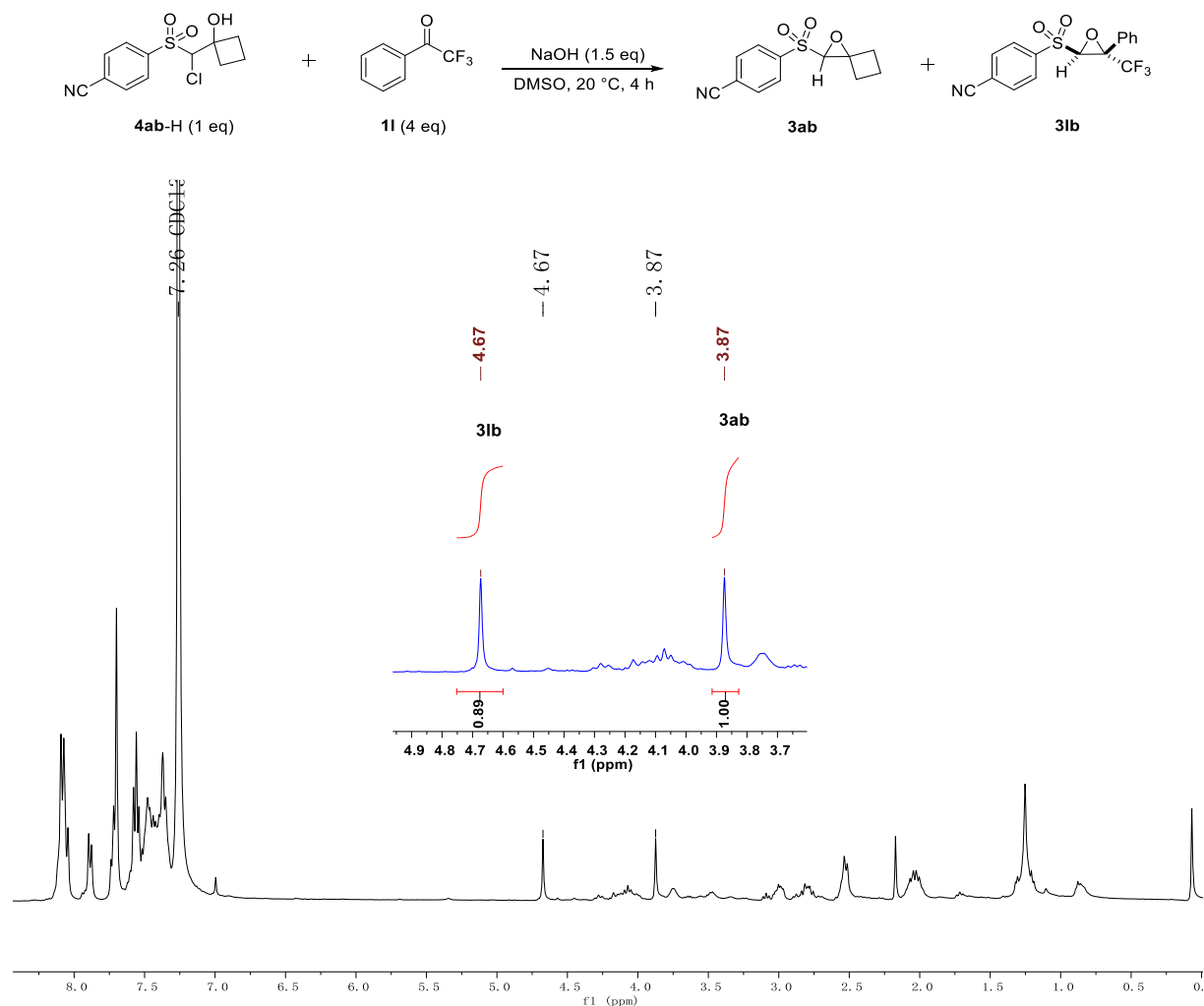
Procedure I for crossover experiments

Chlorohydrin **4-H** (0.050 mmol) and trapping reagent **1** (0.15 mmol) were dissolved in *d*₆-DMSO (1.0 mL). Then NaOH (0.075 mmol) was added at 20 °C. After the given time, the reaction mixture was analyzed by ¹H NMR spectroscopy.

Chapter 3: Kinetics and mechanism of oxirane-formation by Darzens condensation of ketones: quantification of the electrophilicities of ketones

Substrate **4ab-H** (with **1I** as trapping agent)

According to Procedure H, **4ab-H** (14 mg, 0.049 mmol), **1I** (35 mg, 0.20 mmol), and NaOH (3.0 mg, 0.075 mmol) were combined. After workup, the residue was analyzed by ^1H NMR spectroscopy.

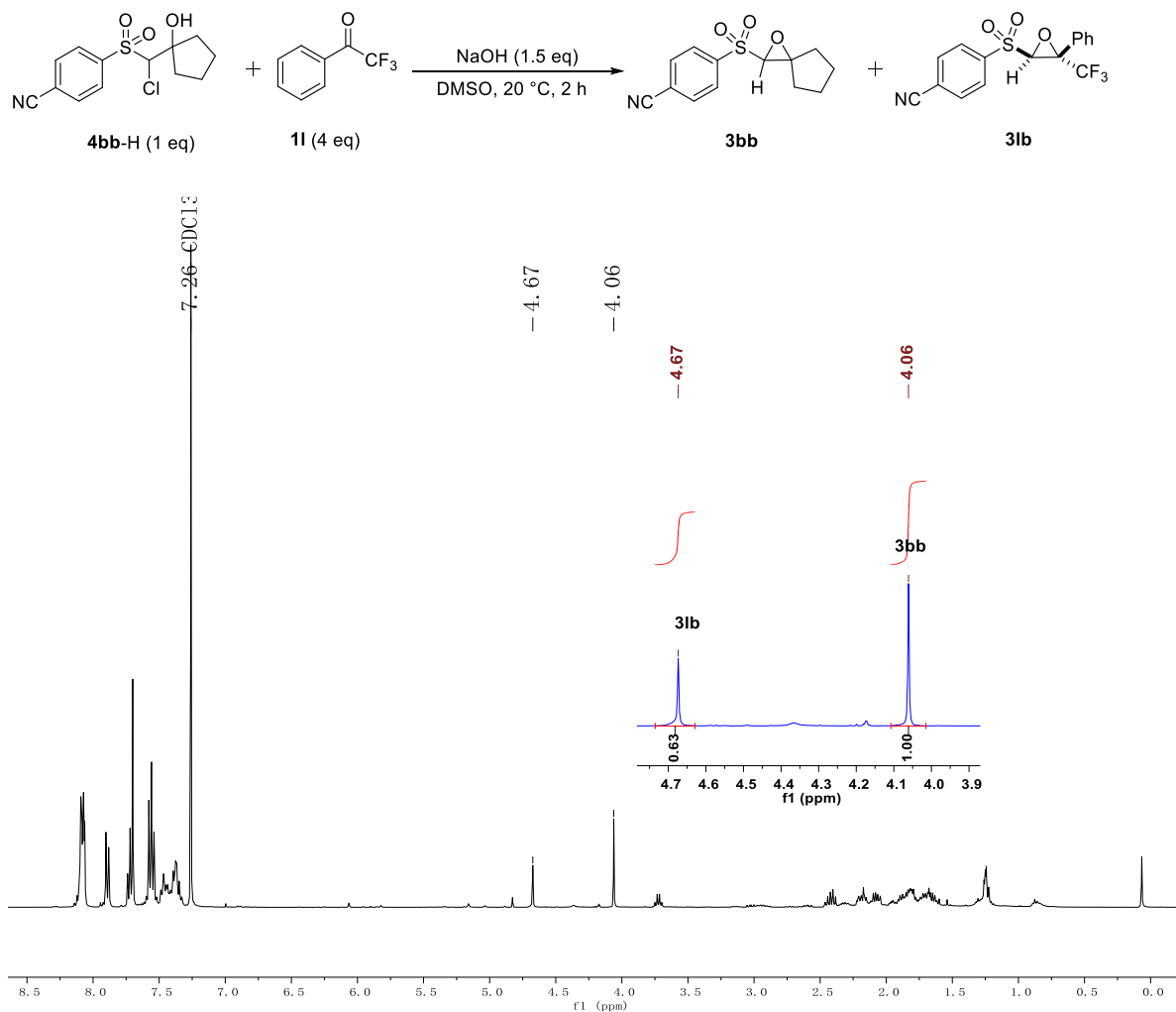


Crossover reaction result: $P_{\text{CC}}/P_{\text{rc}} = [\mathbf{3Ib}]/[\mathbf{3ab}] = 0.89$

Chapter 3: Kinetics and mechanism of oxirane-formation by Darzens condensation of ketones: quantification of the electrophilicities of ketones

Substrate **4bb**-H (with **1l** as trapping agent)

According to Procedure H, **4bb**-H (15 mg, 0.050 mmol), **1l** (35 mg, 0.20 mmol), and NaOH (3.0 mg, 0.075 mmol) were combined. After workup, the residue was analyzed by ^1H NMR spectroscopy.

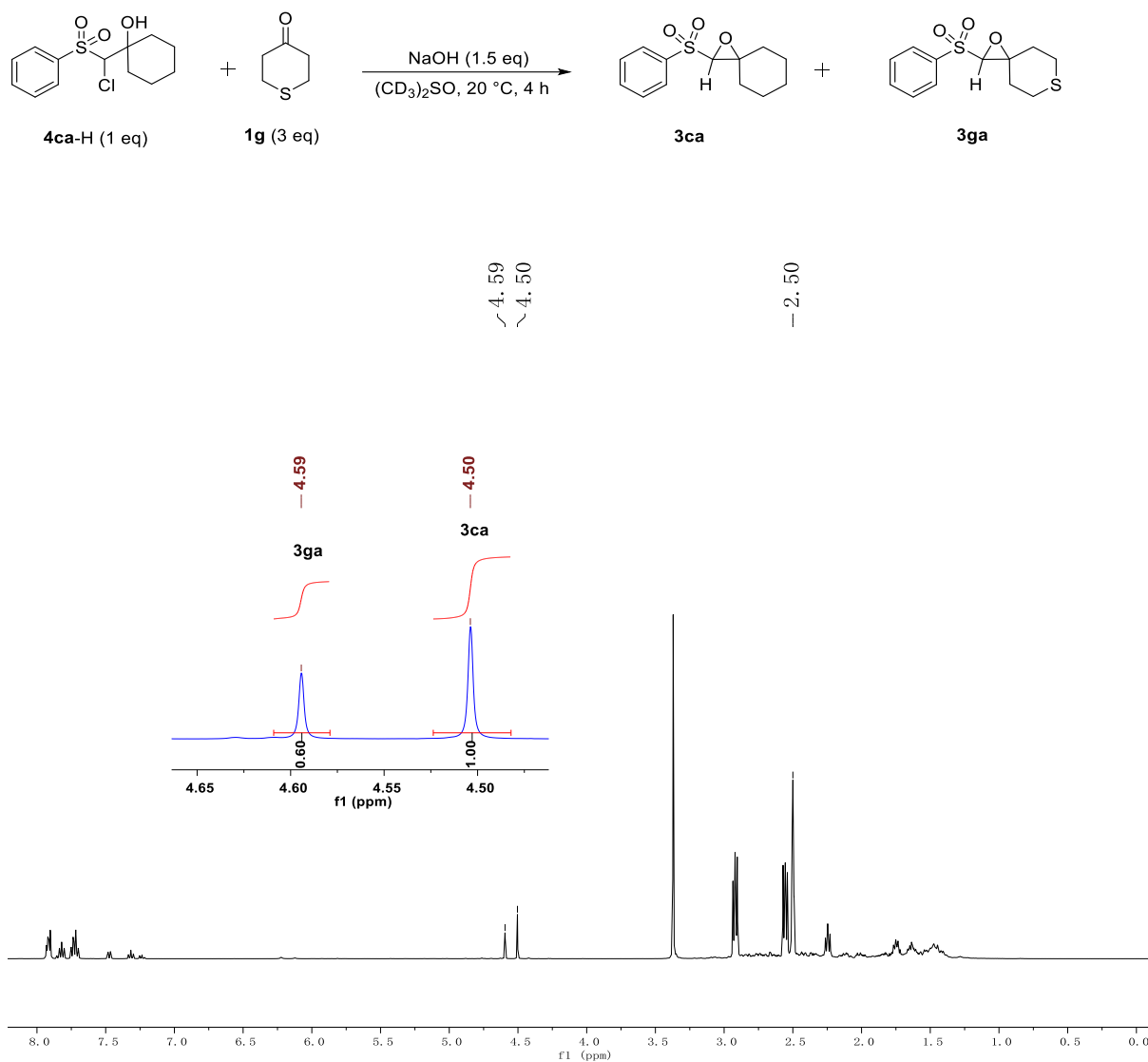


Crossover reaction result: $P_{\text{CC}}/P_{\text{rc}} = [\mathbf{3lb}]/[\mathbf{3bb}] = 0.63$

Chapter 3: Kinetics and mechanism of oxirane-formation by Darzens condensation of ketones: quantification of the electrophilicities of ketones

Substrate **4ca-H** (with **1g** as trapping agent)

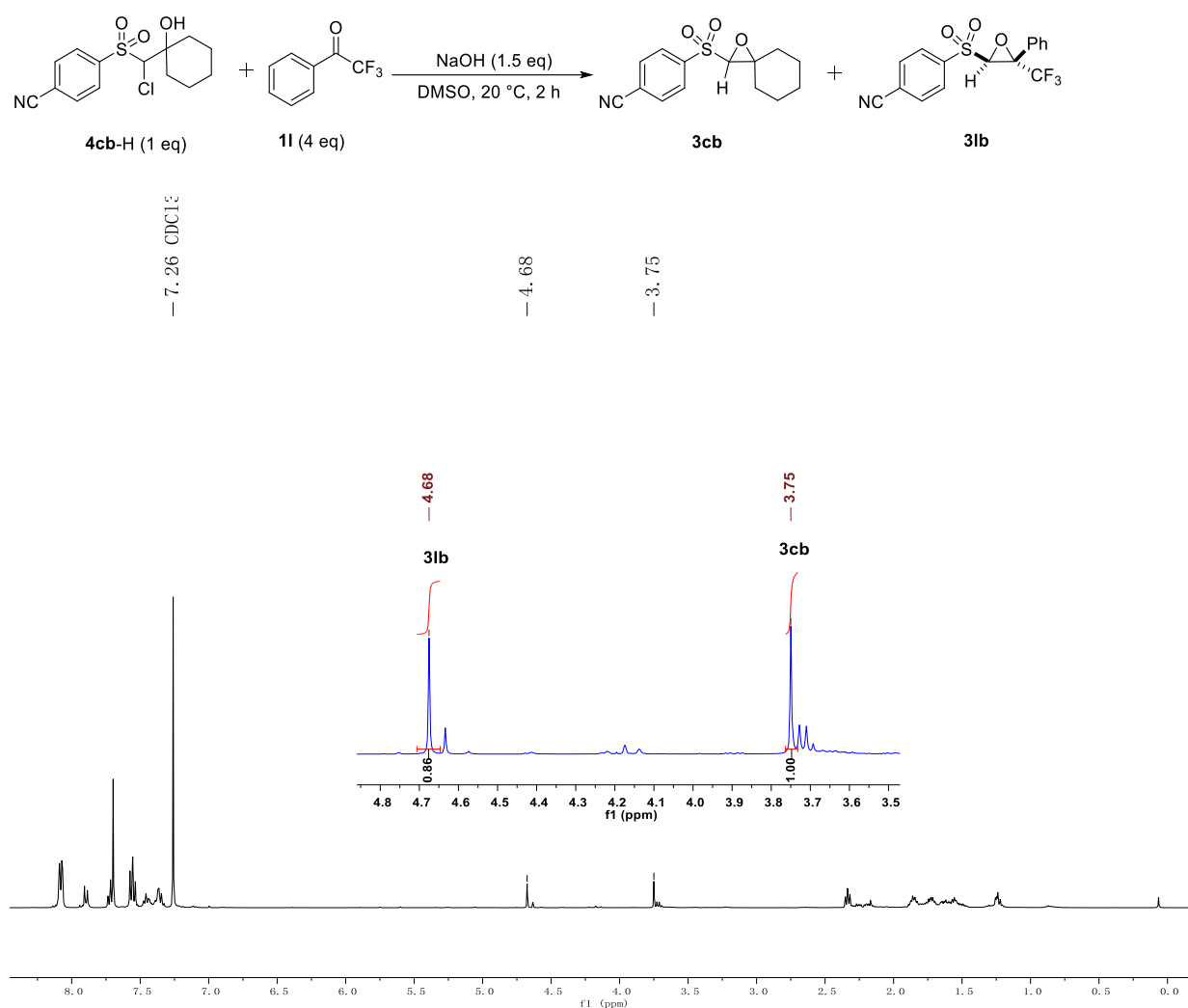
According to Procedure I, **4ca-H** (14 mg, 0.049 mmol), **1g** (17 mg, 0.15 mmol), and NaOH (3.0 mg, 0.075 mmol) were combined and analyzed by ¹H NMR spectroscopy.



Crossover reaction result: $P_{-CC}/P_{rc} = [\mathbf{3ga}]/[\mathbf{3ca}] = 0.60$

Substrate **4cb-H** (with **1I** as trapping agent)

According to Procedure H, **4cb-H** (16 mg, 0.051 mmol), **1I** (35 mg, 0.20 mmol), and NaOH (3.0 mg, 0.075 mmol) were combined. After workup, the residue was analyzed by ^1H NMR spectroscopy.

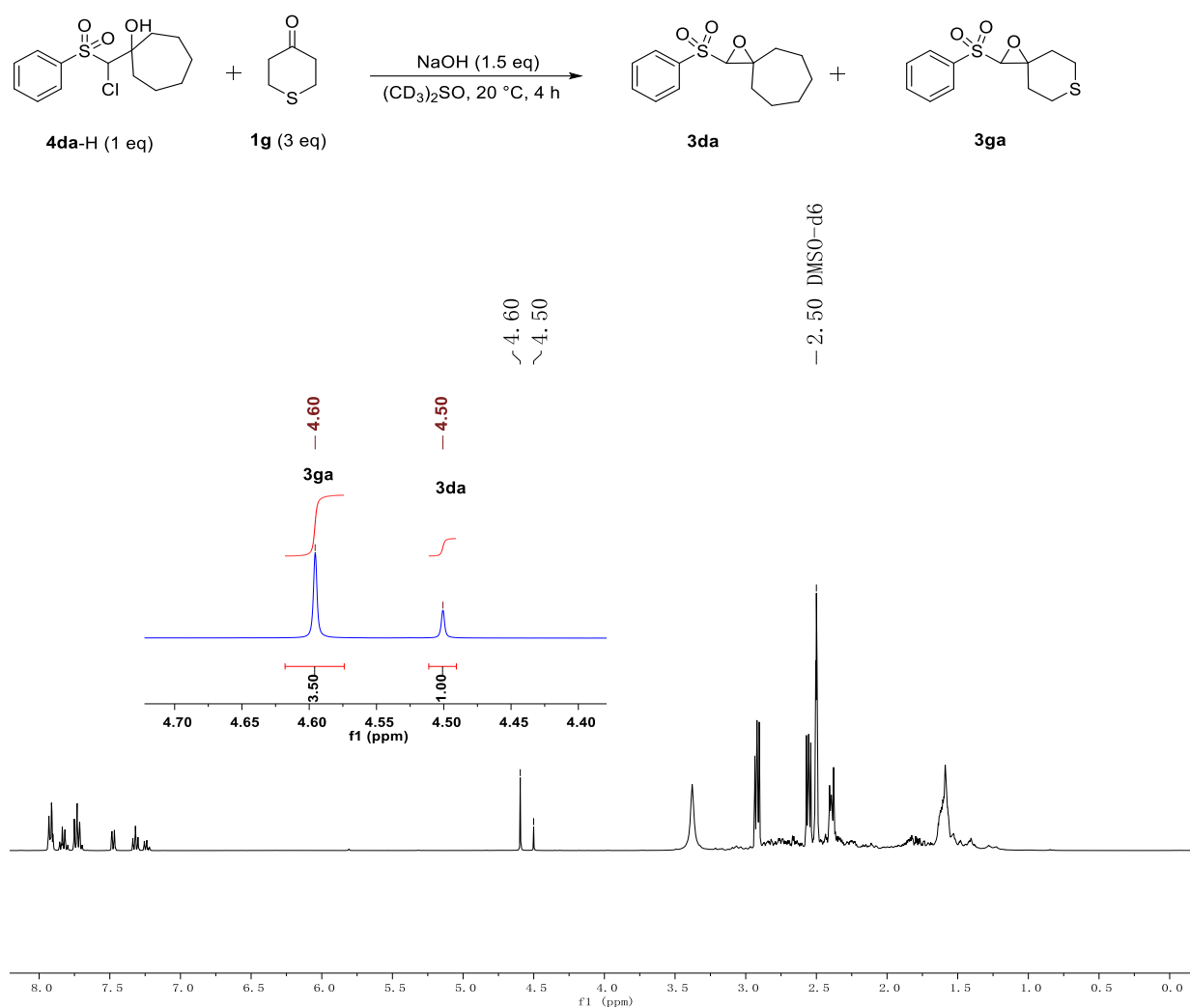


Crossover reaction result: $P_{\text{CC}}/P_{\text{rc}} = [\mathbf{3Ib}]/[\mathbf{3cb}] = 0.86$

Chapter 3: Kinetics and mechanism of oxirane-formation by Darzens condensation of ketones: quantification of the electrophilicities of ketones

Substrate **4da-H** (with **1g** as trapping agent)

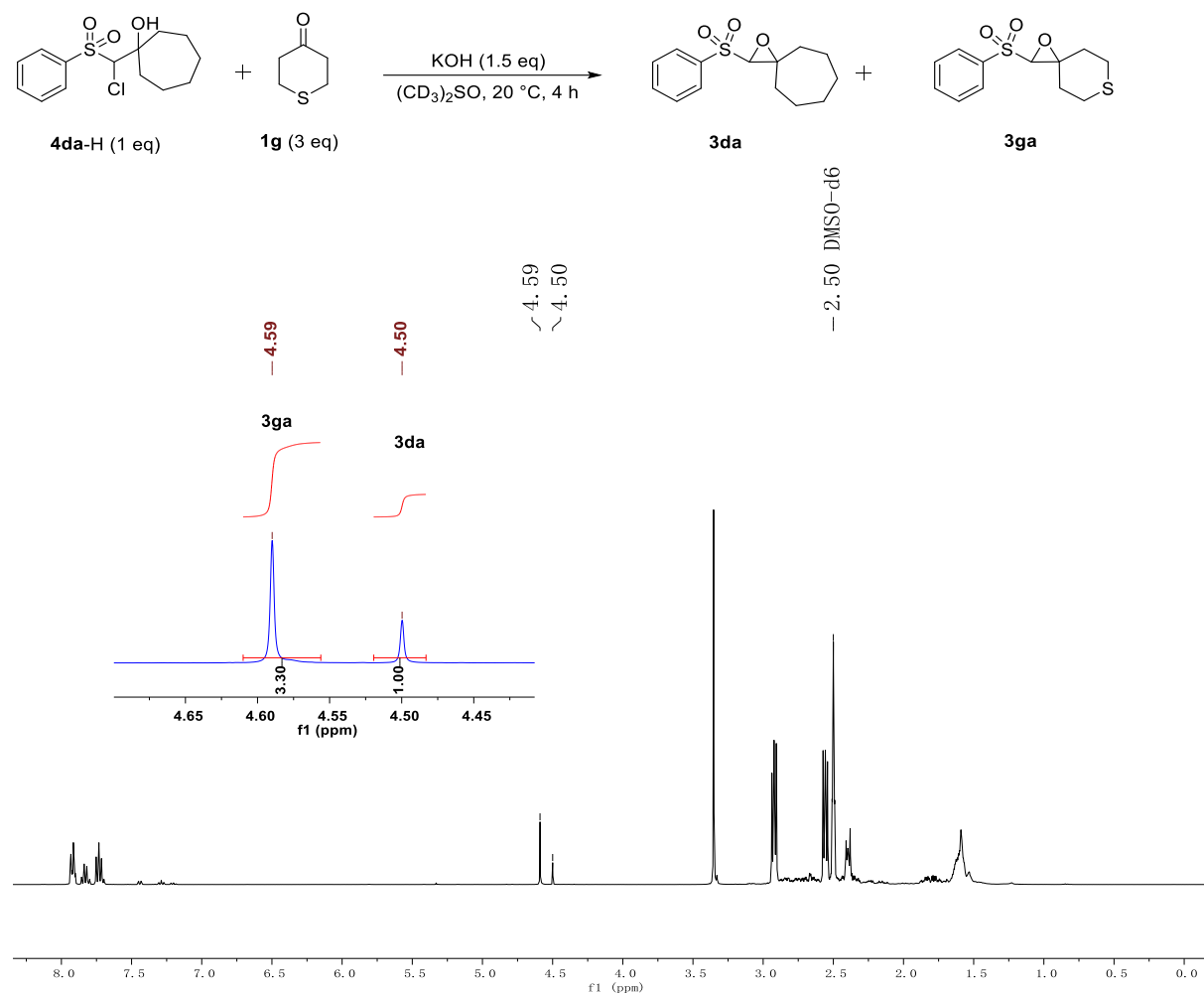
According to Procedure I, **4da-H** (15 mg, 0.050 mmol), **1g** (17 mg, 0.15 mmol), and NaOH (3.0 mg, 0.075 mmol) were combined and analyzed by ^1H NMR spectroscopy.



Crossover reaction result: $P_{\text{CC}}/P_{\text{rc}} = [\mathbf{3ga}]/[\mathbf{3da}] = 3.50$

Substrate **4da-H** (with **1g** as trapping agent, KOH as base)

In analogy to Procedure I, **4da-H** (15 mg, 0.050 mmol), **1g** (17 mg, 0.15 mmol), and KOH (4.0 mg, 0.071 mmol) were combined and analyzed by ^1H NMR spectroscopy.

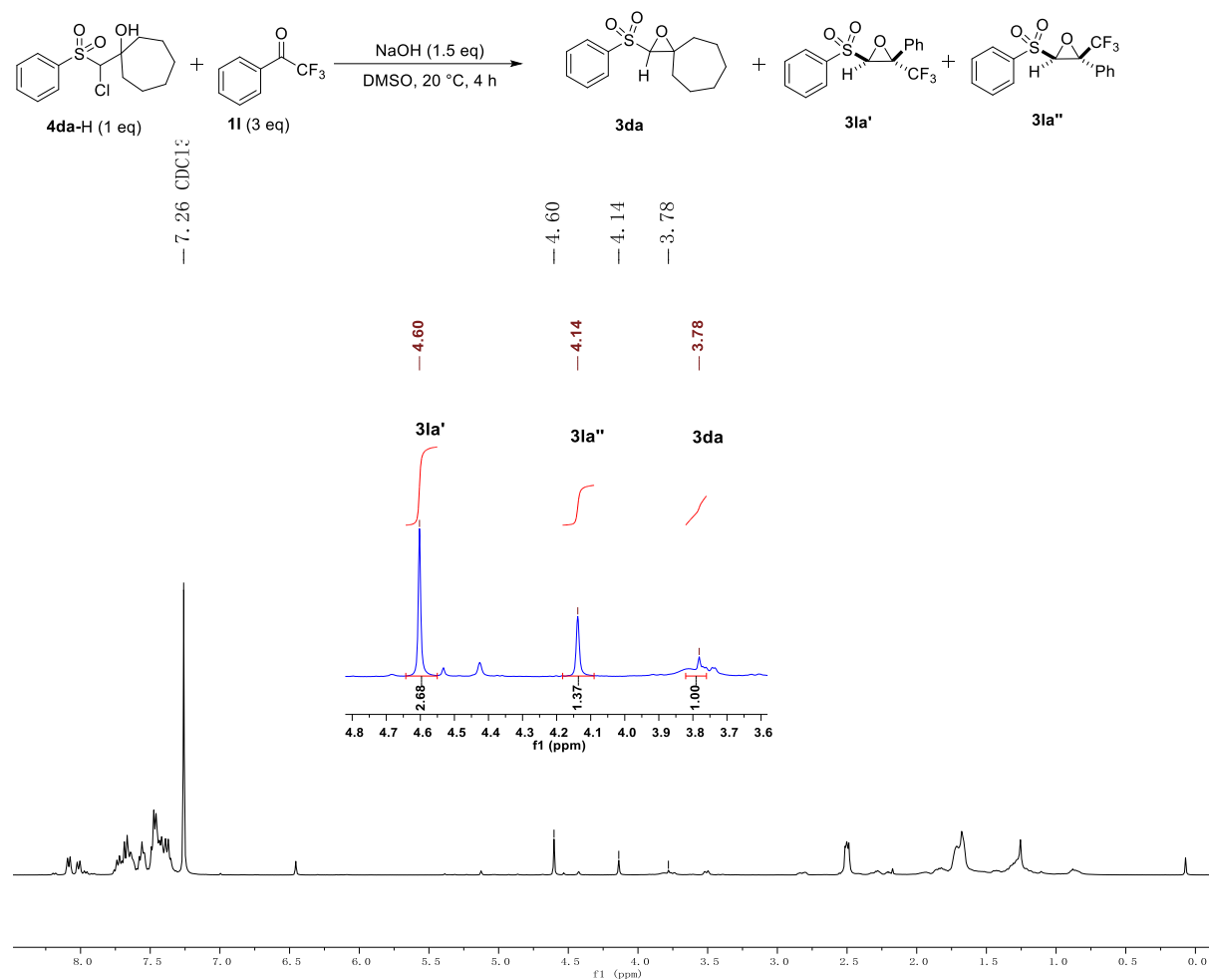


Crossover reaction result: $P_{\text{CC}}/P_{\text{rc}} = [\mathbf{3ga}]/[\mathbf{3da}] = 3.30$

Chapter 3: Kinetics and mechanism of oxirane-formation by Darzens condensation of ketones: quantification of the electrophilicities of ketones

Substrate **4da-H** (with **1I** as trapping agent)

In analogy to Procedure H, **4da-H** (15 mg, 0.050 mmol), **1I** (26 mg, 0.15 mmol), and NaOH (3.0 mg, 0.075 mmol) were combined. After workup, the residue was analyzed by ^1H NMR spectroscopy.

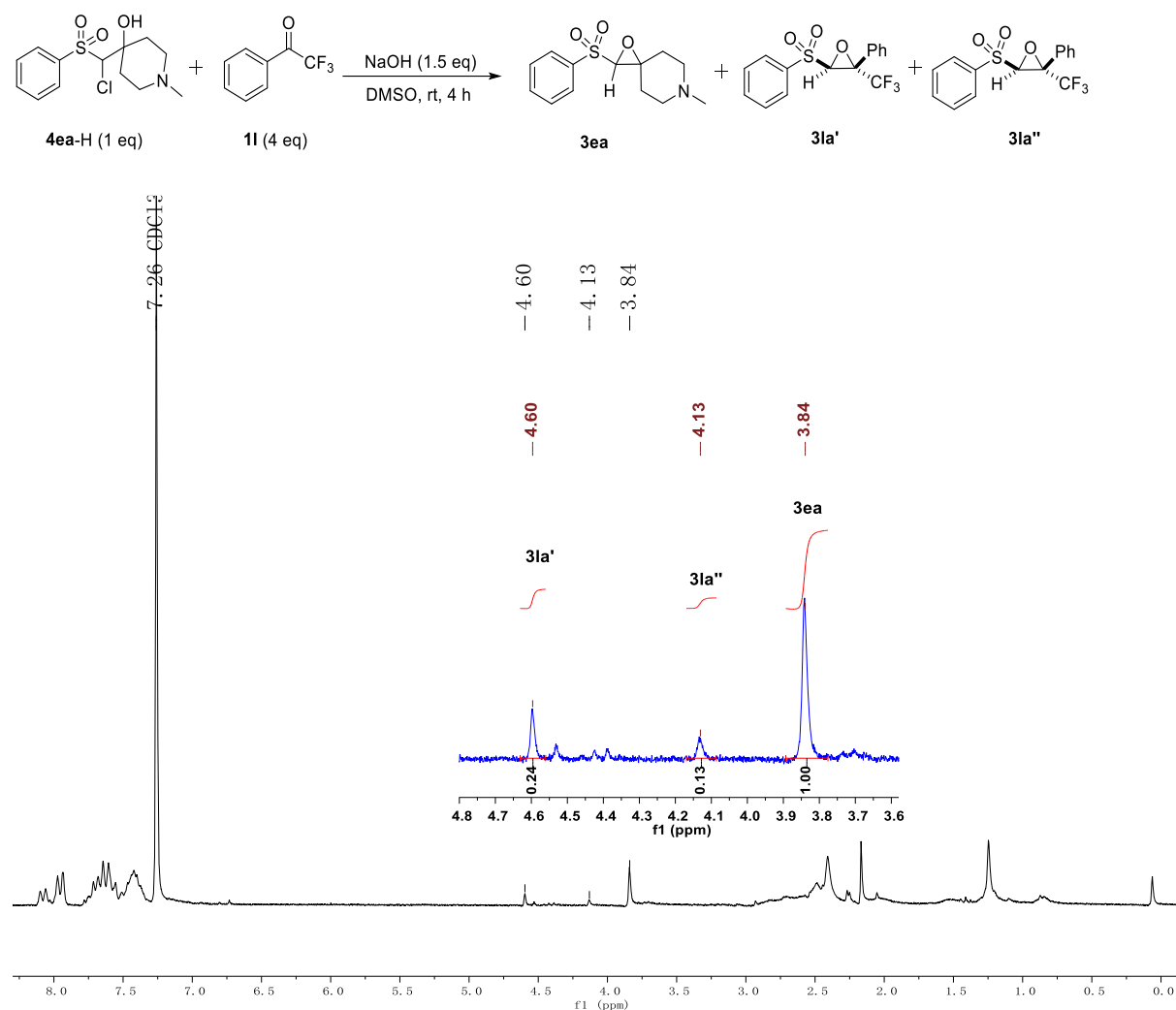


Crossover reaction result: $P_{\text{CC}}/P_{\text{rc}} = ([\mathbf{3la'}] + [\mathbf{3la''}])/[\mathbf{3da}] = 4.05$

Chapter 3: Kinetics and mechanism of oxirane-formation by Darzens condensation of ketones: quantification of the electrophilicities of ketones

Substrate **4ea-H** (with **11** as trapping agent)

In analogy to Procedure H but workup by saturated NH_4Cl solution instead of 2% aq HCl , **4ea-H** (15 mg, 0.050 mmol), **11** (35 mg, 0.20 mmol), and NaOH (3.0 mg, 0.075 mmol) were combined. After workup, the residue was analyzed by ^1H NMR spectroscopy.

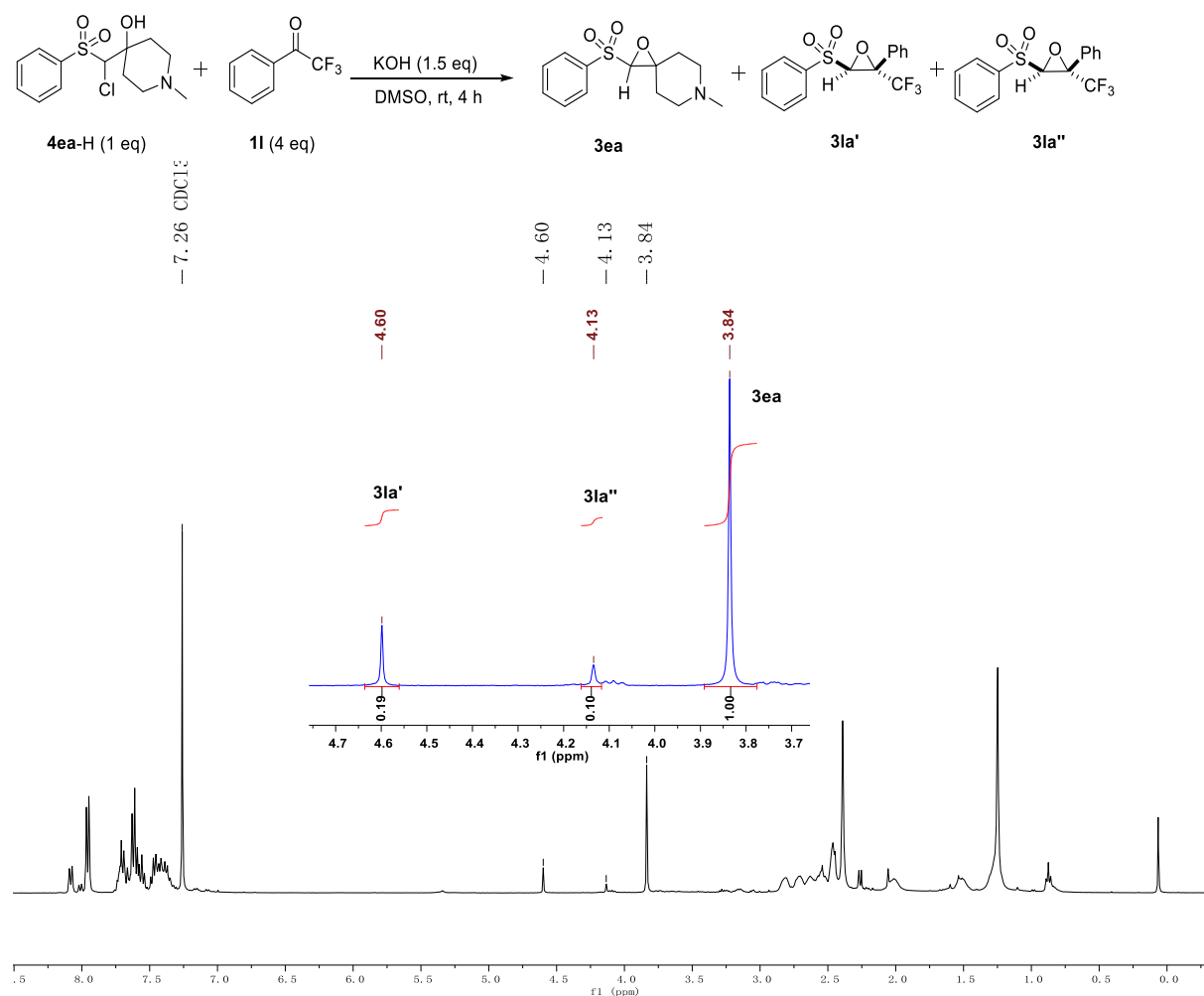


Crossover reaction result: $P_{\text{CC}}/P_{\text{rc}} = ([\mathbf{3la}'] + [\mathbf{3la}''])/[\mathbf{3ea}] = 0.37$

Chapter 3: Kinetics and mechanism of oxirane-formation by Darzens condensation of ketones: quantification of the electrophilicities of ketones

Substrate **4ea-H** (with **11** as trapping agent, KOH as base)

In analogy to Procedure H but workup by saturated NH₄Cl solution instead of 2% aq HCl, **4ea-H** (15 mg, 0.050 mmol), **11** (35 mg, 0.20 mmol), and KOH (4.0 mg, 0.071 mmol) were combined. After workup, the residue was analyzed by ¹H NMR spectroscopy.

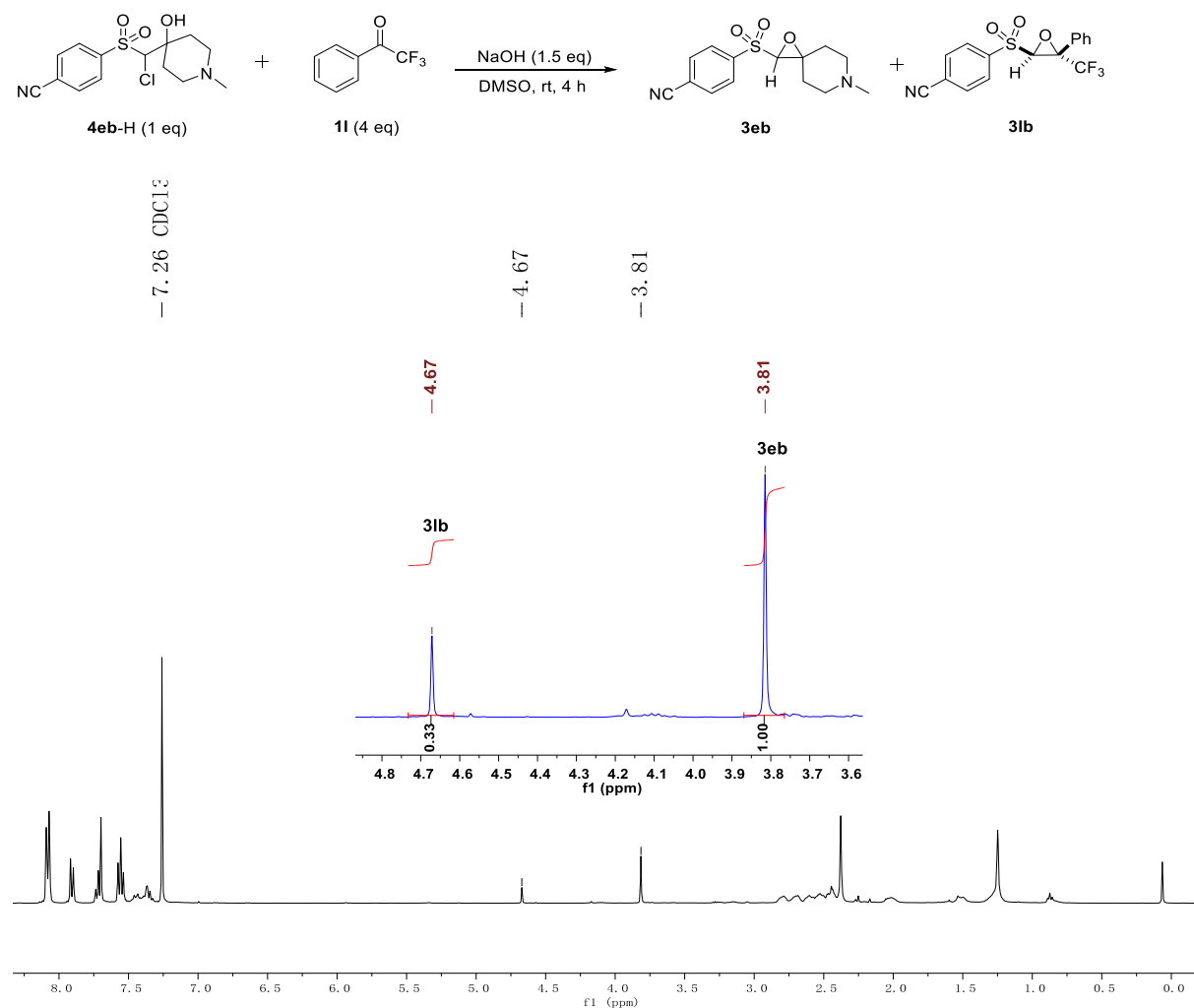


Crossover reaction result: $P_{CC}/P_{rc} = ([3la'] + [3la''])/[3ea] = 0.29$

Chapter 3: Kinetics and mechanism of oxirane-formation by Darzens condensation of ketones: quantification of the electrophilicities of ketones

Substrate **4eb**-H (with **1I** as trapping agent)

In analogy to Procedure H but workup by saturated NH_4Cl solution instead of 2% aq HCl , **4eb**-H (16 mg, 0.049 mmol), **1I** (35 mg, 0.20 mmol), and NaOH (3.0 mg, 0.075 mmol) were combined. After workup, the residue was analyzed by ^1H NMR spectroscopy.

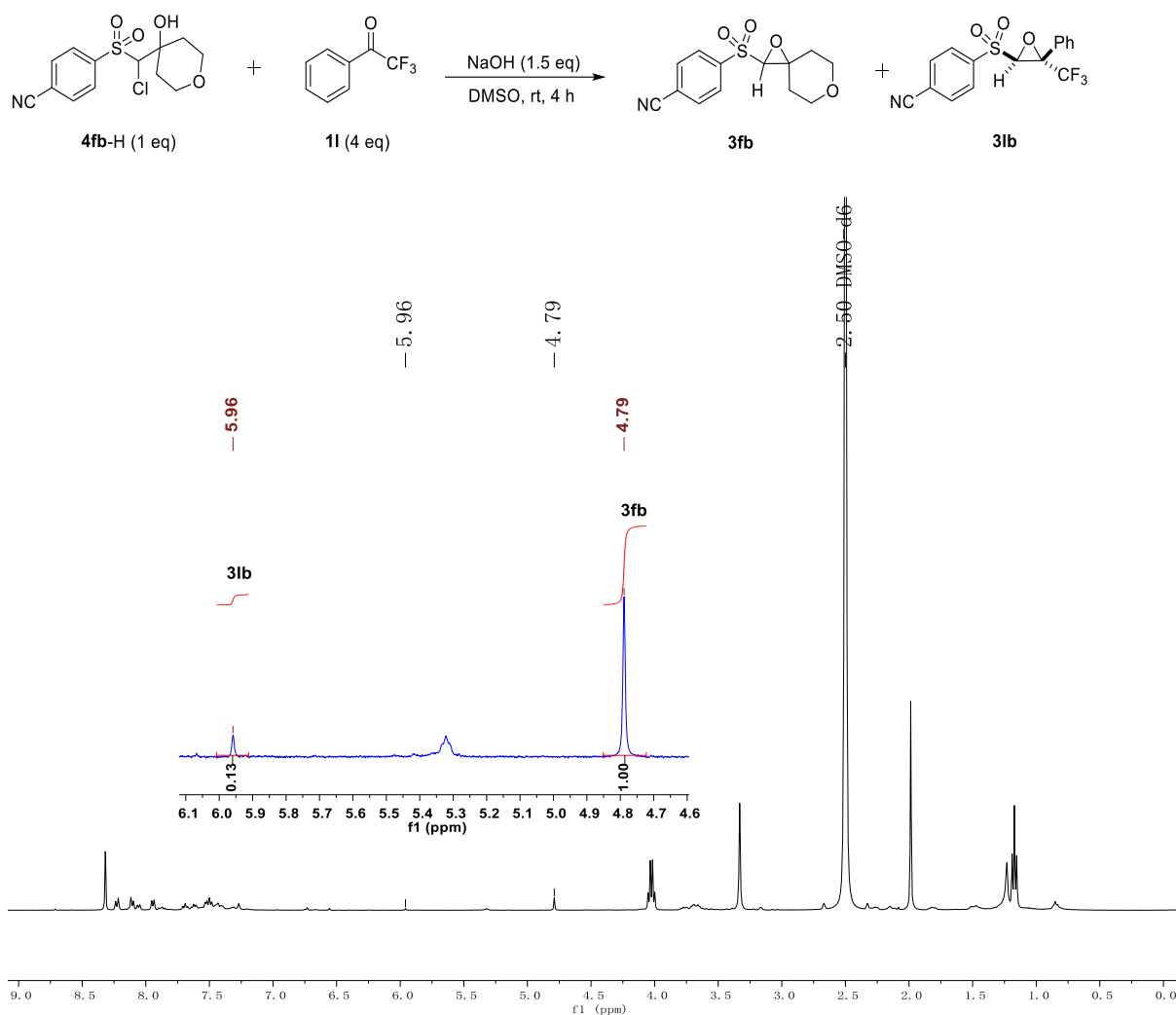


Crossover reaction result: $P_{\text{CC}}/P_{\text{rc}} = [\mathbf{3Ib}]/[\mathbf{3eb}] = 0.33$

Chapter 3: Kinetics and mechanism of oxirane-formation by Darzens condensation of ketones: quantification of the electrophilicities of ketones

Substrate **4fb**-H (with **11** as trapping agent)

In analogy to Procedure H, **4fb**-H (8.0 mg, 0.025 mmol), **11** (17 mg, 0.10 mmol), and NaOH (1.5 mg, 0.038 mmol) were combined. After workup, the residue was analyzed by ^1H NMR spectroscopy (in d_6 -DMSO).

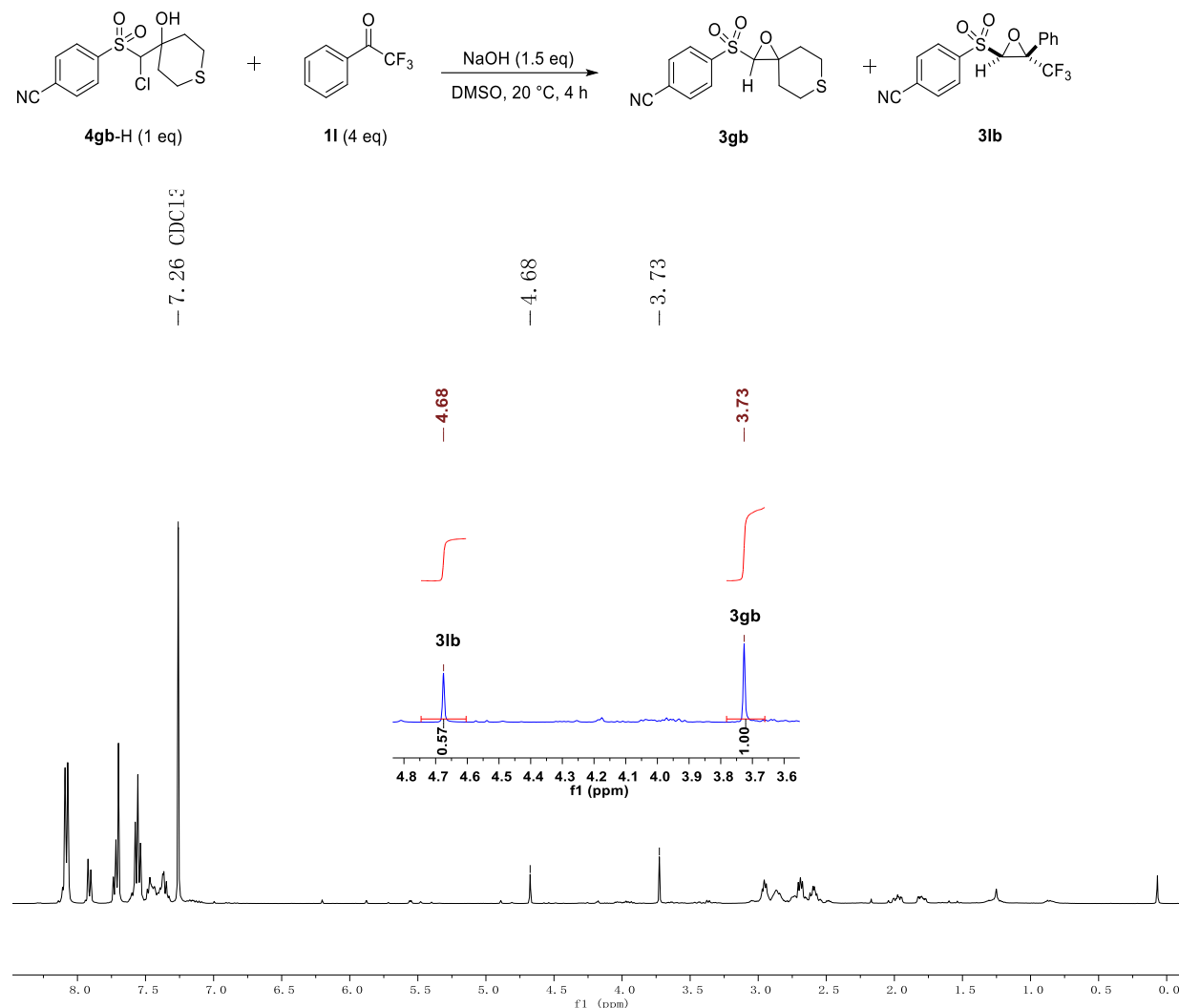


Crossover reaction result: $P_{\text{CC}}/P_{\text{rc}} = [\mathbf{3lb}]/[\mathbf{3fb}] = 0.13$

Chapter 3: Kinetics and mechanism of oxirane-formation by Darzens condensation of ketones: quantification of the electrophilicities of ketones

Substrate **4gb-H** (with **1I** as trapping agent)

According to Procedure H, **4gb-H** (17 mg, 0.051 mmol), **1I** (35 mg, 0.20 mmol), and NaOH (3.0 mg, 0.075 mmol) were combined. After workup, the residue was analyzed by ^1H NMR spectroscopy.

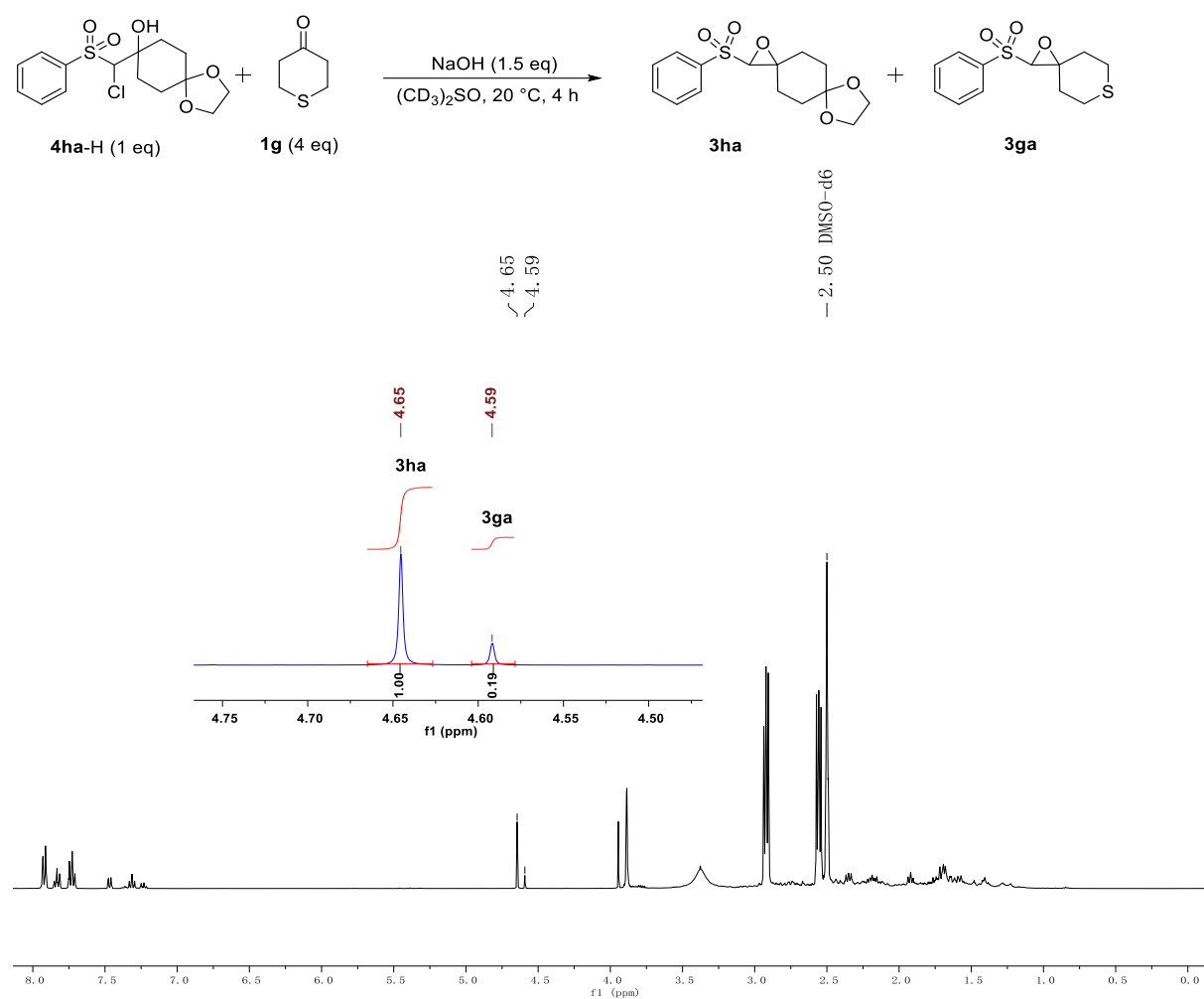


Crossover reaction result: $P_{\text{CC}}/P_{\text{rc}} = [\mathbf{3Ib}]/[\mathbf{3gb}] = 0.57$

Chapter 3: Kinetics and mechanism of oxirane-formation by Darzens condensation of ketones: quantification of the electrophilicities of ketones

Substrate **4ha-H** (with **1g** as trapping agent)

In analogy to Procedure I, **4ha-H** (9.0 mg, 0.026 mmol), **1g** (12 mg, 0.10 mmol), and NaOH (1.5 mg, 0.038 mmol) were combined and analyzed by ¹H NMR spectroscopy.

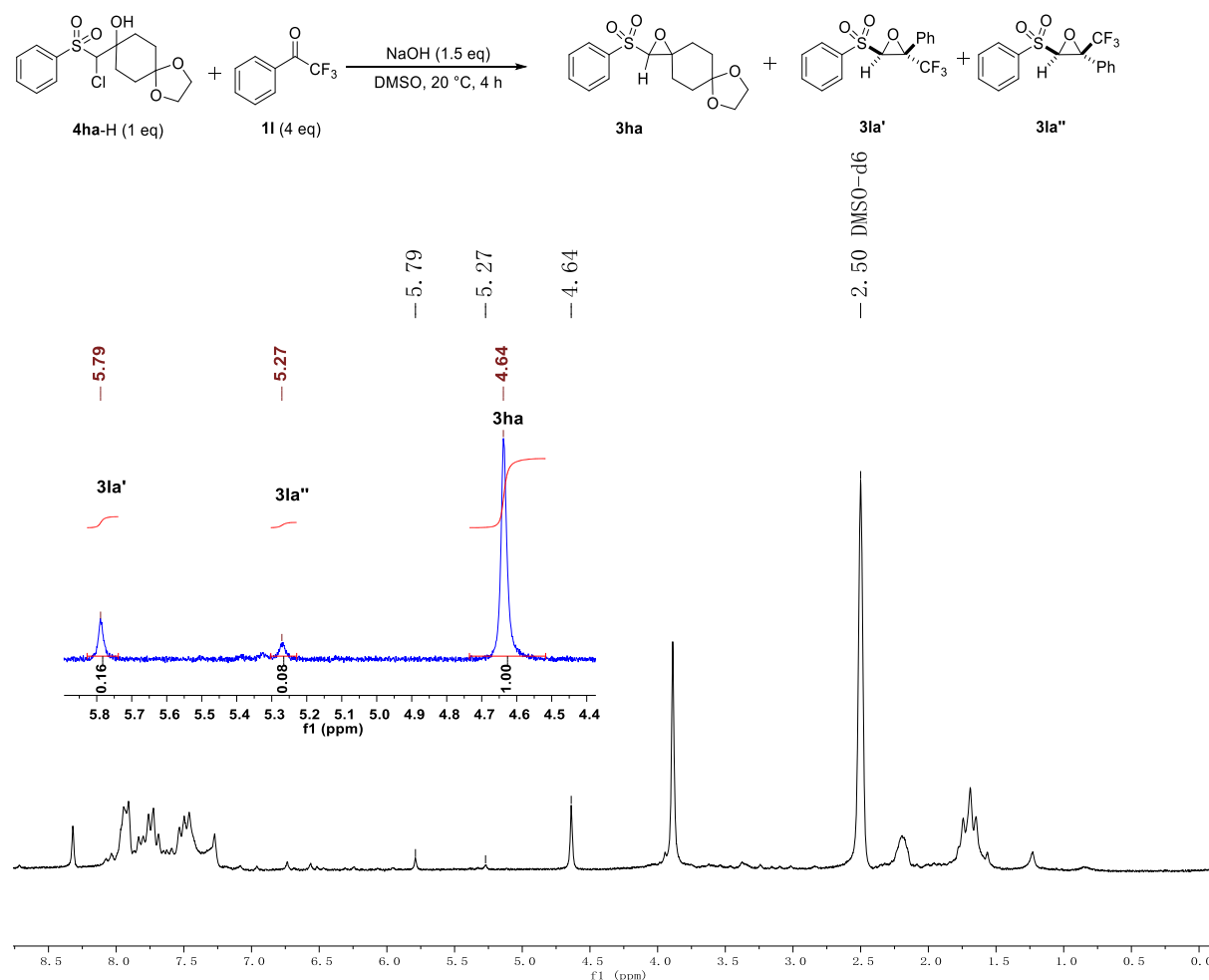


Crossover reaction result: $P_{CC}/P_{rc} = [3ga]/[3ha] = 0.19$

Chapter 3: Kinetics and mechanism of oxirane-formation by Darzens condensation of ketones: quantification of the electrophilicities of ketones

Substrate **4ha-H** (with **1l** as trapping agent)

In analogy to Procedure H, **4ha-H** (9.0 mg, 0.026 mmol), **1l** (17 mg, 0.10 mmol), and NaOH (1.5 mg, 0.038 mmol) were combined. After workup, the residue was analyzed by ^1H NMR spectroscopy.

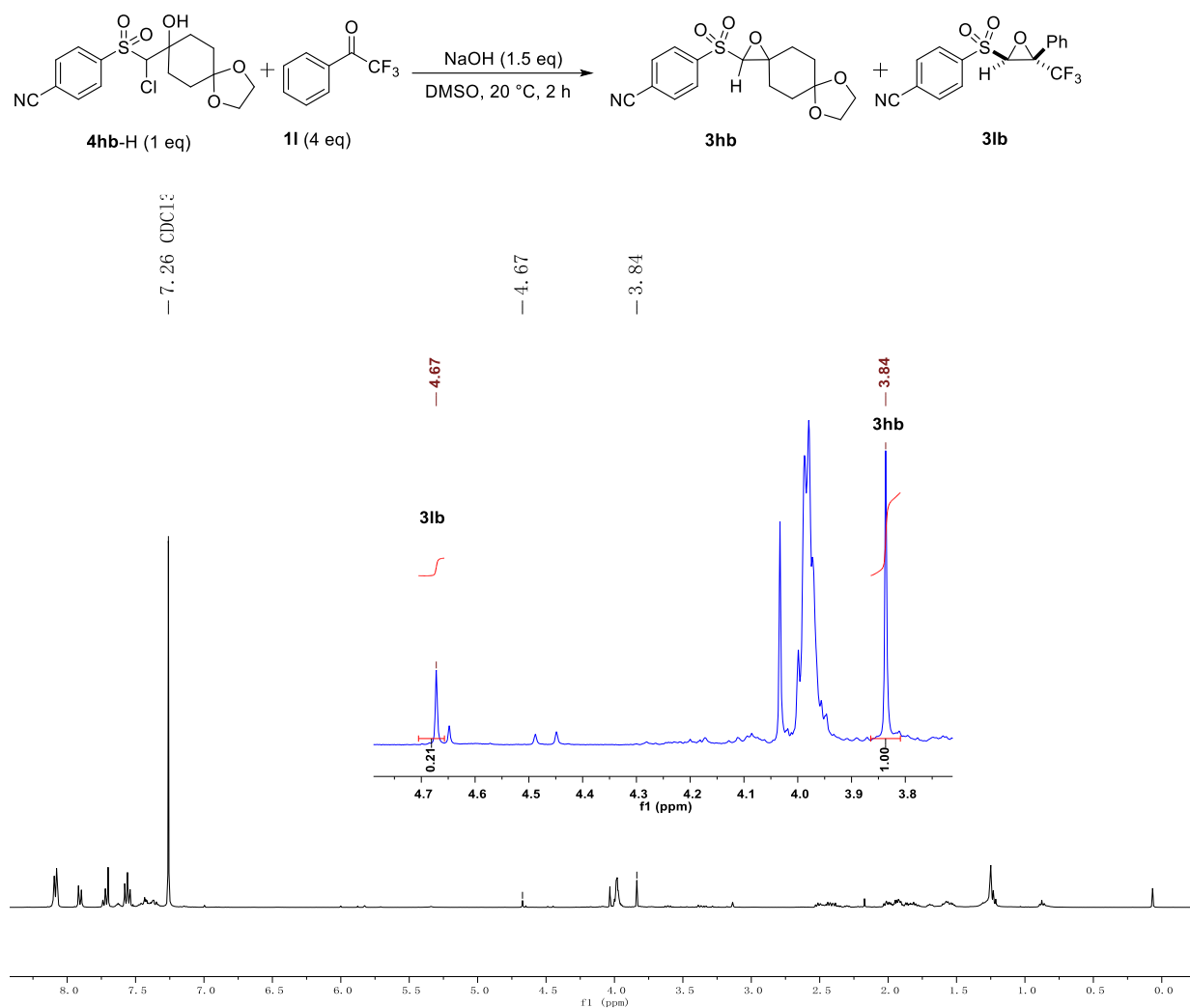


Crossover reaction result: $P_{\text{CC}}/P_{\text{rc}} = ([\mathbf{3la}'] + [\mathbf{3la}''])/[\mathbf{3ha}] = 0.24$

Chapter 3: Kinetics and mechanism of oxirane-formation by Darzens condensation of ketones: quantification of the electrophilicities of ketones

Substrate **4hb-H** (with **1l** as trapping agent)

In analogy to Procedure H, **4hb-H** (9.0 mg, 0.024 mmol), **1l** (17 mg, 0.10 mmol), and NaOH (1.5 mg, 0.038 mmol) were combined. After workup, the residue was analyzed by ^1H NMR spectroscopy.

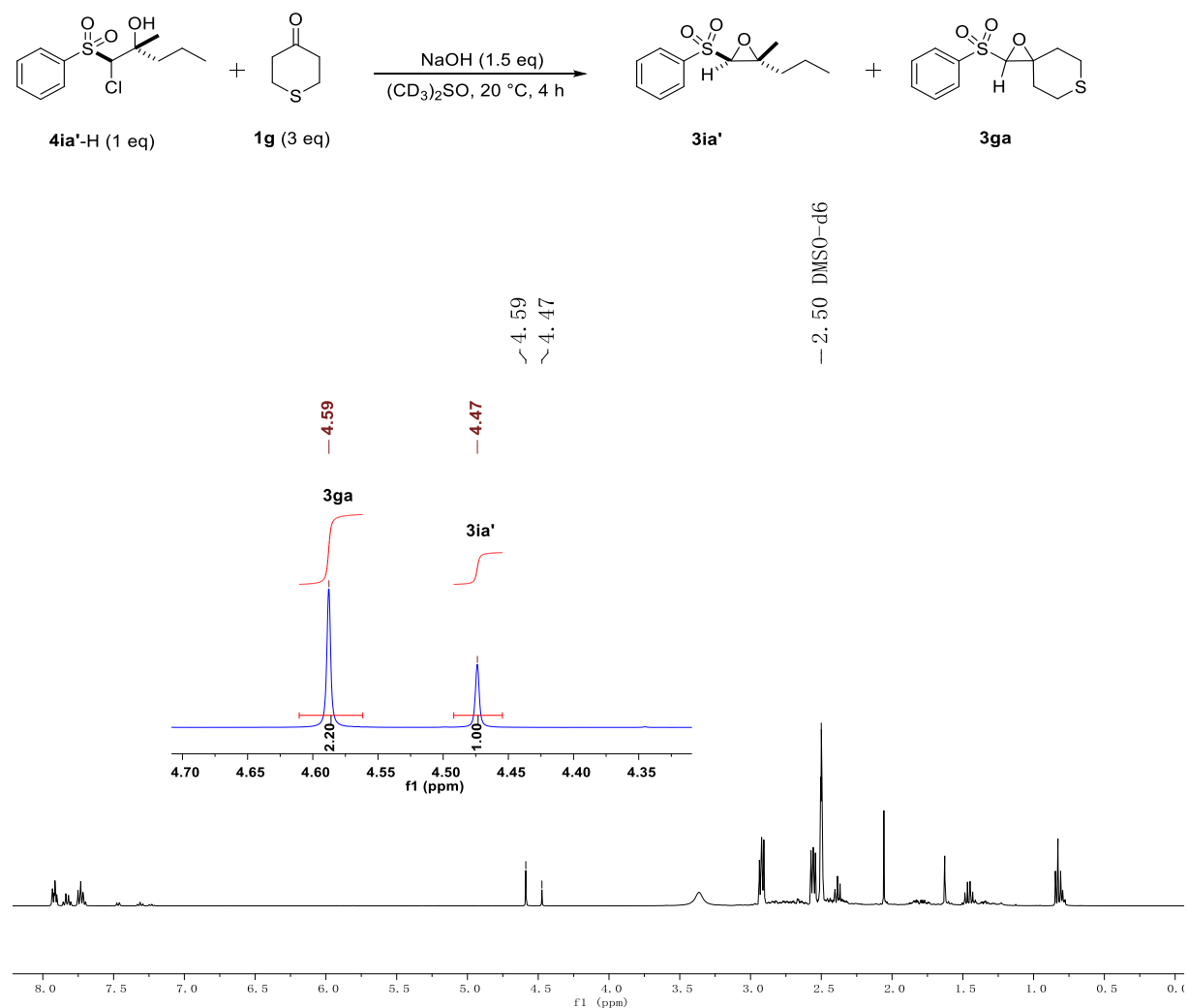


Crossover reaction result: $P_{\text{CC}}/P_{\text{rc}} = [\mathbf{3lb}]/[\mathbf{3hb}] = 0.21$

Chapter 3: Kinetics and mechanism of oxirane-formation by Darzens condensation of ketones: quantification of the electrophilicities of ketones

Substrate **4ia'**-H (with **1g** as trapping agent)

According to Procedure I, **4ia'**-H (14 mg, 0.051 mmol), **1g** (17 mg, 0.15 mmol), and NaOH (3.0 mg, 0.075 mmol) were combined and analyzed by ¹H NMR spectroscopy.

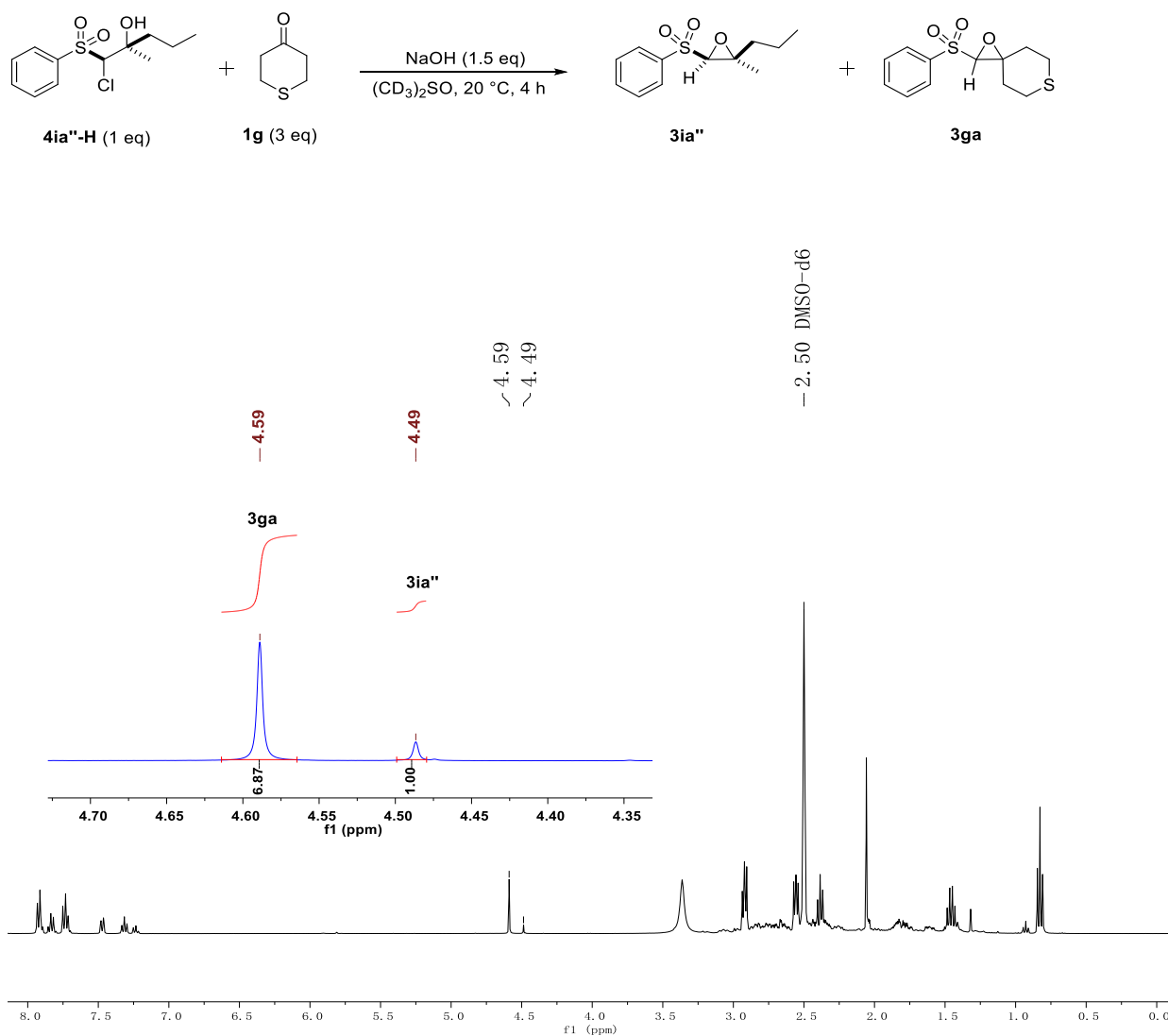


Crossover reaction result: $P_{CC}/P_{rc} = [3ga]/[3ia'] = 2.20$

Chapter 3: Kinetics and mechanism of oxirane-formation by Darzens condensation of ketones: quantification of the electrophilicities of ketones

Substrate **4ia''**-H (with **1g** as trapping agent)

According to Procedure I, **4ia''**-H (14 mg, 0.051 mmol), **1g** (17 mg, 0.15 mmol), and NaOH (3.0 mg, 0.075 mmol) were combined and analyzed by ¹H NMR spectroscopy.

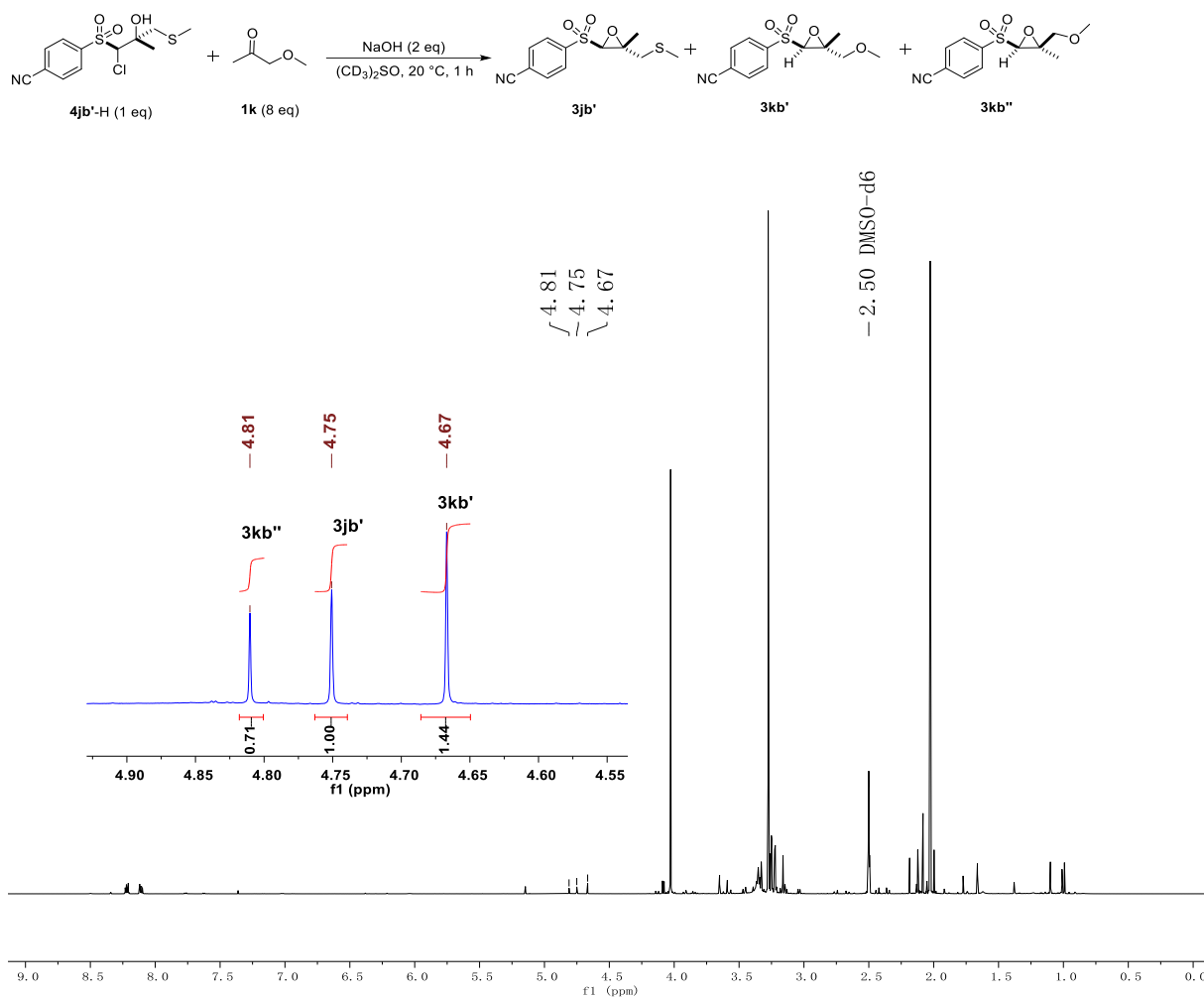


Crossover reaction result: $P_{CC}/P_{rc} = [3ga]/[3ia''] = 6.87$

Chapter 3: Kinetics and mechanism of oxirane-formation by Darzens condensation of ketones: quantification of the electrophilicities of ketones

Substrate **4jb'**-H (with **1k** as trapping agent)

In analogy to Procedure I, **4jb'**-H (8.0 mg, 0.025 mmol), **1k** (18 mg, 0.20 mmol), and NaOH (2.0 mg, 0.050 mmol) were combined and analyzed by ¹H NMR spectroscopy.

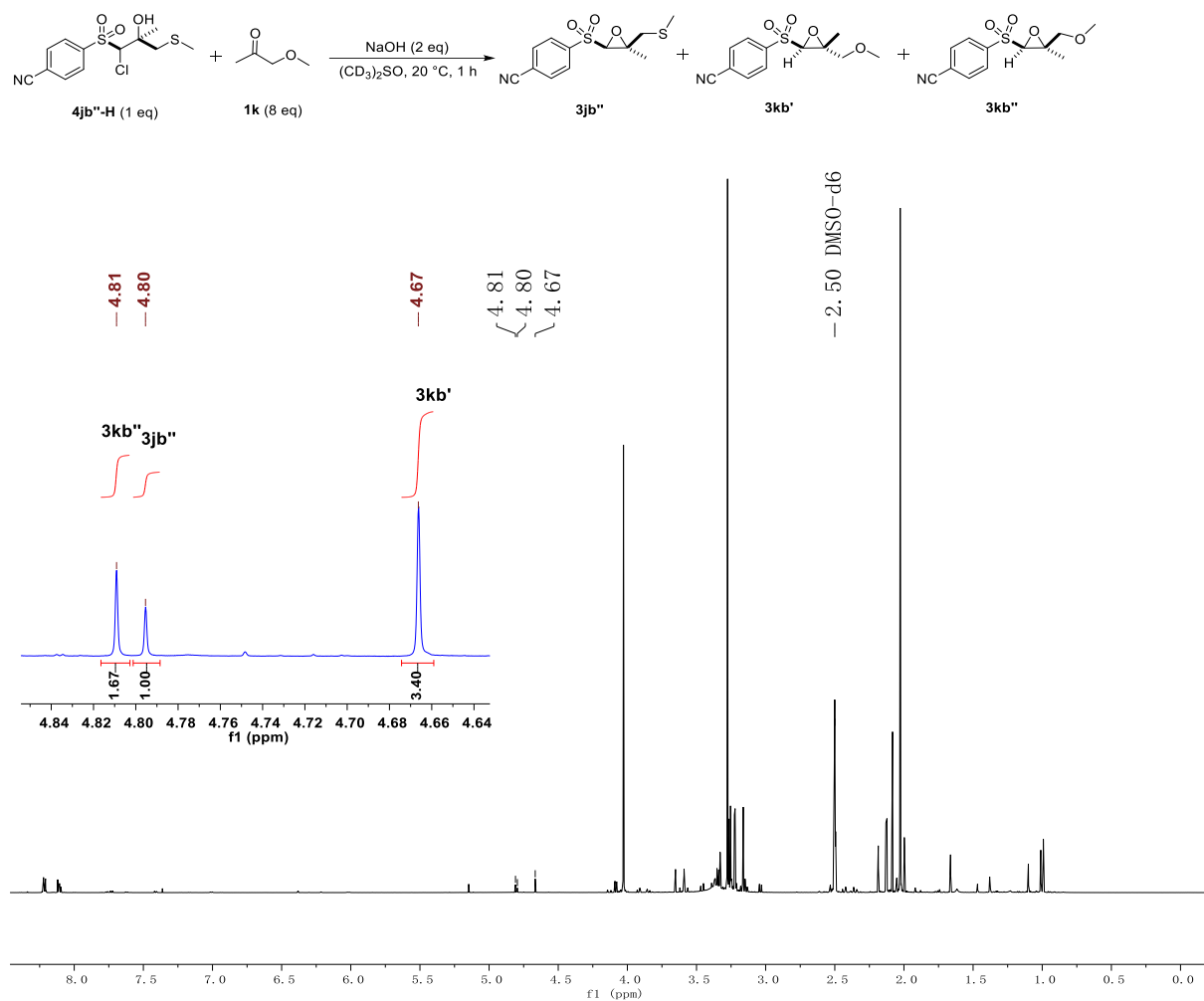


Crossover reaction result: $P_{\text{-CC}}/P_{\text{rc}} = ([\mathbf{3kb}'] + [\mathbf{3kb}''])/[\mathbf{3jb}'] = 2.15$

Chapter 3: Kinetics and mechanism of oxirane-formation by Darzens condensation of ketones: quantification of the electrophilicities of ketones

Substrate **4jb''**-H (with **1k** as trapping agent)

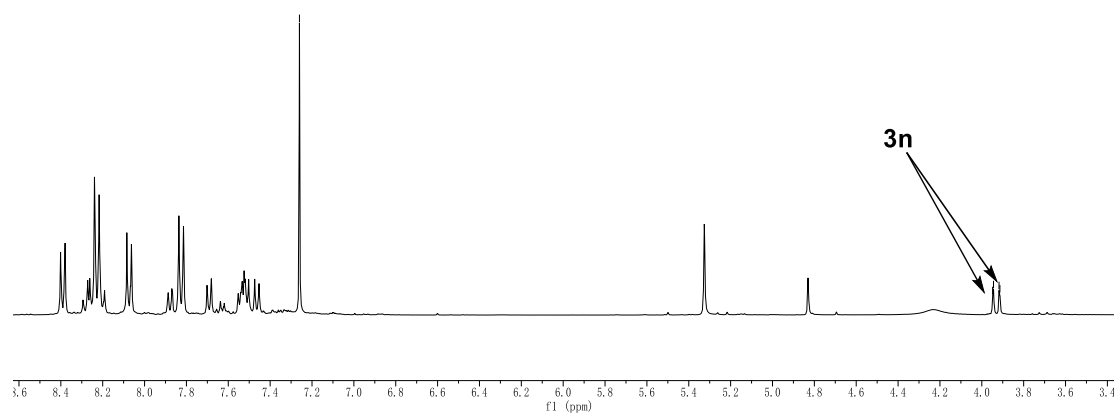
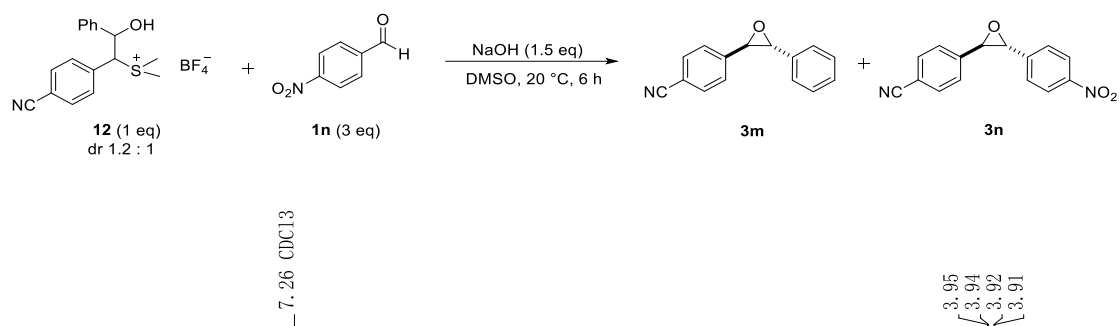
In analogy to Procedure I, **4jb''**-H (8.0 mg, 0.025 mmol), **1k** (18 mg, 0.20 mmol), and NaOH (2.0 mg, 0.050 mmol) were combined and analyzed by ¹H NMR spectroscopy.



Crossover reaction result: $P_{\text{CC}}/P_{\text{rc}} = ([\mathbf{3kb'}] + [\mathbf{3kb''}])/[\mathbf{3jb''}] = 5.07$

Substrate **12** (with **1n** as trapping agent) (main text, Scheme 10)

In analogy to procedure H, **12** (19 mg, 0.051 mmol), **1n** (23 mg, 0.15 mmol), and NaOH (3.0 mg, 0.075 mmol) were combined. After workup, the residue was analyzed by ^1H NMR spectroscopy.



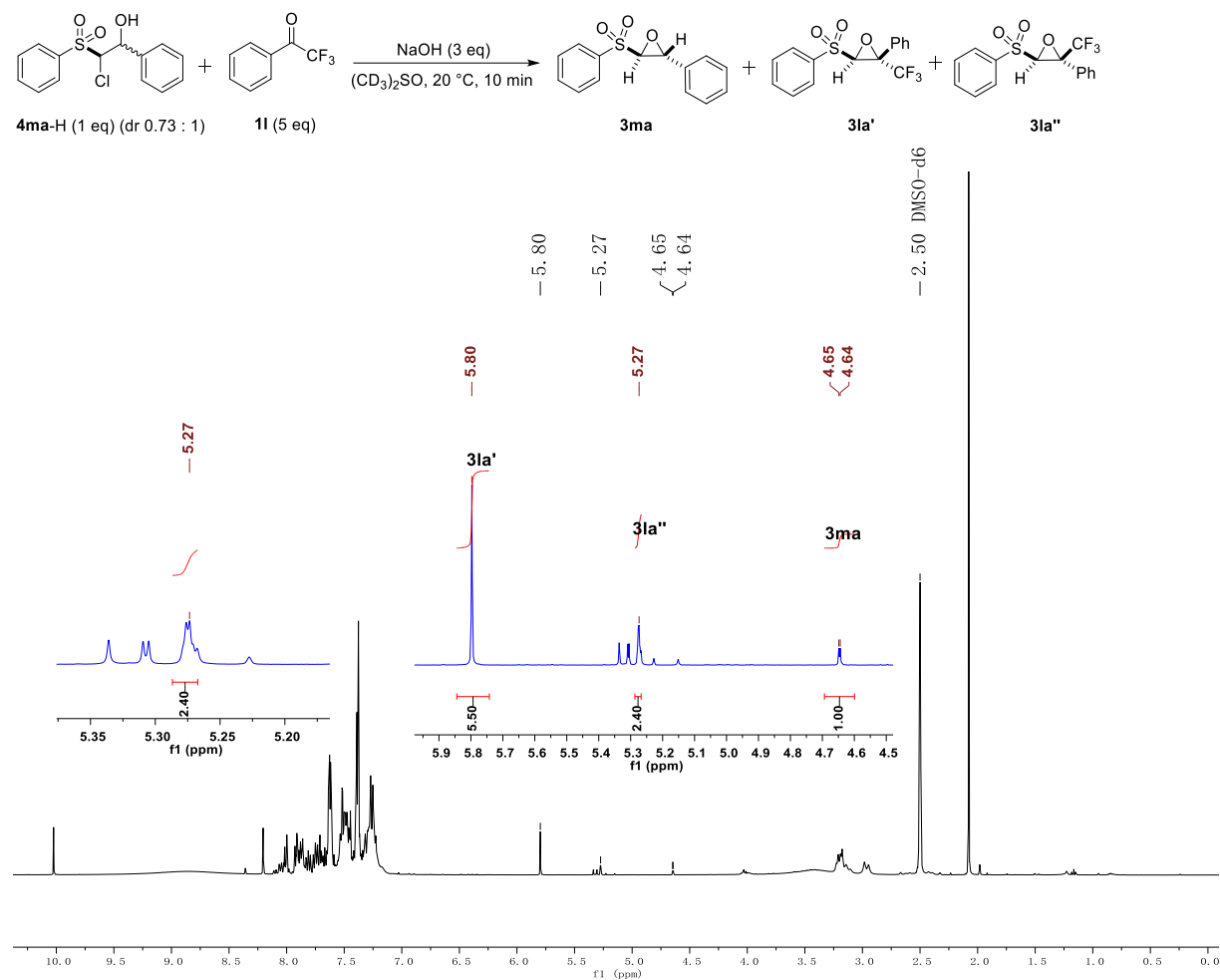
Only **3n**, no **3m** detected.

Crossover reaction result: $P_{\text{-CC}}/P_{\text{rc}} = [\mathbf{3n}]/[\mathbf{3m}] > 99$

Chapter 3: Kinetics and mechanism of oxirane-formation by Darzens condensation of ketones: quantification of the electrophilicities of ketones

Substrate **4ma**-H (with **11** as trapping agent) (main text, Scheme 13)

In analogy to Procedure I, **4ma**-H (8.0 mg, 0.027 mmol), **11** (24 mg, 0.14 mmol), and NaOH (3.2 mg, 0.080 mmol) were combined and analyzed by ¹H NMR spectroscopy.

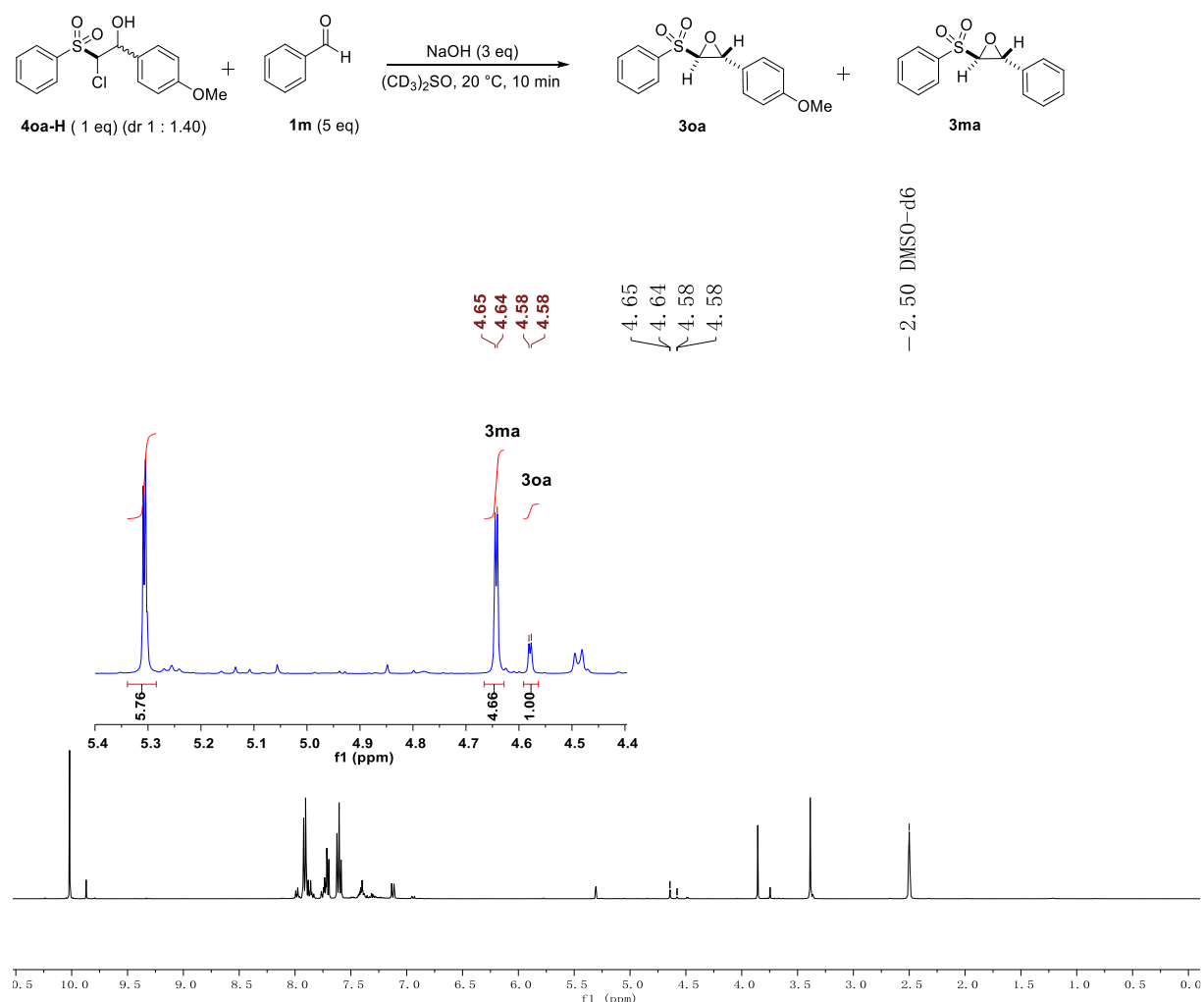


Crossover reaction result: $P_{CC}/P_{rc} = ([\mathbf{3la}'] + [\mathbf{3la}''])/[\mathbf{3ma}] = 7.90$

Chapter 3: Kinetics and mechanism of oxirane-formation by Darzens condensation of ketones: quantification of the electrophilicities of ketones

Substrate **4oa-H** (with **1m** as trapping agent) (main text, Scheme 13)

In analogy to Procedure I, **4oa-H** (8.0 mg, 0.024 mmol), **1m** (13 mg, 0.12 mmol), and NaOH (3.0 mg, 0.075 mmol) were combined and analyzed by ^1H NMR spectroscopy.



Crossover reaction result: $P_{\text{CC}}/P_{\text{rc}} = [\mathbf{3ma}]/[\mathbf{3oa}] = 4.66$

Determination of yields in crossover experiments

a) Chlorohydrin **4ca**-H (7.5 mg, 0.026 mmol) and trapping reagent **1g** (9.1 mg, 0.078 mmol) were dissolved in *d*₆-DMSO (0.6 mL). Then NaOH (1.6 mg, 0.040 mmol) was added at 20 °C. After 4 h, the reaction mixture was mixed with 1,3,5-trimethoxybenzene (1.6 mg, 0.0095 mmol) and then analyzed by ¹H NMR spectroscopy to determine that products **3ca** and **3ga** formed in a total yield of 85%.

b) Chlorohydrin **4cb**-H (15.5 mg, 0.0494 mmol) and trapping reagent **1l** (34.4 mg, 0.198 mmol) were dissolved in DMSO (0.6 mL). Then NaOH (3.0 mg, 0.075 mmol) was added at 20 °C. After 2 h at 20 °C, 2% aq HCl (10 mL) was added, and the mixture was extracted with CHCl₃ (3 × 15 mL). The organic phases were combined, subsequently washed with water (2 × 30 mL) and brine (1 × 30 mL) to remove remaining DMSO, and then dried over anhydrous MgSO₄, and filtered. The solvent was evaporated under reduced pressure and the residue was mixed with 1,3,5-trimethoxybenzene (3.1 mg, 0.018 mmol) in *d*₆-DMSO and then analyzed by ¹H NMR spectroscopy to determine that products **3cb** and **3lb** formed in a total yield of 94%.

c) Chlorohydrin **4da**-H (7.5 mg, 0.025 mmol) and trapping reagent **1g** (8.6 mg, 0.074 mmol) were dissolved in *d*₆-DMSO (0.6 mL). Then NaOH (1.5 mg, 0.038 mmol) was added at 20 °C. After 4 h, the reaction mixture was mixed with 1,3,5-trimethoxybenzene (1.5 mg, 0.0089 mmol) and then analyzed by ¹H NMR spectroscopy to determine that products **3da** and **3ga** formed in a total yield of 70%.

d) Chlorohydrin **4ia'**-H (14.4 mg, 0.0522 mmol) and trapping reagent **1g** (18.5 mg, 0.159 mmol) were dissolved in *d*₆-DMSO (1.0 mL). Then NaOH (3.2 mg, 0.080 mmol) was added at 20 °C. After 4 h, the reaction mixture was mixed with 1,3,5-trimethoxybenzene (3.1 mg, 0.018 mmol) and then analyzed by ¹H NMR spectroscopy to determine that products **3ia'** and **3ga** formed in a total yield of 95%.

(7) Crystallographic data

Single crystals of **4ca-H** of suitable quality for X-ray analysis were obtained by dissolving about 10 mg of solid **4ca-H** in CH₂Cl₂ (0.5 mL) in a smaller vial. Then this smaller vial was placed in a bigger vial, which contained pentane (2 mL). After 1 day, vapor diffusion led to the formation of crystalline **4ca-H** in the smaller vial.

Crystallographic data have been deposited with the Cambridge Crystallographic Data Centre (CCDC 1590395). These supplementary crystallographic data can be obtained free of charge from The Cambridge Crystallographic Data Centre via www.ccdc.cam.ac.uk/data_request/cif.

Table S21. Crystallographic data for **4ca-H**

	4ca-H
net formula	C ₁₃ H ₁₇ ClO ₃ S
$M_r/\text{g mol}^{-1}$	288.77
crystal size/mm	0.070 × 0.050 × 0.030
T/K	103.(2)
radiation	MoK α
diffractometer	'Bruker D8 Venture TXS'
crystal system	monoclinic
space group	'P 1 21/n 1'
$a/\text{\AA}$	19.6959(5)
$b/\text{\AA}$	6.9198(2)
$c/\text{\AA}$	21.5771(6)
$\alpha/^\circ$	90
$\beta/^\circ$	114.9120(10)
$\gamma/^\circ$	90
$V/\text{\AA}^3$	2667.16(13)
Z	8
calc. density/g cm ⁻³	1.438
μ/mm^{-1}	0.440
absorption correction	Multi-Scan

Chapter 3: Kinetics and mechanism of oxirane-formation by Darzens condensation of ketones: quantification of the electrophilicities of ketones

transmission factor range	0.92–0.99
refls. measured	41776
R_{int}	0.0512
mean $\sigma(I)/I$	0.0302
θ range	3.157–26.371
observed refts.	4562
x, y (weighting scheme)	0.0288, 2.1533
hydrogen refinement	H(C) constr, H(O) refall
refls in refinement	5441
parameters	333
restraints	0
$R(F_{\text{obs}})$	0.0324
$R_w(F^2)$	0.0803
S	1.066
shift/error _{max}	0.001
max electron density/e \AA^{-3}	0.356
min electron density/e \AA^{-3}	−0.399

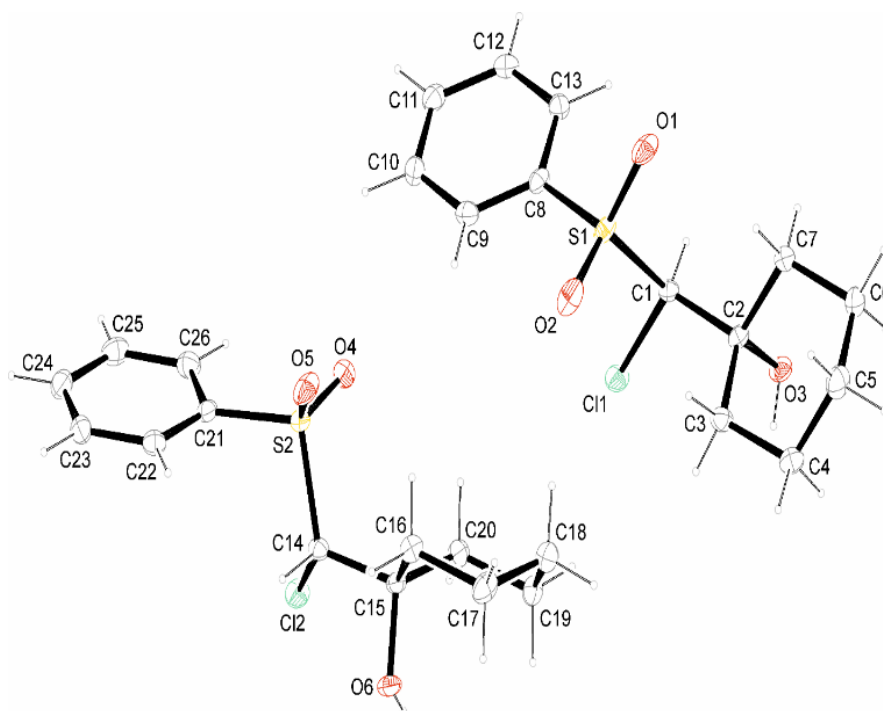
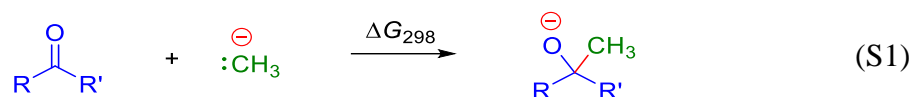


Figure S1. ORTEP drawing of the crystal structure of **4ca-H**. The ellipsoid probability level is 50%.

(8) Computational analysis (completed by Harish Jangra)

8.1 Methodology

Methyl anion affinities (MAA) in the gas phase have been calculated using the same methodology employed successfully in earlier studies^{S8-S10} as the negative of the gas phase free energy at 298.15 K (ΔG_{298}) for the addition reaction shown in equation S1. [MAA = ($-\Delta G_{298}$ of equation S1)].



Geometry optimizations have been performed with a combination of the B3LYP hybrid functional^{S11} and the 6-31G(d,p) basis set.^{S12,S13} Thermochemical corrections to Gibbs energies (corr. ΔG) at 298.15 K have been calculated using the rigid rotor/harmonic oscillator model without any scaling. Gibbs energies (ΔG_{298}) at B3LYP/6-31G(d,p) level have been obtained through addition of ΔE_{tot} and corr. ΔG . Single point total electronic energies (ΔE_{tot}) have subsequently been calculated using a combination of the B3LYP hybrid functional and the larger 6-311++G(3df,2pd) basis set.^{S12-S14} Final Gibbs energies (ΔG_{298}) have been obtained through a combination of ΔE_{tot} with the thermochemical corrections to Gibbs energies (corr. ΔG) calculated at a lower level. In the following these will be designated as ΔG_{gas} at [B3LYP/6-311++G(3df,2pd)//B3LYP/6-31G(d,p)].

Solvent effects on MAA values have first been estimated by adding single point solvation corrections (ΔG_{Solv}) to ΔG_{gas} for equation S1. ΔG_{Solv} was calculated for gas phase optimized geometries using the SMD^{S15} continuum solvation model and subsequently added to gas phase Gibbs energies (ΔG_{gas}) to obtain solution phase Gibbs energies that will be designated single point solvation free energies ($\Delta G_{\text{sol-sp}}$). In an alternative approached geometry optimization was carried out in the presence of the SMD continuum solvation model for DMSO at B3LYP/6-31G(d,p) level. The Gibbs energies calculated using the implicit DMSO optimized geometry are designated as $\Delta G_{\text{sol-opt}}$.

Electrophilicity indices like the electronic chemical potential (μ), the chemical hardness (η), and the global electrophilicity index (ω) were calculated from orbital energies using equations S2, S3, and S4.^{S16-S18}

$$\mu \approx \frac{\text{HOMO}_E + \text{LUMO}_E}{2} \quad (\text{S2})$$

$$\eta \approx \text{LUMO}_E - \text{HOMO}_E \quad (\text{S3})$$

$$\omega = \frac{\mu^2}{2\eta} \quad (\text{S4})$$

Local electrophilicity indices at the carbonyl carbon atom for electrophiles (see equation S1) were calculated using the nucleophilic Fukui function (f_k^+) as defined in equation S5.

$$\omega_k = \omega f_k^+ \quad (\text{S5})$$

In this work, we calculated the nucleophilic Fukui function (f^+) using two different approaches. First, the condensed nucleophilic Fukui function (f_k^+) for atom k was calculated using a procedure described by Contreras and co-workers,^{S19} where f_k^+ was calculated from the Gaussian 09 output files by the Fukui function program available at <https://github.com/dmsteglenko/Fukui-function-calculation>.

In a second approach we used the Yang and Mortier method,^{S20} where the Fukui function for the nucleophilic attack is defined as the change of partial charge q at a certain atom k by adding an electron to the corresponding molecule, that is:

$$f_k^+ = q(k, N+1) - q(k, N) \quad (\text{S6})$$

with N = total number of electrons in the neutral molecule. We calculated f_k^+ as defined in equation S6 using Mulliken charges.

The methodology used for the calculation of potential energy surfaces (PES) for nucleophilic additions to electrophiles follows suggestions recently made for this type of reaction in ref S21. This includes geometry optimizations for all stationary points (minima, complexes and transition states) along the PES at the PCM(DMSO,UA0)/B3LYP-D3/6-31+G(d,p) level of theory. The PCM variant used here is based on the Integral Equation Formalism for the Polarizable Continuum Model (IEFPCM) solvation model employing United Atom Topological Model (UA0) radii derived from the UFF force field

[scrf=(iefpcm,read,solvent=dmsolvent), radii=ua0].^{S22,S23} The dispersion model is that proposed by Grimme as the "GD3" model [empiricaldispersion=gd3].^{S24,S25}

All stationary points were confirmed by vibrational frequency calculation with 0, 0, and 1 imaginary frequencies, respectively. All stationary points were checked for wavefunction stability (stable=opt). The nature of transition states was further confirmed by IRC calculations [20 steps in both directions (reverse/forward) with stepsize=3] followed by geometry optimization to the next minima. In cases of very flat PES(s), manual displacement away from the TS(s) followed by geometry optimization was employed. PES surfaces were re-evaluated at PCM(DMSO,UA0)/B2PLYP^{S26}-D3/Def2TZVPP level of theory.^{S27,S28} All calculations were performed with Gaussian 09, Rev. D.^{S29}

8.2 Potential Energy Surface(s)

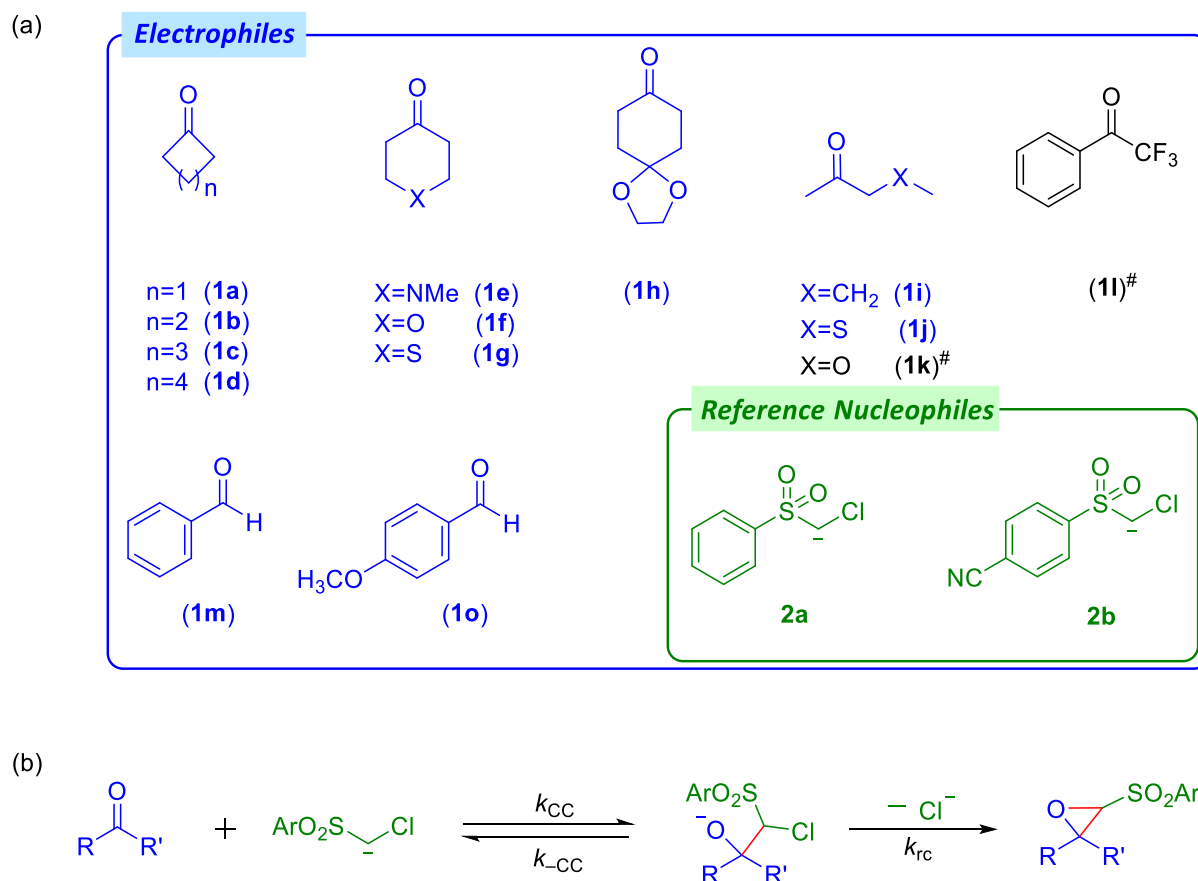


Figure S2. (a) List of electrophiles and reference nucleophiles. (b) The proposed mechanism of the reactions of reference nucleophiles with ketones. [#] Exclusively used as trapping agents for crossover reactions.

8.2.1 1c with 2a

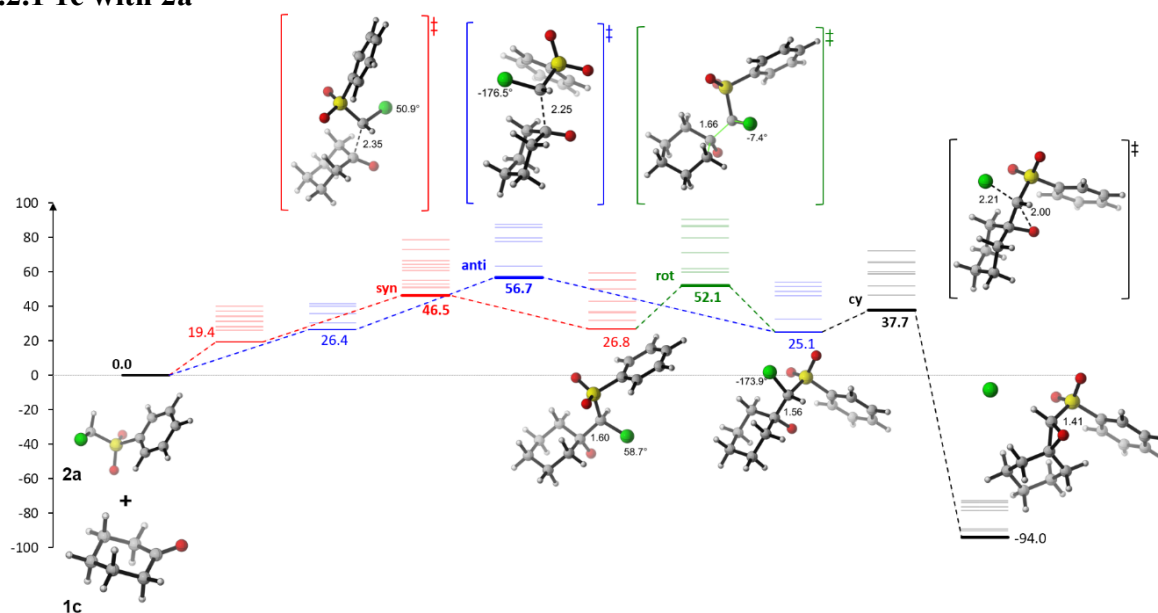


Figure S3. PES ($\Delta G_{\text{sol-opt}}$, kJ/mol) for the reaction of arylsulfonyl-substituted chloromethyl anions **2a** with Ketone **1c** calculated at B3LYP-D3/6-31+G(d,p)/PCM(UA0,DMSO) level of theory. Thick bars with bold font are used to distinguish TSs from reactant complex, intermediates and products along PES. Faded bars are used to show the conformational space screened for each point along PES.

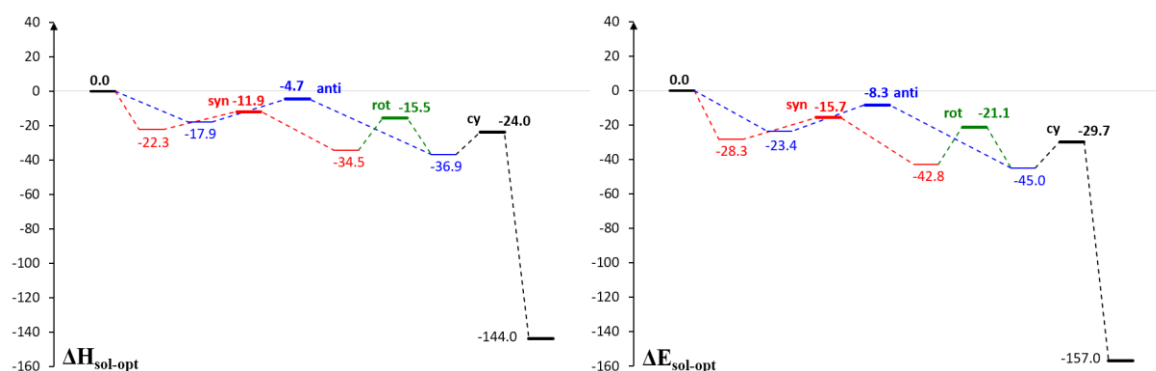


Figure S4. Lowest energy pathways (kJ/mol) for the reaction **2a** with **1c** in terms of $\Delta H_{\text{sol-opt}}$ (a) and $\Delta E_{\text{sol-opt}}$ (b) calculated at B3LYP-D3/6-31+G(d,p)/PCM(UA0,DMSO) level of theory. Thick bars with bold font are used to distinguish TSs from reactant complex, intermediates and products along PES.

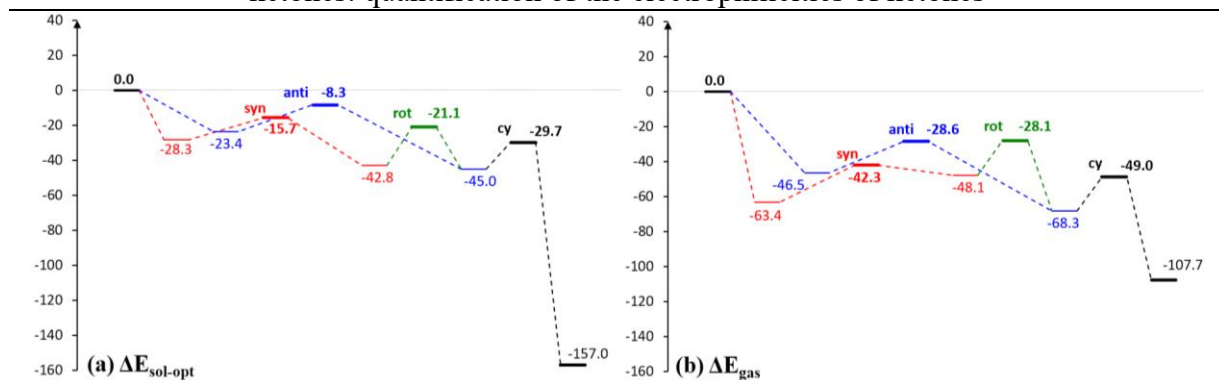


Figure S5. Lowest energy pathways (kJ/mol) for the reaction **2a** with **1c** in terms of $\Delta E_{\text{sol-opt}}$ (a) and ΔE_{gas} (b). PES $\Delta E_{\text{sol-opt}}$ (a) calculated at B3LYP-D3/6-31+G(d,p)/PCM(UA0,DMSO) level of theory. PES ΔE_{gas} (b) was obtained from single point gas phase calculation over PES $\Delta E_{\text{sol-opt}}$ (a) [at B3LYP-D3/6-31+G(d,p)//B3LYP-D3/6-31+G(d,p)/PCM(UA0,DMSO) level of theory]. Thick bars with bold font are used to distinguish TSs from reactant complex, intermediates and products along PES.

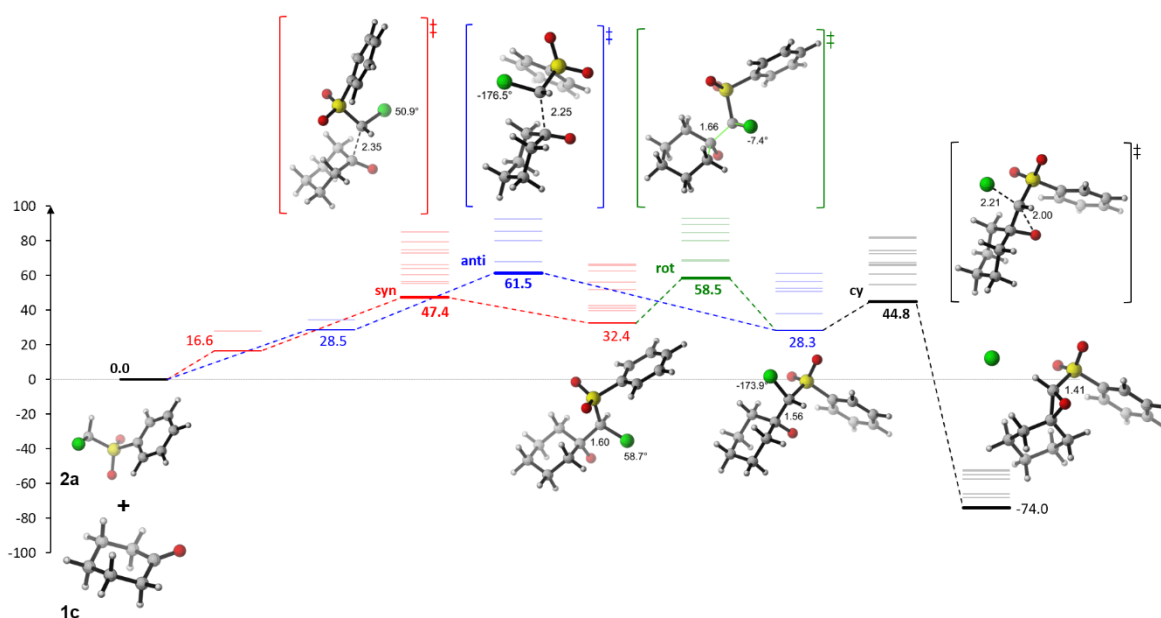


Figure S6. PES ($\Delta G_{\text{sol-opt}}$, kJ/mol) for the reaction of **2a** with **1c** calculated at B2PLYP-D3/def2TZVPP/PCM(UA0,DMSO)//B3LYP-D3/6-31+G(d,p)/PCM(UA0,DMSO) level of theory. Thick bars with bold font are used to distinguish TSs from reactant complex, intermediates and products along PES. Faded bars are used to show the conformational space screened for each point along PES.

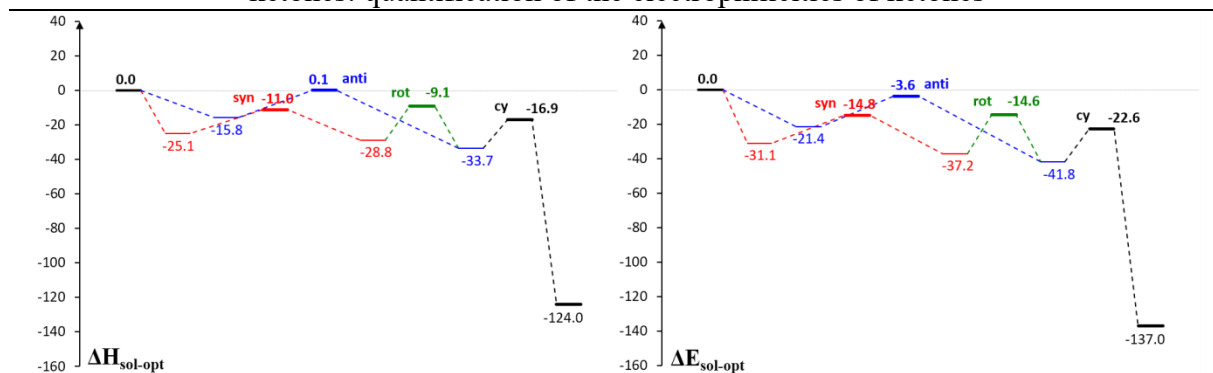


Figure S7. Lowest energy pathways (kJ/mol) for the reaction **2a** with **1c** in terms of $\Delta H_{\text{sol-opt}}$ (a) and $\Delta E_{\text{sol-opt}}$ (b) calculated at B2PLYP-D3/def2TZVPP/PCM(UA0,DMSO)//B3LYP-D3/6-31+G(d,p)/PCM(UA0,DMSO) level of theory. Thick bars with bold font are used to distinguish TSs from reactant complex, intermediates and products along PES.

8.2.2 1g with 2a

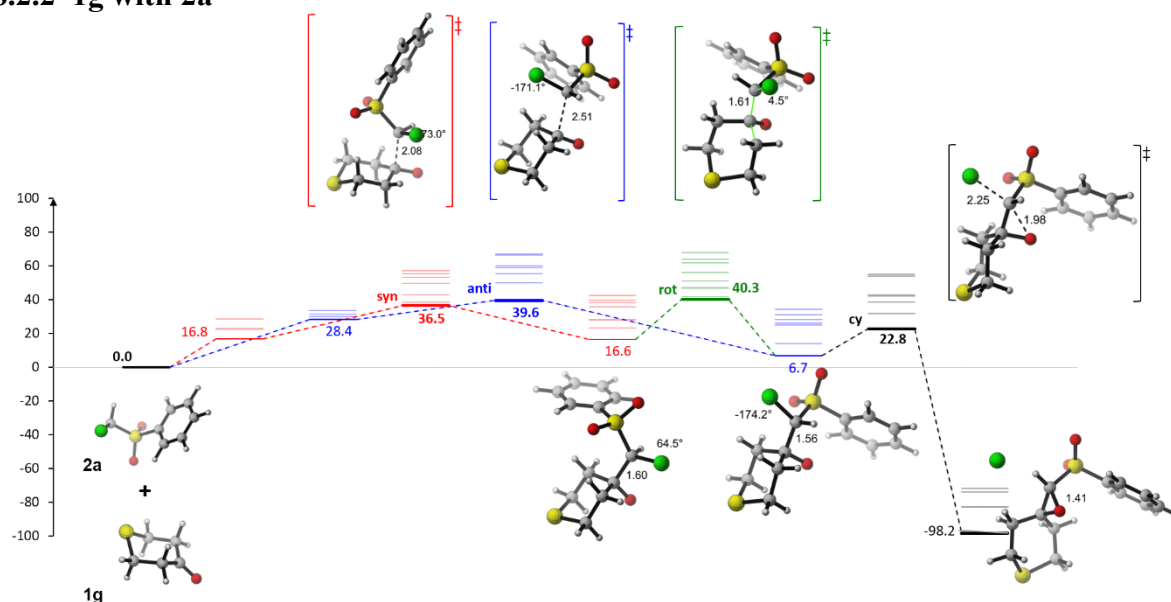


Figure S8. PES ($\Delta G_{\text{sol-opt}}$, kJ/mol) for the reaction of **2a** with **1g** calculated at B3LYP-D3/6-31+G(d,p)/PCM(UA0,DMSO) level of theory. Thick bars with bold font are used to distinguish TSs from reactant complex, intermediates and products along PES. Faded bars are used to show the conformational space screened for each point along PES.

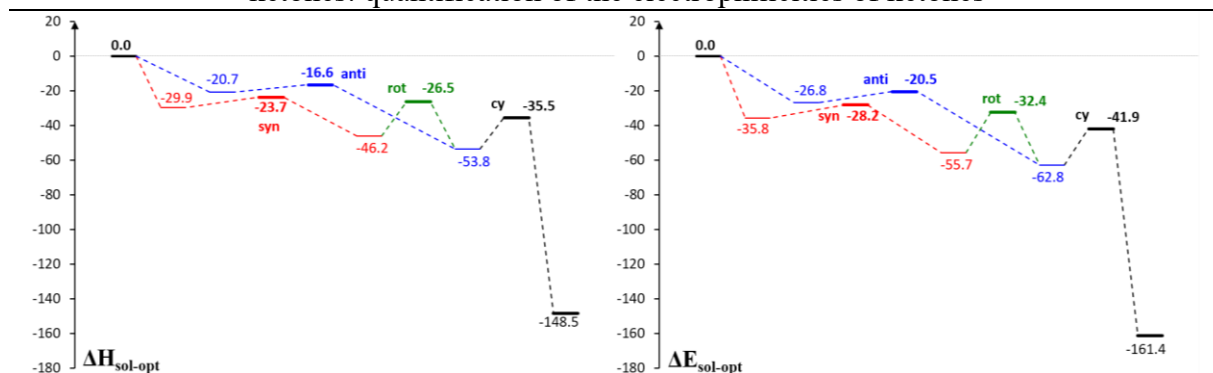


Figure S9. Lowest energy pathways (kJ/mol) for the reaction **2a** with **1g** in terms of $\Delta H_{\text{sol-opt}}$ (a) and $\Delta E_{\text{sol-opt}}$ (b) calculated at B3LYP-D3/6-31+G(d,p)/PCM(UA0,DMSO) level of theory. Thick bars with bold font are used to distinguish TSs from reactant complex, intermediates and products along PES.

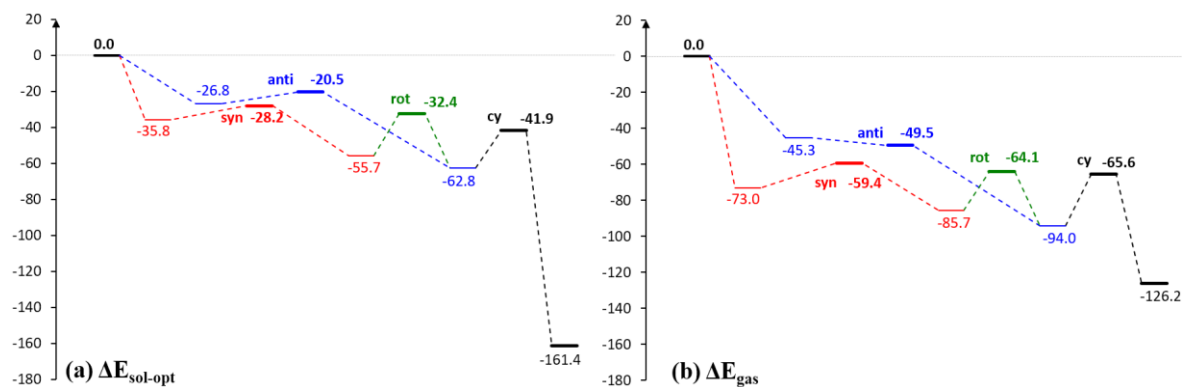


Figure S10. Lowest energy pathways (kJ/mol) for the reaction **2a** with **1g** in terms of $\Delta E_{\text{sol-opt}}$ (a) and ΔE_{gas} (b). PES $\Delta E_{\text{sol-opt}}$ (a) calculated at B3LYP-D3/6-31+G(d,p)/PCM(UA0,DMSO) level of theory. PES ΔE_{gas} (b) was obtained from single point gas phase calculation over PES $\Delta E_{\text{sol-opt}}$ (a) [at B3LYP-D3/6-31+G(d,p)//B3LYP-D3/6-31+G(d,p)/PCM(UA0,DMSO) level of theory]. Thick bars with bold font are used to distinguish TSs from reactant complex, intermediates and products along PES.

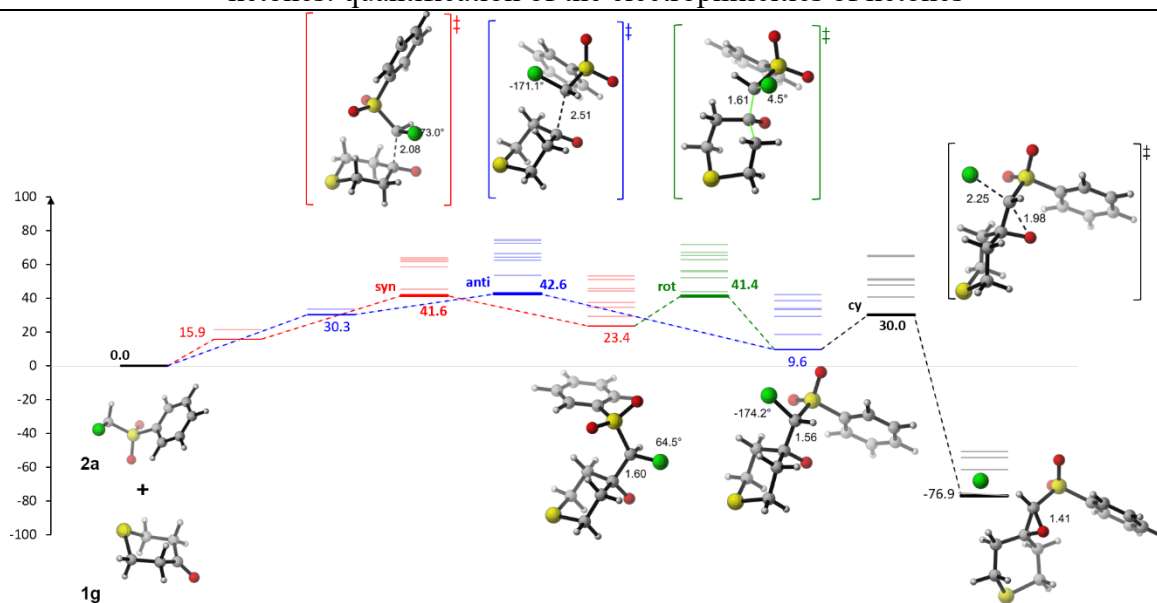


Figure S11. PES ($\Delta G_{\text{sol-opt}}$, kJ/mol) for the reaction of **2a** with **1g** calculated at B2PLYP-D3/def2TZVPP/PCM(UA0,DMSO)//B3LYP-D3/6-31+G(d,p)/PCM(UA0,DMSO) level of theory. Thick bars with bold font are used to distinguish TSs from reactant complex, intermediates and products along PES. Faded bars are used to show the conformational space screened for each point along PES.

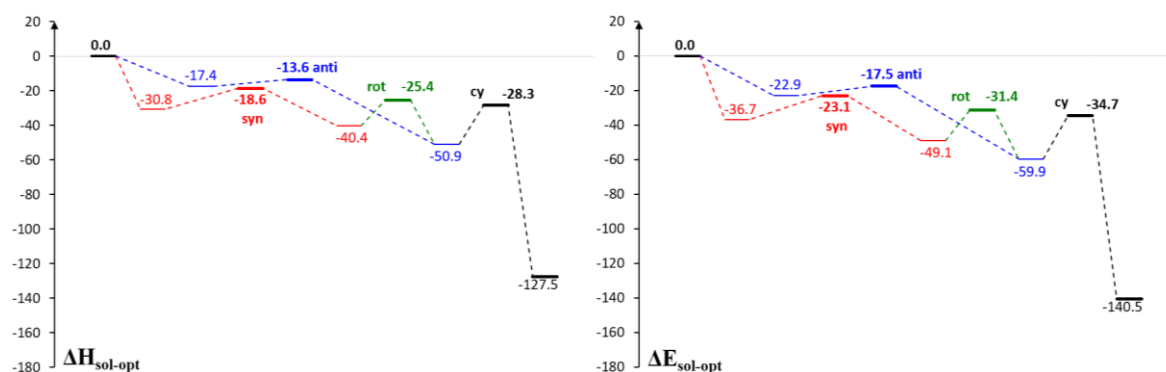


Figure S12. Lowest energy pathways (kJ/mol) for the reaction **2a** with **1g** in terms of $\Delta H_{\text{sol-opt}}$ (a) and $\Delta E_{\text{sol-opt}}$ (b) calculated at B2PLYP-D3/def2TZVPP/PCM(UA0,DMSO)//B3LYP-D3/6-31+G(d,p)/PCM(UA0,DMSO) level of theory. Thick bars with bold font are used to distinguish TSs from reactant complex, intermediates and products along PES.

8.2.3 5* with 2a

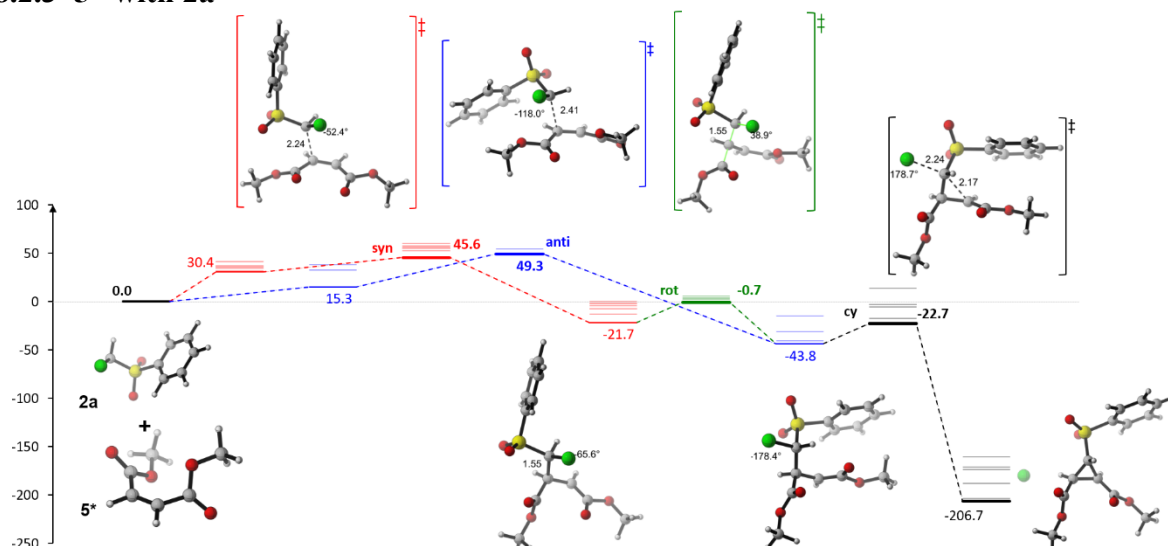


Figure S13. PES ($\Delta G_{\text{sol-opt}}$, kJ/mol) for the reaction of arylsulfonyl-substituted chloromethyl anions **2a** with dimethyl maleate **5*** calculated at B3LYP-D3/6-31+G(d,p)/PCM(UA0,DMSO) level of theory. Thick bars with bold font are used to distinguish TSs from reactant complex, intermediates and products along PES. Faded bars are used to show the conformational space screened for each point along PES. Dimethyl maleate **5*** is used as model substrate for diethyl maleate **5**.

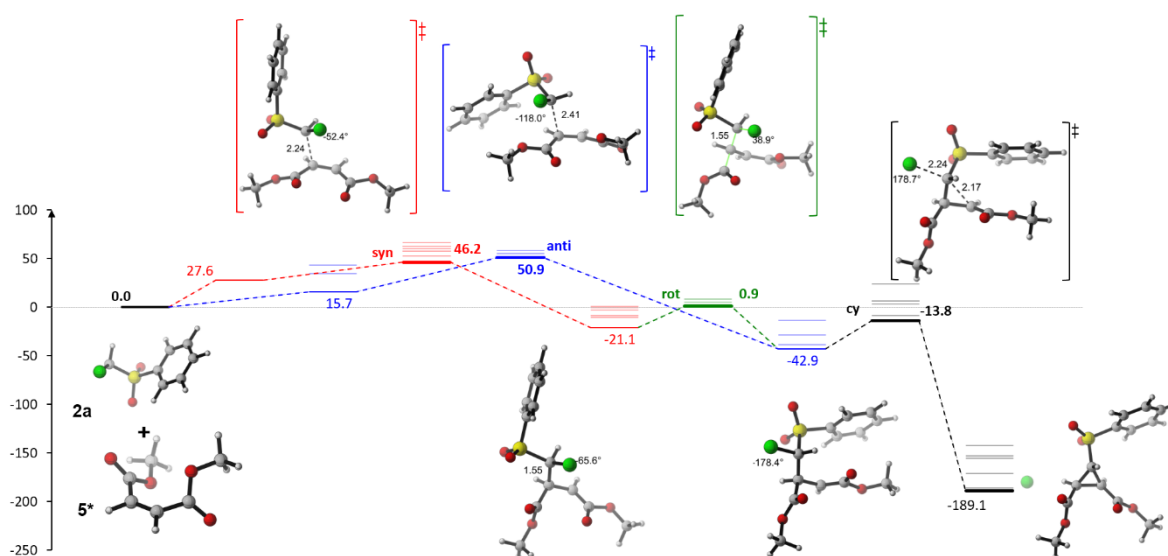


Figure S14. PES ($\Delta G_{\text{sol-opt}}$, kJ/mol) for the reaction of **2a** with **5*** calculated at B2PLYP-D3/def2TZVPP/PCM(UA0,DMSO)//B3LYP-D3/6-31+G(d,p)/PCM(UA0,DMSO) level of theory. Thick bars with bold font are used to distinguish TSs from reactant complex, intermediates and products along PES. Faded bars are used to show the conformational space screened for each point along PES. Dimethyl maleate **5*** is used as a model substrate for diethyl maleate **5**.

8.2.4 Halohydrins conformational distribution

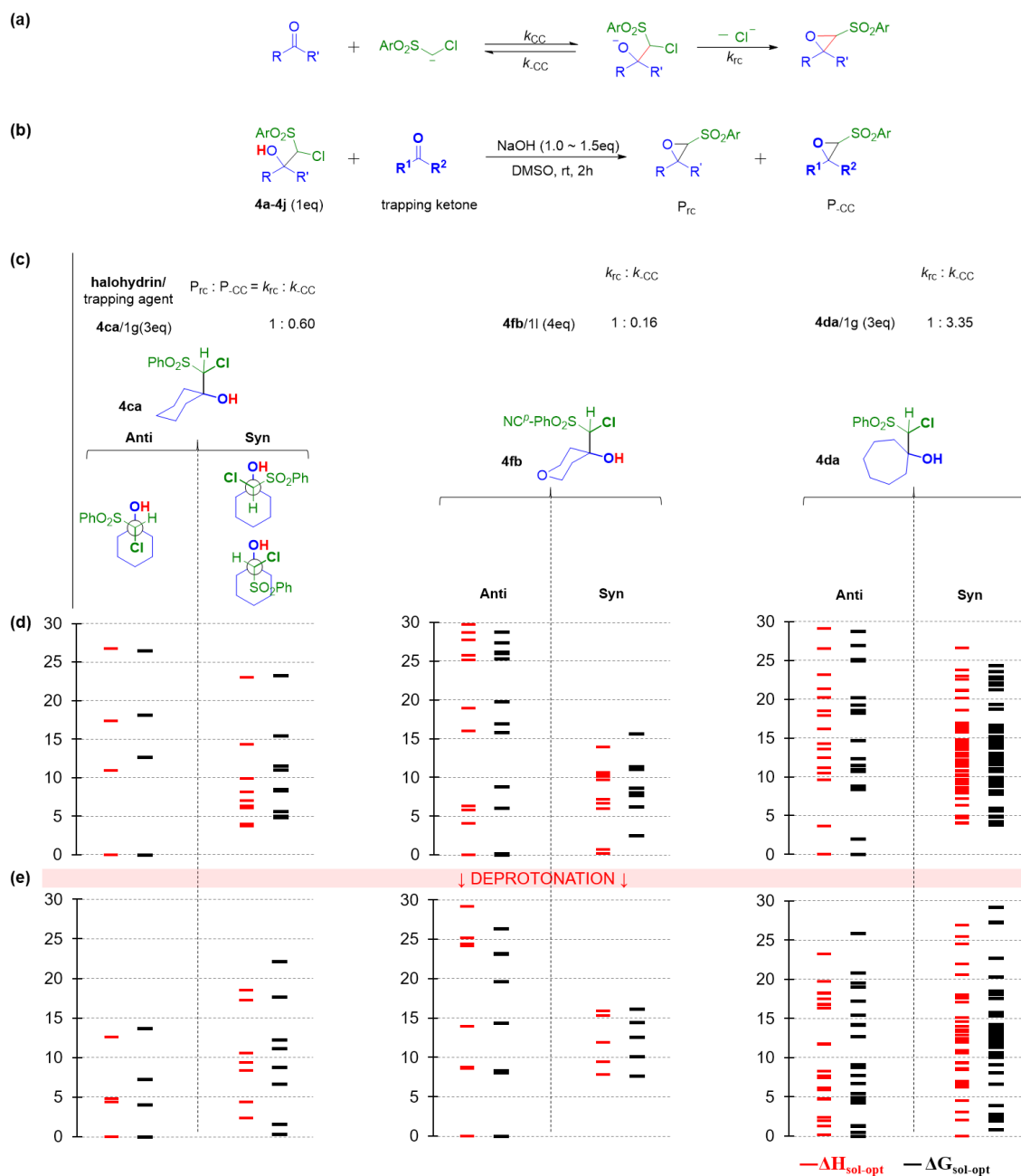


Figure S15. (a) The proposed mechanism of the reactions of reference nucleophiles with ketones. (b) Crossover reaction. (c) The experimentally derived ratio of k_{RC}/k_{CC} . Conformational distribution of halohydrins in (d) neutral and (e) anionic (deprotonated) form calculated at B3LYP-D3/6-31+G(d,p)/PCM(UA0,DMSO) level of theory. Energetics is reported in kJ/mol.

8.2.5 QM data for PESs

Table S22. Transition state (TS), reactant complex (RC) and product complex (PC) barriers ($\Delta G_{\text{sol-opt}}$, kJ/mol) used for plotting PESs for the reaction of arylsulfonyl-substituted chloromethyl anions **2a** with electrophiles [ketones (**1c** and **1g**) and dimethyl maleate **5***] calculated from QM data in Table S23.

System	Filename	Path	B3LYP-D3/6-31G+(d,p)/PCM(DMSO,UA0)			B3LYP-D3/6-31G+(d,p) //B3LYP-D3/6-31G+(d,p)/PCM(DMSO,UA0)			B2PLYP-D3/def2TZVPP/PCM(UA0)		
			RC	TS	PC	RC	TS	PC	RC	TS	PC
1c+2a	au_c1_9	syn	19.4	46.5	26.8	-23.7	11.9	13.6	16.6	47.4	32.4
	au_c1_10	syn	26.0	50.8	31.8	-11.0	19.9	19.4	28.0	56.3	39.5
	c1_1	syn	28.1	51.1	42.8	-	-	-	-	55.2	51.6
	c1_2	syn	31.4	52.7	36.9	-	-	-	-	55.5	42.5
	c1_19	syn	27.8	55.1	36.8	-	-	-	-	60.5	42.6
	c1_5	syn	34.0	60.8	36.2	-	-	-	-	66.0	41.2
	au_c1_5	syn	31.1	62.6	50.0	-	-	-	-	64.0	55.9
	au_c1_12	syn	30.9	64.2	55.2	-	-	-	-	72.8	66.3
	c1_7	syn	34.4	66.5	55.4	-	-	-	-	74.6	65.9
	au_c1_14	syn	37.0	72.9	54.9	-	-	-	-	79.3	62.6
	au_c1_2	syn	40.0	78.7	59.3	-	-	-	-	85.1	66.4
	c1_34	anti	26.4	56.7	32.3	-4.5	28.5	2.8	28.5	61.5	37.7
	c1_37	anti	30.4	63.2	25.1	-3.8	34.2	-6.1	34.4	67.8	28.3
	c1_31	anti	35.7	77.6	51.3	-	-	-	-	80.0	56.6
	c1_35	anti	40.1	79.8	53.8	-	-	-	-	85.3	60.9
	au_c1_1	anti	41.4	85.8	46.0	-	-	-	-	92.4	50.6
	c1_39	anti	-	87.3	48.7	-	-	-	-	92.4	52.3
	c1_2_19	cy	25.1	37.7	-89.1	-6.1	10.5	-21.6	28.3	44.8	-66.0
	c1_2_14	cy	40.9	46.6	-94.0	11.0	17.4	-52.6	47.5	54.5	-74.0
	c1_2_7	cy	32.3	51.8	-90.2	-	-	-	37.7	60.8	-68.3
	c1_2_23	cy	45.9	58.7	-76.4	-	-	-	50.6	66.6	-55.0
	c1_2_3	cy	50.1	59.0	-78.6	-	-	-	52.7	65.6	-57.4
	c1_2_25	cy	48.7	60.1	-74.1	-	-	-	52.3	67.5	-52.0
	c1_2_1	cy	51.4	65.2	-72.8	-	-	-	56.6	72.5	-53.0
	c1_2_2	cy	52.5	65.9	-	-	-	-	60.1	74.2	-
	c1_2_11	cy	54.7	72.1	-78.6	-	-	-	60.6	81.3	-57.4
	c1_2_12	cy	53.8	72.1	-76.4	-	-	-	60.9	82.0	-55.0
	c1_3_4	rot	26.7	52.1	29.1	13.5	37.1	23.4	32.4	58.5	35.1
	c1_3_5	rot	31.8	60.1	36.8	19.4	45.1	26.2	39.5	68.9	43.7
	c1_3_26	rot	34.0	61.6	25.1	26.7	45.6	-6.1	41.4	68.2	28.3
	c1_3_11	rot	42.8	59.6	44.6	-	-	-	51.6	68.2	51.4
	c1_3_17	rot	53.8	79.7	51.3	-	-	-	58.6	84.5	56.5
	c1_3_14	rot	55.4	71.0	40.9	-	-	-	65.9	79.9	47.6
	c1_3_2	rot	59.3	86.0	48.3	-	-	-	66.4	92.9	53.3
	c1_3_1	rot	63.9	86.8	48.3	-	-	-	67.9	89.2	53.3
	c1_3_20	rot	71.1	90.3	48.1	-	-	-	72.4		51.2

Chapter 3: Kinetics and mechanism of oxirane-formation by Darzens condensation of ketones: quantification of the electrophilicities of ketones

c1_3_7	rot	-	59.6	-	-	-	-	-	68.2	-
c1_3_15	rot	-	61.6	-	-	-	-	-	-	-
c1_3_25	rot	-	62.7	-	-	-	-	-	-	-
c1_3_12	rot	-	63.2	-	-	-	-	-	-	-
c1_3_13	rot	-	69.6	-	-	-	-	-	-	-
c1_3_6	rot	-	75.2	-	-	-	-	-	-	-
c1_3_3	rot	-	77.1	-	-	-	-	-	-	-
c1_3_28	rot	-	86.0	-	-	-	-	-	-	-
c1_3_9	rot	-	86.0	-	-	-	-	-	-	-
c1_3_10	rot	-	86.3	-	-	-	-	-	-	-
c1_3_18	rot	-	86.3	-	-	-	-	-	-	-
c1_3_24	rot	-	88.8	-	-	-	-	-	-	-
c1_3_19	rot	-	89.6	-	-	-	-	-	-	-
c1_3_30	rot	-	89.9	-	-	-	-	-	-	-
c1_3_8	rot	-	90.0	-	-	-	-	-	-	-

1g+2a	Filename	Path	RC	TS	PC	RC	TS	PC	RC	TS	PC
	g1_1	syn	16.8	36.5	28.1	-28.3	-2.6	9.8	15.9	41.6	37.7
	g1_3	syn		36.6	28.1	-	-	-	-	41.7	37.7
	g1_2	syn	22.9	38.7	23.3	-13.4	13.8	31.3	21.5	41.8	29.5
	g1_4	syn	22.8	38.8	23.3	-	-	-	-	41.8	29.5
	au_g1_5	syn	-	43.2	28.2	-	-	-	-	45.5	34.8
	au_g1_12	syn	-	49.9	40.0	-	-	-	-	59.0	51.3
	au_g1_11	syn	28.9	53.5	42.6	-	-	-	-	62.0	53.4
	au_g1_14	syn	-	55.5	36.0	-	-	-	-	63.0	44.6
	au_g1_2	syn	-	57.5	38.3	-	-	-	-	64.3	45.8
	g1_6	anti	28.4	39.6	14.0		2.7	-21.8	30.3	42.6	18.8
	g1_5	anti	30.0	50.4	6.7	7.0	16.7	-32.5	33.8	53.7	9.6
	g1_7	anti	28.9	55.8	26.1	-	-	-	-	62.8	33.5
	g1_11	anti	31.5	59.0	31.4	-	-	-	-	64.5	38.7
	g1_10	anti	33.7	60.1	34.3	-	-	-	-	66.6	42.2
	au_g1_4	anti	33.9	66.9	25.0	-	-	-	-	72.9	29.5
	g1_9	anti	33.8	66.9	25.0	-	-	-	-	72.9	29.5
	g1_8	anti	-	67.0	28.4	-	-	-	-	74.8	34.1
	au_g1_1	anti	-	67.5	28.4	-	-	-	-	75.1	34.1
	g1_2_4	cy	6.8	22.8	-98.2	-32.4	-8.8	-73.5	9.7	30.0	-76.9
	g1_2_2	cy	-	32.1	-97.8	-	-	-	-	40.9	-76.8
	g1_2_6	cy	14.0	38.9	-	-	-	-	-	48.2	-
	g1_2_8	cy	27.5	42.3	-82.9	-7.4	9.7	-57.4	33.4	51.0	-61.5
	g1_2_9	cy	25.0	43.2	-72.1	-	-	-	-	51.7	-51.0
	g1_2_10	cy	34.3	54.3	-83.0	-	-	-	-	65.1	-61.6
	g1_2_11	cy	31.4	55.3	-74.2	-	-	-	-	65.8	-54.3
	g1_3_14	rot	28.6	40.3	6.7	3.8	10.9	-32.5	30.2	41.4	9.5
	g1_3_16	rot	21.3	42.1	14.0	-20.7	2.1	-21.8	23.8	44.0	18.8
	g1_3_15	rot	16.6	46.9	6.7	1.5	23.2	-32.5	23.4	52.5	9.5

Chapter 3: Kinetics and mechanism of oxirane-formation by Darzens condensation of ketones: quantification of the electrophilicities of ketones

g1_3_27	rot	28.0	47.3	29.7	-	-	-	-	56.7	37.5
g1_3_30	rot	32.8	51.2	22.2	-	-	-	-	55.8	29.3
g1_3_7	rot	28.2	56.2	31.1	-	-	-	-	63.1	39.0
g1_3_5	rot	45.6	62.1	25.0	-	-	-	-	65.5	29.5
g1_3_4	rot	44.2	64.2	27.0	-	-	-	-	67.3	33.0
g1_3_22	rot	39.1	68.0	34.3	-	-	-	-	72.2	42.2
g1_3_12	rot	-	47.3	-	-	-	-	-	-	-
g1_3_26	rot	-	47.3	-	-	-	-	-	-	-
g1_3_13	rot	-	51.5	-	-	-	-	-	-	-
g1_3_29	rot	-	54.5	-	-	-	-	-	-	-
g1_3_9	rot	-	54.5	-	-	-	-	-	-	-
g1_3_20	rot	-	62.1	-	-	-	-	-	-	-
g1_3_1	rot	-	63.2	-	-	-	-	-	-	-
g1_3_18	rot	-	63.3	-	-	-	-	-	-	-
g1_3_10	rot	-	63.7	-	-	-	-	-	-	-
g1_3_19	rot	-	64.6	-	-	-	-	-	-	-
g1_3_3	rot	-	64.7	-	-	-	-	-	-	-
g1_3_2	rot	-	64.7	-	-	-	-	-	-	-
g1_3_23	rot	-	64.8	-	-	-	-	-	-	-
g1_3_11	rot	-	64.9	-	-	-	-	-	-	-
g1_3_8	rot	-	65.2	-	-	-	-	-	-	-
g1_3_21	rot	-	67.5	-	-	-	-	-	-	-
g1_3_6	rot	-	67.5	-	-	-	-	-	-	-

5*+2a	Filename	Path	RC	TS	PC	RC	TS	PC	RC	TS	PC
	a5_19	syn	30.4	45.6	-21.7	-	-	-	27.6	46.2	-21.1
	a5_9	syn	32.0	52.7	-0.3	-	-	-	28.3	52.8	0.1
	a5_13	syn	35.1	54.7	-1.8	-	-	-	-	60.1	-0.4
	a5_2	syn	34.6	55.1	-7.5	-	-	-	-	57.5	-8.7
	a5_1	syn	36.4	55.1	-7.5	-	-	-	-	57.6	-8.7
	a5_18	syn	41.5	56.3	-13.1	-	-	-	-	62.6	-10.4
	a5_7	syn	36.7	57.7	-4.6	-	-	-	-	62.5	-3.2
	a5_3	syn	36.0	60.3	-2.5	-	-	-	-	66.2	0.4
	a5_6	anti	32.7	49.3	-15.1	-	-	-	34.2	54.7	-14.0
	a5_8	anti	15.3	49.6	-31.4	-	-	-	15.7	50.9	-28.6
	a5_5	anti	37.9	54.3	-40.5	-	-	-	42.8	58.2	-39.0
	a5_2_2	cy	-43.8	-22.7	-206.7	-	-	-	-42.9	-13.8	-189.1
	a5_2_7	cy	-40.6	-17.8	-203.8	-	-	-	-39.0	-8.8	-186.0
	a5_2_1	cy	-37.2	-5.8	-173.9	-	-	-	-37.1	3.4	-155.5
	a5_2_4	cy	-34.8	-3.2	-171.4	-	-	-	-34.2	6.1	-153.4
	a5_2_10	cy	-27.3	-2.9	-188.2	-	-	-	-25.9	6.2	-171.1
	a5_2_6	cy	-19.2	13.5	-160.4	-	-	-	-18.5	23.5	-142.3
	a5_3_8	rot	-19.9	-0.7	-31.4	-	-	-	-17.3	0.9	-28.6
	a5_3_3	rot	-2.6	2.2	-35.8	-	-	-	0.3	2.7	-32.8
	a5_3_2	rot	-5.5	3.8	-34.8	-	-	-	-7.0	4.9	-32.7

a5_3_9 rot -0.8 5.7 -29.8 - - - 0.7 8.0 -25.5

Table S23. QM data used for PESs for the reaction of arylsulfonyl-substituted chloromethyl anions **2a** with electrophiles [ketones (**1c** and **1g**) and dimethyl maleate **5a***] calculated at different levels of theory.

System	Filename	B3LYP-D3/6-31G+(d,p)/PCM(DMSO,UA0)							B3LYP-D3/ 6-31G+(d,p)	B2PLYP-D3 /def2TZVPP /PCM(UA0)	
		Type	Low Frequencies			corr. ZPE	corr. ΔH	corr. ΔG	ΔE _{tot} (hartree)	//B3LYP-D3/6-31G+(d,p)/PCM(DMSO,UA0)	
Reference											
2a	ref_2a_1	nu	-18.8	-5.3	0.0	0.115058	0.126202	0.077398	-1279.2758941	-1279.1876384	-1278.8910872
2a	ref_2a_5	nu	-28.3	-21.1	-14.3	0.114614	0.124953	0.079062	-1279.2714861	-1279.1843610	-1278.8852537
1c	ref_c1_1	el(c1)	-34.5	0.0	0.0	0.150819	0.158206	0.120447	-309.9368880	-309.9297127	-309.7525739
1c	ref_c1_2	el(c1)	-34.8	-22.5	-19.2	0.150349	0.157948	0.119396	-309.9311343	-309.9238362	-309.7467345
1g	ref_g1_1	el(g1)	-25.7	-14.3	0.0	0.123352	0.131069	0.092028	-668.8052751	-668.7969649	-668.5398771
1g	ref_g1_2	el(g1)	-28.2	-19.5	0.0	0.122991	0.130876	0.090915	-668.8016361	-668.7928595	-668.5358418
5a*	ref_a5_3	el(a5*)	-14.2	-4.5	0.0	0.137883	0.149837	0.098628	-534.3936779	-	-534.1778933
5a*	ref_a5_1	el(a5*)	-13.7	-8.9	0.0	0.137874	0.149788	0.099897	-534.3943032	-	-534.1768910
1c+2a Transition State											
	au_c1_9	syn	-64.8	0.0	0.0	0.267812	0.285828	0.221509	-1589.2157279	-1589.1334617	-1588.6462676
	au_c1_10	syn	-90.5	-2.9	0.0	0.267839	0.285788	0.222458	-1589.2150172	-1589.1313660	-1588.6438171
	c1_1	syn	-128.4	-11.1	-3.9	0.268031	0.285813	0.222144	-1589.2146013	-	-1588.6439094
	au_c1_13	syn	-128.5	-10.6	-3.8	0.268032	0.285813	0.222156	-1589.2146010	-	-1588.6439095
	c1_2	syn	-117.4	-1.9	0.0	0.267986	0.285732	0.222512	-1589.2143546	-	-1588.6441648
	c1_19	syn	-85.8	-18.5	0.0	0.267787	0.285839	0.221519	-1589.2124562	-	-1588.6412777
	c1_5	syn	-114.2	0.0	0.0	0.268063	0.285772	0.223129	-1589.2118953	-	-1588.6407836
	au_c1_5	syn	-110.2	-16.6	-3.8	0.267611	0.285748	0.220565	-1589.2086297	-	-1588.6389672
	au_c1_12	syn	-217.0	-13.5	-10.3	0.268205	0.285843	0.223729	-1589.2112049	-	-1588.6388123
	c1_7	syn	-180.4	-19.6	-8.2	0.268507	0.286124	0.223439	-1589.2100424	-	-1588.6378309
	au_c1_14	syn	-111.9	-16.1	0.0	0.267719	0.285802	0.221833	-1589.2059673	-	-1588.6344374
	au_c1_2	syn	-127.6	-16.1	-12.0	0.267942	0.285870	0.222602	-1589.2045433	-	-1588.6329896
	c1_32	syn	-110.2	-16.5	-3.7	0.267612	0.285748	0.220571	-1589.2086297	-	-1588.6389678
	c1_36	syn	-180.6	-19.3	-8.1	0.268509	0.286125	0.223449	-1589.2100426	-	-1588.6378310
	c1_38	syn	-127.7	-16.1	-11.9	0.267943	0.285871	0.222605	-1589.2045432	-	-1588.6329856
	c1_34	anti	-91.9	0.0	0.0	0.267954	0.285788	0.222621	-1589.2129302	-1589.1282572	-1588.6420022
	c1_37	anti	-89.7	-9.0	-4.4	0.267467	0.285539	0.221329	-1589.2091676	-1589.1248077	-1588.6383005
	c1_31	anti	-113.1	0.0	0.0	0.267665	0.285747	0.221145	-1589.2035104	-	-1588.6334755
	c1_35	anti	-136.0	-12.6	-7.7	0.267542	0.285610	0.221513	-1589.2030533	-	-1588.6318027
	au_c1_1	anti	-125.1	-8.4	0.0	0.267871	0.285777	0.222441	-1589.2016676	-	-1588.6300631
	c1_39	anti	-128.9	-1.9	0.0	0.267856	0.285737	0.222736	-1589.2013980	-	-1588.6303464

Chapter 3: Kinetics and mechanism of oxirane-formation by Darzens condensation of ketones: quantification of the electrophilicities of ketones

c1_25	anti	-128.9	-0.9	0.0	0.267857	0.285738	0.222740	-1589.2013980	-	-1588.6303484
c1_2_19	cy	-353.4	-10.2	0.0	0.268821	0.286585	0.223526	-1589.2210912	-1589.1360012	-1588.6492568
c1_2_14	cy	-324.0	-2.6	0.0	0.269080	0.286675	0.224321	-1589.2185041	-1589.1342001	-1588.6463770
c1_2_7	cy	-370.9	-11.1	0.0	0.269018	0.286692	0.224315	-1589.2165220	-	-1588.6439470
c1_2_23	cy	-350.2	-14.6	-10.1	0.268544	0.286472	0.222807	-1589.2123660	-	-1588.6402488
c1_2_3	cy	-346.7	-15.5	-10.7	0.268473	0.286487	0.222306	-1589.2117366	-	-1588.6401222
c1_2_25	cy	-350.5	-12.1	0.0	0.268663	0.286598	0.222654	-1589.2116782	-	-1588.6397535
c1_2_1	cy	-354.1	-17.3	-10.5	0.268552	0.286547	0.222354	-1589.2094301	-	-1588.6375379
c1_2_2	cy	-359.9	-15.0	-10.0	0.268654	0.286540	0.222994	-1589.2098256	-	-1588.6375156
c1_2_11	cy	-370.1	-11.2	0.0	0.268769	0.286646	0.223526	-1589.2079941	-	-1588.6353509
c1_2_12	cy	-372.9	-11.6	-5.3	0.268710	0.286604	0.223298	-1589.2077525	-	-1588.6348578
c1_3_4	rot	-48.3	-4.4	0.0	0.269515	0.286529	0.225704	-1589.2177832	-1589.1280460	-1588.6462133
c1_3_11	rot	-54.3	-23.5	-6.1	0.269605	0.286564	0.225888	-1589.2150975	-	-1588.6427111
c1_3_7	rot	-54.6	-23.6	-6.0	0.269605	0.286564	0.225890	-1589.2150968	-	-1588.6427101
c1_3_5	rot	-55.0	-13.3	-7.2	0.269753	0.286680	0.226358	-1589.2153804	-1589.1256759	-1588.6429070
c1_3_26	rot	-51.7	-19.3	-10.1	0.269651	0.286643	0.226077	-1589.2145243	-1589.1251812	-1588.6429126
c1_3_15	rot	-51.7	-19.4	-10.0	0.269652	0.286643	0.226083	-1589.2145244	-	-
c1_3_25	rot	-44.8	-8.0	-4.8	0.269361	0.286277	0.225990	-1589.2140237	-	-
c1_3_12	rot	-48.4	-16.4	-1.0	0.269278	0.286225	0.225865	-1589.2137158	-	-
c1_3_13	rot	-43.0	-16.5	-5.7	0.269488	0.286231	0.226738	-1589.2121369	-	-
c1_3_14	rot	-48.5	-1.9	0.0	0.269882	0.286740	0.226825	-1589.2117026	-	-1588.6391777
c1_3_6	rot	-42.6	-9.7	0.0	0.269937	0.286779	0.226898	-1589.2101626	-	-
c1_3_3	rot	-43.3	-17.8	-11.4	0.269271	0.286469	0.224815	-1589.2073504	-	-
c1_3_17	rot	-60.5	-21.5	-15.4	0.268775	0.286229	0.223965	-1589.2055128	-	-1588.6345687
c1_3_2	rot	-43.8	-16.3	-4.0	0.269608	0.286691	0.225929	-1589.2051107	-	-1588.6333458
c1_3_28	rot	-43.8	-16.2	-3.9	0.269609	0.286691	0.225931	-1589.2051107	-	-
c1_3_9	rot	-43.6	-16.2	-3.8	0.269612	0.286693	0.225942	-1589.2051107	-	-
c1_3_10	rot	-44.6	-10.6	0.0	0.269089	0.286222	0.225031	-1589.2040885	-	-
c1_3_18	rot	-44.3	-10.1	0.0	0.269094	0.286225	0.225043	-1589.2040905	-	-
c1_3_1	rot	-50.8	-10.6	0.0	0.269080	0.286214	0.225100	-1589.2039528	-	-1588.6339414
c1_3_24	rot	-46.4	-34.8	-12.0	0.268854	0.286051	0.224875	-1589.2029623	-	-
c1_3_19	rot	-46.5	-9.8	0.0	0.269369	0.286596	0.225634	-1589.2034421	-	-
c1_3_30	rot	-41.2	-16.3	-8.1	0.269293	0.286446	0.225451	-1589.2031373	-	-
c1_3_8	rot	-43.7	-12.4	-7.9	0.269389	0.286597	0.225785	-1589.2034222	-	-
c1_3_20	rot	-40.1	0.0	0.0	0.268962	0.286209	0.225041	-1589.2025602	-	-
Reactant (Complex)										
c1_31_r	rc	0.0	0.0	0.0	0.266617	0.286428	0.215441	-1589.2137663	-	-
au_c1_13_r	rc	0.0	0.0	0.0	0.266954	0.286381	0.217564	-1589.2187745	-	-
au_c1_5_r	rc	-21.8	-7.4	0.0	0.266405	0.286323	0.213951	-1589.2140372	-	-
au_c1_1_r	rc	-9.1	0.0	0.0	0.266359	0.286258	0.215484	-1589.2116175	-	-
au_c1_14_r	rc	-16.7	-5.8	0.0	0.266672	0.286390	0.216313	-1589.2141320	-	-
c1_34_r	rc	0.0	0.0	0.0	0.266904	0.286515	0.216842	-1589.2186889	-1589.1350435	-1588.6487821
au_c1_9_r	rc	-12.4	-6.5	0.0	0.267059	0.286679	0.216011	-1589.2205379	-1589.1415161	-1588.6524863
c1_1_r	rc	0.0	0.0	0.0	0.266954	0.286381	0.217564	-1589.2187746	-	-
au_c1_12_f	rc	-17.8	-6.8	0.0	0.266717	0.286195	0.217593	-1589.2177462	-	-

Chapter 3: Kinetics and mechanism of oxirane-formation by Darzens condensation of ketones: quantification of the electrophilicities of ketones

	c1_38_r	rc	-16.5	-8.8	-5.8	0.266158	0.286102	0.215208	-1589.2116796	-	-
	c1_36_r	rc	-35.7	-14.1	0.0	0.269962	0.287730	0.224953	-1589.2157685	-	-
	c1_7_r	rc	-13.7	-9.6	0.0	0.266853	0.286433	0.217097	-1589.2158979	-	-
	c1_35_r	rc	0.0	0.0	0.0	0.266474	0.286267	0.215758	-1589.2123945	-	-
	c1_2_r	rc	-13.2	0.0	0.0	0.266883	0.286319	0.217040	-1589.2169812	-	-
	au_c1_2_r	rc	-16.9	-13.2	-7.6	0.266132	0.286094	0.214987	-1589.2116679	-	-
	c1_5_r	rc	0.0	0.0	0.0	0.266922	0.286439	0.217495	-1589.2164582	-	-
	c1_37_r	rc	-10.4	0.0	0.0	0.266816	0.286511	0.215610	-1589.2159678	-1589.1335292	-1588.6453152
	c1_32_r	rc	-6.3	0.0	0.0	0.266362	0.286271	0.213968	-1589.2138520	-	-
	au_c1_10_r	rc	-7.1	-2.8	0.0	0.266993	0.286519	0.217447	-1589.2194578	-1589.1381349	-1588.6495730
	c1_19_r	rc	-7.5	0.0	0.0	0.266751	0.286494	0.215714	-1589.2170268	-	-
	c1_2_19_r	rc	-14.3	0.0	0.0	0.269669	0.287520	0.224550	-1589.2269186	-1589.1433744	-1588.6565754
	c1_2_7_r	rc	-4.5	0.0	0.0	0.269825	0.287510	0.225471	-1589.2250779	-	-1588.6539040
	c1_2_14_r	rc	-15.3	0.0	0.0	0.269900	0.287655	0.225217	-1589.2215588	-1589.1375107	-1588.6499042
	c1_2_23_r	rc	-11.4	0.0	0.0	0.269432	0.287484	0.223229	-1589.2176638	-	-1588.6467605
	c1_2_25_r	rc	-6.2	-3.3	0.0	0.269507	0.287476	0.224358	-1589.2177201	-	-1588.6472171
	c1_2_3_r	rc	-15.7	0.0	0.0	0.269409	0.287479	0.223799	-1589.2166447	-	-1588.6465155
	c1_2_1_r	rc	-19.3	-11.4	0.0	0.269177	0.287349	0.222824	-1589.2151744	-	-1588.6440546
	c1_2_2_r	rc	-7.8	0.0	0.0	0.269484	0.287464	0.224140	-1589.2160477	-	-1588.6440638
	c1_2_12_r	rc	-16.3	0.0	0.0	0.269425	0.287396	0.224222	-1589.2156469	-	-1588.6438089
	c1_2_11_r	rc	-14.2	0.0	0.0	0.269730	0.287619	0.224645	-1589.2157283	-	-1588.6443709
	c1_3_4_r	rc	-8.2	0.0	0.0	0.269804	0.287599	0.224340	-1589.2260802	-1589.1356760	-1588.6548062
	c1_3_5_r	rc	0.0	0.0	0.0	0.270003	0.287678	0.225596	-1589.2254085	-1589.1346960	-1588.6533344
	c1_3_26_r	rc	-12.8	0.0	0.0	0.270019	0.287773	0.225002	-1589.2239894	-1589.1313220	-1588.6520125
	c1_3_11_r	rc	-22.4	-3.0	0.0	0.269793	0.287574	0.224772	-1589.2203880	-	-1588.6479007
	c1_3_17_r	rc	0.0	0.0	0.0	0.269485	0.287489	0.223521	-1589.2149670	-	-1588.6440097
	c1_3_14_r	rc	-35.7	-14.1	0.0	0.269963	0.287731	0.224966	-1589.2157685	-	-1588.6426694
	c1_3_2_r	rc	-14.7	-9.0	0.0	0.269625	0.287585	0.224448	-1589.2137632	-	-1588.6419557
	c1_3_1_r	rc	-28.5	-18.7	0.0	0.269686	0.287546	0.224660	-1589.2122214	-	-1588.6416107
	c1_3_20_r	rc	-9.2	0.0	0.0	0.269696	0.287541	0.224920	-1589.2097418	-	-1588.6401556
Product (Complex)	c1_37_f	pc	-14.4	0.0	0.0	0.269669	0.287520	0.224552	-1589.2269186	-1589.1433734	-1588.6565754
	c1_34_f	pc	-4.1	0.0	0.0	0.269825	0.287509	0.225477	-1589.2250778	-1589.1408951	-1588.6539018
	au_c1_1_f	pc	-11.5	0.0	0.0	0.269434	0.287485	0.223253	-1589.2176638	-	-1588.6467655
	c1_25_f	pc	-5.0	0.0	0.0	0.269506	0.287474	0.224355	-1589.2177201	-	-1588.6472206
	c1_39_r	pc	-4.8	0.0	0.0	0.269506	0.287474	0.224356	-1589.2177201	-	-1588.6472218
	c1_31_f	pc	-20.0	-11.3	0.0	0.269173	0.287347	0.222797	-1589.2151745	-	-1588.6440525
	c1_35_f	pc	-16.2	0.0	0.0	0.269424	0.287395	0.224218	-1589.2156470	-	-1588.6438153
	au_c1_9_f	pc	-8.0	0.0	0.0	0.269807	0.287600	0.224357	-1589.2260804	-1589.1356735	-1588.6548060
	au_c1_10_f	pc	0.0	0.0	0.0	0.270002	0.287677	0.225594	-1589.2254086	-1589.1346988	-1588.6533308
	c1_5_f	pc	-16.4	-12.1	0.0	0.270047	0.287615	0.225317	-1589.2234400	-	-1588.6524409
	c1_19_f	pc	-8.5	0.0	0.0	0.269800	0.287537	0.225227	-1589.2231455	-	-1588.6518174
	c1_2_f	pc	-12.8	-7.2	0.0	0.270111	0.287716	0.224997	-1589.2228455	-	-1588.6516024
	c1_1_f	pc	-22.5	-3.3	0.0	0.269791	0.287573	0.224768	-1589.2203880	-	-1588.6479010

Chapter 3: Kinetics and mechanism of oxirane-formation by Darzens condensation of ketones: quantification of the electrophilicities of ketones

	au_c1_13_f	pc	-22.5	-3.3	0.0	0.269791	0.287573	0.224768	-1589.2203880	-	-1588.6479011
	c1_32_f	pc	-20.5	-4.5	0.0	0.269632	0.287583	0.223924	-1589.2167823	-	-1588.6454203
	au_c1_5_f	pc	-20.5	-4.4	0.0	0.269633	0.287584	0.223925	-1589.2167823	-	-1588.6454208
	au_c1_14_f	pc	-13.6	0.0	0.0	0.269862	0.287687	0.225265	-1589.2162880	-	-1588.6442336
	au_c1_12_r	pc	-14.8	0.0	0.0	0.269995	0.287681	0.225837	-1589.2167262	-	-1588.6433638
	c1_36_f	pc	-35.7	-14.1	0.0	0.269962	0.287731	0.224964	-1589.2157685	-	-1588.6426700
	c1_7_f	pc	-35.7	-14.1	0.0	0.269963	0.287732	0.224964	-1589.2157684	-	-1588.6426723
	au_c1_2_f	pc	-14.7	-9.0	0.0	0.269624	0.287584	0.224447	-1589.2137632	-	-1588.6419532
	c1_38_f	pc	-14.8	-9.1	0.0	0.269624	0.287584	0.224448	-1589.2137632	-	-1588.6419598
	c1_2_14_ircf	pc	-10.4	0.0	0.0	0.270769	0.289334	0.221834	-1589.2695508	-1589.1583634	-1588.6928127
	c1_2_7_ircr	pc	-12.8	0.0	0.0	0.270409	0.289127	0.221162	-1589.2674492	-	-1588.6899888
	c1_2_19_ircr	pc	0.0	0.0	0.0	0.270265	0.289032	0.220792	-1589.2666569	-1589.1455040	-1588.6887441
	c1_2_11_ircr	pc	-17.7	0.0	0.0	0.270241	0.289155	0.219776	-1589.2616306	-	-1588.6844418
	c1_2_3_ircr	pc	-17.6	0.0	0.0	0.270242	0.289156	0.219785	-1589.2616308	-	-1588.6844435
	c1_2_23_ircr	pc	-9.6	-7.2	0.0	0.270273	0.289144	0.220589	-1589.2616164	-	-1588.6843435
	c1_2_12_ircf	pc	-9.6	-7.2	0.0	0.270274	0.289144	0.220594	-1589.2616164	-	-1588.6843434
	c1_2_25_ircr	pc	-5.9	0.0	0.0	0.270120	0.289083	0.219795	-1589.2599185	-	-1588.6823927
	c1_2_1_ircf	pc	-8.9	-7.1	0.0	0.270446	0.289217	0.221972	-1589.2616244	-	-1588.6849708
	c1_2_11_ircf	pc	-8.1	-5.4	0.0	0.270196	0.289077	0.221009	-1589.2602268	-	-1588.6831752
	c1_3_26_f	pc	-14.2	0.0	0.0	0.269668	0.287519	0.224553	-1589.2269187	-1589.1433744	-1588.6565727
	c1_3_4_f	pc	-17.3	0.0	0.0	0.269647	0.287509	0.224394	-1589.2252302	-1589.1319588	-1588.6538173
	c1_3_5_f	pc	-10.5	-3.8	0.0	0.269632	0.287504	0.224381	-1589.2222652	-1589.1308997	-1588.6505459
	c1_3_14_f	pc	-15.2	0.0	0.0	0.269901	0.287656	0.225224	-1589.2215588	-	-1588.6499087
	c1_3_11_f	pc	-15.8	0.0	0.0	0.269558	0.287398	0.224192	-1589.2191148	-	-1588.6474177
	c1_3_20_f	pc	-13.5	-9.4	0.0	0.269277	0.287421	0.223073	-1589.2166732	-	-1588.6463634
	c1_3_1_f	pc	-12.6	-4.0	0.0	0.269552	0.287523	0.224142	-1589.2176642	-	-1588.6466471
	c1_3_2_f	pc	-12.6	-3.6	0.0	0.269554	0.287524	0.224155	-1589.2176642	-	-1588.6466481
	c1_3_17_f	pc	-20.1	-11.3	0.0	0.269172	0.287347	0.222790	-1589.2151745	-	-1588.6440520
1g+2a Transition State	g1_1	syn	-111.6	-7.7	0.0	0.240839	0.258965	0.194054	-1948.0888831	-1948.0072111	-1947.4367340
	g1_3	syn	-111.7	-9.8	0.0	0.240842	0.258965	0.194101	-1948.0888871	-	-1947.4367378
	g1_2	syn	-114.0	-16.8	-5.7	0.240646	0.258826	0.193741	-1948.0877221	-1948.0006598	-1947.4363568
	g1_4	syn	-114.0	-16.7	-5.7	0.240646	0.258826	0.193758	-1948.0877221	-	-1947.4363569
	au_g1_5	syn	-97.5	-14.9	-8.4	0.240467	0.258905	0.192596	-1948.0848796	-	-1947.4337788
	au_g1_12	syn	-208.1	-11.9	0.0	0.241047	0.259004	0.195859	-1948.0855763	-	-1947.4319046
	au_g1_11	syn	-156.4	-10.8	0.0	0.241166	0.259159	0.195521	-1948.0838792	-	-1947.4304344
	au_g1_14	syn	-116.2	-3.3	0.0	0.240720	0.259013	0.194241	-1948.0818409	-	-1947.4287521
	au_g1_2	syn	-123.1	-15.0	-8.4	0.240457	0.258816	0.194012	-1948.0808252	-	-1947.4280459
	g1_6	anti	-46.4	-23.3	-11.2	0.240178	0.258748	0.192318	-1948.0859510	-1948.0034516	-1947.4346101
	g1_5	anti	-40.3	-9.2	0.0	0.239951	0.258593	0.192305	-1948.0818347	-1947.9981204	-1947.4303603
	g1_7	anti	-122.3	-18.3	-15.9	0.240424	0.258740	0.193555	-1948.0810284	-	-1947.4281607
	g1_11	anti	-96.8	-10.8	-7.3	0.240385	0.258789	0.193384	-1948.0796183	-	-1947.4273216

Chapter 3: Kinetics and mechanism of oxirane-formation by Darzens condensation of ketones: quantification of the electrophilicities of ketones

	gl_10	anti	-126.2	-14.3	-8.9	0.240427	0.258784	0.193431	-1948.0792464	-	-1947.4265654
	au_gl_4	anti	-117.3	-12.3	-4.9	0.240498	0.258775	0.194328	-1948.0775722	-	-1947.4250900
	gl_9	anti	-117.3	-12.2	-4.8	0.240499	0.258775	0.194328	-1948.0775721	-	-1947.4250913
	gl_8	anti	-102.6	-13.4	0.0	0.240961	0.259101	0.194226	-1948.0774417	-	-1947.4242749
	au_gl_1	anti	-111.9	0.0	0.0	0.240798	0.259016	0.194545	-1948.0775499	-	-1947.4244511
	gl_2_4	cy	-371.9	-14.6	0.0	0.241452	0.259701	0.194074	-1948.0941068	-1948.0095882	-1947.4411593
	gl_2_2	cy	-337.9	-18.4	-16.3	0.241706	0.259751	0.195514	-1948.0920249	-	-1947.4384595
	gl_2_6	cy	-385.7	-10.9	0.0	0.241644	0.259775	0.195325	-1948.0892216	-	-1947.4354871
	gl_2_8	cy	-369.4	0.0	0.0	0.241535	0.259703	0.195307	-1948.0879056	-1948.0037639	-1947.4343857
	gl_2_9	cy	-364.8	-14.1	-6.7	0.241608	0.259800	0.195012	-1948.0872796	-	-1947.4338466
	gl_2_10	cy	-383.8	-10.8	-5.1	0.241562	0.259768	0.194752	-1948.0827828	-	-1947.4284699
	gl_2_11	cy	-383.6	-6.5	-2.9	0.241537	0.259758	0.195068	-1948.0827403	-	-1947.4285401
	gl_3_14	rot	-58.0	-24.4	-13.4	0.242124	0.259531	0.197134	-1948.0904982	-1948.0051310	-1947.4398874
	gl_3_16	rot	-37.2	-14.9	0.0	0.242071	0.259379	0.197646	-1948.0903335	-1948.0090173	-1947.4394082
	gl_3_15	rot	-48.8	-9.7	-4.2	0.242394	0.259761	0.198103	-1948.0889766	-1948.0014435	-1947.4366095
	gl_3_27	rot	-41.6	-3.7	0.0	0.242439	0.259738	0.198291	-1948.0889943	-	-1947.4352320
	gl_3_12	rot	-41.2	-2.9	0.0	0.242442	0.259740	0.198301	-1948.0889952	-	-
	gl_3_26	rot	-41.1	-2.6	0.0	0.242443	0.259740	0.198303	-1948.0889954	-	-
	gl_3_30	rot	-36.7	0.0	0.0	0.242159	0.259393	0.198373	-1948.0875917	-	-1947.4356249
	gl_3_13	rot	-34.0	-5.1	0.0	0.242177	0.259411	0.198184	-1948.0872915	-	-
	gl_3_29	rot	-46.9	-18.4	-6.5	0.242435	0.259803	0.197532	-1948.0855125	-	-
	gl_3_9	rot	-46.8	-18.4	-6.2	0.242437	0.259803	0.197549	-1948.0855126	-	-
	gl_3_7	rot	-49.8	-15.1	-9.7	0.242105	0.259560	0.197341	-1948.0846627	-	-1947.4318243
	gl_3_5	rot	-69.6	-20.0	-11.3	0.242041	0.259471	0.197160	-1948.0822489	-	-1947.4307233
	gl_3_20	rot	-69.6	-20.0	-11.3	0.242042	0.259471	0.197161	-1948.0822490	-	-
	gl_3_1	rot	-59.6	-23.6	0.0	0.241750	0.259282	0.196442	-1948.0810766	-	-
	gl_3_18	rot	-59.6	-24.0	0.0	0.241747	0.259280	0.196458	-1948.0810768	-	-
	gl_3_10	rot	-49.8	-7.8	0.0	0.242627	0.259837	0.198996	-1948.0834755	-	-
	gl_3_4	rot	-53.2	-16.8	0.0	0.241796	0.259291	0.196823	-1948.0810772	-	-1947.4296921
	gl_3_19	rot	-45.5	-13.6	0.0	0.242496	0.259839	0.198202	-1948.0823064	-	-
	gl_3_3	rot	-45.4	-13.5	0.0	0.242499	0.259841	0.198208	-1948.0823065	-	-
	gl_3_2	rot	-45.5	-13.6	0.0	0.242501	0.259842	0.198210	-1948.0823065	-	-
	gl_3_23	rot	-32.2	-6.2	0.0	0.242062	0.259349	0.198068	-1948.0820938	-	-
	gl_3_11	rot	-44.1	-8.7	0.0	0.242439	0.259751	0.198345	-1948.0823498	-	-
	gl_3_8	rot	-43.0	0.0	0.0	0.241961	0.259378	0.197323	-1948.0812012	-	-
	gl_3_21	rot	-45.3	-15.0	-7.9	0.242264	0.259704	0.197506	-1948.0805281	-	-
	gl_3_6	rot	-45.1	-14.9	-7.8	0.242266	0.259705	0.197511	-1948.0805284	-	-
	gl_3_22	rot	-42.7	-9.5	0.0	0.241943	0.259298	0.197656	-1948.0804768	-	-1947.4286906
Reactant (Complex)	gl_1_r	rc	-18.5	-3.8	0.0	0.239870	0.259539	0.189461	-1948.0917886	-1948.0124114	-1947.4419418
	gl_4_r	rc	-8.9	0.0	0.0	0.239850	0.259540	0.189541	-1948.0895830	-	-
	gl_2_r	rc	-9.1	0.0	0.0	0.239855	0.259540	0.189591	-1948.0895837	-1948.0068476	-1947.4399388
	gl_6_r	rc	-10.6	0.0	0.0	0.239518	0.259387	0.189689	-1948.0876119	-1948.0018452	-1947.4366785
	au_gl_11_r	rc	-7.7	0.0	0.0	0.239954	0.259592	0.190620	-1948.0883512	-	-
	gl_7_r	rc	-8.1	0.0	0.0	0.239953	0.259590	0.190631	-1948.0883509	-	-

Chapter 3: Kinetics and mechanism of oxirane-formation by Darzens condensation of ketones: quantification of the electrophilicities of ketones

	gl_5_r	rc	-10.0	-5.9	0.0	0.239362	0.259359	0.187262	-1948.0845564	-1947.9967654	-1947.4329072
	gl_11_r	rc	0.0	0.0	0.0	0.239543	0.259411	0.189813	-1948.0865368	-	-
	gl_10_r	rc	-9.3	0.0	0.0	0.239350	0.259297	0.189171	-1948.0850417	-	-
	gl_9_r	rc	-5.4	0.0	0.0	0.239371	0.259380	0.188732	-1948.0845701	-	-
	au_gl_4_r	rc	-4.6	0.0	0.0	0.239376	0.259382	0.188753	-1948.0845698	-	-
	gl_2_8_ircf	rc	-13.5	0.0	0.0	0.242442	0.260695	0.196302	-1948.0945612	-1948.0112631	-1947.4421061
	gl_2_10_ircf	rc	-11.3	0.0	0.0	0.242515	0.260703	0.196788	-1948.0924366	-	-
	gl_2_9_ircf	rc	-17.0	-5.4	0.0	0.242200	0.260576	0.195454	-1948.0946452	-	-
	gl_2_4_ircf	rc	-13.9	0.0	0.0	0.242448	0.260700	0.195923	-1948.1020605	-1948.0204140	-1947.4507648
	gl_2_11_ircf	rc	-11.2	0.0	0.0	0.242449	0.260641	0.196496	-1948.0932723	-	-
	gl_2_6_ircf	rc	-11.6	-6.1	0.0	0.242503	0.260668	0.196791	-1948.1001792	-	-
	gl_3_15_r	rc	-16.3	-5.5	0.0	0.242753	0.260876	0.196943	-1948.0993616	-1948.0085358	-1947.4465352
	gl_3_16_r	rc	0.0	0.0	0.0	0.242497	0.260556	0.197164	-1948.0977814	-1948.0172258	-1947.4466367
	gl_3_27_r	rc	0.0	0.0	0.0	0.242658	0.260772	0.196939	-1948.0949848	-	-
	gl_3_7_r	rc	-6.7	0.0	0.0	0.242599	0.260800	0.196297	-1948.0942715	-	-
	gl_3_14_r	rc	-26.2	-11.4	0.0	0.242480	0.260630	0.196722	-1948.0945390	-1948.0074165	-1947.4437329
	gl_3_30_r	rc	-11.2	-4.5	0.0	0.242948	0.260866	0.197770	-1948.0940087	-	-
	gl_3_22_r	rc	0.0	0.0	0.0	0.242564	0.260617	0.197084	-1948.0909125	-	-
	gl_3_4_r	rc	-21.0	-12.7	0.0	0.242363	0.260549	0.196457	-1948.0883511	-	-
	gl_3_5_r	rc	-10.0	0.0	0.0	0.242662	0.260786	0.196515	-1948.0878528	-	-
Product (Complex)	gl_2_f	pc	-20.9	-12.3	0.0	0.242943	0.260862	0.197317	-1948.0971723	-1947.9975436	-1947.4445916
	gl_4_f	pc	-20.9	-12.3	0.0	0.242943	0.260862	0.197317	-1948.0971723	-	-1947.4445915
	gl_3_f	pc	0.0	0.0	0.0	0.242661	0.260774	0.196950	-1948.0949860	-	-1947.4411159
	gl_1_f	pc	0.0	0.0	0.0	0.242662	0.260774	0.196951	-1948.0949860	-1948.0053605	-1947.4411159
	au_gl_5_f	pc	-6.7	0.0	0.0	0.242599	0.260799	0.196302	-1948.0942716	-	-1947.4415647
	au_gl_14_f	pc	-6.5	0.0	0.0	0.242761	0.260861	0.197159	-1948.0921705	-	-1947.4386946
	au_gl_2_f	pc	-7.9	0.0	0.0	0.242705	0.260870	0.197116	-1948.0912427	-	-1947.4381765
	au_gl_12_f	pc	-16.1	-12.2	0.0	0.242563	0.260672	0.197399	-1948.0908941	-	-1947.4363975
	au_gl_11_f	pc	-9.1	-4.3	0.0	0.242728	0.260836	0.197373	-1948.0898628	-	-1947.4355461
	gl_5_f	pc	-14.1	0.0	0.0	0.242445	0.260699	0.195889	-1948.1020604	-1948.0204126	-1947.4507646
	gl_6_f	pc	-11.5	-6.2	0.0	0.242506	0.260671	0.196796	-1948.1001792	-1948.0172508	-1947.4481515
	au_gl_4_f	pc	-17.0	-6.3	0.0	0.242199	0.260575	0.195439	-1948.0946451	-	-1947.4427271
	gl_9_f	pc	-17.0	-6.3	0.0	0.242199	0.260575	0.195441	-1948.0946452	-	-1947.4427262
	gl_7_f	pc	-5.7	0.0	0.0	0.242675	0.260782	0.197176	-1948.0959426	-	-1947.4429335
	gl_8_f	pc	-12.4	0.0	0.0	0.242528	0.260731	0.196586	-1948.0944872	-	-1947.4421258
	au_gl_1_f	pc	-12.2	0.0	0.0	0.242527	0.260730	0.196590	-1948.0944872	-	-1947.4421239
	gl_11_f	pc	-11.2	0.0	0.0	0.242448	0.260640	0.196494	-1948.0932719	-	-1947.4402619
	gl_10_f	pc	-11.3	0.0	0.0	0.242515	0.260704	0.196785	-1948.0924365	-	-1947.4392335
	gl_2_11_ircr	pc	0.0	0.0	0.0	0.243556	0.262356	0.195015	-1948.1320009	-	-1947.4742342
	gl_2_2_ircf	pc	-10.2	0.0	0.0	0.243264	0.262194	0.193657	-1948.1396417	-	-1947.4814415
	gl_2_4_ircr	pc	-11.4	0.0	0.0	0.242946	0.262049	0.192502	-1948.1386395	-1948.0326705	-1947.4803264
	gl_2_8_ircr	pc	-5.2	0.0	0.0	0.243107	0.262171	0.193111	-1948.1334104	-1948.0271251	-1947.4750527

Chapter 3: Kinetics and mechanism of oxirane-formation by Darzens condensation of ketones: quantification of the electrophilicities of ketones

	g1_2_9_ircr	pc	-14.2	0.0	0.0	0.243351	0.262206	0.194649	-1948.1308226	-	-1947.4726000
	g1_2_10_ircr	pc	-5.2	0.0	0.0	0.243104	0.262171	0.193081	-1948.1334103	-	-1947.4750522
	g1_3_14_f	pc	-14.2	0.0	0.0	0.242444	0.260699	0.195875	-1948.1020604	-1948.0204127	-1947.4507659
	g1_3_15_f	pc	-14.1	0.0	0.0	0.242444	0.260699	0.195879	-1948.1020604	-1948.0204137	-1947.4507642
	g1_3_16_f	pc	-11.5	-6.2	0.0	0.242506	0.260671	0.196795	-1948.1001793	-1948.0172452	-1947.4481510
	g1_3_30_f	pc	-14.6	0.0	0.0	0.242475	0.260665	0.196227	-1948.0965138	-	-1947.4436011
	g1_3_5_f	pc	-17.0	-6.1	0.0	0.242199	0.260575	0.195442	-1948.0946451	-	-1947.4427274
	g1_3_4_f	pc	-21.3	-5.6	0.0	0.242440	0.260719	0.196113	-1948.0945585	-	-1947.4420808
	g1_3_27_f	pc	-26.1	-5.9	0.0	0.242318	0.260512	0.196120	-1948.0935156	-	-1947.4403505
	g1_3_7_f	pc	-20.9	-5.0	0.0	0.242347	0.260648	0.196040	-1948.0929338	-	-1947.4397219
	g1_3_22_f	pc	-11.3	0.0	0.0	0.242516	0.260704	0.196789	-1948.0924369	-	-1947.4392234
5*+2a											
Transition State											
	a5_19	syn	-121.8	-10.0	-7.1	0.254544	0.277250	0.200700	-1813.6738476	-	-1813.0720522
	a5_9	syn	-137.0	-19.7	0.0	0.254972	0.277450	0.201919	-1813.6723682	-	-1813.0707496
	a5_13	syn	-133.8	-12.1	-6.3	0.254635	0.277316	0.201950	-1813.6716301	-	-1813.0679807
	a5_2	syn	-148.4	-15.6	0.0	0.255235	0.277598	0.203190	-1813.6727388	-	-1813.0702073
	a5_1	syn	-148.8	18.4	37.1	0.255238	0.277599	0.203206	-1813.6727389	-	-1813.0702085
	a5_18	syn	-100.0	-8.7	0.0	0.254622	0.277358	0.200684	-1813.6697693	-	-1813.0657760
	a5_7	syn	-148.8	-7.2	0.0	0.254865	0.277447	0.202474	-1813.6710255	-	-1813.0675908
	a5_3	syn	-91.1	-21.4	0.0	0.254717	0.277363	0.202346	-1813.6699098	-	-1813.0660725
	a5_6	anti	-77.3	-15.8	-3.8	0.254049	0.276977	0.199886	-1813.6716535	-	-1813.0679825
	a5_8	anti	-93.8	0.0	0.0	0.254312	0.277094	0.200514	-1813.6721538	-	-1813.0700641
	a5_5	anti	-121.9	-5.1	0.0	0.254587	0.277198	0.202272	-1813.6721001	-	-1813.0690274
	a5_2_2	cy	-363.5	-13.5	-8.6	0.255534	0.278208	0.202112	-1813.7012808	-	-1813.0963204
	a5_2_7	cy	-353.7	-12.2	0.0	0.255738	0.278306	0.203223	-1813.7005246	-	-1813.0954903
	a5_2_1	cy	-372.0	-9.8	0.0	0.256143	0.278393	0.204422	-1813.6971749	-	-1813.0920708
	a5_2_4	cy	-368.2	-1.0	0.0	0.256316	0.278507	0.204939	-1813.6966836	-	-1813.0915437
	a5_2_10	cy	-365.5	-9.0	-4.4	0.255728	0.278176	0.203586	-1813.6952226	-	-1813.0901767
	a5_2_6	cy	-379.1	0.0	0.0	0.256264	0.278382	0.205229	-1813.6906109	-	-1813.0852119
	a5_3_8	rot	-38.7	-11.9	0.0	0.256343	0.278253	0.204540	-1813.6953484	-	-1813.0931299
	a5_3_3	rot	-25.6	-8.9	0.0	0.256544	0.278318	0.206213	-1813.6958896	-	-1813.0941004
	a5_3_2	rot	-36.1	-13.9	0.0	0.256810	0.278445	0.206689	-1813.6957847	-	-1813.0937374
	a5_3_9	rot	-26.6	-14.7	-13.0	0.256489	0.278306	0.205420	-1813.6937721	-	-1813.0913160
Reactant (Complex)											
	a5_8_r	rc	-3.6	0.0	0.0	0.253961	0.278124	0.195112	-1813.6798186	-	-1813.0780725
	a5_19_r	rc	0.0	0.0	0.0	0.254046	0.277996	0.197166	-1813.6760964	-	-1813.0755793
	a5_9_r	rc	-18.9	0.0	0.0	0.254058	0.277951	0.198107	-1813.6764443	-	-1813.0762449
	a5_6_r	rc	-19.8	0.0	0.0	0.253887	0.277835	0.196905	-1813.6749823	-	-1813.0728262
	a5_2_r	rc	-14.4	-11.2	0.0	0.254373	0.278174	0.198889	-1813.6762343	-	-

Chapter 3: Kinetics and mechanism of oxirane-formation by Darzens condensation of ketones: quantification of the electrophilicities of ketones

Product (Complex)	a5_13_r	rc	-11.9	-6.8	0.0	0.254794	0.278603	0.199174	-1813.6763396	-	-
	a5_3_r	rc	-11.9	0.0	0.0	0.253761	0.277998	0.196513	-1813.6733194	-	-
	a5_1_r	rc	-11.6	-6.8	0.0	0.254498	0.278220	0.199526	-1813.6762036	-	-
	a5_7_r	rc	-5.9	0.0	0.0	0.254002	0.278035	0.197983	-1813.6745498	-	-
	a5_5_r	rc	-3.1	0.0	0.0	0.254319	0.278081	0.199712	-1813.6757938	-	-1813.0723282
	a5_18_r	rc	-6.8	0.0	0.0	0.254125	0.278083	0.197264	-1813.6719743	-	-
	a5_2_2_ircf_opt	rc	-11.0	0.0	0.0	0.256816	0.279437	0.204322	-1813.7115334	-	-1813.1095945
	a5_2_7_ircf_opt	rc	-10.3	0.0	0.0	0.256875	0.279481	0.204767	-1813.7107414	-	-1813.1085733
	a5_2_1_ircf_opt	rc	-10.3	0.0	0.0	0.257268	0.279623	0.205606	-1813.7103114	-	-1813.1086528
	a5_2_4_ircf_opt	rc	-5.2	0.0	0.0	0.257344	0.279691	0.205779	-1813.7095448	-	-1813.1077219
	a5_2_10_ircf_opt	rc	-16.1	-2.5	0.0	0.256875	0.279361	0.205069	-1813.7059953	-	-1813.1038691
	a5_2_6_ircf_opt	rc	-12.1	-4.4	0.0	0.257655	0.279724	0.206930	-1813.7047657	-	-1813.1028967
	a5_3_8_r	rc	-15.4	-9.6	0.0	0.256337	0.279074	0.202664	-1813.7007741	-	-1813.0981714
	a5_3_2_r	rc	0.0	0.0	0.0	0.256929	0.279302	0.205940	-1813.6985736	-	-1813.0975444
	a5_3_3_r	rc	-1.8	0.0	0.0	0.257055	0.279360	0.205844	-1813.6973437	-	-1813.0946599
	a5_3_9_r	rc	-11.5	-8.7	0.0	0.256661	0.279245	0.204135	-1813.6949839	-	-1813.0927843
	a5_19_f	pc	-13.8	0.0	0.0	0.256301	0.279081	0.202794	-1813.7016049	-	-1813.0997526
	a5_18_f	pc	-12.7	0.0	0.0	0.256435	0.279252	0.202869	-1813.6983809	-	-1813.0957734
	a5_1_f	pc	-12.8	-3.3	0.0	0.256819	0.279288	0.205172	-1813.6985720	-	-1813.0974378
	a5_2_f	pc	-12.7	-3.5	0.0	0.256825	0.279289	0.205207	-1813.6985723	-	-1813.0974377
	a5_7_f	pc	-12.6	-4.5	0.0	0.256860	0.279336	0.204681	-1813.6969590	-	-1813.0948439
	a5_3_f	pc	-2.4	0.0	0.0	0.257057	0.279360	0.205861	-1813.6973431	-	-1813.0946575
	a5_13_f	pc	-3.1	0.0	0.0	0.257057	0.279422	0.205786	-1813.6970069	-	-1813.0948672
	a5_9_f	pc	0.0	0.0	0.0	0.256912	0.279321	0.205155	-1813.6957808	-	-1813.0940475
	a5_5_f	pc	-9.9	0.0	0.0	0.256879	0.279482	0.204792	-1813.7107415	-	-1813.1085722
	a5_8_f	pc	-5.2	0.0	0.0	0.256604	0.279336	0.203606	-1813.7060998	-	-1813.1034237
	a5_6_f	pc	-11.5	0.0	0.0	0.256487	0.279195	0.203794	-1813.7000584	-	-1813.0980499
	a5_2_2_ircr_opt	pc	-9.6	0.0	0.0	0.257791	0.281241	0.199916	-1813.7691651	-	-1813.1608755
	a5_2_7_ircr_opt	pc	-10.6	-6.2	0.0	0.257837	0.281248	0.200220	-1813.7683806	-	-1813.1599999
	a5_2_6_ircr_opt	pc	-4.8	0.0	0.0	0.258664	0.281439	0.204586	-1813.7562083	-	-1813.1477369
	a5_2_4_ircr_opt	pc	-8.7	0.0	0.0	0.258313	0.281341	0.203607	-1813.7594185	-	-1813.1509547
	a5_2_1_ircr_opt	pc	-3.7	0.0	0.0	0.258243	0.281309	0.202928	-1813.7596788	-	-1813.1511066
	a5_2_10_ircr_opt	pc	-8.4	0.0	0.0	0.258206	0.281314	0.202166	-1813.7643927	-	-1813.1562500
	a5_3_9_f	pc	-9.4	0.0	0.0	0.256490	0.279318	0.203141	-1813.7050006	-	-1813.1017753
	a5_3_3_f	pc	-4.2	0.0	0.0	0.256925	0.279480	0.205008	-1813.7091556	-	-1813.1064336
	a5_3_8_f	pc	-5.1	0.0	0.0	0.256603	0.279336	0.203604	-1813.7060998	-	-1813.1034229
	a5_3_2_f	pc	-21.7	-11.2	0.0	0.256530	0.279318	0.203342	-1813.7071414	-	-1813.1047419

Chapter 3: Kinetics and mechanism of oxirane-formation by Darzens condensation of ketones: quantification of the electrophilicities of ketones

Table S24. QM data used for plotting the conformational distribution of halohydrins in neutral (n) and anionic (a) form calculated at B3LYP-D3/6-31+G(d,p)/PCM(UA0,DMSO) level of theory.

System (Type)	FileName	ΔE_{tot}	B3LYP-D3/6-31G+(d,p)/PCM(DMSO,UA0)						Dihedral (OCCCl)
			Low Frequencies			corr. ZPE	corr. ΔH	corr. ΔG	
Neutral									
4ca									
anti	n_ca4_180_3	-1589.7313124	-9.0	-7.0	0.0	0.283995	0.301917	0.238707	192.9
anti	n_ca4_180_1	-1589.7271995	-6.1	0.0	0.0	0.284059	0.301961	0.239417	191.7
anti	n_ca4_180_2	-1589.7244023	0.0	0.0	0.0	0.283561	0.301625	0.238718	171.8
anti	n_ca4_180_4	-1589.7208033	-22.8	0.0	0.0	0.283508	0.301603	0.238280	192.8
syn	n_ca4_270_6	-1589.7299300	-8.1	-7.7	0.0	0.284085	0.301951	0.239187	301.4
syn	n_ca4_60_6	-1589.7281632	-13.7	-9.7	-4.2	0.283934	0.301882	0.237460	65.3
syn	n_ca4_60_4	-1589.7299395	0.0	0.0	0.0	0.284313	0.302065	0.239473	54.2
syn	n_ca4_270_1	-1589.7290678	-5.0	0.0	0.0	0.284176	0.301989	0.239622	293.6
syn	n_ca4_60_1	-1589.7289680	0.0	0.0	0.0	0.284245	0.301981	0.239603	61.8
syn	n_ca4_60_3	-1589.7289524	-16.4	0.0	0.0	0.284614	0.302229	0.240552	56.7
syn	n_ca4_270_4	-1589.7277079	-10.4	-5.9	0.0	0.284221	0.302068	0.239484	293.1
syn	n_ca4_60_5	-1589.7257953	-28.5	-22.1	-7.8	0.283994	0.301856	0.239060	57.0
syn	n_ca4_270_7	-1589.7225385	-11.3	0.0	0.0	0.283988	0.301896	0.238787	289.1
Anionic									
4ca									
anti	a_ca4_180_1	-1589.2269186	-14.3	0.0	0.0	0.269671	0.287521	0.224553	173.9
anti	a_ca4_180_3	-1589.2252304	-17.0	0.0	0.0	0.269646	0.287507	0.224400	175.0
anti	a_ca4_180_2	-1589.2250780	-4.2	0.0	0.0	0.269824	0.287509	0.225473	173.4
anti	a_ca4_180_4	-1589.2221429	-6.8	0.0	0.0	0.269791	0.287551	0.225010	173.7
syn	a_ca4_270_6	-1589.2260760	-17.6	-10.1	0.0	0.269765	0.287587	0.223844	300.6
syn	a_ca4_270_2	-1589.2260802	-8.4	0.0	0.0	0.269803	0.287598	0.224330	301.2
syn	a_ca4_270_1	-1589.2254086	0.0	0.0	0.0	0.270004	0.287678	0.225599	294.5
syn	a_ca4_270_5	-1589.2239894	-12.9	0.0	0.0	0.270017	0.287772	0.224989	293.1
syn	a_ca4_60_2	-1589.2234400	-16.4	-12.1	0.0	0.270047	0.287615	0.225316	70.1
syn	a_ca4_60_6	-1589.2231660	0.0	0.0	0.0	0.270271	0.287803	0.225465	70.7
syn	a_ca4_270_7	-1589.2203880	-22.4	-3.0	0.0	0.269792	0.287573	0.224770	288.5
syn	a_ca4_60_3	-1589.2200239	-13.0	0.0	0.0	0.270185	0.287686	0.226093	54.8
Neutral									
4fb									
anti	n_fb4_180_3	-1717.8682863	-6.9	0.0	0.0	0.258389	0.277919	0.210429	193.3
anti	n_fb4_180_4	-1717.8682863	-6.5	0.0	0.0	0.258396	0.277920	0.210501	193.3
anti	n_fb4_180_6	-1717.8668600	-6.9	-1.7	0.0	0.258649	0.278044	0.211312	191.7
anti	n_fb4_180_7	-1717.8658320	-4.6	0.0	0.0	0.258444	0.277878	0.211348	164.3
anti	n_fb4_180_1	-1717.8653196	-35.3	0.0	0.0	0.258687	0.277147	0.213487	175.0
anti	n_fb4_180_12	-1717.8622310	-12.1	-3.7	0.0	0.258518	0.277970	0.210840	198.9
anti	n_fb4_180_5	-1717.8606375	-20.0	0.0	0.0	0.257793	0.277501	0.210314	171.7
anti	n_fb4_180_2	-1717.8584524	-11.9	-4.7	0.0	0.258002	0.277669	0.210255	190.7
anti	n_fb4_180_14	-1717.8570101	-22.8	0.0	0.0	0.257855	0.277593	0.209079	205.2
anti	n_fb4_180_8	-1717.8575790	-6.3	0.0	0.0	0.258090	0.277802	0.209690	184.8
anti	n_fb4_180_11	-1717.8585174	-4.4	0.0	0.0	0.258559	0.277977	0.211108	174.5
anti	n_fb4_180_10	-1717.8568677	-5.6	0.0	0.0	0.258136	0.277827	0.209987	173.7
anti	n_fb4_180_13	-1717.8560433	0.0	0.0	0.0	0.258102	0.277649	0.210898	168.3
syn	n_fb4_60_4	-1717.8679211	-5.9	0.0	0.0	0.258347	0.277830	0.211008	67.4
syn	n_fb4_270_8	-1717.8658931	-6.8	-4.7	0.0	0.258252	0.277806	0.210415	301.5
syn	n_fb4_60_5	-1717.8641973	-14.9	-4.8	0.0	0.257703	0.277509	0.209285	69.1
syn	n_fb4_60_2	-1717.8656542	-9.1	0.0	0.0	0.258445	0.277835	0.210780	65.8
syn	n_fb4_270_2	-1717.8672016	-31.1	-6.5	-4.6	0.258241	0.276910	0.212396	296.9
syn	n_fb4_270_3	-1717.8655939	-8.3	0.0	0.0	0.258501	0.277960	0.211029	291.9
syn	n_fb4_270_1	-1717.8655939	-8.2	0.0	0.0	0.258501	0.277960	0.211033	291.9
syn	n_fb4_60_3	-1717.8640027	-6.3	0.0	0.0	0.258177	0.277704	0.210373	71.4
syn	n_fb4_270_7	-1717.8643559	-13.5	-2.8	0.0	0.258346	0.277839	0.210822	297.0
syn	n_fb4_270_6	-1717.8644454	-13.6	-6.9	0.0	0.258525	0.278007	0.210922	292.3
syn	n_fb4_270_10	-1717.8629879	-10.7	0.0	0.0	0.258445	0.277920	0.211086	297.0
syn	n_fb4_270_9	-1717.8556946	-4.5	0.0	0.0	0.258217	0.277780	0.210803	297.7
Anionic									
4fb									
anti	a_fb4_180_1	-1717.3724964	0.0	0.0	0.0	0.244487	0.263847	0.197101	174.1
anti	a_fb4_180_7	-1717.3691113	-25.1	-10.7	-4.2	0.244315	0.263726	0.196805	173.0
anti	a_fb4_180_4	-1717.3690331	-7.7	0.0	0.0	0.244321	0.263718	0.196817	175.4
anti	a_fb4_180_9	-1717.3690327	-7.7	0.0	0.0	0.244319	0.263717	0.196818	175.4
anti	a_fb4_180_12	-1717.3670961	-12.3	-6.9	0.0	0.244398	0.263757	0.197174	171.6
anti	a_fb4_180_10	-1717.3629018	-26.0	-7.1	-2.4	0.243852	0.263547	0.194978	177.3
anti	a_fb4_180_8	-1717.3630946	0.0	0.0	0.0	0.244107	0.263630	0.196520	170.2
anti	a_fb4_180_13	-1717.3627076	-16.8	-12.4	-6.1	0.244208	0.263662	0.196149	172.1
anti	a_fb4_180_14	-1717.3612043	-12.1	-3.9	0.0	0.244176	0.263661	0.195854	187.6
syn	a_fb4_270_5	-1717.3694789	0.0	0.0	0.0	0.244464	0.263806	0.197000	296.7
syn	a_fb4_60_5	-1717.3686518	-14.2	0.0	0.0	0.244314	0.263596	0.197127	67.1

Chapter 3: Kinetics and mechanism of oxirane-formation by Darzens condensation of ketones: quantification of the electrophilicities of ketones

syn	a_fb4_270_7	-1717.3679416	-15.5	0.0	0.0	0.244513	0.263832	0.197353	293.6
syn	a_fb4_270_10	-1717.3665233	-15.7	-8.8	0.0	0.244554	0.263941	0.196619	293.7
syn	a_fb4_60_2	-1717.3664246	-17.4	-8.7	0.0	0.244414	0.263606	0.197181	69.6
syn	a_fb4_270_9	-1717.3579979	-16.3	0.0	0.0	0.244174	0.263616	0.196940	298.7
Neutral 4da									
anti	n_da4_180_12	-1629.0428643	-18.7	-3.9	0.0	0.312808	0.331852	0.266292	194.1
anti	n_da4_180_13	-1629.0415723	-11.2	-4.7	0.0	0.312713	0.331961	0.265754	193.5
anti	n_da4_180_16	-1629.0393417	-7.5	-5.4	0.0	0.312891	0.331997	0.265980	187.1
anti	n_da4_180_17	-1629.0384769	-33.2	-8.8	-2.3	0.312532	0.331725	0.265259	170.8
anti	n_da4_180_6	-1629.0388893	-8.2	-6.9	0.0	0.312804	0.331871	0.266410	171.0
anti	n_da4_180_3	-1629.0382576	0.0	0.0	0.0	0.312751	0.331983	0.265874	168.7
anti	n_da4_180_4	-1629.0368569	-14.8	0.0	0.0	0.311815	0.331294	0.264680	170.7
anti	n_da4_180_1	-1629.0373038	0.0	0.0	0.0	0.312109	0.331481	0.265454	188.4
anti	n_da4_180_7	-1629.0362283	-17.3	-8.3	0.0	0.312017	0.331372	0.265262	167.7
anti	n_da4_180_5	-1629.0359942	-15.1	-4.4	0.0	0.312759	0.332038	0.266369	191.5
anti	n_da4_180_10	-1629.0337314	-22.2	-9.5	0.0	0.311825	0.331542	0.264157	174.8
anti	n_da4_180_9	-1629.0347976	-15.4	0.0	0.0	0.312153	0.331494	0.265297	174.4
anti	n_da4_180_24	-1629.0364194	-11.5	-4.9	0.0	0.313249	0.332217	0.267177	195.4
anti	n_da4_180_8	-1629.0344906	-12.1	0.0	0.0	0.312198	0.331599	0.265612	167.5
anti	n_da4_180_19	-1629.0312172	-11.6	-8.7	0.0	0.312198	0.331798	0.264178	187.1
anti	n_da4_180_23	-1629.0305343	-32.5	-21.3	-7.0	0.312310	0.331753	0.263523	171.3
anti	n_da4_180_11	-1629.0326640	-22.3	0.0	0.0	0.312309	0.331762	0.265669	174.5
anti	n_da4_180_14	-1629.0312467	-6.0	0.0	0.0	0.312337	0.331792	0.264948	174.5
anti	n_da4_180_20	-1629.0316610	-6.3	0.0	0.0	0.312404	0.331739	0.266069	199.2
anti	n_da4_180_15	-1629.0314489	-9.9	-8.5	0.0	0.312655	0.331882	0.266386	190.0
anti	n_da4_180_22	-1629.0294484	-9.9	-2.3	0.0	0.312047	0.331471	0.265092	163.4
anti	n_da4_180_21	-1629.0298869	-3.0	0.0	0.0	0.312562	0.331799	0.265825	169.9
syn	n_da4_270_34	-1629.0412874	-19.0	0.0	0.0	0.312715	0.331813	0.266160	293.1
syn	n_da4_270_3	-1629.0412874	-18.3	0.0	0.0	0.312737	0.331819	0.266322	293.1
syn	n_da4_60_14	-1629.0410845	-7.5	-3.3	0.0	0.312829	0.331865	0.266364	51.3
syn	n_da4_270_6	-1629.0410488	-15.7	-6.1	-3.6	0.312804	0.331911	0.266371	308.3
syn	n_da4_270_8	-1629.0396162	-14.2	0.0	0.0	0.312594	0.331910	0.265205	299.8
syn	n_da4_60_15	-1629.0405685	-9.2	0.0	0.0	0.312881	0.331957	0.266246	55.7
syn	n_da4_60_30	-1629.0389557	-14.3	-3.5	0.0	0.312366	0.331615	0.264669	79.1
syn	n_da4_270_18	-1629.0387728	-5.4	0.0	0.0	0.312671	0.331889	0.265182	293.2
syn	n_da4_270_31	-1629.0387728	-5.4	0.0	0.0	0.312671	0.331889	0.265182	293.2
syn	n_da4_60_3	-1629.0397372	-8.4	-5.3	0.0	0.312700	0.331774	0.266183	61.8
syn	n_da4_60_24	-1629.0390870	0.0	0.0	0.0	0.312639	0.331769	0.265660	54.2
syn	n_da4_60_1	-1629.0401360	-11.6	-7.8	0.0	0.313173	0.332133	0.266917	63.6
syn	n_da4_270_27	-1629.0389982	-8.1	-4.5	0.0	0.312677	0.331908	0.265810	303.7
syn	n_da4_270_26	-1629.0390599	-4.7	0.0	0.0	0.312736	0.331964	0.265896	303.2
syn	n_da4_60_17	-1629.0396670	-7.6	0.0	0.0	0.313059	0.332114	0.266518	65.0
syn	n_da4_60_13	-1629.0398064	-7.9	0.0	0.0	0.312894	0.331934	0.266658	55.6
syn	n_da4_60_6	-1629.0396606	-6.9	0.0	0.0	0.312836	0.331850	0.266522	64.4
syn	n_da4_270_35	-1629.0398136	-7.5	0.0	0.0	0.312845	0.331900	0.266721	296.7
syn	n_da4_60_8	-1629.0404720	-6.4	0.0	0.0	0.313269	0.332200	0.267534	71.2
syn	n_da4_60_16	-1629.0398234	-12.8	-3.5	0.0	0.313136	0.332097	0.266900	53.7
syn	n_da4_60_25	-1629.0400162	0.0	0.0	0.0	0.313273	0.332239	0.267228	73.3
syn	n_da4_60_5	-1629.0379774	-18.4	-6.9	0.0	0.312738	0.331932	0.265489	63.3
syn	n_da4_270_1	-1629.0393847	-7.0	0.0	0.0	0.312943	0.331906	0.267032	299.7
syn	n_da4_60_18	-1629.0385970	-9.8	-2.1	0.0	0.312858	0.332004	0.266257	53.2
syn	n_da4_270_7	-1629.0391860	-7.1	0.0	0.0	0.312888	0.332020	0.267036	292.6
syn	n_da4_270_5	-1629.0387695	-11.2	-6.5	0.0	0.312955	0.332078	0.266653	296.5
syn	n_da4_270_4	-1629.0381022	-15.3	0.0	0.0	0.312440	0.331676	0.266128	293.1
syn	n_da4_270_29	-1629.0381022	-15.3	0.0	0.0	0.312440	0.331676	0.266130	293.1
syn	n_da4_270_9	-1629.0376552	-10.3	-3.0	0.0	0.312849	0.332039	0.265763	299.0
syn	n_da4_60_20	-1629.0379270	-13.9	-9.7	0.0	0.313043	0.332199	0.266073	58.9
syn	n_da4_270_14	-1629.0389006	-7.5	-1.6	0.0	0.312987	0.331978	0.267102	292.1
syn	n_da4_270_19	-1629.0389006	-7.5	-1.8	0.0	0.312987	0.331978	0.267103	292.1
syn	n_da4_60_10	-1629.0383719	-17.5	-5.9	0.0	0.312877	0.332019	0.266662	69.4
syn	n_da4_60_4	-1629.0376116	-7.8	0.0	0.0	0.312618	0.331792	0.266009	75.2
syn	n_da4_60_12	-1629.0401680	-7.4	0.0	0.0	0.313695	0.332470	0.268581	58.4
syn	n_da4_270_13	-1629.0379208	-0.9	0.0	0.0	0.312969	0.332118	0.266574	293.9
syn	n_da4_270_15	-1629.0379208	-1.1	0.0	0.0	0.312971	0.332119	0.266577	293.9
syn	n_da4_60_27	-1629.0365989	0.0	0.0	0.0	0.312454	0.331714	0.265259	56.7
syn	n_da4_60_2	-1629.0374936	-6.9	0.0	0.0	0.312453	0.331629	0.266180	61.5
syn	n_da4_270_16	-1629.0385810	0.0	0.0	0.0	0.313176	0.332164	0.267304	298.0
syn	n_da4_270_11	-1629.0386509	-11.9	-8.0	0.0	0.313133	0.332084	0.267448	294.9
syn	n_da4_270_21	-1629.0381324	-6.6	0.0	0.0	0.312923	0.331980	0.267049	303.5
syn	n_da4_60_29	-1629.0370834	-8.9	0.0	0.0	0.312857	0.332055	0.266019	62.3
syn	n_da4_270_23	-1629.0374577	0.0	0.0	0.0	0.312995	0.332078	0.266511	292.5
syn	n_da4_60_23	-1629.0374974	-12.5	0.0	0.0	0.312945	0.332000	0.266740	53.3
syn	n_da4_60_26	-1629.0385528	-16.8	-9.9	0.0	0.313502	0.332342	0.267996	61.0
syn	n_da4_270_25	-1629.0370033	-7.7	0.0	0.0	0.312936	0.332069	0.266489	304.0

Chapter 3: Kinetics and mechanism of oxirane-formation by Darzens condensation of ketones: quantification of the electrophilicities of ketones

syn	n_da4_270_17	-1629.0368432	0.0	0.0	0.0	0.312861	0.332063	0.266344	296.4
syn	n_da4_270_28	-1629.0368542	-13.4	0.0	0.0	0.313153	0.332234	0.266494	297.0
syn	n_da4_60_9	-1629.0357255	-9.4	0.0	0.0	0.312451	0.331784	0.265395	61.2
syn	n_da4_60_22	-1629.0373456	-6.0	0.0	0.0	0.312923	0.331951	0.267031	57.7
syn	n_da4_60_19	-1629.0377271	-11.4	-7.1	0.0	0.313280	0.332229	0.267522	56.9
syn	n_da4_60_21	-1629.0367379	-7.8	-3.7	0.0	0.313151	0.332178	0.267303	61.5
syn	n_da4_270_36	-1629.0367147	-11.2	-3.7	0.0	0.313074	0.332038	0.267519	298.8
syn	n_da4_60_28	-1629.0349324	-16.5	-13.5	0.0	0.312775	0.331985	0.266459	58.7
syn	n_da4_270_20	-1629.0351914	-7.0	0.0	0.0	0.312727	0.331867	0.266968	294.9
syn	n_da4_60_32	-1629.0348887	-6.6	0.0	0.0	0.312730	0.331897	0.266737	55.8
syn	n_da4_60_31	-1629.0343830	-13.1	0.0	0.0	0.312770	0.331961	0.266425	58.2
syn	n_da4_270_24	-1629.0341260	0.0	0.0	0.0	0.312711	0.331860	0.266288	313.4
syn	n_da4_60_11	-1629.0339815	0.0	0.0	0.0	0.312891	0.332033	0.266403	64.4
syn	n_da4_270_22	-1629.0326996	0.0	0.0	0.0	0.312321	0.331825	0.265412	298.5
Anionic									
4da									
anti	a_da4_180_6	-1628.5374250	-18.5	-6.7	0.0	0.298228	0.317331	0.251560	169.8
anti	a_da4_180_3	-1628.5369289	-15.7	-7.8	0.0	0.298342	0.317516	0.251246	170.1
anti	a_da4_180_1	-1628.5371650	-17.4	0.0	0.0	0.298462	0.317514	0.251799	176.5
anti	a_da4_180_2	-1628.5367301	-6.6	0.0	0.0	0.298329	0.317498	0.251377	178.5
anti	a_da4_180_12	-1628.5350732	-12.0	-6.9	0.0	0.298126	0.317274	0.250849	191.7
anti	a_da4_180_7	-1628.5356572	-13.9	-5.3	0.0	0.298280	0.317330	0.251594	170.4
anti	a_da4_180_17	-1628.5357991	-5.0	0.0	0.0	0.298372	0.317432	0.251810	170.4
anti	a_da4_180_5	-1628.5348087	-3.3	0.0	0.0	0.298320	0.317583	0.251026	174.4
anti	a_da4_180_8	-1628.5353845	-15.4	0.0	0.0	0.298436	0.317468	0.252085	170.3
anti	a_da4_180_10	-1628.5344489	-16.3	-9.8	0.0	0.298276	0.317449	0.251534	176.2
anti	a_da4_180_18	-1628.5330361	-16.4	-4.6	0.0	0.298042	0.317386	0.250532	176.7
anti	a_da4_180_9	-1628.5348543	0.0	0.0	0.0	0.298547	0.317522	0.252460	176.4
anti	a_da4_180_11	-1628.5330721	-6.7	0.0	0.0	0.298280	0.317392	0.252043	175.9
anti	a_da4_180_14	-1628.5315352	-20.0	0.0	0.0	0.298388	0.317606	0.251081	171.9
anti	a_da4_180_19	-1628.5312613	-17.3	-10.4	0.0	0.298632	0.317790	0.250823	174.3
anti	a_da4_180_20	-1628.5312449	-19.0	-12.8	-1.8	0.298289	0.317506	0.251282	192.5
anti	a_da4_180_22	-1628.5312263	-12.6	0.0	0.0	0.298328	0.317436	0.251919	164.1
anti	a_da4_180_15	-1628.5311003	-5.3	0.0	0.0	0.298962	0.317879	0.252478	179.4
anti	a_da4_180_23	-1628.5303212	-10.6	0.0	0.0	0.298653	0.317674	0.251912	173.5
anti	a_da4_180_21	-1628.5310343	-8.0	0.0	0.0	0.298985	0.317844	0.253119	169.0
anti	a_da4_180_24	-1628.5292261	-5.5	0.0	0.0	0.299099	0.317937	0.253202	180.5
syn	a_da4_270_29	-1628.5377490	-12.1	0.0	0.0	0.298653	0.317597	0.252214	294.2
syn	a_da4_270_18	-1628.5352200	-23.1	-9.3	0.0	0.298339	0.317464	0.250106	295.1
syn	a_da4_270_12	-1628.5365012	-5.7	0.0	0.0	0.298390	0.317525	0.251448	298.8
syn	a_da4_270_6	-1628.5369323	-10.2	0.0	0.0	0.298568	0.317550	0.252014	310.9
syn	a_da4_270_26	-1628.5350546	-32.0	-12.0	0.0	0.298209	0.317470	0.250268	303.2
syn	a_da4_270_27	-1628.5348730	-24.8	-3.2	0.0	0.298088	0.317382	0.250508	305.3
syn	a_da4_270_7	-1628.5360380	-11.9	0.0	0.0	0.298615	0.317621	0.252718	294.4
syn	a_da4_270_5	-1628.5352040	-10.3	0.0	0.0	0.298543	0.317597	0.252432	297.7
syn	a_da4_270_14	-1628.5353508	0.0	0.0	0.0	0.298720	0.317560	0.252978	294.1
syn	a_da4_270_13	-1628.5347077	-5.6	0.0	0.0	0.298879	0.317837	0.252676	295.3
syn	a_da4_270_16	-1628.5342361	0.0	0.0	0.0	0.298595	0.317643	0.252285	298.7
syn	a_da4_270_21	-1628.5340653	-4.0	0.0	0.0	0.298444	0.317481	0.252272	305.4
syn	a_da4_270_23	-1628.5335149	-9.2	-5.8	0.0	0.298529	0.317540	0.251971	293.8
syn	a_da4_270_9	-1628.5337848	-11.3	0.0	0.0	0.298597	0.317677	0.252282	297.2
syn	a_da4_270_20	-1628.5347294	-18.9	0.0	0.0	0.298957	0.317793	0.253382	295.2
syn	a_da4_60_27	-1628.5330382	-10.0	0.0	0.0	0.298524	0.317454	0.251807	49.6
syn	a_da4_270_17	-1628.5331357	-5.5	0.0	0.0	0.298606	0.317701	0.252041	297.8
syn	a_da4_60_3	-1628.5335450	-14.1	0.0	0.0	0.298711	0.317538	0.252629	65.2
syn	a_da4_270_25	-1628.5328590	-5.7	0.0	0.0	0.298492	0.317615	0.251986	300.3
syn	a_da4_60_14	-1628.5330436	0.0	0.0	0.0	0.298738	0.317564	0.252271	54.4
syn	a_da4_270_28	-1628.5325106	0.0	0.0	0.0	0.298562	0.317680	0.251782	299.9
syn	a_da4_270_24	-1628.5325085	-15.6	0.0	0.0	0.298362	0.317419	0.251850	299.9
syn	a_da4_60_17	-1628.5334545	-10.0	0.0	0.0	0.299265	0.318060	0.252901	62.5
syn	a_da4_60_25	-1628.5340438	-7.0	0.0	0.0	0.299332	0.318035	0.253570	70.2
syn	a_da4_60_5	-1628.5333182	-17.6	-14.0	0.0	0.298934	0.317762	0.252892	64.6
syn	a_da4_60_30	-1628.5327024	0.0	0.0	0.0	0.298933	0.317719	0.252689	64.2
syn	a_da4_60_4	-1628.5319144	0.0	0.0	0.0	0.298666	0.317517	0.252068	57.7
syn	a_da4_60_7	-1628.5311286	-11.6	0.0	0.0	0.298736	0.317708	0.251970	62.7
syn	a_da4_60_2	-1628.5322063	-17.4	-10.0	0.0	0.298840	0.317622	0.253225	51.3
syn	a_da4_60_18	-1628.5310077	-6.5	0.0	0.0	0.298791	0.317730	0.252215	59.5
syn	a_da4_60_23	-1628.5313871	-7.6	0.0	0.0	0.298996	0.317757	0.253263	49.0
syn	a_da4_60_11	-1628.5301454	-16.7	-6.0	0.0	0.299029	0.317819	0.252919	66.8
syn	a_da4_60_13	-1628.5312491	0.0	0.0	0.0	0.299133	0.317783	0.254038	54.2
syn	a_da4_60_12	-1628.5298756	0.0	0.0	0.0	0.299435	0.318081	0.254374	57.6
syn	a_da4_60_28	-1628.5286547	-16.2	-2.9	0.0	0.298960	0.317826	0.253197	55.2
syn	a_da4_60_19	-1628.5276732	-19.6	0.0	0.0	0.298888	0.317780	0.252939	53.6
syn	a_da4_60_26	-1628.5284983	-14.2	0.0	0.0	0.299451	0.318052	0.254610	59.6

8.3 Correlations

Table S25. Methyl anion affinities ($-\Delta G$, in kJ/mol) calculated at different levels of theory for electrophiles as listed in Figure S2.

SI	Mark er	E	Gas Phase Optimized MAA(ΔG_{gas}) ^a B3LYP		Single Point Implicit Solvation Corrected MAA ($\Delta G_{\text{sol-sp}}$) ^b B3LYP		Implicit Solvation Optimized MAA ($\Delta G_{\text{sol-opt}}$) ^c B3LYP	
			6-31G (d,p) ^d		6-31G (d,p) ^d		6-31G (d,p) ^e	
				6-311++G (3df,2pd) ^d		6-311++G (3df,2pd) ^d		6-311++G (3df,2pd) ^e
1	1a	-17.5	191.0	131.6	67.5	8.0	69.4	5.7
2	1b	-21.0	180.5	114.2	49.0	-14.6	48.9	-17.9
3	1c	-19.9	201.3	126.7	62.3	-11.7	62.9	-15.0
4	1d	-22.1	194.3	116.3	50.4	-26.8	51.6	-29.3
5	1e	-18.4	208.6	136.2	69.5	-2.9	71.0	-4.7
6	1f	-17.9	219.7	147.3	73.8	1.4	74.6	-1.4
7	1g	-16.9	236.4	158.3	82.2	4.1	82.4	0.6
8	1h	-18.2	213.5	138.5	69.7	-5.3	69.5	-8.4
9	1i	-22.3	180.6	114.3	48.5	-16.4	51.5	-18.0
10	1j	-15.6	222.9	144.4	70.1	5.9	72.0	-1.0
11	1m*	-12.9	221.9	155.2	94.5	27.8	93.6	23.0
12	1o*	-15.4	212.7	143.7	82.2	13.2	78.6	6.0
Micheel Acceptors (compound labelling refers to the labels used in ref S9)								
13	17a	-19.49	334.9	246.9	181.7	93.1	187.1	95.4
14	17b	-17.79	309.3	223.1	160.4	74.2	164.4	75.7
15	17c	-15.71	343.1	264.1	211.5	132.4	214.1	130.0
16	17d	-14.07	341.7	260.8	194.7	113.9	196.5	111.2
17	17e	-11.31	382.2	301.9	230.0	149.8	230.6	145.7
18	17f	-7.50	454.1	355.3	273.6	174.8	268.3	165.2
19	17g	-20.55	382.9	284.5	204.8	104.8	205.3	98.9
20	17h	-19.36	349.8	266.3	159.8	75.2	160.9	73.3
21	17i	-17.33	370.4	281.9	175.2	86.8	180.0	88.1
22	17j	-13.30	379.9	290.2	231.0	141.3	232.3	138.9
23	17k	-12.93	440.2	344.3	251.7	155.9	255.7	155.7
24	17l	-12.76	402.7	311.2	226.8	135.3	231.1	135.2
25	17m	-11.32	404.7	318.9	232.8	147.1	233.0	142.6
26	17n	-10.80	400.8	311.1	251.5	161.9	255.8	162.2
27	17o	-10.28	422.0	330.7	245.9	154.4	247.2	151.1
28	17p	-10.11	416.3	331.9	245.1	160.7	245.1	156.0
29	17q	-9.42	413.7	325.4	265.7	177.4	270.9	178.5
30	17r	-9.15	434.8	344.7	259.7	169.6	261.6	166.1
31	17s	-17.90	397.3	295.6	221.9	120.4	222.3	116.5
32	17t	-17.29	398.5	297.7	224.0	123.2	224.3	119.3
33	17u	-16.36	374.1	284.6	220.4	130.7	217.8	123.9
34	17v	-16.11	413.2	312.1	238.2	137.4	241.9	137.5
35	17w	-15.83	415.9	314.8	242.4	141.3	241.9	136.5
36	17x	-13.39	427.9	329.6	245.6	147.3	249.8	146.9
37	17y	-12.18	442.8	344.2	261.5	163.6	262.0	159.4
38	17z	-11.87	451.9	354.2	272.0	174.6	272.1	170.0
39	1a	-18.84	287.3	205.5	162.5	80.7	163.7	80.2
40	1b	-19.07	287.8	203.4	159.7	75.1	167.6	79.4
41	1c	-20.22	293.4	205.7	159.2	71.6	158.0	66.2
42	1d	-23.54	266.1	187.1	138.6	59.6	138.7	55.3
43	1e	-18.36	333.2	246.0	184.0	96.8	184.5	91.6
44	1f	-19.05	279.4	205.1	183.8	109.4	185.4	106.3
45	1g	-16.76	293.3	222.8	176.4	104.2	178.3	102.4
46	1h	-15.25	331.4	251.9	196.2	116.7	197.9	113.6
47	1i	-22.77	280.0	189.9	142.0	51.9	144.5	50.3
48	1j	-12.09	387.4	295.9	251.1	160.5	251.1	156.5
49	2a	-23.59	271.7	187.1	134.4	49.8	133.5	45.2
50	2b	-24.52	274.7	186.9	123.7	36.1	131.4	43.7
51	2c	-24.69	311.5	219.7	141.4	51.8	144.7	50.6
52	2d	-24.60	270.9	190.0	145.2	66.1	151.4	68.7
53	2e	-23.01	285.5	207.7	139.3	60.4	141.6	59.4
54	2f	-19.39	316.6	231.4	157.2	74.8	160.7	76.9
55	2g	-16.63	363.9	268.2	207.9	113.3	214.4	121.0
56	2h	-13.85	342.1	264.6	199.6	123.8	202.2	122.9

^aMAA(ΔG_{gas}) calculated using ΔG_{298} values of gas phase optimized geometries.

^bMAA($\Delta G_{\text{sol-sp}}$) calculated using ΔG_{298} of gas phase geometries + single point implicit DMSO solvation energies (SMD) for same.

^cMAA($\Delta G_{\text{sol-opt}}$) calculated using ΔG_{298} values for an implicit DMSO optimized geometries (SMD).

^dUsing gas phase optimized B3LYP/6-31G(d,p) geometries.

Chapter 3: Kinetics and mechanism of oxirane-formation by Darzens condensation of ketones: quantification of the electrophilicities of ketones

^aUsing solution phase optimized [smd,solvent=dmsol,B3LYP/6-31G(d,p)] geometries.

Table S26. Methyl anion affinities (MAAs, in terms of ΔE and ΔH , in kJ/mol) calculated at different levels of theory for electrophiles as listed in Figure S2.

Sl	Marker	<i>E</i>	Gas Phase Optimized				Implicit Solvation Optimized			
			ΔE_{gas}^a		ΔH_{gas}^b		$\Delta E_{\text{solv-opt}}^c$		$\Delta H_{\text{solv-opt}}^d$	
			B3LYP		B3LYP		B3LYP		B3LYP	
			sb	lb ^e	sb	lb ^e	sb	lb ^f	sb	lb ^f
1	1a	-17.5	262.2	202.7	247.0	187.5	137.7	74.0	123.3	59.6
2	1b	-21.0	246.6	180.3	231.5	165.3	114.3	45.7	100.1	32.3
3	1c	-19.9	269.2	194.6	255.4	180.8	129.5	51.6	116.7	38.8
4	1d	-22.1	262.8	184.7	246.2	168.5	118.3	37.0	105.3	24.3
5	1e	-18.4	277.1	204.7	262.9	190.5	137.3	61.6	124.3	48.6
6	1f	-17.9	288.5	216.0	273.6	201.1	141.8	65.8	128.5	52.5
7	1g	-16.9	305.9	227.7	290.6	212.5	151.1	69.4	137.1	55.4
8	1h	-18.2	281.5	206.5	267.5	192.5	138.2	60.4	124.9	47.0
9	1i	-22.3	252.5	185.9	238.2	171.9	119.4	49.4	106.2	36.2
10	1j	-15.6	292.6	212.7	278.0	198.2	144.9	69.0	133.3	57.7
11	1m*	-12.9	286.7	220.0	272.1	205.4	158.5	88.0	144.8	74.3
12	1o*	-15.4	276.7	207.7	262.3	193.3	146.4	73.9	132.5	60.0

sb is 6-31G(d,p) and lb is 6-311++G(3df,2pd)

^a ΔE_{gas} calculated using ΔE_{tot} values of gas phase optimized geometries.

^b ΔH_{gas} calculated using ΔH_{298} values of gas phase optimized geometries.

^c $\Delta E_{\text{solv-opt}}$ calculated using ΔE_{tot} values for an implicit DMSO optimized geometries (SMD).

^d $\Delta H_{\text{solv-opt}}$ calculated using ΔH_{298} values for an implicit DMSO optimized geometries (SMD).

^eUsing gas phase optimized B3LYP/6-31G(d,p) geometries.

^fUsing solution phase optimized [smd,solvent=dmsol,B3LYP/6-31G(d,p)] geometries.

8.3.1 Method Analysis

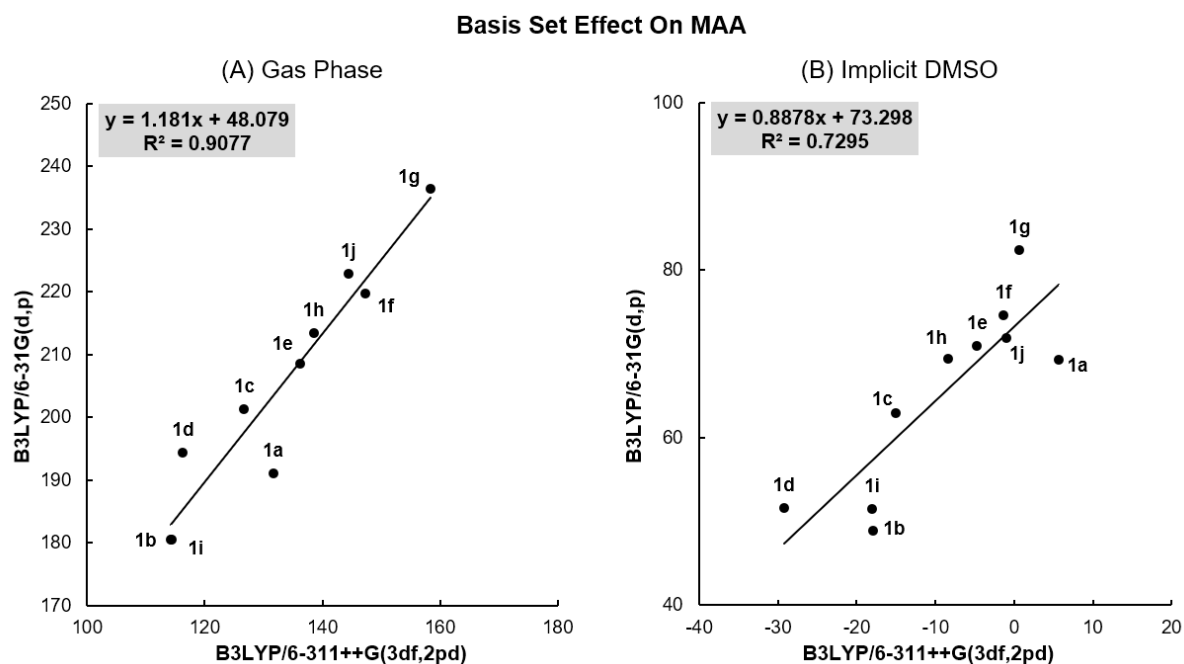


Figure S16. (A) Correlation between gas phase MAA ($-\Delta G_{\text{gas}}$, kJ/mol) calculated at B3LYP/6-31G(d,p) and B3LYP/6-311++G(3df,2pd)//B3LYP/6-31G(d,p) levels of theory and (B) correlation between implicit solvent phase (dmso) optimized MAA ($-\Delta G_{\text{sol-opt}}$, kJ/mol) calculated at B3LYP/6-31G(d,p)/SMD(DMSO) and B3LYP/6-311++G(3df,2pd)/SMD(DMSO)//B3LYP/6-31G(d,p)/SMD(DMSO) levels of theory for electrophiles listed in Figure S2.

8.3.2 Experiment Electrophilicity (E) vs Methyl Anion Affinity (MAA)

8.3.2.1 Gas phase MAA

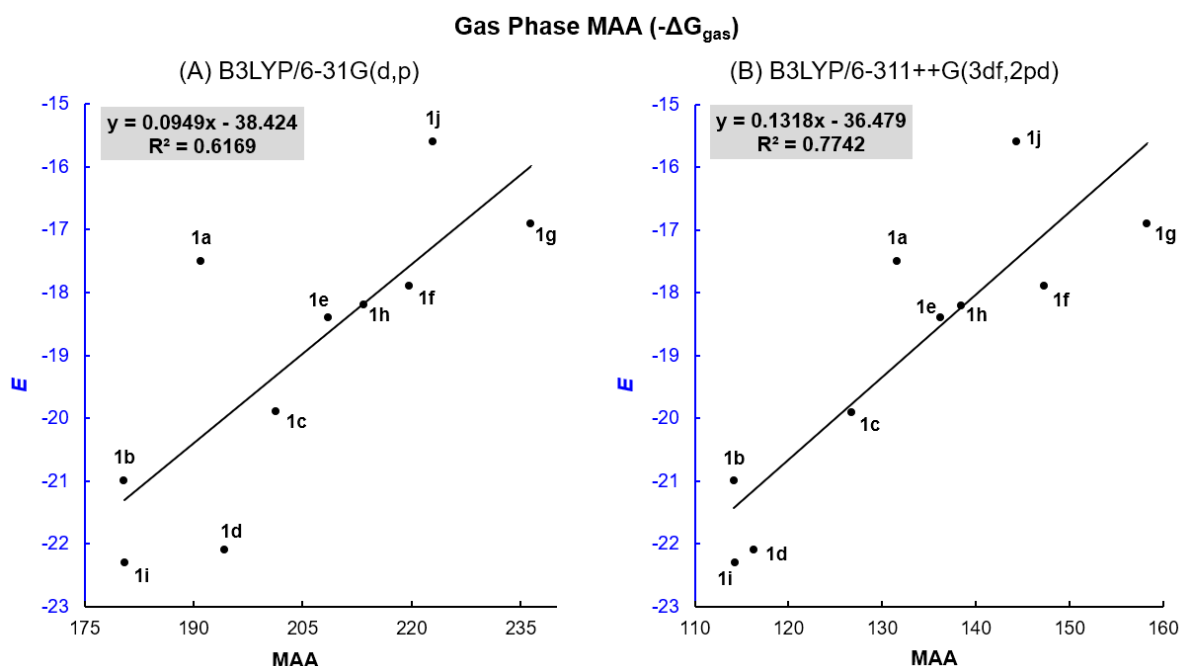


Figure S17. Correlation between E and gas phase MAA ($-\Delta G_{\text{gas}}$, kJ/mol) calculated at (A) B3LYP/6-31G(d,p) and (B) B3LYP/6-311++G(3df,2pd)//B3LYP/6-31G(d,p) level of theory for electrophiles listed in Figure S2.

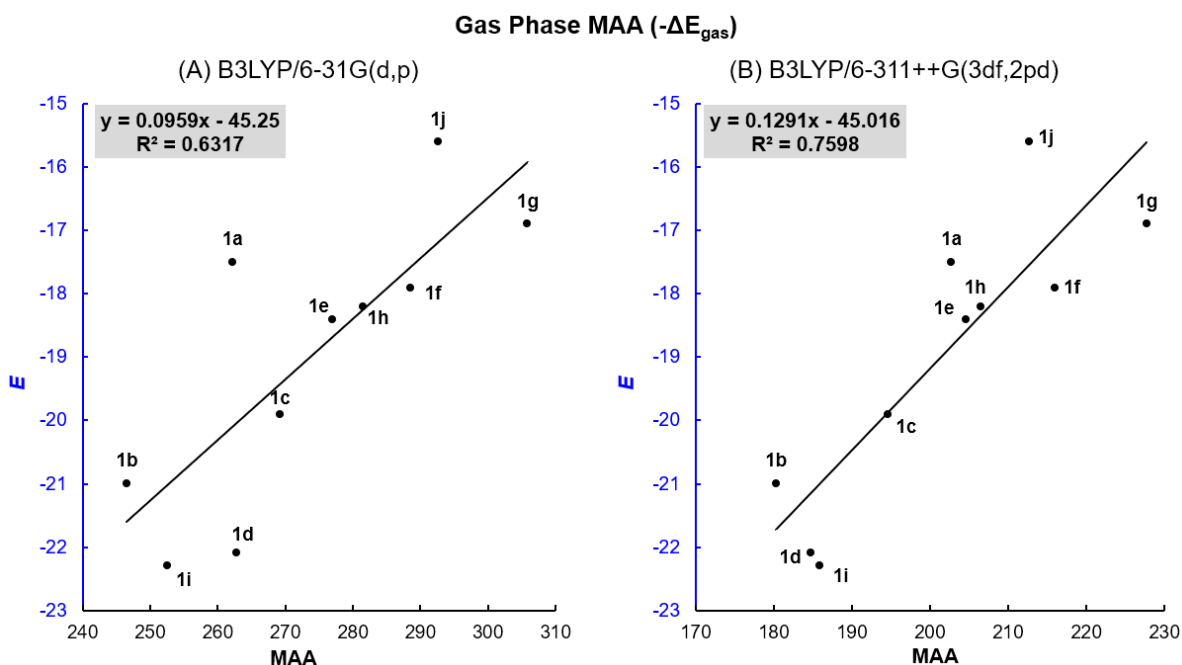


Figure S18. Correlation between E and gas phase MAA ($-\Delta E_{\text{gas}}$, kJ/mol) calculated at (A) B3LYP/6-31G(d,p) and (B) B3LYP/6-311++G(3df,2pd)//B3LYP/6-31G(d,p) levels of theory for electrophiles listed in Figure S2.

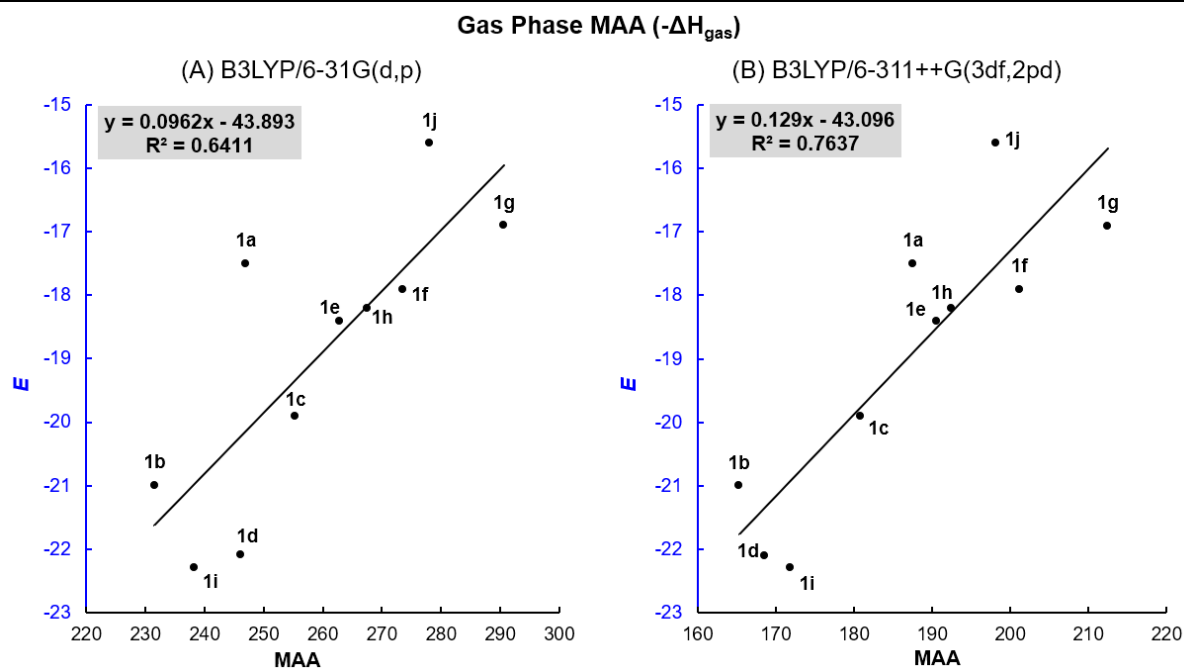


Figure S19. Correlation between E and gas phase MAA ($-\Delta H_{\text{gas}}$, kJ/mol) calculated at (A) B3LYP/6-31G(d,p) and (B) B3LYP/6-311++G(3df,2pd)//B3LYP/6-31G(d,p) levels of theory for electrophiles listed in Figure S2.

8.3.2.2 Single point implicit-solvation (DMSO) corrected MAA

Single point implicit-solvation MAA ($-\Delta G_{\text{sp-sol}}$)

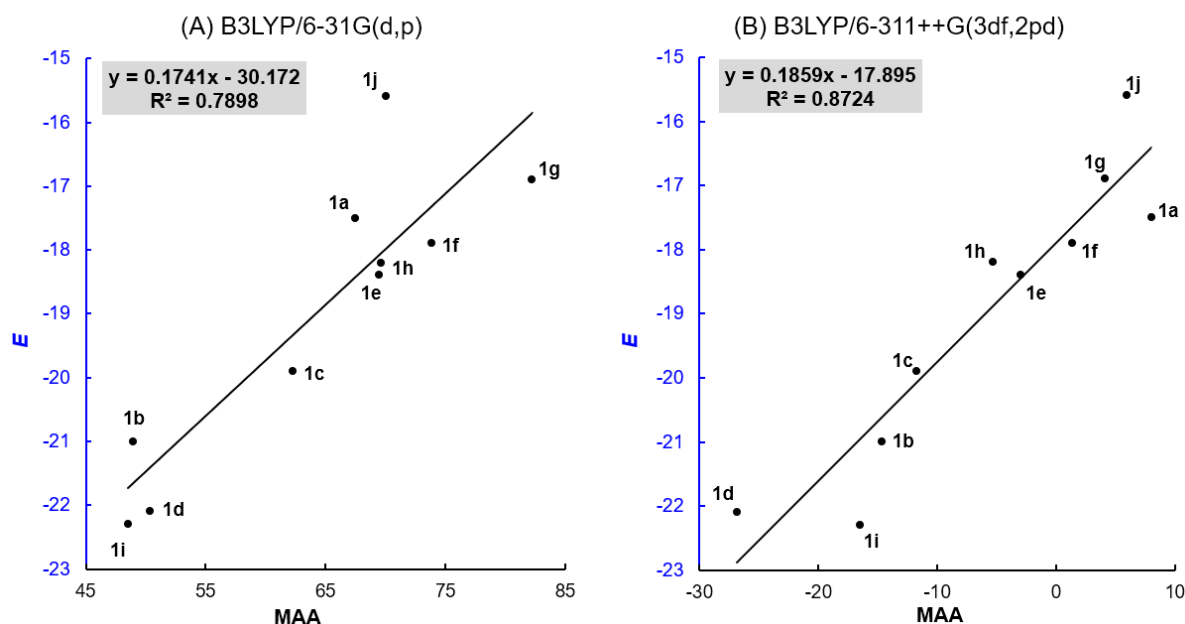


Figure S20. Correlation between E and MAA [$-\Delta G_{\text{sol-sp}}$ ($\Delta G_{298} + \Delta G_{\text{Solv}}$) kJ/mol] calculated at (A) B3LYP/6-31G(d,p) and (B) B3LYP/6-311++G(3df,2pd)//B3LYP/6-31G(d,p) levels of theory for electrophiles listed in Figure S2. B3LYP/6-311++G(3df,2pd)/SMD(DMSO)//B3LYP/6-31G(d,p) values were obtained by adding B3LYP/6-311++G(3df,2pd)//B3LYP/6-31G(d,p) and ΔG_{Solv} [single point solvation energy calculated at B3LYP/6-31G(d,p)/SMD(DMSO)//B3LYP/6-31G(d,p)].

8.3.2.3 Implicit-solvation (DMSO) optimized MAA

Implicit-solvation (DMSO) optimized MAA ($-\Delta G_{\text{sol-opt}}$)

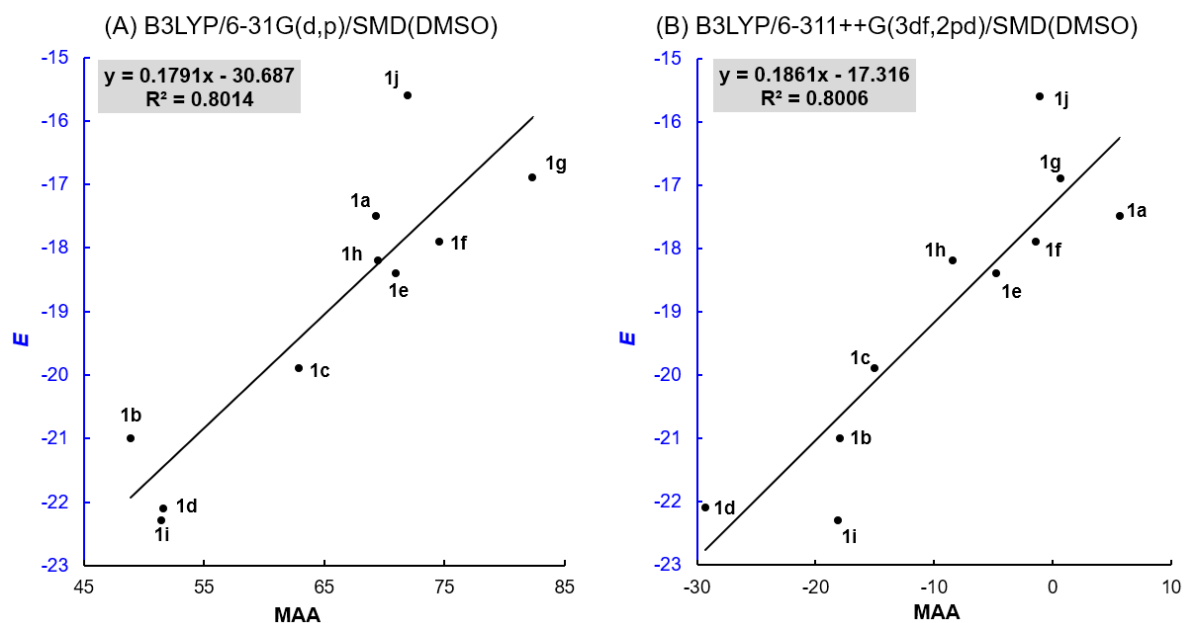


Figure S21. Correlation between E and MAA ($-\Delta G_{\text{sol-opt}}$, kJ/mol) calculated at (A) B3LYP/6-31G(d,p)/SMD(DMSO) and (B) B3LYP/6-311++G(3df,2pd)/SMD(DMSO)//B3LYP/6-31G(d,p)/SMD(DMSO) levels of theory for electrophiles listed in Figure S2. B3LYP/6-311++G(3df,2pd)/SMD(DMSO) values were obtained by adding B3LYP/6-311++G(3df,2pd)//B3LYP/6-31G(d,p)/SMD(DMSO) and ΔG_{Solv} [single point solvation energy calculated at B3LYP/6-31G(d,p)/SMD(DMSO)].

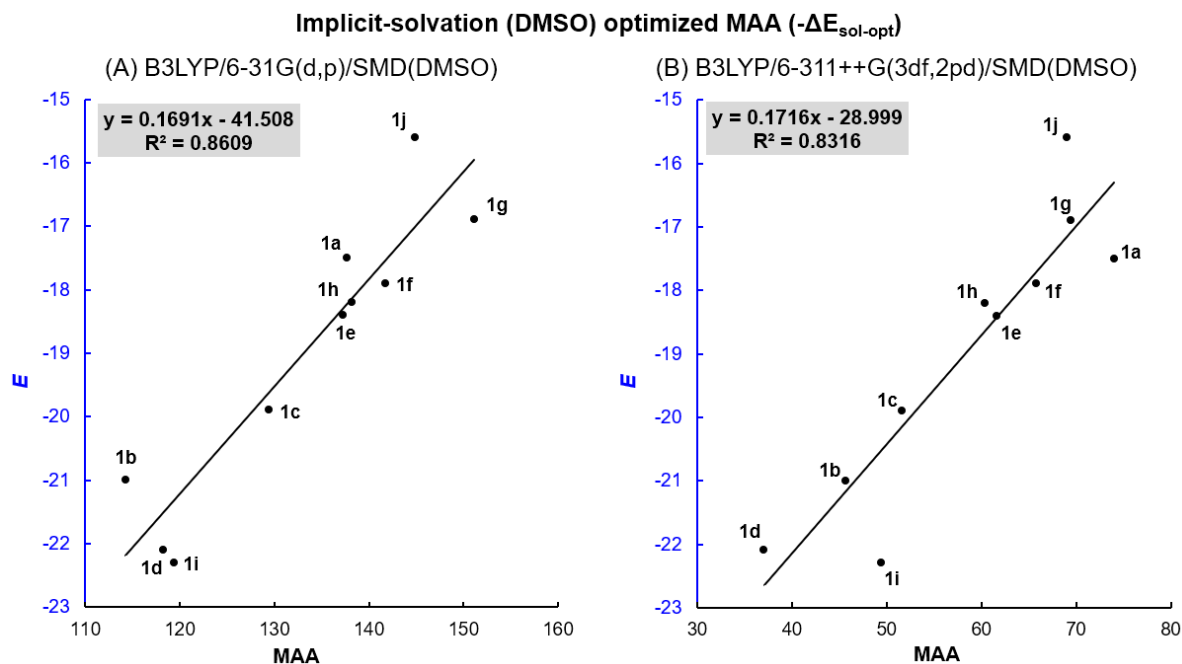


Figure S22. Correlation between E and MAA ($-\Delta E_{\text{sol-opt}}$, kJ/mol) calculated at (A) B3LYP/6-31G(d,p)/SMD(DMSO) and (B) B3LYP/6-311++G(3df,2pd)/SMD(DMSO)//B3LYP/6-31G(d,p)/SMD(DMSO) levels of theory for electrophiles listed in Figure S2. B3LYP/6-311++G(3df,2pd)/SMD(DMSO) values were obtained by adding B3LYP/6-311++G(3df,2pd)//B3LYP/6-31G(d,p)/SMD(DMSO) and ΔG_{Solv} [single point solvation energy calculated at B3LYP/6-31G(d,p)/SMD(DMSO)].

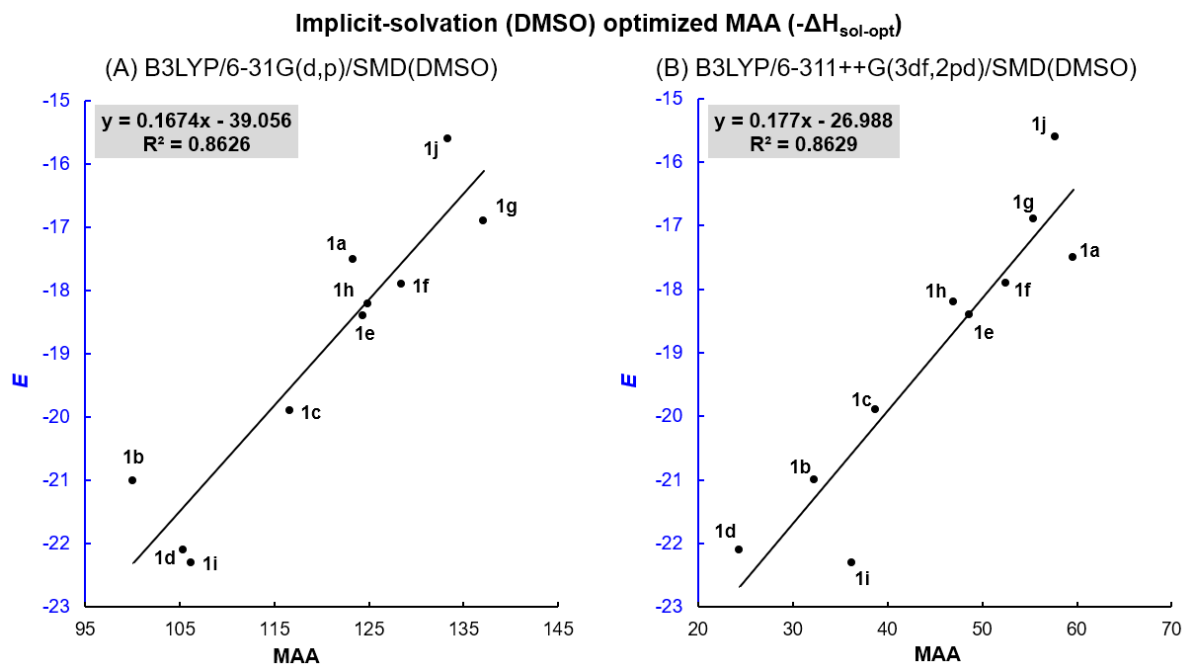


Figure S23. Correlation between E and MAA ($-\Delta H_{\text{sol-opt}}$, kJ/mol) calculated at (A) B3LYP/6-31G(d,p)/SMD(DMSO) and (B) B3LYP/6-311++G(3df,2pd)/SMD(DMSO)//B3LYP/6-31G(d,p)/SMD(DMSO) levels of theory for electrophiles listed in Figure S2. B3LYP/6-311++G(3df,2pd)/SMD(DMSO) values were obtained by adding B3LYP/6-311++G(3df,2pd)//B3LYP/6-31G(d,p)/SMD(DMSO) and ΔG_{Solv} [single point solvation energy calculated at B3LYP/6-31G(d,p)/SMD(DMSO)].

8.3.2.4 Effects of solvation energies on conformational selection

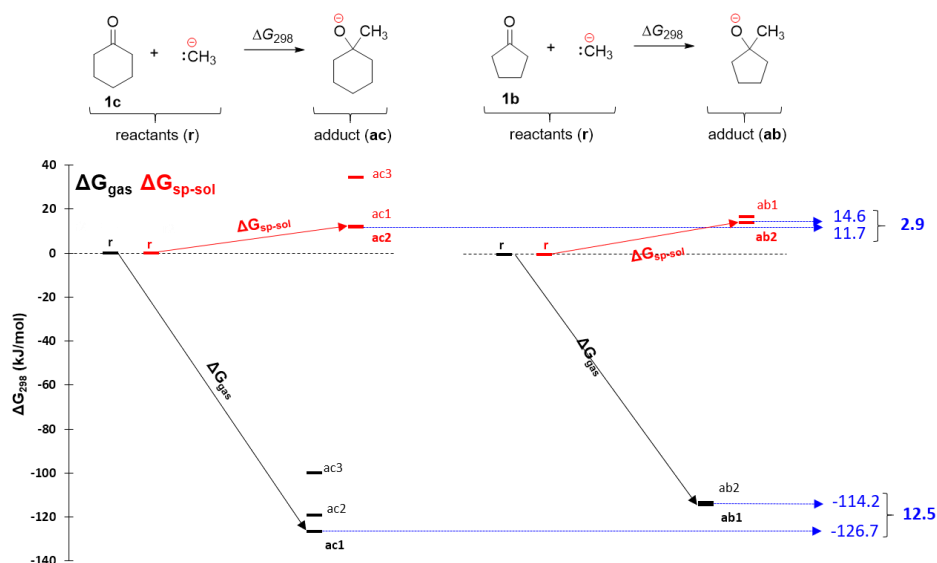


Figure S24. Free energies for CH_3^- addition to **1c** and **1b** in gas (ΔG_{gas}) and solvent phase ($\Delta G_{\text{sp-sol}}$) calculated at B3LYP/6-311++G(3df,2pd)//B3LYP/6-31G(d,p) and B3LYP/6-311++G(3df,2pd)/SMD(DMSO)//B3LYP/6-31G(d,p) levels of theory respectively.

The correlation between MAA and E improves when gas phase values (ΔG_{gas}) of the former were corrected by solvation energies (ΔG_{solv}) obtained in single point SMD calculations. It is important to mention that this improvement in the correlation depends heavily on finding the lowest energy conformer both in the gas and solvent phase. This observation is illustrated in Figure S24 for the example of cyclohexanone **1c**, which has a 12.5 kJ/mol higher MAA than cyclopentanone **1b** in the gas phase (ΔG_{gas}), which is reduced to 2.9 kJ/mol in DMSO ($\Delta G_{\text{sp-sol}}$). This 9.6 kJ/mol change results from two important factors. First, a change in conformational preference for the adducts from the gas phase to DMSO and second the differences in the absolute solvation energies of both ketones and their corresponding adducts.

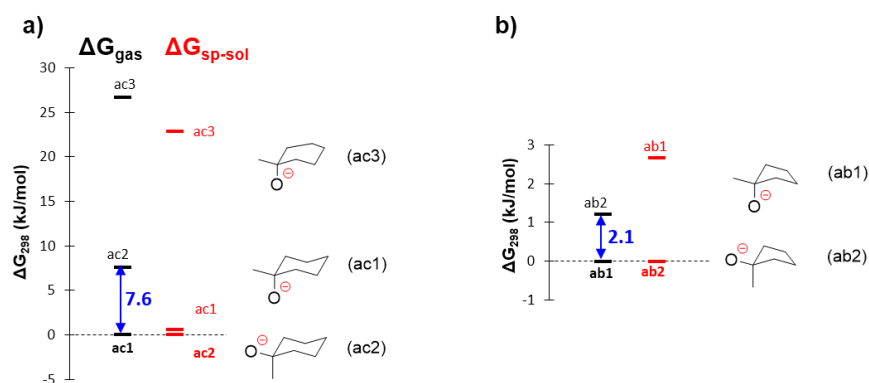


Figure S25. Conformational energetics for CH_3^- adducts (a) **ac** (of **1c**) and (b) **ab** (of **1b**) in gas (ΔG_{gas}) and solvent phase ($\Delta G_{\text{sp-sol}}$) calculated at B3LYP/6-311++G(3df,2pd)//B3LYP/6-31G(d,p) and B3LYP/6-311++G(3df,2pd)/SMD(DMSO)//B3LYP/6-31G(d,p) levels of theory respectively.

Chapter 3: Kinetics and mechanism of oxirane-formation by Darzens condensation of ketones: quantification of the electrophilicities of ketones

Conformation preference: In case of ketones, **1b** and **1c** prefer conformations where the carbonyl oxygen is equatorially oriented (gas phase and DMSO). Adduct of these ketone have difference conformation preference in gas and DMSO: **ab1** and **ac1** preferred in gas phase, **ab2** and **ac2** in DMSO. For cyclohexanone adduct the conformer **ac2** has a 8.2 kJ/mol higher solvation energy than conformer **ac1** and thus becomes the global minimum in DMSO [see Figure S25a, for solvation energies see column 4 of Table S27]. Because of this change, the driving force for CH₃⁻ addition to ketone **1c** is reduced by 7.6 kJ/mol in DMSO relative to the gas phase (**ac2** is 7.6 kJ/mol higher in gas phase). A similar conformational switch can be observed for the reaction of cyclopentanone **1b**, where adduct conformer **ab2** becomes the global minimum in DMSO due to a 3.9 kJ/mol higher solvation energy as compared to conformer **ab1**. Taken together this change in conformational preference leads to loss of 1.2 kJ/mol driving force for CH₃⁻ addition to **1b** in DMSO relative to the gas phase. Overall, because of the changes in conformation preferences, it becomes 6.4 (7.6-1.2) kJ/mol more difficult to add CH₃⁻ to **1c** in DMSO relative to gas phase when comparing it with **1b**.

The absolute solvation free energy of ketone **1c** (-26.8 kJ/mol) is 0.9 kJ/mol higher than that for **1b** (25.9 kJ/mol), while for the methyl anion adducts **ab2** (-228.0 kJ/mol) is 2.3 kJ/mol better solvated than **ac2** (-225.7 kJ/mol). [see column 4 of Table S27]. Taking these solvation effects together the CH₃⁻ addition to **1c** is reduced relative to **1b** by 3.2 kJ/mol in DMSO solution.

Combination of both factors (change in conformational preference with 6.4 kJ/mol, and difference in absolute solvation energies of 3.2 kJ/mol) results in a 9.6 kJ/mol reduction of CH₃⁻ addition reaction energy for **1c** relative to **1b** in DMSO when compared to the gas phase.

Table S27. Relative energies (in kJ/mol) for **1b** and **1c** along with their adducts.

Marker	FileName	Rel. ΔG_{gas} B3LYP	ΔG_{solv} SMD(DMSO)/B3LYP/6-31G(d,p)	Rel. $\Delta G_{\text{sp-sol}}$ SMD(DMSO)/B3LYP
		/6-311++G(3df,2pd) //B3LYP/6-31G(d,p)	//B3LYP/6-31G(d,p)	/6-311++G(3df,2pd) //B3LYP/6-31G(d,p)
1b	b1_cs_1	0.0	-25.9	0.0
ab1	b1_add_cs_1	0.0	-224.2	2.7
ab2	b1_add_cs_2	1.2	-228.0	0.0
1c	c1_1	0.0	-26.8	0.0
1c	c1_2	12.5	-27.1	12.1
ac1	me_c1_1	0.0	-217.5	0.6
ac2	me_c1_2	7.6	-225.7	0.0
ac3	me_c1_3	26.7	-221.9	22.9

8.3.2.5 Comparison of ketones and Michael acceptors electrophilic reactivity

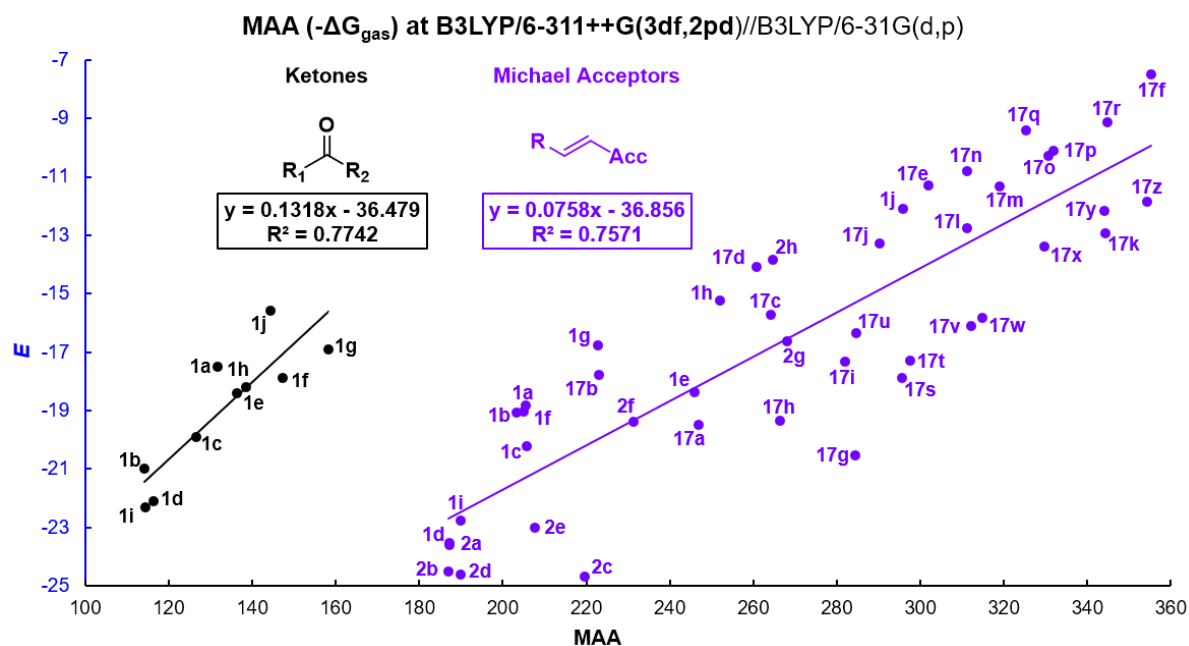


Figure S26. Correlation between E and gas phase MAA ($-\Delta G_{\text{gas}}$, kJ/mol) of ketones and Michael acceptors at B3LYP/6-311++G(3df,2pd)//B3LYP/6-31G(d,p) levels of theory (compound labelling for Michael acceptors refers to the labels used in ref S9)

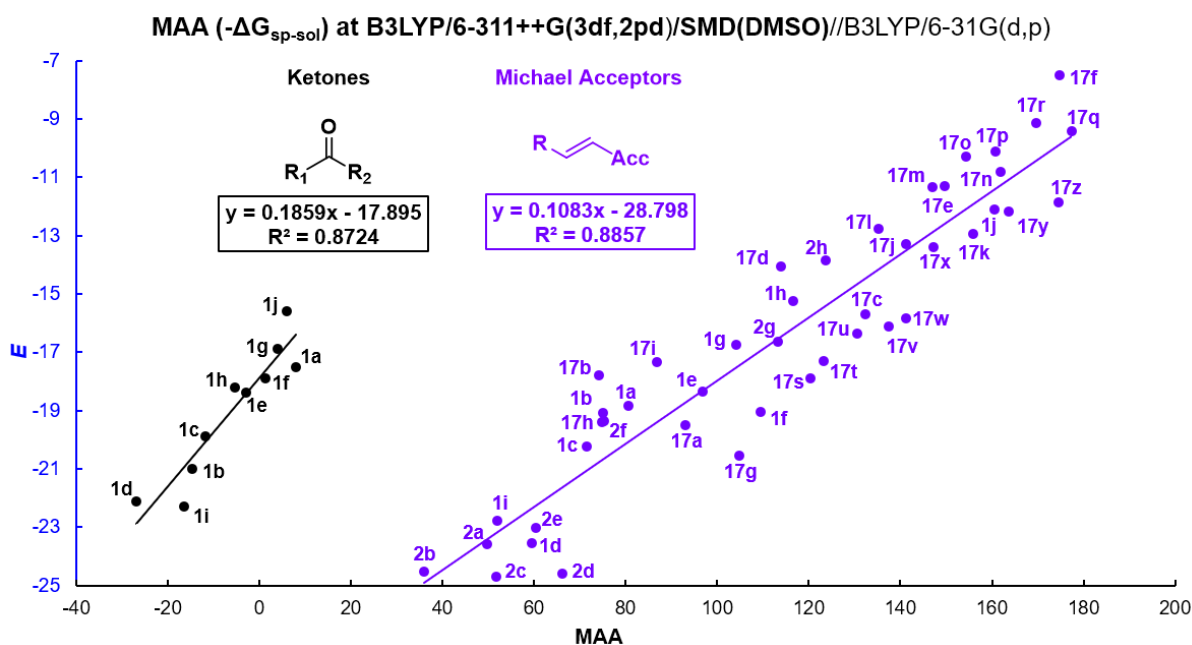


Figure S27. Correlation between E and MAA ($-\Delta G_{\text{sol-sp}}$, in kJ/mol) of ketones and Michael acceptors at B3LYP/6-311++G(3df,2pd)/SMD(DMSO)//B3LYP/6-31G(d,p) level of theory (compound labelling for Michael acceptors refers to the labels used in ref S9). $\Delta G_{\text{sol-sp}}$ values at B3LYP/6-311++G(3df,2pd)/SMD(DMSO)//B3LYP/6-31G(d,p) were obtained by adding ΔG_{298} at B3LYP/6-311++G(3df,2pd)//B3LYP/6-31G(d,p) and ΔG_{Solv} [single point solvation energy calculated at B3LYP/6-31G(d,p)/SMD(DMSO)//B3LYP/6-31G(d,p)]

8.3.3 *E* vs Frontier Molecular Orbital Energies (FMO_E)Table S28. FMO_E for electrophiles listed in Figure S2.

Marker	E	Gas phase optimization						Implicit-solvation phase optimization			
		B3LYP/ 6-31G(d,p)		B3LYP/ 6-31G(d,p)/SMD(DMSO) //B3LYP/6-31G(d,p)		B3LYP/ 6-311++G(3df,2pd) //B3LYP/6-31G(d,p)		FileName	B3LYP/ 6-31G(d,p)/SMD(DMSO)		
		HOMO _E	LUMO _E	HOMO _E	LUMO _E	HOMO _E	LUMO _E		HOMO _E	LUMO _E	
											FileName
1a	-17.5		-0.24245	-0.02117	-0.23629	-0.01179	-0.25743	-0.03994	a1_cs_1	-0.23653	-0.01248
1b	-21.0	a1_cs_1	-0.23597	-0.01449	-0.23076	-0.00600	-0.25073	-0.03336	b1_cs_1	-0.23074	-0.00688
1c	-19.9	b1_cs_1	-0.23443	-0.01201	-0.22980	-0.00432	-0.24879	-0.03383	c1_1	-0.22976	-0.00511
1d	-22.1	c1_1	-0.23483	-0.01104	-0.23104	-0.00427	-0.24950	-0.03153	d1_cs_2	-0.23016	-0.00267
1e	-18.4	d1_cs_1	-0.22444	-0.01456	-0.21284	-0.00768	-0.23805	-0.03542	e1_1	-0.21392	-0.00844
1f	-17.9	e1_1	-0.24378	-0.02071	-0.23565	-0.00941	-0.25848	-0.04045	f1_1	-0.23564	-0.01020
1g	-16.9	f1_1	-0.23250	-0.02310	-0.22327	-0.01134	-0.24075	-0.04213	g1_1	-0.22291	-0.01208
1h	-18.2	g1_1	-0.23481	-0.01233	-0.23238	-0.00757	-0.24970	-0.03238	h1_cs_1	-0.23242	-0.00823
1i	-22.3	h1_cs_1	-0.24272	-0.00948	-0.23665	-0.00012	-0.25646	-0.02730	i1_cs_1	-0.23639	-0.00070
1j	-15.6	i1_cs_1	-0.22563	-0.02762	-0.22018	-0.01957	-0.23476	-0.04346	j1_cs_6	-0.21847	-0.00976
1m*	-12.9	j1_cs_1	-0.25521	-0.06342	-0.25209	-0.05735	-0.26952	-0.08083	k1_cs_1	-0.25174	-0.05820
1o*	-15.4	k1_cs_1	-0.23442	-0.05149	-0.22737	-0.04826	-0.24806	-0.06825	l1_cs_2	-0.22681	-0.04886

8.3.3.1 Gas phase optimized geometries

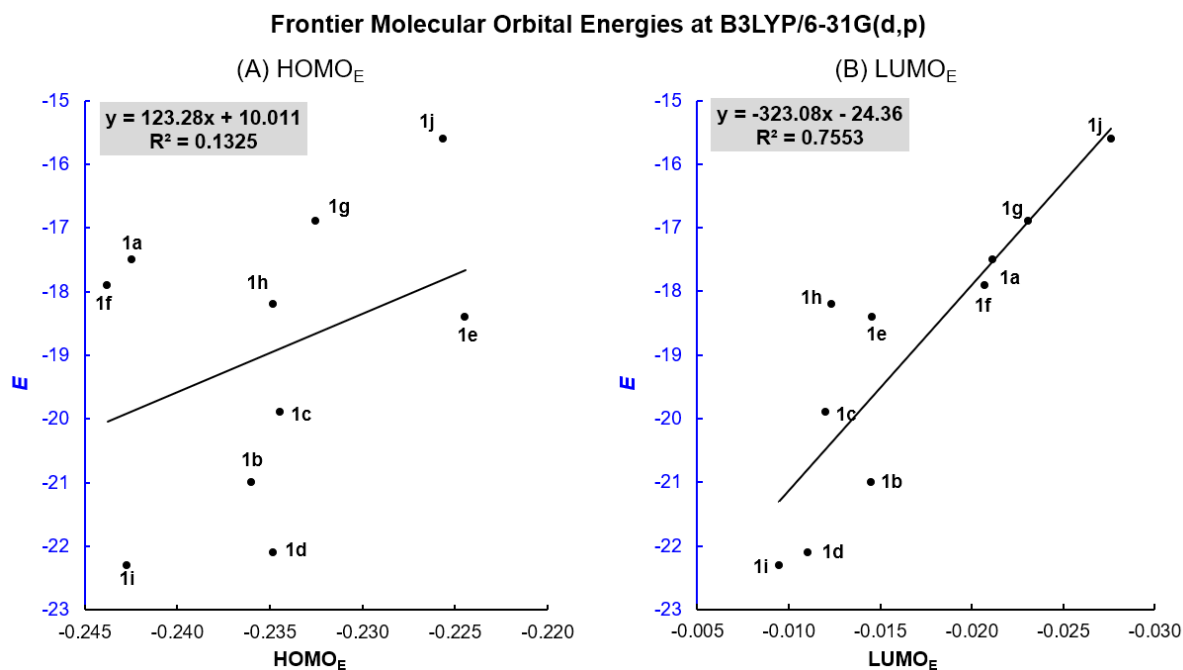


Figure S28. Correlation between E and frontier molecular orbital energies (A) HOMO_E and (B) LUMO_E from gas phase optimized geometries at B3LYP/6-31G(d,p) level of theory for electrophiles listed in Figure S2. FMO energies are reported in Hartree.

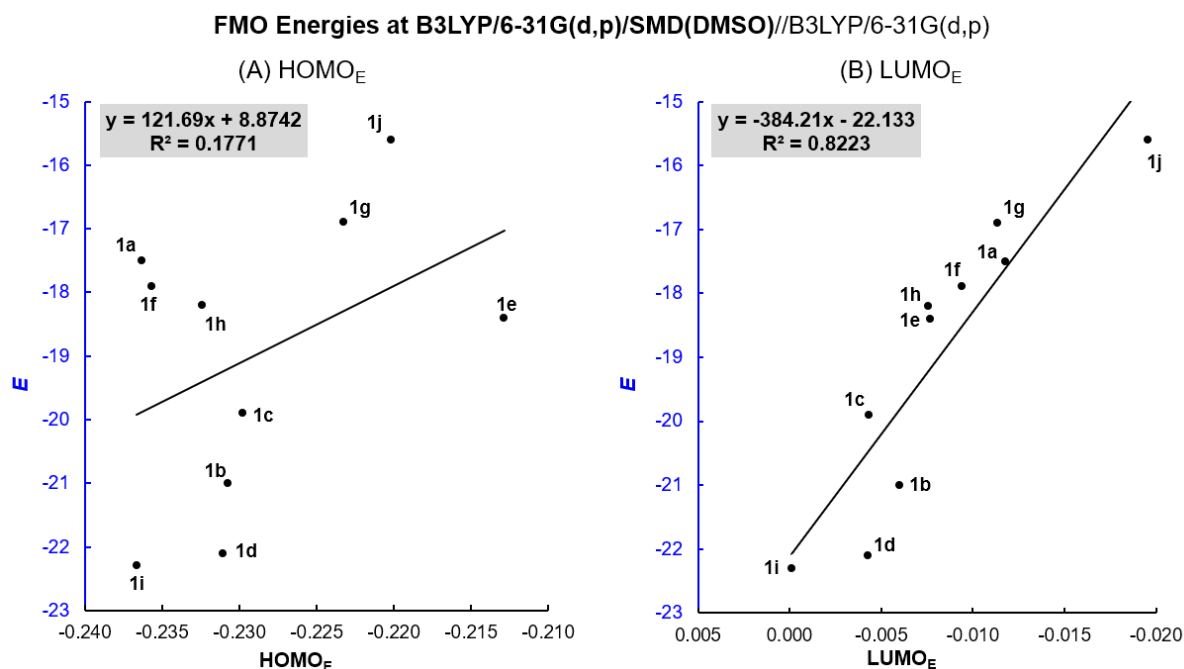


Figure S29. Correlation between E and frontier molecular orbital energies (A) HOMO_E and (B) LUMO_E calculated at B3LYP/6-31G(d,p)/SMD(DMSO)//B3LYP/6-31G(d,p) level of theory for electrophiles listed in Figure S2. FMO energies are reported in Hartree.

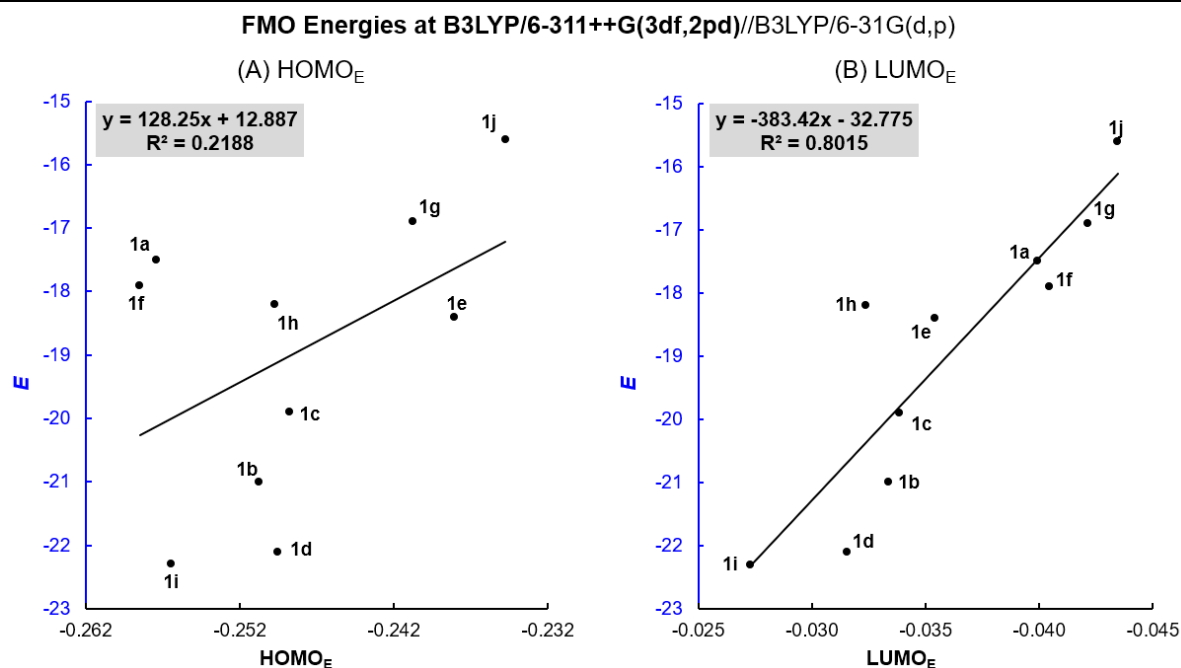


Figure S30. Correlation between E and frontier molecular orbital energies (A) HOMO_E and (B) LUMO_E calculated at B3LYP/6-311++G(3df,2pd)// B3LYP/6-31G(d,p) level of theory for electrophiles listed in Figure S2. FMO energies are reported in Hartree.

8.3.3.2 Implicit solvation (DMSO) optimized geometries

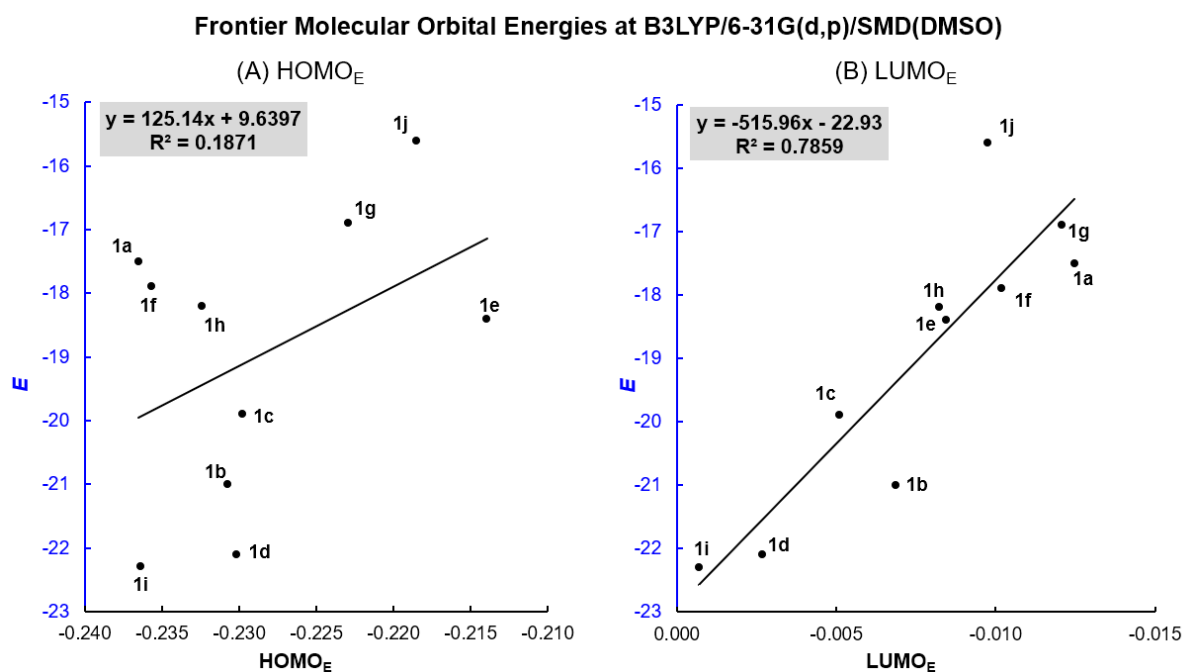


Figure S31. Correlation between E and frontier molecular orbital energies (A) HOMO_E and (B) LUMO_E from implicit solvation (DMSO) optimized geometries at B3LYP/6-31G(d,p)/SMD(DMSO) level of theory for electrophiles listed in Figure S2. FMO energies are reported in Hartree.

8.3.4 *E* vs Electrophilicity Indices

Table S29. Electrophilicity indices calculated at B3LYP/6-31G(d,p) for electrophiles listed in Figure S2.

SI	Marker	E	B3LYP/6-31G(d,p)		Chemical Potential $\mu \approx (E_H + E_L)/2$	Chemical Hardness $\eta \approx (E_L - E_H)$	Global Electrophilicity Index $\omega = \mu^2/2\eta$	Local Electrophilicity (ω_k), Yang and Mortier				ω_k Contreras	
			HOMO _E (E_H)	LUMO _E (E_L)				q_k (N)	q_k (N+1)	f_k^+	ω_k ($\omega^* f_k^+$)	f_k^+	ω_k ($\omega^* f_k^+$)
1	1a	-17.5	-0.24245	-0.02117	-0.13181	0.22128	1.07	0.395103	0.242452	0.15	0.16	0.48	0.51
2	1b	-21.0	-0.23597	-0.01449	-0.12523	0.22148	0.96	0.416329	0.260839	0.16	0.15	0.50	0.48
3	1c	-19.9	-0.23443	-0.01201	-0.12322	0.22242	0.93	0.426145	0.261355	0.16	0.15	0.50	0.47
4	1d	-22.1	-0.23483	-0.01104	-0.12294	0.22379	0.92	0.421597	0.271794	0.15	0.14	0.51	0.47
5	1e	-18.4	-0.22444	-0.01456	-0.11950	0.20988	0.93	0.415529	0.252644	0.16	0.15	0.50	0.46
6	1f	-17.9	-0.24378	-0.02071	-0.13225	0.22307	1.07	0.413215	0.241469	0.17	0.18	0.50	0.53
7	1g	-16.9	-0.23250	-0.02310	-0.12780	0.20940	1.06	0.429222	0.251864	0.18	0.19	0.51	0.54
8	1h	-18.2	-0.23481	-0.01233	-0.12357	0.22248	0.93	0.422973	0.257594	0.17	0.15	0.51	0.47
9	1i	-22.3	-0.24272	-0.00948	-0.12610	0.23324	0.93	0.420833	0.254655	0.17	0.15	0.53	0.49
10	1j	-15.6	-0.22563	-0.02762	-0.12663	0.19801	1.10	0.431925	0.305401	0.13	0.14	0.46	0.51
11	1m*	-12.9	-0.25521	-0.06342	-0.15932	0.19179	1.80	0.258182	0.137644	0.12	0.22	0.26	0.48
12	1o*	-15.4	-0.23442	-0.05149	-0.14296	0.18293	1.52	0.253321	0.132615	0.12	0.18	0.28	0.42

For Yang and Mortier method: $f_k^+ = |q_k(N+1) - q_k(N)|$, where, q_k is partial charge at k^{th} atom and N is a number of electron in the neutral system.

8.3.4.1 E vs global electrophilicity index (ω)

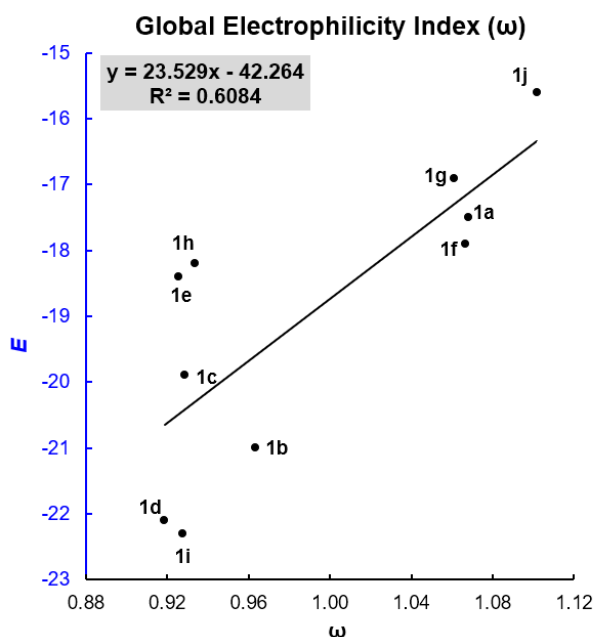


Figure S32. Correlation between E and gas phase global electrophilicity index (ω , in eV) calculated at B3LYP/6-31G(d,p) level of theory for electrophiles listed in Figure S2.

8.3.4.2 E vs local electrophilicity index at β position (ω_k)

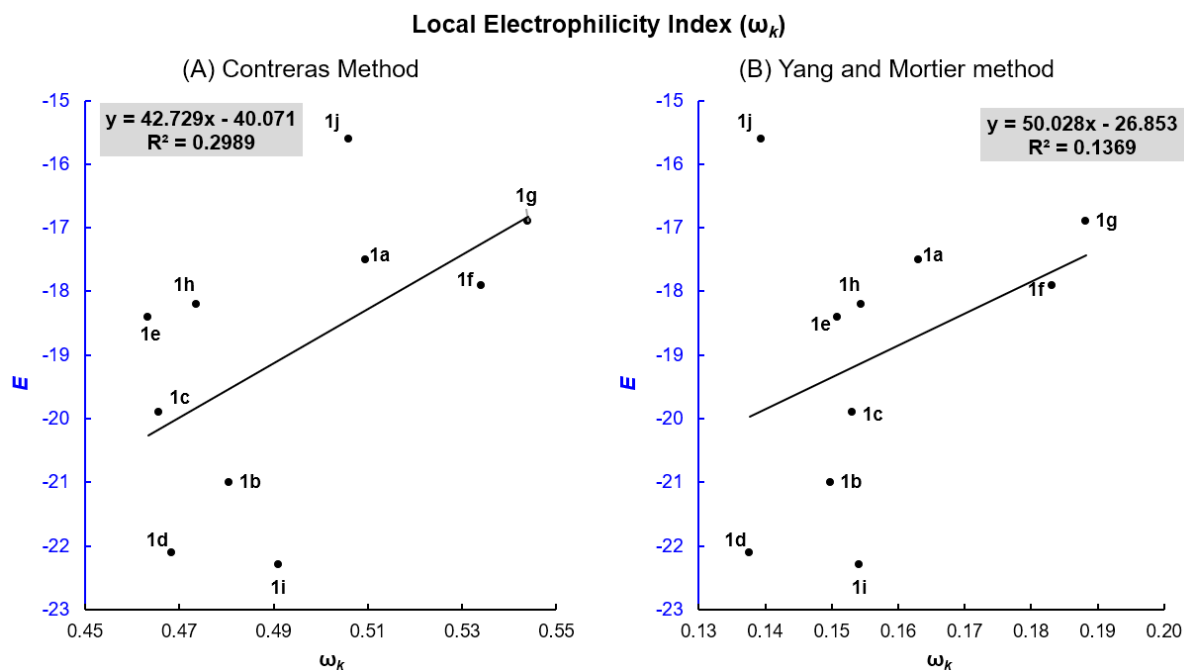


Figure S33. Correlation between E and gas phase local electrophilicity index (ω_k) calculated at B3LYP/6-31G(d,p) level of theory for electrophiles listed in Figure S2 using (A) Contreras method and (B) Yang and Mortier method. Fukui function for nucleophilic attach (f_k^+) calculated using Mulliken charges for Yang and Mortier method.

8.4 Individual calculations

Table S30. QM properties for gas phase optimized conformers of neutral electrophiles (Figure S2) and their corresponding methyl anion adducts (maa).

Marker	File Name	Low Frequency			HOMO _E (hartree)	LUMO _E (hartree)	B3LYP/6-31G(d,p)		corr. ΔG (hartree)	ΔG _{Solv} (kcal/mol)	ΔE _{tot} (hartree)	ΔE _{tot} (hartree) [B3LYP/6-311++G(3df,2pd) //B3LYP/6-31G(d)]
							corr. ZPE (hartree)	corr. ΔH (hartree)				
CH ₃ ⁻¹	ch3anion	-29	0	0	0.13514	0.37353	0.027840	0.031650	0.008651	-78.9	-39.7960280	-39.8566374
1a ^{abcd}	a1_cs_1	-12	-11	0	-0.24245	-0.02117	0.090904	0.096832	0.062130	-5.68	-231.2371532	-231.3138638
maa_1a ^{abcd}	a1_add_cs_1	0	0	0	0.04646	0.25510	0.127047	0.134270	0.097881	-55.00	-271.1330435	-271.2477231
1b ^{abcd}	b1_cs_1	-8	0	0	-0.23597	-0.01449	0.121440	0.127945	0.092357	-6.19	-270.5841570	-270.6712723
maa_1b ^{abc}	b1_add_cs_1	0	0	0	0.04683	0.24788	0.157154	0.165316	0.126186	-53.63	-310.4740988	-310.5965808
maa_1b ^d	b1_add_cs_2	0	0	0	0.04889	0.23193	0.156905	0.165131	0.125929	-54.55	-310.4711888	-310.5958638
1c ^{abcd}	c1_1	-32	-10	0	-0.23443	-0.01201	0.151148	0.158585	0.120742	-6.40	-309.9052322	-310.0023493
1c	c1_2	-36	-29	-21	-0.23412	-0.00921	0.150819	0.158467	0.119768	-6.49	-309.8993796	-309.9966087
maa_1c ^{abc}	me_c1_1	-30	0	0	0.03883	0.24169	0.186642	0.195495	0.155247	-52.04	-349.8037850	-349.9330986
maa_1c ^d	me_c1_2	-35	-13	0	0.04723	0.22725	0.186331	0.195249	0.154816	-53.99	-349.7962078	-349.9297814
maa_1c	me_c1_3	-15	-9	0	0.04479	0.23003	0.186307	0.195384	0.154238	-53.09	-349.7897370	-349.9219254
1d ^{abcd}	d1_cs_1	-22	0	0	-0.23483	-0.01104	0.180022	0.188651	0.147561	-6.58	-349.2162954	-349.3236608
1d	d1_cs_2	-26	-14	-8	-0.23431	-0.00855	0.179587	0.187447	0.148646	-6.60	-349.2161694	-349.3233795
1d	d1_cs_3	-23	-10	0	-0.23438	-0.01338	0.180241	0.188994	0.147852	-6.44	-349.2124739	-349.3200753
1d	d1_cs_4	-13	-4	0	-0.23404	-0.00953	0.180190	0.188905	0.147812	-6.53	-349.2122920	-349.3197159
1d	d1_cs_5	-20	0	0	-0.23387	-0.00983	0.180071	0.188784	0.147477	-6.62	-349.2114665	-349.3189288
maa_1d ^{abc}	d1_add_cs_2	-17	0	0	0.03199	0.22438	0.215440	0.225546	0.182279	-51.04	-389.1124022	-389.2506544
maa_1d ^d	d1_add_cs_1	-20	0	0	0.04251	0.21909	0.215186	0.225343	0.181646	-52.58	-389.1059765	-389.2478766
maa_1d	d1_add_cs_7	-14	-8	0	0.03608	0.22950	0.215474	0.225700	0.182072	-50.19	-389.1028568	-389.2404664
maa_1d	d1_add_cs_3	-22	-7	0	0.04515	0.21256	0.215104	0.225354	0.181699	-53.50	-389.1014513	-389.2450191
maa_1d	d1_add_cs_4	-16	-12	0	0.04545	0.21267	0.215144	0.225389	0.181833	-53.54	-389.1012614	-389.2445929
maa_1d	d1_add_cs_5	0	0	0	0.04241	0.21771	0.215509	0.225768	0.181370	-52.61	-389.1006012	-389.2425681
maa_1d	d1_add_cs_6	-23	-17	0	0.04482	0.21420	0.215204	0.225587	0.180881	-53.35	-389.0909761	-389.2340404
1e ^{abcd}	e1_1	-16	-14	0	-0.22444	-0.01456	0.167437	0.176137	0.135409	-7.01	-365.2410462	-365.3583211
1e	e1_2	-16	-3	0	-0.21692	-0.01330	0.167648	0.176296	0.135726	-7.59	-365.2375889	-365.3540043
1e	e1_3	-11	0	0	-0.21893	-0.00956	0.167116	0.176003	0.134585	-7.26	-365.2343402	-365.3517572
1e	e1_4	-18	0	0	-0.20950	-0.01371	0.166826	0.175740	0.134068	-7.34	-365.2315912	-365.3487132
maa_1e ^{abcd}	me_e1_4	0	0	0	0.03599	0.22894	0.203089	0.213186	0.170136	-52.62	-405.1425989	-405.2929144
maa_1e	me_e1_3	-18	0	0	0.03388	0.22375	0.203289	0.213332	0.170446	-51.89	-405.1391436	-405.2877620
maa_1e	me_e1_1	-11	0	0	0.04363	0.21201	0.202704	0.212831	0.169676	-54.39	-405.1352438	-405.2889540
maa_1e	me_e1_2	0	0	0	0.04295	0.21661	0.203042	0.213155	0.170047	-53.65	-405.1312625	-405.2841987
maa_1e	me_e1_8	-24	-14	0	0.03965	0.21889	0.202483	0.212783	0.168835	-53.07	-405.1268901	-405.2788782
maa_1e	me_e1_7	-15	0	0	0.03969	0.22445	0.202593	0.212918	0.168774	-52.85	-405.1268180	-405.2786262

Chapter 3: Kinetics and mechanism of oxirane-formation by Darzens condensation of ketones: quantification of the electrophilicities of ketones

1f ^{abcd}	f1_1	-15	-11	0	-0.24378	-0.02071	0.127195	0.134351	0.097014	-7.42	-345.7913289	-345.9093248
1f	f1_2	-22	-19	0	-0.24522	-0.02125	0.126375	0.133876	0.095218	-7.76	-345.7835501	-345.9020055
maa_1f ^{abcd}	me_f1_1	0	0	0	0.03366	0.25618	0.163085	0.171676	0.131851	-51.41	-385.6972390	-385.8482513
maa_1f	me_f1_2	-14	-13	0	0.04082	0.23744	0.162561	0.171234	0.131189	-53.21	-385.6895749	-385.8440555
maa_1f	me_f1_3	-15	0	0	0.03736	0.24130	0.162272	0.171167	0.130232	-52.12	-385.6836150	-385.8370636
maa_1f	me_f1_4	-7	0	0	0.04144	0.23576	0.162336	0.171261	0.130267	-53.29	-385.6801809	-385.8348855
1g ^{abcd}	g1_1	0	0	0	-0.23250	-0.02310	0.123772	0.131493	0.092502	-8.33	-668.7731478	-668.8935009
1g	g1_2	-27	-22	-3	-0.22690	-0.02311	0.123357	0.131274	0.091246	-8.71	-668.7690290	-668.8892255
maa_1g ^{abcd}	me_g1_1	-6	0	0	0.02306	0.19542	0.159793	0.168952	0.127595	-50.34	-708.6856747	-708.8368715
maa_1g	me_g1_2	-32	-15	0	0.03464	0.18287	0.159193	0.168480	0.126729	-52.85	-708.6755408	-708.8312876
maa_1g	me_g1_3	-21	0	0	0.03087	0.18620	0.159344	0.168699	0.126529	-51.57	-708.6728149	-708.8267716
1h ^{abcd}	h1_cs_1	-16	-10	0	-0.23481	-0.01233	0.195529	0.206140	0.159990	-8.92	-537.7521363	-537.9293339
1h	h1_cs_3	-12	-11	0	-0.23646	-0.01074	0.195133	0.205753	0.159380	-9.21	-537.7478915	-537.9257182
1h	h1_cs_2	-9	0	0	-0.23642	-0.01079	0.194965	0.205754	0.158007	-9.17	-537.7460967	-537.9238619
1h	h1_cs_5	-21	-10	0	-0.23276	-0.00993	0.195136	0.205892	0.158784	-9.29	-537.7459518	-537.9234935
maa_1h ^{abcd}	h1_add_cs_1	-12	0	0	0.03189	0.20298	0.231067	0.243128	0.194553	-53.41	-577.6553878	-577.8646258
maa_1h	h1_add_cs_3	-29	-11	0	0.04194	0.19429	0.230477	0.242692	0.193585	-55.94	-577.6460346	-577.8595332
maa_1h	h1_add_cs_6	-14	-8	0	0.03767	0.20035	0.230473	0.242685	0.193339	-54.67	-577.6424220	-577.8545184
maa_1h	h1_add_cs_5	-10	0	0	0.03684	0.19332	0.230499	0.242838	0.192869	-54.27	-577.6411149	-577.8538581
1i ^{abcd}	i1_cs_1	-5	0	0	-0.24272	-0.00948	0.141093	0.149962	0.107973	-5.10	-271.7982944	-271.8863111
1i	i1_cs_2	-13	0	0	-0.24332	-0.01053	0.141402	0.150055	0.109404	-4.83	-271.7980310	-271.8858735
1i	i1_cs_3	0	0	0	-0.23903	-0.01203	0.141687	0.150320	0.109476	-5.10	-271.7955688	-271.8839563
maa_1i ^{abc}	i1_add_1	-11	-9	0	0.04243	0.24000	0.176916	0.186974	0.143909	-52.39	-311.6903942	-311.8137694
maa_1i	i1_add_5	-20	-12	0	0.03897	0.24586	0.177183	0.187076	0.144105	-51.24	-311.6905062	-311.8116997
maa_1i	i1_add_3	-10	-9	0	0.04132	0.23917	0.177019	0.187060	0.143831	-52.22	-311.6875001	-311.8104352
maa_1i ^d	i1_add_2	-4	0	0	0.04855	0.22827	0.176896	0.187015	0.143645	-53.78	-311.6853354	-311.8117927
maa_1i	i1_add_4	-27	-9	0	0.04804	0.22980	0.177046	0.187056	0.144049	-53.58	-311.6818892	-311.8080310
1j ^{ac}	j1_cs_1	-12	-3	0	-0.22563	-0.02762	0.114031	0.123015	0.081127	-5.88	-630.6652109	-630.7768767
1j	j1_cs_3	-16	-11	0	-0.21876	-0.02150	0.113518	0.122587	0.080271	-7.21	-630.6626927	-630.7733217
1j ^{bd}	j1_cs_6	-27	-13	-10	-0.22098	-0.02006	0.113187	0.122451	0.078868	-8.39	-630.6612771	-630.7722619
1j	j1_cs_2	-12	0	0	-0.23055	-0.02387	0.113598	0.122779	0.079721	-6.71	-630.6607001	-630.7728974
1j	j1_cs_4	-15	0	0	-0.22756	-0.02511	0.113776	0.122816	0.080468	-7.10	-630.6607481	-630.7728145
maa_1j ^{ac}	j1_add_1	-10	0	0	0.02345	0.20605	0.150008	0.160215	0.116315	-49.66	-670.5726875	-670.7145446
maa_1j ^{bd}	j1_add_3	-15	-3	0	0.02988	0.18835	0.149311	0.160097	0.114089	-52.68	-670.5655513	-670.7128251
maa_1j	j1_add_2	0	0	0	0.02748	0.19278	0.149831	0.160339	0.115695	-51.78	-670.5665256	-670.7132313
maa_1j	j1_add_4	-22	-14	-4	0.03058	0.20822	0.149527	0.159965	0.115535	-53.55	-670.5644642	-670.7087647
maa_1j	j1_add_5	-14	-9	-4	0.03621	0.19712	0.149399	0.159936	0.114951	-53.66	-670.5606522	-670.7077292
1m ^{abcd}	k1_cs_1	-6	-4	0	-0.25521	-0.06342	0.110034	0.117271	0.079513	-5.86	-345.5826850	-345.6941066
maa_1m ^{abcd}	k1_add_cs_1	-13	-2	0	0.02925	0.15315	0.145551	0.154468	0.112841	-54.27	-385.4879001	-385.6345414
1o ^{abcd}	l1_cs_2	-9	-6	0	-0.23442	-0.05149	0.142702	0.152478	0.108731	-7.12	-460.1103734	-460.2627691
1o	l1_cs_1	-3	0	0	-0.23370	-0.05201	0.142750	0.152517	0.108791	-7.11	-460.1103480	-460.2626696
maa_1o ^{abcd}	l1_add_cs_1	-10	-3	0	0.02856	0.14848	0.178099	0.189611	0.141771	-54.80	-500.0117866	-500.1985231
maa_1o	l1_add_cs_2	-8	0	0	0.02870	0.14769	0.178075	0.189599	0.141671	-54.95	-500.0113725	-500.1981003

^aLowest energy conformer in term of $\Delta G_{298} \{=\Delta E_{\text{tot}}[\text{B3LYP/6-31G(d,p)}] + \text{Coord. } \Delta G[\text{B3LYP/6-31G(d,p)}]\}$ at B3LYP/6-31G(d,p)

^bLowest energy conformer in term of $\Delta G_{\text{sol-sp}} (= \Delta G_{298}^{\text{a}} + \Delta G_{\text{Solv}})$ at B3LYP/6-31G(d,p).

^cLowest energy conformer in term of $\Delta G_{298} \{=\Delta E_{\text{tot}}[\text{B3LYP/6-311++G(3df,2pd)}//\text{B3LYP/6-31G(d,p)}] + \text{Coord. } \Delta G[\text{B3LYP/6-31G(d,p)}]\}$ at B3LYP/6-311++G(3df,2pd)//B3LYP/6-31G(d,p).

^dLowest energy conformer in term of $\Delta G_{\text{sol-sp}} (\Delta G_{298}^{\text{c}} + \Delta G_{\text{Solv}})$ at B3LYP/6-311++G(3df,2pd)//B3LYP/6-31G(d,p).

Table S31. QM properties for solvent phase (implicit DMSO) optimized conformers of neutral electrophiles (Figure S2) and their corresponding methyl anion adducts (maa).

Marker	File Name	Low Frequency			HOMO _E (hartree)	LUMO _E (hartree)	B3LYP/6-31G(d,p) Corr. ZPE (hartree)	Corr. ΔH (hartree)	Corr. ΔG (hartree)	ΔG_{Solv} (kcal/mol)	ΔE_{tot} (hartree)	ΔE_{tot} (hartree) [B3LYP/6-311++G(3df,2pd) //B3LYP/6-31G(d)]
CH ₃ ⁻¹	ch3anion	-286	-270	-79	-0.11861	0.15572	0.028670	0.032485	0.009517	-79.41	-39.9221619	-39.8583319
1a	a1_cs_1	-29	0	0	-0.23653	-0.01248	0.090925	0.096724	0.063001	-5.81	-231.2463040	-231.3137010
maa_1a	a1_add_cs_1	-25	0	0	-0.11512	0.11410	0.127602	0.134702	0.098548	-55.28	-271.2209148	-271.2479399
1b ^{ab}	b1_cs_1	-20	-16	0	-0.23074	-0.00688	0.121221	0.127702	0.092184	-6.30	-270.5941108	-270.6711392
maa_1b ^a	b1_add_cs_1	-22	0	0	-0.11095	0.11047	0.157497	0.165602	0.126609	-53.93	-310.5597995	-310.5969630
maa_1b ^b	b1_add_cs_2	-53	-21	0	-0.10958	0.09895	0.157042	0.165302	0.125940	-54.85	-310.5583622	-310.5960597
1c ^{ab}	c1_1	-13	0	0	-0.22976	-0.00511	0.150866	0.158292	0.120469	-6.53	-309.9155601	-310.0022605
1c	c1_2	-38	-35	-23	-0.22949	-0.00247	0.150543	0.158156	0.119660	-6.61	-309.9098148	-309.9964919
maa_1c ^{ab}	me_c1_1	-23	-11	-8	-0.11424	0.10955	0.186786	0.195652	0.155348	-52.46	-349.8870336	-349.9335870
maa_1c	me_c1_2	-119	-68	-25	-0.10859	0.10209	0.187454	0.196412	0.155670	-54.24	-349.8823976	-349.9299326
maa_1c	me_c1_3	0	0	0	-0.10969	0.10213	0.186709	0.195702	0.154790	-53.51	-349.8746915	-349.9225273
1d ^{ab}	d1_cs_2	-16	-7	0	-0.23016	-0.00267	0.179314	0.187988	0.146866	-6.72	-349.2268008	-349.3232966
1d	d1_cs_1	-22	-11	0	-0.23089	-0.00505	0.179530	0.188160	0.147123	-6.69	-349.2268651	-349.3235537
1d	d1_cs_4	-21	-15	0	-0.23006	-0.00343	0.179675	0.188428	0.147116	-6.64	-349.2227867	-349.3196107
1d	d1_cs_3	-31	-14	0	-0.23072	-0.00801	0.179823	0.188538	0.147583	-6.54	-349.2228099	-349.3199636
1d	d1_cs_5	-18	0	0	-0.22996	-0.00415	0.179695	0.188366	0.147280	-6.72	-349.2220929	-349.3188147
maa_1d ^{ab}	d1_add_cs_2	-30	-8	0	-0.11747	0.10082	0.215234	0.225472	0.181838	-51.49	-389.1940775	-389.2511407
maa_1d	d1_add_cs_1	-10	0	0	-0.10948	0.10086	0.215367	0.225460	0.182079	-53.11	-389.1902016	-389.2484985
maa_1d	d1_add_cs_3	-31	-15	0	-0.10868	0.09582	0.215377	0.225566	0.182019	-53.82	-389.1869719	-389.2451848
maa_1d	d1_add_cs_4	-19	-17	0	-0.10819	0.09343	0.215235	0.225477	0.181898	-53.86	-389.1868373	-389.2447651
maa_1d	d1_add_cs_5	0	0	0	-0.10992	0.09612	0.215790	0.225959	0.182145	-53.07	-389.1848047	-389.2430046
maa_1d	d1_add_cs_7	-55	-27	0	-0.11221	0.10077	0.215104	0.224625	0.182743	-50.59	-389.1831531	-389.2408072
maa_1d	d1_add_cs_6	-28	-23	-19	-0.10883	0.09589	0.215537	0.225843	0.181531	-53.70	-389.1762703	-389.2342237
1e ^{ab}	e1_1	-37	0	0	-0.21392	-0.00844	0.167164	0.175820	0.135281	-7.16	-365.2523471	-365.3581774
1e	e1_2	-36	-10	-4	-0.20634	-0.00493	0.167390	0.176038	0.135419	-7.80	-365.2498425	-365.3537784

Chapter 3: Kinetics and mechanism of oxirane-formation by Darzens condensation of ketones: quantification of the electrophilicities of ketones

le	e1_3	0	0	0	-0.20961	-0.00478	0.166961	0.175792	0.134563	-7.45	-365.2460581	-365.3515527
le	e1_4	-11	0	0	-0.20006	-0.00586	0.166624	0.175467	0.134038	-7.54	-365.2434439	-365.3484955
maa_le ^{ab}	me_e1_4	-36	-30	-19	-0.11562	0.11113	0.203109	0.213242	0.170049	-53.09	-405.2267966	-405.2933203
maa_le	me_e1_1	-24	0	0	-0.11068	0.10002	0.203075	0.213174	0.170061	-54.80	-405.2222488	-405.2890249
maa_le	me_e1_3	-16	0	0	-0.11630	0.10095	0.203595	0.213625	0.170741	-52.30	-405.2221685	-405.2881535
maa_le	me_e1_2	-26	0	0	-0.10979	0.09687	0.203371	0.213454	0.170405	-54.05	-405.2170955	-405.2843917
maa_le	me_e1_8	-21	0	0	-0.11220	0.10067	0.202903	0.213146	0.169309	-53.52	-405.2118213	-405.2792607
maa_le	me_e1_7	-8	0	0	-0.11174	0.10240	0.202911	0.213154	0.169374	-53.49	-405.2115419	-405.2793577
lf ^{ab}	fl_1	-33	-30	0	-0.23564	-0.01020	0.127006	0.134175	0.096801	-7.60	-345.8032969	-345.9091472
lf	fl_2	-31	-27	0	-0.23431	-0.00926	0.126305	0.133791	0.095175	-7.92	-345.7960416	-345.9018388
maa_lf ^{ab}	me_fl_1	-31	-21	0	-0.11723	0.11920	0.163145	0.171726	0.131901	-51.79	-385.7794579	-385.8486616
maa_lf	me_fl_2	-27	-15	-3	-0.11226	0.10856	0.162856	0.171511	0.131471	-53.57	-385.7746243	-385.8442402
maa_lf	me_fl_3	0	0	0	-0.11402	0.11000	0.162699	0.171523	0.130726	-52.48	-385.7669718	-385.8374967
maa_lf	me_fl_4	-34	-19	0	-0.11193	0.10459	0.162912	0.171734	0.131075	-53.73	-385.7654259	-385.8348046
lg ^{ab}	gl_1	-20	-9	0	-0.22291	-0.01208	0.123562	0.131329	0.092114	-8.51	-668.7865568	-668.8932901
maa_lg ^{ab}	me_gl_1	-21	-8	0	-0.12242	0.06321	0.160011	0.169148	0.127820	-50.77	-708.7662790	-708.8372596
maa_lg	me_gl_2	-35	-25	-10	-0.11439	0.05944	0.159617	0.168845	0.127153	-53.15	-708.7599931	-708.8314024
maa_lg	me_gl_3	0	0	0	-0.11629	0.05882	0.159889	0.169136	0.127247	-51.94	-708.7552893	-708.8271900
lh ^{ab}	hl_cs_1	-26	-17	0	-0.23242	-0.00823	0.195243	0.205899	0.159190	-9.13	-537.7665206	-537.9291948
lh	hl_cs_3	-34	-28	-16	-0.23315	-0.00533	0.194712	0.205443	0.157836	-9.40	-537.7627199	-537.9255488
lh	hl_cs_5	-30	-11	-7	-0.22950	-0.00612	0.194986	0.205717	0.158917	-9.62	-537.7610283	-537.9232046
maa_lh ^{ab}	hl_add_cs_1	-21	0	0	-0.11583	0.10448	0.231436	0.243472	0.194894	-54.45	-577.7413289	-577.8648431
maa_lh	hl_add_cs_3	-32	-18	0	-0.10972	0.09660	0.231110	0.243214	0.194508	-56.77	-577.7358397	-577.8594182
maa_lh	hl_add_cs_6	-11	0	0	-0.11181	0.10416	0.231099	0.243206	0.194263	-55.62	-577.7302996	-577.8547661
maa_lh	hl_add_cs_5	-29	0	0	-0.11177	0.10224	0.231135	0.243294	0.194226	-55.43	-577.7285408	-577.8538542
li ^{ab}	il_cs_1	-15	0	0	-0.23639	-0.00070	0.140996	0.149661	0.109056	-5.27	-271.8065786	-271.8861892
li	il_cs_2	-23	0	0	-0.23640	-0.00129	0.141085	0.149655	0.109375	-5.02	-271.8058864	-271.8857742
li	il_cs_3	-36	-28	0	-0.23358	-0.00399	0.141247	0.149876	0.109008	-5.42	-271.8039412	-271.8838893
maa_li ^a	il_add_1	-12	0	0	-0.11402	0.11036	0.177235	0.187177	0.144463	-52.81	-311.7742303	-311.8141348
maa_li	il_add_5	0	0	0	-0.11452	0.10794	0.177654	0.187407	0.145153	-51.70	-311.7725842	-311.8118173
maa_li ^b	il_add_2	-41	-9	0	-0.10970	0.10628	0.177184	0.187235	0.144060	-54.08	-311.7712698	-311.8118985
maa_li	il_add_3	-19	0	0	-0.11475	0.10680	0.177344	0.187261	0.144575	-52.63	-311.7710538	-311.8107844
maa_li	il_add_4	-27	0	0	-0.11015	0.10372	0.177281	0.187251	0.144279	-53.91	-311.7675408	-311.8081644
lj ^a	j1_cs_6	-20	0	0	-0.21847	-0.00976	0.113431	0.122542	0.080095	-8.67	-630.6748733	-630.7720686
lj ^b	j1_cs_1	-26	0	0	-0.22049	-0.01987	0.113741	0.122781	0.080558	-6.13	-630.6747791	-630.7768005
lj	j1_cs_3	-50	0	0	-0.21785	-0.00866	0.113660	0.122619	0.080475	-7.74	-630.6745596	-630.7730722
lj	j1_cs_2	0	0	0	-0.22258	-0.01814	0.113658	0.122705	0.080393	-6.85	-630.6715008	-630.7727460
lj	j1_cs_4	0	0	0	-0.22008	-0.01847	0.114197	0.123030	0.081386	-7.58	-630.6724276	-630.7725871
maa_lj ^a	j1_add_1	-50	-28	-21	-0.12307	0.06904	0.149927	0.159438	0.117389	-50.18	-670.6522179	-670.7149830
maa_lj	j1_add_4	-38	-26	0	-0.11991	0.07573	0.150077	0.160453	0.116042	-54.17	-670.6503027	-670.7091758
maa_lj	j1_add_2	-38	0	0	-0.12093	0.06719	0.150223	0.160580	0.116241	-52.30	-670.6494817	-670.7135661
maa_lj ^b	j1_add_3	-68	-29	0	-0.12098	0.06340	0.149856	0.159569	0.116749	-53.10	-670.6498482	-670.7131126
lm ^{ab}	kl_cs_1	-40	-23	-17	-0.25174	-0.05820	0.110029	0.117347	0.079246	-5.96	-345.5921016	-345.6939236

maa_1m ^{ab}	k1_add_cs_1	-16	0	0	-0.12608	0.01639	0.146180	0.155039	0.113488	-54.60	-385.5746388	-385.6347907
1o ^{ab}	l1_cs_2	-50	-28	-11	-0.22681	-0.04886	0.142328	0.152383	0.107254	-7.36	-460.1219030	-460.2625146
1o	l1_cs_1	0	0	0	-0.22657	-0.04956	0.143003	0.152675	0.109340	-7.35	-460.1218660	-460.2624157
maa_1o ^{ab}	l1_add_cs_1	-15	0	0	-0.12503	0.01605	0.178720	0.190137	0.142601	-55.70	-500.0998162	-500.1984906
maa_1o	l1_add_cs_2	0	0	0	-0.12488	0.01522	0.178802	0.190179	0.142931	-55.91	-500.0997097	-500.1980352

^aLowest energy conformer in term of $\Delta G_{\text{sol-opt}} \{=\Delta E_{\text{tot}} + \text{Coor. } \Delta G \}$ at B3LYP/6-31G(d,p), (smd, solvent=dmsol). Since optimization is carried out under implicit solvation, ΔE_{tot} term include ΔG_{Solv} :

^bLowest energy conformer in term of $\Delta G_{\text{sol-opt}} \{=\Delta E_{\text{tot}}[\text{B3LYP/6-311++G(3df,2pd)}/\text{B3LYP/6-31G(d,p)}] + \text{Coor. } \Delta G [\text{B3LYP/6-31G(d,p)}] + \Delta G_{\text{Solv}} \text{B3LYP/6-31G(d,p), smd, solvent=dmsol} \}$ at B3LYP/6-311++G(3df,2pd)//B3LYP/6-31G(d,p).

(9) References

- (1) Li, Z.; Chen, Q.; Mayer, P.; Mayr, H. *J. Org. Chem.* **2017**, *82*, 2011–2017.
- (2) Appel, R.; Hartmann, N.; Mayr, H. *J. Am. Chem. Soc.* **2010**, *132*, 17894.
- (3) Zhang, X. S.; Zhang, Y. F.; Li, Z. W.; Luo, F. X.; Shi, Z. J. *Angew. Chem., Int. Ed.* **2015**, *54*, 5478.
- (4) Hewkin, C. T.; Jackson, R. F. W.; Clegg, W. *J. Chem. Soc., Perkin Trans. I* **1991**, 3091.
- (5) Durst, T.; Tin, K. C.; Hirtzbach, F.; Decesare, J. M.; Ryan, M. D. *Can. J. Chem.* **1979**, *57*, 258.
- (6) Wan, X.; Meng, Q.; Zhang, H.; Sun, Y.; Fan, W.; Zhang, Z. *Org. Lett.* **2007**, *9*, 5613.
- (7) Hayasi, Y.; Nozaki, H. *Bull. Chem. Soc. Jpn.* **1972**, *45*, 198.
- (8) Mayr, H.; Ammer, J.; Baidya, M.; Maji, B.; Nigst, T. A.; Ofial, A. R.; Singer, T. *J. Am. Chem. Soc.* **2015**, *137*, 2580.
- (9) Allgäuer, D. S.; Jangra, H.; Asahara, H.; Li, Z.; Chen, Q.; Zipse, H.; Ofial, A. R.; Mayr, H. *J. Am. Chem. Soc.* **2017**, *139*, 13318.
- (10) Byrne, P. A.; Kobayashi, S.; Würthwein, E.-U.; Ammer, J.; Mayr, H. *J. Am. Chem. Soc.* **2017**, *139*, 1499.
- (11) Becke, A. D. *J. Chem. Phys.* **1993**, *98*, 5648.
- (12) Ditchfield, R.; Hehre, W. J.; Pople, J. A. *J. Chem. Phys.* **1971**, *54*, 724.
- (13) Krishnan, R.; Binkley, J. S.; Seeger, R.; Pople, J. A. *J. Chem. Phys.* **1980**, *72*, 650.
- (14) Clark, T.; Chandrasekhar, J.; Spitznagel, G. W.; Schleyer, P. v. R. *J. Comput. Chem.* **1983**, *4*, 294.
- (15) Marenich, A. V.; Cramer, C. J.; Truhlar, D. G. *J. Phys. Chem. B* **2009**, *113*, 6378.
- (16) Domingo, L. R.; Pérez, P.; Contreras, R. *Tetrahedron* **2004**, *60*, 6585.
- (17) Parr, R. G.; Yang, W. *Density-Functional Theory of Atoms and Molecules*; Oxford University Press: New York, 1989.
- (18) Parr, R. G.; Szentpaly, L. v.; Liu, S. *J. Am. Chem. Soc.* **1999**, *121*, 1922.
- (19) Contreras, R. R.; Fuentealba, P.; Galván, M.; Pérez, P. *Chem. Phys. Lett.* **1999**, *304*, 405.
- (20) Yang, W.; Mortier, W. J. *J. Am. Chem. Soc.* **1986**, *108*, 5708.

- (21) Mayer, R. J.; Tokuyasu, T.; Mayer, P.; Gomar, J.; Sabelle, S.; Mennucci, B.; Mayr, H.; Ofial, A. R. *Angew. Chem., Int. Ed.* **2017**, *56*, 13279.
- (22) Cances, E.; Mennucci, B.; Tomasi, J. *J. Chem. Phys.* **1997**, *107*, 3032.
- (23) Tomasi, J.; Mennucci, B.; Cammi, R. *Chem. Rev.* **2005**, *105*, 2999.
- (24) Grimme, S. *J. Comput. Chem.* **2006**, *27*, 1787.
- (25) Grimme, S.; Antony, J.; Ehrlich, S.; Krieg, H. *J. Chem. Phys.* **2010**, *132*, 154104.
- (26) Grimme, S. *J. Chem. Phys.* **2006**, *124*, 034108.
- (27) Weigend, F. *Phys. Chem. Chem. Phys.* **2006**, *8*, 1057.
- (28) Weigend, F.; Ahlrichs, R. *Phys. Chem. Chem. Phys.* **2005**, *7*, 3297.
- (29) Gaussian 09, Revision D.01, Frisch, M. J.; Trucks, G. W.; Schlegel, H. B.; Scuseria, G. E.; Robb, M. A.; Cheeseman, J. R.; Scalmani, G.; Barone, V.; Mennucci, B.; Petersson, G. A.; Nakatsuji, H.; Caricato, M.; Li, X.; Hratchian, H. P.; Izmaylov, A. F.; Bloino, J.; Zheng, G.; Sonnenberg, J. L.; Hada, M.; Ehara, M.; Toyota, K.; Fukuda, R.; Hasegawa, J.; Ishida, M.; Nakajima, T.; Honda, Y.; Kitao, O.; Nakai, H.; Vreven, T.; Montgomery, Jr., J. A.; Peralta, J. E.; Ogliaro, F.; Bearpark, M.; Heyd, J. J.; Brothers, E.; Kudin, K. N.; Staroverov, V. N.; Keith, T.; Kobayashi, R.; Normand, J.; Raghavachari, K.; Rendell, A.; Burant, J. C.; Iyengar, S. S.; Tomasi, J.; Cossi, M.; Rega, N.; Millam, J. M.; Klene, M.; Knox, J. E.; Cross, J. B.; Bakken, V.; Adamo, C.; Jaramillo, J.; Gomperts, R.; Stratmann, R. E.; Yazyev, O.; Austin, A. J.; Cammi, R.; Pomelli, C.; Ochterski, J. W.; Martin, R. L.; Morokuma, K.; Zakrzewski, V. G.; Voth, G. A.; Salvador, P.; Dannenberg, J. J.; Dapprich, S.; Daniels, A. D.; Farkas, O.; Foresman, J. B.; Ortiz, J. V.; Cioslowski, J.; Fox, D. J.; Gaussian, Inc.: Wallingford CT, 2013.

Chapter 4 Quantification of electrophilicities of carbon dioxide and other heteroallenes

4.1 Introduction

Heteroallenes¹ are important compounds in organic synthesis, which include ketenes,² isocyanates,³ isothiocyanates,⁴ carbodiimide,⁵ carbon disulfide,⁶ carbon dioxide,⁷ etc. We attempted to quantify the electrophilic reactivities of various heteroallenes to understand how the variation of hetero atoms affects their electrophilicities. With this information it would be possible to design new reactions and to predict the mechanisms of cycloaddition reactions between heteroallenes and π -nucleophiles, such as alkenes, enamines, and enol ethers.

Carbon dioxide is the most common heteroallene and is an important and useful C1 building block in organic synthesis because of its abundance, availability, and sustainability.⁸ However, carbon dioxide is difficult to activate and utilize under mild conditions because it is thermodynamically stable, although it is rather electrophilic. We have attempted to quantify the electrophilicity of CO₂ and hope that our investigation will guide chemists how to utilize CO₂ as a substrate in organic synthesis.

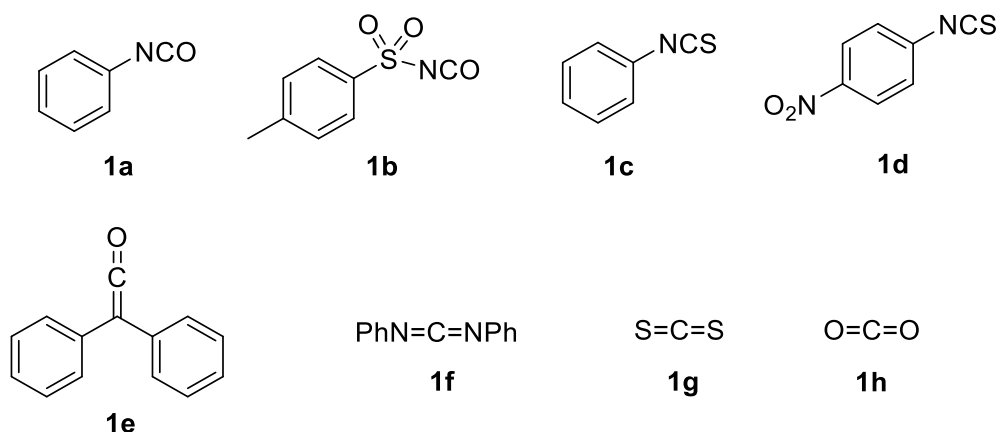


Figure 1. Heteroallenes **1a–1h** studied in this work

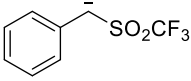
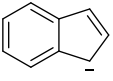
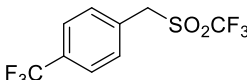
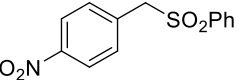
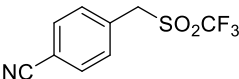
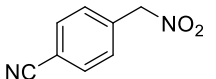
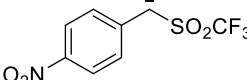
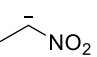
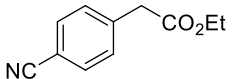
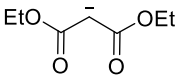
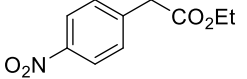
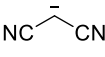
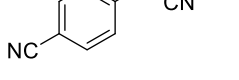
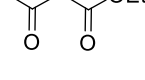
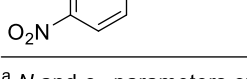
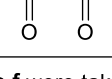
In previous work, we had developed scales of nucleophilicity and electrophilicity on the basis of eq 1, which can be used to predict scope and selectivities of reactions of electrophiles with nucleophiles. This linear free-energy relationship characterizes electrophiles by one parameter (electrophilicity E), and nucleophiles by two solvent-dependent parameters (nucleophilicity N and susceptibility s_N).⁹

$$\log k_2(20\text{ }^\circ\text{C}) = s_N(N + E) \quad (1)$$

4.2 Results

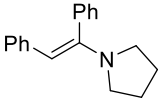
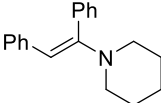
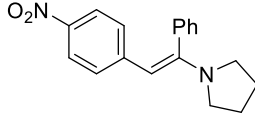
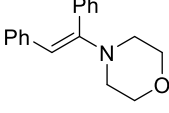
To quantify the electrophilicities of **1a–1h**, we now investigated the kinetics of the reactions of **1** with reference nucleophiles^{10,11} (carbanions **2** from Table 1 and enamines **3** from Table 2). All kinetic investigations were performed in DMSO or CH₃CN solution at 20 °C by following the disappearance of the UV/Vis absorptions of the nucleophiles **2** and **3** or formation of the UV/Vis absorptions of the products **4** under pseudo-first-order conditions ($[1]_0/[2(\text{or } 3)]_0 > 10$ or $[2]_0/[1]_0 > 10$). The first-order rate constants k_{obs} were obtained by least-squares fitting of the exponential function $A = A_0 \exp(-k_{\text{obs}}t) + C$ to the observed time-dependent absorbances of **2** or **4** (Figure 2a). The slopes of the linear correlations between k_{obs} and the different concentrations of the excess components (Figure 2b) correspond to the second-order rate constants k_2^{exp} listed in Table 3. As heteroallenes **1a**, **1b**, and **1e** are not persistent in DMSO solution, we performed the corresponding kinetic investigations in CH₃CN solution. The reaction of p-nitrophenyl isothiocyanate **1d** with carbanion **2c** was found to be 1.3 times faster in CH₃CN solution than in DMSO solution (Table 3). Since this difference is small with respect to the error limits of eq 1, we have applied N and s_N of the carbanions which were parameterized for DMSO solution also for deriving the electrophilicity parameters of heteroallenes in CH₃CN. Carbon dioxide is a gas under ambient conditions, and according to Henry's law the amount of dissolved gas in a liquid is directly proportional to the partial pressure of the gas. The preparation of different concentrations of solutions of carbon dioxide in DMSO is explicitly described in experimental section of this chapter. Titration with NaOH standard solution and phenolphthalein as indicator showed a concentration which is 5.6% higher than calculated from the solubility of CO₂ in DMSO under the atmospheric pressure of CO₂ by Henry's law. (detailed procedures of titration experiment are described in experimental section)

Table 1. Nucleophiles **2a–2p** and Their Reactivity Parameters N and s_N in DMSO

Nucleophile	N (s_N) ^a	Nucleophile	N (s_N) ^a
 2a	18.67 (0.68)	 2i	24.16 (0.68)
 2b	17.33 (0.74)	 2j	18.50 (0.75)
 2c	16.28 (0.75)	 2k	16.96 (0.73)
 2d	14.49 (0.86)	 2l	21.54 (0.62)
 2e	23.64 (0.65)	 2m	20.22 (0.65)
 2f	20.00 (0.71)	 2n	19.36 (0.67)
 2g	25.11 (0.54)	 2o	18.82 (0.69)
 2h	19.67 (0.68)	 2p	17.64 (0.73)

^a N and s_N parameters of **2a–d** were taken from ref 10a, those of **2e,f** were taken from 10b, those of **2g,h** were taken from 10c, those of **2i** were taken from 10d, those of **2j** were taken from ref 10e, those of **2k** were taken from ref 10f, those of **2l** were taken from ref 10g, those of **2m–p** were taken from ref 9b.

Table 2. Nucleophiles **3a–d** and Their Reactivity Parameters N and s_N in CH_3CN

Nucleophile	N (s_N) ^a	Nucleophile	N (s_N) ^a
 3a	11.66 (0.82)	 3c	9.94 (0.86)
 3b	10.42 (0.82)	 3d	8.78 (0.83)

^a N and s_N parameters of **3a–d** were taken from ref 10h.

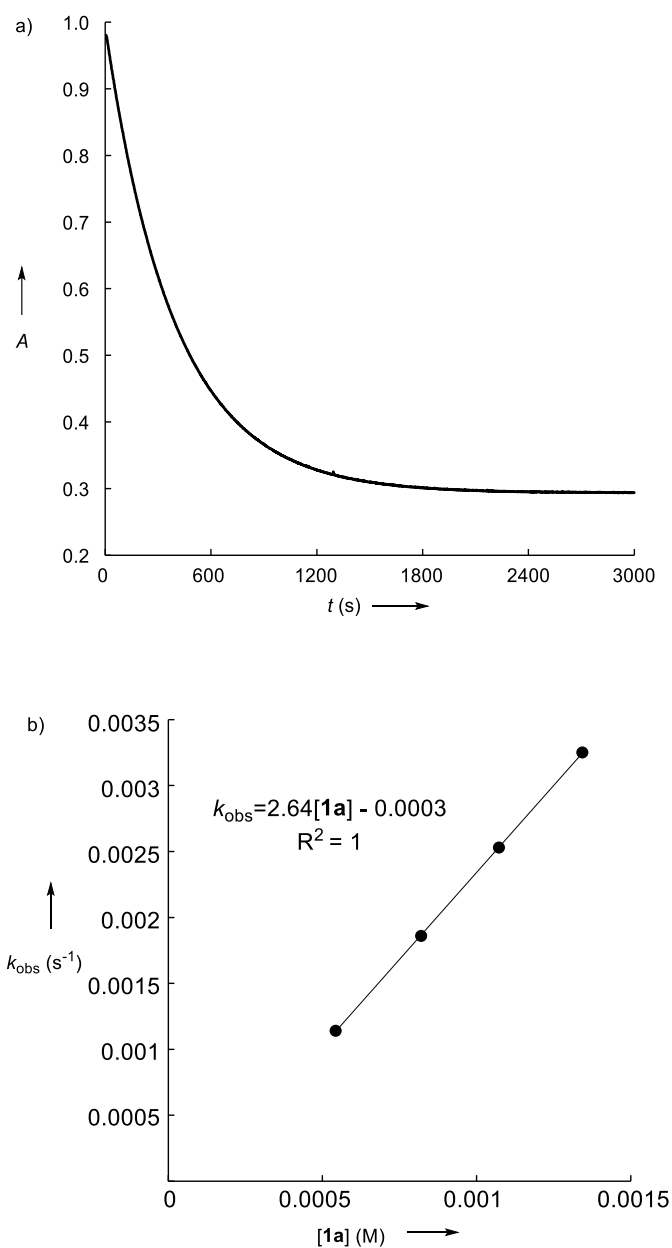
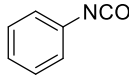
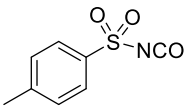
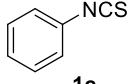
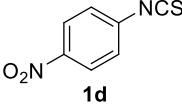
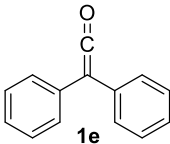


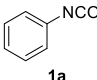
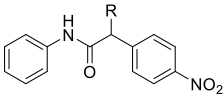
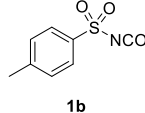
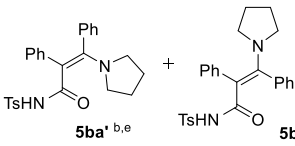
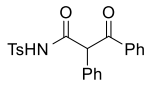
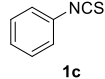
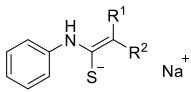
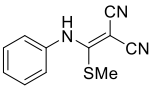
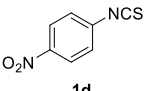
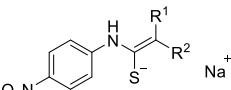
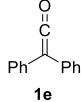
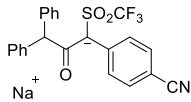
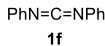
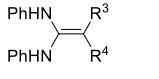
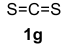
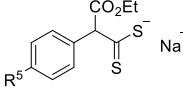
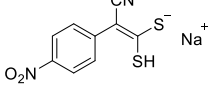
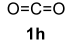
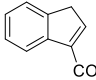
Figure 2. a) Monoexponential decay of the absorbance A of **2c** (at 344 nm) during the reaction of **1a** (1.07×10^{-3} mol L⁻¹) with **2c** (5.00×10^{-5} mol L⁻¹) in CH₃CN at 20 °C. b) Plot of k_{obs} for the reaction of **1a** with **2c** versus the concentration of **1a**.

Table 3. Second-Order Rate Constants k_2^{exp} (20 °C) and Calculated Values k_2^{cald} from Equation 1 for the Reactions of Heteroallenes **1** with Nucleophiles **2** and **3**.

Heteroallene	<i>E</i> parameter	Nucleophile	k_2^{exp} (M ⁻¹ s ⁻¹)	k_2^{cald} (M ⁻¹ s ⁻¹)	$k_2^{\text{exp}}/k_2^{\text{cald}}$
 1a	-15.55 (in CH ₃ CN)	2b	2.49×10^1	2.08×10^1	1.20
		2c	2.65×10^0	3.52×10^0	0.75
		2d	3.29×10^{-1}	1.23×10^{-1}	2.67
		2h	2.35×10^2	6.33×10^2	0.37
		2j	2.95×10^2	1.63×10^2	1.81
 1b	-7.68 (in CH ₃ CN)	3a	2.03×10^3	1.83×10^3	1.11
		3b	1.80×10^2	1.77×10^2	1.02
		3c	7.56×10^1	8.78×10^1	0.86
		3d	7.96×10^0	8.18×10^0	0.97
 1c	-18.18 (in DMSO)	2a	2.03×10^0	2.15×10^0	0.94
		2l	5.36×10^1	1.21×10^2	0.44
		2n	2.69×10^1	6.17×10^0	4.36
		2o	1.15×10^0	2.76×10^0	0.42
		2p	6.45×10^{-1}	4.03×10^{-1}	1.60
 1d	-15.87 (in DMSO)	2c	2.47×10^0 ^a	2.03×10^0	1.22
		2m	2.72×10^2	6.72×10^2	0.40
		2n	1.24×10^3	2.18×10^2	5.69
		2o	9.08×10^1	1.09×10^2	0.83
		2p	7.72×10^0	1.96×10^1	0.39
 1e	-11.21 (in CH ₃ CN)	2a	2.32×10^4	1.18×10^5	0.20
		2c	1.87×10^3	6.35×10^3	0.29
		2d	1.22×10^3	6.62×10^2	1.84
		2k	2.20×10^5	1.58×10^4	13.9
PhN=C=NPh 1f	-20.19 (in DMSO)	2a	2.80×10^{-1}	9.26×10^{-2}	3.02
		2e	1.42×10^2	1.74×10^2	0.82
		2g	2.65×10^2	4.54×10^2	0.58
		2m	5.96×10^{-1}	1.05×10^0	0.57
		2o	2.41×10^{-1}	1.13×10^{-1}	2.13
S=C=S 1g	-17.90 (in DMSO)	2a	9.95×10^0	3.34×10^0	2.98
		2b	4.19×10^{-1}	3.79×10^{-1}	1.11
		2f	2.19×10^1	3.10×10^1	0.71
		2e	1.97×10^3	5.38×10^3	0.37
		2h	2.60×10^1	1.60×10^1	1.63
O=C=O 1h	-16.54 (in DMSO)	2i	1.51×10^5		

^a $k_2^{\text{exp}} = 3.19 \times 10^0$ in CH₃CN

Table 4. Product Studies of Heteroallenes **1** with Nucleophiles **2** and **3**.

heteroallens	nucleophiles	reaction conditions	products
 1a	2d 2h 2j	(1) 1a , <i>t</i> -BuOK, CH ₃ CN, 20 °C (2) 2-H , 4 h (3) NH ₄ Cl	 4ad (87%) ^a 4ah (80%) ^a 4aj (90%) ^a
 1b	3a	(a) CD ₃ CN, 20 °C (b) 5ba , 2 % HCl	 5ba ^{a, b, e} + 5ba'' ^{a, b, e}  6ba (70%) ^a
 1c	2n 2o 2p	(a) 2-H , NaOH, (CD ₃) ₂ SO 2 h, 20 °C (b) 4cn ⁻ Na ⁺ , CH ₃ I, (CD ₃) ₂ SO	 4cn ⁻ Na ⁺ ^{a, b, c} 4co ⁻ Na ⁺ ^{a, b, d} 4cp ⁻ Na ⁺ ^{a, b, c}  7cn (80%) ^a
 1d	2n 2o 2p	2-H , NaOH, (CD ₃) ₂ SO 2 h, 20 °C	 4dn ⁻ Na ⁺ ^{a, b, e} 4do ⁻ Na ⁺ ^{a, b, d} 4dp ⁻ Na ⁺ ^{a, b, e}
 1e	2c	2c-H , NaOH, 20 °C, 2 h CD ₃ CN/(CD ₃) ₂ SO (5:1) ^g	 4ec ⁻ Na ⁺ ^{a, b, c}
 1f	2a 2e 2g 2m 2o	(1) 2-H , <i>t</i> -BuOK, DMSO, 20 °C (2) 1f , 4 h (3) NH ₄ OAc (aq) (pH = 7.10)	 4fa (95%) ^a 4fe (75%) ^a 4fg (85%) ^a 4fm (90%) ^a 4fo (80%) ^a
 1g	2e 2f 2h	2-H , NaOH, (CD ₃) ₂ SO 20 °C, 2 h	 4ge ⁻ Na ⁺ ^{a, b, f} 4gf ⁻ Na ⁺ ^{a, b, e}  4gh ⁻ Na ⁺ ^{a, b, c}
 1h	2i	(1) 2i-H , <i>t</i> -BuOK, DMSO, 20 °C (2) 1h (solid), 30 min (3) 2 M HCl	 4hi (80%) ^a

^a Isolated yield obtained after chromatographic purification and products are characterized by ¹H NMR, ¹³C NMR, IR, and HRMS. ^b Products are formed in deuterated solvents and analyzed without purification. ^c Products are identified by ¹H NMR and HRMS. ^d Products are identified by ¹H NMR, ¹³C NMR, and HRMS. ^e Products are identified by ¹H NMR. ^f Product is identified by ¹H NMR and ¹³C NMR. ^g Mixed solvents were used because of poor solubility of product **4ec**⁻Na⁺ in CD₃CN.

The reactions of heteroallenes **1** with nucleophiles **2** or **3** in DMSO or CH₃CN proceeded smoothly at 20 °C (Table 4); in some cases the products were unstable and decomposed

immediately. The carbanions **2d,h,j** generated by treatment of (**2d,h,j**)-H with *t*-BuOK, reacted with phenyl isocyanate (**1a**) to form an adduct, which was treated with NH₄Cl solution to give the isolated products **4**. Analogously, the products **4** of reactions of diphenyl carbodiimide (**1f**) with various carbanions **2** were obtained in good yield after treatment with NH₄OAc solution.

While reactions of phenyl isocyanate with 1-pyrrolidino-2-methyl-prop-1-ene have been reported to give [2+2] cycloaddition products,¹² the β -pyrrolidino- α,β -unsaturated amides **5ba'** and **5ba''** were formed through nucleophilic addition of **3a** to tosyl isocyanate (**1b**) and subsequent proton shift, in analogy to reported reactions of tosyl isocyanate (**1b**) with other enamines.¹³ The mixture of *E* and *Z* isomers was identified by two sets of pyrrolidino protons in the ¹H NMR spectrum (δ 2.93, 1.78 and δ 2.73, 1.63). As **5ba'** and **5ba''** were difficult to isolate, the mixture of enamines was treated with 2% aqueous HCl to give the hydrolysis product **6ba**, which was isolated in moderate yield.

The adduct **4cn**⁻Na⁺ formed from phenyl isothiocyanate (**1c**) and **2n** was identified by the NH resonance in the ¹H NMR spectrum (δ = 8.89 ppm in (CD₃)₂SO) and the molecular anion peak in the high resolution mass spectrum (ESI method). Further confirmation of its structure was obtained by treatment of **4cn**⁻Na⁺ with CH₃I to yield the methylation product **7cn** in 80% yield. Analogously, the products formed by addition of carbanions to *p*-nitrophenyl isothiocyanate (**1d**), diphenyl ketene (**1e**), and carbon disulfide (**1g**) were analyzed directly by NMR spectroscopy as they could not be isolated. Since the adduct **4ec**⁻Na⁺ was not well dissolved in CD₃CN, 0.2 equivalent of (CD₃)₂SO with respect to CD₃CN was added.

The indenide ion **2i** (generated in DMSO solution from **2i**-H and *t*-BuOK) reacted with solid CO₂ in DMSO, and 1*H*-indene-3-carboxylic acid (**4hi**) was isolated in 80% yield after treatment with 2 M HCl. On the other hand, none of the carbanions listed in Scheme 1 reacted with CO₂ under similar conditions; Only fluorenyl ion **2t** gave a trace of fluorene-9-carboxylic acid (Scheme 1). Since the failure of forming carboxylation products also includes carbanions with similar p*K*_{aH} values as indenide (**2i**), we assume that isomerization of **4hi**⁻, initially formed from **2i** and CO₂, to the conjugated carboxylate ion **4hi**⁻ provides the necessary thermodynamic driving force (Scheme 2). Probably carbanions with p*K*_{aH} > 22.6 (fluorenyl **2t**) are needed to give carboxylation products under the conditions of our kinetic experiments, if subsequent isomerization is not possible.

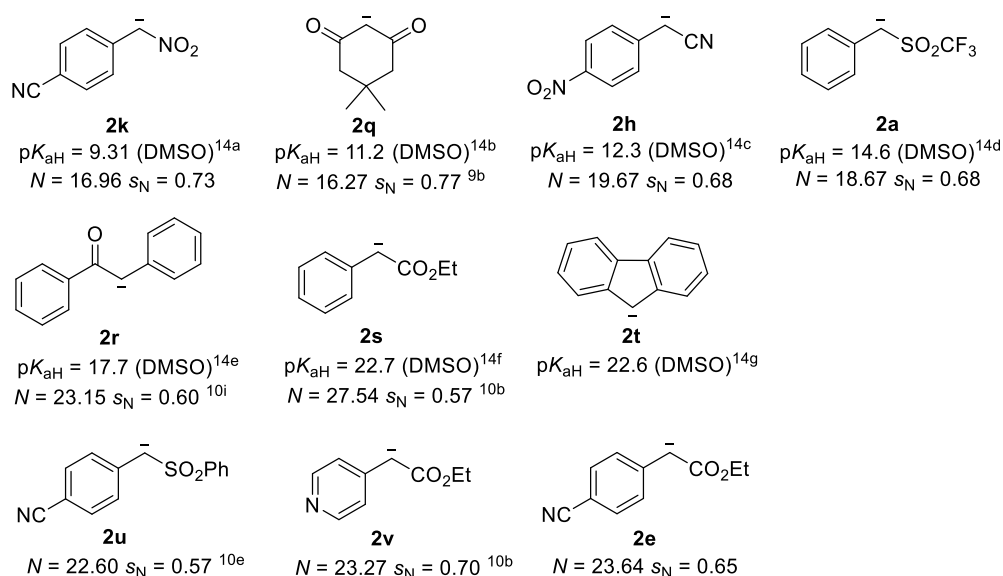
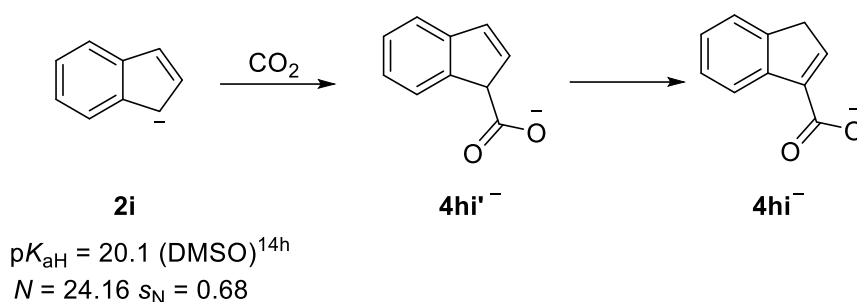
Scheme 1. Carbanions not reacting with CO₂ in DMSO**Scheme 2.** Carboxylation of indenide **2i**

Figure 3 shows that the correlations of $(\log k_2)/s_N$ for the reactions of heteroallenes **1** with carbanions **2** and enamines **3** versus the corresponding nucleophilicity parameters N are linear with a slope of roughly 1.0 as required by eq 1. It indicates that the reactions of cumulative π systems with enamines and carbanions follow the linear free-energy relationship (1) as the corresponding reactions of benzhydrylium ions and other π electrophiles.¹ Electrophilicity parameters E for heteroallenes **1** in the second column of Table 3 were determined by least-squares minimization [minimization of $\Delta^2 = \sum(\log k_2 - s_N(N + E))^2$] based on the rate constants of their reactions with carbanions **2** and enamines **3**.

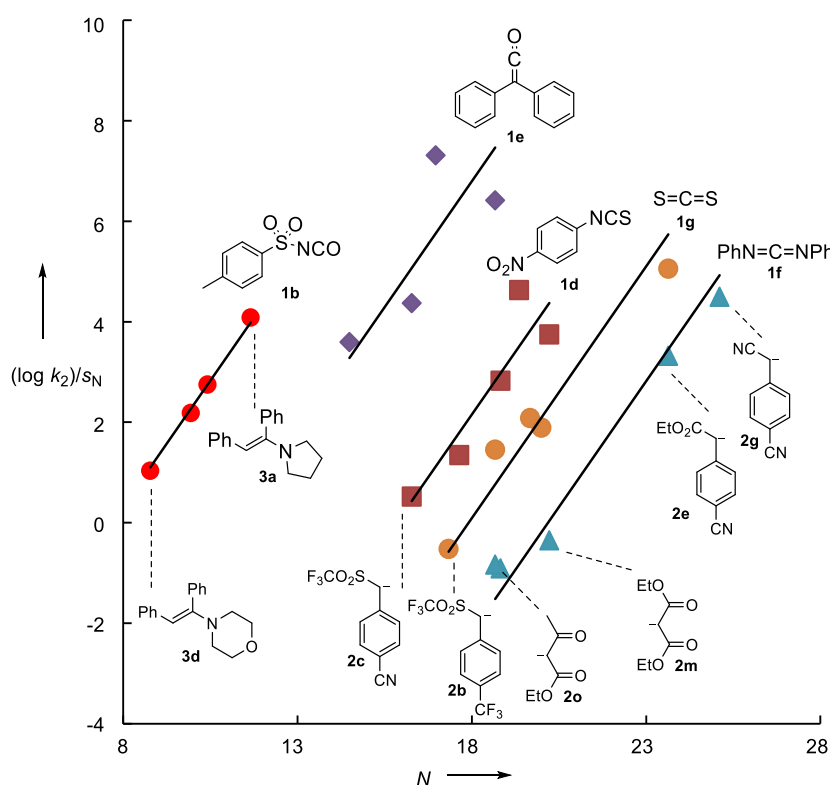


Figure 3. Plot of $(\log k_2)/s_N$ vs N for the reactions of heteroallenes **1** with carbanions **2** and enamines **3** in DMSO or CH_3CN at 20 °C (the slope is enforced to 1). For the sake of clarity, the correlation lines for **1a** and **1c** are shown only in the experimental section.

Figure 4 compares the electrophilicities E of the heteroallenes which have been investigated in this work. For the phenyl-substituted compounds, one can see the general ordering of electrophilic reactivities: ketene > isocyanate > isothiocyanate > carbodiimide. Phenyl isocyanate (**1a**) is 2.5 orders of magnitude more reactive than phenyl isothiocyanate (**1c**), and diphenyl ketene (**1e**) is around 4.5 orders of magnitude more reactive than phenyl isocyanate (**1a**). Although carbon dioxide (**1h**) doesn't react with most carbanions of Scheme 1, our kinetic measurements indicate that it is more electrophilic than carbon disulfide (**1g**), phenyl isothiocyanate (**1c**), and diphenyl carbodiimide (**1f**) (Figure 4). Since these heteroallenes react smoothly with several of the carbanions of Scheme 1 (Table 4), we must conclude that the high electrophilicity of CO_2 is due to a low intrinsic barriers. From tosyl isocyanate (**1b**) to diphenyl carbodiimide (**1f**), the electrophilicities scale cover almost 13 orders of magnitude.

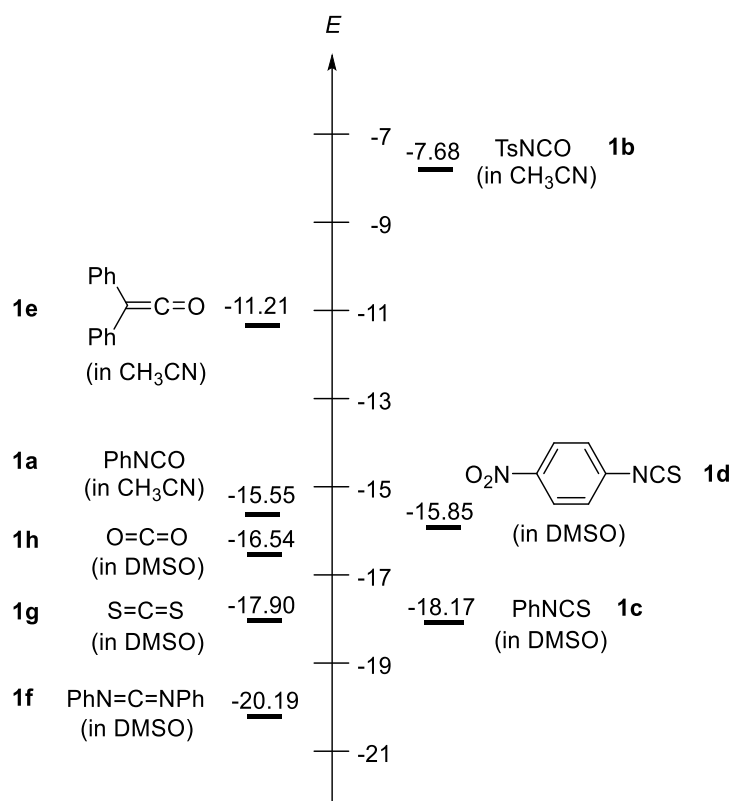


Figure 4. Comparison of the electrophilicities of heteroallenes

4.3 Quantum Chemical Calculations

In order to probe the origin of the different electrophilic reactivities of the heteroallenes, we have performed quantum chemical calculations (Table 5). We calculated Parr's global electrophilicity indices ω and local electrophilicity indices ω_c at the central sp-hybridized carbon atoms using the same methods described previously.¹⁵ Furthermore, methyl anion affinities (MAAs) which are defined as the negative of the reaction Gibbs energies for the addition of methyl anion to heteroallenes (eq 2) have been calculated by the previously reported methods.¹⁵

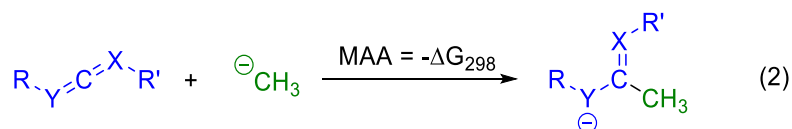
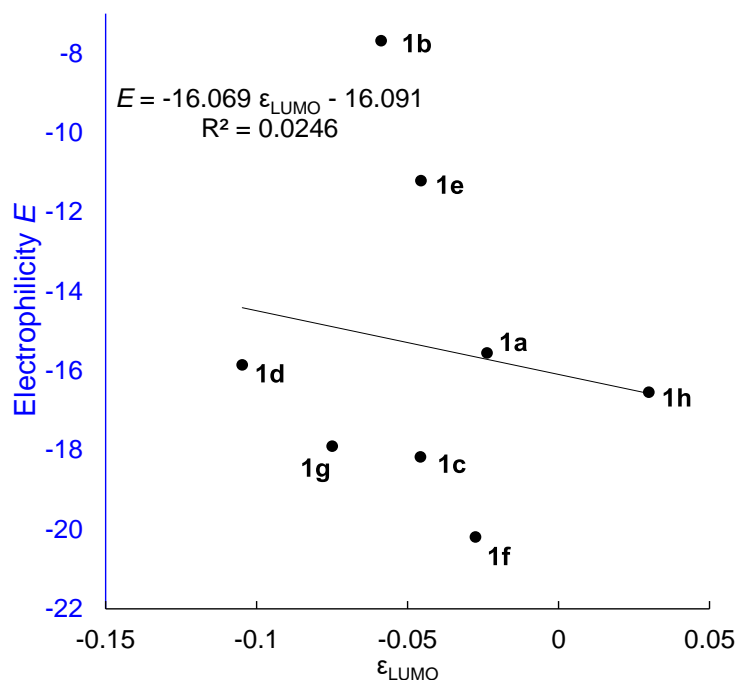


Table 5. DFT calculated Frontier Orbital Energies (Hartree), Global (ω) and Local (ω_C) Parr Electrophilicity Indices (in eV) as well as Methyl Anion Affinities (MAAs, in kJ mol⁻¹) of Heteroallenes

Electrophile	E^a	ϵ_{HOMO}^b	ϵ_{LUMO}^b	Global ω^b	Local ω_C^b	$\Delta G_{\text{gas}}(-\text{MAA})^c$	$\Delta G_{\text{sol-sp}}(-\text{MAA})^d$
1a	-15.55	-0.23744	-0.02371	1.09	0.17	-261.0	-133.4
1b	-7.68	-0.27376	-0.05875	1.75	0.23	-336.9	-201.7
1c	-18.18	-0.23182	-0.04576	1.41	0.15	-276.1	-148.4
1d	-15.87	-0.25644	-0.10474	2.92	0.16	-342.3	-171.9
1e	-11.21	-0.20205	-0.04555	1.33	0.27	-297.5	-144.6
1f	-20.19	-0.22394	-0.02753	1.10	0.16	-281.6	-129.7
1g	-17.90	-0.27776	-0.07494	2.09	0.21	-277.0	-174.7
1h	-16.54	-0.36997	0.02992	0.98	0.55	-209.4	-118.3

^a Empirical electrophilicity parameters from Table 4, as defined in equation 1. ^b Calculated at B3LYP/6-31G(d,p) level in the gas phase. ^c Calculated at B3LYP/6-311+G(3df,2pd)¹⁶//B3LYP/6-31G(d,p) level in the gas phase. ^d Based on methyl anion affinities (ΔG_{gas}), which were corrected for solvent effects by adding single point solvation energies calculated at B3LYP/6-31G(d,p) using the SMD (solvent = DMSO) solvation model¹⁷ on gas phase optimized geometries at the same level.

**Figure 5.** Correlation of the electrophilicities (E) of heteroallenes with their gas-phase lowest unoccupied molecular orbital energies (ϵ_{LUMO} , Hartree) calculated at the B3LYP/6-31G(d,p) level of theory.

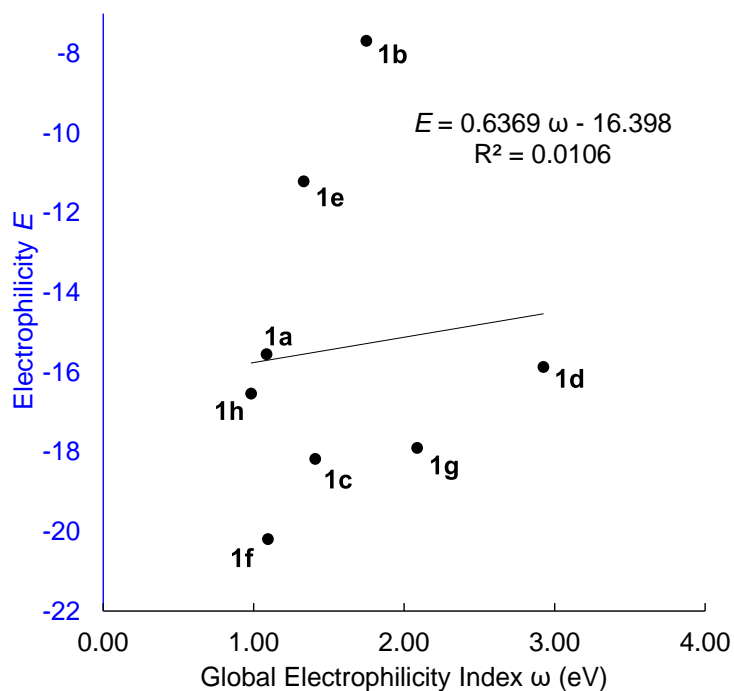


Figure 6. Correlation of the electrophilicities (E) of heteroallenes with Parr's global electrophilicity index (ω) calculated at the B3LYP/6-31G(d,p) level of theory.

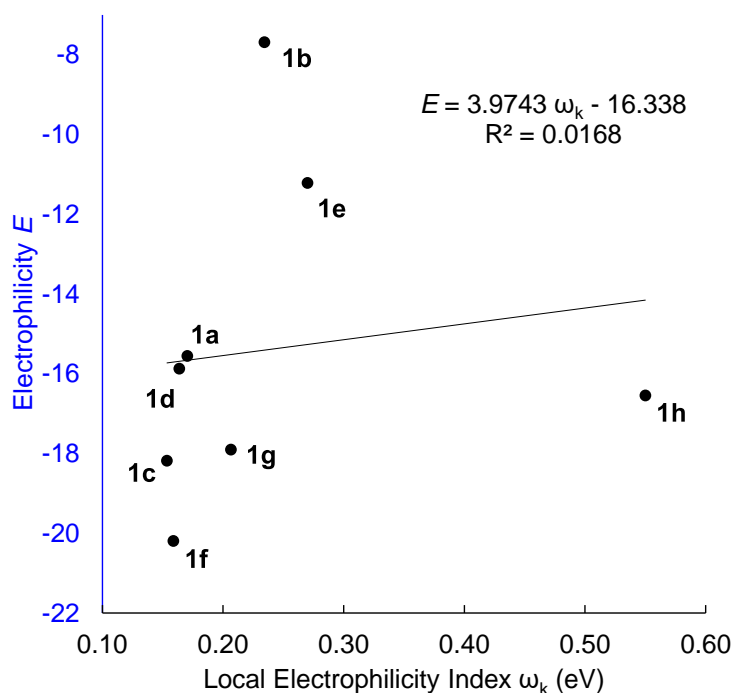


Figure 7. Correlation of the electrophilicities (E) of heteroallenes with local electrophilicity index (ω_k) calculated at the B3LYP/6-31G(d,p) level of theory.

Figure 5 shows that the electrophilicity parameters E of heteroallenes do not correlate with LUMO energies in the gas phase. Neither Parr's global electrophilicity index ω nor local

electrophilicity index ω_k is adequate to predict electrophilic reactivities of heteroallenes, since their correlations with empirical electrophilicities E are awful (Figure 6 and Figure 7).

Whereas the electrophilic reactivities of acceptor substituted ethylenes^{15a} and ketones^{15b} correlate fairly with the calculated methyl anion affinities (MAA, eq 2), Figure 8 shows that the corresponding correlation is very poor for nucleophilic additions to heteroallenes. One can see, however, that all compounds comprising a C=O double bond are above the correlation line, whereas those with only C=N and C=S double bonds react more slowly than expected from their thermodynamic driving force. Whereas it is obvious that nucleophilic attack at the carbodiimide **1f** initially yields a perpendicular azaallyl anion which must undergo internal rotation to gain full resonance stabilization, the same situation is encountered when the nucleophilic attack at the isothiocyanates **1c** and **1d** occurs at the C=N double bond. Transition state calculations are needed to clarify whether nucleophiles attack at π^*_{CN} or π^*_{CS} .

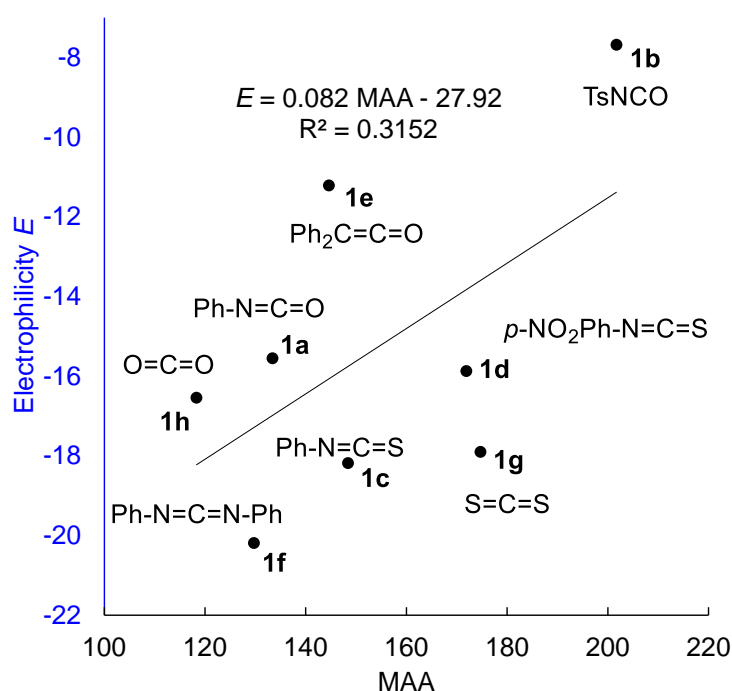


Figure 8. Correlation between electrophilicities (E) of heteroallenes **1** with their MAA_{sol-sp} values ($-\Delta G_{sol-sp}$, kJ mol^{-1}) calculated at SMD (DMSO)/B3LYP/6-311++G(3df,2pd)//B3LYP/6-31G(d,p) level of theory.

Conclusion

The rate constants for the reactions of heteroallenes **1** with the carbanions **2** and enamines **3** in DMSO or CH₃CN follow the linear free-energy relationship eq 1, which allowed us to determine the electrophilicity parameters E for heteroallenes from these rate constants and the previously reported reactivity parameters N and s_N for the carbanions **2** and enamines **3**. Fair correlations were neither obtained with the calculated methyl anion affinities nor with their LUMO energies and Parr's electrophilicity indices.

4.4 Experimental section

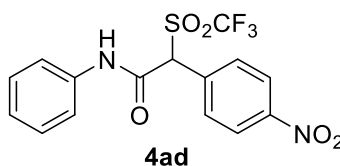
(1) Product study

Procedure A for the synthesis of **4**. To a solution of *t*-BuOK (22 mg, 0.20 mmol) in anhydrous CH₃CN (1 mL) at room temperature were added a solution of **2**-H (0.20 mmol) in anhydrous CH₃CN (0.5 mL) and then a solution of **1** (0.20 mmol) in anhydrous CH₃CN (0.5 mL). After 4 h, 10 mL of saturated NH₄Cl solution was added and the mixture was extracted with CHCl₃ (3 × 20 mL). The combined organic phase was washed with brine (1 × 30 mL), dried with anhydrous MgSO₄, and filtered. The solvent was evaporated under reduced pressure, and the residue was purified by column chromatography to give product.

Procedure B for the synthesis of **4**. To a solution of **1** (0.20 mmol) and **2**-H (0.20 mmol) in anhydrous (CD₃)₂SO (0.6 mL) at room temperature was added NaOH (8.0 mg, 0.20 mmol). After 2 h, the reaction mixture was analyzed by ¹H NMR spectroscopy without further workup.

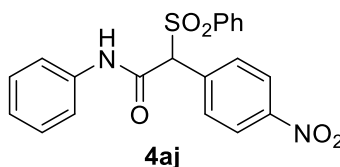
Procedure C for the synthesis of **4**. To a solution of *t*-BuOK (22 mg, 0.20 mmol) in anhydrous DMSO (1 mL) at room temperature were added a solution of **2**-H (0.20 mmol) in anhydrous DMSO (0.5 mL) and then a solution of **1** (0.20 mmol) in anhydrous DMSO (0.5 mL). After 4 h, 10 mL of NH₄OAc solution (pH ≈ 7) was added and the mixture was extracted with CHCl₃ (3 × 20 mL). The combined organic phase was washed with water (2 × 30 mL) and brine (1 × 30 mL), dried with anhydrous MgSO₄, and filtered. The solvent was evaporated under reduced pressure, and the residue was purified by column chromatography to give product.

2-(4-Nitrophenyl)-N-phenyl-2-((trifluoromethyl)sulfonyl)acetamide (4ad) was obtained according to Procedure A from **1a** (24 mg, 0.20 mmol) and **2d-H** (54 mg, 0.20 mmol): yellow solid (66 mg, 0.17 mmol, 85%), mp 175–180 °C.



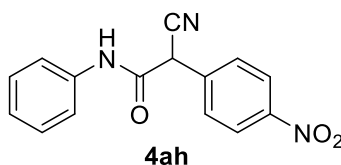
¹H NMR (400 MHz, CD₃CN) δ 8.99 (s, 1H), 8.32 (d, *J* = 8.9 Hz, 2H), 8.02 (d, *J* = 8.9 Hz, 2H), 7.54 (d, *J* = 7.5 Hz, 2H), 7.37 (t, *J* = 8.4 Hz, 2H), 7.20 (t, *J* = 7.4 Hz, 1H), 5.87 (s, 1H). **¹³C NMR** (101 MHz, CD₃CN) δ 159.4 (C=O), 150.4 (C), 138.1 (C), 133.5 (C), 133.0 (CH), 130.1 (CH), 126.5 (CH), 124.9 (CH), 121.2 (q, *J*_{CF} = 232 Hz), 121.1 (CH), 70.8 (CH). **HRMS** (EI) *m/z*: [*M*⁺] calcd for [C₁₅H₁₁F₃N₂O₅S]⁺ 388.0335, found 388.0355. **IR** (ATR) *ν* (cm⁻¹) = 3318, 2954, 2199, 1664, 1601, 1494, 1448, 1367, 1195, 1110, 978, 854, 740, 688.

2-(4-Nitrophenyl)-N-phenyl-2-(phenylsulfonyl)acetamide (4aj) was obtained according to Procedure A from **1a** (24 mg, 0.20 mmol) and **2j-H** (55 mg, 0.20 mmol): pale yellow solid (71 mg, 0.18 mmol, 90%), mp 188–193 °C.



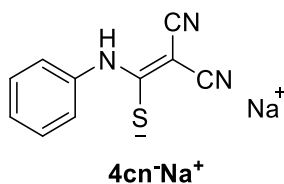
¹H NMR (400 MHz, CD₃CN) δ 8.75 (s, 1H), 8.16 (d, *J* = 8.9 Hz, 2H), 7.76 (d, *J* = 8.9 Hz, 2H), 7.69 (m, 3H), 7.57 – 7.50 (m, 2H), 7.46 (d, *J* = 7.4 Hz, 2H), 7.36 – 7.29 (m, 2H), 7.15 (t, *J* = 7.4 Hz, 1H), 5.40 (s, 1H). **¹³C NMR** (101 MHz, CD₃CN) δ 161.8 (C=O), 149.6 (C), 138.5 (C), 137.7 (C), 136.7 (C), 135.7 (CH), 132.8 (CH), 130.4 (CH), 130.1 (CH), 130.0 (CH), 126.0 (CH), 124.2 (CH), 120.9 (CH), 75.4 (CH). **HRMS** (EI) *m/z*: [*M*⁺] calcd for [C₂₀H₁₆N₂O₅S]⁺ 396.0774, found 396.0773. **IR** (ATR) *ν* (cm⁻¹) = 3351, 2953, 1693, 1673, 1600, 1518, 1444, 1344, 1145, 1080, 975, 847, 747, 683.

2-Cyano-2-(4-nitrophenyl)-N-phenylacetamide (4ah) was obtained according to Procedure A from **1a** (24 mg, 0.20 mmol) and **2h-H** (32 mg, 0.20 mmol): yellow solid (45 mg, 0.16 mmol, 80%), mp 150–155 °C.



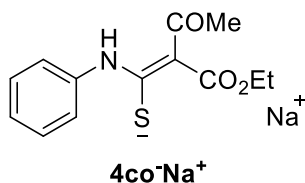
^1H NMR (400 MHz, CD_3CN) δ 8.81 (s, 1H), 8.27 (d, $J = 8.9$ Hz, 2H), 7.79 (d, $J = 8.8$ Hz, 2H), 7.50 (d, $J = 7.7$ Hz, 2H), 7.34 (t, $J = 7.9$ Hz, 2H), 7.15 (t, $J = 7.4$ Hz, 1H), 5.16 (s, 1H). **^{13}C NMR** (101 MHz, CD_3CN) δ 162.6 (C=O), 149.3 (C), 139.6 (C), 138.6 (C), 130.3 (CH), 130.0 (CH), 126.0 (CH), 125.3 (CH), 121.0 (CH), 117.3 (C), 45.7 (CH). **HRMS** (EI) m/z : $[\text{M}^+]$ calcd for $[\text{C}_{15}\text{H}_{11}\text{N}_3\text{O}_3]^+$ 281.0795, found 281.0792. **IR** (ATR) ν (cm^{-1}) = 3309, 2930, 1669, 1598, 1517, 1444, 1344, 1251, 1110, 943, 863, 751, 730, 688.

Sodium 2,2-dicyano-1-(phenylamino)ethene-1-thiolate ($4\text{cn}^-\text{Na}^+$) was obtained according to Procedure B from **1c** (24 mg, 0.20 mmol) and **2n-H** (13 mg, 0.20 mmol).



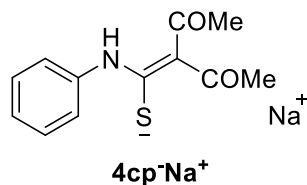
^1H NMR (400 MHz, $(\text{CD}_3)_2\text{SO}$) δ 8.89 (s, 1H), 7.49 (d, $J = 7.4$ Hz, 2H), 7.27 – 7.18 (m, 2H), 7.01 (t, $J = 7.4$ Hz, 1H). **HRMS** (ESI^-) m/z : $[\text{M}-\text{Na}^+]$ calcd for $[\text{C}_{10}\text{H}_6\text{N}_3\text{S}]^-$ 200.0288, found 200.0288.

Sodium (Z)-2-(ethoxycarbonyl)-3-oxo-1-(phenylamino)but-1-ene-1-thiolate ($4\text{co}^-\text{Na}^+$) was obtained according to Procedure B from **1c** (24 mg, 0.20 mmol) and **2o-H** (26 mg, 0.20 mmol).



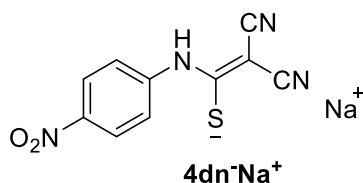
^1H NMR (400 MHz, $(\text{CD}_3)_2\text{SO}$) δ 14.44 (s, 1H), 7.79 (d, $J = 7.4$ Hz, 2H), 7.28 – 7.14 (m, 2H), 6.96 (t, $J = 7.3$ Hz, 1H), 4.02 (q, $J = 7.1$ Hz, 2H), 1.77 (s, 3H), 1.21 (t, $J = 7.1$ Hz, 3H). **^{13}C NMR** (101 MHz, $(\text{CD}_3)_2\text{SO}$) δ 184.4 (C), 178.6 (C=O), 172.1 (C=O), 142.0 (C), 127.9 (CH), 122.3 (CH), 122.1 (CH), 112.3 (C), 59.2 (CH_2), 26.5 (CH_3), 14.1 (CH_3). **HRMS** (ESI^-) m/z : $[\text{M}-\text{Na}^+]$ calcd for $[\text{C}_{13}\text{H}_{14}\text{NO}_3\text{S}]^-$ 264.0700, found 264.0701.

Sodium 2-acetyl-3-oxo-1-(phenylamino)but-1-ene-1-thiolate (4cp⁻Na⁺) was obtained according to Procedure B from **1c** (24 mg, 0.20 mmol) and **2p-H** (20 mg, 0.20 mmol).



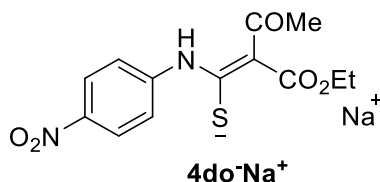
¹H NMR (400 MHz, (CD₃)₂SO) δ 14.60 (s, 1H), 7.77 (d, J = 7.3 Hz, 2H), 7.28 – 7.19 (m, 2H), 6.97 (t, J = 7.3 Hz, 1H), 2.11 (s, 6H). **HRMS** (ESI⁻) m/z : [M-Na⁺]⁻ calcd for [C₁₂H₁₂NO₂S]⁻ 234.0594, found 234.0595.

Sodium 2,2-dicyano-1-((4-nitrophenyl)amino)ethene-1-thiolate (4dn⁻Na⁺) was obtained according to Procedure B from **1d** (36 mg, 0.20 mmol) and **2n-H** (13 mg, 0.20 mmol).



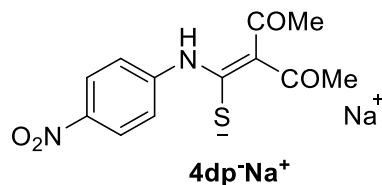
¹H NMR (400 MHz, (CD₃)₂SO) δ 9.71 (s, 1H), 8.09 (d, J = 8.8 Hz, 2H), 7.81 (d, J = 8.9 Hz, 2H).

Sodium (Z)-2-(ethoxycarbonyl)-1-((4-nitrophenyl)amino)-3-oxobut-1-ene-1-thiolate (4do⁻Na⁺) was obtained according to Procedure B from **1d** (36 mg, 0.20 mmol) and **2o-H** (26 mg, 0.20 mmol).



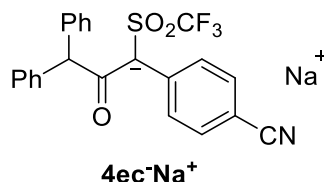
¹H NMR (400 MHz, (CD₃)₂SO) δ 15.00 (s, 1H), 8.22 (d, J = 9.4 Hz, 2H), 8.11 (d, J = 9.4 Hz, 2H), 4.05 (q, J = 7.1 Hz, 2H), 1.81 (s, 3H), 1.21 (t, J = 7.1 Hz, 3H). **¹³C NMR** (101 MHz, (CD₃)₂SO) δ 183.8 (C), 180.8 (C=O), 171.4 (C=O), 148.8 (C), 140.6 (C), 124.4 (CH), 119.9 (CH), 114.6 (C), 59.4 (CH₂), 26.7 (CH₃), 14.0 (CH₃). **HRMS** (ESI⁻) m/z : [M-Na⁺]⁻ calcd for [C₁₃H₁₃N₂O₅S]⁻ 309.0551, found 309.0554.

Sodium 2-acetyl-1-((4-nitrophenyl)amino)-3-oxobut-1-ene-1-thiolate (4dp⁻Na⁺) was obtained according to Procedure B from **1d** (36 mg, 0.20 mmol) and **2p-H** (20 mg, 0.20 mmol).



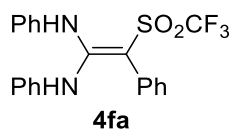
¹H NMR (400 MHz, (CD₃)₂SO) δ 15.15 (s, 1H), 8.20 (d, *J* = 9.4 Hz, 2H), 8.11 (d, *J* = 9.4 Hz, 2H), 2.11 (s, 6H).

Sodium 1-(4-cyanophenyl)-2-oxo-3,3-diphenyl-1-((trifluoromethyl)sulfonyl)propan-1-ide (4ec⁻Na⁺) was obtained in analogy to Procedure B from **1e** (19 mg, 0.10 mmol) and **2c-H** (25 mg, 0.10 mmol) in 0.6 mL CD₃CN/(CD₃)₂SO (5 : 1).



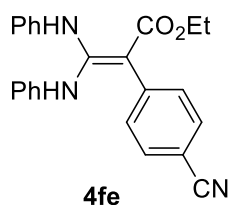
¹H NMR (400 MHz, CD₃CN) δ 7.37 – 7.15 (m, 14H), 4.98 (s, 1H). **HRMS** (ESI⁻) *m/z*: [M–Na⁺]⁻ calcd for [C₂₃H₁₅F₃NO₃S]⁻ 442.0730, found 442.0733.

N,N',2-Triphenyl-2-((trifluoromethyl)sulfonyl)ethene-1,1-diamine (4fa) was obtained according to Procedure C from **1f** (39 mg, 0.20 mmol) and **2a-H** (45 mg, 0.20 mmol): white solid (79 mg, 0.19 mmol, 95%), mp 129–134 °C.



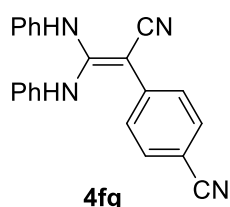
¹H NMR (400 MHz, (CD₃)₂SO) δ 9.13 (s, 2H), 7.20 – 7.13 (m, 4H), 7.13 – 7.03 (m, 5H), 7.02 – 6.96 (m, 4H), 6.87 (t, *J* = 7.3 Hz, 2H). **¹³C NMR** (101 MHz, (CD₃)₂SO) δ 155.5 (C), 139.1 (C), 133.2 (C), 131.8 (CH), 128.6 (CH), 127.8 (CH), 126.0 (CH), 123.6 (CH), 120.78 (q, *J*_{CF} = 330 Hz), 120.75 (CH), 81.5 (q, *J*_{CF} = 2.02 Hz). **HRMS** (EI) *m/z*: [M⁺] calcd for [C₂₁H₁₇F₃N₂O₂S]⁺ 418.0957, found 418.0955. **IR** (ATR) ν (cm⁻¹) = 3390, 3346, 1598, 1576, 1495, 1440, 1378, 1313, 1195, 1115, 951, 751, 689, 660.

Ethyl 2-(4-cyanophenyl)-3,3-bis(phenylamino)acrylate (4fe) was obtained in analogy to Procedure C but independently synthesized **2e-K** was used rather than generation in-situ by *t*-BuOK with **2e-H**. The product was obtained from **1f** (39 mg, 0.20 mmol) and **2e-K** (45 mg, 0.20 mmol): pale yellow solid (57 mg, 0.15 mmol, 75%), mp 150–155 °C.



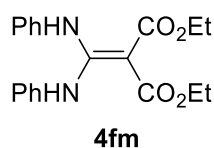
¹H NMR (400 MHz, (CD₃)₂SO) δ 9.08 (s, 2H), 7.52 (d, *J* = 8.4 Hz, 2H), 7.31 (d, *J* = 8.4 Hz, 2H), 7.15 – 7.03 (m, 4H), 6.97 (d, *J* = 7.5 Hz, 4H), 6.79 (t, *J* = 7.3 Hz, 2H), 3.92 (q, *J* = 7.1 Hz, 2H), 1.03 (t, *J* = 7.1 Hz, 3H). **¹³C NMR** (101 MHz, (CD₃)₂SO) δ 168.3 (C=O), 152.0 (C), 144.1 (C), 141.1 (C), 131.4 (CH), 131.1 (CH), 128.7 (CH), 121.8 (CH), 119.6 (C), 118.8 (CH), 106.1 (C), 90.4 (C), 58.8 (CH₂), 14.3 (CH₃). **HRMS** (EI) *m/z*: [*M*⁺] calcd for [C₂₄H₂₁N₃O₂]⁺ 383.1628, found 383.1627. **IR** (ATR) *ν* (cm⁻¹) = 3336, 2229, 1628, 1612, 1596, 1579, 1497, 1370, 1226, 1202, 1059, 749, 698.

4-(1-Cyano-2,2-bis(phenylamino)vinyl)benzonitrile (4fg) was obtained according to Procedure C from **1f** (39 mg, 0.20 mmol) and **2g-H** (28 mg, 0.20 mmol): yellow solid (57 mg, 0.17 mmol, 85%), mp 235–240 °C.



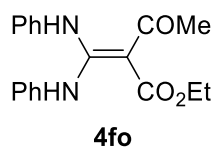
¹H NMR (400 MHz, (CD₃)₂SO) δ 9.47 (s, 2H), 7.57 (d, *J* = 8.5 Hz, 2H), 7.33 (d, *J* = 8.5 Hz, 2H), 7.17 (m, 4H), 7.03 (m, 4H), 6.88 (m, 2H). **¹³C NMR** (101 MHz, (CD₃)₂SO) δ 151.5 (C), 141.5 (C), 140.4 (C), 132.1 (CH), 129.0 (CH), 125.5 (CH), 122.4 (CH), 121.5 (C), 119.4 (C), 118.8 (CH), 104.9 (C), 70.4 (C). **HRMS** (EI) *m/z*: [*M*⁺] calcd for [C₂₂H₁₆N₄]⁺ 336.1369, found 336.1378. **IR** (ATR) *ν* (cm⁻¹) = 3308, 3050, 2224, 2191, 1611, 1594, 1569, 1528, 1496, 1480, 1362, 1249, 1178, 844, 739.

Diethyl 2-(bis(phenylamino)methylene)malonate (4fm) was obtained according to Procedure C from **1f** (39 mg, 0.20 mmol) and **2m-H** (32 mg, 0.20 mmol): white solid (64 mg, 0.18 mmol, 90%), mp 171–173 °C.



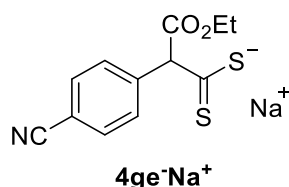
¹H NMR (400 MHz, CDCl₃) δ 11.24 (s, 2H), 7.03 – 6.95 (m, 4H), 6.90 (d, *J* = 7.4 Hz, 4H), 6.82 (t, *J* = 7.3 Hz, 2H), 4.24 (q, *J* = 7.1 Hz, 4H), 1.34 (t, *J* = 7.1 Hz, 6H). **¹³C NMR** (101 MHz, CDCl₃) δ 171.5 (C=O), 159.0 (C), 138.3 (C), 128.6 (CH), 124.3 (CH), 122.4 (CH), 80.1 (C), 60.3 (CH₂), 14.5 (CH₃). **HRMS** (EI) *m/z*: [*M*⁺] calcd for [C₂₀H₂₂N₂O₄]⁺ 354.1574, found 354.1578. **IR** (ATR) *ν* (cm⁻¹) = 2978, 1626, 1585, 1512, 1438, 1398, 1373, 1342, 1223, 1176, 1086, 1066, 1024, 748, 704.

Ethyl 2-(bis(phenylamino)methylene)-3-oxobutanoate (4fo) was obtained according to Procedure C from **1f** (39 mg, 0.20 mmol) and **2o-H** (26 mg, 0.20 mmol): white solid (52 mg, 0.16 mmol, 80%), mp 107–112 °C.



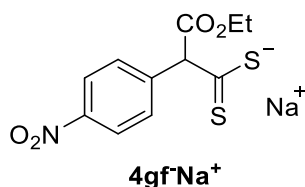
¹H NMR (400 MHz, (CD₃)₂SO) δ 11.95 (s, 2H), 7.07 (t, *J* = 7.7 Hz, 4H), 6.99 (d, *J* = 7.9 Hz, 4H), 6.88 (t, *J* = 7.3 Hz, 2H), 4.08 (q, *J* = 7.1 Hz, 2H), 2.35 (s, 3H), 1.21 (t, *J* = 7.1 Hz, 3H). **¹³C NMR** (101 MHz, (CD₃)₂SO) δ 196.2 (C=O), 170.3 (C=O), 158.0 (C), 137.7 (C), 128.6 (CH), 124.4 (CH), 122.0 (CH), 91.4 (C), 59.7 (CH₂), 31.5 (CH₃), 14.2 (CH₃). **HRMS** (EI) *m/z*: [*M*⁺] calcd for [C₁₉H₂₀N₂O₃]⁺ 324.1468, found 324.1471. **IR** (ATR) *ν* (cm⁻¹) = 2976, 1623, 1572, 1516, 1333, 1247, 1225, 1170, 1086, 971, 786, 748, 690.

Sodium 2-(4-cyanophenyl)-3-ethoxy-3-oxopropanedithioate (4ge^{-Na}⁺) was obtained in analogy to Procedure B but independently synthesized **2e-K** was used rather than generation in-situ by NaOH with **2e-H**. The product was obtained from **1g** (15 mg, 0.20 mmol) and **2e-K** (45 mg, 0.20 mmol).



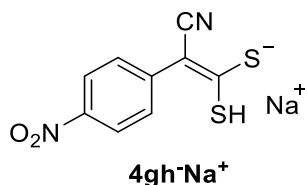
¹H NMR (400 MHz, (CD₃)₂SO) δ 7.77 (d, J = 8.5 Hz, 2H), 7.69 (d, J = 8.6 Hz, 2H), 5.42 (s, 1H), 4.03 (m, 2H), 1.16 (t, J = 7.1 Hz, 3H). **¹³C NMR** (101 MHz, (CD₃)₂SO) δ 192.7 (C=S), 168.6 (C=O), 144.0 (C), 131.0 (CH), 130.1 (CH), 119.2 (C), 109.1 (C), 79.0 (CH), 59.9 (CH₂), 14.0 (CH₃).

Sodium 2-(4-nitrophenyl)-3-ethoxy-3-oxopropanedithioate (4gf⁻Na⁺) was obtained in analogy to Procedure B but independently synthesized **2f-K** was used rather than generation in-situ by NaOH with **2f-H**. The product was obtained from **1g** (15 mg, 0.20 mmol) and **2f-K** (49 mg, 0.20 mmol).

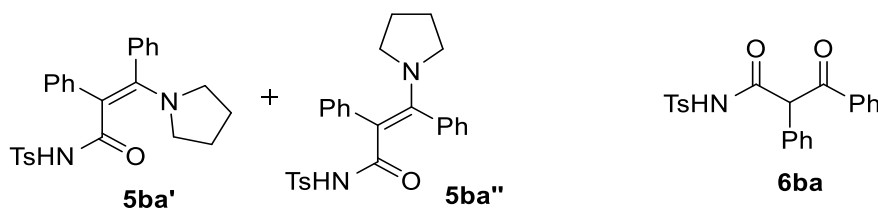


¹H NMR (400 MHz, (CD₃)₂SO) δ 8.12 (d, J = 8.4 Hz, 2H), 7.85 (d, J = 8.4 Hz, 2H), 5.50 (s, 1H), 4.04 (m, 2H), 1.17 (t, J = 7.0 Hz, 3H).

Sodium (E)-2-cyano-1-mercapto-2-(4-nitrophenyl)ethene-1-thiolate (4gh⁻Na⁺) was obtained according to Procedure B from **1g** (15 mg, 0.20 mmol) and **2h-H** (32 mg, 0.20 mmol).



¹H NMR (400 MHz, (CD₃)₂SO) δ 8.52 (d, J = 9.2 Hz, 2H), 7.98 (d, J = 9.3 Hz, 2H), 5.44 (br s, 1H). **HRMS** (ESI⁻) m/z : [M-Na⁺-H⁺]²⁻ calcd for [C₉H₄N₂O₂S₂]²⁻ 235.9725, found 235.9722.



To a solution of **1b** (39 mg, 0.20 mmol) in anhydrous CD_3CN (0.5 mL) at room temperature was added a solution of **3a** (50 mg, 0.20 mmol) in anhydrous CD_3CN (0.5 mL). After 10 min, the products **2,3-diphenyl-3-(pyrrolidin-1-yl)-N-tosylacrylamide (5ba)** was analyzed by ^1H NMR spectroscopy without workup. After the ^1H NMR measurement, the **5ba** solution was quenched by 2% aq HCl (5 mL) and the mixture was extracted with CHCl_3 (3×20 mL). The combined organic phase was washed with brine (1×30 mL), dried with anhydrous MgSO_4 , and filtered. The solvent was evaporated under reduced pressure, and the residue was purified by column chromatography to give product **3-oxo-2,3-diphenyl-N-tosylpropanamide (6ba)**: pale yellow liquid (55 mg, 0.14 mmol, 70%).

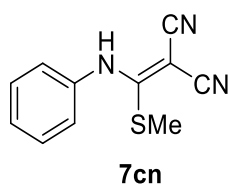
2,3-Diphenyl-3-(pyrrolidin-1-yl)-N-tosylacrylamide (5ba)

^1H NMR (599 MHz, CD_3CN) δ 8.03 (m, 2H), 7.89 (d, $J = 7.9$ Hz, 2H), 7.59 (d, $J = 8.0$ Hz, 2H), 7.41 (m, 3H), 7.38 – 7.29 (m, 8H), 7.26 (m, 2H), 7.19 – 7.09 (m, 6H), 6.99 (m, 3H), 6.86 (d, $J = 7.5$ Hz, 2H), 2.93 (s, 4H), 2.73 (s, 4H), 2.46 (s, 3H), 2.42 (s, 3H), 1.78 (s, 4H), 1.63 (s, 4H).

3-Oxo-2,3-diphenyl-N-tosylpropanamide (6ba)

^1H NMR (400 MHz, $(\text{CD}_3)_2\text{SO}$) δ 12.54 (s, 1H), 7.87 (d, $J = 7.1$ Hz, 2H), 7.78 (d, $J = 8.3$ Hz, 2H), 7.57 (t, $J = 7.4$ Hz, 1H), 7.47 – 7.39 (m, 4H), 7.31 – 7.21 (m, 5H), 5.94 (s, 1H), 2.40 (s, 3H).

^{13}C NMR (101 MHz, $(\text{CD}_3)_2\text{SO}$) δ 193.4 (C=O), 166.7 (C=O), 144.2 (C), 136.1 (C), 135.2 (C), 133.4 (CH), 132.5 (C), 129.8 (CH), 129.5 (CH), 128.7 (CH), 128.6 (CH), 128.4 (CH), 127.8 (CH), 127.5 (CH), 60.2 (CH), 21.1 (CH_3). HRMS (ESI $^-$) m/z : $[\text{M}-\text{H}]^-$ calcd for $[\text{C}_{22}\text{H}_{18}\text{NO}_4\text{S}]^-$ 392.0962, found 392.0965. IR (ATR) ν (cm^{-1}) = 3236, 2925, 1717, 1678, 1596, 1448, 1341, 1169, 1085, 889, 813, 761, 698, 658.



To a solution of **1c** (54 mg, 0.40 mmol) and **2m-H** (27 mg, 0.41 mmol) in anhydrous DMSO (3 mL) at room temperature was added NaOH (16 mg, 0.40 mmol). After 2 h, a solution of CH_3I (57

mg, 0.40 mmol) in anhydrous DMSO (1 mL) was added at room temperature. After 2 h, 20 mL of saturated NH_4Cl solution was added and the mixture was extracted with EtOAc (3×20 mL). The combined organic phase was washed with water (2×30 mL) and brine (1×30 mL), dried with anhydrous MgSO_4 , and filtered. The solvent was evaporated under reduced pressure, and the residue was purified by column chromatography to give product **2-((methylthio)(phenylamino)methylene)malononitrile (7cn)**: white solid (69 mg, 0.32 mmol, 80%), mp 173–178 °C.

^1H NMR (400 MHz, $(\text{CD}_3)_2\text{SO}$) δ 10.54 (s, 1H), 7.42 (t, $J = 7.7$ Hz, 2H), 7.30 (d, $J = 8.4$ Hz, 2H), 7.27 (t, $J = 7.2$ Hz, 1H), 2.52 (s, 3H). **^{13}C NMR** (101 MHz, $(\text{CD}_3)_2\text{SO}$) δ 171.5 (C), 138.3 (C), 129.2 (CH), 126.6 (CH), 123.9 (CH), 52.9 (C), 15.8 (CH_3). (one carbon missing) **HRMS** (EI) m/z : $[\text{M}^+]$ calcd for $[\text{C}_{11}\text{H}_9\text{N}_3\text{S}]^+$ 215.0512, found 215.0504. **IR** (ATR) ν (cm^{-1}) = 3285, 2194, 2179, 1594, 1520, 1489, 1448, 1425, 1262, 965, 757, 699. **Elemental analysis**: C 61.37, H 4.21, N 19.52, S 14.89; Found C 60.93, H 4.45, N 18.96, S 14.89.

(2) Kinetics of the reactions of the heteroallenes 1 with the carbanions 2 and enamines 3.

The rates of all investigated reactions were determined spectrophotometrically (UV-Vis) by following the disappearance of the UV/Vis absorptions of the nucleophiles **2** and **3** or formation of the UV/Vis absorptions of the products **4**. The temperature of the solutions during all kinetics studies was kept constant (20.0 ± 0.1 °C) by using a circulating bath thermostat. The kinetics investigations were performed with a high excess of the one component over the other to achieve first-order kinetics. The kinetics were followed by conventional UV/Vis diode array spectrophotometer (slow kinetics, $\tau_{1/2} > 10$ s) or commercial stopped-flow spectrophotometer system (fast kinetics, $\tau_{1/2} < 10$ s). Rate constants k_{obs} (s^{-1}) were obtained by fitting the single exponential decay $A_t = A_0 \exp(-k_{\text{obs}}t) + C$ (exponential decrease) to the observed time-dependent absorbance (in the case of the stopped-flow spectrophotometer, at least 5 kinetic runs for each nucleophile concentration were averaged). Second-order rate constants k_2 ($\text{M}^{-1} \text{s}^{-1}$) were derived from the slopes of the linear correlations of k_{obs} with electrophile concentrations.

Table S1. Kinetics of the reactions of **1a** with **2b** in CH_3CN at 20 °C (deprotonated with 1.00–1.05 equiv. *t*-BuOK, conventional UV-Vis spectrometer, $\lambda = 320$ nm).

[2b]/mol L ⁻¹	[1a]/mol L ⁻¹	$k_{\text{obs}}/\text{s}^{-1}$
5.00×10^{-5}	4.59×10^{-4}	9.23×10^{-3}
5.00×10^{-5}	6.93×10^{-4}	1.44×10^{-2}
5.00×10^{-5}	9.04×10^{-4}	2.08×10^{-2}
5.00×10^{-5}	1.13×10^{-3}	2.54×10^{-2}
5.00×10^{-5}	1.34×10^{-3}	3.11×10^{-2}

$k_2 = 2.49 \times 10^1 \text{ L mol}^{-1} \text{s}^{-1}$

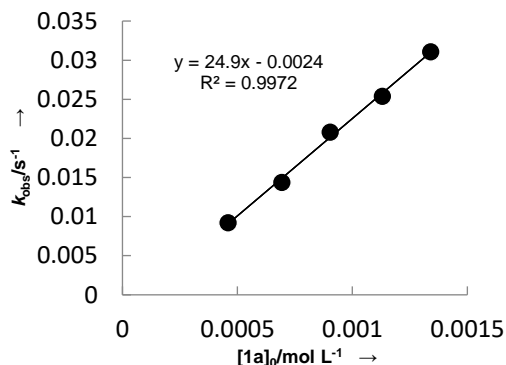


Table S2. Kinetics of the reactions of **1a** with **2c** in CH_3CN at 20 °C (deprotonated with 1.00–1.05 equiv. *t*-BuOK, conventional UV-Vis spectrometer, $\lambda = 344$ nm).

[2c]/mol L ⁻¹	[1a]/mol L ⁻¹	$k_{\text{obs}}/\text{s}^{-1}$
5.00×10^{-5}	5.43×10^{-4}	1.14×10^{-3}
5.00×10^{-5}	8.20×10^{-4}	1.86×10^{-3}
5.00×10^{-5}	1.07×10^{-3}	2.53×10^{-3}
5.00×10^{-5}	1.34×10^{-3}	3.25×10^{-3}

$k_2 = 2.65 \times 10^0 \text{ L mol}^{-1} \text{s}^{-1}$

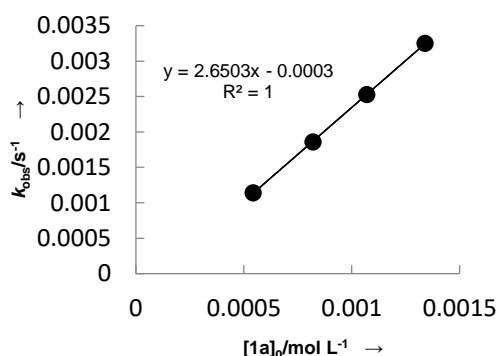
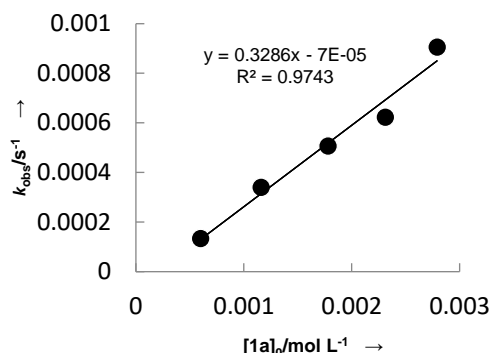


Table S3. Kinetics of the reactions of **1a** with **2d** in CH₃CN at 20 °C (deprotonated with 1.00–1.05 equiv. *t*-BuOK, conventional UV-Vis spectrometer, $\lambda = 464$ nm).

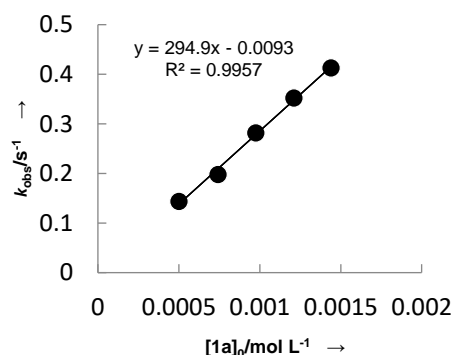
[2d]/mol L ⁻¹	[1a]/mol L ⁻¹	$k_{\text{obs}}/\text{s}^{-1}$
5.00×10^{-5}	6.00×10^{-4}	1.33×10^{-4}
5.00×10^{-5}	1.16×10^{-3}	3.39×10^{-4}
5.00×10^{-5}	1.78×10^{-3}	5.06×10^{-4}
5.00×10^{-5}	2.31×10^{-3}	6.22×10^{-4}
5.00×10^{-5}	2.79×10^{-3}	9.05×10^{-4}

$k_2 = 3.29 \times 10^{-1} \text{ L mol}^{-1} \text{ s}^{-1}$

Table S4. Kinetics of the reactions of **1a** with **2j** in CH₃CN at 20 °C (deprotonated with 1.00–1.05 equiv. *t*-BuOK, conventional UV-Vis spectrometer, $\lambda = 527$ nm).

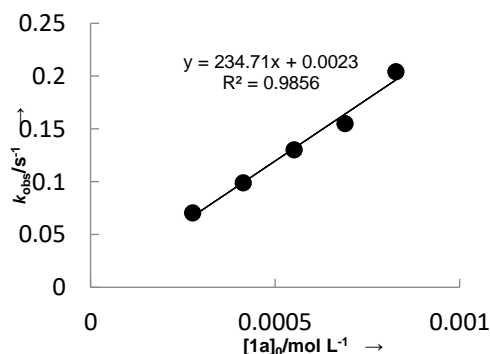
[2j]/mol L ⁻¹	[1a]/mol L ⁻¹	$k_{\text{obs}}/\text{s}^{-1}$
5.00×10^{-5}	5.01×10^{-4}	1.44×10^{-1}
5.00×10^{-5}	7.42×10^{-4}	1.98×10^{-1}
5.00×10^{-5}	9.74×10^{-4}	2.82×10^{-1}
5.00×10^{-5}	1.21×10^{-3}	3.52×10^{-1}
5.00×10^{-5}	1.44×10^{-3}	4.13×10^{-1}

$k_2 = 2.95 \times 10^2 \text{ L mol}^{-1} \text{ s}^{-1}$

Table S5. Kinetics of the reactions of **1a** with **2h** in CH₃CN at 20 °C (deprotonated with 1.00–1.05 equiv. *t*-BuOK, stopped-flow UV-Vis spectrometer, $\lambda = 540$ nm).

[2h]/mol L ⁻¹	[1a]/mol L ⁻¹	$k_{\text{obs}}/\text{s}^{-1}$
2.50×10^{-5}	2.76×10^{-4}	7.04×10^{-2}
2.50×10^{-5}	4.13×10^{-4}	9.88×10^{-2}
2.50×10^{-5}	5.51×10^{-4}	1.30×10^{-1}
2.50×10^{-5}	6.89×10^{-4}	1.55×10^{-1}
2.50×10^{-5}	8.27×10^{-4}	2.04×10^{-1}

$k_2 = 2.35 \times 10^2 \text{ L mol}^{-1} \text{ s}^{-1}$

Table S6. Kinetics of the reactions of **1b** with **3a** in CH₃CN at 20 °C (stopped-flow UV-Vis spectrometer, $\lambda = 317$ nm).

[3a]/mol L ⁻¹	[1b]/mol L ⁻¹	$k_{\text{obs}}/\text{s}^{-1}$
5.00×10^{-5}	4.96×10^{-4}	1.03×10^0
5.00×10^{-5}	7.54×10^{-4}	1.47×10^0
5.00×10^{-5}	9.92×10^{-4}	1.97×10^0
5.00×10^{-5}	1.25×10^{-3}	2.49×10^0
5.00×10^{-5}	1.49×10^{-3}	3.04×10^0

$k_2 = 2.03 \times 10^3 \text{ L mol}^{-1} \text{ s}^{-1}$

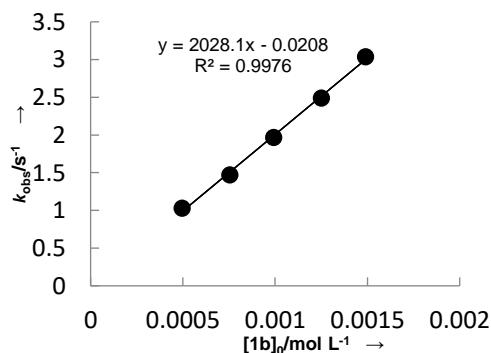
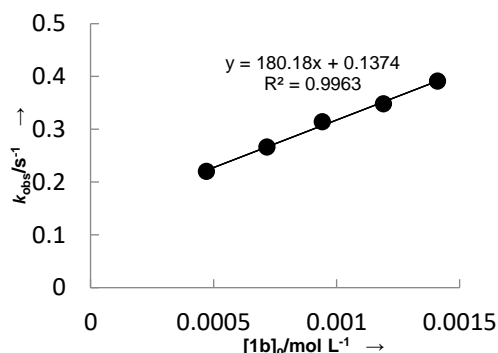
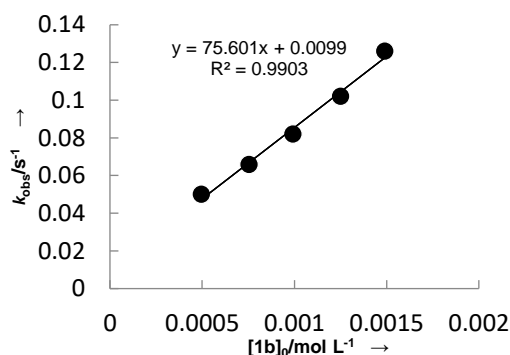


Table S7. Kinetics of the reactions of **1b** with **3b** in CH₃CN at 20 °C (stopped-flow UV-Vis spectrometer, $\lambda = 465$ nm).

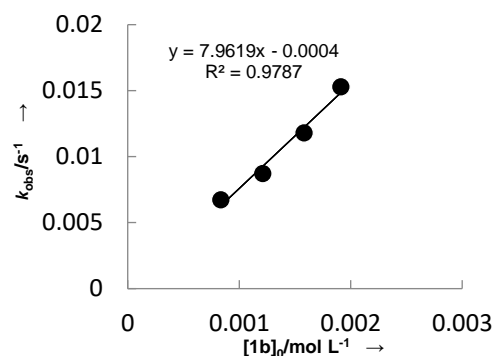
[3b]/mol L ⁻¹	[1b]/mol L ⁻¹	$k_{\text{obs}}/\text{s}^{-1}$
5.00×10^{-5}	4.71×10^{-4}	2.20×10^{-1}
5.00×10^{-5}	7.16×10^{-4}	2.66×10^{-1}
5.00×10^{-5}	9.42×10^{-4}	3.14×10^{-1}
5.00×10^{-5}	1.19×10^{-3}	3.48×10^{-1}
5.00×10^{-5}	1.41×10^{-3}	3.91×10^{-1}
$k_2 = 1.80 \times 10^2 \text{ L mol}^{-1} \text{ s}^{-1}$		

Table S8. Kinetics of the reactions of **1b** with **3c** in CH₃CN at 20 °C (stopped-flow UV-Vis spectrometer, $\lambda = 316$ nm).

[3c]/mol L ⁻¹	[1b]/mol L ⁻¹	$k_{\text{obs}}/\text{s}^{-1}$
5.00×10^{-5}	4.96×10^{-4}	5.01×10^{-2}
5.00×10^{-5}	7.54×10^{-4}	6.59×10^{-2}
5.00×10^{-5}	9.92×10^{-4}	8.20×10^{-2}
5.00×10^{-5}	1.25×10^{-3}	1.02×10^{-1}
5.00×10^{-5}	1.49×10^{-3}	1.26×10^{-1}
$k_2 = 7.56 \times 10^1 \text{ L mol}^{-1} \text{ s}^{-1}$		

Table S9. Kinetics of the reactions of **1b** with **3d** in CH₃CN at 20 °C (conventional UV-Vis spectrometer, $\lambda = 306$ nm).

[3d]/mol L ⁻¹	[1b]/mol L ⁻¹	$k_{\text{obs}}/\text{s}^{-1}$
1.00×10^{-4}	8.33×10^{-4}	6.73×10^{-3}
1.00×10^{-4}	1.21×10^{-3}	8.72×10^{-3}
1.00×10^{-4}	1.58×10^{-3}	1.18×10^{-2}
1.00×10^{-4}	1.91×10^{-3}	1.53×10^{-2}
$k_2 = 7.96 \times 10^0 \text{ L mol}^{-1} \text{ s}^{-1}$		

Table S10. Kinetics of the reactions of **1c** with **2a** in DMSO at 20 °C (deprotonated with 1.00–1.05 equiv. *t*-BuOK, conventional UV-Vis spectrometer, $\lambda = 300$ nm).

[2a]/mol L ⁻¹	[1c]/mol L ⁻¹	$k_{\text{obs}}/\text{s}^{-1}$
5.00×10^{-5}	6.43×10^{-4}	1.58×10^{-3}
5.00×10^{-5}	9.55×10^{-4}	2.30×10^{-3}
5.00×10^{-5}	1.26×10^{-3}	2.77×10^{-3}
5.00×10^{-5}	1.56×10^{-3}	3.53×10^{-3}
5.00×10^{-5}	1.85×10^{-3}	4.03×10^{-3}
$k_2 = 2.03 \times 10^0 \text{ L mol}^{-1} \text{ s}^{-1}$		

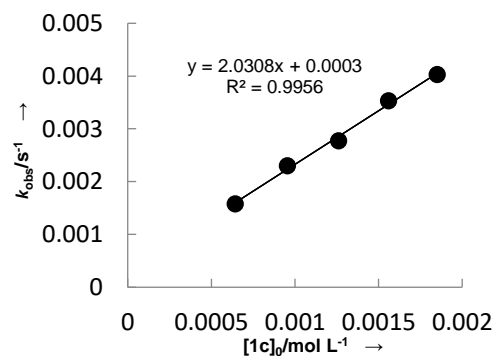
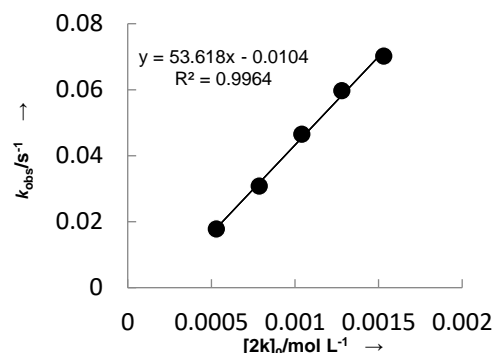


Table S11. Kinetics of the reactions of **1c** with **2l** in DMSO at 20 °C (deprotonated with 0.5 equiv. *t*-BuOK, conventional UV-Vis spectrometer, $\lambda = 326$ nm).

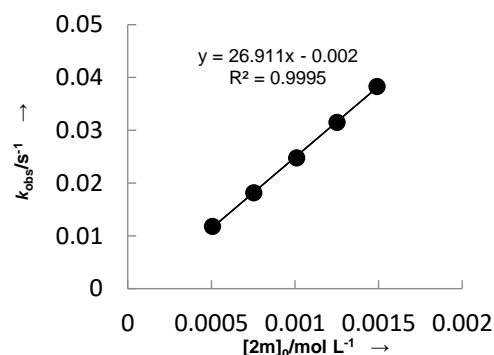
[1c]/mol L ⁻¹	[2l]/mol L ⁻¹	$k_{\text{obs}}/\text{s}^{-1}$
5.00×10^{-5}	5.30×10^{-4}	1.78×10^{-2}
5.00×10^{-5}	7.86×10^{-4}	3.08×10^{-3}
5.00×10^{-5}	1.04×10^{-3}	4.65×10^{-3}
5.00×10^{-5}	1.28×10^{-3}	5.97×10^{-3}
5.00×10^{-5}	1.53×10^{-3}	7.02×10^{-3}

$k_2 = 5.36 \times 10^1 \text{ L mol}^{-1} \text{ s}^{-1}$

Table S12. Kinetics of the reactions of **1c** with **2n** in DMSO at 20 °C (deprotonated with 0.5 equiv. *t*-BuOK, conventional UV-Vis spectrometer, $\lambda = 320$ nm).

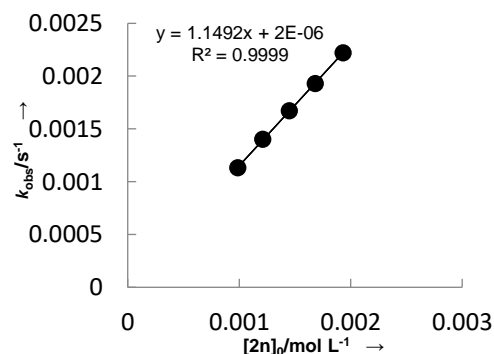
[1c]/mol L ⁻¹	[2n]/mol L ⁻¹	$k_{\text{obs}}/\text{s}^{-1}$
5.00×10^{-5}	5.07×10^{-4}	1.18×10^{-2}
5.00×10^{-5}	7.53×10^{-4}	1.82×10^{-2}
5.00×10^{-5}	1.01×10^{-3}	2.48×10^{-2}
5.00×10^{-5}	1.25×10^{-3}	3.15×10^{-2}
5.00×10^{-5}	1.49×10^{-3}	3.83×10^{-2}

$k_2 = 2.69 \times 10^1 \text{ L mol}^{-1} \text{ s}^{-1}$

Table S13. Kinetics of the reactions of **1c** with **2o** in DMSO at 20 °C (deprotonated with 0.5 equiv. *t*-BuOK, conventional UV-Vis spectrometer, $\lambda = 350$ nm).

[1c]/mol L ⁻¹	[2o]/mol L ⁻¹	$k_{\text{obs}}/\text{s}^{-1}$
5.00×10^{-5}	9.86×10^{-4}	1.13×10^{-3}
5.00×10^{-5}	1.21×10^{-3}	1.40×10^{-3}
5.00×10^{-5}	1.45×10^{-3}	1.67×10^{-3}
5.00×10^{-5}	1.68×10^{-3}	1.93×10^{-3}
5.00×10^{-5}	1.93×10^{-3}	2.22×10^{-3}

$k_2 = 1.15 \times 10^0 \text{ L mol}^{-1} \text{ s}^{-1}$

Table S14. Kinetics of the reactions of **1c** with **2p** in DMSO at 20 °C (deprotonated with 0.5 equiv. *t*-BuOK, conventional UV-Vis spectrometer, $\lambda = 350$ nm).

[1c]/mol L ⁻¹	[2p]/mol L ⁻¹	$k_{\text{obs}}/\text{s}^{-1}$
5.00×10^{-5}	1.12×10^{-3}	8.21×10^{-4}
5.00×10^{-5}	1.41×10^{-3}	1.00×10^{-3}
5.00×10^{-5}	1.67×10^{-3}	1.16×10^{-3}
5.00×10^{-5}	1.94×10^{-3}	1.31×10^{-3}
5.00×10^{-5}	2.21×10^{-3}	1.54×10^{-3}

$k_2 = 6.45 \times 10^{-1} \text{ L mol}^{-1} \text{ s}^{-1}$

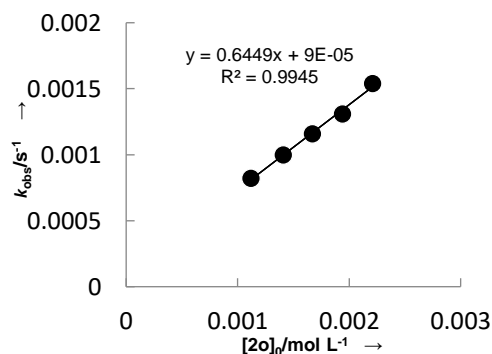
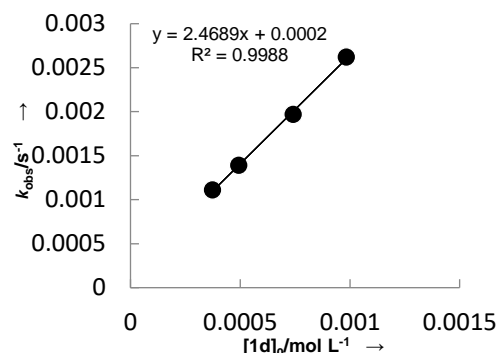


Table S15. Kinetics of the reactions of **1d** with **2c** in DMSO at 20 °C (deprotonated with 1.00–1.05 equiv. *t*-BuOK, conventional UV-Vis spectrometer, $\lambda = 344$ nm).

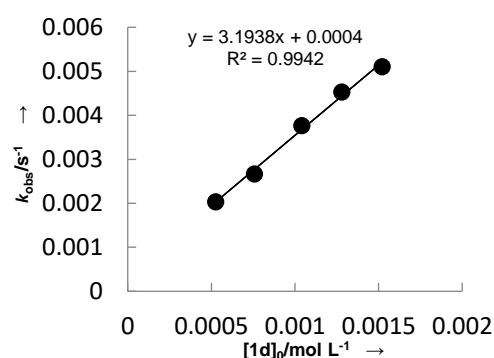
[2c]/mol L ⁻¹	[1d]/mol L ⁻¹	$k_{\text{obs}}/\text{s}^{-1}$
5.00×10^{-5}	3.74×10^{-4}	1.11×10^{-3}
5.00×10^{-5}	4.93×10^{-4}	1.39×10^{-3}
5.00×10^{-5}	7.41×10^{-4}	1.97×10^{-3}
5.00×10^{-5}	9.83×10^{-4}	2.62×10^{-3}

$k_2 = 2.47 \times 10^0 \text{ L mol}^{-1} \text{ s}^{-1}$

Table S16. Kinetics of the reactions of **1d** with **2c** in CH₃CN at 20 °C (deprotonated with 1.00–1.05 equiv. *t*-BuOK, conventional UV-Vis spectrometer, $\lambda = 344$ nm).

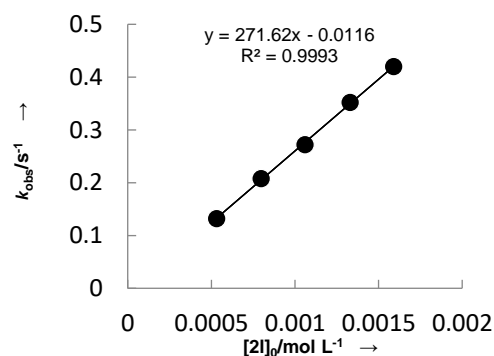
[2c]/mol L ⁻¹	[1d]/mol L ⁻¹	$k_{\text{obs}}/\text{s}^{-1}$
5.00×10^{-5}	5.26×10^{-4}	2.04×10^{-3}
5.00×10^{-5}	7.58×10^{-4}	2.67×10^{-3}
5.00×10^{-5}	1.04×10^{-3}	3.77×10^{-3}
5.00×10^{-5}	1.28×10^{-3}	4.53×10^{-3}
5.00×10^{-5}	1.52×10^{-3}	5.11×10^{-3}

$k_2 = 3.19 \times 10^0 \text{ L mol}^{-1} \text{ s}^{-1}$

Table S17. Kinetics of the reactions of **1d** with **2m** in DMSO at 20 °C (deprotonated with 0.5 equiv. *t*-BuOK, conventional UV-Vis spectrometer, $\lambda = 439$ nm).

[1d]/mol L ⁻¹	[2m]/mol L ⁻¹	$k_{\text{obs}}/\text{s}^{-1}$
5.00×10^{-5}	5.31×10^{-4}	1.32×10^{-1}
5.00×10^{-5}	7.97×10^{-4}	2.08×10^{-1}
5.00×10^{-5}	1.06×10^{-3}	2.72×10^{-1}
5.00×10^{-5}	1.33×10^{-3}	3.52×10^{-1}
5.00×10^{-5}	1.59×10^{-3}	4.20×10^{-1}

$k_2 = 2.72 \times 10^2 \text{ L mol}^{-1} \text{ s}^{-1}$

Table S18. Kinetics of the reactions of **1d** with **2n** in DMSO at 20 °C (deprotonated with 0.5 equiv. *t*-BuOK, stopped-flow UV-Vis spectrometer, $\lambda = 414$ nm).

[1d]/mol L ⁻¹	[2n]/mol L ⁻¹	$k_{\text{obs}}/\text{s}^{-1}$
1.00×10^{-4}	1.01×10^{-3}	1.13×10^0
1.00×10^{-4}	1.52×10^{-3}	1.73×10^0
1.00×10^{-4}	2.03×10^{-3}	2.35×10^0
1.00×10^{-4}	2.53×10^{-3}	3.00×10^0
1.00×10^{-4}	3.04×10^{-3}	3.64×10^0

$k_2 = 1.24 \times 10^3 \text{ L mol}^{-1} \text{ s}^{-1}$

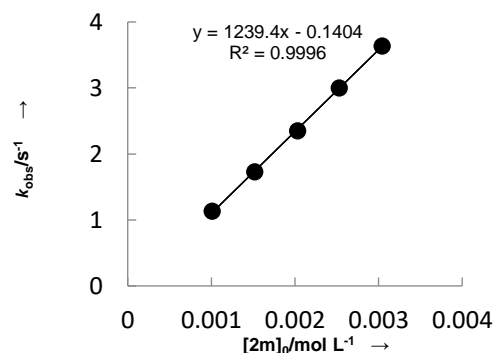
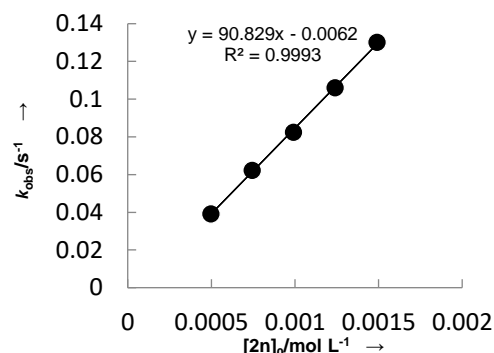


Table S19. Kinetics of the reactions of **1d** with **2o** in DMSO at 20 °C (deprotonated with 0.5 equiv. *t*-BuOK, stopped-flow UV-Vis spectrometer, $\lambda = 426$ nm).

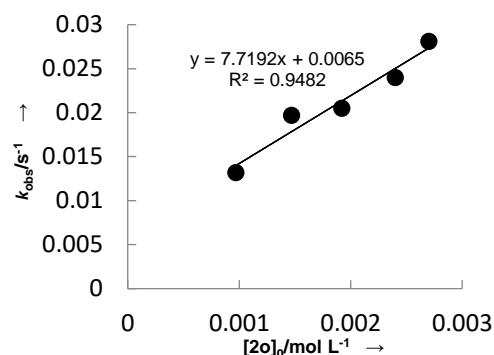
[1d]/mol L ⁻¹	[2o]/mol L ⁻¹	$k_{\text{obs}}/\text{s}^{-1}$
5.00×10^{-5}	4.96×10^{-4}	3.91×10^{-2}
5.00×10^{-5}	7.43×10^{-4}	6.21×10^{-2}
5.00×10^{-5}	9.91×10^{-4}	8.24×10^{-2}
5.00×10^{-5}	1.24×10^{-3}	1.06×10^{-1}
5.00×10^{-5}	1.49×10^{-3}	1.30×10^{-1}

$k_2 = 9.08 \times 10^1 \text{ L mol}^{-1} \text{ s}^{-1}$

Table S20. Kinetics of the reactions of **1d** with **2p** in DMSO at 20 °C (deprotonated with 0.5 equiv. *t*-BuOK, conventional UV-Vis spectrometer, $\lambda = 402$ nm).

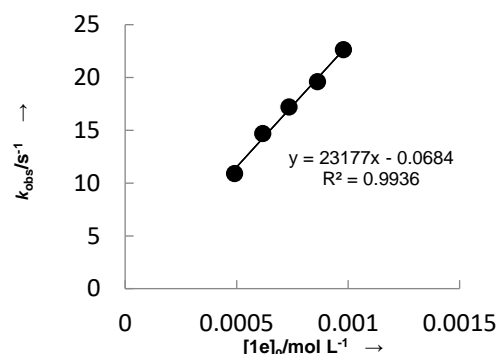
[1d]/mol L ⁻¹	[2p]/mol L ⁻¹	$k_{\text{obs}}/\text{s}^{-1}$
1.00×10^{-4}	9.68×10^{-4}	1.32×10^{-2}
1.00×10^{-4}	1.47×10^{-3}	1.97×10^{-2}
1.00×10^{-4}	1.92×10^{-3}	2.05×10^{-2}
1.00×10^{-4}	2.40×10^{-3}	2.40×10^{-2}
1.00×10^{-4}	2.70×10^{-3}	2.81×10^{-2}

$k_2 = 7.72 \times 10^0 \text{ L mol}^{-1} \text{ s}^{-1}$

Table S21. Kinetics of the reactions of **1e** with **2a** in CH₃CN at 20 °C (deprotonated with 1.00–1.05 equiv. *t*-BuOK, stopped-flow UV-Vis spectrometer, $\lambda = 295$ nm).

[2a]/mol L ⁻¹	[1e]/mol L ⁻¹	$k_{\text{obs}}/\text{s}^{-1}$
2.50×10^{-5}	4.90×10^{-4}	1.09×10^1
2.50×10^{-5}	6.17×10^{-4}	1.47×10^1
2.50×10^{-5}	7.35×10^{-4}	1.72×10^1
2.50×10^{-5}	8.62×10^{-4}	1.96×10^1
2.50×10^{-5}	9.79×10^{-4}	2.26×10^1

$k_2 = 2.32 \times 10^4 \text{ L mol}^{-1} \text{ s}^{-1}$

Table S22. Kinetics of the reactions of **1e** with **2c** in CH₃CN at 20 °C (deprotonated with 1.00–1.05 equiv. *t*-BuOK, stopped-flow UV-Vis spectrometer, $\lambda = 344$ nm).

[2c]/mol L ⁻¹	[1e]/mol L ⁻¹	$k_{\text{obs}}/\text{s}^{-1}$
2.50×10^{-5}	2.84×10^{-4}	7.83×10^{-1}
2.50×10^{-5}	4.31×10^{-4}	1.09×10^0
2.50×10^{-5}	5.67×10^{-4}	1.38×10^0
2.50×10^{-5}	7.14×10^{-4}	1.66×10^0
2.50×10^{-5}	8.51×10^{-4}	1.82×10^0

$k_2 = 1.87 \times 10^3 \text{ L mol}^{-1} \text{ s}^{-1}$

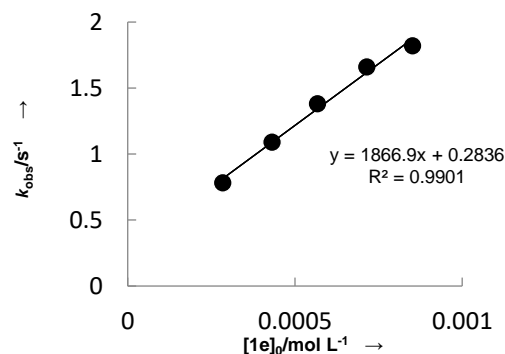
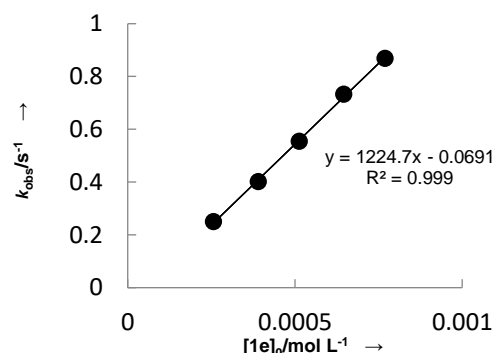


Table S23. Kinetics of the reactions of **1e** with **2d** in CH₃CN at 20 °C (deprotonated with 1.00–1.05 equiv. *t*-BuOK, stopped-flow UV-Vis spectrometer, λ = 464 nm).

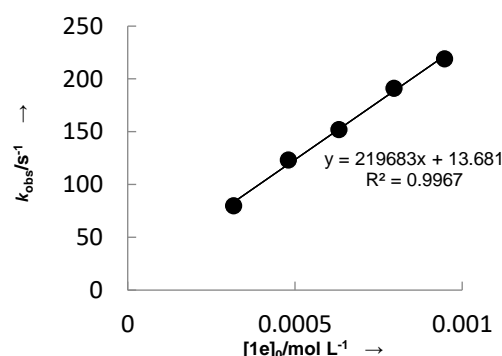
[2d]/mol L ⁻¹	[1e]/mol L ⁻¹	$k_{\text{obs}}/\text{s}^{-1}$
2.50×10^{-5}	2.56×10^{-4}	2.50×10^{-1}
2.50×10^{-5}	3.90×10^{-4}	4.01×10^{-1}
2.50×10^{-5}	5.13×10^{-4}	5.54×10^{-1}
2.50×10^{-5}	6.46×10^{-4}	6.46×10^{-1}
2.50×10^{-5}	7.69×10^{-4}	7.69×10^{-1}

$$k_2 = 1.22 \times 10^3 \text{ L mol}^{-1} \text{ s}^{-1}$$

Table S24. Kinetics of the reactions of **1e** with **2k** in CH₃CN at 20 °C (deprotonated with 1.00–1.05 equiv. *t*-BuOK, stopped-flow UV-Vis spectrometer, λ = 400 nm).

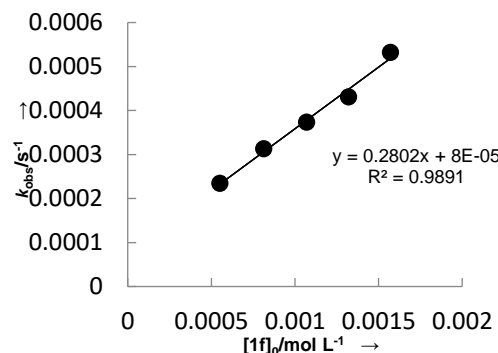
[2k]/mol L ⁻¹	[1e]/mol L ⁻¹	$k_{\text{obs}}/\text{s}^{-1}$
2.50×10^{-5}	3.16×10^{-4}	7.98×10^1
2.50×10^{-5}	4.80×10^{-4}	1.23×10^1
2.50×10^{-5}	6.31×10^{-4}	1.52×10^1
2.50×10^{-5}	7.96×10^{-4}	1.91×10^1
2.50×10^{-5}	9.47×10^{-4}	2.19×10^1

$$k_2 = 2.20 \times 10^5 \text{ L mol}^{-1} \text{ s}^{-1}$$

Table S25. Kinetics of the reactions of **1f** with **2a** in DMSO at 20 °C (deprotonated with 1.00–1.05 equiv. *t*-BuOK, conventional UV-Vis spectrometer, λ = 320 nm).

[2a]/mol L ⁻¹	[1f]/mol L ⁻¹	$k_{\text{obs}}/\text{s}^{-1}$
5.00×10^{-5}	5.50×10^{-4}	2.34×10^{-4}
5.00×10^{-5}	8.13×10^{-4}	3.13×10^{-4}
5.00×10^{-5}	1.07×10^{-3}	3.73×10^{-4}
5.00×10^{-5}	1.32×10^{-3}	4.31×10^{-4}
5.00×10^{-5}	1.57×10^{-3}	5.32×10^{-4}

$$k_2 = 2.80 \times 10^{-1} \text{ L mol}^{-1} \text{ s}^{-1}$$

Table S26. Kinetics of the reactions of **1f** with **2e** in DMSO at 20 °C (deprotonated with 1.00–1.05 equiv. *t*-BuOK, stopped-flow UV-Vis spectrometer, λ = 405 nm).

[2e]/mol L ⁻¹	[1f]/mol L ⁻¹	$k_{\text{obs}}/\text{s}^{-1}$
2.50×10^{-5}	2.63×10^{-4}	8.36×10^{-2}
2.50×10^{-5}	4.00×10^{-4}	1.16×10^{-1}
2.50×10^{-5}	5.26×10^{-3}	1.22×10^{-1}
2.50×10^{-5}	6.62×10^{-3}	1.37×10^{-1}
2.50×10^{-5}	7.89×10^{-3}	1.66×10^{-1}

$$k_2 = 1.42 \times 10^2 \text{ L mol}^{-1} \text{ s}^{-1}$$

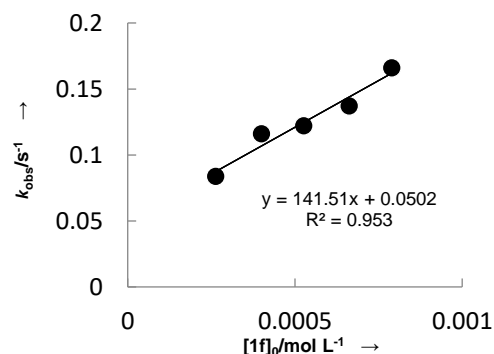
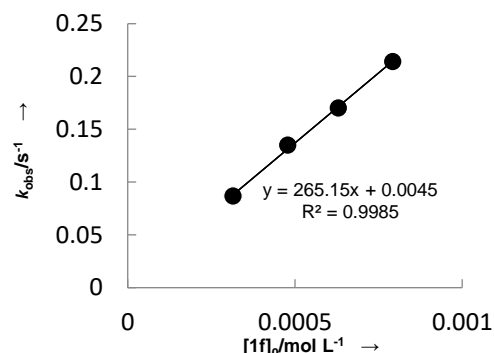


Table S27. Kinetics of the reactions of **1f** with **2g** in DMSO at 20 °C (deprotonated with 1.00–1.05 equiv. *t*-BuOK, stopped-flow UV-Vis spectrometer, λ = 395 nm).

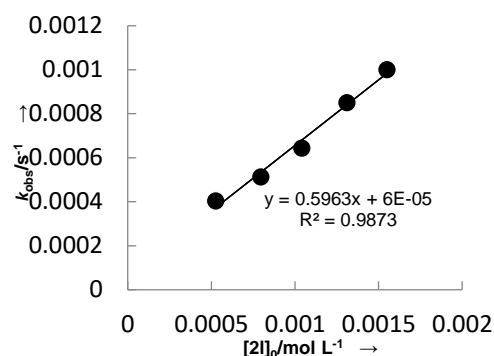
[2g]/mol L ⁻¹	[1f]/mol L ⁻¹	$k_{\text{obs}}/\text{s}^{-1}$
2.50×10^{-5}	3.14×10^{-4}	8.67×10^{-2}
2.50×10^{-5}	4.78×10^{-4}	1.35×10^{-1}
2.50×10^{-5}	6.29×10^{-3}	1.70×10^{-1}
2.50×10^{-5}	7.92×10^{-3}	2.14×10^{-1}

$k_2 = 2.65 \times 10^2 \text{ L mol}^{-1} \text{ s}^{-1}$

Table S28. Kinetics of the reactions of **1f** with **2m** in DMSO at 20 °C (deprotonated with 0.5 equiv. *t*-BuOK, conventional UV-Vis spectrometer, λ = 295 nm).

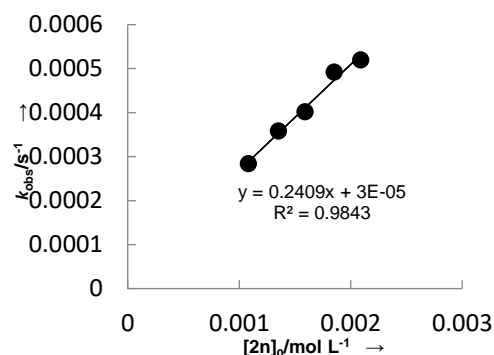
[1f]/mol L ⁻¹	[2m]/mol L ⁻¹	$k_{\text{obs}}/\text{s}^{-1}$
5.00×10^{-5}	5.26×10^{-4}	4.04×10^{-4}
5.00×10^{-5}	7.95×10^{-4}	5.13×10^{-4}
5.00×10^{-5}	1.04×10^{-3}	6.44×10^{-4}
5.00×10^{-5}	1.31×10^{-3}	8.50×10^{-4}
5.00×10^{-5}	1.55×10^{-3}	1.00×10^{-3}

$k_2 = 5.96 \times 10^{-1} \text{ L mol}^{-1} \text{ s}^{-1}$

Table S29. Kinetics of the reactions of **1f** with **2o** in DMSO at 20 °C (deprotonated with 0.5 equiv. *t*-BuOK, conventional UV-Vis spectrometer, λ = 315 nm).

[1f]/mol L ⁻¹	[2o]/mol L ⁻¹	$k_{\text{obs}}/\text{s}^{-1}$
5.00×10^{-5}	1.08×10^{-3}	2.84×10^{-4}
5.00×10^{-5}	1.35×10^{-3}	3.58×10^{-4}
5.00×10^{-5}	1.59×10^{-3}	4.02×10^{-4}
5.00×10^{-5}	1.85×10^{-3}	4.92×10^{-4}
5.00×10^{-5}	2.09×10^{-3}	5.20×10^{-4}

$k_2 = 2.41 \times 10^{-1} \text{ L mol}^{-1} \text{ s}^{-1}$

Table S30. Kinetics of the reactions of **1g** with **2a** in DMSO at 20 °C (deprotonated with 1.00–1.05 equiv. *t*-BuOK, conventional UV-Vis spectrometer, λ = 295 nm).

[2a]/mol L ⁻¹	[1g]/mol L ⁻¹	$k_{\text{obs}}/\text{s}^{-1}$
5.00×10^{-5}	4.98×10^{-4}	4.46×10^{-3}
5.00×10^{-5}	7.36×10^{-4}	6.62×10^{-3}
5.00×10^{-5}	9.77×10^{-4}	9.05×10^{-3}
5.00×10^{-5}	1.21×10^{-3}	1.14×10^{-2}
5.00×10^{-5}	1.45×10^{-3}	1.39×10^{-2}

$k_2 = 9.95 \times 10^0 \text{ L mol}^{-1} \text{ s}^{-1}$

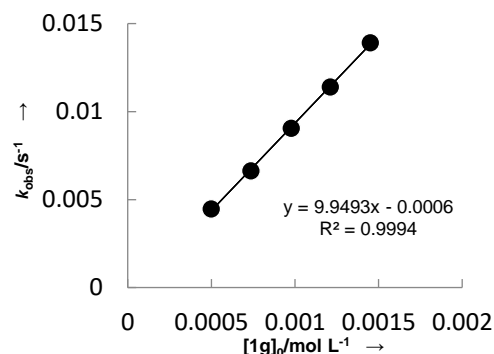
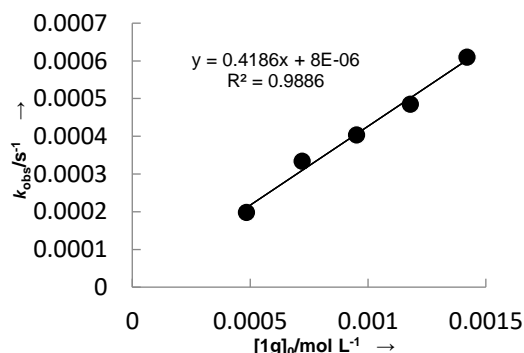


Table S31. Kinetics of the reactions of **1g** with **2b** in DMSO at 20 °C (deprotonated with 1.00–1.05 equiv. *t*-BuOK, conventional UV-Vis spectrometer, λ = 320 nm).

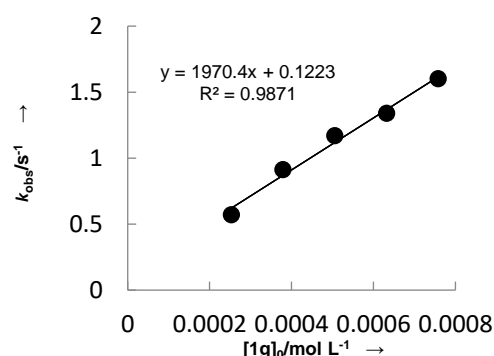
[2b]/mol L ⁻¹	[1g]/mol L ⁻¹	$k_{\text{obs}}/\text{s}^{-1}$
5.00×10^{-5}	4.84×10^{-4}	1.98×10^{-3}
5.00×10^{-5}	7.21×10^{-4}	3.34×10^{-3}
5.00×10^{-5}	9.52×10^{-4}	4.04×10^{-3}
5.00×10^{-5}	1.18×10^{-3}	4.85×10^{-2}
5.00×10^{-5}	1.42×10^{-3}	6.10×10^{-2}

$$k_2 = 4.19 \times 10^{-1} \text{ L mol}^{-1} \text{ s}^{-1}$$

Table S32. Kinetics of the reactions of **1g** with **2e** in DMSO at 20 °C (deprotonated with 1.00–1.05 equiv. *t*-BuOK, stopped-flow UV-Vis spectrometer, λ = 405 nm).

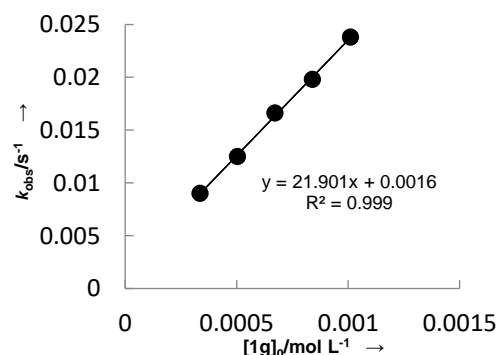
[2e]/mol L ⁻¹	[1g]/mol L ⁻¹	$k_{\text{obs}}/\text{s}^{-1}$
2.50×10^{-5}	2.53×10^{-4}	5.70×10^{-1}
2.50×10^{-5}	3.79×10^{-4}	9.11×10^{-1}
2.50×10^{-5}	5.05×10^{-4}	1.17×10^0
2.50×10^{-5}	6.32×10^{-3}	1.34×10^0
2.50×10^{-5}	7.58×10^{-3}	1.60×10^0

$$k_2 = 1.97 \times 10^3 \text{ L mol}^{-1} \text{ s}^{-1}$$

Table S33. Kinetics of the reactions of **1g** with **2f** in DMSO at 20 °C (deprotonated with 1.00–1.05 equiv. *t*-BuOK, stopped-flow UV-Vis spectrometer, λ = 550 nm).

[2f]/mol L ⁻¹	[1g]/mol L ⁻¹	$k_{\text{obs}}/\text{s}^{-1}$
2.50×10^{-5}	3.36×10^{-4}	9.01×10^{-3}
2.50×10^{-5}	5.03×10^{-4}	1.25×10^{-2}
2.50×10^{-5}	6.71×10^{-4}	1.66×10^{-2}
2.50×10^{-5}	8.39×10^{-4}	1.98×10^{-2}
2.50×10^{-5}	1.01×10^{-3}	2.38×10^{-2}

$$k_2 = 2.19 \times 10^1 \text{ L mol}^{-1} \text{ s}^{-1}$$

Table S34. Kinetics of the reactions of **1g** with **2h** in DMSO at 20 °C (deprotonated with 1.00–1.05 equiv. *t*-BuOK, conventional UV-Vis spectrometer, λ = 540 nm).

[2h]/mol L ⁻¹	[1g]/mol L ⁻¹	$k_{\text{obs}}/\text{s}^{-1}$
5.00×10^{-5}	4.54×10^{-4}	1.23×10^{-2}
5.00×10^{-5}	6.75×10^{-4}	1.90×10^{-2}
5.00×10^{-5}	8.92×10^{-4}	2.45×10^{-2}
5.00×10^{-5}	1.10×10^{-3}	2.95×10^{-2}
5.00×10^{-5}	1.31×10^{-3}	3.48×10^{-2}

$$k_2 = 2.60 \times 10^1 \text{ L mol}^{-1} \text{ s}^{-1}$$

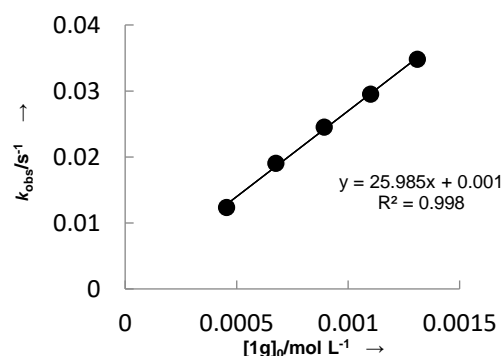
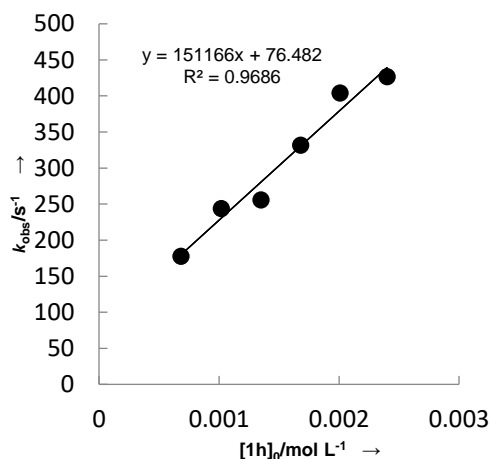


Table S35. Kinetics of the reactions of **1h** with **2i** in DMSO at 20 °C (deprotonated with 1.00–1.05 equiv. *t*-BuOK, conventional UV-Vis spectrometer, $\lambda=265$ nm).

[2i]/mol L ⁻¹	[1h]/mol L ⁻¹	$k_{\text{obs}}/\text{s}^{-1}$
7.00×10^{-5}	6.83×10^{-4}	1.78×10^2
7.00×10^{-5}	1.02×10^{-3}	2.44×10^2
7.00×10^{-5}	1.35×10^{-3}	2.56×10^2
7.00×10^{-5}	1.68×10^{-3}	3.32×10^2
7.00×10^{-5}	2.01×10^{-3}	4.04×10^2
7.00×10^{-5}	2.40×10^{-3}	4.27×10^2

$k_2 = 1.51 \times 10^5 \text{ L mol}^{-1} \text{ s}^{-1}$



(3) Correlation of the $\log k_2/s_N$ for the reactions of heteroallenes **1a and **1c** with carbanions versus the corresponding nucleophilicity parameters N**

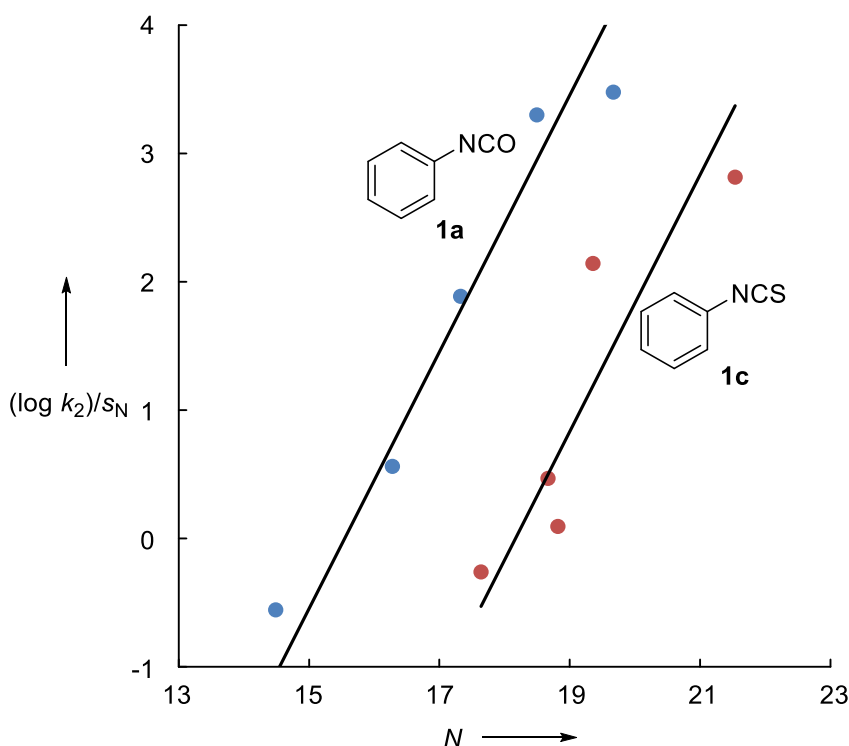


Figure S1. Plot of $(\log k_2)/s_N$ vs N for the reactions of phenylisocyanate **1a** with carbanions **2** in CH_3CN and phenylisothiocyanate **1c** with carbanions **2** in DMSO at 20 °C (the slope is enforced to 1).

(4) Detailed experiments for investigation of carbon dioxide

I. Deriving solubility of carbon dioxide in DMSO at 20 °C under 1 atm (101 kPa) CO₂ partial pressure

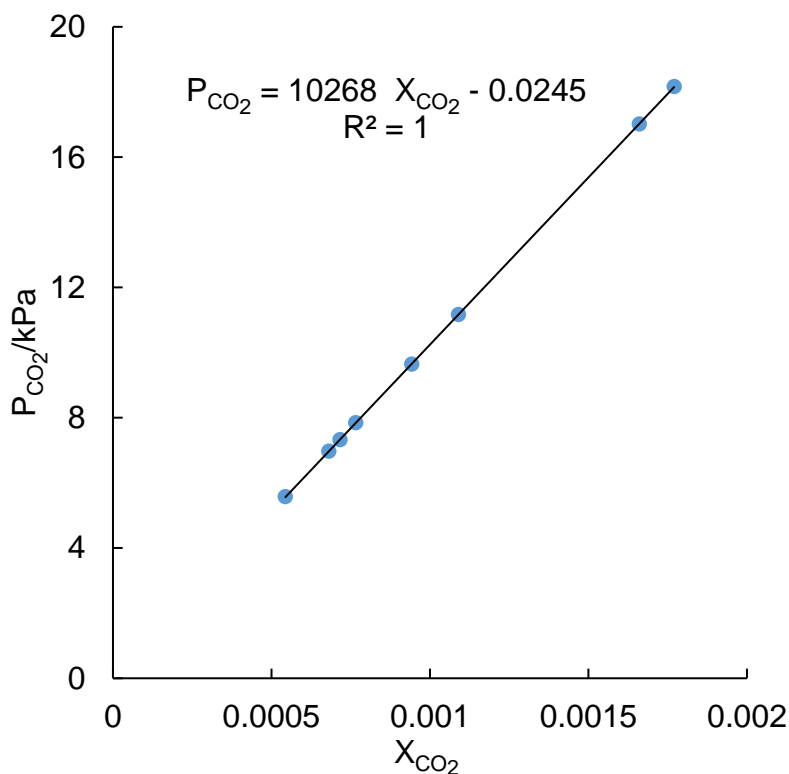


Figure S2. Plot of partial pressure of CO₂ (P_{CO_2} kPa) with mole fraction of CO₂ in DMSO solution (X_{CO_2}) at 20 °C

Li Hua group has reported a correlation between the partial pressure of CO₂ in the gas phase and the solubility of CO₂ in DMSO solution at 20 °C (Figure S2).¹⁸ This correlation allowed to calculate the molar ratio of CO₂ in DMSO solution when P_{CO_2} is 1 atm (101 kPa).

$$101 = 10268 X_{CO_2} - 0.0245 \quad \text{so} \quad X_{CO_2} = n(CO_2) / [n(CO_2) + n(DMSO)] = 9.8 \times 10^{-3}$$

$n(CO_2)$ is mole of CO₂ dissolved in DMSO solution and $n(DMSO)$ is mole of DMSO liquid.

As $n(CO_2)$ is much smaller than $n(DMSO)$, $X_{CO_2} = n(CO_2)/n(DMSO)$

$$9.8 \times 10^{-3} = n(CO_2)/n(DMSO) = n(CO_2) / \{ [v(DMSO) L \times 1100 g \cdot L^{-1}] / 78.13 g \cdot mol^{-1} \}$$

The concentration of CO₂ in DMSO is thus given by $[CO_2] = n(CO_2)/v(DMSO) = 1.38 \times 10^{-1} M$

II. Preparation of a stock solution with $[\text{CO}_2]_s = 1.38 \times 10^{-1} \text{ M}$

- 25-mL volumetric flask was dried by heat gun under reduced pressure, evacuated and then filled with pure CO_2 . This operation is repeated three times using CO_2 from sublimation of dry ice and passed through drying agent system (CaCl_2 and silica gel).
- Then 10 mL of anhydrous DMSO were filled into a 25-mL volumetric flask containing pure CO_2 . Afterwards a stream of pure CO_2 is passed through the DMSO solution for 30 min to generate a saturated CO_2 solution (Picture 1).

Picture 1 (left) and picture 2 (right)



- Afterwards a balloon with pure CO_2 was placed on the flask to maintain a pressure of 1 atm CO_2 .

III. Preparation of a series of dilute solutions with different $[\text{CO}_2]$

- In six 5-mL volumetric flasks filled with Ar gas was added 6 mL anhydrous DMSO that the gas phase above the liquid is less than 1 mL (Picture 2). Variable amounts ($V_n = 0.06 - 0.18 \text{ mL}$) of CO_2 stock solution were transferred into these six volumetric flasks to get dilute solutions which are used for kinetic measurements directly.

b. Most of transferred CO_2 from stock solution is dissolved in DMSO of 5-mL volumetric flask, we thus derive the concentration of dilute solution $[\text{CO}_2]_n = V_n \times [\text{CO}_2]_s / (V_n + 6)$. This conclusion can be verified by equations shown below:

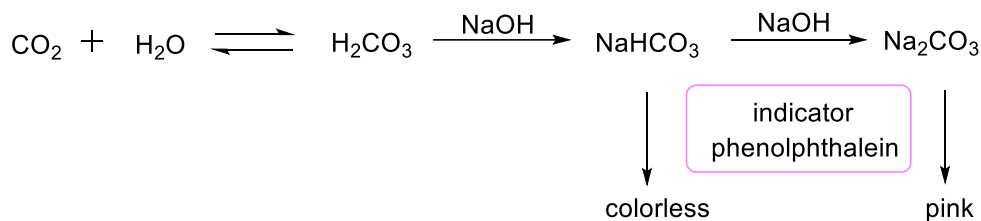
Ideal gas law is $PV = 8.31(\text{kPa} \cdot \text{L} \cdot \text{mol}^{-1} \cdot \text{K}^{-1}) \cdot n \cdot T$. In our case, it can be expressed by $P_{\text{CO}_2} V_{\text{gas}} = 8.31(\text{kPa} \cdot \text{L} \cdot \text{mol}^{-1} \cdot \text{K}^{-1}) \cdot n(\text{CO}_2)_{\text{gas}} \cdot T$.

Henry law is $P_{\text{CO}_2} = 10268 X_{\text{CO}_2} - 0.0245$, namely $P_{\text{CO}_2} = 10268 n(\text{CO}_2) / \{ [v(\text{DMSO}) \times 1100 \text{ g} \cdot \text{L}^{-1}] / 78 \text{ g} \cdot \text{mol}^{-1} \} - 0.0245$. Since 0.0245 is very small and can be neglected in my case, we derive $n(\text{CO}_2)_{\text{DMSO}} / n(\text{CO}_2)_{\text{gas}} = 3.34 \cdot (V_{\text{DMSO}} / V_{\text{gas}})$

In my case $V_{\text{DMSO}} = 6 \text{ mL}$, $V_{\text{gas}} < 1 \text{ mL}$, so $n(\text{CO}_2)_{\text{DMSO}} / n(\text{CO}_2)_{\text{gas}} > 20$. It indicates that most of transferred CO_2 from stock solution will be dissolved in DMSO of 5-mL volumetric flask, the amount of CO_2 going to gas phase can be neglected.

IV. Titration of the dilute solution of $[\text{CO}_2]_n$ in DMSO

a. Principle of titration method



End point is light pink.

b. Preparation of degassed water: Ar was passed through a distilled water for 1 h in order to remove dissolved CO_2 completely.

c. 0.18 mL of a stock solution ($[\text{CO}_2]_s = 1.38 \times 10^{-1} \text{ M}$) was transferred into 6 mL of DMSO solution in the 5 mL volumetric flask. Then 4 mL of this solution was transferred into 10 mL degassed water.

d. This mixed solution of CO_2 in water and DMSO was titrated by NaOH standard solution (0.1 M) using phenolphthalein as indicator (7.4 ‰). (The titration was preformed in a closed system to ensure that atmospheric CO_2 does not influence the results)

V(NaOH) (mL)	n(CO ₂) (mmol)
0.16	0.016
0.17	0.017
0.18	0.018
average	0.017

Our way: $n(\text{CO}_2) = [0.18 \text{ mL} \times 1.38 \times 10^{-1} \text{ M} / (0.18 + 6) \text{ mL}] \times 4 \text{ mL} = 0.0161 \text{ mmol}$

Deviation = $(0.017 - 0.0161) / 0.0161 = 5.6\%$

(5) Computational analysis (completed by Robert J. Mayer)

Methyl anion affinities were calculated following the previously published protocol as the negative free energy for the methyl anion addition reaction (eq 2).¹⁵

Conformers for reactants and products were searched with the OPLS3 force field as implemented in the MacroModel software. All conformers were then optimized in Gaussian 16 employing the B3LYP/6-31G(d,p) method in gas phase. Thermochemical corrections to Gibbs energies (corr. ΔG) at 298.15 K have been calculated using the rigid rotor/harmonic oscillator model without any scaling. Gibbs energies (ΔG_{298}) at B3LYP/6-31G(d,p) level have been obtained through addition of ΔE_{tot} and corr. ΔG . Single point total electronic energies (ΔE_{tot}) have subsequently been calculated using a combination of the B3LYP hybrid functional and the larger 6-311++G(3df,2pd) basis set. Final Gibbs energies (ΔG_{298}) have been obtained through a combination of ΔE_{tot} with the thermochemical corrections to Gibbs energies (corr. ΔG) calculated at a lower level. In the following these will be designated as ΔG_{gas} at [B3LYP/6-311++G(3df,2pd)//B3LYP/6-31G(d,p)]. Solvent effects on MAA values have first been estimated by adding single point solvation corrections (ΔG_{Solv}) to ΔG_{gas} for equation S1. ΔG_{Solv} was calculated for gas phase optimized geometries using the SMD continuum solvation model and subsequently added to gas phase Gibbs energies (ΔG_{gas}) to obtain solution phase Gibbs energies that will be designated single point solvation free energies ($\Delta G_{\text{sol-sp}}$).

In analogy to previous studies, we tested the applicability of frontier molecular orbital energies as well as global and local electrophilicity indices to predict experimental electrophilicity parameters.

$$\mu \approx \frac{\text{HOMO}_E + \text{LUMO}_E}{2}$$

$$\eta \approx \text{LUMO}_E - \text{HOMO}_E$$

$$\omega = \frac{\mu^2}{2\eta}$$

Local electrophilicities were calculated based on the nucleophilic Fukui function (f_k^+) as defined in equation S2.

$$\omega_k = \omega f_k^+ \quad (\text{S2})$$

We used Yang and Mortier's method¹⁹ in which f_k^+ is defined as change of partial charge q at the reaction center k by adding an electron to the molecule with N being the total number of electrons in the neutral species.

$$f_k^+ = q(k, N + 1) - q(k, N)$$

In this work, we applied Mulliken charges for this procedure.

4.5 References

- (1) (a) Brandsma, L. *Eur. J. Org. Chem.* **2001**, 4569–4581. (b) Louie, J. *Curr. Org. Chem.* **2005**, 9, 605–623. (c) Schenk, S.; Notni, J.; Köhn, U.; Wermann, K.; Anders, E. *Dalton Trans.* **2006**, 4191–4206.
- (2) (a) Tidwell, T. T. *Acc. Chem. Res.* **1990**, 23, 273–279. (b) Tidwell, T. T. *Eur. J. Org. Chem.* **2006**, 563–576. (c) Allen, A. D.; Tidwell, T. T. *Eur. J. Org. Chem.* **2012**, 1081–1096. (d) Allen, A. D.; Tidwell, T. T. *Arkivoc* **2016**, (i) 415–490.
- (3) (a) Ozaki, S. *Chem. Rev.* **1972**, 72, 457–496. (b) Arnold, R. G.; Nelson, J. A.; Verbanc, J. J. *Chem. Rev.* **1957**, 57, 47–76. (c) Rasmussen, J. K.; Hassner, A. *Chem. Rev.* **1976**, 76, 389–408.
- (4) Ashare, R.; Mukerjee, A. K. *Chem. Rev.* **1991**, 91, 1–24.
- (5) Williams, A.; Ibrahim, I. T. *Chem. Rev.* **1981**, 81, 589–636.
- (6) (a) Yokoyama, M.; Imamoto, T. *Synthesis* **1984**, 797–824. (b) Rudolf, W. D. *Sulfur Reports* **1991**, 11, 51–141. (c) Rudolf, W. D. *J. Sulfur. Chem.* **2007**, 28, 295–339. (d) Iglesias-Sigüenza, F. J. *Synlett* **2009**, 157–158.
- (7) (a) Sakakura, T.; Choi, J.-C.; Yasuda, H. *Chem. Rev.* **2007**, 107, 2365–2387. (b) Liu, Q.; Wu, L.; Jackstell, R.; Beller, M. *Nat. Commun.* **2005**, 6, 5933.
- (8) (a) Aresta, M. *Carbon Dioxide as Chemical Feedstock*; Wiley-VCH: Weinheim, 2010. (b) Centi, G.; Perathoner, S. *Green Carbon Dioxide: Advances in CO₂ Utilization*; Wiley-VCH: Weinheim, 2014.
- (9) (a) Mayr, H.; Bug, T.; Gotta, M. F.; Hering, N.; Irrgang, B.; Janker, B.; Kempf, B.; Loos, R.; Ofial, A. R.; Remennikov, G.; Schimmel, H. *J. Am. Chem. Soc.* **2001**, 123, 9500–9512. (b) Lucius, R.; Loos, R.; Mayr, H. *Angew. Chem., Int. Ed.* **2002**, 41, 91–95. (c) Mayr, H.; Kempf, B.; Ofial, A. R. *Acc. Chem. Res.* **2003**, 36, 66–77.
- (10) (a) Berger, S. T. A.; Ofial, A. R.; Mayr, H. *J. Am. Chem. Soc.* **2007**, 129, 9753–9761. (b) Corral-Bautista, F.; Mayr, H. *Eur. J. Org. Chem.* **2013**, 4255–4261. (c) Kaumanns, O.; Appel, R.; Lemek, T.; Seeliger, F.; Mayr, H. *J. Org. Chem.* **2009**, 74, 75–81. (d) Corral-Bautista, F.; Klier, L.; Knochel, P.; Mayr, H. *Angew. Chem., Int. Ed.* **2015**, 54, 12497–12500. (e) Seeliger, F.; Mayr, H. *Org. Biomol. Chem.* **2008**, 6, 3052–3058. (f) Bug, T.; Lemek, T.; Mayr, H. *J. Org. Chem.* **2004**, 69, 7565–7576. (g) Lemek, T.; Mayr, H. *J. Org. Chem.* **2003**, 68, 6880–6886. (h) Timofeeva, D. S.; Mayer, R.; Mayer, P.; Ofial, A.; Mayr, H. *Chem. - Eur. J.* **2018**, 24, 5901–5910. (i) Corral-Bautista, F.; Appel, R.; Frickel, J. S.; Mayr, H. *Chem. - Eur. J.* **2015**, 21, 875–884.

- (11) For a comprehensive database of nucleophilicity parameters N and s_N as well as electrophilicity parameters E , see <http://www.cup.lmu.de/oc/mayr/DBintro.html>.
- (12) Opitz, G.; Koch, J. *Angew. Chem.* **1963**, 75, 167.
- (13) (a) Shvydenko, T.; Nazarenko, K.; Shvydenko, K.; Boron, S.; Gutov, O.; Tolmachev, A.; Kostyuk, A. *Tetrahedron* **2017**, 73, 6942–6953. (b) Lyutenko, N. V.; Gerus, I. I.; Kacharov, A. D.; Kukhar, V. P. *Tetrahedron* **2003**, 59, 1731–1738. (c) Sugiura, M.; Kashiwagi, T.; Ito, M.; Kotani, S.; Nakajima, M. *J. Org. Chem.* **2017**, 82, 10968–10979. (d) Kostyuk, A. N.; Volochnyuk, D. M.; Lupiha, L. N.; Pinchuk, A. M.; Tolmachev, A. A. *Tetrahedron Lett.* **2002**, 43, 5423–5425. (e) Vilsmaier, E.; Adam, R.; Altmeier, P.; Fath, J.; Scherer, H. J.; Maas, G.; Wagner, O. *Tetrahedron* **1989**, 45, 6683–6696.
- (14) (a) Keeffe, J. R.; Palmer, C. A.; Lee, J. C. *J. Am. Chem. Soc.* **1979**, 101, 1295–1297. (b) Olmstead, W. N.; Bordwell, F. G. *J. Org. Chem.* **1980**, 45, 3299–3305. (c) Bordwell, F. G.; Cheng, J-P.; Bausch, M. J. Bares, J. E. *J. Phys. Org. Chem.* **1988**, 1, 209–223. (d) Bordwell, F. G. *Acc. Chem. Res.* **1988**, 21, 456–463. (e) Bordwell, F. G.; Harrelson, J. A. *Can. J. Chem.* **1990**, 68, 1714–1718. (f) Bordwell, F. G.; Fried, H. E. *J. Org. Chem.* **1981**, 46, 4327–4331. (g) Matthews, W. S.; Bares, J. E.; Bartmess, J. E.; Bordwell, F. G.; Cornforth, F. J.; Drucker, G. E.; Margolin, Z.; McCallum, R. J.; McCollum, G. J.; Vanier, N. R. *J. Am. Chem. Soc.* **1975**, 97, 7006–7014. (h) Bordwell, F. G.; Drucker, G. E. *J. Org. Chem.* **1980**, 45, 3325–3328.
- (15) (a) Allgäuer, D. S.; Jangra, H.; Asahara, H.; Li, Z.; Chen, Q.; Zipse, H.; Ofial, A. R.; Mayr, H. *J. Am. Chem. Soc.* **2017**, 139, 13318–13329. (b) Li, Z.; Jangra, H.; Chen, Q.; Mayer, P.; Ofial, A. R.; Zipse, H.; Mayr, H. *J. Am. Chem. Soc.* **2018**, 140, 5500–5515.
- (16) Clark, T.; Chandrasekhar, J.; Spitznagel, G. W.; Schleyer, P. v. R. *J. Comput. Chem.* **1983**, 4, 294–301.
- (17) Marenich, A. V.; Cramer, C. J.; Truhlar, D. G. *J. Phys. Chem. B.* **2009**, 113, 6378–6396.
- (18) Hua, L. *Phys. Chem. Liq.* **2009**, 47, 296–301.
- (19) Yang, W.; Mortier, W. *J. Am. Chem. Soc.* **1986**, 108, 5708–5711.

Chapter 5 Kinetics and Mechanism of Corey-Chaykovsky Reactions of Acceptor-substituted Ketones

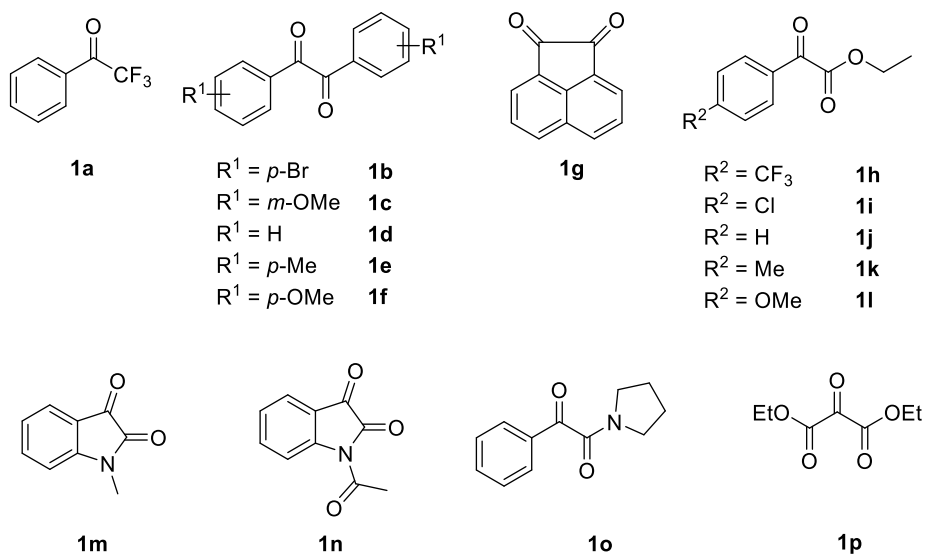
5.1 Introduction

Previously, we have developed scales of nucleophilicity and electrophilicity based on equation 1, where electrophiles are characterized by one parameter, E , and nucleophiles are characterized by two solvent-dependent parameters, N and s_N . Reactions of carbenium ions and other C_{sp^2} -centered electrophiles with different classes of σ -, π -, and n -nucleophiles are applicable to this linear free-energy relationship 1.¹

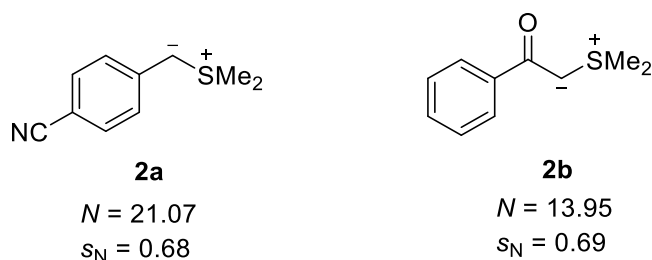
$$\log k_2(20\text{ }^\circ\text{C}) = s_N(N + E) \quad (1)$$

Carbonyl compounds belong to the most common electrophiles, which are widely employed in organic synthesis. We have already quantified aldehydes and aliphatic ketones previously.² As acceptor-substituted ketones are highly reactive and undergo numerous reactions with various nucleophiles under mild conditions, we tried to quantify their electrophilic reactivities and compare their electrophilicities with those of aliphatic ketones. Since the alkoxide anions initially formed by additions of nucleophiles to carbonyl groups are highly basic ($pK_{aH} = 29.0$ for MeO^- in DMSO),^{3,4} the reactions of ketones with acceptor-stabilized carbanions (e. g. malonate anions) are highly endergonic in aprotic solvents and only proceed in the presence of a suitable proton source. Thus we employed sulfonium ylides⁵ as reference nucleophiles which react with ketones to yield intermediates that undergo subsequent irreversible reactions with formation of stable epoxides.

Scheme 1. Activated Ketones Studied in This Work



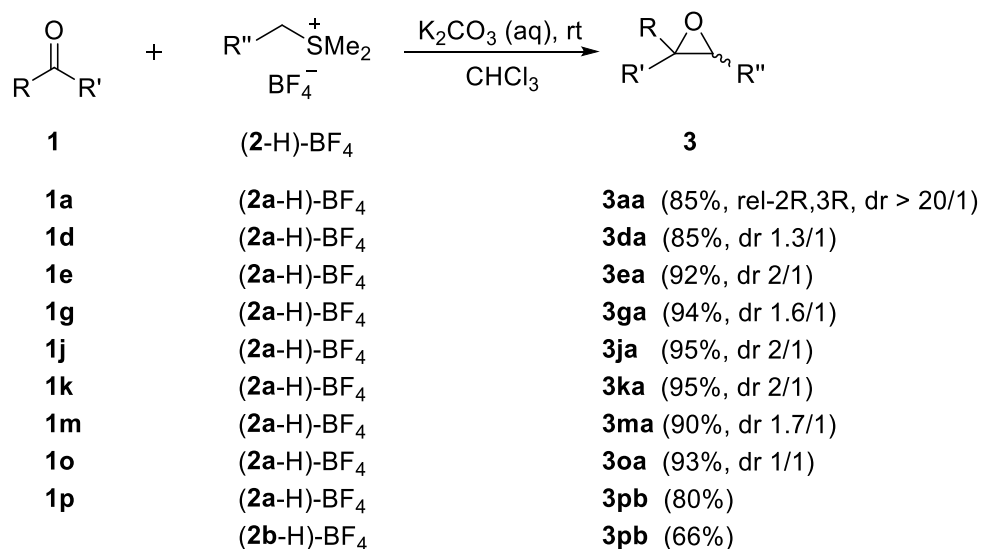
Scheme 2. Reference Nucleophiles Sulfonium Ylides **2** and their N and s_N Values.



5.2 Results

Product study. The reactions of the activated ketones **1** (Scheme 1) with the sulfonium ylides **2** (Scheme 2) proceeded smoothly at room temperature under phase transfer conditions (CHCl_3 /aqueous solution of K_2CO_3) to give the epoxides **3** in good yields. Unsymmetrical ketones generally reacted with low diastereoselectivity; Only **1a** gave one diastereomer exclusively.

Scheme 3. Reactions of Sulfur Ylides **2** with Activated Ketones **1**.



Kinetic investigations. The rates of the reactions of **1** with **2** were determined in DMSO at 20 °C by following the disappearance of the UV/Vis absorption of sulfonium ylides **2** under pseudo-first-order conditions ($[\mathbf{1}]_0/[\mathbf{2}]_0 > 10$). As the ylide **2a** decomposes slowly at 20 °C, it was generated by treatment of the corresponding sulfonium ion with 1.00–1.05 equiv of *t*-BuOK in dry THF at –78 °C. Small amounts of these solutions were then dissolved in DMSO at 20 °C immediately before the ketones **1** were added. The first-order rate constants k_{obs} were obtained by least-squares fitting of the exponential function $A = A_0 \exp(-k_{\text{obs}}t) + C$ to the observed time-dependent absorbances A of **2** (Figure 1a). The slopes of the linear correlations between k_{obs} and

the different concentrations of **1a-j** (Figure 1b) correspond to the second-order rate constants k_2^{exp} listed in Table 1.

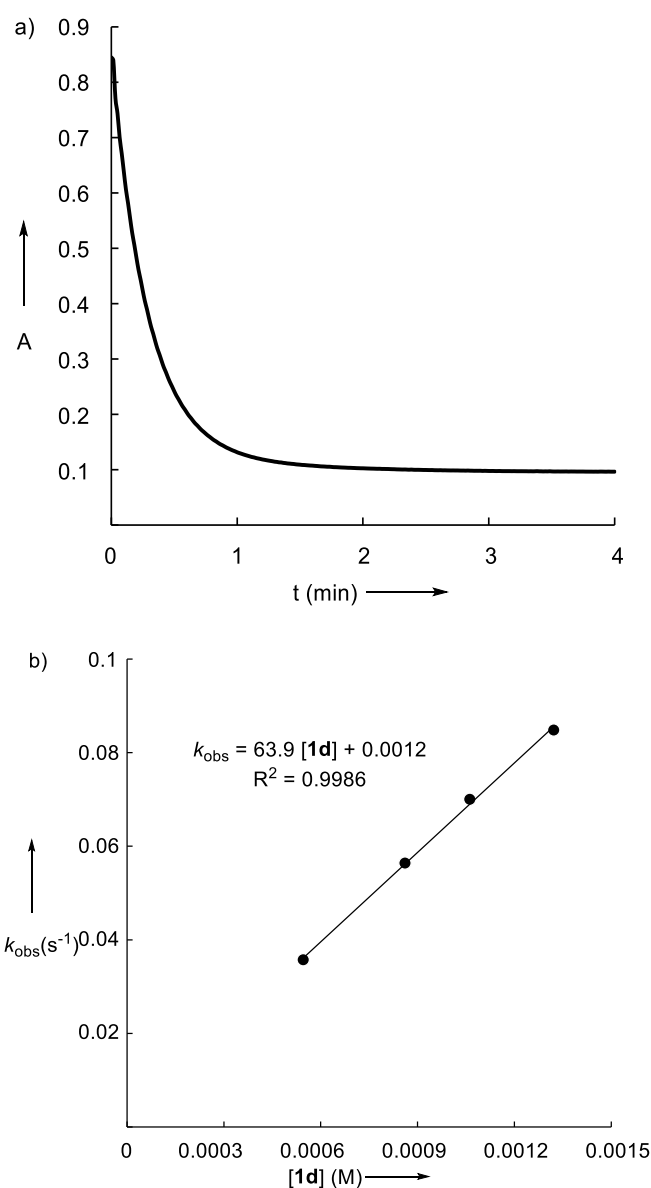


Figure 1. a) Monoexponential decay of the absorbance A of **2a** ($5.00 \times 10^{-5} \text{ mol L}^{-1}$) at 380 nm during its reaction with **1d** ($8.62 \times 10^{-4} \text{ mol L}^{-1}$) in DMSO at 20 °C. b) Plot of k_{obs} for the reaction of **1d** with **2a** versus the concentration of **1d**.

Table 1. Second-Order Rate Constants k_2^{exp} (20 °C) for the Reactions of Activated Ketones **1** with Sulfonium Ylides **2**.

Electrophile	Nucleophile	k_2^{exp}
1a	2a	1.51×10^4
1b	2a	6.58×10^2
1c	2a	1.12×10^2
1d	2a	6.96×10^1
1e	2a	1.54×10^1
1f	2a	1.71×10^0
1g	2a	1.80×10^2
1h	2a	3.38×10^2
1i	2a	2.66×10^3
1j	2a	3.47×10^0
1k	2a	2.37×10^1
1l	2a	6.24×10^0
1m	2a	1.40×10^2
1n	2a	5.97×10^3
1o	2a	1.12×10^2
1p	2a	too fast
1p	2b	1.26×10^2

The Hammett correlation for the reactions of the benzil derivatives **1b–f** with the sulfonium ylide **2a** is of good quality and gives rise to the Hammett reaction constants $\rho = 3.89$ (Figure 2). A similar Hammett reaction constant $\rho = 3.10$ is obtained for the reactions of activated ketones **1h–l** with **2a** (Figure 3).

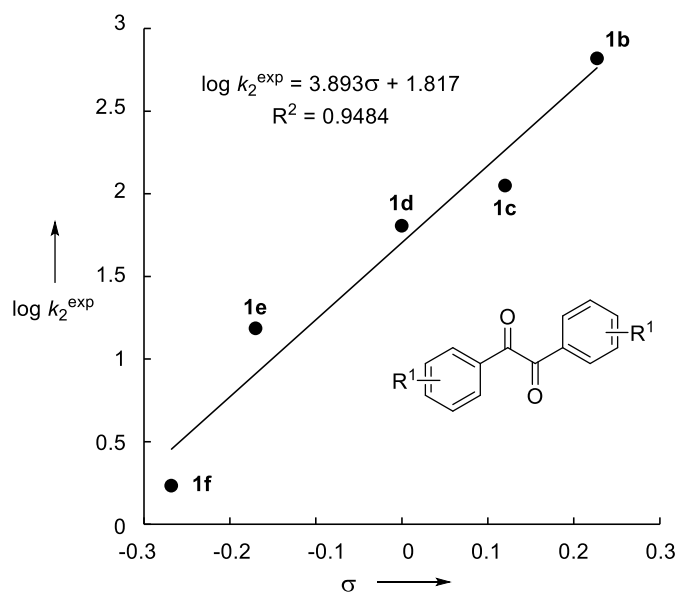


Figure 2. Correlation of the second-order rate constants $\log k_2^{\text{exp}}$ for the reactions of the benzil derivatives **1b–f** with the sulfonium ylide **2a** vs Hammett's σ values for R^1 .⁶

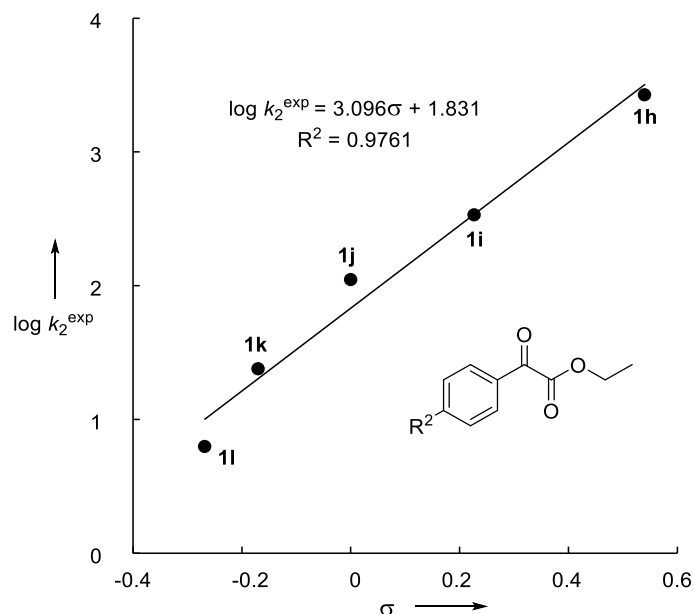
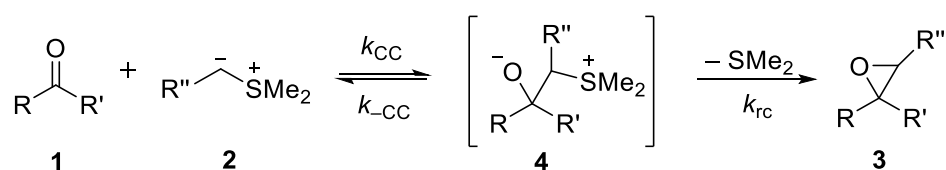


Figure 3. Correlation of the second-order rate constants $\log k_2^{\text{exp}}$ for the reactions of the activated ketones **1h-l** with the sulfonium ylide **2a** vs vs Hammett's σ values for R^2 .⁶

The negative deviation of the methoxy-substituted derivatives **1f** and **1l** indicates that resonance stabilization of the ground states is contributing. We abstained to analyze this effect in more detail by using the Yukawn-Tsuno treatment because the following discussion shows that k_2^{exp} is not an elementary rate constant.

Reaction mechanism

Scheme 4. Mechanism of the Reactions of Sulfonium Ylides with Ketones

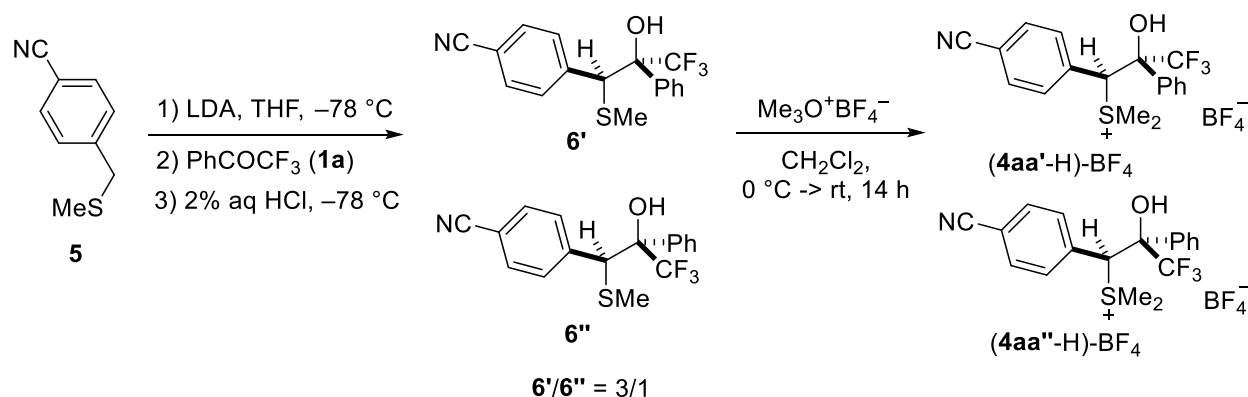


As shown in Scheme 4, the sulfur ylide mediated epoxidations (Corey-Chaykovsky reaction) proceed via initial nucleophilic attack of sulfonium ylide **2** at ketone **1** to give the zwitterion **4** which either undergoes retroaddition (k_{-CC}) or intramolecular substitution with elimination of dimethyl sulfide and formation of epoxide **3**. Aggarwal have reported seminal works about mechanism of these reactions previously.⁷ As derived for the mechanistically analogous Darzens condensation in the preceding chapter, k_2^{exp} is a function of k_{CC} , k_{-CC} , and k_{rc} as shown by equation 2.^{2b}

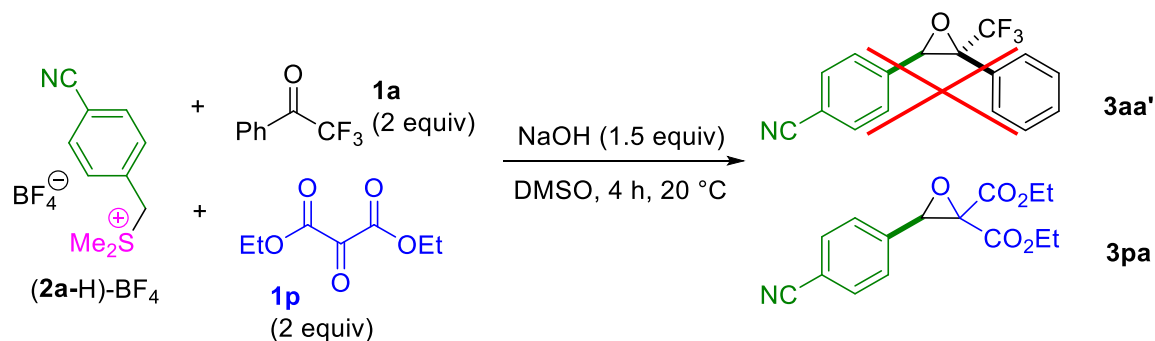
$$k_2^{\text{exp}} = k_{CC}/(k_{-CC}/k_{rc} + 1) \quad (2)$$

According to equation 2, we can derive the rate of nucleophilic attack of **2** at the carbonyl group (k_{CC}) from the measured rate constant k_2^{exp} and the ratio k_{CC}/k_{rc} , which can be determined from crossover experiments using independently synthesized **4-H**. 2,2,2-Trifluoroacetophenone **1a** was selected as example to illustrate the principle of the crossover experiments.

Scheme 5. Synthesis of the **4aa-H**



Scheme 6. Competition Experiment Demonstrating the much Higher Reactivity of Ketone **1p** Compared to Ketone **1a**

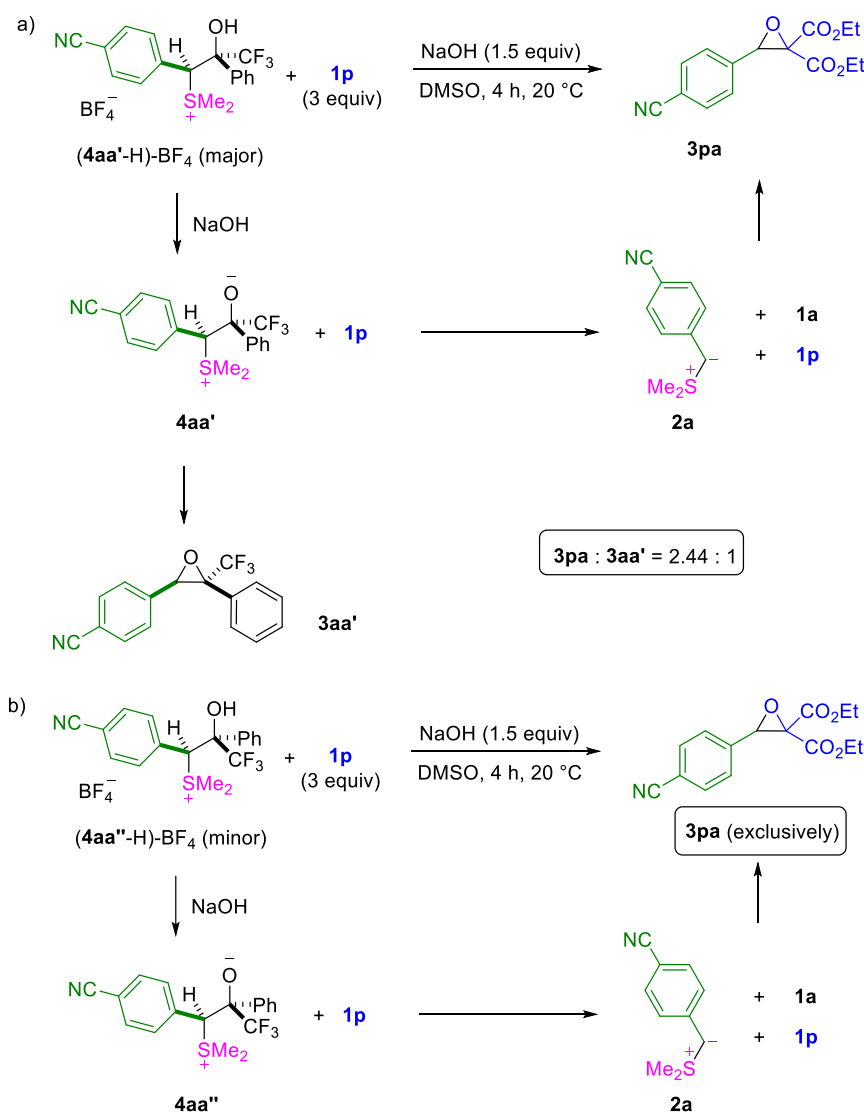


Treatment of the benzylthioether **5** with LDA and ketone **1a** yielded two diastereoisomers of the β -methylthio substituted alcohols **6'** and **6''** which were separated by column chromatography.⁷ Treatment of **6'** and **6''** with trimethyloxonium tetrafluoroborate generated the corresponding sulfonium tetrafluoroborates **4aa'-H** and **4aa''-H** respectively.⁸ The relative stereochemistry of two diastereoisomers are determined by the stereospecific cyclization product of **3aa**.

Scheme 6 shows that the reactions of sulfonium ylide **2a** with a mixture of ketones **1a** and **1p** (2 equivalents each) exclusively gave product **3pa**, indicating that **1p** is much more reactive than **1a**. Ketone **1p** can therefore be used as a trapping agent for the crossover experiments with **4aa'-H** and **4aa''-H**. As shown in Scheme 7a, when **4aa'-H** was treated with NaOH in the presence of **1p**, crossover product **3pa** and cyclization product **3aa'** were formed in the ratio 2.4/1. Analogously, treatment of the other diastereomer (**4aa''-H**) with NaOH in the presence of **1p**

yielded the crossover product **3pa** exclusively (Scheme 7b). The results of the crossover experiments suggest the preferred formation of product **3aa'** with Ar and CF₃ trans to each other, since the rate of cyclization of **4aa''** is much slower than the rate of retroaddition with regeneration of **1a** and **2a**. We can split the measured gross second order rate constant $k_2^{\text{exp}} = 1.51 \times 10^4 \text{ M}^{-1} \text{ s}^{-1}$ for the reaction of **1a** with **2a** (Table 1) into the partial rate constants $k_2^{\text{exp}'}$ and $k_2^{\text{exp}''}$ for the formation of **3aa'** and **3aa''**, respectively. As **3aa''** was not observed ($k_2^{\text{exp}''} = 0$), we could derive $k_2^{\text{exp}'} = k_2^{\text{exp}} = 1.51 \times 10^4 \text{ M}^{-1} \text{ s}^{-1}$. Applying equation 2 with $k_{\text{CC}}'/k_{\text{re}}' = 2.4$ (Scheme 7) we obtain $k_{\text{CC}}' = (2.4 + 1) \times (1.51 \times 10^4) \text{ M}^{-1} \text{ s}^{-1} = 5.1 \times 10^4 \text{ M}^{-1} \text{ s}^{-1}$. Since the diastereoselectivity of initial attack of sulfonium ylide **2a** at the ketone **1a** is unknown in DMSO solution at 20 °C under the conditions of the kinetic experiments, we cannot derive k_{CC}'' and subsequently derive the *E* parameter.

Scheme 7. Crossover Experiments of **4aa'**-H and **4aa''**-H



5.3 Conclusion

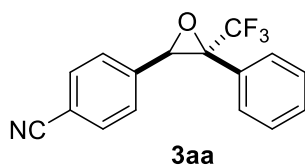
We have investigated the kinetics of reactions of activated ketones **1** with sulfonium ylides **2** in DMSO at 20 °C and obtained the corresponding gross second-order rate constants k_2^{exp} . Crossover experiments with the independently generated zwitterions **4aa'** and **4aa''** showed that **4aa'** underwent cyclization to the epoxide 2.4 times slower than retroaddition while its diastereomer **4aa''** did not cyclize at all and exclusively reacted with retroaddition.

5.4 Experimental section

(1) Product study

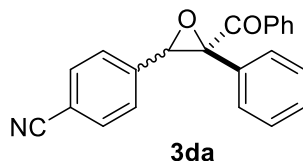
Procedure A for the synthesis of **3**. Saturated aqueous K_2CO_3 -solution (5 mL) was added to a vigorously stirred solution of sulfonium tetrafluoroborate (**2a-H**)- BF_4 (133mg, 0.501 mmol) and ketones **1** (0.50 mmol) in CHCl_3 (15 mL). The resulting biphasic mixture was vigorously stirred for 3 h. During this reaction further portions of (**2a-H**)- BF_4 were added after 1h (133mg, 0.501 mmol) and 2.5 h (67 mg, 0.25 mmol). The reaction was subsequently treated with water, the organic layer was separated and the aqueous phase additionally extracted by CHCl_3 . The combined organic layers were washed with water and brine, dried over Na_2SO_4 , and evaporated under reduced pressure. Purification of the crude product by column chromatography on silica gel.

4-((rel-2R,3S)-3-Phenyl-3-(trifluoromethyl)oxiran-2-yl)benzonitrile was obtained according to Procedure A from **1a** (87 mg, 0.50 mmol): white solid (124 mg, 0.429 mmol, 86%), mp 125–130 °C.



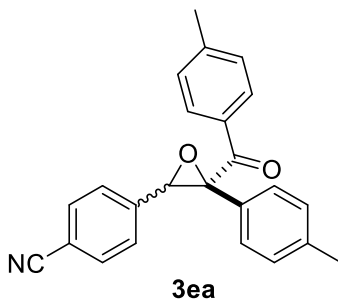
^1H NMR (400 MHz, CDCl_3) δ 7.43 (d, $J = 8.4$ Hz, 2H), 7.33 – 7.24 (m, 5H), 7.13 (d, $J = 8.0$ Hz, 2H), 4.64 (s, 1H). **^{13}C NMR** (101 MHz, CDCl_3) δ 137.5 (C), 131.9 (CH), 129.9 (CH), 129.1 (CH), 128.5 (CH), 127.5 (CH), 127.4 (C), 122.9 (q, $J_{\text{CF}} = 281$ Hz), 118.3 (C), 112.7 (C), 65.1 (q, $J_{\text{CF}} = 36.4$ Hz), 59.7 (q, $J_{\text{CF}} = 2.02$ Hz). **HRMS** (EI) m/z : $[\text{M}^+]$ calcd for $[\text{C}_{16}\text{H}_{10}\text{F}_3\text{NO}]^+$ 289.0709, found 289.0707. **IR** (ATR) ν (cm^{-1}) = 2924, 2229, 1612, 1321, 1280, 1172, 1152, 952, 830, 726, 700, 664, 612.

4-(3-Benzoyl-3-phenyloxiran-2-yl)benzonitrile was obtained according to Procedure A from **1d** (105 mg, 0.500 mmol): white solid (137 mg, 0.421 mmol, 84%), dr 1.3 : 1.



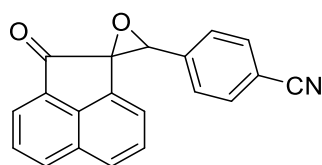
¹H NMR (400 MHz, CDCl₃) δ 8.16 – 8.10 (m, 2H), 7.95 – 7.93 (m, 2H), 7.62 – 7.51 (m, 6H), 7.50 – 7.37 (m, 10H), 7.35 – 7.28 (m, 4H), 7.21 (m, 4H), 4.57 (s, 1H), 4.26 (s, 1H). **¹³C NMR** (101 MHz, CDCl₃) δ 194.5, 193.0, 140.0, 139.0, 135.3, 134.9, 134.3, 134.2, 133.8, 132.3, 131.8, 131.3, 130.1, 130.0, 129.8, 129.25, 129.16, 128.84, 128.77, 128.5, 127.5, 127.3, 127.0, 125.5, 118.63, 118.62, 112.3, 112.0, 71.6, 70.8, 66.2, 62.4. **HRMS** (EI) m/z: [M⁺] calcd for [C₂₂H₁₅NO₂]⁺ 325.1097, found 325.1097. **IR** (ATR) ν (cm⁻¹) = 3062, 2925, 1677, 1611, 1597, 1580, 1318, 1274, 1214, 1174, 1021, 828, 755, 697, 638.

4-(3-(4-Methylbenzoyl)-3-(p-tolyl)oxiran-2-yl)benzonitrile was obtained according to Procedure A from **1e** (119 mg, 0.500 mmol): white solid (163 mg, 0.461 mmol, 92%), dr 2 : 1.



¹H NMR (400 MHz, CDCl₃) δ 8.03 (d, *J* = 7.9 Hz, 2H), 7.85 (d, *J* = 7.9 Hz, 2H), 7.48 (m, 6H), 7.38 – 7.14 (m, 12H), 7.00 (d, *J* = 7.9 Hz, 2H), 4.54 (s, 1H), 4.26 (s, 1H), 2.38 (s, 3H), 2.37 (s, 3H), 2.35 (s, 3H), 2.21 (s, 3H). **¹³C NMR** (101 MHz, CDCl₃) δ 194.0, 192.6, 145.3, 145.1, 140.2, 139.2, 139.1, 138.6, 132.9, 132.2, 132.1, 131.8, 131.3, 130.1, 129.8, 129.7, 129.5, 129.4, 129.2, 128.4, 127.5, 127.2, 126.9, 125.5, 118.6, 112.1, 111.8, 71.6, 70.8, 66.0, 62.3, 21.88, 21.86, 21.3, 21.2. **HRMS** (EI) m/z: [M⁺] calcd for [C₂₄H₁₉NO₂]⁺ 353.1410, found 353.1394. **IR** (ATR) ν (cm⁻¹) = 3031, 2921, 2228, 1675, 1604, 1512, 1408, 1274, 1171, 1019, 896, 809, 730, 685.

4-(2-Oxo-2H-spiro[acenaphthylene-1,2'-oxiran]-3'-yl)benzonitrile was obtained according to Procedure A from **1g** (91 mg, 0.50 mmol): (141 mg, 0.47 mmol, 94%), dr 1.6 : 1.



3ga

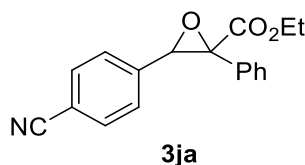
3ga' yellow solid

¹H NMR (400 MHz, CDCl₃) δ 8.17 (d, *J* = 8.2 Hz, 1H), 7.99 (d, *J* = 8.4 Hz, 1H), 7.88 (d, *J* = 7.1 Hz, 1H), 7.80 – 7.66 (m, 6H), 7.54 (d, *J* = 6.9 Hz, 1H), 4.85 (s, 1H). **¹³C NMR** (101 MHz, CDCl₃) δ 195.5 (C=O), 142.0 (C), 137.8 (C), 132.8 (C), 132.1 (CH), 131.8 (C), 131.7 (CH), 130.4 (C), 128.7 (CH), 128.6 (CH), 128.2 (CH), 126.5 (CH), 122.2 (CH), 118.8 (C), 118.5 (CH), 112.5 (C), 67.2 (CH), 66.6 (C). **HRMS** (EI) *m/z*: [*M*⁺] calcd for [C₂₀H₁₁NO₂]⁺ 297.0784, found 289.0776. **IR** (ATR) *ν* (cm⁻¹) = 3049, 2233, 1716, 1609, 1434, 1276, 1205, 1013, 893, 829, 782, 735.

3ga'' yellow solid.

¹H NMR (400 MHz, CDCl₃) δ 8.16 (d, *J* = 8.2 Hz, 1H), 8.08 (d, *J* = 7.1 Hz, 1H), 7.88 (d, *J* = 8.4 Hz, 1H), 7.79 (dd, *J* = 8.2, 7.1 Hz, 1H), 7.76 – 7.71 (m, 2H), 7.66 – 7.59 (m, 2H), 7.39 (dd, *J* = 8.4, 7.1 Hz, 1H), 6.68 (d, *J* = 7.1 Hz, 1H), 4.94 (s, 1H). **¹³C NMR** (101 MHz, CDCl₃) δ 197.1 (C=O), 143.3 (C), 139.5 (C), 132.6 (CH), 132.5 (CH), 130.7 (C), 130.6 (C), 129.8 (C), 128.42 (CH), 128.38 (CH), 127.7 (CH), 126.7 (CH), 122.5 (CH), 120.5 (CH), 118.5 (C), 112.7 (C), 66.5 (C), 64.5 (CH). **HRMS** (EI) *m/z*: [*M*⁺] calcd for [C₂₀H₁₁NO₂]⁺ 297.0784, found 289.0791. **IR** (ATR) *ν* (cm⁻¹) = 3049, 2229, 1714, 1607, 1421, 1268, 1079, 1026, 820, 783, 692.

Ethyl 3-(4-cyanophenyl)-2-phenyloxirane-2-carboxylate was obtained according to Procedure A from **1g** (89 mg, 0.50 mmol): (140 mg, 0.478 mmol, 96%), dr 2 : 1.



3ja

3ja' white solid, mp 75–80 °C.

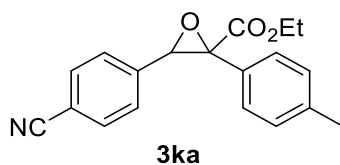
¹H NMR (400 MHz, CDCl₃) δ 7.42 (d, *J* = 8.0 Hz, 2H), 7.28 – 7.19 (m, 5H), 7.15 (d, *J* = 8.1 Hz, 2H), 4.61 (s, 1H), 4.35 – 4.20 (m, 2H), 1.29 (t, *J* = 7.1 Hz, 3H). **¹³C NMR** (101 MHz, CDCl₃) δ 168.7 (C=O), 138.6 (C), 131.8 (CH), 130.6 (C), 128.7 (C), 128.7 (CH), 128.0 (CH), 127.5 (CH),

118.5 (C), 112.2 (C), 65.5 (C), 62.7 (CH), 62.6 (CH₂), 14.2 (CH₃). **HRMS** (EI) m/z: [M⁺] calcd for [C₁₈H₁₅NO₃]⁺ 293.1046, found 293.1048. **IR** (ATR) ν (cm⁻¹) = 2984, 2229, 1733, 1612, 1448, 1262, 1184, 1020, 836, 748, 698, 571.

3ja'' white solid, mp 60–65 °C.

¹H NMR (400 MHz, CDCl₃) δ 7.67 (d, *J* = 8.3 Hz, 2H), 7.64 – 7.60 (m, 2H), 7.54 (d, *J* = 7.9 Hz, 2H), 7.45 – 7.39 (m, 3H), 4.18 (s, 1H), 4.08 – 3.96 (m, 2H), 1.00 (t, *J* = 7.1 Hz, 3H). **¹³C NMR** (101 MHz, CDCl₃) δ 166.0 (C=O), 139.2 (C), 134.1 (C), 132.2 (CH), 129.3 (C), 128.8 (CH), 127.1 (CH), 126.3 (CH), 118.6 (C), 112.5 (C), 67.2 (C), 64.8 (CH), 61.8 (CH₂), 14.0 (CH₃). **HRMS** (EI) m/z: [M⁺] calcd for [C₁₈H₁₅NO₃]⁺ 293.1046, found 293.1051. **IR** (ATR) ν (cm⁻¹) = 2983, 2229, 1734, 1612, 1305, 1214, 1184, 1096, 1019, 938, 855, 829, 761, 695, 638, 595.

Ethyl 3-(4-cyanophenyl)-2-(p-tolyl)oxirane-2-carboxylate was obtained according to Procedure A from **1k** (96 mg, 0.50 mmol): (146 mg, 0.475 mmol, 95%), dr 2 : 1.



3ka' pale yellow liquid

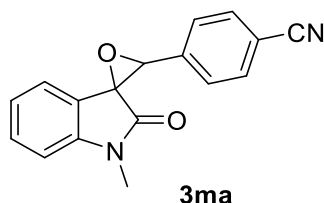
¹H NMR (400 MHz, CDCl₃) δ 7.42 (d, *J* = 8.3 Hz, 2H), 7.18 – 7.11 (m, 4H), 7.01 (d, *J* = 8.5 Hz, 2H), 4.58 (s, 1H), 4.26 (m, 2H), 2.26 (s, 3H), 1.28 (t, *J* = 7.1 Hz, 3H). **¹³C NMR** (101 MHz, CDCl₃) δ 168.8 (C=O), 138.8 (C), 138.5 (C), 131.7 (CH), 128.8 (CH), 128.5 (CH), 127.5 (CH), 118.6 (C), 112.1 (C), 65.5 (C), 62.62 (CH₂), 62.57 (CH), 21.3 (CH₃), 14.2 (CH₃). (one carbon may overlap with other carbons) **HRMS** (EI) m/z: [M⁺] calcd for [C₁₉H₁₇NO₃]⁺ 307.1203, found 307.1200. **IR** (ATR) ν (cm⁻¹) = 2982, 2229, 1736, 1611, 1513, 1305, 1215, 1181, 1095, 1018, 830, 810, 753, 667.

3ka'' pale yellow liquid

¹H NMR (400 MHz, CDCl₃) δ 7.66 (d, *J* = 8.2 Hz, 2H), 7.56 – 7.46 (m, 4H), 7.22 (d, *J* = 8.0 Hz, 2H), 4.18 (s, 1H), 4.07 – 3.96 (m, 2H), 2.38 (s, 3H), 0.99 (t, *J* = 7.1 Hz, 3H). **¹³C NMR** (101 MHz, CDCl₃) δ 166.1 (C=O), 139.3 (C), 139.2 (C), 132.2 (CH), 131.1 (C), 129.5 (CH), 127.0 (CH), 126.2 (C), 118.5 (C), 112.4 (C), 67.2 (C), 64.7 (CH), 61.7 (CH₂), 21.3 (CH₃), 14.0 (CH₃).

HRMS (EI) m/z : $[M^+]$ calcd for $[C_{19}H_{17}NO_3]^+$ 307.1203, found 307.1203. **IR** (ATR) ν (cm^{-1}) = 2983, 2229, 1733, 1612, 1516, 1368, 1261, 1217, 1179, 1019, 803, 756, 696.

4-(1-Methyl-2-oxospiro[indoline-3,2'-oxiran]-3'-yl)benzonitrile was obtained according to Procedure A from **1m** (81 mg, 0.50 mmol): (124 mg, 0.449 mmol, 90%), dr 1.7 : 1.



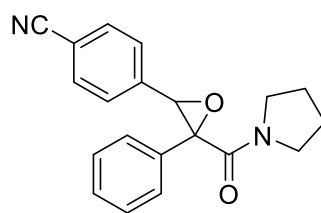
3ma' white solid.

1H NMR (400 MHz, $CDCl_3$) δ 7.72 (d, J = 7.9 Hz, 2H), 7.59 (d, J = 7.9 Hz, 2H), 7.31 (t, J = 7.8 Hz, 1H), 6.89 (d, J = 7.8 Hz, 1H), 6.80 (t, J = 7.6 Hz, 1H), 6.36 (d, J = 7.4 Hz, 1H), 4.82 (s, 1H), 3.30 (s, 3H). **^{13}C NMR** (101 MHz, $CDCl_3$) δ 171.0 (C=O), 145.4 (C), 138.6 (C), 132.4 (CH), 130.8 (CH), 127.7 (CH), 123.3 (CH), 122.7 (CH), 120.0 (C), 118.4 (C), 112.7 (C), 109.1 (CH), 64.2 (CH), 61.9 (C), 26.8 (CH_3). **HRMS** (EI) m/z : $[M^+]$ calcd for $[C_{17}H_{12}N_2O_2]^+$ 276.0893, found 276.0892. **IR** (ATR) ν (cm^{-1}) = 2923, 2230, 1718, 1613, 1472, 1425, 1373, 1349, 1256, 1126, 1106, 1023, 889, 822, 764, 697, 584, 557.

3ma'' white solid.

1H NMR (400 MHz, $CDCl_3$) δ 7.72 (d, J = 8.0 Hz, 2H), 7.66 (d, J = 7.9 Hz, 2H), 7.43 (t, J = 7.7 Hz, 1H), 7.24 (d, J = 7.4 Hz, 1H), 7.15 (t, J = 7.4 Hz, 1H), 6.92 (d, J = 7.8 Hz, 1H), 4.69 (s, 1H), 3.15 (s, 3H). **^{13}C NMR** (101 MHz, $CDCl_3$) δ 169.4 (C=O), 144.7 (C), 137.1 (C), 131.5 (CH), 130.8 (CH), 128.3 (CH), 123.0 (CH), 122.7 (C), 121.9 (CH), 118.8 (C), 112.4 (C), 109.0 (CH), 66.1 (CH), 62.1 (C), 26.6 (CH_3). **HRMS** (EI) m/z : $[M^+]$ calcd for $[C_{17}H_{12}N_2O_2]^+$ 276.0893, found 276.0890. **IR** (ATR) ν (cm^{-1}) = 3056, 2229, 1725, 1618, 1466, 1310, 1130, 903, 872, 809, 727, 698, 567.

4-(3-Phenyl-3-(pyrrolidine-1-carbonyl)oxiran-2-yl)benzonitrile was obtained according to Procedure A from **1o** (102 mg, 0.502 mmol): (148 mg, 0.465 mmol, 93%), dr 1 : 1.



3oa

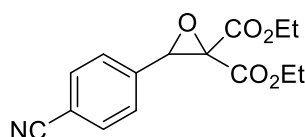
3oa' white solid, mp 157–162 °C.

¹H NMR (400 MHz, CDCl₃) δ 7.62 (d, *J* = 8.0 Hz, 2H), 7.57 – 7.49 (m, 2H), 7.46 – 7.36 (m, 5H), 4.15 (s, 1H), 3.72 (m, 1H), 3.47 – 3.16 (m, 3H), 1.90 (m, 1H), 1.83 – 1.71 (m, 2H), 1.65 (m, 1H). **¹³C NMR** (101 MHz, CDCl₃) δ 163.6 (C=O), 140.4 (C), 134.5 (C), 132.2 (CH), 129.1 (CH), 128.9 (CH), 126.7 (CH), 125.6 (CH), 118.7 (C), 112.2 (C), 68.7 (C), 66.7 (CH), 46.3 (CH₂), 45.7 (CH₂), 26.0 (CH₂), 23.8 (CH₂). **HRMS** (EI) *m/z*: [*M*⁺] calcd for [C₂₀H₁₈N₂O₂]⁺ 318.1363, found 318.1360. **IR** (ATR) *ν* (cm⁻¹) = 3070, 2971, 2224, 1638, 1442, 1194, 931, 831, 770, 716, 697, 654, 601, 562.

3oa'' white solid, mp 176–181 °C.

¹H NMR (400 MHz, CDCl₃) δ 7.43 – 7.35 (m, 4H), 7.27 (d, *J* = 8.4 Hz, 2H), 7.17 (m, 3H), 4.62 (s, 1H), 3.88 – 3.75 (m, 1H), 3.56 – 3.37 (m, 2H), 3.27 (m, 1H), 1.98 – 1.86 (m, 1H), 1.85 – 1.70 (m, 3H). **¹³C NMR** (101 MHz, CDCl₃) δ 166.0 (C=O), 139.2 (C), 131.6 (CH), 131.4 (C), 128.5 (CH), 128.2 (CH), 127.4 (CH), 127.0 (CH), 118.6 (C), 111.6 (C), 69.0 (C), 63.8 (CH), 46.4 (CH₂), 45.7 (CH₂), 26.0 (CH₂), 23.7 (CH₂). **HRMS** (EI) *m/z*: [*M*⁺] calcd for [C₂₀H₁₈N₂O₂]⁺ 318.1363, found 318.1359. **IR** (ATR) *ν* (cm⁻¹) = 2975, 2876, 2228, 1638, 1438, 1166, 1077, 932, 827, 774, 708, 652, 625.

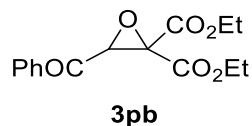
Diethyl 3-(4-cyanophenyl)oxirane-2,2-dicarboxylate was obtained according to Procedure A from **1p** (87 mg, 0.50 mmol): pale yellow liquid (116 mg, 0.401 mmol, 80%).



3pa

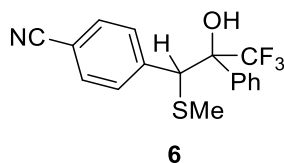
¹H NMR (400 MHz, CDCl₃) δ 7.64 (d, *J* = 7.9 Hz, 2H), 7.47 (d, *J* = 7.9 Hz, 2H), 4.60 (s, 1H), 4.33 (q, *J* = 7.1 Hz, 2H), 4.04 (m, 2H), 1.34 (t, *J* = 7.1 Hz, 3H), 1.00 (t, *J* = 7.1 Hz, 3H). **¹³C NMR** (101 MHz, CDCl₃) δ 164.9 (C=O), 163.1 (C=O), 137.5 (C), 132.3 (CH), 127.2 (CH), 118.4

(C), 113.1 (C), 63.3 (CH₂), 63.2 (C), 62.3 (CH₂), 61.1 (CH), 14.1 (CH₃), 13.9 (CH₃). **HRMS** (EI) *m/z*: [M⁺] calcd for [C₁₅H₁₅NO₅]⁺ 289.0945, found 289.0936. **IR** (ATR) ν (cm⁻¹) = 2985, 2231, 1744, 1371, 1266, 1230, 1201, 1112, 1045, 1018, 856, 834, 730.



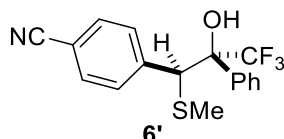
To a solution of (**2b**-H)-Br (196 mg, 0.751 mmol) in anhydrous DMSO (3 mL) was added a solution of *t*-BuOK (84 mg, 0.75 mmol) in anhydrous DMSO (3 mL) at room temperature. After 2 min, a solution of **1p** (87 mg, 0.50 mmol) in anhydrous DMSO (3 mL) was added to the resulting solution. The completion of the reaction was checked by TLC and quenched by 20 mL 2% aqueous HCl followed with CHCl₃ extraction. The organic extract was washed by water (3 × 30) to remove remaining DMSO, dried with anhydrous MgSO₄ and filtered. The solvent was evaporated under reduced pressure and the crude product was purified by column chromatography to obtain **diethyl 3-benzoyloxirane-2,2-dicarboxylate (3pb)**: liquid (110 mg, 0.376 mmol, 75%).

¹H NMR (400 MHz, CDCl₃) δ 8.03 – 7.97 (m, 2H), 7.67 – 7.61 (m, 1H), 7.54 – 7.48 (m, 2H), 4.67 (s, 1H), 4.36 (qd, *J* = 7.1, 1.4 Hz, 2H), 4.17 (qd, *J* = 7.1, 2.1 Hz, 2H), 1.36 (t, *J* = 7.1 Hz, 3H), 1.14 (t, *J* = 7.1 Hz, 3H). **¹³C NMR** (101 MHz, CDCl₃) δ 189.8 (C=O), 164.7 (C=O), 163.0 (C=O), 135.1 (C), 134.5 (CH), 129.1 (CH), 128.7 (CH), 63.5 (CH₂), 62.7 (CH₂), 60.9 (C), 60.0 (CH), 14.1 (CH₃), 13.8 (CH₃). **HRMS** (EI) *m/z*: [M⁺] calcd for [C₁₅H₁₅O₆]⁺ 292.0941, found 292.0950. **IR** (ATR) ν (cm⁻¹) = 2985, 1747, 1693, 1597, 1450, 1370, 1223, 1108, 1038, 1003, 956, 858, 766, 692.



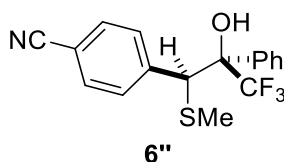
To a solution of **5** (82 mg, 0.50 mmol) in anhydrous THF (3 mL) at -78 °C was dropwise added a freshly prepared solution of LDA (0.60 mmol) in anhydrous THF (1 mL). After 10 min, a solution of **1a** (131 mg, 0.753 mmol) in anhydrous THF (1mL) was added at -78 °C dropwise. Then the cooling bath was removed and the reaction was stirred for 30 min at room temperature. Afterwards, 2% aq HCl (10 mL) was added, and the mixture was extracted with CHCl₃. The

organic phase was washed with brine, dried over anhydrous MgSO_4 , and filtered. The solvent was evaporated under reduced pressure, and the residue was purified by column chromatography to give **4-((rel-1S,2R)-3,3,3-trifluoro-2-hydroxy-1-(methylthio)-2-phenylpropyl)benzonitrile (6')** (101 mg, 0.300 mmol, 60%) and **4-((rel-1S,2S)-3,3,3-trifluoro-2-hydroxy-1-(methylthio)-2-phenylpropyl)benzonitrile (6'')** (34 mg, 0.10 mmol, 20%).



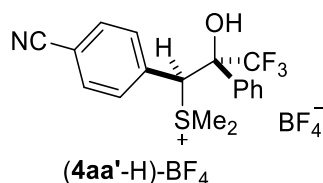
White solid, mp 144–147 °C

¹H NMR (400 MHz, CDCl_3) δ 7.68 – 7.63 (m, 4H), 7.59 (d, J = 8.3 Hz, 2H), 7.50 – 7.43 (m, 3H), 4.48 (s, 1H), 3.37 (s, 1H), 1.63 (s, 3H). **¹³C NMR** (101 MHz, CDCl_3) δ 142.7 (C), 136.7 (C), 132.2 (CH), 130.6 (CH), 129.4 (CH), 128.7 (CH), 126.1 (CH), 124.6 (q, J_{CF} = 273 Hz), 118.6 (C), 112.1 (C), 78.0 (q, J_{CF} = 30.3 Hz), 58.6 (CH), 15.9 (CH₃). **HRMS** (EI) m/z : $[\text{M}^+]$ calcd for $[\text{C}_{17}\text{H}_{14}\text{F}_3\text{NOS}]^+$ 337.0743, found 337.0725. **IR** (ATR) ν (cm^{-1}) = 3488, 2926, 2221, 1604, 1500, 1417, 1255, 1155, 1104, 1076, 985, 838, 762, 701.



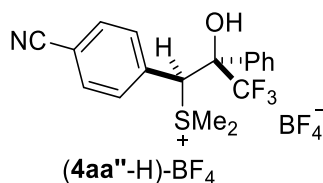
liquid

¹H NMR (400 MHz, CDCl_3) δ 7.35 (d, J = 8.0 Hz, 2H), 7.33 – 7.29 (m, 2H), 7.18 (m, 5H), 4.55 (s, 1H), 3.92 (s, 1H), 2.05 (s, 3H). **¹³C NMR** (101 MHz, CDCl_3) δ 142.9 (C), 135.5 (C), 131.8 (CH), 130.1 (CH), 128.7 (CH), 128.3 (CH), 125.9 (CH), 125.2 (q, J_{CF} = 288 Hz), 118.6 (C), 111.3 (C), 78.7 (q, J_{CF} = 27.2 Hz), 57.4 (C), 16.4 (CH₃). **HRMS** (FAB⁺) m/z : $[\text{M}+\text{H}]^+$ calcd for $[\text{C}_{17}\text{H}_{15}\text{F}_3\text{NOS}]^+$ 338.0821, found 338.0813. **IR** (ATR) ν (cm^{-1}) = 3042, 2923, 2229, 1606, 1502, 1451, 1240, 1155, 1073, 992, 912, 846, 753, 702.



To a suspension of trimethyloxonium tetrafluoroborate (30 mg, 0.20 mmol) in CH₂Cl₂ (1 mL) was added a solution of sulfide **6'** (67 mg, 0.20 mmol) in CH₂Cl₂ (1 mL) at 0 °C. The reaction mixture was stirred for 1 h at 0 °C and then for 14 h at room temperature. After removal of the solvent, the solid residue was washed with CH₂Cl₂ to give the ((**rel-1S,2R**)-1-(4-cyanophenyl)-3,3,3-trifluoro-2-hydroxy-2-phenylpropyl)dimethylsulfonium tetrafluoroborate ((4aa'-H)-BF₄): white solid (79 mg, 0.18 mmol, 90%), 200–205 °C.

¹H NMR (400 MHz, CD₃CN) δ 8.17 (d, *J* = 8.2 Hz, 1H), 7.91 (d, *J* = 7.3 Hz, 2H), 7.79 (d, *J* = 8.3 Hz, 2H), 7.69 (d, *J* = 7.8 Hz, 1H), 7.65 – 7.55 (m, 3H), 6.26 (d, *J* = 2.3 Hz, 1H), 5.35 (d, *J* = 2.0 Hz, 1H), 2.51 (s, 3H), 2.20 (s, 3H). **¹³C NMR** (101 MHz, CD₃CN) δ 135.9, 134.2, 133.0, 132.6, 131.7, 130.5, 127.2, 125.1, 118.8, 115.7, 81.8, 65.1, 25.9, 25.2. **HRMS** (ESI[−]) *m/z*: [M+BF₄][−] calcd for [C₁₈H₁₇B₂F₁₁NOS][−] 526.1047, found 526.1059. **IR** (ATR) ν (cm^{−1}) = 3042, 2234, 1429, 1256, 1173, 1052, 992, 840, 766, 730, 702.



To a suspension of trimethyloxonium tetrafluoroborate (15 mg, 0.10 mmol) in CH₂Cl₂ (0.5 mL) was added a solution of sulfide **6''** (34 mg, 0.10 mmol) in CH₂Cl₂ (0.5 mL) at 0 °C. The reaction mixture was stirred for 1 h at 0 °C and then for 14 h at room temperature. After removal of the solvent, the solid residue was washed with CH₂Cl₂ to give the ((**rel-1S,2S**)-1-(4-cyanophenyl)-3,3,3-trifluoro-2-hydroxy-2-phenylpropyl)dimethylsulfonium tetrafluoroborate ((4aa''-H)-BF₄): white solid (40 mg, 0.091 mmol, 91%), 220–223 °C.

¹H NMR (400 MHz, CD₃CN) δ 7.77 – 7.51 (m, 2H), 7.45 (d, *J* = 8.0 Hz, 2H), 7.39 – 7.32 (m, 2H), 7.31 – 7.25 (m, 3H), 6.49 (d, *J* = 2.2 Hz, 1H), 5.60 (d, *J* = 2.2 Hz, 1H), 2.70 (s, 3H), 2.58 (s, 3H). **¹³C NMR** (101 MHz, CD₃CN) δ 135.2, 133.7, 133.4, 131.5, 130.5, 129.6, 127.5, 125.7, 118.5, 114.9, 81.6, 61.8, 26.0, 25.5. **HRMS** (ESI[−]) *m/z*: [M+BF₄][−] calcd for [C₁₈H₁₇B₂F₁₁NOS][−]

526.1047, found 526.1064. **IR** (ATR) ν (cm⁻¹) = 3394, 3030, 2234, 1664, 1507, 1432, 1236, 1169, 1058, 1006, 852, 714, 702.1

Competition experiment: **1a** (87 mg, 0.50 mmol), (**2a**-H)-BF₄ (66 mg, 0.25 mmol), and **1p** (87 mg, 0.50 mmol) were dissolved in DMSO (5.0 mL). Then NaOH (15 mg, 0.38 mmol) was added. After 4 h at 20 °C, 2% aq HCl (30 mL) was added, and the mixture was extracted with CHCl₃ (3 × 30 mL). The organic phases were combined and subsequently washed with water (2 × 30 mL) and brine (1 × 30 mL) to remove remaining DMSO. After drying with anhydrous MgSO₄ and filtration, the solvent was evaporated under reduced pressure. The residue was dissolved in CDCl₃ and analyzed by ¹H NMR spectroscopy.

Crossover experiment: A solution of (**4aa'**-H)-BF₄ (or (**4aa''**-H)-BF₄) (15 mg, 0.034 mmol) and trapping reagent **1p** (18 mg, 0.10 mmol) in DMSO (0.6 mL) was prepared. Then NaOH (2.0 mg, 0.050 mmol) was added at 20 °C. After 40h at 20 °C, 2% aq HCl (10 mL) was added, and the mixture was extracted with CHCl₃ (3 × 15 mL). The organic phases were combined, subsequently washed with water (2 × 30 mL) and brine (1 × 30 mL) to remove remaining DMSO, and then dried over anhydrous MgSO₄, and filtered. The solvent was evaporated under reduced pressure and the residue (in CDCl₃) was analyzed by ¹H NMR spectroscopy.

(2) Kinetics of the reactions of the ketones **1** with sulfonium ylides **2**

The rates of all investigated reactions were determined spectrophotometrically (UV-Vis) by following the disappearance of the colored carbanions **2a,b**. The temperature of the solutions during all kinetics studies was kept constant (20.0 ± 0.1 °C) by using a circulating bath thermostat. The kinetics investigations were performed with a high excess of the electrophiles over the carbanions to achieve first-order kinetics. The carbanions **2a** decompose slowly at room temperature. Thus we prepared stock solutions of the carbanions **2a** by deprotonation of the corresponding CH acids **2a**-H in dry THF at -78 °C with 1.00–1.05 equiv *t*-BuOK. Small amounts of these stock solutions were dissolved in DMSO at room temperature directly before each kinetic experiment. The kinetics were followed by conventional UV/Vis diode array spectrophotometer (slow kinetics, $\tau_{1/2} > 10$ s) or commercial stopped-flow spectrophotometer system (fast kinetics, $\tau_{1/2} < 10$ s). Rate constants k_{obs} (s⁻¹) were obtained by fitting the single exponential decay $A_t = A_0 \exp(-k_{\text{obs}}t) + C$ (exponential decrease) to the observed time-dependent absorbance (in the case of the stopped-flow spectrophotometer, at least 5 kinetic runs for each

nucleophile concentration were averaged). Second-order rate constants k_2 ($\text{M}^{-1} \text{s}^{-1}$) were derived from the slopes of the linear correlations of k_{obs} with electrophile concentrations.

Table S1. Kinetics of the reactions of **1a** with **2a** in DMSO at 20 °C (deprotonated with 1.00–1.05 equiv. *t*-BuOK, stopped-flow UV-Vis spectrometer, $\lambda = 380$ nm).

[2a]/mol L ⁻¹	[1a]/mol L ⁻¹	$k_{\text{obs}}/\text{s}^{-1}$
5.00×10^{-5}	5.00×10^{-4}	9.67×10^0
5.00×10^{-5}	7.50×10^{-4}	1.42×10^1
5.00×10^{-5}	1.00×10^{-3}	1.80×10^1
5.00×10^{-5}	1.25×10^{-3}	2.10×10^1
$k_2 = 1.51 \times 10^4 \text{ L mol}^{-1} \text{s}^{-1}$		

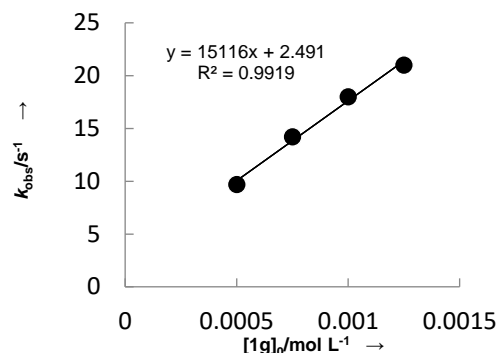


Table S2. Kinetics of the reactions of **1b** with **2a** in DMSO at 20 °C (deprotonated with 1.00–1.05 equiv. *t*-BuOK, stopped-flow UV-Vis spectrometer, $\lambda = 380$ nm).

[2a]/mol L ⁻¹	[1a]/mol L ⁻¹	$k_{\text{obs}}/\text{s}^{-1}$
5.00×10^{-5}	4.57×10^{-4}	3.65×10^{-1}
5.00×10^{-5}	6.85×10^{-4}	5.40×10^{-1}
5.00×10^{-5}	9.13×10^{-4}	7.00×10^{-1}
5.00×10^{-5}	1.14×10^{-3}	8.12×10^{-1}
$k_2 = 6.59 \times 10^2 \text{ L mol}^{-1} \text{s}^{-1}$		

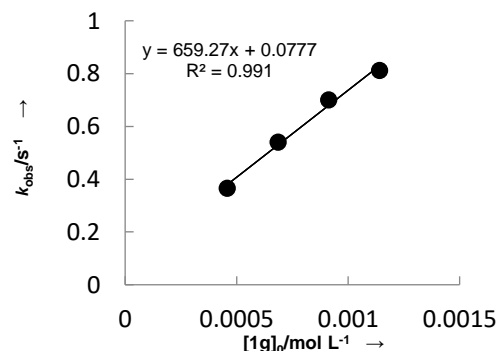


Table S3. Kinetics of the reactions of **1c** with **2a** in DMSO at 20 °C (deprotonated with 1.00–1.05 equiv. *t*-BuOK, stopped-flow UV-Vis spectrometer, $\lambda = 380$ nm).

[2a]/mol L ⁻¹	[1a]/mol L ⁻¹	$k_{\text{obs}}/\text{s}^{-1}$
5.00×10^{-5}	5.14×10^{-4}	6.73×10^{-2}
5.00×10^{-5}	1.03×10^{-3}	1.28×10^{-1}
5.00×10^{-5}	1.54×10^{-3}	1.87×10^{-1}
5.00×10^{-5}	2.06×10^{-3}	2.40×10^{-1}
$k_2 = 1.12 \times 10^2 \text{ L mol}^{-1} \text{s}^{-1}$		

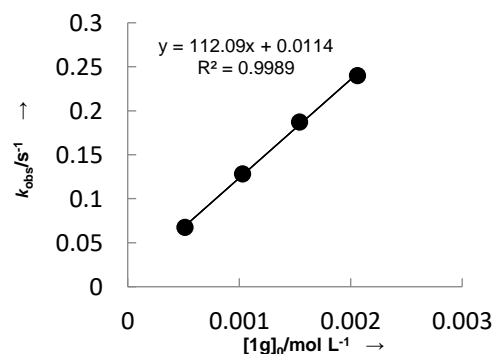


Table S4. Kinetics of the reactions of **1d** with **2a** in DMSO at 20 °C (deprotonated with 1.00–1.05 equiv. *t*-BuOK, conventional UV-Vis spectrometer, λ = 380 nm).

[2a]/mol L ⁻¹	[1a]/mol L ⁻¹	$k_{\text{obs}}/\text{s}^{-1}$
5.00×10^{-5}	5.46×10^{-4}	3.57×10^{-2}
5.00×10^{-5}	8.62×10^{-4}	5.64×10^{-2}
5.00×10^{-5}	1.06×10^{-3}	7.00×10^{-2}
5.00×10^{-5}	1.32×10^{-3}	8.48×10^{-2}
$k_2 = 6.39 \times 10^1 \text{ L mol}^{-1} \text{ s}^{-1}$		

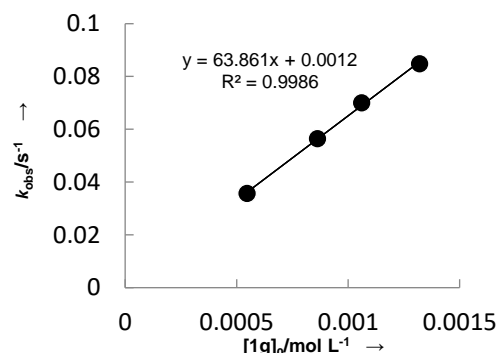


Table S5. Kinetics of the reactions of **1e** with **2a** in DMSO at 20 °C (deprotonated with 1.00–1.05 equiv. *t*-BuOK, conventional UV-Vis spectrometer, λ = 380 nm).

[2a]/mol L ⁻¹	[1a]/mol L ⁻¹	$k_{\text{obs}}/\text{s}^{-1}$
5.00×10^{-5}	5.17×10^{-4}	8.43×10^{-3}
5.00×10^{-5}	7.65×10^{-4}	1.13×10^{-2}
5.00×10^{-5}	1.01×10^{-3}	1.58×10^{-2}
5.00×10^{-5}	1.27×10^{-3}	1.97×10^{-2}
$k_2 = 1.53 \times 10^1 \text{ L mol}^{-1} \text{ s}^{-1}$		

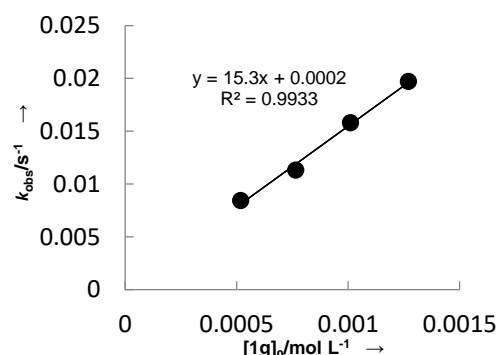


Table S6. Kinetics of the reactions of **1f** with **2a** in DMSO at 20 °C (deprotonated with 1.00–1.05 equiv. *t*-BuOK, conventional UV-Vis spectrometer, λ = 380 nm).

[2a]/mol L ⁻¹	[1a]/mol L ⁻¹	$k_{\text{obs}}/\text{s}^{-1}$
5.00×10^{-5}	5.13×10^{-4}	2.88×10^{-3}
5.00×10^{-5}	1.02×10^{-3}	3.94×10^{-3}
5.00×10^{-5}	2.00×10^{-3}	5.56×10^{-3}
5.00×10^{-5}	2.46×10^{-3}	6.24×10^{-3}
$k_2 = 1.71 \times 10^0 \text{ L mol}^{-1} \text{ s}^{-1}$		

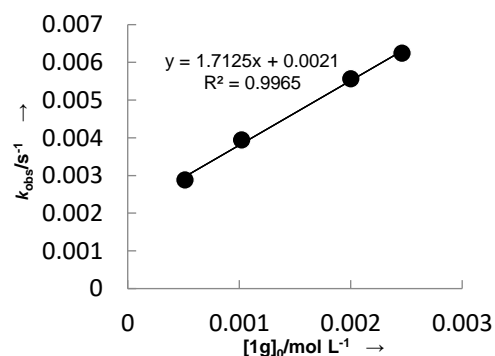


Table S7. Kinetics of the reactions of **1g** with **2a** in DMSO at 20 °C (deprotonated with 1.00–1.05 equiv. *t*-BuOK, stopped-flow UV-Vis spectrometer, λ = 380 nm).

[2a]/mol L ⁻¹	[1a]/mol L ⁻¹	$k_{\text{obs}}/\text{s}^{-1}$
5.00×10^{-5}	4.74×10^{-4}	8.51×10^{-2}
5.00×10^{-5}	9.49×10^{-4}	1.51×10^{-1}
5.00×10^{-5}	1.42×10^{-3}	2.41×10^{-1}
5.00×10^{-5}	1.90×10^{-3}	3.30×10^{-1}
$k_2 = 1.74 \times 10^2 \text{ L mol}^{-1} \text{ s}^{-1}$		

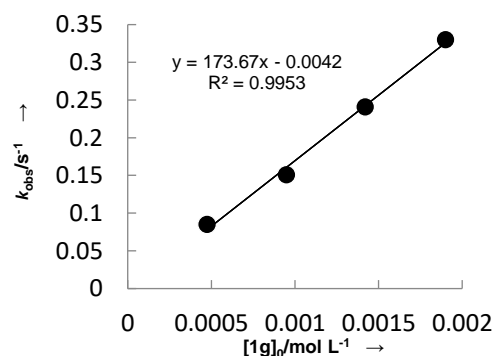


Table S8. Kinetics of the reactions of **1h** with **2a** in DMSO at 20 °C (deprotonated with 1.00–1.05 equiv. *t*-BuOK, stopped-flow UV-Vis spectrometer, $\lambda = 380$ nm).

[2a]/mol L ⁻¹	[1a]/mol L ⁻¹	$k_{\text{obs}}/\text{s}^{-1}$
5.00×10^{-5}	5.45×10^{-4}	1.23×10^0
5.00×10^{-5}	8.17×10^{-4}	1.86×10^0
5.00×10^{-5}	1.09×10^{-3}	2.51×10^0
5.00×10^{-5}	1.63×10^{-3}	4.12×10^0
$k_2 = 2.67 \times 10^3 \text{ L mol}^{-1} \text{ s}^{-1}$		

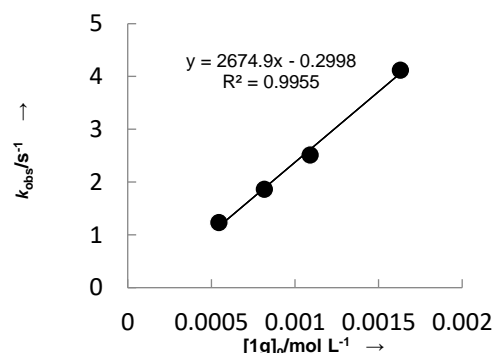


Table S9. Kinetics of the reactions of **1i** with **2a** in DMSO at 20 °C (deprotonated with 1.00–1.05 equiv. *t*-BuOK, stopped-flow UV-Vis spectrometer, $\lambda = 380$ nm).

[2a]/mol L ⁻¹	[1a]/mol L ⁻¹	$k_{\text{obs}}/\text{s}^{-1}$
5.00×10^{-5}	4.76×10^{-4}	1.77×10^{-1}
5.00×10^{-5}	7.15×10^{-4}	2.49×10^{-1}
5.00×10^{-5}	9.53×10^{-4}	3.28×10^{-1}
5.00×10^{-5}	1.19×10^{-3}	4.08×10^{-1}
5.00×10^{-5}	1.43×10^{-3}	5.00×10^{-1}
$k_2 = 3.38 \times 10^2 \text{ L mol}^{-1} \text{ s}^{-1}$		

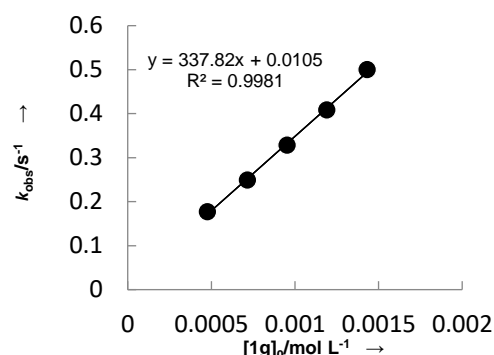


Table S10. Kinetics of the reactions of **1j** with **2a** in DMSO at 20 °C (deprotonated with 1.00–1.05 equiv. *t*-BuOK, conventional UV-Vis spectrometer, $\lambda = 380$ nm).

[2a]/mol L ⁻¹	[1a]/mol L ⁻¹	$k_{\text{obs}}/\text{s}^{-1}$
5.00×10^{-5}	9.05×10^{-4}	6.38×10^{-2}
5.00×10^{-5}	1.17×10^{-3}	9.49×10^{-2}
5.00×10^{-5}	1.40×10^{-3}	1.19×10^{-1}
5.00×10^{-5}	1.63×10^{-3}	1.45×10^{-1}
$k_2 = 1.11 \times 10^2 \text{ L mol}^{-1} \text{ s}^{-1}$		

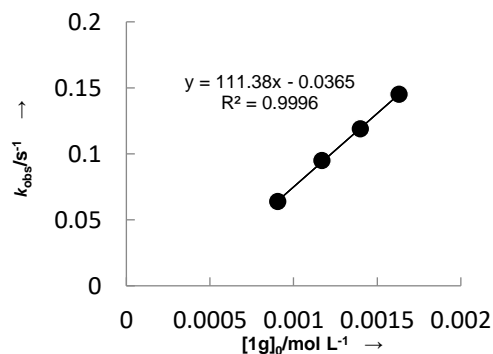


Table S11. Kinetics of the reactions of **1k** with **2a** in DMSO at 20 °C (deprotonated with 1.00–1.05 equiv. *t*-BuOK, conventional UV-Vis spectrometer, $\lambda = 380$ nm).

[2a]/mol L ⁻¹	[1a]/mol L ⁻¹	$k_{\text{obs}}/\text{s}^{-1}$
5.00×10^{-5}	5.13×10^{-4}	1.57×10^{-2}
5.00×10^{-5}	7.65×10^{-4}	2.09×10^{-2}
5.00×10^{-5}	1.25×10^{-3}	3.25×10^{-2}
5.00×10^{-5}	1.52×10^{-3}	3.97×10^{-2}
$k_2 = 2.39 \times 10^1 \text{ L mol}^{-1} \text{ s}^{-1}$		

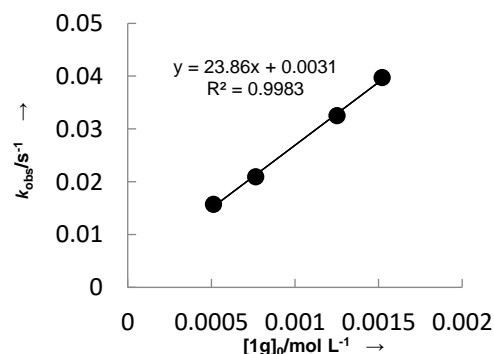


Table S12. Kinetics of the reactions of **1l** with **2a** in DMSO at 20 °C (deprotonated with 1.00–1.05 equiv. *t*-BuOK, conventional UV-Vis spectrometer, λ = 380 nm).

[2a]/mol L ⁻¹	[1a]/mol L ⁻¹	$k_{\text{obs}}/\text{s}^{-1}$
5.00×10^{-5}	5.14×10^{-4}	5.39×10^{-3}
5.00×10^{-5}	7.62×10^{-4}	7.03×10^{-3}
5.00×10^{-5}	1.00×10^{-3}	8.72×10^{-3}
5.00×10^{-5}	1.25×10^{-3}	9.93×10^{-3}

$k_2 = 6.26 \times 10^0 \text{ L mol}^{-1} \text{ s}^{-1}$

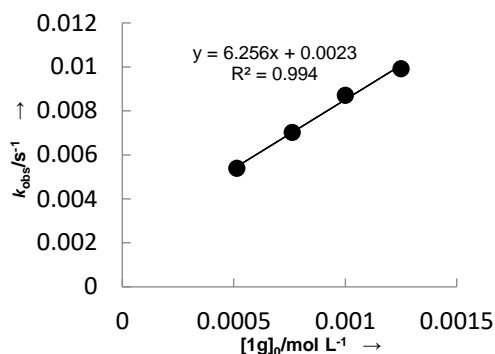


Table S13. Kinetics of the reactions of **1m** with **2a** in DMSO at 20 °C (deprotonated with 1.00–1.05 equiv. *t*-BuOK, stopped-flow UV-Vis spectrometer, λ = 380 nm).

[2a]/mol L ⁻¹	[1a]/mol L ⁻¹	$k_{\text{obs}}/\text{s}^{-1}$
5.00×10^{-5}	4.47×10^{-4}	6.17×10^{-2}
5.00×10^{-5}	8.94×10^{-4}	1.22×10^{-1}
5.00×10^{-5}	1.34×10^{-3}	1.83×10^{-1}
5.00×10^{-5}	1.79×10^{-3}	2.42×10^{-1}
5.00×10^{-5}	2.23×10^{-3}	3.15×10^{-1}

$k_2 = 1.40 \times 10^2 \text{ L mol}^{-1} \text{ s}^{-1}$

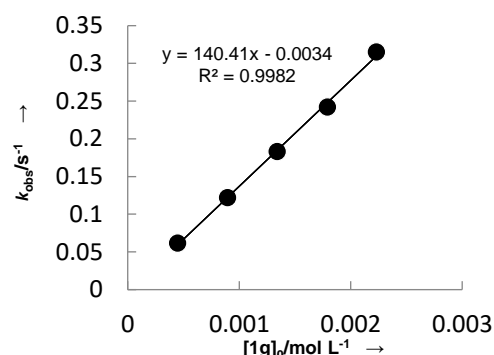


Table S14. Kinetics of the reactions of **1n** with **2a** in DMSO at 20 °C (deprotonated with 1.00–1.05 equiv. *t*-BuOK, stopped-flow UV-Vis spectrometer, λ = 380 nm).

[2a]/mol L ⁻¹	[1a]/mol L ⁻¹	$k_{\text{obs}}/\text{s}^{-1}$
5.00×10^{-5}	7.81×10^{-4}	3.31×10^0
5.00×10^{-5}	1.04×10^{-3}	4.47×10^0
5.00×10^{-5}	1.30×10^{-3}	5.95×10^0
5.00×10^{-5}	1.56×10^{-3}	8.00×10^0

$k_2 = 5.99 \times 10^3 \text{ L mol}^{-1} \text{ s}^{-1}$

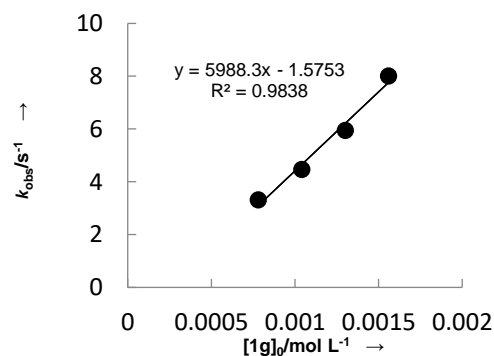


Table S15. Kinetics of the reactions of **1o** with **2a** in DMSO at 20 °C (deprotonated with 1.00–1.05 equiv. *t*-BuOK, stopped-flow UV-Vis spectrometer, λ = 380 nm).

[2a]/mol L ⁻¹	[1a]/mol L ⁻¹	$k_{\text{obs}}/\text{s}^{-1}$
5.00×10^{-5}	5.54×10^{-4}	2.62×10^{-3}
5.00×10^{-5}	1.08×10^{-3}	4.72×10^{-3}
5.00×10^{-5}	1.59×10^{-3}	6.74×10^{-3}
5.00×10^{-5}	2.06×10^{-3}	7.87×10^{-3}
5.00×10^{-5}	2.52×10^{-3}	9.55×10^{-3}

$k_2 = 3.47 \times 10^0 \text{ L mol}^{-1} \text{ s}^{-1}$

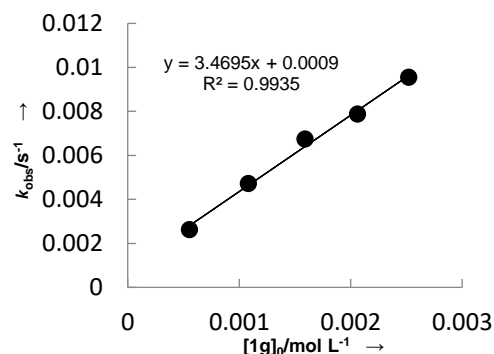
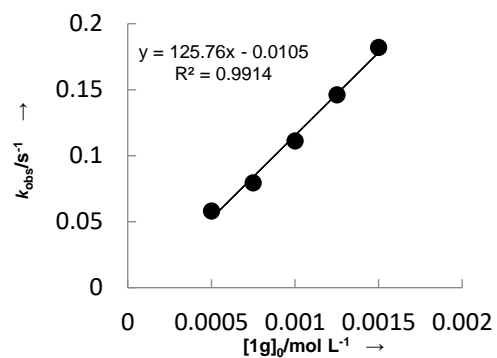


Table S16. Kinetics of the reactions of **1p** with **2b** in DMSO at 20 °C (deprotonated with 1.00–1.05 equiv. *t*-BuOK, stopped-flow UV-Vis spectrometer, $\lambda = 320$ nm).

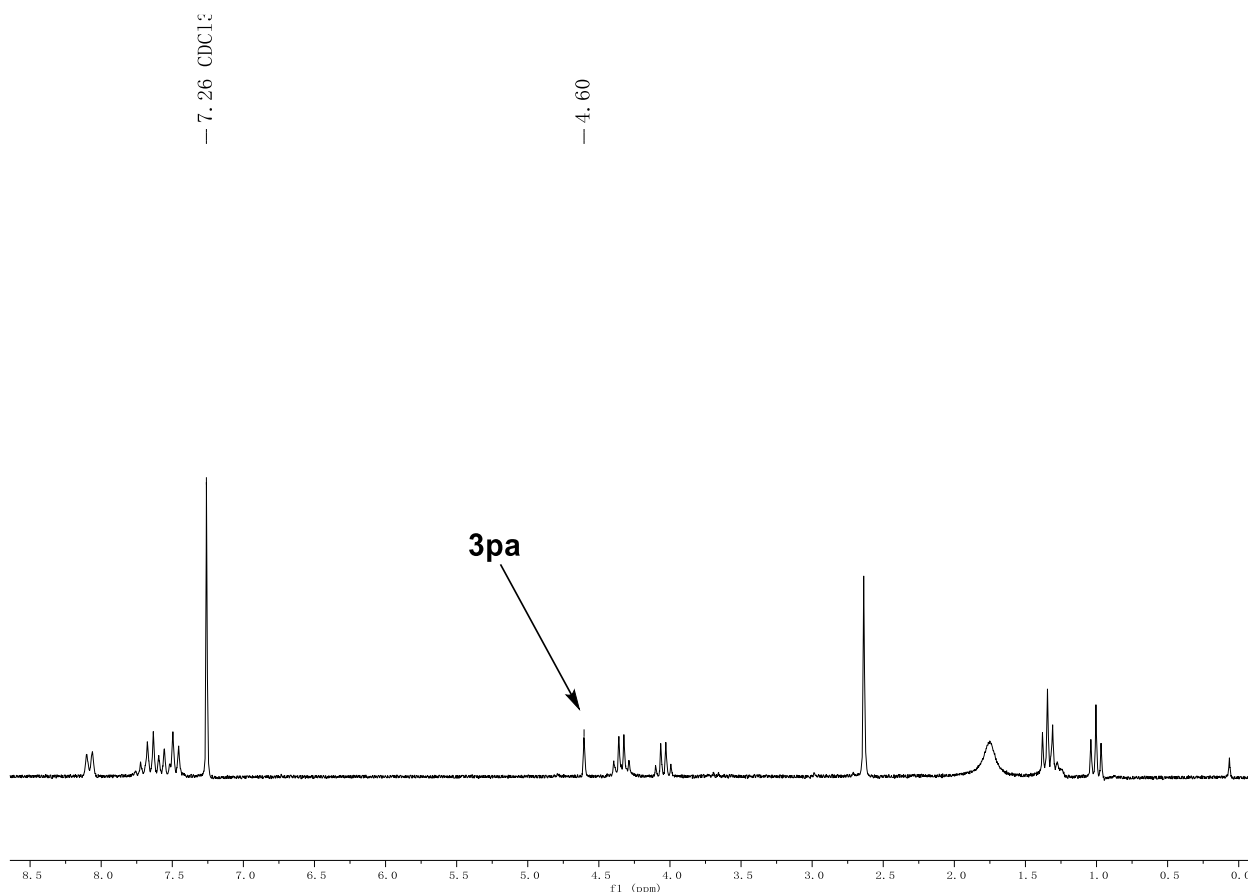
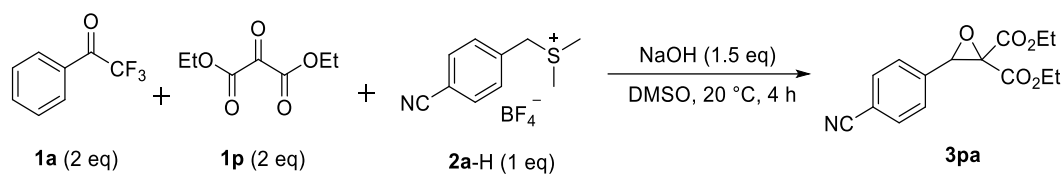
[2a]/mol L ⁻¹	[1a]/mol L ⁻¹	$k_{\text{obs}}/\text{s}^{-1}$
5.00×10^{-5}	5.00×10^{-4}	5.81×10^{-2}
5.00×10^{-5}	7.50×10^{-4}	7.94×10^{-2}
5.00×10^{-5}	1.00×10^{-3}	1.11×10^{-1}
5.00×10^{-5}	1.25×10^{-3}	1.46×10^{-1}
5.00×10^{-5}	1.50×10^{-3}	1.82×10^{-1}

$k_2 = 1.26 \times 10^2 \text{ L mol}^{-1} \text{ s}^{-1}$



(3) competition experiment and crossover experiments

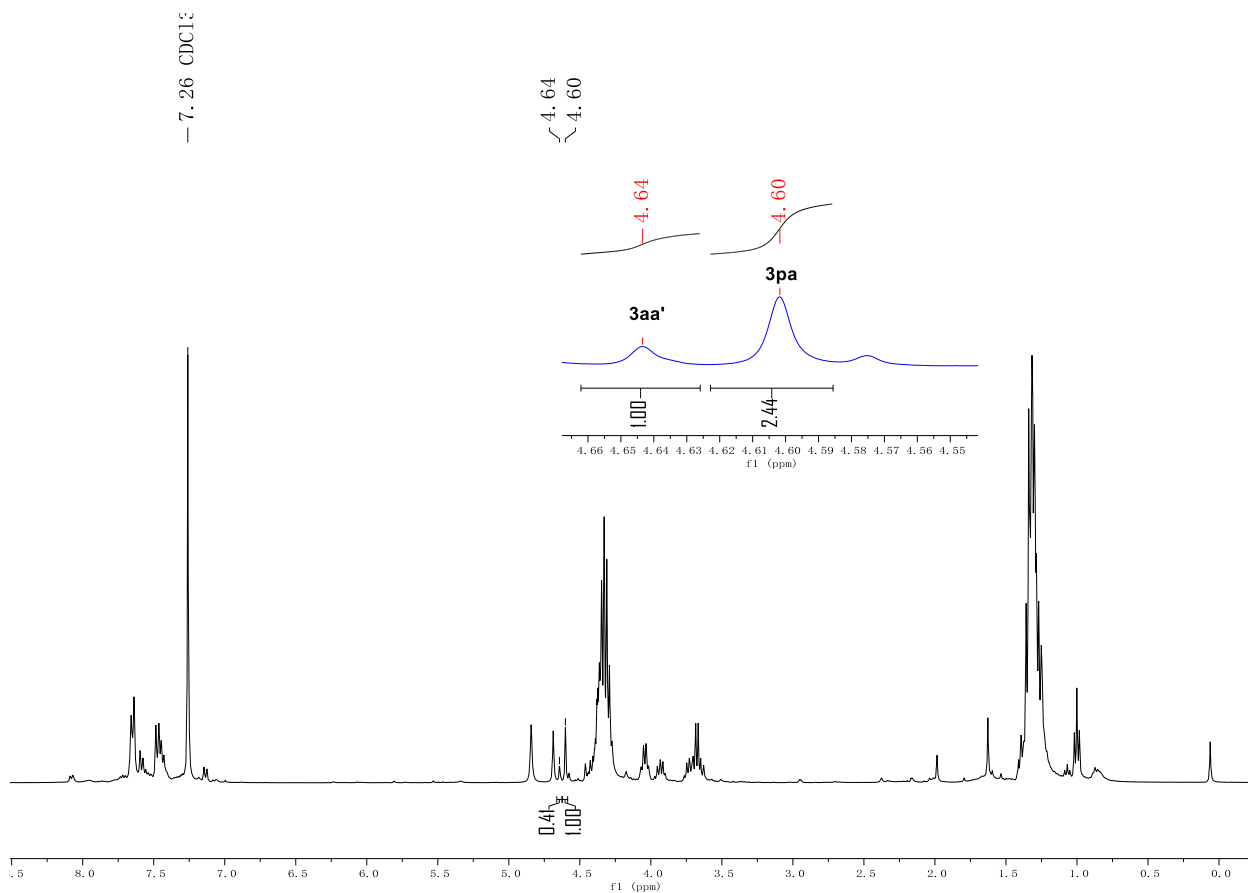
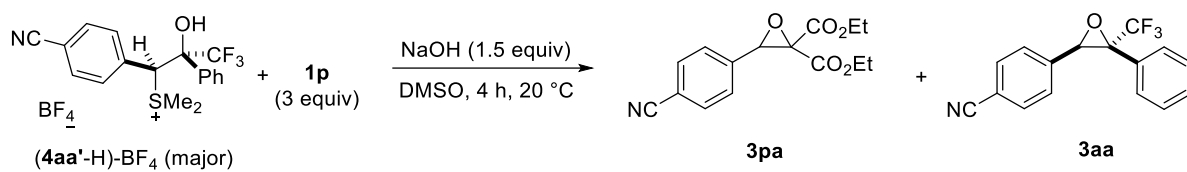
Competition between **1a** and **1p** (trapping agent) for sulfonium ylide **2a**



^1H NMR spectroscopy shows selective formation of **3pa** (from **1p**) under the above mentioned experimental conditions ($[\mathbf{1l}]_0/[\mathbf{1m}]_0 = 1$).

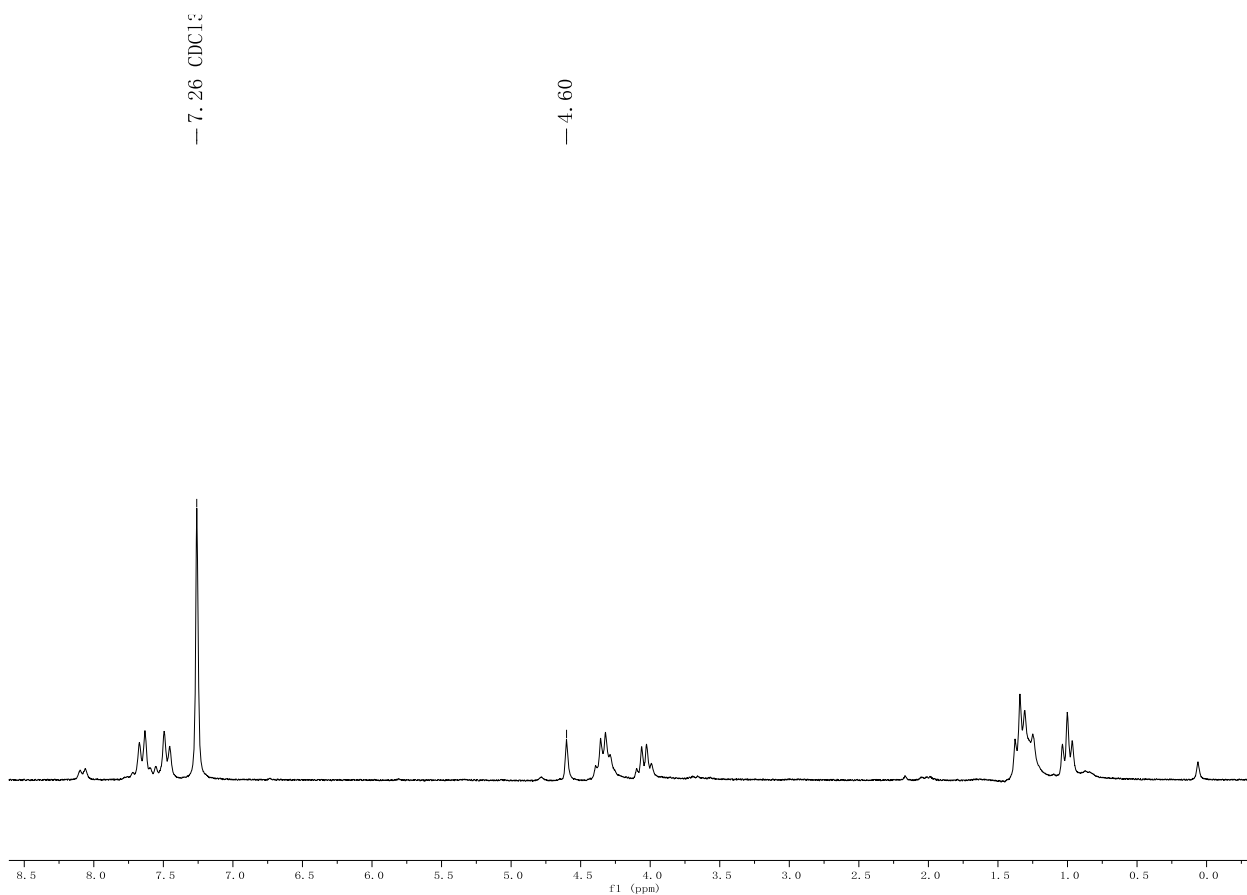
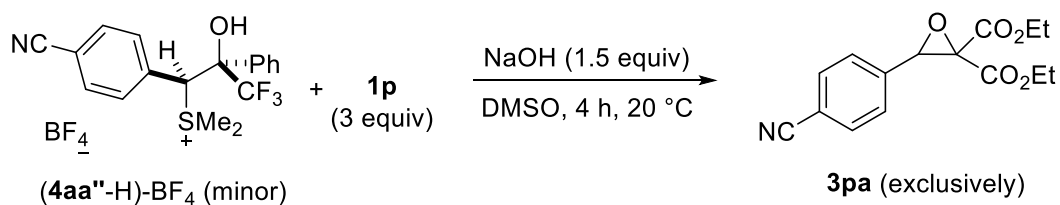
Crossover experiments

Substrate (**4aa'**-H)-BF₄ (with **1p** as trapping agent)



Crossover reaction result: $P_{\text{CC}}/P_{\text{rc}} = [\mathbf{3pa}]/[\mathbf{3aa}'] = 2.44$

Substrate (**4aa''**-H)-BF₄ (with **1p** as trapping agent)



Crossover reaction result: only P_{CC}

5.5 References

- (1) (a) Mayr, H.; Bug, T.; Gotta, M. F.; Hering, N.; Irrgang, B.; Janker, B.; Kempf, B.; Loos, R.; Ofial, A. R.; Remennikov, G.; Schimmel, H. *J. Am. Chem. Soc.* **2001**, *123*, 9500–9512. (b) Lucius, R.; Loos, R.; Mayr, H. *Angew. Chem., Int. Ed.* **2002**, *41*, 91–95. (c) Mayr, H.; Kempf, B.; Ofial, A. R. *Acc. Chem. Res.* **2003**, *36*, 66–77.
- (2) (a) Appel, R.; Mayr, H. *J. Am. Chem. Soc.* **2011**, *133*, 8240–8251. (b) Li, Z.; Jangra, H.; Chen, Q.; Mayer, P.; Ofial, A. R.; Zipse, H.; Mayr, H. *J. Am. Chem. Soc.* **2018**, *140*, 5500–5515.
- (3) (a) Olmstead, W. N.; Margolin, Z.; Bordwell, F. G. *J. Org. Chem.* **1980**, *45*, 3295–3299. (b) Bordwell, F. G. *Acc. Chem. Res.* **1988**, *21*, 456–463.
- (4) For a comprehensive list of pK_a values, see <http://ibond.nankai.edu.cn/>.
- (5) Appel, R.; Hartmann, N.; Mayr, H. *J. Am. Chem. Soc.* **2010**, *132*, 17894–17900.
- (6) Hansch, C.; Leo, A.; Taft, R. W. *Chem. Rev.* **1991**, *91*, 165–195.
- (7) (a) Aggarwal, V. K.; Calamai, S.; Ford, J. G. *J. Chem. Soc., Perkin Trans. 1* **1997**, 593–599. (b) Aggarwal, V. K.; Richardson, J. *Chem. Commun.* **2003**, 2644–2651.
- (8) Müller, P.; Bernardinelli, G.; Thi, H. C. G. *Helvetica Chimica Acta* **1989**, *72*, 1627–1638.

Curriculum Vitae

Personal information

Name: Li, Zhen
Citizenship: Chinese
Gender: Male
Date of birth: May, 05, 1988
Place of birth: Baotou, Nei Mongol, China

Education

Ph.D. in Organic Chemistry: (2014-2018) Department Chemie und Biochemie
Ludwig-Maximilians-Universität München, Germany
Thesis Supervisor: Prof. Dr. Herbert Mayr
Thesis Title: Quantification of electrophilic reactivities of ketones and heteroallenes
Master of Science: (2011-2014) Department of Chemistry
Nankai University, China
Thesis Supervisor: Prof. Dr. Zhongwen Wang
Thesis Title: Total synthesis of (-)-quinocarcin
Bachelor of Science: (2007-2011) Department of Chemistry
Nankai University, China
Thesis Supervisor: Prof. Dr. Zhongwen Wang
Thesis Title: The synthesis of Donor-Acceptor cyclopropanes and investigation of their [3 +2] cycloaddition reactions

Fellowship

PhD fellowship by the China Scholarship Council (2014-2018)